Investigating the anti-amyloidogenic activities of functionalized polyphenolic compounds and metal oxide nanoparticles on the structure and the fibrillation of β-lactoglobulin.

Thesis submitted by

RAMKRISHNA DALUI

DOCTOR OF PHILOSOPHY (SCIENCE)

Department of Chemistry

Faculty Council of Science

Jadavpur University

2024

JADAVPUR UNIVERSITY
KOLKATA-700032, INDIA

INDEX NO. 49/17/Chem./25

1. Title of the thesis: Investigating the anti-amyloidogenic activities of functionalized polyphenolic compounds and metal oxide nanoparticles on the structure and the fibrillation of β-lactoglobulin.

2. Name, Designation, and institution of supervisor:

Professor (Dr.) Umesh Chandra Halder

Professor,

Department of Chemistry,

Jadavpur University,

Kolkata-700032, India.

List of Publications

1. **Ramkrishna Dalui**, Shahnaz Begum, Hasan Parvej, Swarnali Paul, Falguni Mondal, Sampa Pal, Nayim Sepay, and Umesh Chandra Halder. Electronic effect of (E)-1-(2-hydroxyphenyl)-3-phenylprop-2-en-1-one derivatives on the promotion and modulation of the aggregation of bovine beta-lactoglobulin. Journal of Molecular Structure (2024). (Under Revision).

2. **Ramkrishna Dalui**, Hasan Parvej, Shahnaz Begum, Subrata Sardar, Sanhita Maity, Nayim Sepay and U. C. Halder. Zinc Oxide nanoparticle assisted refolding of alkali denatured bovine β-lactoglobulin: A useful technique for protein renaturation (Communicated).

3. **Ramkrishna Dalui**, Shahnaz Begum, Hasan Parvej, Subrata Sardar, Nayim Sepay and U. C. Halder. Amyloid aggregates of bovine beta-lactoglobulin are inhibited by highly dispersed copper oxide nanoparticles prepared by a quick-precipitation method: An approach to therapeutics for protein misfolding diseases (Communicated).

4. **Ramkrishna Dalui**, Hasan Parvej, Shahnaz Begum, Subrata Sardar, Nayim Sepay and U. C. Halder. Self-assembly formation and acceleration of thermal aggregation of bovine β-lactoglobulin in the presence of synthesized zinc oxide nanoparticles (Communicated).

5. Hasan Parvej, **Ramkrishna Dalui**, Shahnaz Begum, Swarnali Paul, Falguni Mondal, Sanhita Maity, Nayim Sepay and Umesh Chandra Halder,2024. Promotion and modulation of amyloid fibrillation of bovine beta-lactoglobulin by hydroxychalcones. Journal of Molecular Structure, 1318, p.139164.

6. Shahnaz Begum, Swarnali Paul, Hasan Parvej, Falguni Mondal, **Ramkrishna Dalui**, Anirban Pradhan, Nayim Sepay, and Umesh Chandra Halder. Anion–Induced Amyloid Fibrillation of Human Insulin In vitro. ChemistrySelect, 9(13), p.e202303699.

7. Swarnali Paul, Shahnaz Begum, Hasan Parvej, **Ramkrishna Dalui**, Subrata Sardar, Falguni Mondal, Nayim Sepay, Umesh Chandra Halder. In vitro retardation and modulation of human insulin amyloid fibrillation by Fe3+ and Cu2+ ions. New Journal of Chemistry, 48(7), pp.3120-3135.

8. Shahnaz Begum, Hasan Parvej, **Ramkrishna Dalui**, Swarnali Paul, Sanhita Maity, Nayim Sepay, Mohd Afzal, Umesh Chandra Halder. Structural modulation of insulin by hydrophobic and hydrophilic molecules. RSC advances, 13(48), pp.34097-34106.
9. Hasan Parvej, Shahnaz Begum, **Ramkrishna Dalui**, Swarnali Paul, Barun Mondal, Subrata Sardar, Nayim Sepay, Gourhari Maiti and Umesh Chandra Halder. Coumarin derivatives inhibit the aggregation of β-lactoglobulin. RSC advances, 12(27), pp.17020-17028.
10. Sampa Pal, Sanhita Maity, Subrata Sardar, Shahnaz Begum, **Ramkrishna Dalui**, Hasan Parvej, Kaushik Bera, Anirban Pradhan, Nayim Sepay, Swarnali Paul and Umesh Chandra Halder. Antioxidant ferulic acid prevents the aggregation of bovine β-lactoglobulin in vitro. Journal of Chemical Sciences, 132, pp.1-13.
11. Subrata Sardar, Md. Anas, Sanhita Maity, Sampa Pal, Hasan Parvej, Shahnaz Begum, **Ramkrishna Dalui**, Nayim Sepay, Umesh Chandra Halder. Silver nanoparticle modulates the aggregation of beta-lactoglobulin and induces to form rod-like aggregates. International journal of biological macromolecules, 125, pp.596-604.
12. Sanhita Maity, Sampa Pal, Subrata Sardar, Nayim Sepay, Hasan Parvej, Shahnaz Begum, **Ramkrishna Dalui**, Niloy Das, Anirban Pradhan and Umesh Chandra Halder. Inhibition of amyloid fibril formation of b-lactoglobulin by natural and synthetic curcuminoids. New Journal of Chemistry, 42(23), pp.19260-19271.

List of Presentations at National/ International Conferences/ Seminars

- Poster presentation at International Conference on Chemistry for Human Development (ICCHD-2018) from 8-10th January 2018 held at Heritage Institute of Technology, Kolkata.
- Participated in the National Seminar on Current Developments in Chemical Sciences (CDCS-2018) On 7th March 2018, Organized by the Department of Chemistry, Jadavpur University.
- Participated in the National Symposium on Emerging Trends in Chemical Science (ETCS-2018) held on 28th March 2018, Organized by the Department of Chemistry, University of Calcutta, Kolkata, India.

- Participated in the National Seminar on Chemical Sciences: Today and Tomorrow (CSTT-2019) held on 14th March 2019, Organized by the Department of Chemistry, Jadavpur University, Kolkata 700032.
- Participated & Poster presentation at the National Conference on 'Recent Advances in Chemistry 2019' (RAC 2019) held in the Department of Chemistry, NIT Meghalaya during October 14-15, 2019.
- Poster Presentation at the National Seminar on Emerging Trends in Chemical Sciences held on 7th January 2020, Organized by the Department of Chemistry, Jadavpur University, Kolkata 700032.

"Statement of Originality"

I, **Ramkrishna Dalui**, registered on June 23, 2017. I hereby declare that this thesis, titled "**Investigating the Anti-Amyloidogenic Activities of Functionalized Polyphenolic Compounds and Metal Oxide Nanoparticles on the Structure and Fibrillation of β-Lactoglobulin**" encompasses both a comprehensive literature review and original research conducted by me as part of my doctoral studies. All information presented within this thesis has been gathered and compiled in accordance with established academic regulations and ethical standards. I affirm that I have duly cited and referenced all materials and results that are not original to this work.

Ramkrishna Dalui

Signature of Candidate

Date: 18.12.2024

যাদবপুর বিশ্ববিদ্যালয়
কলকাতা-৭০০ ০৩২, ভারত

JADAVPUR UNIVERSITY
KOLKATA-700 032, INDIA

FACULTY OF SCIENCE DEPARTMENT OF CHEMISTRY ORGANIC CHEMISTRY SECTION

CERTIFICATE FROM THE SUPERVISOR

This is to certify that the thesis entitled *"Investigating the anti-amyloidogenic activities of functionalized polyphenolic compounds and metal oxide nanoparticles on the structure and the fibrillation of β-lactoglobulin"* submitted by **Ramkrishna Dalui** who got his name registered on **23.06.2017** for the award of Ph. D. (Science) Degree of Jadavpur University, is absolutely based upon his own work under the supervision of **Prof. (Dr.) Umesh Chandra Halder** and neither this thesis nor any part of it has been submitted for either any degree/diploma or any other academic award anywhere before.

Umesh Chandra Halder. 18/12/2024.
(Signature of the Supervisor date with official seal)

DR. UMESH CHANDRA HALDER
Professor of Chemistry
Department of Chemistry
Jadavpur University
Kolkata-700032

Telephone : 91-033-2414-6223 Internet : http:// www.jadavpur.edu Fax : 91-033-2414-6484

Acknowledgments

While words may often fall short in fully expressing gratitude and emotions, I wish to take this moment to extend my heartfelt appreciation to those who supported me throughout my academic journey. First and foremost, I humbly express my gratitude to the 'Almighty' for granting me this invaluable opportunity and for instilling in me the strength to fulfill my responsibilities.

I would like to express my sincere appreciation and deep gratitude to my esteemed supervisor, ***Prof. Umesh Chandra Halder****, from the Department of Chemistry, Organic Chemistry Division, at Jadavpur University, Jadavpur, India. His consistent support, kind encouragement, and the exchange of immensely valuable ideas and suggestions have been pivotal in shaping my academic and research experience. I have been remarkably fortunate to have had a supervisor who not only provided unwavering attention but also empowered me with the freedom to independently explore and interpret research findings. This guidance has been invaluable in my academic and personal growth, and I am truly grateful for the mentorship I have received.*

I would like to take this opportunity to express my sincere and wholehearted gratitude to ***Prof. K. K. Rajak****, Head of the Department of Chemistry at Jadavpur University, for graciously providing me with access to a wide range of departmental facilities and unwavering moral support throughout this duration. Additionally, I extend my sincere appreciation to* ***Prof. A. Saha****,* ***Prof. P. Roy****, and* ***Prof. A. Gayen****, present Sectional Heads of the Department of Chemistry at Jadavpur University in Kolkata, for their continuous support, encouragement,*

and for facilitating the necessary resources that allowed me to conduct my research seamlessly. Their invaluable scientific, academic, and administrative assistance significantly contributed to the successful completion of my work, and for this, I am truly grateful.

I would like to take this opportunity to express my sincere gratitude to ***Prof. C.R. Sinha****, the esteemed Dean of the Faculty of Science at Jadavpur University in Kolkata. His unwavering administrative assistance, invaluable advice, and constant encouragement have been instrumental in my journey, and I am truly thankful for his support.*

I am deeply appreciative of the invaluable support, guidance, and encouragement provided by ***Prof. S. Bhar, Prof. G. Maiti, Prof. U. Jana, Dr. S. Haldar, Dr. T. Bhowmik, Dr. S Guha, Dr. A. Thakur, Dr. M. A. Mondal, Dr. A. Saha, Dr. T Ghosh, Dr. S. Waiba, Dr.R.K. Nandi*** *and all the esteemed faculty members of the Department of Chemistry at Jadavpur University, Kolkata. Their unwavering assistance has been instrumental in shaping my academic journey, and I am grateful for their mentorship and support.*

I wish to extend my sincere appreciation to my esteemed colleagues at the laboratory, namely ***Dr. Hasan Parvej, Dr. Shahnaz Begum, Ms. Swarnali Paul, Ms. Falguni Mondal, Mr. Rajibul Islam,*** *and* ***Ms. Debosmita Mukherjee****. Additionally, I would like to express my gratitude to the senior members of the lab,* ***Dr. Subrata Sardar, Dr. Barun Mondal, Dr. Sanhita Maity****, and* ***Dr. Sampa Pal****, for their exemplary collaborative approach and unwavering readiness to provide their expertise whenever I encountered challenges in my research methodologies and data analysis. I am truly thankful for the cohesive community that we have collectively fostered. I will always*

cherish the memories of my laboratory colleagues. Our shared experiences were characterized by moments of lightheartedness, laughter, and strengthened connections.

I wish to express my sincere gratitude to ***Mrs. Sraboni Halder*** *(Madam) for her unwavering moral support, warmth, and guidance.*

I am deeply grateful to ***Dr. Nayim Sepay****, Assistant Professor of the Department of Chemistry at Lady Brabourne College, Kolkata, for his indispensable technical assistance, invaluable scientific expertise, and unwavering moral support.*

I would like to express my profound gratitude to my parents, with special mention of my late father, ***Nabakumar Dalui****, and my mother,* ***Mrs. Maharani Dalui****. I extend my sincere appreciation to my in-laws,* ***Mr. Sadhan Chandra Mandal*** *and* ***Mrs. Radharani Mandal****, as well as my entire family, for their unwavering love, support, prayers, care, and sacrifices. Their invaluable contributions have significantly influenced and shaped my educational and professional endeavors. Their steadfast encouragement has served as a crucial foundation for my perseverance and achievements. I wish to express my heartfelt gratitude to my supportive and caring wife,* ***Mrs. Pritilata Mandal****, for her unwavering encouragement during challenging times. I deeply appreciate her willingness to manage the care of our little sweetheart,* ***'Rishik'****, which provided me with a great sense of comfort and relief as I focused on my academic pursuits.*

I also wish to convey my sincere appreciation to my esteemed confidants and mentors, ***Dr. Krishnagopal Maiti*** *and* ***Mr. Krishendu Barik****, for their invaluable counsel, empathy, and dedicated*

commitment in assisting me to successfully navigate the completion of this thesis.

Last, but certainly not least, I express my sincere gratitude to all my colleagues at Bartala Madhyamik Vidyalaya (H.S), specifically ***Mr. Ratan Mistry, Mr. Kunal Mukherjee, Mr. Palash Mandal,*** *and* ***Mr. Shantanu Senapati*** *for their relentless encouragement and moral support.*

Date: (RAMKRISHNA DALUI)

Place: Research Scholar

Jadavpur University

Dedicated to my late Father, who made me stronger, better, and more fulfilled.

PREFACE

The research pertaining to the Doctor of Philosophy (Science) degree thesis was conducted under the guidance of Prof. (Dr.) Umesh Chandra Halder at the Department of Chemistry, Jadavpur University, Kolkata, India.

Proteins, ubiquitous bio-molecules, are integral to a wide spectrum of biological processes. Serving as the structural foundation of living cells, they comprise a linear sequence of amino acids synthesized on ribosomes. Demonstrating exceptional adaptability, proteins function independently or in conjunction with other proteins or cellular components. Biological processes encompass a diverse range of phenomena, including intricate developmental and differentiation processes, enzymatic reaction catalysis, modulation of gene expression, signal transduction, molecular transport and storage, neurological activity, cell death, and apoptosis. The multifaceted functionality of proteins stems from the intricate folding of their polypeptide chains into highly ordered structures. These folds are meticulously structured to minimize energy conformations of individual amino acid residues while maximizing the formation of hydrogen bonds between polar groups, resulting in a compact, three-dimensional atomic structure with strategically concealed hydrophobic residues from the surrounding aqueous environment.

Protein misfolding is a prevalent occurrence within cellular processes, arising from various factors including genetic mutations, errors in protein synthesis, abnormal protein modifications, exposure to elevated temperatures or oxidative stress, and incomplete protein complex formation. When a protein misfolds, it exposes its hydrophobic regions, leading to the development of protein aggregates. These aggregates have the potential to disrupt normal cellular functions by sequestering functional proteins and inciting a sequence of malfunctions. Protein instability presents a formidable challenge for biopharmaceutical formulations, necessitating a comprehensive understanding of the underlying physical mechanisms and available protective measures for proteins. Misfolding of proteins leads to the conversion of native states to non-native structures, which may further progress into organized fibrils. This phenomenon is associated with over 35 human diseases, including Alzheimer's disease, Parkinson's disease, Huntington's disease, and sickle cell anemia, thereby imposing significant challenges on medical technology and industries. Additionally, the potential formation of intermediates such as protofibrils and oligomers must not be overlooked. Notably, 20 homologous proteins and several associated proteins, including Aβ1–40, β-lactoglobulin,

lysozymes, and insulin, have been identified as forming amyloid fibrils, which are implicated in causing incurable conditions such as Parkinson’s disease and type-2 diabetes.

The distinct properties and applications of nanoparticles arise from their large surface area and small size, setting them apart from bulk materials. Nanoparticles possess the capacity to influence protein folding and aggregation, which is of interest due to both potential beneficial applications and potential risks to human health and the environment. Therefore, it is crucial to comprehensively understand the impact of nanoparticles on fundamental biological processes such as protein folding. While the binding of proteins to planar surfaces often induces significant changes in their secondary structure, the high curvature of nanoparticles can facilitate the retention of proteins' original structure. However, studies have revealed that interactions between proteins and various nanoparticle surfaces can still lead to perturbations in protein structure. Numerous studies have documented a loss of α-helical content in proteins upon adsorption onto nanoparticles, often accompanied by an increase in β-sheet content. The small size of nanoparticles enables them to access nearly every part of the human body, including crossing the blood-brain barrier, suggesting the potential use of nanoparticles to inhibit fibril formation or disaggregate amyloid fibrils for the treatment of neurodegenerative diseases such as Alzheimer's.

Proteins can attach to nanoparticle surfaces through various mechanisms, including electrostatic interactions, van der Waals forces, and hydrophobic, hydrophilic, structural, and steric interactions. The modification of nanoparticles through their association with specific proteins affects the functional properties of the nanoparticle and the attached protein molecule It is widely acknowledged that upon adsorption onto nanoparticles, the structure of proteins is perturbed to varying extents. However, it is also pertinent to investigate whether certain nanoparticles may function as chaperones, thereby enhancing the efficiency of protein folding. In the native state of a protein, the hydrophobic core is shielded, and the protein surface is typically rich in hydrophilic residues, which interact favorably with the surrounding aqueous environment. Unfolding of the protein exposes hydrophobic surfaces, consequently leading to protein aggregation. Chaperones such as GroEL and GroES selectively bind to unfolded proteins through hydrophobic or electrostatic interactions, preventing aggregation and facilitating their folding into the native conformation. Chaperones find widespread application in biotechnology for the production of biologically active recombinant proteins.

Chapter 1 provides a brief overview of bovine β-lactoglobulin, covering its origin, isolation, purification, structural characteristics, chemical modification, and biological functions. This protein is particularly important in the field of structural biology due to its well-defined crystal structure. The chapter also explores amyloid fibril formation, a process associated with various neurodegenerative diseases, and investigates the factors influencing amyloid fibrillation resulting from aggregation.

Chapter 2 offers an in-depth literature review of polyphenolic compounds, specifically focusing on chalcone analogs.

In Chapter 3, the synthesis of four distinct chalcone derivatives (SC1, SC2, SC3, and SC4) is discussed, each featuring different substituents positioned relative to the chalcone nucleus. The impact of these chalcone derivatives on the structural and aggregation properties of β-lactoglobulin is examined using multispectroscopic and morphological analyses. The synthesized compounds were found to promote β-lactoglobulin aggregation in the following order: SC3 > SC2 > SC1 > SC4.

Chapter 4 presents an extensive literature review on nanoparticles and nanotechnology, focusing on their diverse impact on the structural modifications of protein aggregation and inhibition.

In Chapter 5, the potential chaperone-like activity of synthesized zinc oxide nanoparticles (ZnO NPs) when interacting with alkaline unfolded bovine β-lactoglobulin at pH 11.0 is investigated. This exploration involves a comprehensive analysis using multispectroscopic and morphological methodologies to understand the interactions between the nanoparticles and the protein.

Chapter 6 delves into the inhibition of amyloid aggregates of thermally incubated bovine β-lactoglobulin by highly dispersed copper oxide nanoparticles (CuO NPs) prepared via a rapid precipitation method. This inhibition is scrutinized through diverse spectroscopic and morphological experiments conducted at physiological pH.

In Chapter 7, the focus is on the self-assembly formation and accelerated thermal aggregation of bovine β-lactoglobulin in the presence of synthesized zinc oxide nanoparticles. These phenomena are studied extensively through a variety of spectroscopic and morphological experiments conducted under physiological pH conditions.

ABBREVIATIONS

°C	:	Degree centigrade
µL	:	Microlitre
µM	:	Micromolar
Abs	:	Absorbance
ANS	:	1-Anilino-8-naphthalene sulphonic acid
APS	:	Ammonium persulfate
AR	:	Analytical reagent
ATP	:	Adenosine triphosphate
BSA	:	Bovine serum albumin
CD	:	Circular dichroism
CR	:	Congo red
Cys	:	Cysteine
DLS	:	Dynamic light Scattering
FA	:	Folic acid
FESEM	:	Field emission scanning electron microscope
FRET	:	Fluorescence resonance energy transfer
Gdn.HCl	:	Guanidine hydrochloride
Gdn.SCN	:	Guanidinum thiocyanate
Gln	:	Glutamine
Glu	:	Glutamic acid
HSA	:	Human serum albumin
HIV-1	:	Human Immunodeficiency Virus 1
Lys	:	Lysine
M	:	Molar
Met	:	Methionine

Mg	:	Milligram
mL	:	Milliliter
mM	:	Millimolar
MRE	:	Mean residue ellipticity
nm	:	Nanometer
ns	:	Nanosecond
PAGE	:	Polyacrylamide gel electrophoresis
PEG	:	Poly (ethylene glycol)
RBP	:	Retinol-binding protein
SDS	:	Sodium dodecyl sulfate
SEM	:	Scanning electron microscope
tBHP	:	tert-Butyl hydroperoxide
TEM	:	Transmission electron microscope
TEMED	:	N, N, N′, N′-Tetramethylenediamine
TFE	:	2, 2, 2-Trifluoroethanol
Th T	:	Thioflavin T
Trp	:	Tryptophan
Tyr	:	Tyrosine
UV	:	Ultraviolet
β	:	Beta
Arg	:	Arginine
β-lg	:	Beta-lactoglobulin
Aβ	:	Amyloid-beta
AD	:	Alzheimer's disease
AFM	:	Atomic force microscopy
DMSO	:	Dimethyl sulfoxide

DTT	:	Dithioerythritol
ER	:	Endoplasmic reticulum
EGCG	:	Epigallocatechin gallate
SOD1	:	Superoxide dismutase 1
SAR	:	Structure-activity relationship
DM	:	Diabetes mellitus
NMR	:	Nuclear magnetic resonance
RLS	:	Rayleigh light scattering
STM	:	Scanning tunneling microscopy
pI	:	Isoelectric point
CuONPs	:	Copper oxide nanoparticles
ZnONPs	:	Zinc oxide nanoparticles
DNA	:	Deoxyribonucleic acid
RNaseA	:	Ribonuclease A
CJD	:	Creutzfeldt–Jakob disease
PD	:	Parkinson's disease
ALS	:	Amyotrophic lateral sclerosis
HPLC	:	High-performance liquid chromatography
ER	:	Endoplasmic reticulum
PDI	:	Protein disulfide isomerase
HD	:	Huntington's disease
XRD	:	X-ray diffraction

CONTENTS

CHAPTER 1

Introduction

1.1. Outline of Protein and its Structure

Proteins are complex macromolecules composed of one or more polypeptide chains, each consisting of a linear sequence of amino acid residues. These biomolecules perform a wide range of vital functions in living organisms, including but not limited to DNA replication, molecular transportation, metabolic catalysis, and structural maintenance of cells. Proteins are macromolecules that dwarf the dimensions of sugar or salt molecules. They are composed of lengthy chains of amino acids, akin to beads arranged on a string. Roughly 20 amino acids o sequence and composition **(Fig.1)** (Taylor, 1986). While not all protein functions can be elucidated by analyzing their amino acid sequence, well-established correlations between protein structure and function can be attributed to the intrinsic properties of the amino acids that constitute them.

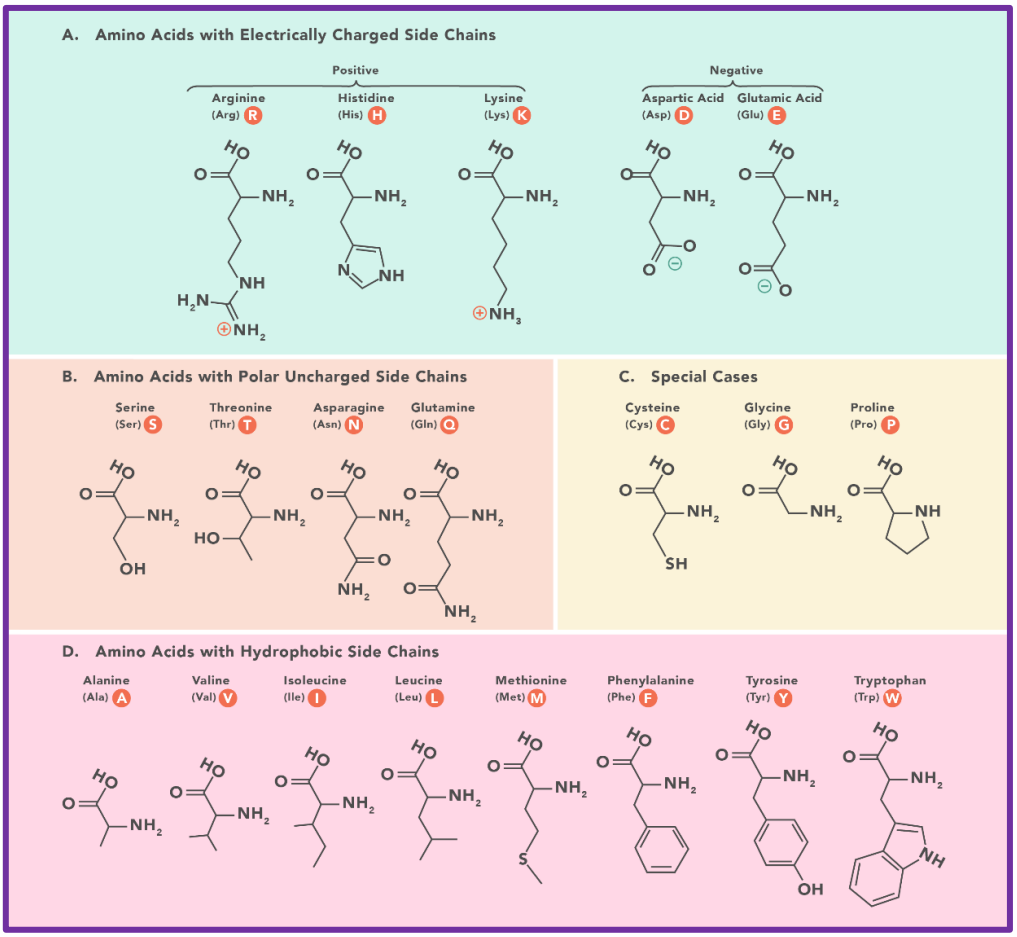

Figure 1: Chemical structures of the 20 amino acids that make up proteins.

It is intriguing to note that plants possess the unique ability to synthesize all the essential amino acids for sustaining life, while animals cannot. Plants are capable of utilizing inorganic nutrients, such as nitrogen and potassium, to grow and create organic compounds, such as carbohydrates, through photosynthesis using carbon dioxide from the air (Rao, 2009). On the other hand, animals cannot produce their organic nutrients, which makes it necessary for them to consume external sources. Although most plant sources have a low protein content, ruminant animals like cows consume large amounts of plant material to fulfill their amino acid requirements. Non-ruminant animals, including humans, primarily obtain proteins through animal-based sources like meat, milk, and eggs (Ahmed et al., 2022). Recently, legume seeds ccur naturally in proteins, and proteins with similar functions share a similar amino acid have gained popularity as an affordable and protein-rich food source, especially in the context of human nutrition. Amino acids hold a pivotal position in the human body as indispensable building blocks for protein synthesis, tissue repair, and nutrient absorption. These fundamental components are critical for the proper physiological functioning of the body. In the realm of biochemistry, amino acids are considered the building blocks of proteins. These organic compounds possess a common fundamental structure yet are distinguished from one another based on the unique side chains, also known as R-groups, that they harbor. Amino acids, the fundamental building blocks of proteins, exist in a state of equilibrium wherein two acids coexist, and the proton (H+) oscillates between the amino group and the carboxyl group. The weaker acid always dominates this equilibrium, and since ammonia is weaker than carboxylic acid, the equilibrium tilts towards the left side (on the "zwitterion" side). While textbooks often depict the right-hand structure, amino acids primarily exist in the left-hand structure. Glycine, the simplest and smallest amino acid, has an R-group consisting of a hydrogen (H) atom. Amino acids can be categorized based on their properties, which are determined by the functional groups they possess. They can be broadly classified based on their charge, hydrophobicity, and polarity (Wood, 2016). These properties play a pivotal role in determining the way amino acids interact with surrounding amino acids in polypeptides and proteins, ultimately influencing protein 3D structure and properties (Yan et al., 2014). The set of nine amino acids, namely histidine, isoleucine, leucine, lysine, methionine, phenylalanine, threonine, tryptophan, and valine, are designated as essential amino acids owing to their lack of endogenous synthesis in human and mammalian cells. Thus, the provision of these amino acids is reliant upon dietary intake from external sources **(Fig.2)**.

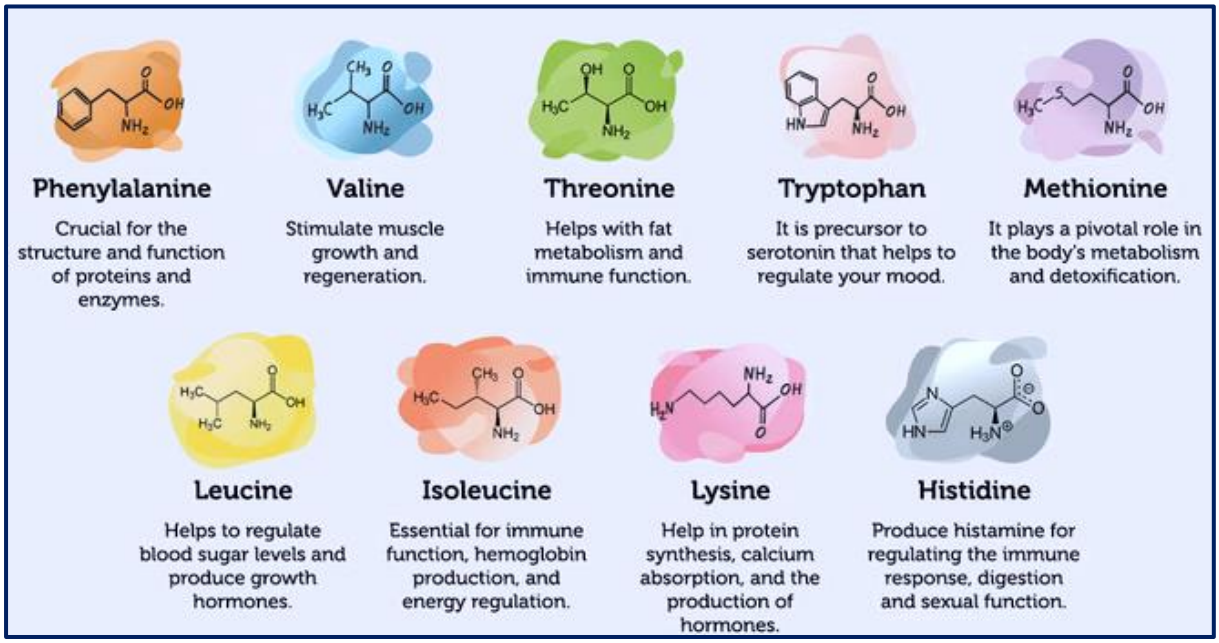

Figure 2: Chemical structures of nine essential amino acids.

1.2. Protein Structure

Protein structures are composed of amino acids that undergo a condensation reaction to form peptide bonds. The linear sequence of amino acids in a protein constitutes its primary structure. Subsequently, the secondary structure of the protein is determined by the dihedral angles of the peptide bonds, while the tertiary structure is formed by the folding of protein chains in three-dimensional space. The association of folded polypeptide molecules results in the quaternary structure of complex functional proteins.

1.2.1. Primary Structure

The primary structure of a protein refers to the linear sequence of amino acids in a polypeptide chain, and it is the most rudimentary level of protein structure. For example, insulin, an endocrine hormone produced in the pancreas, consists of two polypeptide chains, A and B, each with a unique set of amino acids arranged in a specific order (Philippe,1991). The A chain commences with glycine at the N-terminus and concludes with asparagine at the C-terminus, while the B chain's sequence differs from that of the A chain **(Fig.3)**. It is worth noting that the insulin molecule depicted in the diagram pertains to cow insulin, albeit its structure is analogous to that of human insulin. The insulin chains are linked together by sulfur-containing bonds between cysteines (Kurouski et al., 2012).

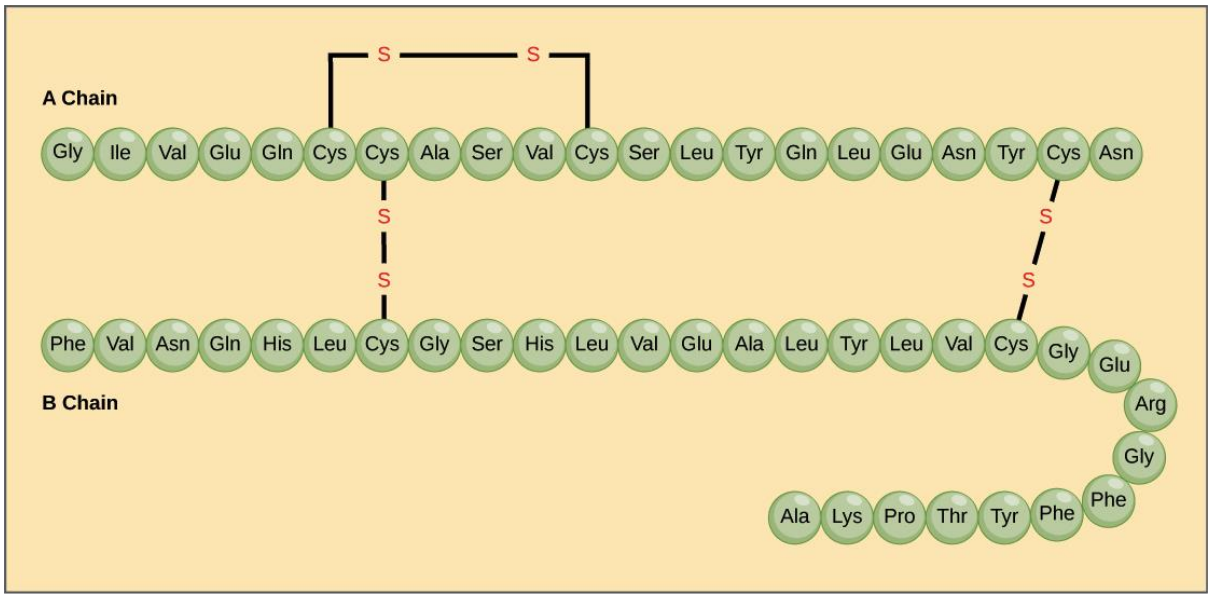

Figure 3: Primary structure: The A chain of insulin is 21 amino acids long and the B chain is 30 amino acids long, and each sequence is unique to the insulin protein.

Proteins play a crucial role in biological processes, and their function is largely determined by their amino acid sequence. This sequence is, in turn, determined by the DNA sequence of the gene that encodes the protein (Fafournoux et al., 2000). Therefore, any alteration in the DNA sequence of the gene can lead to a consequential change in the amino acid sequence of the protein. It is worth noting that even a single amino acid substitution can significantly affect the protein's overall structure and function. For instance, sickle cell anaemia is a hereditary disease that adversely affects red blood cells (Nader et al., 2020). The disease is linked to a slight sequence change in one of the polypeptide chains that make up haemoglobin, the protein responsible for carrying oxygen in the blood. Specifically, the sixth amino acid of the haemoglobin β chain, one of the two types of protein chains that make up haemoglobin, is substituted with valine instead of glutamic acid **(Fig.4)**.

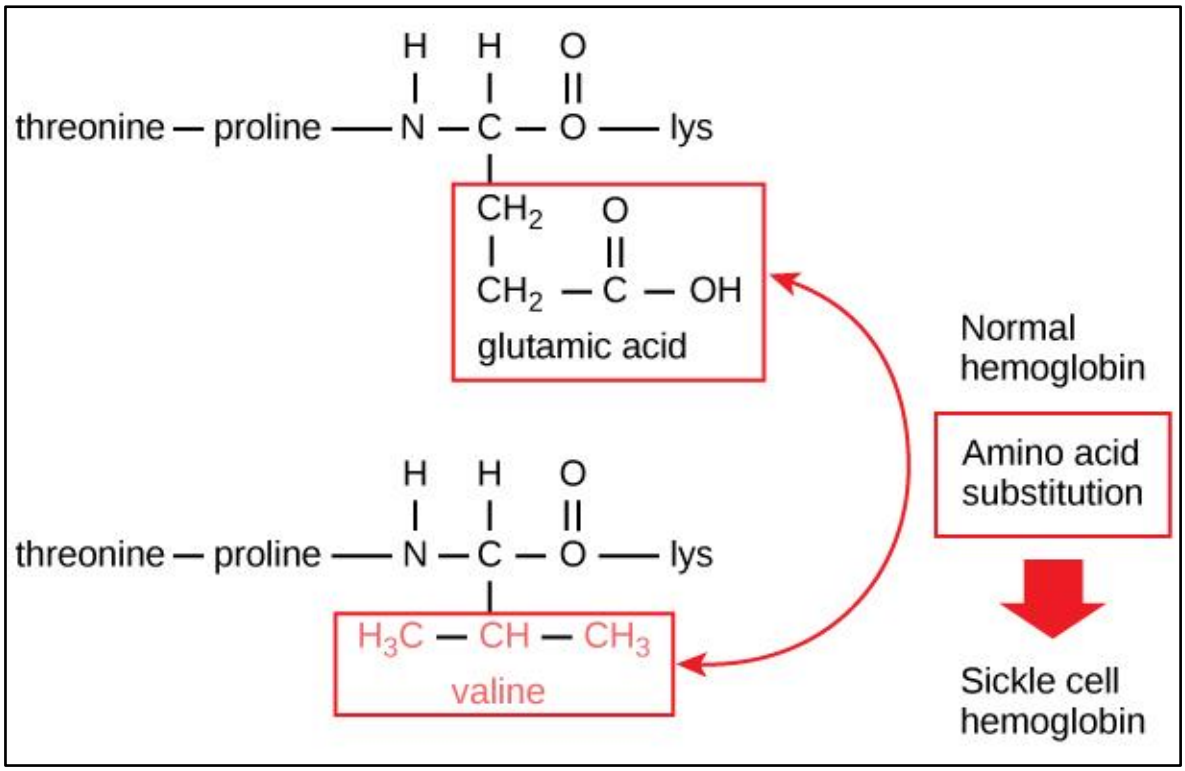

Figure 4: The representation of this substitution for a fragment of the β chain is demonstrated in the diagram below.

It is noteworthy to consider that a haemoglobin molecule comprises two α chains and two β chains, each encompassing approximately 150 amino acids, resulting in a total of nearly 600 amino acids in the complete protein. Remarkably, the distinguishing feature between a normal haemoglobin molecule and a sickle cell molecule is merely two amino acids out of the approximately 600. In individuals who exclusively produce sickle cell haemoglobin, the manifestation of sickle cell anaemia symptoms is inevitable. This is due to the substitution of glutamic acid with valine, which results in the assembly of haemoglobin molecules into elongated fibers. Consequently, the fibers contort the shape of discoid red blood cells, thus causing them to adopt a crescent-like morphology. The blood sample presented below displays various instances of 'sickled' cells, intermixed with normally shaped, discoid cells **(Fig.5)**.

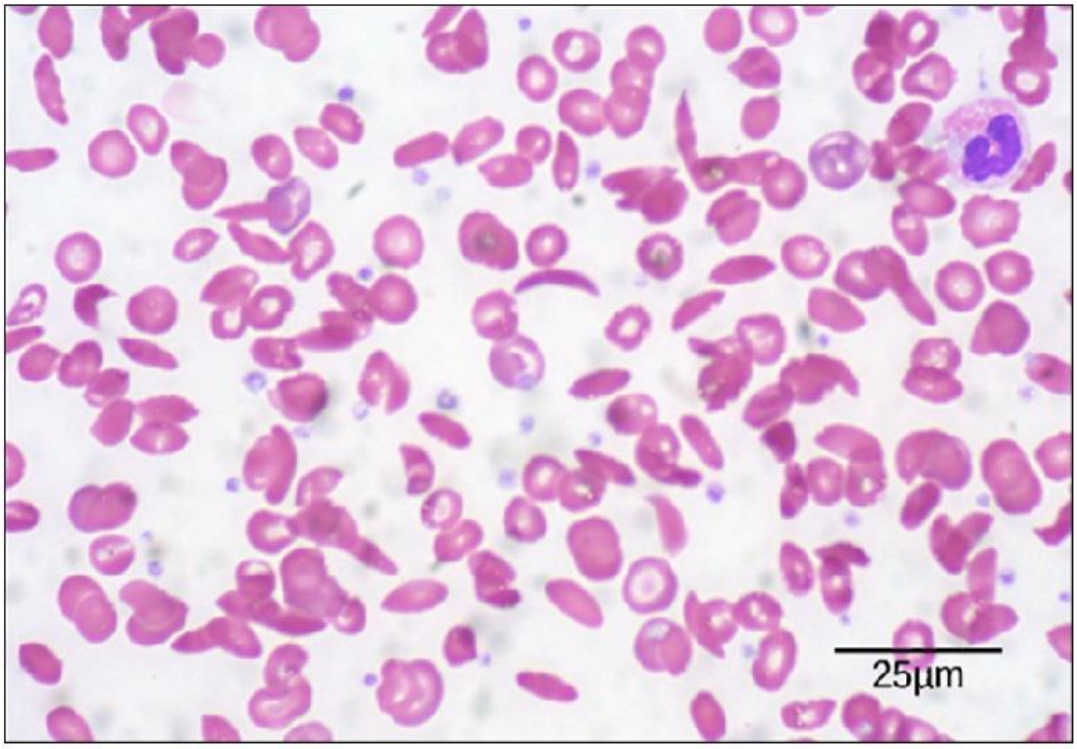

Figure 5: Sickle cell disease: Sickle cells are crescent-shaped, while normal cells are disc-shaped.

1.2.2. Secondary Structure

The subsequent level of protein structure is referred to as secondary structure, which alludes to the local folded structures that emerge within a polypeptide as a result of the interactions between atoms of the backbone. The backbone, in this context, denotes the polypeptide chain apart from the R groups, and, therefore, the secondary structure does not entail the participation of R group atoms. The most widespread types of secondary structures are the α helix and the β pleated sheet (Seebach et al., 2006). These structures are held in conformation by hydrogen bonds that arise from the interaction between the carbonyl 'O'of one amino acid and the amino 'H' of another.

The α-helix is a fundamental secondary structure of proteins, wherein the carbonyl (C=O) of an amino acid residue forms a hydrogen bond with the amino H (N-H) of another residue located four residues down the polypeptide chain. Specifically, the carbonyl group of amino acid 1 is involved in hydrogen bonding with the N-H group of amino acid 5. This pattern of hydrogen bonding results in a helical conformation that is reminiscent of a curled ribbon, with each helical turn being composed of 3.6 amino acid residues. The R-groups of the amino acids extend outward from the α-helix, allowing for various interactions with the surrounding

environment. In the realm of protein structure, a β pleated sheet is a sheet-like structure formed through the alignment of two or more segments of a polypeptide chain, held together by hydrogen bonds. In this secondary structure, the hydrogen bonds form between the carbonyl and amino groups of the protein backbone, while the R groups extend above and below the sheet's plane **(Fig.6)**. The strands of a β pleated sheet can either be parallel or antiparallel, with the former pointing in the same direction, and the latter pointing in opposite directions (Chou et al., 1982).

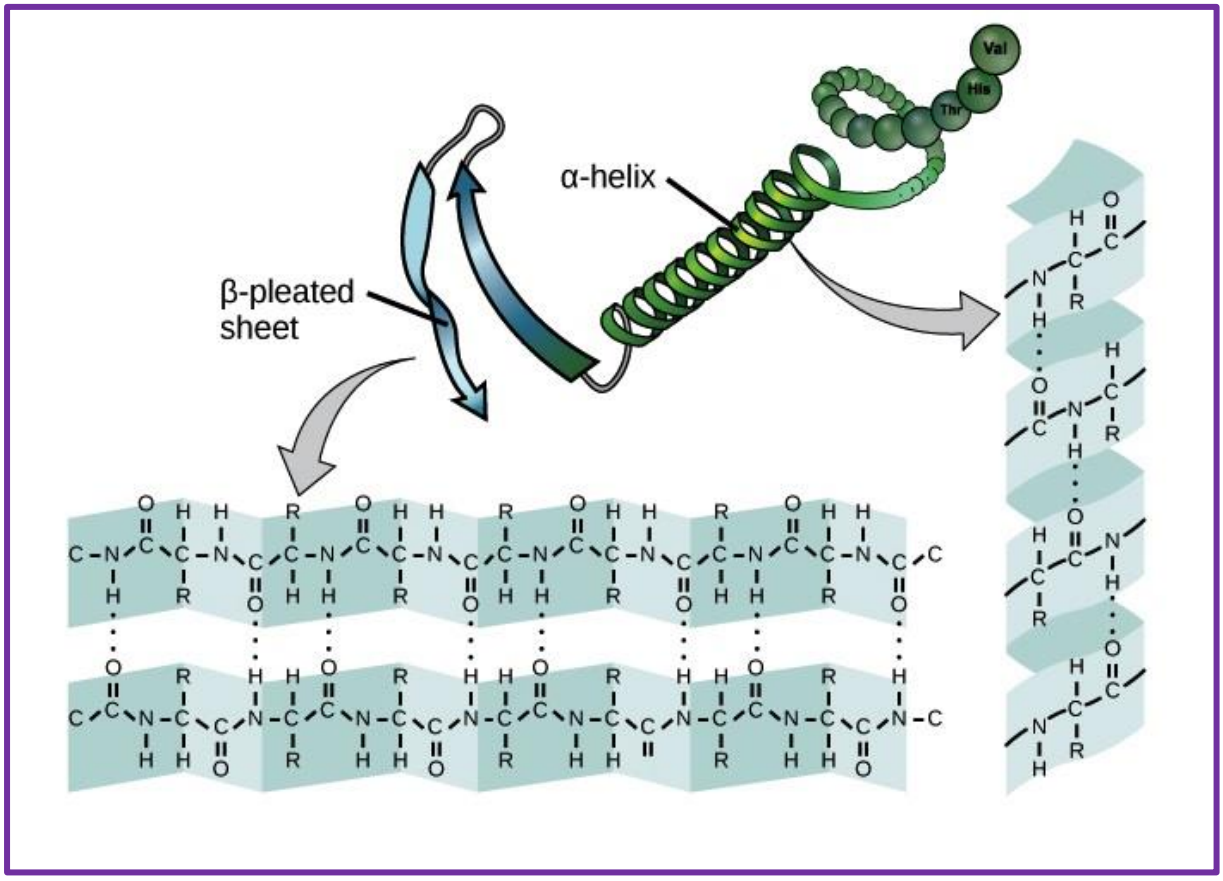

Figure 6: Secondary structure: The α-helix and β-pleated sheet form because of hydrogen bonding between carbonyl and amino groups in the peptide backbone. Certain amino acids have a propensity to form an α-helix, while others have a propensity to form a β-pleated sheet.

Certain amino acids exhibit a higher or lower propensity for forming α-helices or β pleated sheets. For example, proline is often referred to as a 'helix breaker' due to its R group's unusual structure, which creates a bend in the chain and prevents helix formation. Consequently, proline is typically found in bends or unstructured regions between secondary structures. Other amino acids, such as tryptophan, tyrosine, and phenylalanine, which have large ring structures in their R groups, favor forming β pleated sheets. This preference may be due to the β pleated sheet structure providing more space for these side chains. While many proteins contain both α

helices and β pleated sheets, some proteins only adopt one type of secondary structure or do not form either type. The diverse array of protein structures and their constituent amino acids have long fascinated researchers and play a critical role in protein function and stability.

1.2.3. Tertiary Structure

The tertiary structure of a polypeptide chain pertains to its comprehensive three-dimensional architecture, which is achieved through the intricate folding of all the secondary structural elements. This intricate folding is facilitated by the interplay of polar, nonpolar, acidic, and basic R groups present within the polypeptide chain. In an aqueous environment, the hydrophobic R groups of nonpolar amino acids preferentially occupy the protein's interior, whereas the hydrophilic R groups are predominantly located on the exterior. In the presence of oxygen, cysteine side chains form disulfide linkages, which represent the sole covalent bond formation during protein folding. The final three-dimensional structure of the protein is determined by a combination of both weak and strong interactions, which collectively shape the protein's conformation (Zhou and Pang, 2018). It is important to note that any loss of this conformation renders the protein functionally inactive.

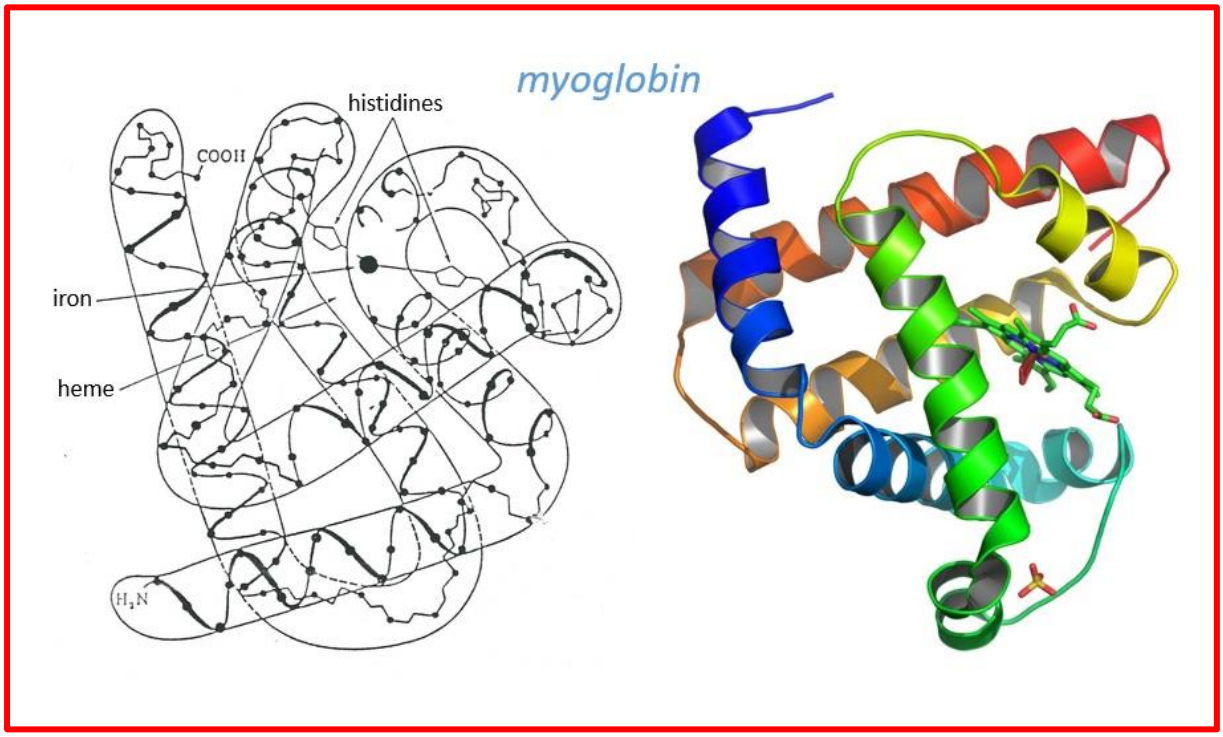

Figure 7: Tertiary structure of myoglobin: Helices are represented by tubes or helices, while β structures are represented by arrows. The chain ends are indicated by NH^{3+} and COO^{-}.

1.2.4. Quaternary Structure

The quaternary structure of a protein is a result of the spatial arrangement of its tertiary structures. Multiple polypeptide chains, known as subunits, are present in some proteins. The configuration of these subunits to each other is recognized as the quaternary structure. It's worth noting that haemoglobin is a prototypical protein that exemplifies quaternary structure, comprised of four subunits (two α and two β). Its primary function is to carry oxygen through the bloodstream. Another example of a protein with a quaternary structure is DNA polymerase, an enzyme that generates new DNA strands and contains ten subunits (Acharya et al., 2020). The subunits are held together by the same types of interactions that contribute to the tertiary structure, primarily weak forces like hydrogen bonding and London dispersion forces.

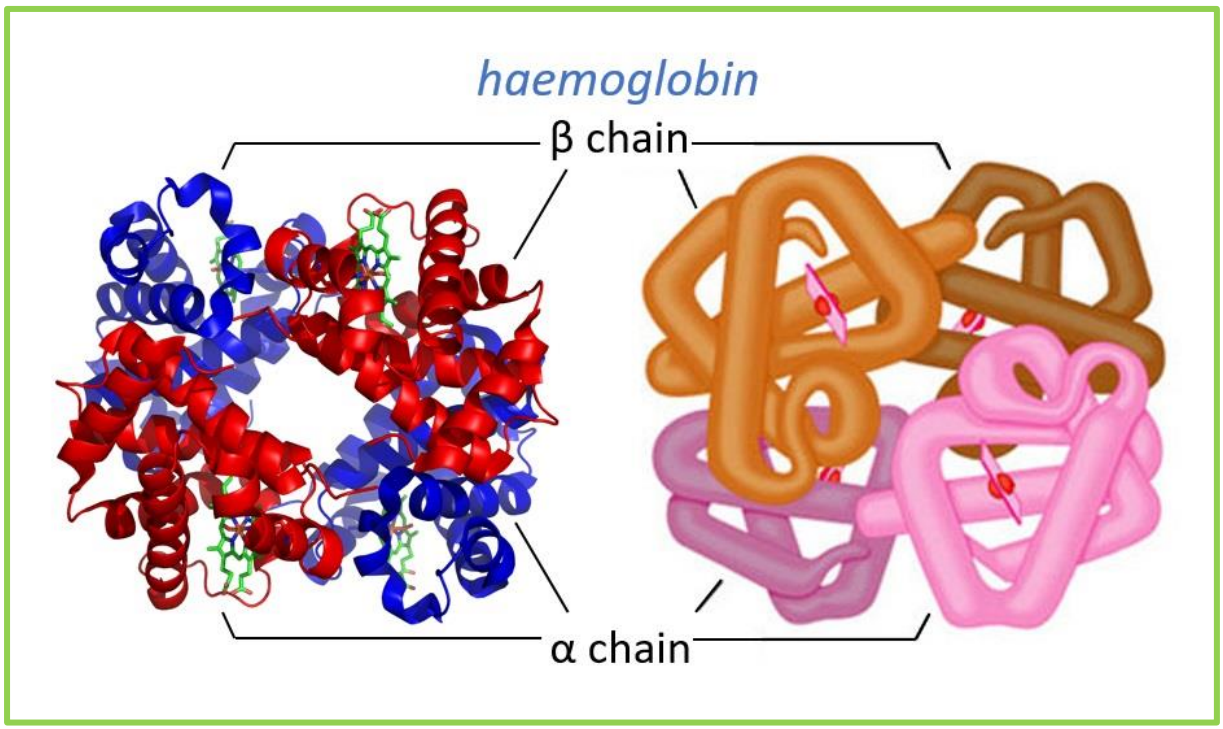

Figure 8: Quaternary structure of haemoglobin: Hemoglobin comprises four protomers, specifically two α and two β subunits. These subunits are integral to the structural composition and functionality of hemoglobin, facilitating its role in the transportation of oxygen within the bloodstream.

1.3. Protein Folding and Unfolding

1.3.1. Perspectives and Overview

Proteins are incredibly important in living organisms, as they serve as the backbone of various cellular and organismal processes. They are composed of intricate chains of amino acid residues, intricately linked by peptide bonds, and undergo a fascinating process called protein folding. This process involves a rapid transformation from a disordered, unstructured state(U) to a highly intricate, specifically structured form(N), represented by **(Fig.9)** (Creighton 1990; Udgaonkar 2008; Dill et al., 2012). The transformation happens within a remarkably short time span for most proteins, ranging from mere microseconds to a few minutes (Finkelstein 2018). What maintains the structured state are the complex intermolecular interactions within the protein, which are relatively weak and non-covalent (Bigman et al., 2020). Unlike conventional chemical reactions, the protein folding process represents a shift from disorder to order, involving a significant reduction in the conformational entropy of the polymer chain, offset by the formation of numerous noncovalent interactions and favorable entropy changes within the surrounding environment. The interplay of these various interactions defines the free energy landscape for each protein, which in turn influences the level of cooperativity in the folding process (Gō,1984; Malhotra et al.,2016).

Protein folding represents a crucial process whereby a protein assumes its functional structure and conformation. Through this physical process, a protein transforms from an irregularly folded state to a specific, functional three-dimensional structure Proteostasis, the state of balance between the folding of newly synthesized proteins and the removal of misfolded proteins, represents a critical objective for the human body (Dobson, 2003). Alas, in some instances, protein misfolding can result in the formation of aggregates, thereby disrupting the state of proteostasis. The aggregation of misfolded proteins can lead to the formation of ordered structures such as amyloid fibrils, which are implicated in amyloidosis, including Alzheimer's disease, Parkinson's disease & Huntington's disease (Das et al.,2020; Roos2010; Ross et al.,2014). Beyond its pathological implications, understanding the protein folding mechanism holds theoretical significance as it represents a crucial pathway to uncovering genetic codes across various species. In a narrower sense, protein folding research entails studying a protein's specific three-dimensional structure, its stability, and the relationship between structure and biological activity. Consequently, protein folding represents a vital indicator of physiological

conditions at the molecular level, enabling us to investigate and predict the states of amyloidosis indirectly.

Proteins are indispensable biomolecules that play critical structural and functional roles in various cellular and organismal processes that underpin life. These macromolecules are synthesized within the cell as unstructured chains of amino acid residues that are covalently connected via peptide bonds. The polypeptide chain undergoes a self-assembly process from an unstructured unfolded state to a distinctly structured native state (Creighton 1990; Udgaonkar 2008; Dill et al., 2012). This folding process typically occurs within microseconds to minutes for most protein (Finkelstein 2018) results in a stable conformation that is maintained by multiple intramolecular interactions of a weak and noncovalent nature (Dill et al., 2012). Unlike simple chemical reactions that involve the formation or breakage of covalent bonds, protein folding represents a "disorder to order" transition. This transition involves a significant reduction in the conformational entropy of the polymer chain, which is compensated by the formation of multiple noncovalent interactions and favorable entropy changes in the solvent. The interplay between diverse interactions defines the free energy landscape of a given protein and, importantly, the degree of cooperativity in the folding process.

Proteins are synthesized in cells as sequential strings of amino acids connected via peptide bonds. However, the linear peptide chains are, in most cases, functionally inactive as proteins exert their biological activities only when they are converted into unique three-dimensional (3D) structures. This process of forming a 3D structure from a polypeptide chain is referred to as protein folding. Small globular proteins have been observed to fold spontaneously in a test tube, but the intermediates, particularly in proteins folded with their disulfide (S-S) bonds intact, are not easily characterized due to the short time constant of the folding reaction, which is usually less than 1 second. Conversely, oxidative folding from the SS-reduced state occurs with a much longer time constant, making S-S coupled protein folding advantageous in detecting folding intermediates. This enables us to delineate a scenario of protein folding. Researchers have expended significant effort to elucidate the folding pathways of various proteins since the pioneering studies (Anfinsen 1972; Anfinsen 1973) and (Levinthal 1968) in the 1960s.

In the early studies of S-S coupled (or oxidative) protein folding, researchers focused on observing and characterizing the folding intermediates. However, due to technical limitations (Arolas et al.,2006) the reactions were frequently monitored under conditions slightly different

from those in vivo, in terms of temperature and pH. In recent decades, thanks to new experimental techniques, including genetic and chemical technologies for synthesizing artificial proteins, as well as new types of oxidants (S-S forming reagents), the study of oxidative folding has moved into a new realm. The new oxidants have allowed for S-S coupled folding to be performed under more biologically relevant conditions. By applying these new techniques, researchers have discovered unprecedented folding pathways for several S-S containing proteins, suggesting that protein folding pathways are much more flexible than previously thought.

This review provides a brief overview of the historical and physicochemical aspects of oxidative protein folding studies. It then compares the recently revised oxidative folding pathways of several representative peptides and proteins with those reported in earlier years, focusing on the flexible nature of protein folding pathways. The review also proposes some intriguing issues in the new realm of oxidative protein folding study, including possible applications of flexible folding to engineering peptide and protein structures.

1.3.2. Historical Background

In the 1920s-30s, Wu (Edsall 1995) conducted extensive studies on protein denaturation processes. Approximately half a century ago, Anfinsen proposed a fundamental principle of protein folding based on his groundbreaking study using bovine pancreatic ribonuclease A (RNaseA) as a model protein. This principle posits that a polypeptide chain ultimately folds into a unique structure, known as a native state. This principle gave rise to the notion that the structural information of a protein is encoded in the amino acid sequence, known as Anfinsen's dogma. Meanwhile, Levinthal discovered that, if a polypeptide chain were to search for the specific native structure by trial and error, the process would require an astronomical amount of time to fold into a protein. However, since the protein folding process typically completes within a second for small globular proteins, the vast timescale gap between the theoretical prediction and the experimental observation led him to propose that proteins fold through defined pathways. In the early stages of protein folding research, scientists endeavored to characterize the folding pathways to decipher the information of the native-state 3D structure from the amino acid sequence.

In the 1990s, it became widely recognized that neurodegenerative disorders, such as Creutzfeldt–Jakob disease (CJD), Alzheimer's disease (AD), Parkinson's disease (PD), amyotrophic lateral sclerosis (ALS), etc., are linked to misfolding of proteins in neurons

(Mossuto 2013; Hartl 2017). This observation suggests that the native structure of a protein is not a unique state for the amino acid sequence but one of the possible stable states. Furthermore, genetic engineering and chemical peptide synthesis technologies have become available for preparing designed artificial proteins in the past few decades. These breakthroughs have ushered the protein folding study into a new realm where researchers can actively control the structures of proteins. The development of methods to prevent or cure protein misfolding diseases, as well as the fabrication of peptide-based medicines, is no longer a distant dream. To achieve this goal, researchers must gain a thorough understanding of the peptide and protein folding pathways, depending on the environment (Khoury et al., 2014).

1.3.3. Phenomenological Frameworks for Protein Folding

When considering the outcomes of experimental studies on protein folding and the subsequent advancements in the experimental comprehension of protein folding reactions, researchers are consistently guided by various phenomenological models **(Fig.9)**. These models delineate different pathways through which the structure may evolve during the process of protein folding (Compiani et al.,2013; Udgaonkar 2013).

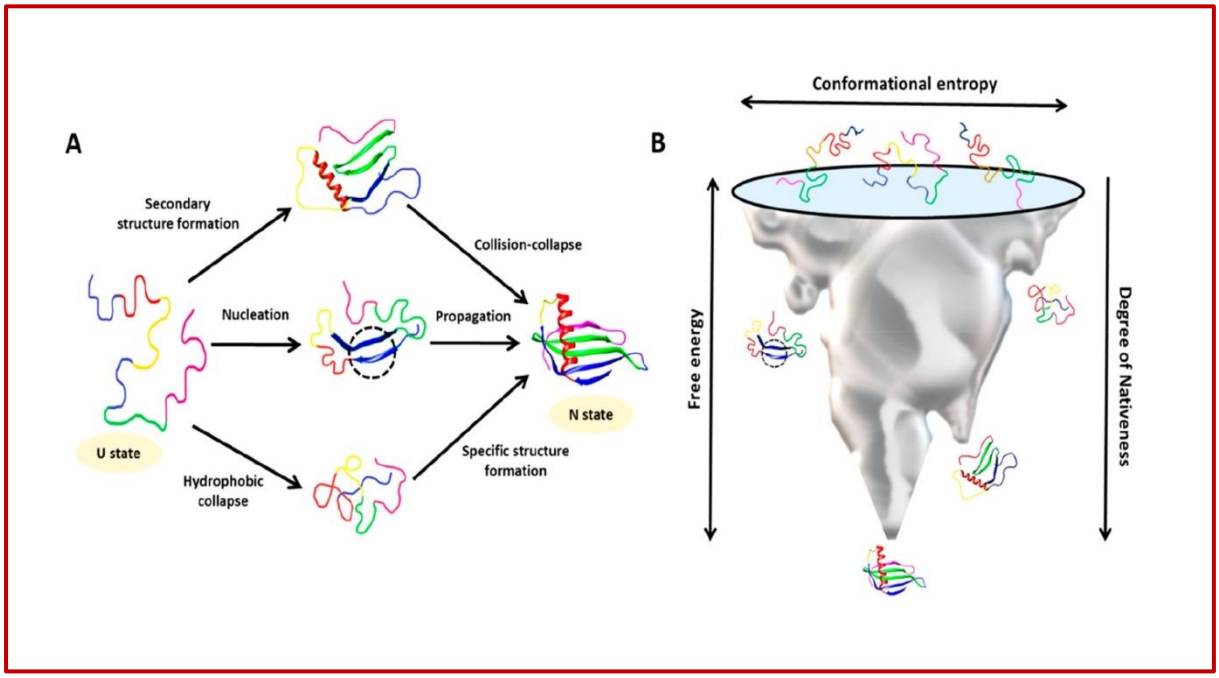

Figure 9: Models for protein folding. (Adapted from Udgaonkar et al., 2022)

1.3.4. Framework Model

According to the hierarchical model, local secondary structural elements form early in the folding process and then come together to create the tertiary structure (Ptitsyn 1973; Kim et

al., 1990; Udgaonkar et al., 1988). The stabilization of the secondary structural units occurs as they associate through random diffusive collision (Karplus et al.,1979; Karplus et al., 1994.). This model recognizes that the coalescence of the secondary structural units can occur in multiple ways, reflecting the observation that protein tertiary structures appear to be assembled from their constituent parts (Bashford et al 1988; Baldwin et al 1999; Baldwin et al., 1999). Experimental studies and computer simulations have consistently observed the early formation of secondary structures during folding (Kuwajima et al., 1987; Kuwajima, et al.,1993; Matthews 1993; Varley et al.,1993; Chamberlain et al.,2000; Lindorff-Larsen et al., 2011; Rollins et al., 2014). More recently, the fundamental concepts of this model have given rise to the idea of foldons, which are sequential assemblies of secondary structural units that form the tertiary structure during folding (Englander et al., 2014; Englander et al., 2017) **(Fig.10).**

1.3.5. Nucleation and Nucleation-condensation Model

In nucleation models, a folding nucleus is thought to originate either locally within a contiguous segment of the sequence (Wetlaufer 1973), conceivably due to hydrophobic interactions (Matheson Jr et al., 1978), or through the diffusive condensation of specific adjacent segments of the polypeptide chain (Tsong et al., 1972). In both scenarios, the nucleus is posited to form during the rate-limiting step, subsequently serving as the focal point for the progressive development of the overall structure, analogous to the process of crystallization. The presence of the folding nucleus in the transition state of folding is anticipated **(Fig.10).** The nucleation-condensation model hypothesizes the creation of an unstable diffuse nucleus in the transition state, with its structure subsequently stabilized in the ensuing rate-limiting step through the concerted condensation of specific secondary and tertiary structures (Itzhaki 1995; Fersht 1997). An alternative proposition suggests that the transition state of folding comprises an extended nucleus, representing an ensemble of structures incorporating some native secondary structure but disrupted native packing interactions (Sánchez et al., 2003; Daggett et al., 2003). Notably, computer simulations have not only contributed significantly to the refinement of the nucleation mechanism (Abkevich et al., 1994; Guo et al., 1995; Faisca 2009; Thirumalai et al., 2010) but have also furnished additional structural characterizations of transition states (Fersht 2002; Mayor 2003).

1.3.6. Hydrophobic Collapse Model

The proposed model postulates that the aggregation of hydrophobic residues is due to their solvent exclusion property, resulting in the rapid initial collapse of the polypeptide chain

(Robson et al., 1971; Dill 1985; Agashe et al., 1995). This collapsed state provides a conducive environment for the conformational search for the formation of native-like secondary and tertiary structures, owing to the reduction in conformational space (reduced chain entropy) (Finkelstein et al., 1987). The use of computer simulations, particularly those utilizing lattice models, has significantly contributed to our comprehension of how the initial chain collapse facilitates subsequent folding (Dill 1990; Alonso et al., 1991; Šali et al.,1994; Gutin et al., 1995A). Both the framework model and the hydrophobic model advocate for the presence of intermediates during (un)folding processes and the potential for folding through multiple pathways **(Fig.10)**. On the contrary, the nucleation model presents the folding reaction as a strictly two-state process, conflicting with the existence of folding intermediates. It is noteworthy that these mechanisms are not mutually exclusive, as the same protein may employ one or more of these mechanisms for folding, dependent on solvent conditions.

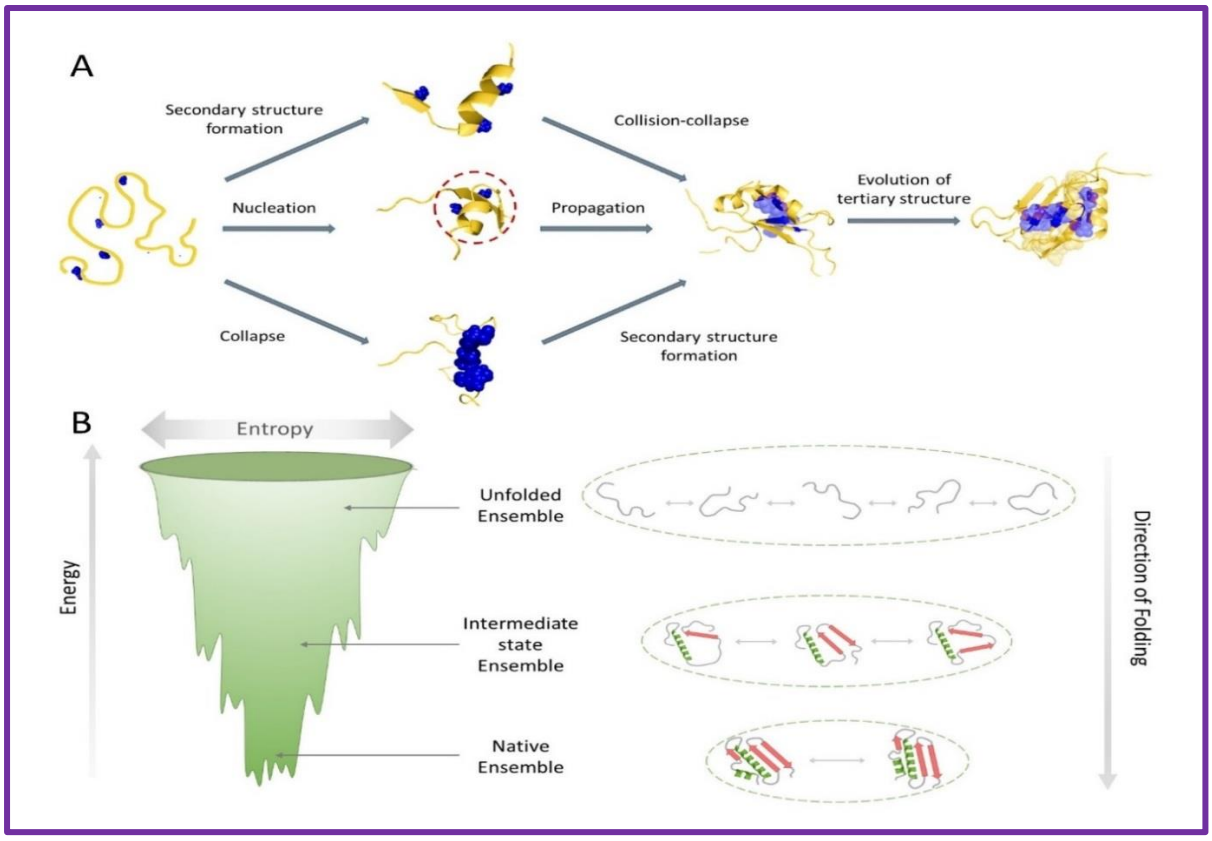

Figure 10: The process of protein folding can be elucidated through four primary models. A) The framework model entails folding via the formation of secondary structural elements, such as α-helices and β-sheets. The hydrophobic collapse model initiates with the aggregation of hydrophobic residues. The nucleation and nucleation-condensation model entails the creation of a nucleation site around which the remainder of the protein folds. B) According to the energy

landscape theory, proteins traverse a funnel-shaped energy landscape in stochastic steps toward their native, lowest-energy state (Adapted from Mishra and Jha.,2022).

1.4. Physicochemical Aspects of S-S Coupled Protein Folding

To comprehensively characterize the folding pathways of a protein, it is imperative to observe the transient intermediates that form during the folding reaction (Englander et al., 2014). However, the inherently conformationally flexible and short-lived nature of these intermediates has made their observation a challenging endeavor, despite numerous attempts in the past. Conversely, the oxidative folding of proteins containing disulfide bonds typically transpires over a more prolonged time frame, commonly spanning minutes to hours. Consequently, the intermediates that arise during this process, such as disulfide intermediates, can be readily characterized by trapping them. This can be accomplished through either acidifying the reaction solution to pH 2-3, which converts the reactive cysteinyl thiolates (S−) to essentially unreactive thiols (SH) (Englander et al., 2014; Bulaj et al., 1998) or by chemically capping the S− with quenching reagents such as iodoacetic acid or iodoacetamide (Tajc et al.,2004).

Subsequently, the isolated SS-intermediates are separated by HPLC, and their chemical structures, including the SS topologies and conformations, are determined using advanced spectroscopic methods as well as proteolytic digestion. This analytical approach has facilitated the elucidation of oxidative folding pathways for numerous disulfide-containing proteins.

Scheraga and his colleagues classified oxidative folding pathways into four typical types, as shown in **(Fig.11)** (Narayan et al., 2000). In each type, a reduced and denatured protein (R) folds through a ‘des’ intermediate, which is produced by the rearrangement of partially and randomly oxidized species, the unstructured precursors **(Fig.11)**. The ‘des’ intermediates are specific disulfide (S-S) intermediates that lack one of the native SS bonds present in the native state. ‘DesU’ lacks a specific structure, while ‘desN’ adopts a native-like structure. These intermediates can be converted to the native state (N) when direct oxidation to form the last native SS bond is possible. However, some of the ‘desN’ intermediates cannot be directly oxidized to N because of their stiff conformation. When local unfolding occurs in ‘desN’ to generate ‘desLU’, the buried SH groups gain enough flexibility to form the final SS linkage by oxidation. Chang, et al., 2006 used a folding funnel as the energetic landscape (Wolynes 1995) to illustrate the relationship between the number of SS bonds and the diversity of conformations (i.e., chain entropy) during oxidative folding.

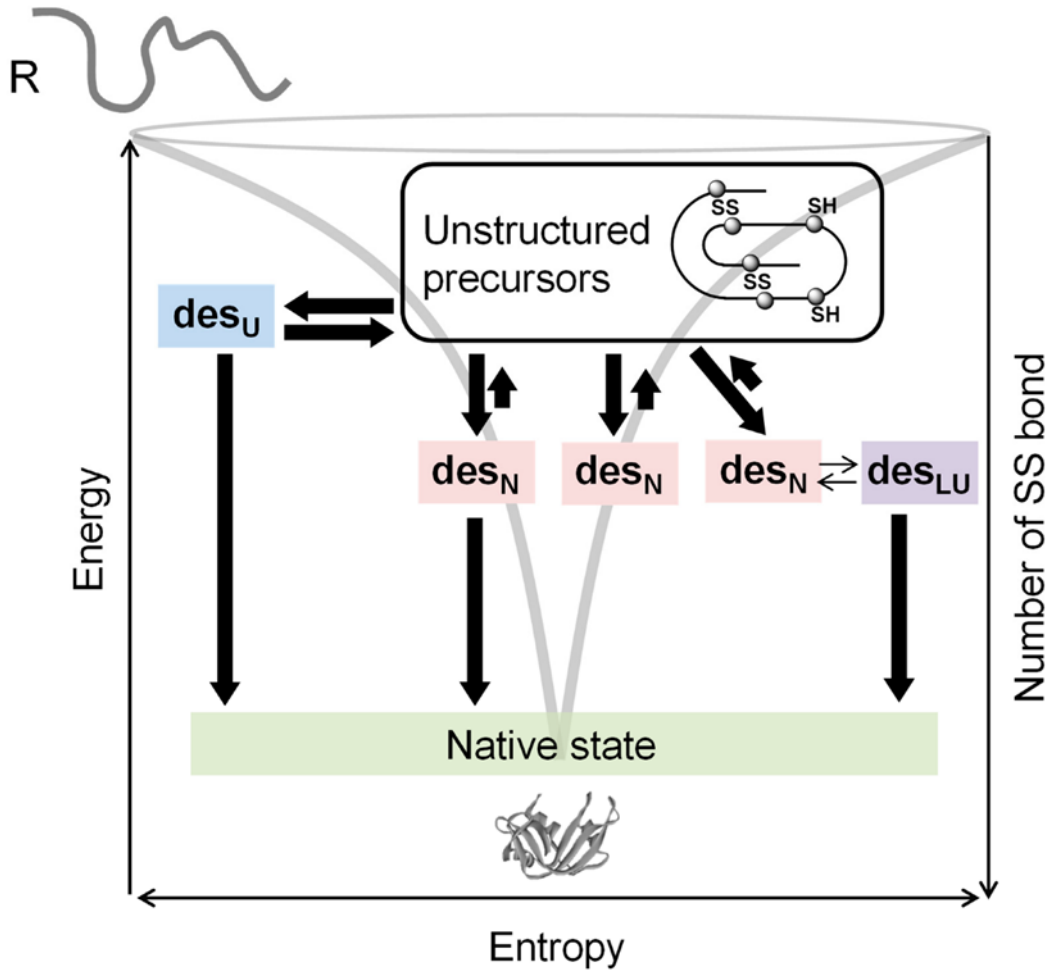

Figure 11: Four typical oxidative folding pathways governed by a folding funnel as the energetic landscape. This figure was made by merging a concept regarding the energetic landscape model (Chang, et al., 2006) with the schematic model demonstrated (Scheraga et al.,2000).

Fig.11 schematically depicts the reaction mechanism of S-S formation, which is a fundamental process of oxidative protein folding. The regeneration of N from the reduced R necessitates S-S bonds to be formed at the correct positions of the native state. However, upon oxidation, S-S formation typically ensues before the structural folding, thereby generating numerous intermediates with randomly formed S-S bonds (Phase I). Subsequently, the partially oxidized species gradually acquire the native-like structure through SS rearrangement, concurrently with the regeneration of the native S-S pairings (Phase II). The latter process is governed by the thermodynamics of the peptide chain under the prevailing conditions **(Fig.12)**. Thus, the formation of the native S-S bonds after the pre-folding event becomes coupled with the conformational shift from the random-coil or collapsed state to the native-like fold (Narayan 2020).

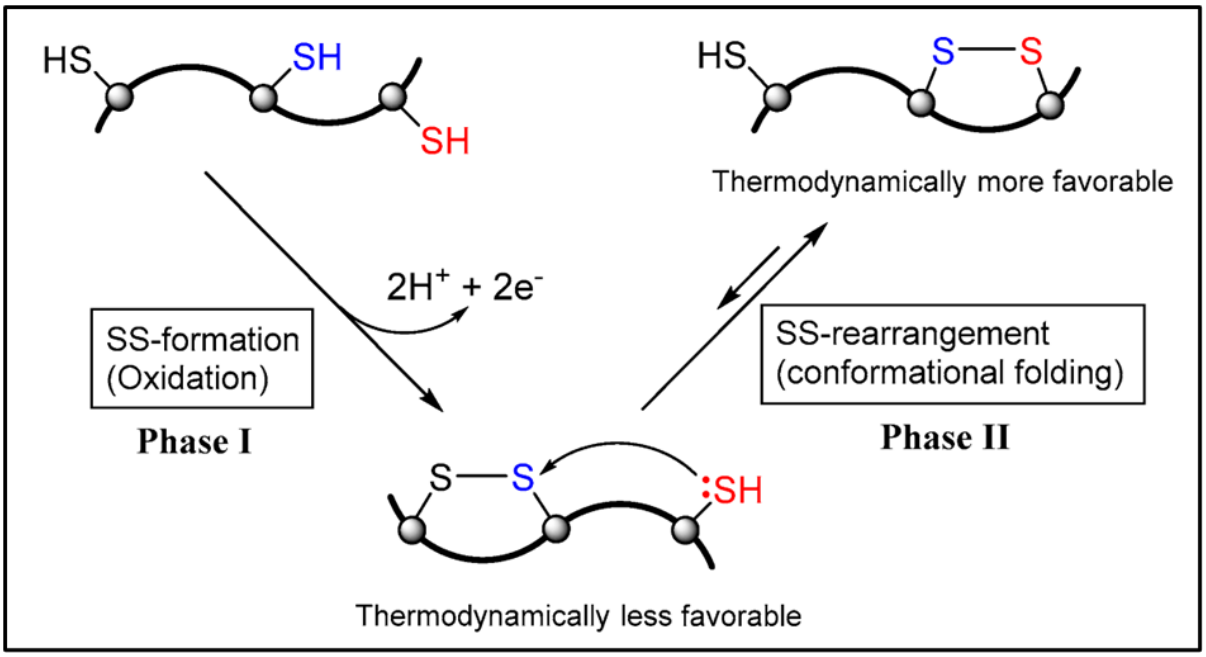

Figure 12: Disulfide formation and reshuffling are governed by thermodynamic stability.

In the study of oxidative folding, the choice of an oxidant (S-S forming agent) is crucial in controlling the protein folding pathways as it significantly affects the reaction rate of S-S formation. This, in turn, controls the amount of SS intermediates that transiently accumulate in the reaction solution. In the early years, aerial oxidation by molecular oxygen(O_2) was frequently used, although the oxidation was too slow with O_2. Therefore, dimeric S-S oxidants, such as glutathione (GSSG), were subsequently employed to perform oxidative folding at a reasonable reaction velocity. As shown in **(Scheme 1a)**, the dimeric SS oxidant induces the formation of an S-S bond in a protein via a mixed S-S intermediate. However, analyzing the folding pathways became difficult due to the generation of such S-S intermediates.

To solve this issue, trans-4,5-dihydroxy-1,2-dithiane (DTTox) was used because the mixed S-S intermediate would not be populated in the reaction solution **(Scheme 1b)**. This significantly reduces the number of detectable folding intermediates (Rothwarf et al.,1993). However, since the oxidation potentials for GSSG and DTTox [$E^{\circ\prime} = -256$ and -327 mV, respectively (Beld et al., 2007)] are close to that for cystine (CysS-SCys) [$E^{\circ\prime} = -238$ mV (Beld et al., 2007)], S-S formation in a peptide chain should be reversible. Hence, an excess amount of the oxidant is required to complete the reaction. Furthermore, the SS-based oxidants are only applicable under weakly basic conditions (pH 7.5~9.0). As a result, clear observation of conformational folding events coupled with S-S rearrangement is still not easy even with these S-S based oxidants.

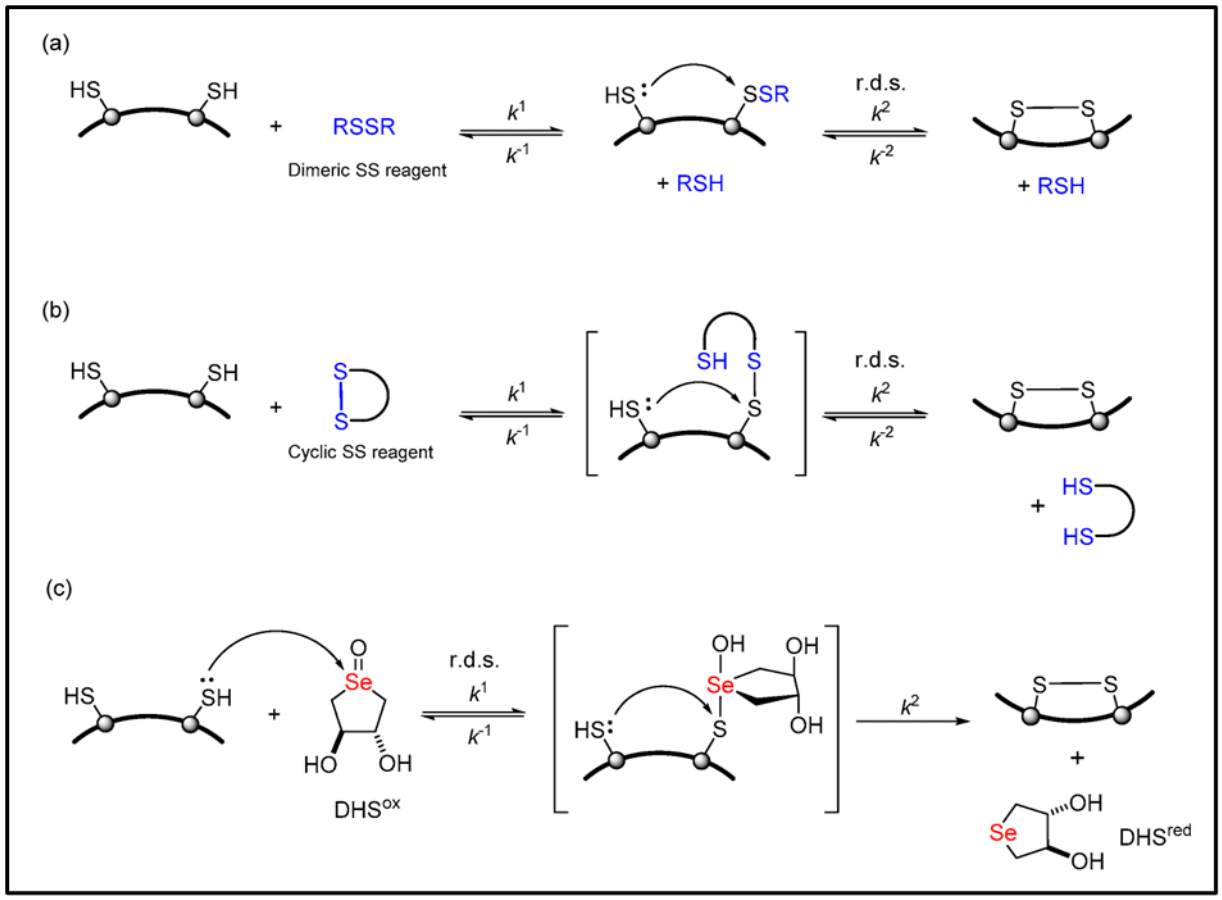

Scheme 1: Mechanisms for SS formation using various oxidants. (a) A dimeric disulfide (S-S) reagent. (b) A cyclic S-S reagent. (c) A selenoxide reagent (Arai et al.,2011).

In oxidative protein folding, it is crucial to differentiate between S-S formation and S-S rearrangement events. To this end, the trans-3,4-dihydroxytetrahydroselenophene-1-oxide (DHSox) reagent was developed for its aforementioned purpose (Arai et al., 2011; Arai et al., 2019). DHSox is a strong S-S forming reagent that selectively oxidizes the SH groups of a reduced protein molecule. The reaction is stoichiometrically conducted within a broad range of pH (i.e., pH 3.0~10.0) through a similar mechanism to that of DTTox. DHSox operates by the SH group of a peptide chain attacking the Se atom of DHSox initially. Then, another SH group of the peptide chain intramolecularly attacks the S atom of the generated thioselenurane intermediate to produce an S-S bond, releasing selenide DHSred. Remarkably, DHSox has a higher oxidation potential than cystine (Arai et al., 2013), making the rate-determining step the first step, thus proceeding irreversibly and stoichiometrically.

The reaction rate of S-S formation was proportional to the number of free SH groups present in the substrate peptide chain (Arai et al., 2011; Arai et al., 2013, Iwaoka et al.,2008). Moreover, the oxidative process of S-S formation is completed before the S-S reshuffling in the oxidized

peptide chain. Consequently, Phases I and II of **(Fig.12**) could be separated, enabling the analysis of the oxidative folding pathways of proteins with ease. In addition to DHSox, inorganic oxidants, such as a platinum complex ($[Pt(en)_2Cl_2]^{2+}$), were employed (Shi et al., 2000; Narayan., 2003; Narayan., 2003). Various diselenide (Se-Se) and SS-based reagents and catalysts were also tested (Arai et al., 2011), as alternative oxidants to accelerate oxidative folding rates (Arai et al., 2013, Iwaoka et al.,2008; Shi et al., 2000; Narayan., 2003; Narayan., 2003; Lees 2008; Madar et al., 2009). Recent studies showed that enzymes that assist protein folding processes in the endoplasmic reticulum (ER), such as protein disulfide isomerase (PDI), can also improve the velocity and yield of oxidative protein folding significantly (Potempa et al., 2010).

In the realm of oxidative folding, the classical approach frequently involved conducting the folding reaction in non-natural environments, thus enabling easy observation of key S-S intermediates. This approach facilitated the characterization of oxidative folding pathways of representative proteins and the proposal of a general model of protein folding. However, it also revealed that folding pathways are highly dependent on both the reaction environment and the protein type. In this review, we present an overview of recent achievements in relevant fields, emphasizing the significant flexibility of peptide and protein folding pathways.

To address protein misfolding diseases, investigating protein folding pathways under conditions that simulate physiological environments, preferably at the organ level, is preferable. Concurrently, the application of state-of-the-art technologies has enabled pathway control, as illustrated in this review. The engineering of peptide and protein structures and functions through the control of folding pathways presents intriguing and pertinent issues in the evolving realm of current protein folding studies.

1.5. Protein Misfolding and Aggregation

Proteins are highly versatile macromolecules ubiquitous in mammalian cells, typically ranging between 10,000 and 20,000 distinct protein variants within the proteome. Preserving proteome integrity and cellular health necessitates a delicate equilibrium in protein synthesis, folding, and degradation, alongside meticulous regulation of the abundance of each protein species. The encoded information governing the tightly folded structure of a protein, imperative for its biological functionality, is embedded in the linear amino acid sequence of the newly synthesized polypeptide chain (Anfinsen 1973), which may extend to several thousand amino acids. Nonetheless, even a modest polypeptide of approximately 100 amino acids possesses the

capacity to assume an astronomically vast number of conformations, estimated to be in the order of 1030 (Dobson et al., 1998). Furthermore, although the biologically active conformation - known as the native state - is thermodynamically favorable, it is often only marginally stable under physiological conditions. Consequently, the folding process is intrinsically error-prone, culminating in misfolded states and off-pathway aggregates **(Fig. 13)**. Over the past two decades, the indispensability of molecular chaperones in guiding numerous proteins toward efficient folding at a biologically pertinent rate has become increasingly evident (Balchin et al., 2016). Diverse chaperone proteins escort the nascent polypeptide chain during translation at the ribosome and subsequent folding phases, effectively averting or rectifying misfolding and aggregation. These chaperones collaborate with protein degradation machineries, contributing to an extensive protein homeostasis network (Balch et al., 2008; Brehme et al., 2014; Hipp et al., 2014).

Amyloid refers to a proteinaceous material that accumulates in organs and tissues. This material is characterized by a cross-β-pleated sheet conformation. Aberrant protein folding is connected to an increasing number of diseases, which fall into two distinct groups: loss-of-function and toxic gain-of-function diseases. The first group is characterized by protein dysfunction resulting from mutations, such as single nucleotide polymorphisms, which can make proteins unstable and prone to degradation. Diseases like cystic fibrosis and various metabolic defects fall into this category (Sahni et al., 2015). In the second group of diseases, unstable proteins aggregate and lead to cellular toxicity, seen in neurodegenerative diseases like Alzheimer's (AD) and Parkinson's (PD), as well as type II diabetes, certain types of heart disease, and cancer. The aggregation of proteins can be caused by inherited mutations in disease-related proteins, as observed in Huntington's disease (HD) and early-onset AD and PD. However, the majority of cases occur sporadically and become evident with age (Hipp et al., 2014; Labbadia et al., 2015; Douglas et al., 2010), possibly due to a decline in the body's proteostasis network. Initially considered an inconvenience by researchers studying protein folding, aggregation has now been recognized as a highly relevant medical process.

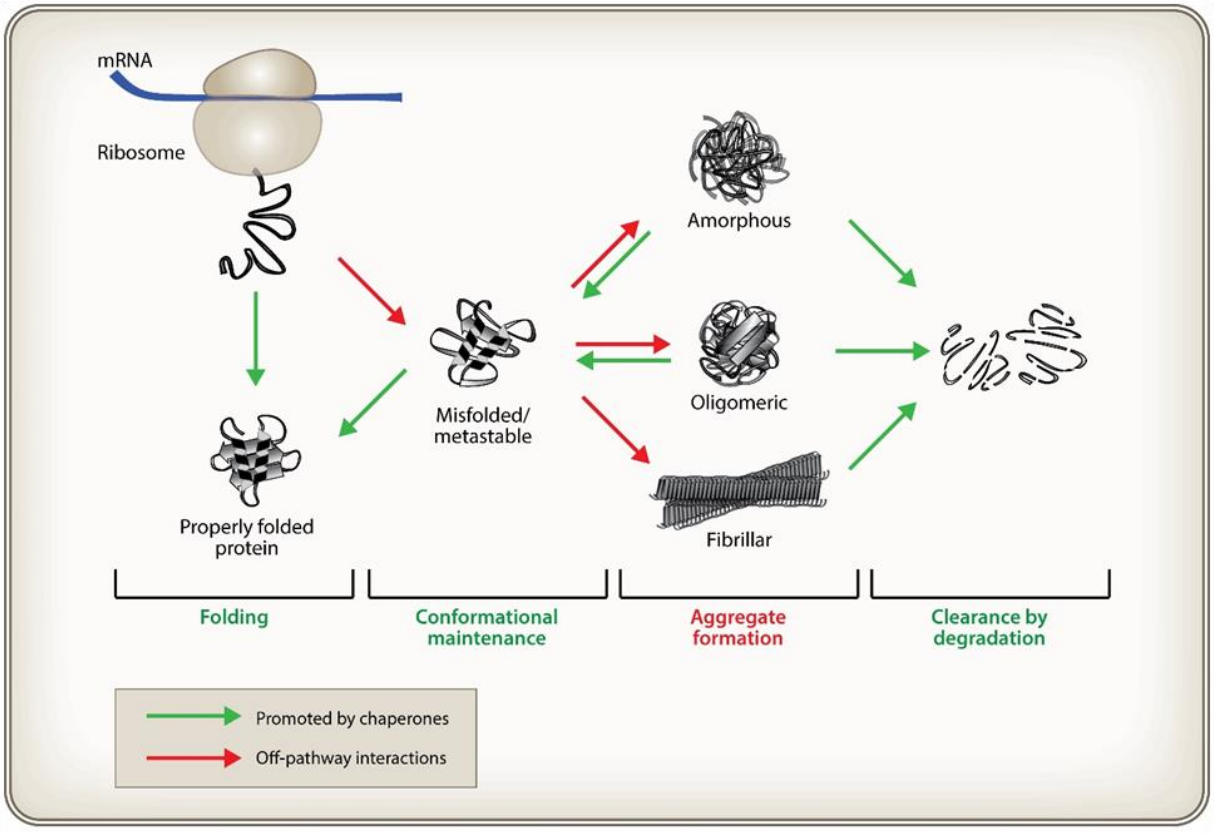

Figure 13: Protein chains undergo a range of conformations during initial folding and throughout their lifecycle in the cell. Molecular chaperones play a crucial role in the cell's proteostasis network, facilitating the folding of newly synthesized proteins, maintaining native conformations, and preventing the formation of harmful aggregates. Additionally, chaperones collaborate with protein degradation systems to remove misfolded and aggregated proteins. (Adapted from Balchin et al., 2016)

The formation of aggregates in partially folded or misfolded proteins is driven by the exposure of hydrophobic amino acid residues and unstructured polypeptide backbones to the solvent. This exposure leads to the concentration-dependent formation of aggregates rich in β-sheet structure (**Fig.13**). While hydrophobic forces stabilize the compact core of proteins during folding, they act between molecules in aggregation. Although most aggregates are amorphous, a subset of non-native proteins aggregate to form amyloid fibrils, which are characterized by β-strands running perpendicular to the long fibril axis i.e. cross-β structure (Chiti et al., 2006). These structural features were first observed by biophysicist William Astbury in 1935 (Astbury et al.,1935) in poached egg white, and are commonly associated with protein aggregates found in neurological tissues, indicative of age-dependent neurodegenerative diseases. It is noteworthy that many amyloid-forming proteins are secreted and form deposits in the extracellular space of the nervous system and various organs (Chiti et al.,2017). Conversely, a

few amyloidogenic polypeptides are cytosolic and form intracellular inclusions, such as α-synuclein and tau, which are linked to Parkinson's disease and Alzheimer's disease, respectively. The proteins containing expanded polyglutamine stretches that cause Huntington's disease and various ataxias also exhibit similar intracellular aggregation.

Remarkably, amyloid-forming disease proteins are often relatively small and intrinsically disordered in their nonaggregated states, including α-synuclein and tau. Despite the lack of significant sequence similarities among these proteins, it is believed that many proteins have an intrinsic ability to undergo fibrillar β-sheet aggregation (Chiti et al.,2017; Fändrich et al., 2002; Eisenberg et al., 2017). Electron microscopy observations reveal that amyloid fibrils are typically 7–13 nm in diameter and often several microns in length. They are generally composed of a few protofilaments that twist around each other or associate laterally as flat ribbons and possess a tensile strength that approaches that of steel (Chiti et al.,2017), attributed primarily to their extended arrangement of hydrogen-bonded β-sheets. Notably, the amyloid form of a protein molecule can be even more stable than the native state.

Insights into the interactions within amyloid fibrils have been elucidated through the application of cryo-electron microscopy, solid-state NMR analysis, and X-ray diffraction studies of microcrystalline arrays of short peptides. Eisenberg & Saway's review (Eisenberg et al., 2017) underscores a substantial body of research wherein a considerable number of amyloid microcrystals have been subjected to high-resolution scrutiny using highly focused X-ray microbeams. These investigations have unveiled, among various findings, the in-register alignment of β-strands in the β-sheet, optimizing intermolecular interactions, and the tightly interdigitated nature of side chains within such pairs. Notably, the ability of small peptide segments to form amyloid fibrils has been pivotal in surmounting the inherent challenge posed by the helical architecture of fibrils, particularly in the context of crystal formation. The initial crystal consisted of a seven-residue segment of the amyloid-forming yeast prion protein Sup35 with the sequence GNNQQNY (Nelson et al., 2005). In these crystals, the amyloid protofilament comprised two flat β-sheets forming a steric zipper, extending throughout the length of the crystal, and consisting of approximately 50,000 layers of short segments. This breakthrough structure facilitated the identification of amyloid-forming segments in other proteins, which were subsequently demonstrated to form fibrils in vitro. Based on these analyses, it was determined that structural features enabling amyloid formation are widespread in the proteome.

The detrimental effects of aggregation stem from common structural properties of the aggregates and may not be related to the normal function of the affected protein (resulting in a gain of toxic function). Prior to forming insoluble end-stage fibrils, disease proteins often aggregate into soluble oligomers, widely considered the primary toxic species **(Fig.13)**. These oligomers expose sticky surfaces (hydrophobic amino acid residues and unpaired β-strands), enabling them to disrupt phospholipid bilayers (Chiti et al.,2017) and engage in aberrant interactions with multiple key cellular proteins (Olzscha et al., 2011; Kim et al., 2016). These toxic surfaces are largely obscured in the regular structure of the fibrils, which explains why fibrils are less interactive than soluble oligomers (Kim et al., 2016). However, it's worth noting that fibrillar aggregates are by no means inert and, while less toxic, contribute to pathology by stably sequestering key cellular factors and by generating oligomers through fragmentation and secondary nucleation (Chiti et al.,2017, Olzscha et al., 2011). The proteins targeted by toxic aggregates are often themselves unstable; they are typically enriched in intrinsically unstructured regions and sequences of low amino acid complexity, characteristic features of many RNA-binding proteins (Olzscha et al., 2011; Kim et al., 2016). Therefore, protein aggregation disrupts nucleocytoplasmic RNA transport and RNA homeostasis (Freibaum et al., 2015; Woerner et al., 2016). Significantly, multiple studies have shown that the aggregates can inhibit protein degradation by the proteasome and autophagy systems (Hipp et al., 2014) and can sequester critical chaperone components (Choe et al.,2016; Park et al., 2013; Yonashiro et al., 2016). Consequently, aggregation directly interferes with general protein quality control and is both a symptom and a cause of proteostasis decline.

Table 1: A summary of the main amyloidoses and the proteins or peptides involved. (Adapted from Stefani et al., 2003).

Disease	Main aggregate component
Alzheimer's disease	Aβ peptides (plaques); tau protein (tangles)
Spongiform encephalopathies	Prion (whole or fragments)
Parkinson's disease	α-synuclein (wt or mutant)
Primary systemic amyloidosis	Ig light chains (whole or fragments)
Secondary systemic amyloidosis	Serum amyloid A (whole or 76-residue fragment)
Fronto-temporal dementias	Tau (wt or mutant)
Senile systemic amyloidosis	Transthyretin (whole or fragments)
Familial amyloid polyneuropathy I	Transthyretin (over 45 mutants)
Hereditary cerebral amyloid angiopathy	Cystatin C (minus a 10-residue fragment)
Haemodialysis-related amyloidosis	β2-microglobulin
Familial amyloid polyneuropathy III	Apolipoprotein AI (fragments)
Finnish Hereditary Systemic Amyloidosis	Gelsolin (71 amino acid fragment)
Type II diabetes	Amylin (fragment)
Medullary carcinoma of the thyroid	Calcitonin (fragment)
Atrial amyloidosis	Atrial natriuretic factor
Hereditary non-neuropathic systemic amyloidosis	Lysozyme (whole or fragments)
Injection-localised amyloidosis	Insulin
Hereditary renal amyloidosis	Fibrinogen α-A chain, transthyretin, apolipoprotein AI, apolipoprotein AII, lysozyme, gelsolin, cystatin C
Amyotrophic lateral sclerosis	Superoxide dismutase 1 (wt or mutant)
Huntington's disease	Huntingtin
Spinal and bulbar muscular atrophy	Androgen receptor [whole or poly(Q) fragments]
Spinocerebellar ataxias	Ataxins [whole or poly(Q) fragments]
Spinocerebellar ataxia 17	TATA box-binding protein [whole or poly(Q) fragments]

1.6. Conformational Properties of Protein Aggregates

The abnormal association of misfolded proteins usually leads to the formation of aggregates. Small aggregates can remain soluble, but large protein aggregates precipitate out of solution under physiological conditions. From a morphological standpoint, we can essentially differentiate between two types of aggregates: amorphous aggregates and amyloid fibrils. Amorphous aggregates display a granular appearance when imaged by electron microscopy and consist mostly of disordered polypeptide chains, even if they exhibit certain regions enriched in β-sheet structures, which bind the macromolecular assembly (Morell et al., 2008; Wang et al., 2008). Amyloid fibrils are highly ordered and repetitive structures where all polypeptides adopt a common fold. In the present and next sections, our focus will be on the properties and mechanisms of formation of these structures, due to their relevance in pathogenic and functional processes **(Table 1)**.

The core region of amyloid fibrils consists of repetitive arrays of β-sheets that are oriented perpendicularly to the fibril axis. This structure, known as cross-β, displays characteristic X-ray diffraction signals forming a 'cross' pattern. The strong meridional reflection at 4.7 °A corresponds to inter-strand distances, while the weaker longitudinal signal at 10 °A results from the stacking of the β-sheets. These fibrils typically have diameters of about 10 nm and often consist of multiple proto-filaments twisted around the fibril axis (Carulla et al., 2005; Chiti and Dobson, 2006; Kodali and Wetzel, 2007).

The presence of a cross-β fold in amyloids was widely accepted even before high-resolution structural data were obtained by X-ray crystallography and solid-state NMR (Wasmer et al., 2008; Nelson et al., 2005). Low-resolution techniques such as staining with specific amyloid dyes like thioflavins (Th) and Congo Red (CR), secondary structure content analysis focused on the detection of newly formed β-sheets by circular dichroism (CD) and Fourier-transformed infrared (FT-IR) spectroscopies, or detection of the cross-β-sheet motif in oriented samples by X-ray diffraction were already available to characterize and follow the formation of this macromolecular assembly. These assays are usually complemented with visualization of the fibril's morphology by transmission electron microscopy (TEM) and atomic force microscopy (AFM), detection of protected amyloid β-sheet cores through limited proteolysis and mass spectroscopy (MS) or by Hydrogen/Deuterium (H/D) exchange using solution NMR or MS, or even monitoring the ability of the aggregates to specifically seed amyloid formation (Dasari et

al., 2011; Hubbell et al., 2000; Kodali and Wetzel, 2007; Pelczer and Carter, 1997; Sawaya et al., 2007; Tycko, 2006, 2011; Wasmer et al., 2008; Sabate et al., 2007).

1.7. Amyloid Aggregation Pathways

The process of amyloid fibrillogenesis, the formation of amyloid fibrils, is commonly modeled as a nucleation-elongation polymerization process. In this process, the reaction rate is dependent on the protein concentration and can be accelerated by introducing homologous pre-aggregated polypeptides, which act as seeds or templates, facilitating the transition from the soluble to the aggregated state (Chiti and Dobson, 2006; Harper and Lansbury, 1997; Jarrett and Lansbury, 1993; Sabate et al., 2003; Nielsen et al., 2001). According to this simplified model, amyloid aggregation can be divided into three primary phases:

1. The thermodynamically disfavored lag phase, in which the soluble species, typically monomers, associate to form nuclei. This poorly characterized state significantly influences the overall kinetics of the amyloid reaction.
2. The population of these transient assemblies triggers the polymerization and fibril growth during the exponential phase.
3. Finally, the exhaustion of monomers leads to the saturation phase, wherein no more soluble species can associate with the ends of preformed fibrils. This phase results in fibril maturation, typically through the lateral association of fibrils **(Fig.14)** (Jarrett and Lansbury, 1993; Bhak et al., 2009).

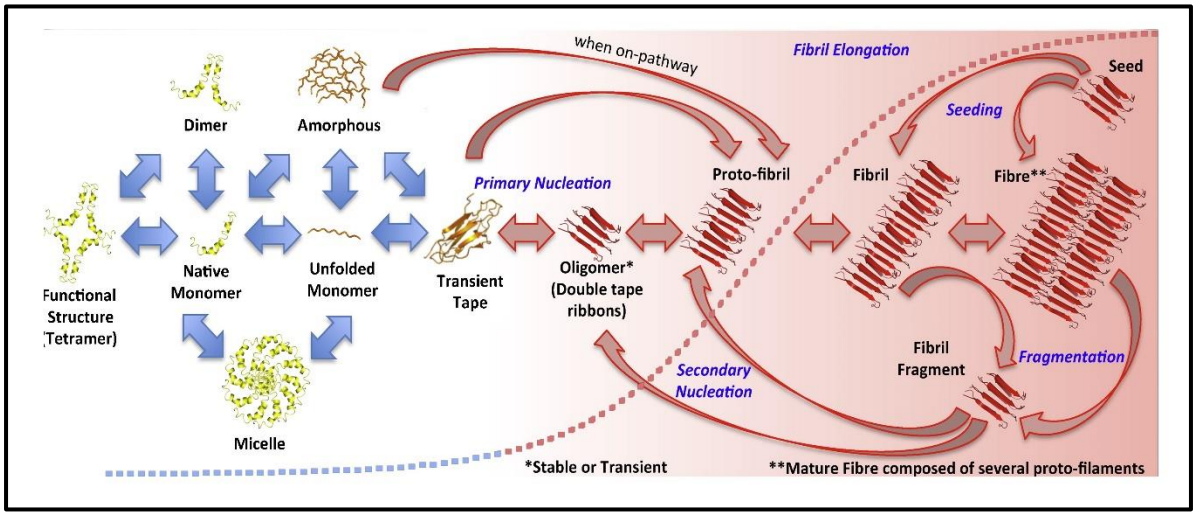

Figure 14: Schematic overview of an amyloid assembly landscape. (Adapted from Invernizzi et al., 2012).

The lag and growth phases are pivotal stages for potential drug interventions, as they offer opportunities for the inhibition of pathological processes through the action of small molecules. In the context of these phases, the lag phase encompasses the transformation from soluble and native structure to the appearance of the initial species exhibiting β-sheet conformation. Oosawa and Asakura described the simplest kinetic model for a nucleation–elongation aggregation reaction, within which nuclei exist in an unfavorable thermodynamic equilibrium with native monomeric species (Oosawa, 1975; Ferrone, 1999). Notably, in certain processes, the fibril mass becomes directly proportional to the square of the elapsed time, leading to the absence of a distinct lag phase. In more intricate scenarios, the nucleation process can be catalyzed by pre-existing aggregates, resulting in the formation of initial nuclei from monomers until a critical number of aggregates are populated, at which point a secondary nucleation pathway predominates the reaction. The duration of the lag phase is chiefly influenced by the rate constant of this secondary step. Alternatively, the lag phase might stem from a nucleus being assembled through successive smaller soluble aggregates or monomers, rather than directly achieving thermodynamic equilibrium with the native conformation. It has been illustrated that soluble monomers can attain equilibrium with dimeric, trimeric, and n-meric soluble species, as well as "micelles" which can function as a reservoir for monomers **(Fig.14)** (Bernstein et al., 2009; Jin et al., 2011; Hu et al., 2008; Sabate and Estelrich, 2005; Yong et al., 2002). According to this model, the initial stages of the reaction follow a power law growth that is contingent on the number of gradual additions/conversions required to form the nucleus. In the context of globular proteins, the destabilization of the native monomer from a thermodynamic standpoint is typically a prerequisite to initiate the aggregation process.

In proteins manifesting a quaternary native structure, the dissociation of the functional oligomer into monomeric subunits is typically necessary (Azevedo et al., 2011; Chiti and Dobson, 2009; Straub and Thirumalai, 2011). The resulting conformational and energetic landscape is extraordinarily intricate and influenced by the propensity of each specific intermediate to associate into disordered or ordered aggregates, thereby leading to on- or off-pathway conversions **(Fig.14)** (Jahn and Radford, 2008; Giurleo et al., 2008). The growth phase encompasses multiple stages in which soluble species are progressively arranged at the termini of preformed β-sheet rich structures through a thermodynamically favorable process (Jarrett and Lansbury, 1993; Bhak et al., 2009). Diverse mechanisms may account for the observed increase in structural order at this stage: the direct growth of fibrils from initially ordered β-sheet oligomers, the conversion of these oligomers into β-sheet enriched non-fibrillar

assemblies prior to fibril formation and elongation, or the growth of large disordered aggregates from initially disordered oligomers, followed by their structural reorganization, initially leading to nonfibrillar β-sheet rich assemblies and ultimately to fibrils **(Fig.14)**. The pathway taken by a given polypeptide appears to be highly contingent upon the specific attributes of the protein.

Molecules with low β-sheet propensity give rise to longer-lived non-fibrillar aggregates, which are considered to be more hazardous (Bellesia and Shea, 2009). As fibrils emerge as the prevailing form of aggregated species in the initial stages of growth, their characteristics critically influence elongation rates. Preformed fibrils have the capacity to facilitate the generation of new fibrils through processes such as fragmentation, branching, and nucleation on the fibril surface. Despite being commonly perceived as rigid entities, mature amyloids frequently undergo fragmentation. This phenomenon significantly impacts the kinetics of amyloid assembly, as the disintegration of preformed fibrils engenders new growth-competent surfaces, effectively accelerating the polymerization reaction. Moreover, a direct correlation has been observed between increased fibril fragmentation rates and cytotoxicity (Xue et al., 2009, 2010). The susceptibility of fibril fragmentation plays a pivotal role in prion dissemination in yeast (Tanaka et al., 2006). It has been postulated that while non-prion amyloids may be too inflexible to undergo in vivo fragmentation, prion fibrils readily undergo fragmentation, leading to an increase in the number of extension-competent sites and the likelihood of seeding events per cell, thereby favoring transmissibility to daughter cells (Castro et al., 2011). Additionally, the presence of aggregation-promoting natural or artificial surfaces and the ability of certain fibrils to generate new fibril ends through continuous branching, which involves secondary nucleation reactions, collectively result in an exponential growth of the total mass of fibrillar species over time, exerting a substantial influence on nucleation kinetics and playing a crucial role in the growth phase. This, in turn, affects the overall kinetics of the reaction as well as the morphological and functional properties of the resulting aggregates (Ferrone, 1999). It is noteworthy that notwithstanding the prevailing perception of mature fibrils as end-point assemblies, events involving dissociation and association occur continuously, leading to molecular recycling within amyloid fibrils (Carulla et al., 2005).

At the molecular level, the initial formation of fibrils can be elucidated by considering that aligned β-strands form a rod-like structure with complementary donor and acceptor groups on opposing sides. The chemical complementarities between the upper and lower surfaces facilitate the generation of extended, twisted, transient, and metastable tapes, which exhibit a

tendency to interconnect through tape-to-tape attraction, giving rise to double-tape-ribbons (Aggeli et al., 2001).

These ribbons, characterized by diameters ranging from 3 to 6 nm and lengths of less than 100 nm, mutually attract each other, leading to the formation of proto-fibrils (Aggeli et al., 2001). These proto-fibrils, termed "rod-like" when short or "worm-like" when longer, are frequently observed experimentally during intermediate stages of the growth phase and are thought to serve as the foundational stable entities in the pathway of fibril formation (Kodali and Wetzel, 2007). The resulting fibrils, typically around 10 nm in diameter and exceeding 100 nm in length, also exhibit mutual attraction between their surfaces, resulting in lateral fibril association and the eventual construction of mature amyloid fibers **(Fig.14)** (Aggeli et al., 2001).

Historically, mature fibers were deemed to be primarily accountable for the toxicity linked to the amyloid process. Nevertheless, there is now a broad consensus suggesting that non-fibrillar assemblies, particularly the oligomeric forms, are instead responsible for exerting cytotoxic effects. These aggregates are prevalent in the initial stages of the growth phase preceding proto-fibril formation and play a substantial role in disrupting membrane homeostasis in diseases such as Alzheimer's or Parkinson's (Uversky, 2010; Bucciantini et al., 2002; Chiti and Dobson, 2006; Kodali and Wetzel, 2007).

The oligomers, featuring small, flexible, and typically spheroid structures, retain essential amyloid characteristics (Aggeli et al., 2001; Uversky, 2010; Kodali and Wetzel, 2007). These inherent properties elucidate their intrinsic toxicity. Their reduced size and spherical shape promote their association with cellular membranes, where their amyloid conformation leads to pore formation and abnormal ion flux, causing cellular dysfunction and potentially triggering apoptosis. The non-specific attachment of non-fibrillar amyloid assemblies to cellular membrane receptors, along with subsequent intracellular mis-signaling, has been proposed as an alternative mechanism for membrane-mediated oligomer toxicity (Glabe, 2006; van Rooijen et al., 2009, 2010).

1.8. Protein Misfolding, Protein Aggregation and Amyloid Formation

In numerous amyloid diseases, the aggregation of proteins outside of cells has been associated with toxic effects (Aguzzi and O'Connor, 2010). Precise coordination of the processes regulating protein production, trafficking, and balance within the early secretory compartment

is crucial for maintaining normal protein function. Disruptions in these processes can lead to the development of diseases (Stefani, 2007). Therapeutic approaches to address protein folding issues include using molecules that target various factors promoting protein misfolding and aggregation (Gandhi et al., 2019; Valastyan and Lindquist, 2014). These therapeutic molecules can help enhance the stability of proteins' natural conformation, thereby increasing the barrier to protein misfolding and misassembly (Cortez and Sim, 2014; Cohen and Kelly, 2003; Lee et al., 2011; Shakya et al., 2010). Another approach involves focusing on the clearance of already-formed misassembled and misfolded protein aggregates. Under specific conditions, such as denaturation conditions, it becomes energetically favorable for a protein to transition into a more stable aggregated state, as depicted in **(Fig.15)**.

The folding of proteins is influenced by various factors, including errors in post-translational modifications, changes in the protein environment (Pagel et al., 2015), increased degradation and accumulation of degradation products, and oxidative stress. Proteins prone to aggregation exhibit increased aggregation at higher protein concentrations (Dasuri et al., 2013). Partially folded or misfolded intermediates display patches of surface hydrophobicity, facilitating an easier and more energetically feasible assembly process, as shown in **(Fig.15)**. This assembly progresses to oligomers, protofibrils, and fibrils of aggregated protein (Stefani, 2010). Amyloid fibrils consist essentially of unbranched bundles of 2–6 filaments twisted together. These fibrils can disrupt biological functions and have been associated with numerous neurodegenerative and cognitive diseases (Evans, 1996). Recently, aggregated oligomers have also been linked to the pathogenicity of protein aggregation. Protein misfolding occurs when molecules are trapped in local energy minima with non-native architecture and properties (Hipp et al., 2019). Under normal conditions, the native structure represents the most stable folded form for a protein. The folding pathway can be depicted as an energy funnel with minimum energy and almost fixed conformation compared to other states. The native state of the protein lies at the bottom of the funnel (Bryngelson et al.,1995; Veitshans et al., 1997; Boczko and Brooks III,1995). The energy of the intermediates decreases as they gain a more ordered structure and approach the native state. The native structure generally exhibits a packed structure with secondary elements and tertiary structure. The attainment of the native structure type depends on the sequence and length of the polypeptide. As the folding progresses, the number of molecules in different structural states decreases as most of them attain a native-like state, and finally, they all conclude in the native state. The native state represents the most stable minimum energy state under a set of conditions. Small proteins fold through nucleation

condensation mechanisms where small regions fold first, guiding the folding of the rest of the structure. In such cases, the nucleus of condensation or the region of the protein that guides the rest of the polypeptide to fold is crucial. Any disruption to this nucleation process can result in the misfolding and aggregation of the protein (Mirny and Shakhnovich, 2001, Finkelstein, 2018). Protein misfolding and aggregation are implicated in numerous human diseases and the aggregation of therapeutic proteins produced by recombinant techniques. Bioanalytical techniques based on the optical readout of the aggregation process and fibril formation have been developed. The recent advancements in analytical method development have led to significant progress in studying the equilibrium between soluble and insoluble proteins and aggregates within living systems. The field of protein aggregation and inclusion body formation has undergone several conceptual shifts, with the emergence of natural and functional amyloids as distinct aspects of the protein aggregation phenomenon. There is a great potential for utilizing amyloids for beneficial purposes, such as generating natural biomaterials for various industrial and medical applications. Recent ambitious research has indicated possible applications of amyloids in water filtration technology (Peydayesh et al., 2022; Zhao et al., 2023; Etale et al., 2023), showing promising potential in water purification and the removal of micropollutants to produce potable water for millions of people.

To fully utilize aggregation, it is essential to understand the process of aggregation itself. Deviant interactions caused by misfolding and misbinding initiate the process of protein aggregation, leading to the exposure of previously hidden regions in polypeptides and the establishment of unwanted contacts. These interactions result in self-assembly and the formation of large, insoluble aggregates.

Morphologically, amyloids exist as amorphous aggregates and fibrils (Ashrafian et al., 2021; Bigi et al., 2022; Chaturvedi et al., 2016). Amorphous aggregates have a granular appearance in electron microscopy and are primarily formed by disordered polypeptide chains (Alam et al., 2017; Zaman et al., 2019).

Amyloid fibrils are ordered and have repetitive structural elements. This unique morphology is significant in the context of the pathogenic and functional roles of amyloids. The prion protein is an important protein in the context of human diseases, and there is a strong link between the misfolding and aggregation of this human protein in pathogenesis. The prion is an anchored helical protein in the cell membrane, and its functions include the modulation of

signal pathways, defense against oxidative stress, embryonic cell adhesion, copper binding, and maintenance of peripheral myelin.

Functional protein aggregates and functional amyloids have been discovered in various organisms, including prokaryotes such as bacteria, and modern animals, including humans. Throughout the course of evolution, functional amyloids have been optimized to self-assemble. They are conformationally more stable and resistant to damage than pathological amyloids, and their assembly is faster. Functional amyloids are kinetically and thermodynamically favored to form ordered aggregated structures, hindering the formation of highly harmful small metastable aggregates before reaching the final aggregated state (Fefilova et al., 2022).

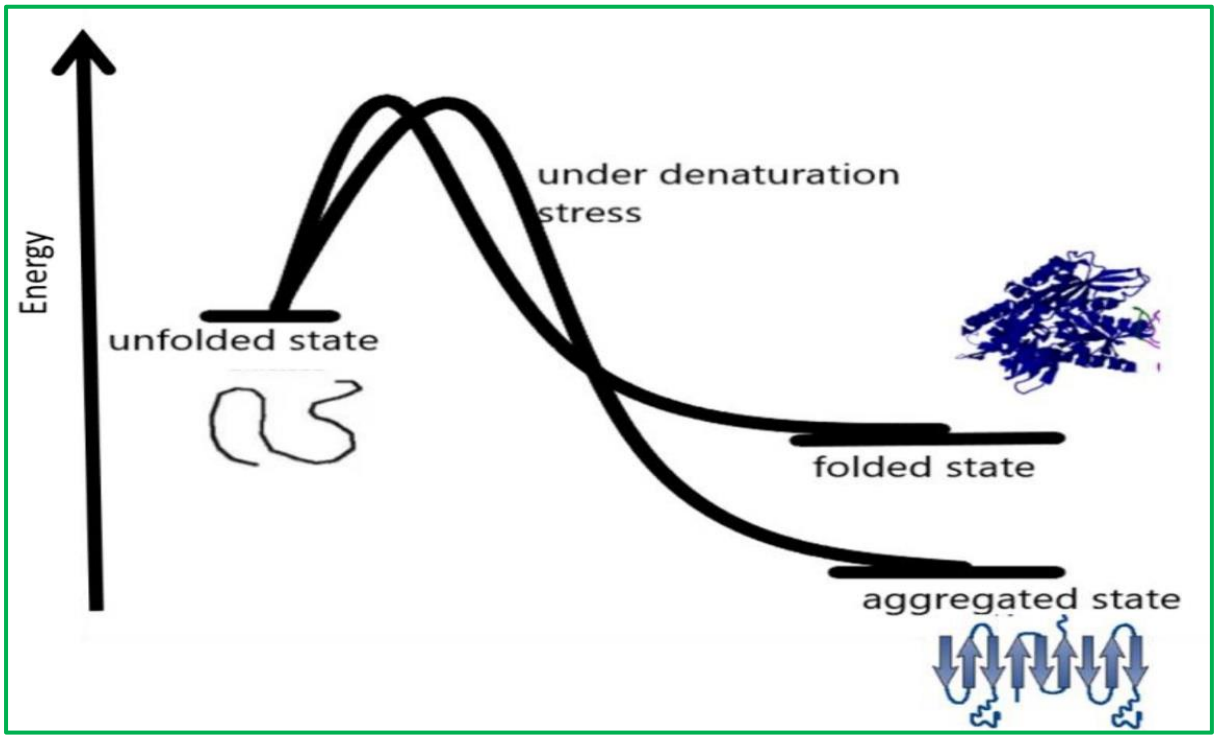

Figure 15: Under specific denaturation conditions, a protein is more likely to change to an aggregated state rather than the native state. (Adapted from Chi et al., 2003).

1.9. Methods for the investigating Protein Aggregation

Over the years, the scientific community has developed numerous methods for the study of protein misfolding and aggregation. It is important to note that each method has its limitations and specific blind spots. Therefore, researchers often integrate several different approaches to thoroughly characterize protein aggregation. We will delve into the various methods used to measure protein stability such as Differential Scanning Calorimetry (DSC), intrinsic dyes, and Nano-Differential Scanning Fluorimetry (Nano-DSF). Moving forward, we will discuss some

of the most widely used tools for predicting protein aggregation, including biophysical, sequence- and structure-based methods **(Fig.16)**. These tools enable the prediction of the aggregation propensity of protein sequences and the identification of Amyloid-Forming Peptide Regions (APRs). We will examine the size and shape through techniques such as Dynamic Light Scattering (DLS), Size Exclusion Chromatography coupled with Multi-angle Light Scattering (SEC-MALS), the use of fluorescent dyes, Transmission Electron Microscopy (TEM), and Atomic Force Microscopy (AFM). We will also explore the monitoring of aggregation kinetics, kinetic modeling, as well as secondary structure characterization using techniques such as Fourier Transform Infrared Spectroscopy (FTIR) and Circular Dichroism (CD). Moreover, we will delve into detailed structural characterization at atomic resolution, accomplished through methods like X-ray Diffraction (XRD), solid-state Nuclear Magnetic Resonance (ssNMR), and Cryo-Electron Microscopy (Cryo-EM). Finally, we will conclude this comprehensive review with a brief discussion of methods to investigate protein aggregation in vivo. These methods are suitable for analyzing the formation of both fibrillar and amorphous aggregates unless specifically stated otherwise.

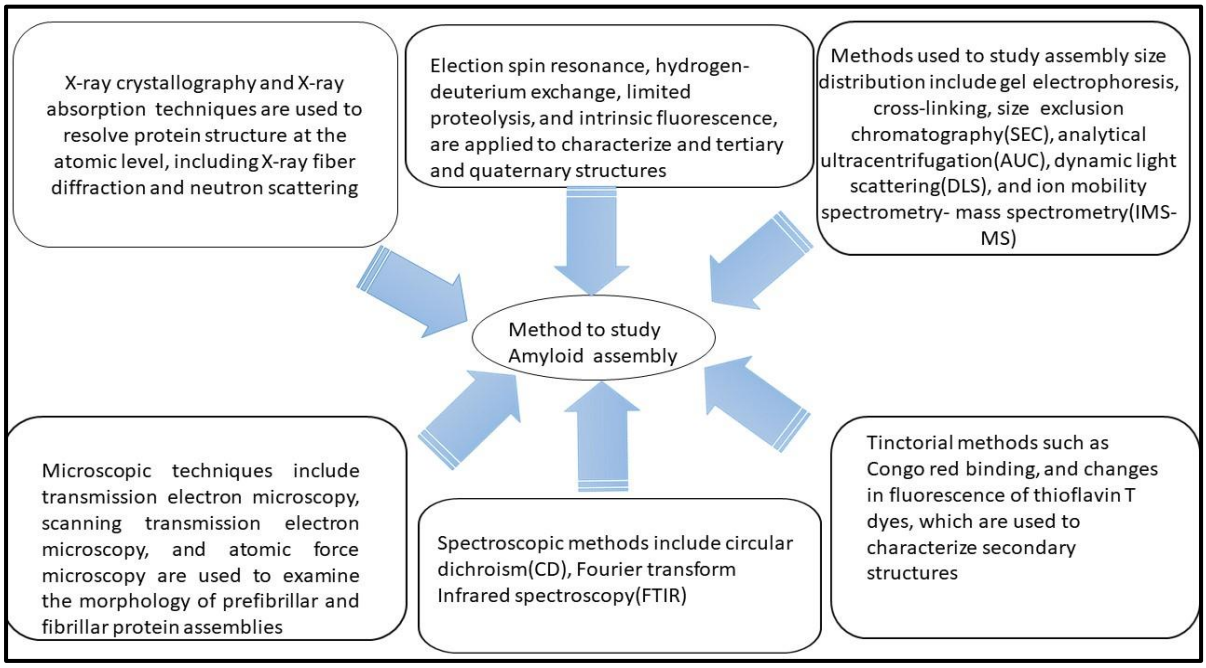

Figure 16: Methods and instrumentation applied to study amyloid formation. (Adapted from Nilsson ,2004)

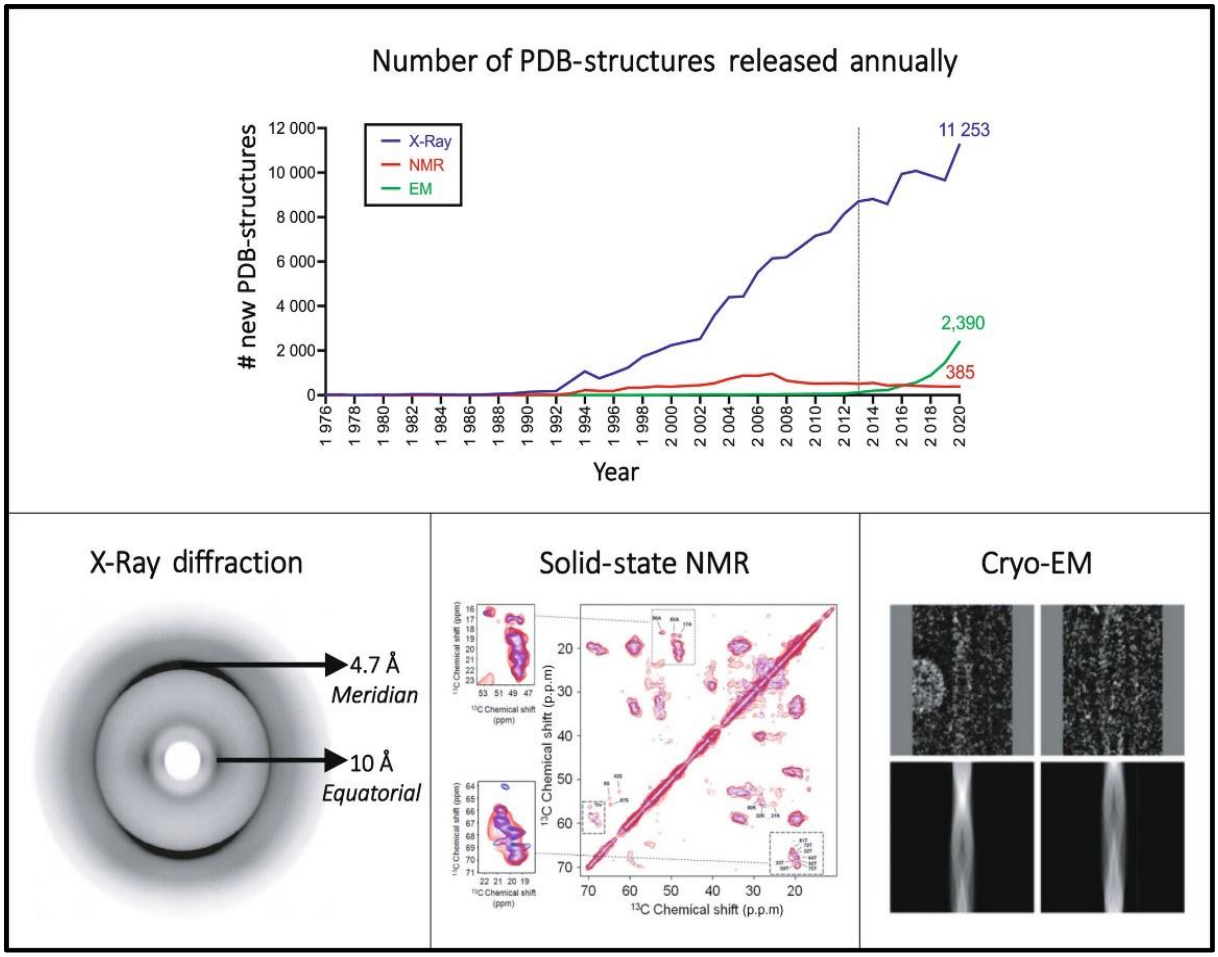

Figure 17: depicts the annual growth of structures in the PDB database, resolved through X-ray, NMR, or EM. The top section illustrates structures solved by X-ray diffraction (XRD), solution NMR (ssNMR), and Cryo-EM. The bottom section showcases experimental data obtained using XRD, ssNMR, and Cryo-EM. "PDB" refers to the Protein Data Base. Source: https://www.rcsb.org/stats/all-released-structures. (Adapted from Morozova-Roche et al., 2000; de Oliveira et al., 2016; Schmidt et al., 2016).

1.10. Protein Misfolding Diseases and Protein Aggregation

A diverse spectrum of human diseases arises from the inability of specific proteins to uphold their native functional conformation. These pathological conditions, commonly termed as protein misfolding diseases (PMDs) (Chiti et al., 2006; Chiti et al.,2017), exhibit a predominant clinical trait marked by the accumulation of amyloid deposits in specific tissues or organs. These amyloid deposits comprise amyloidogenic proteins or peptides, such as amyloid β (Aβ) in Alzheimer's disease (AD) (Ma et al., 2021; Jeremy et al., 1990), α-Synuclein (α-Syn) in Parkinson's disease (PD) (Lashuel et al., 2013; Li et al., 2020), huntingtin protein (HTT) in Huntington's disease (HD) (Bates et al., 2015), transactive response DNA binding protein 43

(TDP-43) in amyotrophic lateral sclerosis and frontotemporal lobar degeneration (ALS and FTLD respectively) (Smethurst et al., 2020; Feneberg et al., 2018), islet amyloid polypeptide (IAPP) in type 2 diabetes mellitus (T2DM) (Westermark et al., 2011), and the prion protein in transmissible spongiform encephalopathies (TSE; prion diseases) (Prusiner et al., 1998). In numerous instances, the misfolded protein aggregates to form amyloid. In pathological conditions, amyloidogenic proteins form fibrils with similar biophysical properties and share similar aggregation kinetics, despite differences in their sequences and sizes (Chiti et al.,2006; Ma et al., 2020; Cheng et al., 2013; Huang et al., 2015). The aggregation process is typically divided into three stages: nucleation, elongation, and plateau (Aguzzi et al., 2010) **(Fig.18A)**. During the nucleation stage, natively folded proteins usually unfold, crossing energy barriers before transforming into β-sheet-rich oligomers/protofibrils (Arosio et al., 2015). Following the nucleation phase, monomers continuously attach to the nuclei, forming long and mature fibrils during the elongation and plateau phases. In amyloidogenic proteins, three crucial blocks with aggregation-regulating potentials are commonly observed, including regions with high fibrillation propensity, α-helical structure, and intramolecular S–S bonds (Li et al.,2018). Consequently, targeting these blocks may be explored to inhibit aggregation. Oligomers rich in β-sheets, primarily formed during the nucleation stage, are considered the primary toxic species during fibrillation and have been shown to have detrimental effects on cells (Sun et al., 2021). Therefore, reducing the production of oligomers has been regarded as a key indicator for estimating aggregation and potential unfavorable pathology. The intermediate oligomers produced during aggregation cause damage to cells through various mechanisms, such as lipid membrane permeabilization, endoplasmic reticulum stress, mitochondrial dysfunction, and oxidative stress **(Fig.18B)** (Ma et al., 2020; Zaman et al., 2019).

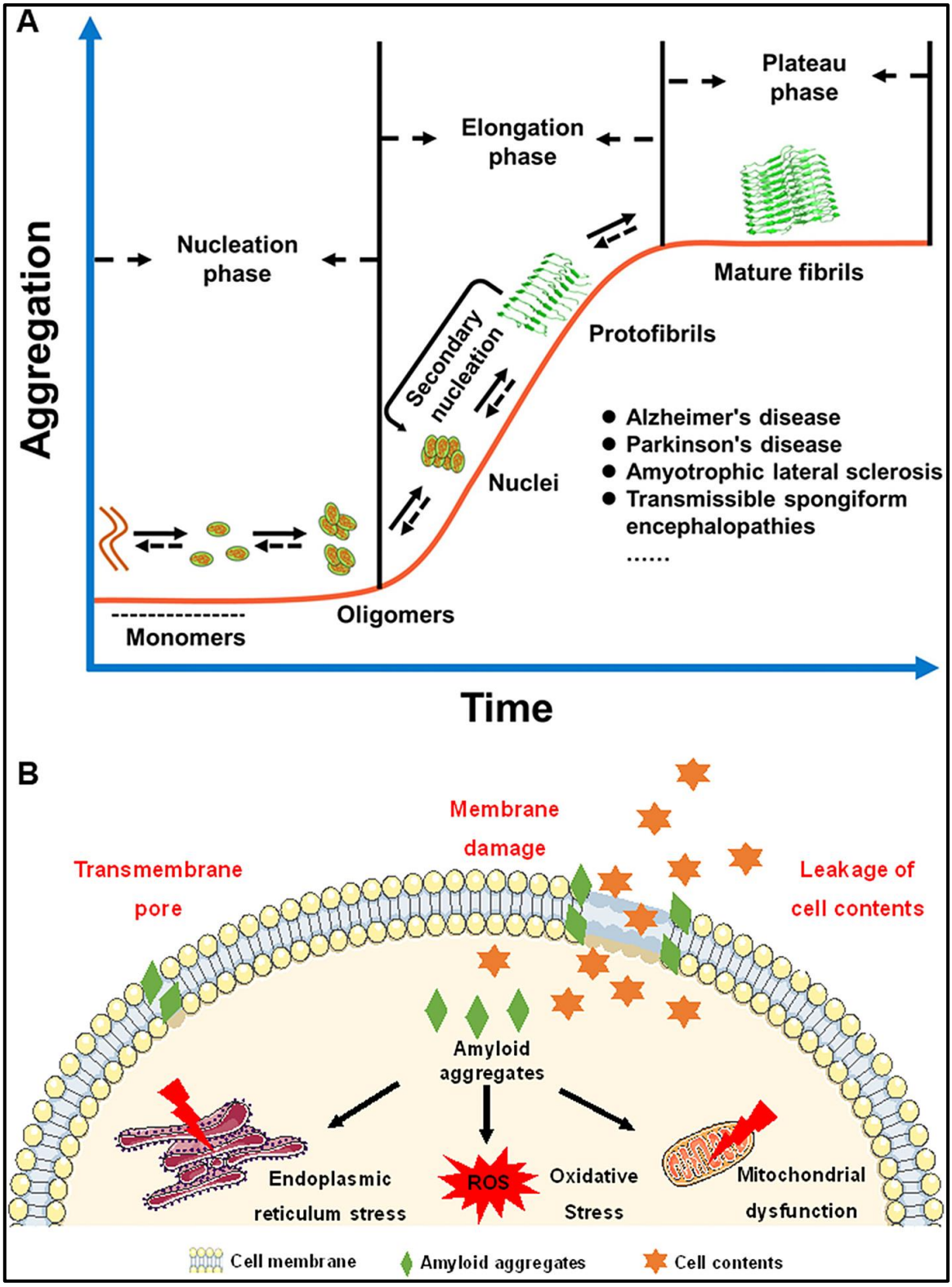

Figure 18: Illustrates the process of aggregation and the cytotoxic mechanisms of amyloidogenic proteins. (A)The aggregation process comprises three distinct stages: a nucleation phase, an elongation phase, and a plateau phase. (B) The resulting aggregates induce cellular damage through lipid membrane permeabilization, endoplasmic reticulum stress, mitochondrial dysfunction, and oxidative stress. (Adapted from Wang et al., 2022).

1.11. Milk Proteins

Milk has been valued for its extensive nutritional benefits since ancient times, serving as a crucial component of a healthy and balanced diet for individuals of all ages, from infants to the elderly. This invaluable source of nutrition is derived from a variety of milch animals, including buffalo, goat, cow, and sheep. Bovine milk, with its approximately 13% total solids and 9% solids without fat, is primarily composed of 87% water, making it a highly hydrating and nourishing liquid food (Yalcin,2006). The proteins present in milk offer a wide array of health benefits and perform various biological functions. These include important therapeutic properties such as antihypertensive effects, anticarcinogenic activities, immune system modulation, and other metabolic features. Furthermore, milk is packed with essential nutrients, including calcium, vitamin A, riboflavin, fortified vitamin D, protein, vitamin B12, potassium, and phosphorus. It also contains a substantial amount of niacin precursor tryptophan, making it an excellent source of niacin equivalents. In addition to these nutrients, milk is rich in various bioactive compounds that possess medicinal (nutraceutical) properties (Davoodi et al.,2016**;** Fox et al., 1998). Bovine milk is a significant source of protein, containing approximately 3.5% protein by weight (36 g/L), which contributes nearly 38% of its total solids and about 21% of its energy (Jensen,1995). Moreover, it is one of the richest natural sources of biologically active peptides, adding to its nutritional value and health benefits. Peptides derived from casein fractions and whey proteins, such as casein phosphopeptides (CPPs), glycomacropeptide (GMP), antihypertensive peptides, opioid peptides, and lactoferrins, exert control over various physiological functions, encompassing antibacterial, antihypertensive, immune-stimulating, opioid-like, antiviral effects, and augmented calcium absorption (Shah, 2000; Meisel,1998; Silva and Malcata,2005; Pan et al., 2006; Expósito and Recio,2006; Jauhiainen and Korpela,2007). Scientific evidence supports a link between milk consumption and reduced susceptibility to cardiovascular diseases, hypertension, cancer, metabolic disorders, and other maladies (Knekt et al., 1996; Davoodi et al., 2013). The major protein families in milk comprise caseins (insoluble) and whey proteins (soluble), with caseins constituting approximately 80% of the total protein content. Casein primarily consists of calcium phosphate-micelle complexes (Yalcin,2006) and is a diverse family of four principal constituents: alpha- (αs1- and αs2-casein), beta-casein, gamma-casein, and kappa-casein (Saxelin et al., 2003; McLachlan,2001; Pihlanto,2011; Séverin and Wenshui,2005). These caseins can be efficiently obtained from skim milk through isoelectric precipitation (the

addition of acid or in situ acid production) or rennet-driven coagulation while yielding whey as a by-product (Madureira et al., 2007).

1.12. Whey Proteins

In recent years, there has been a growing recognition of the functional benefits of milk constituents, which are now acknowledged as functional foods due to their direct and measurable impact on health outcomes (Gill and Cross, 2000). Within the realm of food products, various proteins exhibit desirable functional properties, including gluten, albumin, gelatin, soy protein, casein, and whey proteins. Notably, milk is endowed with a protein system consisting of two major families of proteins: caseins (insoluble) and whey proteins (soluble). Caseins constitute 80% (w/w) of the total protein inventory and can be readily extracted from skim milk through methods such as isoelectric precipitation induced by the addition of acid or rennet-driven coagulation, which also yields whey as a by-product. Meanwhile, whey proteins (WP) are renowned for their nutritional value and versatile functional properties, making them widely utilized in the food industry. It is estimated that approximately 700,000 tonnes (De Wit, 1998) of true whey proteins are made available annually for use as food ingredients globally, with whey accounting for about 20-24% of the total milk protein, the specific amount depending on its source. Historically, whey, being a by-product of cheese making, has not received as much attention as the source of milk. However, in recent decades, there has been a surge in interest in whey protein products owing to their nutritional significance and, increasingly, their active role in promoting human health. Commercially, whey proteins are available in the forms of whey protein isolates (WPI, 90-95% protein) and whey protein concentrates (WPC, 35-75% protein). Whey proteins are characterized by their globular molecular structure, substantial content of α-helix motifs, and a fairly balanced distribution of acidic/basic and hydrophobic/hydrophilic amino acids along their polypeptide chains (Fox et al., 1982). Whey proteins demonstrate numerous health-promoting effects, encompassing anti-inflammatory, antioxidant, and antiviral activities (Zhao et al., 2022). Furthermore, whey protein complements the augmentation of lean mass and the fortification of exercise endurance. Owing to their elevated leucine content, whey proteins have substantiated their capacity to drive muscle protein synthesis more effectively than alternative proteins (Pennings et al., 2011). Prevalent constituents of whey proteins comprise α-lactalbumin and β-lactoglobulin, in conjunction with lactoferrin, immunoglobulins, glycomacropeptide, and bovine serum albumin (Master and Macedo, 2021). These soluble protein fractions sourced from milk and whey

effortlessly traverse the gastric milieu, liberating amino acids into the systemic circulation (Hall et al., 2003; Boirie et al.,1997).

1.12.1 Introduction of Bovine β-lactoglobulin (β-lg)

Bovine β-lactoglobulin (β-lg) is the predominant whey protein, comprising approximately 55% (w/w) of the total whey protein content. This protein was first identified in 1934 and is primarily found in the whey protein of ruminant species, although it is notably absent in human milk (L. Sawyer,2003). Interestingly, in monogastric species such as dolphins, horses, and pigs, β-lg exists in a monomeric form with an approximate molecular weight of 18300 Da. However, in the milk of ruminants like cows, sheep, and reindeer, β-lg is predominantly found in a dimeric form (Hambling et al. 1992). The process of isolating β-lg from cow's milk involved salt fractionation (Palmer,1933**)**. The preparation of a crystalline globulin from the albumin fraction of cow's milk and its crystalline structure was first captured in an X-ray photograph by Crowfoot (Crowfoot and Riley, 1938). Additionally, ultra-centrifugal studies of milk and whey revealed multiple peaks in the sedimentation pattern, with Pederson (Pedersen, 1936) designating them as α, β, γ and identifying the β-peak as originating from α Palmer's protein. Subsequently, Svedberg named it β-lactoglobulin (Svedberg,1939). Furthermore, the existence of genetic variants A and B in milk proteins was first reported by R. Aschaffenburg and J. Drewry (Aschaffenburg and Drewry,1955). The intricate structure of β-lg has been extensively explored using X-ray crystallography and NMR techniques. β-lactoglobulin (β-lg) is capable of binding to a diverse array of small hydrophobic ligands. These include calcium, retinol, various fatty acids, protoporphyrin IX, triacylglycerols, alkanes, aliphatic ketones, aromatic chemicals, vitamin D, cholesterol, and palmitic acid (Kontopidis et al., 2002). This property of β-lg to interact with such a wide range of molecules contributes to its versatility and potential applications in various fields, including food science and pharmaceuticals. Owing to its abundance and the availability of various crystal forms, β-lg has emerged as a key model protein for a wide range of biophysical studies due to the ease of different preparation methods (Brownlow et al., 1997).

Table 2: Chronological development of isolation, purification, and structural elucidation of bovine of β-lactoglobulin (β-lg).

Year	Isolation, Purification, and X-ray Crystallographic Study	Reference
1933	Precipitation at pH 5.8 followed by Na2SO4 precipitation at 30ºC, dialysis, and crystallization.	Palmer, 1933
1938	X-ray Crystallographic Study of Palmer's lactoglobulin.	Crowfoot et al., 1938
1941	X-ray work on β-lg crystal.	Crowfoot, 1941
1957	Na2SO4 precipitation at 40ºC followed by acidic precipitation at pH 2, dialysis, and crystallization.	Aschaffenburg & Drewry, 1957
1959	X-ray diffraction study of derivatives of β-lactoglobulin	Green, 1959
1965	X-ray Crystallographic Study of β-lactoglobulin.	Aschaffenburg et al., 1965
1967	•$(NH_4)_2SO_4$ precipitation at 20ºC, acidic precipitation at pH 2 followed by Na_2SO_4 precipitation at pH 6, dialysis and crystallization. •Separation of β-lactoglobulin by trichloroacetic acid.	Armstrong et al., 1967 Fox et al., 1967
1986	Crystal structure of orthorhombic lattice Y form.	Papiz et al., 1986
1987	Centrifugation, CaCl2 precipitation at pH 6.6, dialysis followed by anion exchange gel filtration and crystallization (lattice Z structure based upon lattice Y).	Monaco et al., 1987
1990	Gel filtration using Sephacryl S-200 and purification by diethyl aminoethyl ion exchange chromatography	Yoshida, 1990
1991	Acidic precipitation at pH 4.6, Centrifugation, filtration followed by bio-affinity column chromatography.	Chiancone & Gattoni, 1991
1994	Large-scale separation of β-lactoglobulin.	Mate & Krochta, 1994

1996	X-ray Crystallographic Study of β-lactoglobulin.	Rocha et al., 1996
1997	• Centrifugation, acidic precipitation at pH 4.6, filtration, dialysis, and gel filtration. • Acidic precipitation at pH 4.6, Centrifugation, and Nretinyl-create affinity chromatography. • Triclinic lattice X at 1.8 Aº resolution and lattice Y at 2.1 Aº resolution. • Isolated by combining a precipitation process and a diafiltration process.	Felipe and Law, 1997 Heddleson et al., 1997 Brownlow et al., 1997 Caessens et al., 1997
1998	Crystallographic presentation of external ligand-binding sites.	Sawyer et al., 1998
1999	Crystallographic three-dimensional aspects of βlactoglobulin and functional properties.	Sawyer et al., 1999
2001	Centrifugation, acidic precipitation at pH 4.4-4.5, base precipitation at pH 7.2, centrifugation followed by anion-exchange and gel filtration Chromatography.	de Jongh et al., 2001
2008	10-90% $(NH_4)_2SO_4$ precipitation, cation-exchange chromatography, dialysis, and lyophilization.	Lozano et al., 2008
2010	Gel filtration Chromatography at low pH using a BioGel P10 column	Naqvi et al., 2010
2012	One-step method by anion exchange chromatography, high-performance liquid chromatography, and mass spectroscopy.	Stojadinovic et al., 2012
2014	Combining ion exchange chromatography and gel filtration by adsorbed on DEAE-Sepharose FF packed column and Sephadex G-75 gel and SDS-PAGE	Buyanbadrakh et al., 2014
2015	Gel filtration chromatography using Sephacryl S-200 at acidic pH 4.6	Aich et al., 2015
2019	The structure of bovine β-lactoglobulin in crystals grown at pH 3.8 Exhibiting Novel Threefold Twinning	Todd et al., 2019

1.12.2 Polymorphic variants of Bovine β -lactoglobulin(β-lg)

The identification of genetic polymorphism in milk proteins was initially documented by Aschaffenburg and Drewry (Aschaffenburg and Drewry,1955). Their observation involved subjecting milk samples from individual cows to electrophoresis on filter paper, revealing distinctly separate bands, later denoted as β-lg A and β-lg B. The amount of caseins in milk is closely related to the amount of β-lactoglobulin (β-lg) protein present. A low concentration of β-lg protein is associated with a high concentration of caseins (Ng-Kwai-Hang et al., 1986; Lunde´n et al., 1997). The variation in β-lg protein levels is largely attributed to different protein variants. There are eleven known variants of β-lg, with variants A and B being common in most cattle breeds (Farrell et al., 2004). Variants A and B differ by two amino acid substitutions: Asp64Gly and Val118Ala. Variant A has a higher β-lg protein concentration in bovine milk compared to variant B (Cerbulis and Farrell, 1975; Hill, 1993). This difference in β-lg protein levels is likely due to varying levels of expression of the corresponding A and B alleles of the β-lg gene, rather than the amino acid substitutions. The differential expression of the A and B alleles of the β-lg gene may be attributed to polymorphisms in regulatory sequences that are in linkage disequilibrium (LD) with the causal genetic polymorphisms of β-lg protein variants A and B. Several polymorphisms have been identified in the promoter region of the bovine β-lg gene, including some within putative regulatory sequences (Wagner et al. 1994; Lum et al. 1997). To date, however, no evidence has emerged to suggest that any of the identified polymorphisms are responsible for the observed disparity in β-lg protein levels between variants A and B. This polymorphism arises from a mutation in the genetic sequence, resulting in an amino acid substitution along the translated polypeptide chain, which has persisted within bovine populations. These disparities yield unique biophysical and biochemical traits of the variants, including heat stability (Manderson et al., 1999), subunit dissociation/denaturation due to hydrostatic pressure (Botelho et al., 2000), self-association properties (Timasheff and Townend,1961), and solubility (Treece et al., 1964). While numerous genetic variants have been identified, our particular focus centers on elucidating the properties of the β-lg B variant.

β-lgA β-lgB

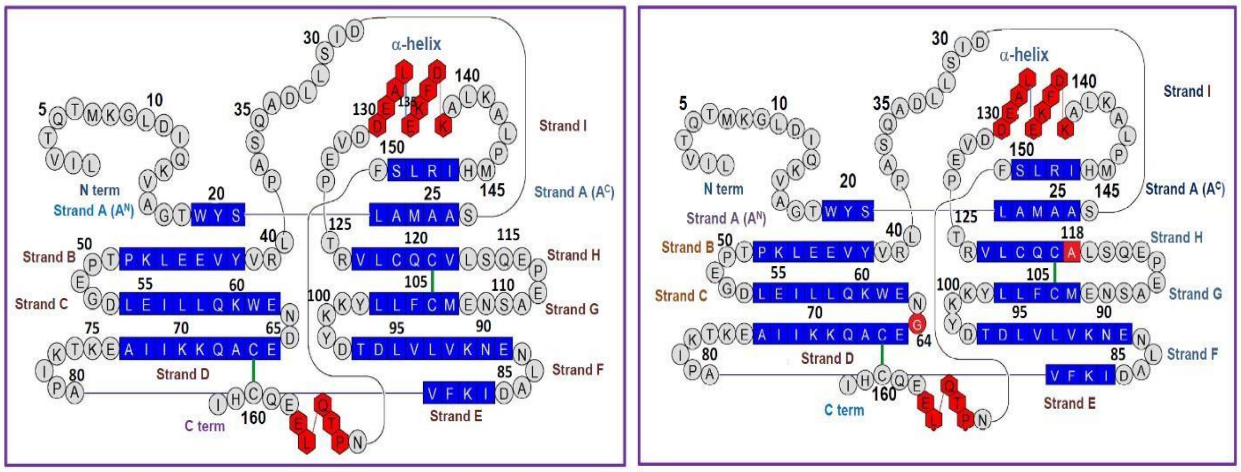

Figure 19: A schematic representation of the amino acid residues of the β-lg A and β-lg B sequence. Residues making up the α-helix, β-sheet, and loop are represented by hexagons in red, squares in blue, and circles in grey, respectively. Green lines indicate the positions of disulfide bonds. The substitutions Val118Ala (A→B) and Asp64Gly (A→B) are shown in red square and red circle, respectively. (Adapted from Qin et al., 1999).

1.12.3. Amino Acid Sequence of Bovine β-lactoglobulin (β-lg)

The amino acid distributions of the A and B variants of bovine β-lactoglobulin were meticulously analyzed (Gordon et al., 1961) and later confirmed (Bell et al., 1968), who also determined the composition of the A, B, and C variants. The amino acid sequences of β-lg (A and B) were initially discovered (Frank and Brannitzer ,1967), as shown in Scheme x Since then, extensive molecular level information has been obtained, including the purification process, amino acid sequencing, and high accurate X-ray diffraction studies.

β-lg A: 1LIVTQTMKGL DIQKVAGTWY SLAMAASDIS LLDAQSAPLR YVEELKPTP

β-lg B: 1LIVTQTMKGL DIQKVAGTWY SLAMAASDIS LLDAQSAPLR YVEELKPTP

β-lgA: 51EGDLEILLQK WENDECAQKK IIAEKTKIPA VFKIDALNEN VLVLDTDYK

β-lgB: 51EGDLEILLQK WENGECAQKK IIAEKTKIPA VFKIDALNEN VLVLDTDYK

β-lgA:101KYLLFCMENS AEPEQSLVCQ CLVRTPEVDD EALEKFDKAL KALPMHIRLS

β-lgB: 101KYLLFCMENS AEPEQSLACQ CLVRTPEVDD EALEKFDKAL KALPMHIRLS

β-lgA: 151FNPTQLEFQC HI

β-lgB: 151FNPTQLEFQC HI

Scheme 2: The Amino Acid sequence of Bovine β-Lactoglobulin A (β-lgA) and B (β-lg B). W-Tryptophan 19; W-Tryptophan61; C-Cystein 121 (free Thiol, -SH); Change in amino acid sequences (position 64 and 118) in variants A and B have been highlighted in green.

It is widely acknowledged that two distinct genetic variants of β-lactoglobulin (β-lg), denoted as A and B, have been identified, differing solely in two specific amino acid positions: Asp 64→Gly64 and Val 118→Ala 118 (Sawyer & Konotopidis, 2000). Variant A and B exhibit isoelectric points of 5.1 and 5.3, respectively. β-lactoglobulin contains two intra-molecular disulfide bonds, namely Cys66-Cys160 and Cys106-Cys119, in addition to a free thiol (-SH) group located at Cys 121 (Sakurai & Goto, 2002). Furthermore, this protein harbors two tryptophan residues (Trp 19 and Trp 61) and four tyrosine residues (Tyr20, Tyr 41, Tyr 99, Tyr 102). Notably, Trp 19, situated within the hydrophobic calyx, is responsible for the principal fluorescence attribute of β-lg (Qin et al., 1998; Uhrinova et al., 2000). Lastly, β-lg consists of 15 lysine residues, which have been found to play vital roles in maintaining the structural integrity of β-lg (Bewley et al., 1997; Brownlow et al., 1997; Chakraborty et al., 2009).

1.12.4. Bio-availability of Bovine β-lactoglobulin(β-lg)

Bovine β-lg, a crucial protein component found in the whey portion of milk, is primarily present in the milk of various animals including cows, dolphins, baboons, and pigs (Buyanbadrakh et al., 2014; Conti et al., 1986), sheep, horses **(**Conti et al., 1984), goats, cats (Halliday et al., 1991), buffaloes (Aich et al., 2014), bison, and others. Notably, it is absent from human milk (Sawyer and Kontopidis, 2000). The average concentration of β-lg in milk is 3 g/L (Kontopidis et al., 2004). The comparison of amino acid sequences within the lipocalin family has revealed that glycodelin, a protein present in the human endometrium during early pregnancy, exhibits the highest similarity to β-lg (Koistinen et al., 1999; Halttunen et al., 2000). Glycodelin is exclusive to the human species, while β-lg is synthesized and secreted by the epithelial cells of the mammary gland under the regulation of the hormone prolactin (Larson, 1972). The mRNA coding for β-lg is initially synthesized in the mammary gland and subsequently translated into pre-β-lg, which comprises 180 amino acids (Yoshikawa et al., 1978). Notably, a highly conserved peptide consisting of 18 amino acids, known as the "signal peptide," precedes the

remaining 162 amino acids in the linear chain of β-lg. These 162 amino acids undergo a refolding process to assume the native conformation of β-lg. Similar to glycodelin, the distinct functional aspects of β-lg remain undisclosed; however, theories have been postulated based on inter-species distribution and its relationship to lipocalin (Kontopidis et al., 2004).

1.12.5. Molecular structure of Bovine β-lactoglobulin(β-lg)

Based on several studies, the monomer exhibits a spherical shape with a block of electron density and a rod-like structure across one face (Green and Aschaffenburg, 1959). The secondary structure of β-lg was estimated to consist of approximately 50% β-sheet, 15% α-helix, and 15–20% reverse turn (Wang et al., 2022). The first medium-resolution structure of β-lg was disclosed in 1986, revealing a predominantly β-sheet structure (Figure 16), with an eight-stranded antiparallel (A-H) β-barrel, a small three-turn α-helix on the outer surface, and a β-strand 'I' immediately before the C-terminal end (Papiz et al., 1986). The crystallographic analysis highlights the presence of an eight-strand antiparallel barrel arranged in an anti-parallel ring structure, wherein hydrophobic ligands/molecules are contained within the hydrophobic calyx (Monaco et al., 1987; Brownlow et al., 1997). β-lg's globular nature is evident from its 162 amino acid residues and an estimated molecular mass of 18400 Da. Notably, β-lg possesses conserved three-dimensional structural domains (sequence motifs) and exhibits a characteristic property of binding and transporting small hydrophobic molecules, typical of the lipocalin family (Sawyer and Kontopidis, 2000). β-lg shares extensive sequence homology with the retinol-binding protein and is thought to be involved in the binding and transportation of retinol in mammals (Redl and Habeler, 2022). Under physiological pH, β-lg exists as a dimer. However, it transitions to a monomeric state below pH 3.0 and above pH 7.0. At pH 2.0, β-lg dissociates into its monomeric form while maintaining its native conformation (Crowther, 2017). X-ray crystallography shows that A—>D strands contribute to one side of the β-barrel's formation, with strands E—>H involved on the other side, while strand 'I' protrudes outward from the calyx, playing a role in dimer interface through ionic strength/salt dependence or hydrogen bonding (Qin et al., 1998; Sakurai and Goto, 2002). Moreover, β-lg exhibits resistance to acid hydrolysis and pepsin digestion (Rahaman et al., 2017). This pH-dependent monomer ↔ dimer transformation is strictly attributed to non-covalent and hydrophobic interactions (Sakurai et al., 2001). The presence of aromatic residues such as two tryptophan, four tyrosine, and four phenylalanine residues make β-lg fluorescence active (Xu et al., 2019). These groups are also responsible for the near UV CD of β-lg spectra, which helps investigate site-specific conformational changes. β-lg has a high helical propensity despite

being a predominantly β-sheet protein. During its refolding from the fully unfolded state, an intermediate with a non-native α-helical structure accumulates because the local interactions between neighboring amino acid residues favor the α-helical structure (Hamada et al., 1996). In particular, the EF loop, consisting of amino acids 85-90, acts as a gate over the binding site. At low pH, it is in the "closed" position, and binding is inhibited or impossible, whereas, at high pH, it is open, allowing ligands to penetrate the hydrophobic binding site.

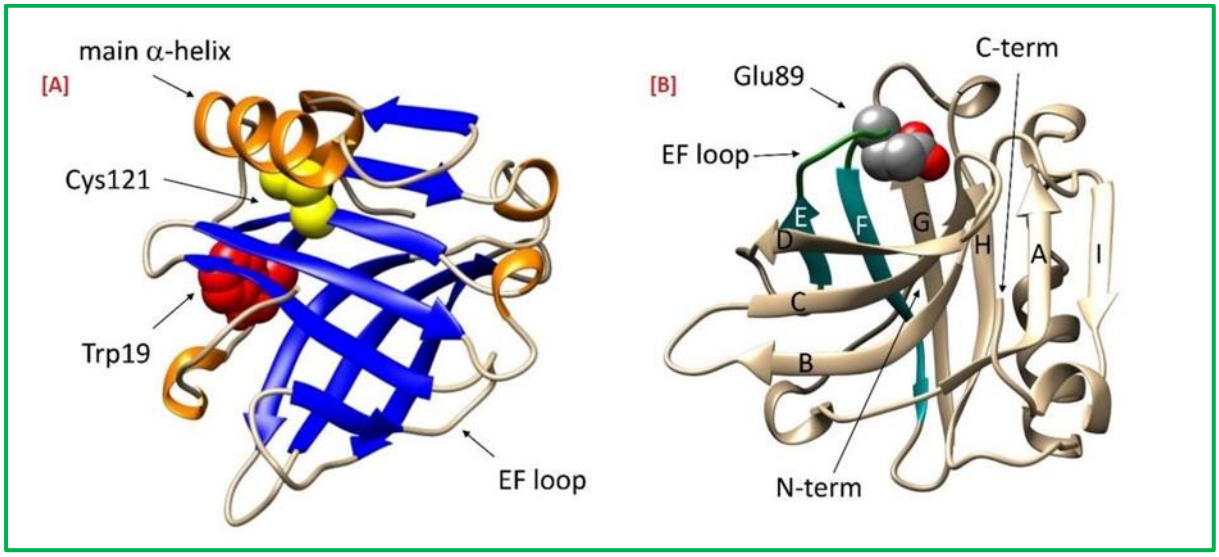

Figure 20: Properties of the native BLG structure that are pertinent to research on folding stability. (A): Trp19 (red) is at the base of the beta-barrelled calyx (blue); Cys121 (yellow) is concealed behind the major alpha-helix (orange). (B): The EF loop forms a "lid," which closes when Glu89, seen in CPK colors, is protonated (dark green). The free graphics program UCSF Chimera (version 1.14, University of California, San Francisco, CA, USA) was used to create the structures.

β-lg forms covalent dimers or oligomers through disulfide links accompanied by the free thiol (Cys121) group, or via disulfide exchange processes during the unfolding/refolding pathway under thermal stress (Hoffmann and van Mil,1997; Qi et al., 1997; Qin et al., 1999, Galani and Owusu,1999; Oliveira et al., 2001). The residues Cys106 and Cys119 form the disulfide bridge in the β-G and β-H strands, allowing the α-helix to remain packed against the exterior of the calyx. However, this disulfide bridge is not solvent-accessible and is shielded from the thiol of Cys121 by the side chains of Phe136, Ala139, and Leu140. Another disulfide bridge, Cys66-Cys160, fastens the C-terminal loop to the exterior of the calyx (Brownlow et al., 1997).

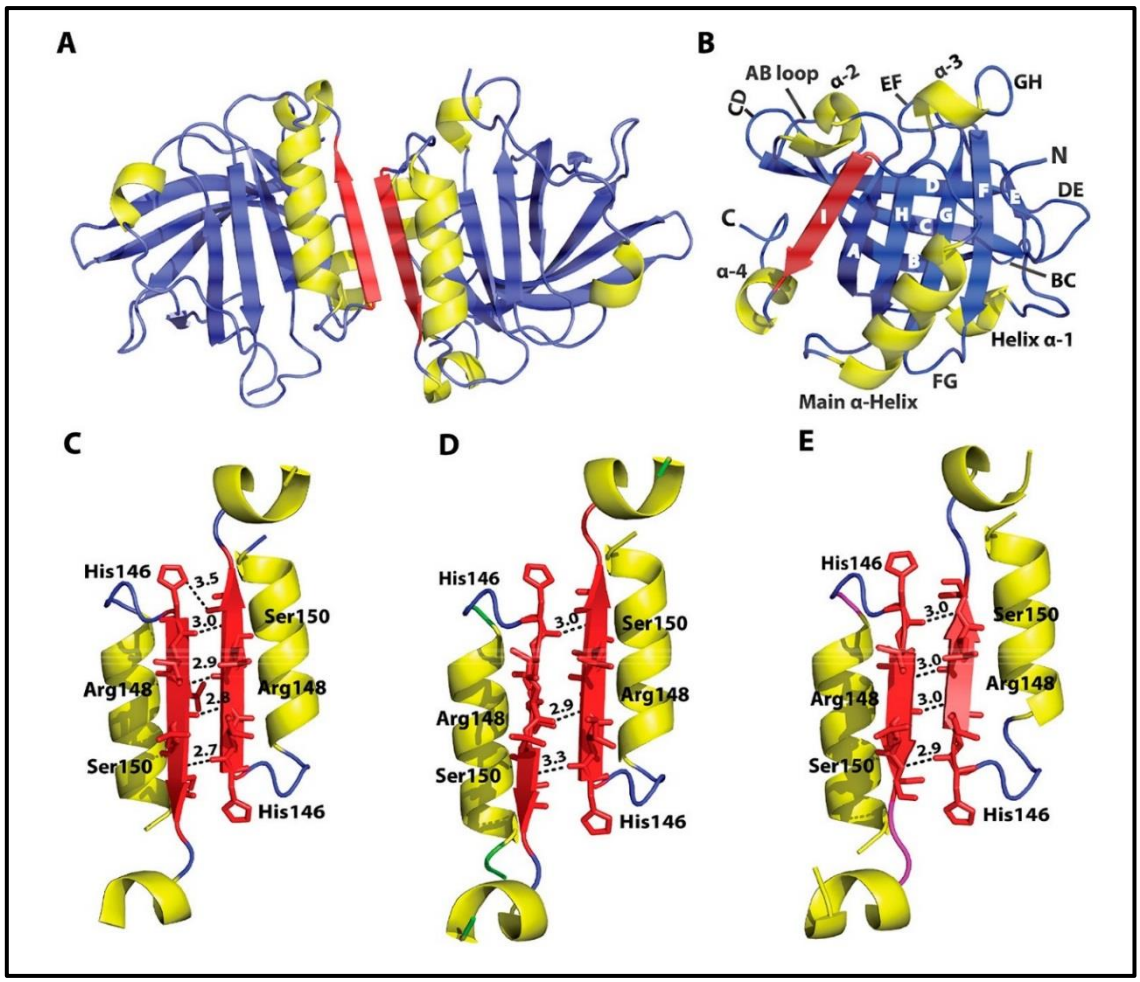

Figure 21: Crystal structure of β-lg A (6FXB) at pH 4.0. (A) Ribbon representation of β-lg A (chains AB) dimer. (B) Ribbon representation of a β-lg A (chain B) monomer with β-strands, α-helices, and loops being labeled. The dimer interface of β-lg A (chains AB) showing hydrogen bonds between β-strands I in (C) the present crystal structure at pH 4.0 and crystal structures (D) at pH 5.2 (2AKQ) and (E) pH 6.5 (1BEB). This figure was generated by PyMOL.51 Hydrogen bond distances are shown in angstroms**.** (Adapted from Khan et al., 2018).

The irreversible denaturation is attributed to thiol-disulfide exchange facilitated by the free thiol of Cys-121. Prior reports have documented the occurrence of intermolecular disulfide bridge formation during heat denaturation at neutral pH (Schokker et al.,1999; Carrotta et al.,2001; Surroca et al., 2002; Croguennec et al., 2003). Notably, even at pH 2.1, an incomplete recovery of circular dichroism (CD) spectra was evident in samples treated with 7 M urea (Ragona et al.,1999). The close proximity of Cys-121 to Cys-119 potentially enables thiol-disulfide exchange even under acidic conditions. Previous efforts to generate a mutant lacking the free thiol group at Cys-121 within the Escherichia coli expression system were unsuccessful.

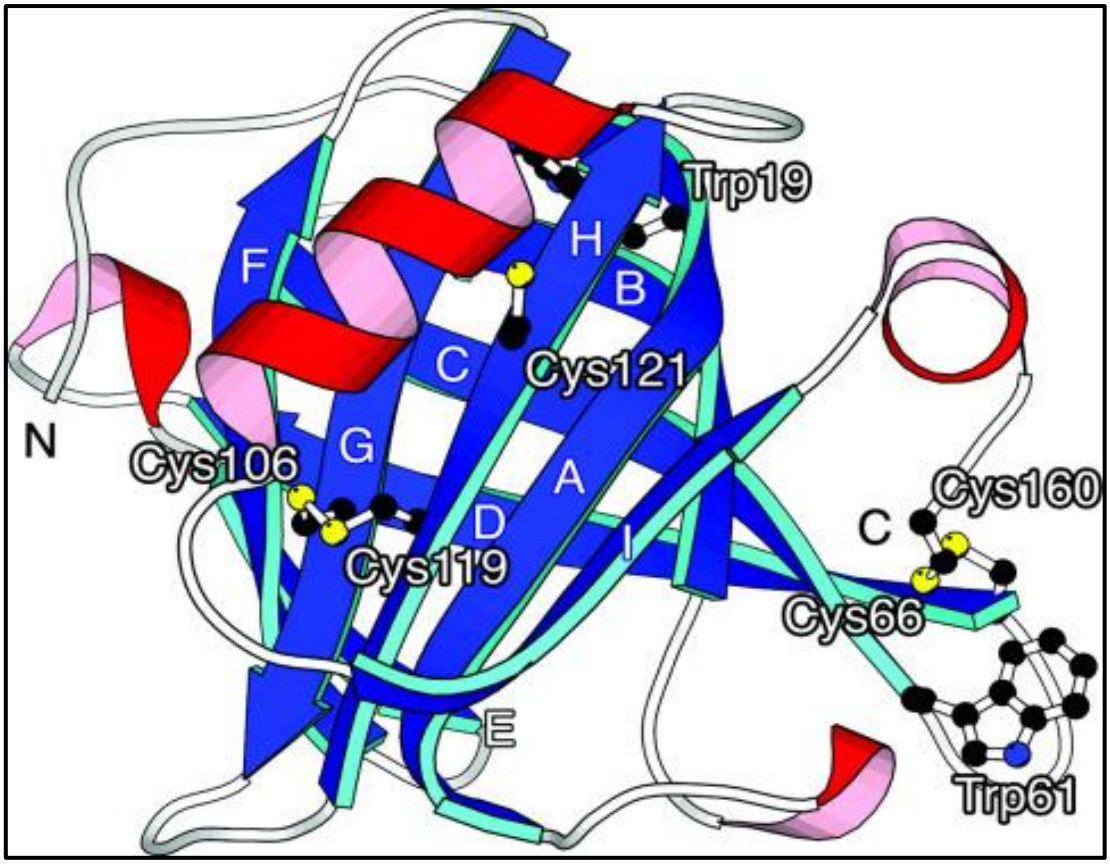

Figure 22: The positions of disulfide bonds (Cys-66/Cys-160, Cys-106/Cys-119), a free cysteine residue (Cys121), tryptophan residues (Trp-19, Trp-61), and-strands (A–I) are indicated in the structure. The diagram was created by Molscript (Kraulis,1991) with the Protein Data Bank code 1BEB (Brownlow et al., 1997). (Adapted from Yagi et al., 2003)

1.12.6. The Lipocalins and β-lactoglobulin: Structure and Function

Lipocalin constitutes a protein family capable of binding to small, predominantly hydrophobic molecules including steroids, bilins, retinoids, lipids, and specific cell surface receptors, resulting in the formation of macromolecular complexes. Proteins exhibiting analogous characteristics in extracellular environments and engaging in the binding of hydrophobic molecules and ligands to specific cell surface receptors are classified as lipocalins. Typically composed of 160-180 amino acids, lipocalins exhibit a conserved crystal structure (sequence motif) while displaying a low degree of sequence similarity (Newcomer et al., 1984; Virtanen, 2001). Selectivity is influenced by the overall dimensions and conformation of the pocket, loop scaffold, and the constituent amino acids. The structural components of the lipocalin fold, specifically a capacious cup-shaped cavity within the β-barrel and an entrance-containing loop scaffold, are particularly well-suited for ligand binding. The antiparallel beta-barrel comprises eight strands and houses an internal ligand binding site with a repeating +1 topology (Cowan et al., 1990).

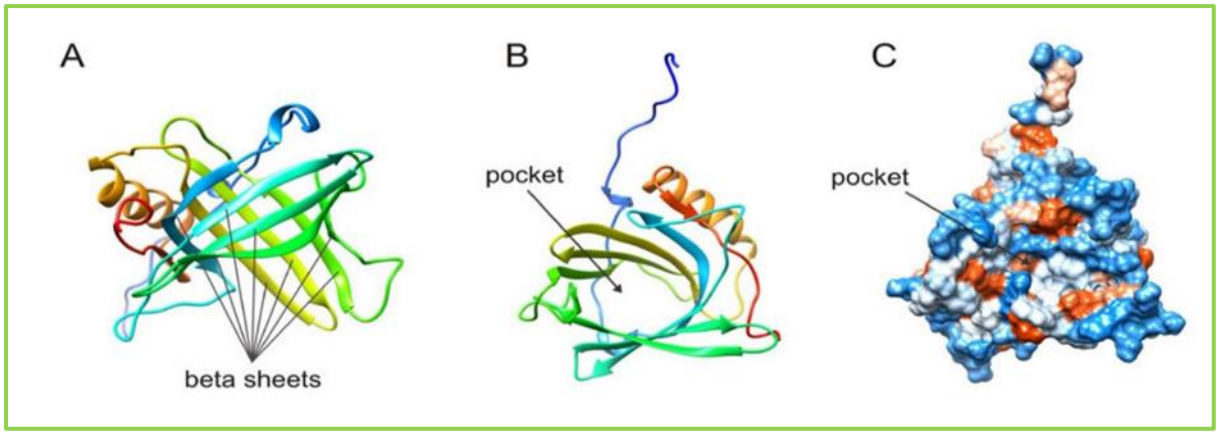

Figure 23: The crystal structures of lipocalin that are highly conserved are made up of an antiparallel β-barrel (A) that is constantly hydrogen-bonded and has eight strands. This barrel defines a calyx shape that indicates the internal ligand binding site (B) and the hydrophobicity surface (C). Using the UCSF Chimera software, which is provided by the University of California, San Francisco's Resource for Biocomputing, Visualization, and Informatics, images were created from the RCSB PDB database (http://www.rcsb.org) (ID: 1NGL). (supported by NIGMS P41-GM103311) (Coles et al., 1999).

1.12.7. Biological Function of Bovine β - lactoglobulin (β-lg)

Beta-lactoglobulin (β-lg) is the predominant whey protein in cow's milk, accounting for approximately 25% of the total protein content. It is renowned for its high nutritional value, serving as an excellent source of essential amino acids, particularly branched-chain amino acids. These attributes make it an essential component in infant formulas, contributing to the growth and development of infants.

Moreover, β-lg has piqued the interest of researchers as a potential candidate for drug delivery. Specifically, its ability to bind with hydrophobic drugs and traverse the gastrointestinal tract effectively positions it as a promising oral drug delivery carrier. Studies have shown that β-lg improves the stability and solubility of drugs, thereby enhancing their bioavailability and therapeutic efficacy. This makes it an attractive option for improving the delivery of poorly soluble drugs and enhancing their therapeutic outcomes.

It exhibits a remarkable ability to bind a diverse array of ligands, particularly small hydrophobic and amphiphilic molecules. These include retinol (vitamin A) (Kontopidis et al., 2004; Fugate and Song, 1980), long-chain fatty acids (Fletcher et al., 1970), palmitate (Therese et al., 2005), and sodium dodecyl sulfate (McMeekin et al., 1949; Ray and Chatterjee, 1967; Jones and Wilkinson, 1976; Lamiot et al., 1994). The X-ray crystallographic studies and amino acid sequence of β-lg (Papiz et al., 1986; Monaco et al., 1987) reveal striking similarities with

plasma retinol-binding protein (Newcomer et al., 1984), which is classified within the lipocalin family (Akerstrom et al., 2000). It is suggested that the role of β-lg involves the transport of small hydrophobic substances and the uptake of retinol in suckling mammals through the small intestine epithelium. However, a specific receptor for β-lg has yet to be characterized. Additionally, it may play a part in lipid digestion as a carrier protein for fatty acids and retinol within the gut (Perez et al., 1992). Native β-lg displays resistance to peptic and chymotryptic digestion (Reddy et al., 1988**)**. In summary, β-lg represents a group of proteins capable of binding a wide variety of amphiphilic or hydrophobic ligands.

1.12.8. Structural Stability of Bovine β-lactoglobulin (β-lg)

1.12.8.1 Effect of pH on Bovine β-lactoglobulin (β-lg)

The conformational transition of proteins is often pH-dependent, leading to changes in their solubility profile. Under different conditions, the protein β-lactoglobulin can aggregate into two distinct forms: amyloid fibrils at pH values far from the isoelectric point, and spherical aggregates near it. At physiological pH, bovine beta-lactoglobulin exists as a dimer. However, it isolates into its monomer form with a native conformation at pH 2.0 (Mckenzie and Sawyer, 1967; Sakai et al., 2000; Uhrinova et al., 2000). Below pH 3.0 and above pH 7.0, it exists as a monomer (Casal et al.,1988) demonstrated changes in secondary structures using infrared spectroscopic studies to analyze the effect of pH and temperature on the conformation-sensitive amide-I bands. Additionally, the mechanism of pH-induced β-lg native state aggregation near the pI, the strong effect of the direction of pH adjustment on both aggregation and disaggregation kinetics, and the nature of the two characteristic rate processes, as well as their relationships to net versus local protein charge, are considered. On the other hand, the structure of β-lg has been investigated by studying the effect of pH, ionic strength, and heat on its intrinsic tryptophan fluorescence properties to monitor tertiary structural aspects (Renard et al., 1998). It is noted that β-lg is resistant to acid hydrolysis and pepsin digestion (Astwood et al., 1996; Renard et al., 1998; Takagi et al., 2003). The pH-dependent monomer ↔ dimer transition is primarily attributed to non-covalent and hydrophobic interactions (Sakurai et al., 2001). The aggregation of β- lg is found to be pH-dependent and can be observed using DLS and CD spectroscopies. In terms of the conformation of β- lg, the EF loop made up of amino acids 85-90, particularly the glutamic acid (Glu 89), plays a crucial role in allowing small hydrophobic molecules to enter the calyx of β- lg. This is accompanied by a 'lid-motion' along with the serine residue (Ser 116) through H-bond formation in a pH-dependent manner (Tanford and Nozaki, 1959; Brownlow et al., 1997; Qin et al., 1998; Uhrinova et al., 2000; Kntopidis et al., 2004).

The 'Tanford transition' occurs at around pH 7.5 (Tanford and Nozaki, 1959). Recent results from combined spectroscopic and volumetric studies reveal that at pH 5, transitions of β- lg occur within the pH range of 1 to 13, as reported (Taulier and Chailikian, 2001**)**. Additionally, recent reports based on PCA of NMR data, where electric field artifacts have been removed, present a different perspective on pH-dependent structural transition. Recent work has also been carried out on the folding and self-assembly of β- lg from a reversible unfolded state at pH 10.5 in the presence of methanol, 2-propanol, t-butanol, and 2,2,2-trifluoroethanol (TFE) (Maity et al., 2016).

Tanford Transition of Bovine β-lactoglobulin (β-lg)

The protein undergoes multiple conformational changes within the pH range of 6 to 8, a phenomenon referred to as the "Tanford transition" (Qin et al., 1998; Sakurai and Goto, 2006). These alterations lead to a noticeable expansion of the protein. Despite this, the specific molecular mechanisms governing these conformational changes in the wild type remain unidentified. The "Tanford transition," named in honor of Tanford and his colleagues who originally discovered it five decades ago, denotes the pH-induced transition of β-lg within the pH range of 6 to 8. Notably, variations in the conformation of the EF loop are evident at the open end of the protein cavity. Moreover, the anomalous protonation of E89 (pKa = 7.5), which is exposed to the solvent at neutral pH and is localized within the EF loop, establishes a hydrogen bond with S116 at acidic pH (Qin et al., 1998). Furthermore, it is probable that the EF loop functions to regulate access to the b-barrel, while the Tanford transition is anticipated to modulate ligand binding to β-lg (Qin et al., 1999). In an energetic study, it was demonstrated that the presence of closed and open states corresponds to the protonation and deprotonation of E89, respectively; however, the conformational transition involving the opening and closing of the EF loop was not observed by the researchers. Subsequently, Goto et al. employed the dimeric β-lg mutant A34C for NMR studies at neutral pH to investigate the conformational change from an open to a closed EF loop. Due to the monomer-dimer equilibrium of wild-type β-lg causing substantial signal broadening, which hindered NMR measurements, a covalent dimeric A34C mutant was utilized (Sakurai and Goto, 2006). Their findings indicate that the Tanford transition can only take place through a conformational shift between the EF and GH loops before the transition of from an open to closed state, utilizing the dimeric β-lg mutant A34C. The movement of the EF loop was observed to occur slowly over milliseconds or rapidly within the micro-to-millisecond range. These earlier investigations provide vital insights, suggesting that the dimeric state serves as a useful model for examining this structural

phenomenon. The primary structural alteration of the protein is the opening of the calyx's interior above a pH of 7.5, a change attributed to the displacement of the EF loop (Qin et al., 1998). It is believed that the Tanford transition is initiated by the protonation of this residue. Both the Tanford transition and the opening of the EF loop, which is closed below a pH of 6.2 and opens above a pH of 7.1, result in the expansion of the protein molecule's volume. As a consequence, the carboxyl group of Glu89, previously buried with an unusually high pKa value, becomes accessible to the solvent (Kontopidis et al., 2004).

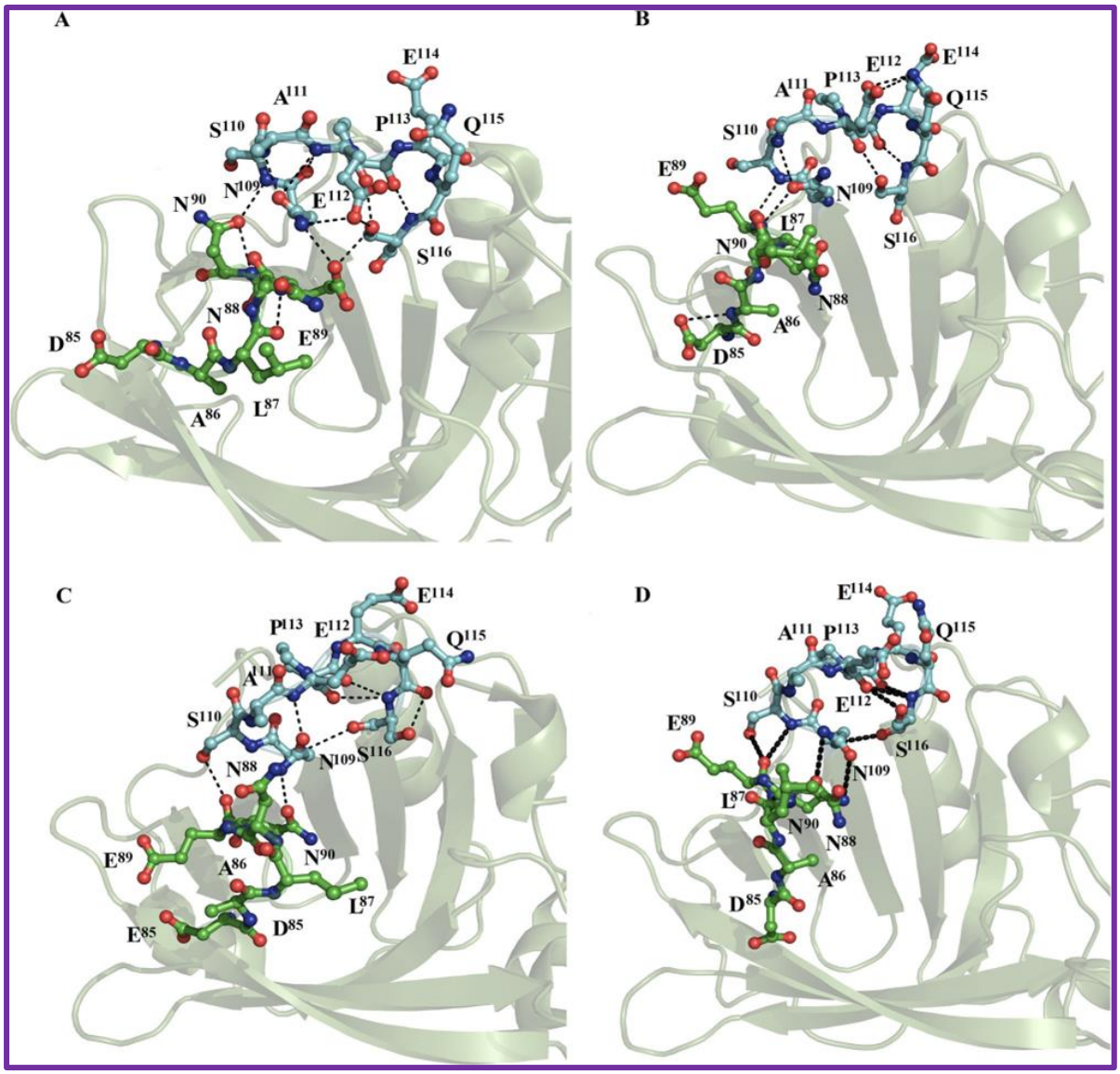

Figure 24: Crystallographic structures of β-lg were solved at different pH levels: 6.2, 7.1, 7.5, and 8.2. The structures at pH 6.2 (A), 7.1 (B), 7.5 (C), and 8.2 (D) show differences that explain the Tanford transition. This transition occurs through conformational changes between the EF and GH loops, represented by green ball-and-stick models. The figures were created using Pymol (DeLano, 2002). (Adapted from Bello, 2022).

1.12.8.2. The effect of Heat and Pressure on Bovine β-lactoglobulin (β-lg)

The structure of bovine β-lactoglobulin changes when the pH or temperature is altered. The naturally occurring form of β-lactoglobulin in milk is a stable dimeric structure held together by noncovalent bonds. However, a small portion of the protein can also exist in less stable, unfolded states. Changes in temperature and other processing conditions can shift this equilibrium by breaking hydrogen bonds in the protein's network. The balance between the monomeric and dimeric forms of β-lactoglobulin is achieved at a pH of 2.5 and in the presence of 100 mM NaCl. Destabilization and partial unfolding of the protein's globular structure exposes residues of histidine, tyrosine, and tryptophan to the surrounding environment, making buried thiol groups more reactive, especially after heating. (Seo et al., 2010; Kuwata et al., 1999; Crowther et al., 2018; Kella and Kinsella, 1988). After undergoing brief and reversible conformational changes, intramolecular interactions break down, leading to the formation of a partially unfolded state known as the "molten globule state". This state is also formed during the refolding of β-lactoglobulin, which exposes the protein's buried hydrophobic core and thiol group **(**Judy and Kishore, 2019; Bhattacharjee et al., 2005). Initial conformational shifts can occur at temperatures as low as 40°C, but reaching the fully denatured state of β-lactoglobulin requires temperatures higher than 130°C, indicating a multistep process. The midpoint of transition between patterns of abrupt large-scale loss of spiral structural elements occurs around 65°C, depending on environmental conditions (Qi et al., 1997). The partially denatured β-lactoglobulin proteins are susceptible to thiol/disulfide exchange reactions, resulting in covalent aggregation, while non-covalent interactions play a minor role (Quevedo et al., 2019). Under conditions of low salt and neutral pH, a quantitative kinetic model has been observed to describe the irreversible aggregation of β-lactoglobulin due to thiol/disulfide exchange reactions at temperatures ranging from 60-75°C (Roefs and De Kruif, 1994), particularly when heated at those temperatures and then with increasing salt levels. This phenomenon is attributed to radical polymerization reactions involving initiation, propagation, and termination steps. These steps correspond to the exposure of a free sulfhydryl group, the exchange of a thiol for a disulfide, and the reaction of two reactive intermediates. Findings from studies conducted in test tube conditions have significantly contributed to our comprehension of the denaturation and aggregation of β-lactoglobulin. However, it is important to note that these conditions significantly differ from the complex environment in milk, which contains lipids, lactose, and other proteins.

β-lactoglobulin (β-lg) is more prone to pressure-induced changes compared to other major whey proteins. This may be attributed to its relatively inefficient packing, characterized by a large solvent-exposed hydrophobic pocket and a lower number of disulfide bonds (two versus four in proteins of similar size, such as α-lactalbumin). Research suggests that bovine β-lg experiences a reduced molar volume at pressures as low as 10 MPa, possibly due to the contraction of its calyx (Hinnenkamp, 2020). Multiple studies have indicated that β-lg becomes more susceptible to enzymatic cleavage under pressure, likely due to pressure-induced conformational changes (Carullo et al., 2020). The tertiary and quaternary structure of β-lg is irreversibly altered by pressures greater than 300 MPa. Moreover, exposure to pressures as high as 900 MPa at neutral pH results in the formation of monomers and subsequent aggregation, with only minor irreversible effects on its tertiary structure as observed through CD and fluorescence spectroscopy (Edwards and Jameson, 2020).

1.12.8.3. Effect of Osmolytes on Bovine β-lactoglobulin (β-lg)

The majority of osmotically active solutes, known as osmolytes or osmoprotectants, are small organic molecules that cells and organisms accumulate to protect against internal or external osmotic stresses, including high concentrations of protein denaturants, freezing, dehydration, temperature fluctuations, variable pH, and high salinity (Yancey and Somero, 1979). These osmolytes are classified into two categories: free amino acids and their derivatives (proline, taurine, and β-alanine), and polyhydric alcohols (polyols), such as trehalose, glycerol, and sucrose. Organic osmolytes, such as sugars and polyols, play a significant role in stress prevention by stabilizing macromolecules and functioning as protein stabilizers, affecting proteins' thermodynamic stability in the face of chemical or thermal denaturation (Sharma et al., 2021). Natural osmolytes actively participate in the folding of proteins and serve as osmoprotectants. Comparative studies have demonstrated that certain osmolytes, like glycine, N-methylglycine (sarcosine), N-trimethylglycine (betaine), trimethylamine N-oxide (TMAO), and myo-inositol, can double protein stability (Rabbani and Choi, 2018). Sarcosine, betaine, and TMAO interact negatively with the unfolded state as protective osmolytes, imparting relative stability to the folded state.

1.12.8.4. Effect of Metal Ions on Bovine β-lactoglobulin (β-lg)

The denaturation of β-lactoglobulin (β-lg) is a complex process influenced by a variety of metal ions. Specifically, the presence of ionic calcium has been found to play a pivotal role in the denaturation and aggregation of β-lg, with significant research conducted on this topic

(Mulvihill and Donovan, 1987; Britten et al., 1988; De Wit, 1990; Anema and McKenna, 1996; Changani et al., 1997; Simmons et al., 2007; Petit et al., 2011). Furthermore, the presence of multiple metal ions in a β-lg solution has been observed to promote the growth of protein aggregates (Verheul et al., 1998; Allen and Smith, 2001; Schmitt et al., 2007) and result in surface fouling (De Wit, 1990; Relkin and Mulvihill, 1996; Simmons et al., 2007) by neutralizing the protein surface charge and subsequently reducing Coulombic repulsion. Researchers have delved into the molecular basis of the influence of Cu^{2+} and Zn^{2+} ions on the thermal aggregation processes of β-lactoglobulin using a range of advanced techniques. In particular, Raman spectroscopy has proven to be a valuable tool in identifying the diverse effects induced by these two metals at a molecular level, including changes in the protonation state of histidine, conformation of disulfide bridges, and microenvironment of aromatic residues. This has shed light on the critical importance of the distribution of protein charge during the aggregation process (Navarra et al., 2014).

1.12.8.5. Interactions of Nanoparticles on Bovine β-lactoglobulin (β-lg)

The unique properties and applications of nanoparticles are derived from their significant surface area relative to their small size, which leads to distinct behaviors compared to bulk materials. One intriguing aspect is the impact of nanoparticles on protein folding and aggregation, which presents both potentially beneficial applications and concerns for human health and the environment. Therefore, it is imperative for us to gain a comprehensive understanding of how nanoparticles affect essential biological processes, such as protein folding. It is worth noting that while the binding of proteins to planar surfaces often results in notable changes in their secondary structure, the high curvature of nanoparticles may offer a supportive environment for proteins to maintain their original structure. However, in-depth studies involving a variety of nanoparticle surfaces and proteins indicate that some level of disturbance to protein structure still occurs, albeit to varying extents. This demonstrates the nuanced and complex relationship between nanoparticles and proteins, highlighting the need for further exploration and understanding.

The kinetics of lysozyme or β-lg unfolding upon adsorption onto silica nanoparticles indicate a rapid conformational change at both secondary and tertiary structure levels (Shang et al., 2007; Wu and Narsimhan,2008). Studies have shown that the adsorption of proteins onto nanoparticles leads to a loss of α-helical content, often accompanied by an increase in β-sheet content (Vertegel et al., 2004). Due to their minute size, nanoparticles can permeate nearly all

bodily tissues, including the blood-brain barrier (Chopra et al., 2008). Consequently, there is potential for nanoparticles to serve as agents for controlling neurodegenerative amyloid diseases like Alzheimer's by inhibiting fibrillogenesis or disaggregating amyloid fibrils (Triulzi et al., 2008). A deeper understanding of the interactions between nanoparticles and amyloid proteins may contribute to unraveling the molecular mechanisms of fibril formation, an area that remains elusive. However, the growing use of nanoparticles in medical applications has raised concerns regarding their potential toxicity (Nie et al., 2007; Marcato and Durán, 2008; McBain et al.,2008; De Jong and Borm, 2008).

Nanoparticles measuring less than 100 nm were fabricated from β-lactoglobulin (β-lg) using a desolvation method and glutaraldehyde for cross-linking, resulting in a narrow size distribution. By preheating the β-lg solution to 60 °C and adjusting the pH to 9.0, nanoparticles of 59 ± 5 nm were achieved with improved uniformity. There is potential to utilize thermally modified β-lg for creating co-assembled nano vehicles for delivering EGCG, serving as a model system for the delivery of polyphenols using heat-modified proteins (Shpigelman et al., 2010). The resulting nano-complexes provided better protection to the vitamin against degradation than β-lg alone, and their stability was significantly better than that of unprotected vitamins dispersed in water **(**Ron et al., 2010). Core-shell nanoparticles of chitosan-coated with β-lg were suggested for delivering nutraceuticals (Chen and Subirade, 2005). Nanosized amine-functionalized KIT-6 [n-PrNH2-KIT-6], which has an average pore diameter of around 6.5 nm, when interacting with β-lactoglobulin B (β-lg-B) with a hydrodynamic radius of 2 nm, causes alterations in the secondary and tertiary structure of this protein. This result also demonstrates the immobilization of this protein onto amine-functionalized mesoporous silica nanoparticles (Falahati et al., 2012).

The research aimed to investigate the impact of neutral cosolvents on the formation and characteristics of biopolymer nanoparticles formed through the thermal treatment of protein-polysaccharide complexes. These biopolymer particles were created by heating an aqueous solution containing a globular protein (β-lg) and an anionic polysaccharide (beet pectin) above the denaturation temperature of the protein (Tm) under pH conditions that enabled the formation of electrostatic complexes (at pH 5). The study examined how two neutral cosolvents (glycerol and sorbitol) affected the self-association of β-lg and the formation of β-lg-pectin complexes under various solution pH levels (ranging from 3 to 7) and temperatures (ranging from 30 to 95 °C). The results showed that the presence of sorbitol favored the folded state of β-lg over the unfolded state more than glycerol (Chanasattru et al., 2009). Researchers have

demonstrated that under specific conditions, β-lg can form nano-complexes with FA (folic acid), which results in changes to the physicochemical properties of both FA and β-lg. These nano-complexes can be utilized for delivering FA in clear beverages with minimal impact on the protein's sensitivity to proteolysis (Pérez et al., 2014). It has been reported that alterations in the secondary and tertiary structure of β-lg occur when it is adsorbed onto nanoparticle surfaces, under varying surface concentrations, ionic strength, temperature, pH, and TFE and DTT concentrations (Wu and Narsimhan,2008). An antibacterial Cu-β-lg nanocomposite is synthesized through the interaction of the free thiol of β-lg and copper ion, causing N-H bending of amide II of this protein (Sardar et al., 2016). The subjection of β-lg to AuNPs at 75 °C yields smaller ragged aggregates. Results indicate that GNPs have the ability to hinder the formation of amyloid fibrillar aggregates of β-lg in a concentration-dependent manner, potentially aiding the refolding into a native-like structure. AgNPs are therefore serving as nano-chaperones to inhibit protein aggregation (Sardar et al., 2014).

1.12.8.6. Effect of Chemical Denaturants and Surfactants on Bovine β-lactoglobulin (β-lg)

A variety of chemical substances can be used to denature proteins. Common denaturants include urea, guanidinium hydrochloride (Gdn.HCl), methanol, ethanol, isopropanol, acetone, dioxane, and dimethylformamide (DMF), which are utilized in protein denaturation studies across different fields. Surfactants also act as denaturants and interact with proteins through various mechanisms depending on their concentrations. In studies on denaturation-renaturation kinetics from different structural perspectives, the protein β-lg has been a subject of interest. Surfactants (anionic, cationic, and non-ionic) interact with bovine β-lg and modulate its heat-induced aggregation (Viseu et al., 2004; Viseu et al., 2007; Magdassi et al., 1996; Waninge et al., 1998; Hansted et al., 2011). Research on the unfolding and refolding of β-lg using was conducted monoclonal antibodies as a probe (Hattori et al. 1933), provides insight into its complete refolding process. Additionally, to identify the unfolding intermediates of β-lg, denaturation in the presence of urea and Gdn.HCl was studied at varying pH using spectroscopic techniques (D'Alfonso et al., 2002). In 2005, D'Alfonso et al. conducted a characterization of the non-native α-helical intermediates in porcine β-lg. Subsequently, The Gdn.HCl-induced unfolding intermediate of bovine β-lg A at pH 2 has been reported to have an increased α-helical structure (Dar et al., 2007). Current literature denotes urea as a more potent destabilizing agent compared to Gdn.HCl is attributed to its capability to form hydrogen bonds with the protein backbone (Lim et al., 2009). Additionally, the denaturant 2,2,2-

trifluoroethanol (TFE) has been evidenced to induce non-native α-helical structure formation, contrary to the prevalent supposition of native-like secondary structures in intermediates (Hamada and Goto, 1997). Uversky et al. (1997) documented the occurrence of two-fold transitions, encompassing the disruption of rigid tertiary structure and subsequent expansion of the helical conformation, instigated by methanol, ethanol, isopropanol, DMF, and dioxane. Intriguingly, the conformational transition stimulated by alcohols suggests a correlation with the dielectric properties of the selected solvents (Babu et al., 2001). The study of β-lg interaction with SDS and other surfactants indicates significant conformational changes dependent on concentration (Jones and Wilkinson, 1976; Damon and Kresheck, 1982). Wahlgren and Arnebrant (1991) demonstrated the effects of surfactants on surface-adsorbed proteins and adsorption from protein/surfactant mixtures. Dickinson and Hong (1994) examined the surface coverage of β-lg at the oil-water interface with various emulsifiers. Maulik et al. (1998) extensively investigated the binding studies of Cetyltrimethylammonium bromide (CTAB) and SDS. Roth et al. (2000) revealed the interfacial shear rheology of adsorbed β-lg films at temperatures ranging from 20-90ºC and varying pH and ionic strength. Kerstens et al. (2006) demonstrated the competitive adsorption of proteins and surfactants in emulsions and the effect of emulsion droplets on the rheology of heat-set protein gels. Hence, conformational transitions induced by prominent denaturants to recently used surfactants have been reported in the last few decades (Viseu et al., 2007).

1.12.8.7. The Effect of Anti-oxidant on Bovine β-lactoglobulin (β-lg)

An antioxidant is a compound that impedes the oxidation of other molecules. Oxidation is a chemical process that generates free radicals, initiating cascading reactions that may harm cells. Antioxidants, such as thiols or ascorbic acid (Vitamin C), halt these cascading reactions. The term ‘antioxidant’ encompasses two primary categories of substances: industrial chemicals added to products to prevent oxidation and natural chemicals present in foods and bodily tissues that purportedly yield beneficial health effects.

To maintain a balanced oxidative state, both plants and animals possess intricate, overlapping antioxidant systems, including internally synthesized glutathione and enzymes (e.g., catalase and superoxide dismutase), as well as dietary antioxidants like Vitamin A, Vitamin C, and Vitamin E. Furthermore, the fibrillation of β-lg is highly deleterious. Curcumin, an antioxidant, inhibits the fibrillation of numerous proteins (Ahmad and Lapidus, 2012; Gautam et al., 2014; Lin et al., 2013) and also suppresses the fibrillation of β-lg (Mazaheri et al., 2015). In addition,

ferulic acid, a natural compound, serves as another antioxidant that functions to forestall neurodegenerative diseases, such as Alzheimer's disease (Sgarbossa et al., 2015). Research indicates that ferulic acid impedes the fibrillation of proteins (Jayamani et al., 2014).

1.12.8.8. The Effect of Solvent on Bovine β-lactoglobulin (β-lg)

The aggregation of proteins can occur in response to various stresses, including changes in solvent conditions. Research has demonstrated that the addition of alcohol can trigger protein aggregation. The impact of alcohol on the structural changes of β-lg in dilute solutions (in the micromolar range) has been extensively studied using spectroscopic methods (Tanford et al., 1960; Towsend et al., 1967; Dufour et al., 1990, 1993, 1994). Across a broad pH range, the protein tends to adopt an α-helical conformation when the solvent's dielectric constant is low (Dufour et al., 1990, 1993, 1994). The reversible transition of β-strand to α-helix induced by alcohol involves at least three conformational states: native protein, an intermediate state, and an α-helix-shaped β-lg (Dufour et al., 1994). The intermediate state observed in 20% (v: v) ethanol, using fluorescence and circular dichroism measurements, was identified as a 'molten globule' state (Dufour et al., 1990, 1994). The β-strand to α-helix transition of β-lg at high protein concentration (in the millimolar range) in water: ethanol solutions has also been investigated using infrared spectroscopy (Dufour et al., 1994). A millimolar solution of β-lg in 50% (v: v) ethanol exhibits a higher α-helix content at pH 8 than at pH 7. Furthermore, β-lg may aggregate and gel at room temperature in hydro-alcoholic solutions, depending on the pH and the protein concentration (Dufour et al., 1994). The aggregation and gelation properties of β-lactoglobulin (β-lg), a globular protein found in milk, were studied in hydro-ethanolic solutions (50:50% (v: v)) at room temperature. Alcohol-induced aggregation of β-lg was characterized by the formation of intermolecular hydrogen-bonded β-sheet structures. Small-angle neutron scattering indicated that the aggregate structures in the final gels were similar at pH 7, 8, and 9 (Renard et al., 1999).

Aside from alcohol, dimethyl sulfoxide (DMSO), renowned as one of the most flexible solvents in biological science, is utilized to reduce protein solubility, thereby inducing precipitation and crystallization (Jacob et al., 1971). Arakawa et al. (2007) investigated the interactions of DMSO with β-lactoglobulin and noted that at low DMSO concentrations, native β-lg exhibited negative preferential DMSO binding or preferential hydration. However, as the DMSO concentration increased, the preferential interaction shifted from preferential hydration to preferential DMSO binding, resulting in structural alterations and protein unfolding. Recently,

Maity et al. (2016) demonstrated that under pH 10.5, the folding and self-assembly of β-lactoglobulin from a reversible unfolded state occurred in the presence of methanol, 2-propanol, t-butanol, and 2,2,2-trifluoroethanol (TFE). Their findings revealed that exposure to an apolar environment induced the aggregation of protein molecules. Specifically, methanol and TFE induced aggregation through the α-helical structure, while isopropanol and t-butanol favored the formation of the β-structure, leading to aggregation at higher concentrations.

1.12.8.9. Effect of Co-solvents on Bovine β-lactoglobulin (β-lg)

A cosolvent is a substance that allows substances that don't normally mix to become mixable by adding them to the mixture. The cosolvent increases the solvent power of the main substance in the mixture. Protein stability can be improved by using cosolvents such as trehalose, sucrose, glycerol, stachyose, and glucose. For example, trehalose can significantly enhance the stability of β-lg against chemical denaturation by guanidinium chloride (Gdn.HCl) (D'Alfonso et al., 2003). When cosolvents like sorbitol, glycerol, and sucrose are added to β-lg, the thermodynamic properties of the proteins change, leading to improved thermal stability. This is due to the preferential hydration of the protein, which causes the exclusion of cosolvent molecules from the protein surface (Anuradha and Prakash, 2008). According to Maity et al. (2016), β-lactoglobulin can undergo folding and self-assembly from a reversible unfolded state at pH 10.5 in the presence of methanol, 2-propanol, t-butanol, and 2,2,2-trifluoroethanol (TFE) (Maity et al., 2016). The degree of secondary and tertiary structure formation follows this order: methanol < 2-propanol < t-butanol < TFE. In the apolar environment of TFE, the exposure of the hydrophobic core of the protein molecules leads to the formation of a higher-order intermolecular cluster. Isopropanol and t-butanol promote the creation of the β-structure, resulting in aggregation at higher concentrations, whereas methanol and TFE induce aggregation through the α-helical structure. The addition of cosolvents such as sorbitol, glycerol, and sucrose to β-lg leads to the formation of hydrogen bonds, resulting in preferential hydration of the protein. This leads to the exclusion of cosolvent molecules from the protein surface and alters the thermodynamic properties of the proteins, resulting in longer thermal stability.

1.12.9. The Effect of Chemical Modification on Bovine β-lactoglobulin (β-lg)

A chemical modification involves chemically reacting a protein with chemical reagents. This process covalently grafts specific amino acid residue side chains with modifying agents of interest. The goal of chemical modification is to understand the relative reactivity of side chain

groups, quantify amino acids individually, and develop various affinity reagents, mechanism-based reagents for pharmaceutical use, cross-linking reagents, bioprosthetic techniques, blocking reagents for peptide synthesis, and cleavage reagents **(**Feeney, 1987). According to Crane (1994), chemical modifications are extensively used in two applications: (a) identifying important groups involved in binding and catalytic sites, and (b) structural analysis (264). In addition to primary structural analysis, the contribution of specific amino acid residues to tertiary and secondary structural components has also been studied. Several chemical transformations available for selective modification of proteins include the studies of protein-protein interaction, protein-ligand interactions, processing of bio-conjugates, and protein microarrays (Baslé et al., 2010). Side chain residues of asparagine, cysteine, glutamine, histidine, lysine, tryptophan, and tyrosine have been chemically modified in different proteins for various purposes. β-lg, a major whey protein abundant in cow's milk, has been extensively studied in this regard in recent years. Modifications of β-lg not only serve the purpose of structural biology as a model protein but also have a significant impact on the field of protein chemistry. The different modifying agents for β-lg's modification have been briefly discussed below.

1.12.9.1. Phosphorylation

Phosphorylation of bovine β-lactoglobulin (β-lg) can occur with the assistance of phosphorus oxychloride or phosphorus pentoxide in phosphoric acid under alkaline pH conditions. This process targets the amino nitrogen groups of amino acids such as lysine, as well as the hydroxyl oxygen groups, such as those in serine. It has been suggested that phosphate groups can also attach to lysine and histidine residues based on ^{31}P NMR spectral data (Woo et al., 1982). Phosphorylation significantly affects the functional properties, such as emulsifying and gelling properties, of β-lg (Woo and Richardson,1983). Similar chemical modifications were later carried out under milder conditions, which had the same impact on the secondary structure and solubility of β-lg (Sitohy et al., 1995). Various efforts have been made to further enhance the functional properties of milk proteins like β-lg for industrial food applications.

1.12.9.2. Glycosylation

The process of glycosylation is a well-established phenomenon within the realm of chemical modification of β-lactoglobulin (β-lg). It involves the covalent attachment of carbohydrates, such as maltose, lactose, glucose, and gluconic acid, to β-lg, thereby inducing significant alterations in its physicochemical properties. This modification impacts crucial traits including

hydrophobicity, viscosity, and fluorescence. Notably, synthetic glycoproteins have displayed heightened solubility and heat stability under iso-electric pH and reduced ionic strength conditions, commensurate with the degree of glycosylation. Furthermore, consequential alterations have been observed in the association behavior governing the multi-step denaturation and aggregation processes of β-lg, consequent to glycation with lactose, whether in a powdered state or in aqueous solution (Waniska and Kinsella, 1984; Kitabatake et al., 1985). Researchers have found that subjecting milk protein to mild heat treatment leads to the binding of lactose to β-lg through the Maillard reaction (Maubois et al., 1995; Burr et al., 1996; Leonil et al., 1997). After glycosylation, the dimer interface of β-lg, involving the AB loop, GH loop, P-strand 'I', and helix part, was characterized using immunochemical methods (Morgan et al., 1999a and b). Glycosylation was observed to reduce the antigenicity and immunogenicity of β-lg (Hattori et al., 2000; Kobayashi et al., 2001; Bu et al., 2010). Recent work suggests that the modification of the lysine group of β-lg by lactose likely affects the enzymatic activity of β-galactosidase, highlighting the importance of lysine ε-amino groups in its ability to activate the enzyme (Del Moral-Ramirez et al., 2008).

1.12.9.3. Free Thiol modification

The unbound thiol group of bovine β-lactoglobulin at Cys121 on the βH strand is completely shielded beneath the C-terminal α-helix. This thiol group has been the focus of studies in both its native and denatured states using a variety of cysteine-specific reagents, including Dithioerithreotol (DTT), 5,5-dithiobis (2-nitrobenzoic acid) (DTNB), 4,4-dithiopyridine, 2-mercaptoethanol (MCE), mercapto propanoic acid, and other maleimide derivatives tagged with fluorescent markers, for the purpose of gaining insights into its structure (Cupo and Pace, 1983; Kella and Kinsella, 1988; Apenten, 1998; Burova et al., 1998; Narayan and Berliner, 1998). Due to its high susceptibility to participating in pathways leading to the formation of disulfide-linked oligomers and aggregates in heat-treated β-lactoglobulin, various thiol-modifying agents have been utilized to investigate its specific role in the aggregation process and to understand the conformation and stability of the pristine protein (Sakai et al., 2000).

1.12.9.4. Alkylation/Acylation

Protein research has transitioned from a predominant focus on the conformational aspects of proteins to an examination of their functional characteristics subsequent to the modification of side chain residues. This interdisciplinary exploration entails collaboration between chemists and biologists, with an emphasis on investigating the structure-activity relationship (SAR) of

small proteins engaging with ligands or small organic molecules. Recent advancements in this domain have facilitated the elucidation of nuanced attributes of β-lg molecules. The chemical or enzymatic modification of β-lg has demonstrated the capacity to induce conformational changes and alter binding properties. Research findings indicate that N-methyllysyl-β-lg and N-ethyllysyl-β-lg, derived through esterification or reductive alkylation, distinctly influence the binding affinity of several terpenes structurally akin to retinol (Dufour and Haertle, 1990).

The adsorption behavior of lysine-modified β-lg through acetylation and succinylation has been extensively studied at the air-water interface and alumina-water interface (Song and Damodaran, 1991; Bhaduri and Das, 1994). These studies suggest that the modified electrostatic forces play a key role in the aggregation and dissociation properties of β-lg. The aggregation behavior was also investigated in another protein system, Concanavalin A, after succinylation. The succinyl derivatives were found to be less likely to participate in the aggregation process and fibril formation (Vetri and Militello, 2005). Results from other researchers also indicated that the succinylation of lysine residues provides indirect evidence that the £-amino groups of specific lysine residues are likely to be the binding sites of β-lg in the activation of β-galactosidase activity (Del Moral-Ramirez et al., 2008). Enzymatic modification has shown a significant impact on biophysical processes. Modification of lysines and glutamines of β-lg with transglutaminase from Streptoverticillium mobaraense (MTgase) can be utilized for various physico-chemical processes such as surface tension, viscosity, etc. (Nieuwenhuizen et al., 2004; Partschefeld et al., 2007).

Previously, the importance of chemical modifications has been associated with improvements in the design of therapeutic agents (Shaw, 1970). Recent reports suggest that modified β-lg, through acetylation, succinylation, and/or hydroxy pthalylation in the lysine residues, exhibit significant antiviral activities (Bon et al., 1999; Lefebvre and Subirade, 2000). Additionally, fine-stranded, transparent gels were formed at a pH away from the isoelectric point and low ionic strength (Kavanagh et al., 2000; Lefebvre and Subirade, 2000; Arnaudov et al., 2003). An increase in β-lg concentration results in increased hardness of the gel. Dynamic Light Scattering (DLS), Nuclear Magnetic Resonance (NMR), and Atomic Force Microscopy (AFM) studies have established an apparent critical concentration of 2.5% (wt/V) (Arnaudov et al., 2003).

1.12.9.5. The Maillard Reaction

When proteins are exposed to heat in the presence of carbonyl compounds, such as reducing sugars, a complex chemical reaction known as the Maillard reaction occurs (Münch et al.,1999). In this reaction, a reducing sugar interacts with the amino group of lysine or the N-terminal group of a protein, leading to the formation of Amadori or Heyn's rearrangement products. This process, initially described by Hodge in 1953 (Hodge,1953), progresses into advanced stages where the Amadori (1-amino-1-deoxy-2-ketose) and Heyn's products go through degradation via a variety of pathways, depending on the specific conditions of the reaction. These pathways may involve the formation of Schiff bases, Strecker degradation, or fission products, ultimately resulting in the formation of copolymers, brown nitrogenous polymers, and melanoidins (Mossine et al., 1994; Röper et al., 1983).

1.12.9.6. Methionine modification

Methionine (Met) is one of the amino acids most susceptible to oxidation. It can undergo various processes, such as UV exposure, metal-catalyzed reactions, and hydrogen peroxide treatment, leading to the formation of methionine sulfoxide or sulfone derivatives. Maity et al. investigated the impact of t-butyl hydroperoxide (tBHP) oxidation on the structure, compactness, and fibrillation tendency of β-lg at physiological pH. The selective oxidation of Met induced by t-BHP alters the structural orientation of β-lg, affecting the protein's internal polarity and reducing its susceptibility to thermal instability. This results in the introduction of internal strain (Maity et al., 2021).

1.12.9.7. Esterification

As the quantity of ionizable carboxyl groups diminishes, proteins undergoing esterification acquire an increased positive charge. Moderate esterification of β-lg leads to subtle alterations in both its secondary and tertiary structures, resulting in the unfolding of the β-lg molecule and the subsequent cleavage of the peptide link. The introduction of 22 additional pepsin cleavage sites through esterification renders esterified β-lg more vulnerable to hydrolysis by pepsin (Chobert, 2012). Structural modifications reveal 14 pepsin-specific cleavage sites, with pepsin identifying eight of these as esterified carboxylates. According to M.I. Halpin, methyl, ethyl, and butyl esters of β-lg exhibit heightened surface activity and increased hydrophobic probe binding activity, with methyl esters demonstrating the most pronounced effect (Halpin and Richardson,1985). The positive charge of protein molecules enables interaction with viral proteins or DNA, thereby influencing viral transcription, translation, replication, and

ultimately, contagiousness. It is noteworthy that at a pH of 7, highly esterified β-lg evidences DNA-binding capabilities akin to those of natural basic proteins such as histones and lysozymes. Esterified β-lg exhibits enhanced antiviral activity against the HSV-1 virus, influenza virus A subtype H1N1, and avian influenza A virus (H5N1), while esterified β-lg peptic hydrolyzates also demonstrate antiviral properties **(**Sitohy et al., 2007).

1.12.10. Modification on Bovine β-lactoglobulin (β-lg) by Physical methods

The molecular structure and stability of β-lg may be subject to alteration due to various physical factors, including electrolysis, high hydrostatic pressure, UV, gamma, and ultrasound radiation. Upon exposure to the sonication method, the β-lg forms demonstrate enhanced hydrophobic surfaces compared to their native conformation, rendering them more conducive to phenol oxidase cross-linking. Notably, the capacity of β-lg to bind to IgE remains minimally influenced by sonication (Zhang et al., 2021). Furthermore, ultrasound-mediated glycation in the Maillard reaction has exhibited augmented reducing power, a heightened ferrous ion-chelating activity, and radical scavenging capability (Stanic-Vucinic et al., 2013).

UV exposure disrupts the ordered structure of β-lg, consequently inducing changes in molecule size distribution and thereby modifying the antigenicity of β-lg and its regulatory influence on immunoglobulin generation. After a 24-hour UV light exposure, it was discerned that 18.8% of the protein had undergone denaturation, with some portion experiencing aggregation, resulting in an alteration of the protein's secondary structure. Additionally, Jia et al. (2019) have reported a reduction in the overall count of sulfhydryl groups during the photo-oxidation process coupled with a concurrent increase in exposed sulfhydryl groups.

The impact of γ-irradiation on the secondary and tertiary structures of β-lg resembles that of mild thermal treatment, leading to increased agglomeration and reduced solubility. Exposure to γ-radiation up to 10 kGy decreased solubility and heightened the antigenicity of β-lg, without affecting its molecular-weight distribution (Kaddouri et al., 2008).

Under high hydrostatic pressure (HHP), β-lg aggregation resulted in the development of only dimers and trimers due to SH/S–S interaction (Reznikov et al., 2011). The thiol group, initially nestled within the native globule, exhibited increased reactivity following high-pressure denaturation of β-lg, attributed to its exposure on the protein surface. This led to enhanced hydrolysis of β-lg by various enzymes under increased hydrostatic pressure (Bamdad et al., 2017).

Application of high-intensity pulsed electric field (PEF) partially denatured and aggregated β-lg, leading to covalent cross-linking. This treatment enhanced β-lg's gelation rate and thermal stability by 4 to 5 °C (Perez and Pilosof, 2004).

Following electrolysis treatment, a noticeable reduction in the allergenic characteristics of β-lg was observed at the cathode, explained by the dislocation of allergenic peptides from the protein surface (Matsumoto,2011).

1.12.11. Enzymatic Modification

Enzymes play a critical role in facilitating modifications within physiological conditions with high specificity and minimal side effects. One notable enzyme, transglutaminase (TG), is responsible for catalyzing the cross-linking of proteins. TG mediates the transfer of an acyl group between the ε-amino group of lysine residues and the γ-carboxamide group of glutaminyl residues in proteins, leading to the formation of an iso-peptide bond. Excessive treatment with TG has been found to enhance the thermostability of β-lactoglobulin (β-lg), potentially due to the partial unfolding of the protein molecule and subsequent conformational rearrangement (Tang and Ma, 2007). The use of laccase in protein cross-linking relies on the presence of phenolic moieties in proteins, which are often limited in availability. Laccase induces irreversible intermolecular cross-links in β-lg and causes oxidative modifications, including the formation of dityrosine, fluorescent tryptophan oxidation products, and carbonyl derivatives of histidine, tryptophan, and methionine. These modifications result in protein molecules with heightened surface tension (Steffensen et al., 2008). Research conducted by Thalmann et al. suggests that only Agaricus bisporus tyrosinase, in the presence of a low molecular weight phenolic compound as a bridging agent between protein subunits, can effectively cross-link β-lg (Thalmann and Lötzbeyer, 2002). Moreover, enzymatic hydrolysis of β-lg under high hydrostatic pressure (HHP) yields a greater quantity of short bioactive peptides with potential antioxidant and anti-inflammatory effects (Bamdad et al., 2017).

1.12.12. Aggregation of Bovine β-lactoglobulin (β-lg)

Thermal aggregation represents a critical phenomenon within the realm of protein science and engineering, yet the precise mechanisms underpinning the formation of protein aggregates and their biological significance remain elusive. Unfolding and aggregation, two discrete processes, entail successive unimolecular reactions and a bimolecular second-order reaction, respectively. Influencing factors, including temperature, pH, protein concentration, and ionic strength, exert distinct effects on these reactions (Mounsey and O'kennedy, 2009). Particular

attention is directed towards proteins such as α-lactoglobulin and β-lactalbumin, prevalent in milk serum, which display susceptibility to temperatures ranging from 60 to 100 degrees Celsius. This thermal exposure results in denaturation, aggregation, and intramolecular reactions. During dairy processing, the heating process induces a conformational alteration in β-lactoglobulin. Furthermore, the partial unfolding of polypeptide chains contributes to the aggregation. Despite extensive research in this area, the absence of a clear physical depiction and a comprehensive understanding of the implicated mechanisms have led to the widespread reliance on heuristic approaches. Under ambient temperature and physiological pH conditions, β-lactoglobulin exists predominantly as a dimer, with noncovalently linked monomers. However, heightened temperatures prompt the dissociation of β-lactoglobulin into monomers, marking a requisite stage within the heat-induced aggregation mechanism. Subsequent to this, further heating (above 50°C) induces a conformational transformation in the protein, leading to the exposure of previously concealed hydrophobic groups and thiol groups. This state, recognized as the 'molten globule state' retains the native-like backbone secondary structure, within which hydrophobic interactions drive the aggregation of protein molecules. Roefs and de Kruif have postulated an analogous polymerization mechanism involving thiol catalysts for β-lactoglobulin when subjected to a temperature of 65°C under neutral pH and low ionic strength conditions. A progressive decline in the β-sheet structure was observed with escalating temperature, while a sudden loss of the helical conformation was detected near 65°C (Roefs and De Kruif, 1994).

In accordance with Jung et al. (2008), β-lg experiences partial denaturation and aggregation at temperatures exceeding 70ºC. In cases where the protein concentration falls below the critical gelation concentration, soluble aggregates form, whereas concentrations above this threshold result in the establishment of a continuous gel network (Jung et al., 2008). Noncovalent interactions assume increasing significance at temperatures surpassing 80ºC, with the aggregation process being governed by both disulfide bond interchange and hydrophobic interactions. The kinetics of protein denaturation/aggregation are contingent on several factors, including heating conditions, temperature, duration, chemical milieu, protein concentration, pH, ionic strength, as well as calcium and lactose concentrations. Experimental kinetics utilizing 1H NMR at 70°C suggest the unfolding of the folded form within minutes while ensuing aggregation and gel formation from the unfolded state represent protracted processes taking several hours.

Protein aggregation is a multifaceted process influenced by various factors, including protein concentration, temperature, and pH. Near the isoelectric point (IEP), the exchange frequency of disulfide bonds diminishes, thereby prompting electrostatic attractions and hydrophobic interactions to dominate the aggregation process (Krebs et al., 2009). Conversely, below the IEP (e.g., pH 2), the constrained reactivity of sulfhydryl groups inhibits covalent bond formation, leading to the predominance of noncovalent interactions like ionic, dipole, van der Waals, and hydrophobic interactions, culminating in aggregate formation. β-lg protein denaturation and aggregation follow a radical-addition polymerization reaction at nearly neutral pH, with the free thiol group of β-lg serving as the radical. The range of optimal pH for maximum aggregation rates has been documented to be between 4.3 and 4.8. Additionally, the folding of alkaline β-lg is contingent upon the presence of non-fluorinated alcohols such as MeOH, i-PrOH, t-BuOH, and a fluorinated alcohol, 2,2,2-trifluoroethanol (TFE). TFE, at lower concentrations, fosters intermolecular hydrogen bonding, while t-BuOH instigates secondary and tertiary structures. Both fluorinated and non-fluorinated alcohols expedite the formation of non-native secondary structures, contributing to protein self-assembly. Intriguingly, the introduction of TFE exclusively induces α-helical structure formation, consequently yielding β-lg aggregation (Maity et al., 2016).

Recombinant variants of a protein can be utilized to comprehend the effects of covalent and non-covalent interactions during aggregation and their influence on aggregation kinetics and resulting morphology (Hoppenreijs et al., 2023). Interactions involving intermolecular disulfide bonds (SS) disrupt the secondary structure, while intramolecular SS stabilizes it. Beta-sheets exhibit greater stability in acidic pH, attributable to carboxyl group protonation, and remain largely preserved under heating. However, intermolecular SS destabilizes β-sheets at both acidic and neutral pH, as well as α-helices. Unstable α-helices convert into intermolecular β-sheets. α-helices are less stable, and β-sheets are more stable at pH 3.5 compared to pH 7.0, with this transformation being augmented. The removal of intramolecular SS accelerates and intensifies conformation changes. Increasing the proportion of non-covalent interactions (either through cysteine removal or adjusting pH) augments the linear growth of aggregates. At pH 7.0, complete elimination of covalent association even leads to the transformation of worm-like aggregates into fibril structures, likely through alignment and entanglement (**Fig D**).

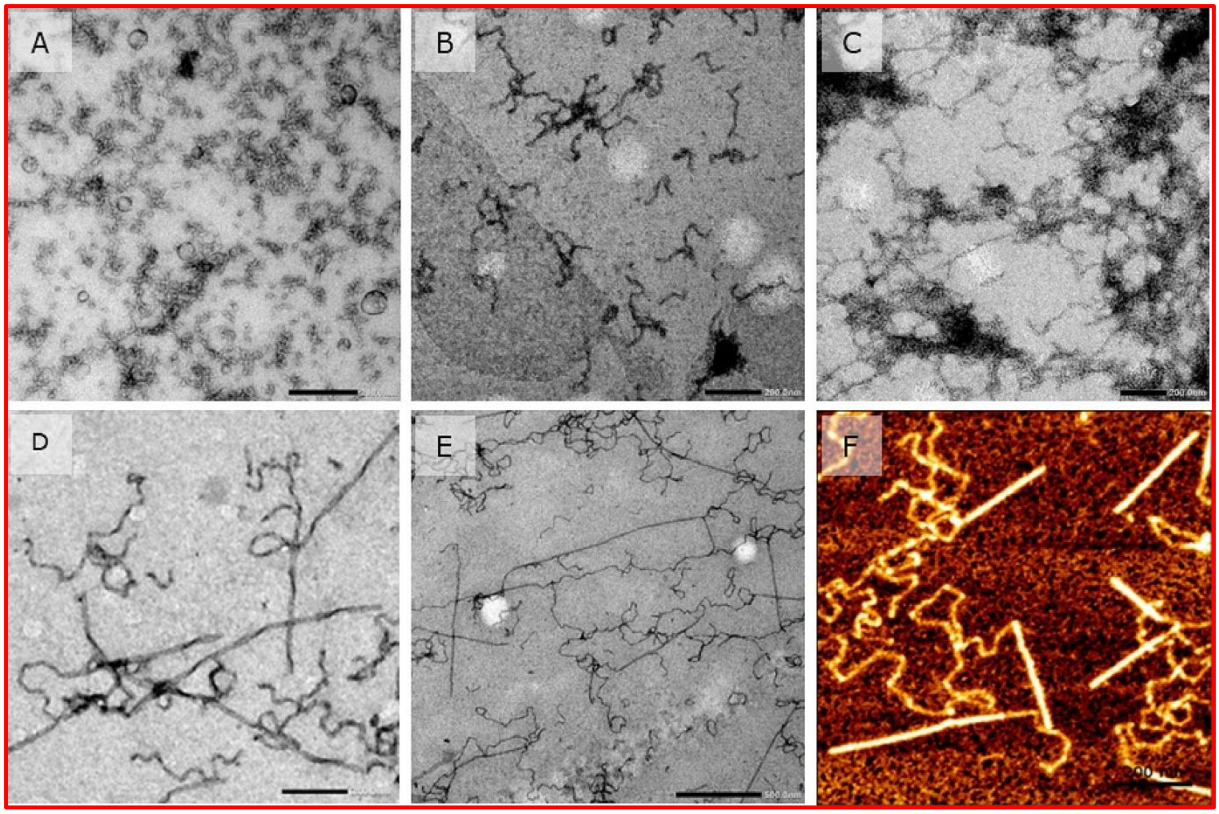

Figure 25: TEM images depict the aggregates of β-lg variants following heating at 80 °C for 24 hours at pH 7.0: (**A**) r β-lg (recombinant β-lactoglobulin), (**B**) r β-lg -SH (thiol), (**C**)r β-lg -SS (disulfide), (D&E) r β-lg -C (cysteine residues). Additionally, sample r β-lg -C was analyzed using AFM. The scale bar represents 200 nm for A–D and F, and 500 nm for E. (Adapted from Hoppenreijs et al., 2023**).**

1.12.13 General Mechanisms of Bovine β-lactoglobulin(β-lg) Aggregation

The forthcoming discourse will encapsulate the process by which engineered functional β-lg nanofibrils are generated through heat-induced elimination of covalent bonds at neutral pH. Additionally, the potential transferability of the function of cysteine residues in β-lg assembly to other proteins will be explored, particularly those implicated in the formation of pathogenic fibrils such as those associated with neurodegenerative diseases like Alzheimer's and Parkinson's, as well as natural functional fibrils like bacterial biofilms. A schematic mechanistic overview is delineated in (**Fig.26)**.

In the initial stages of heating (less than 5 hours at 80°C), intact β-lg formed worm-like aggregates. The removal of intramolecular SS bonds destabilized the secondary structures of BLG, increasing flexibility and accelerating the transition from α-helix to β-sheet. Additionally, the absence of the inner SS bond exposed amyloidogenic regions. A recent review by Mitra and Sarkar (Mitra and Sarkar,2022) concluded that the removal of

intramolecular SS bonds disrupts the structure and stimulates the pathogenic fibrillation of various proteins, including insulin (Li et al.,2012), superoxide dismutase (Chattopadhyay et al., 2008), amyloid β (Shivaprasad and Wetzel,2004), and α-synuclein (Jiang and Chang,2007). For globular proteins, Marinelli et al. (Marinelli et al.,2018) also suggested that oxidative stress induced by reactive oxygen species can cleave intramolecular SS bonds, causing destabilization and initiating pathogenic fibrillation. The same principle was observed in natural functional bacterial fibrils formed by CsgA (Balistreri et al.,2020): introducing an engineered intramolecular SS bond 'locked' the structure and hindered β-sheet formation, while its reduction led to amyloid formation similar to the wild-type within hours. While intramolecular SS bonds generally hinder fibril formation, there is no clear indication in the literature whether proteins with a low amount of these bonds would be a preferred choice for engineering fibrils.

The presence of intermolecular disulfide (SS) bonds has been observed to either promote or inhibit the formation of β-sheets, depending on the specific aggregation conditions. Notably, suppressing the formation of SS bonds in the cysteine mutants resulted in the formation of longer aggregates. The impact of intermolecular SS bonds on fibrillation is more subject to debate compared to intramolecular SS bonds. Interactions facilitated by intermolecular SS bonds allow for the close proximity of peptide chains, thereby stimulating oligomerization (Mitra and Sarkar,2022). This has been reported for proteins associated with amyloid disorders, such as prion proteins (Tompa et al., 2002) and transthyretin (Nakanishi et al., 2010**)**. It's worth noting that while the intensity or concentration of β-sheets is often used as a measure of fibrillation, it may not necessarily correspond to the shape of fibrillar aggregates.

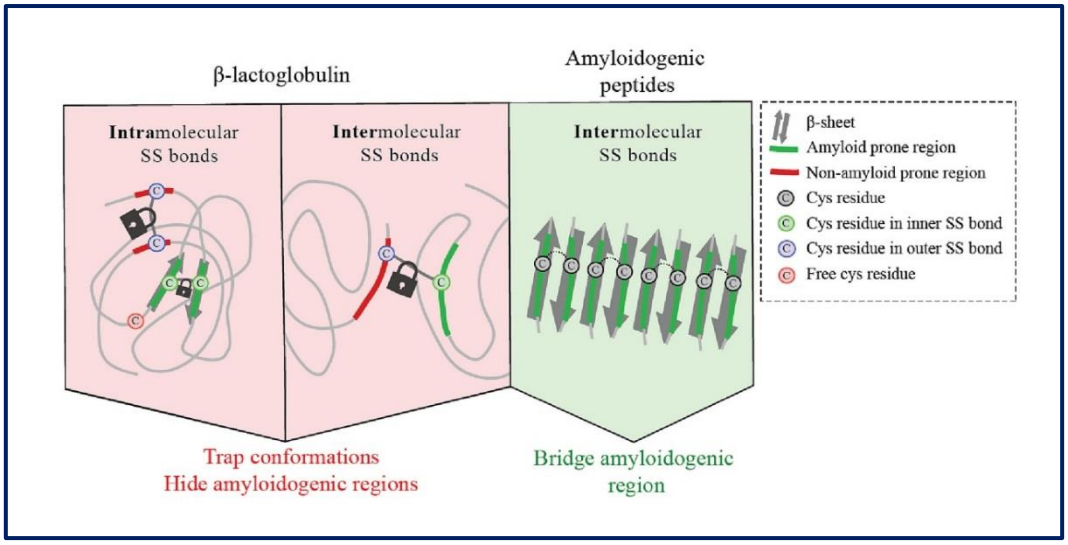

Figure 26: A scheme that succinctly details the essential role of disulfide (SS) bonds in the process of assembling into β-sheets.

1.12.14 Amyloid Fibrils of Bovine β-lactoglobulin (β-lg)

In its native state, it has been observed that β-lg predominantly forms a β-sheet structure (Hamada et al.,2009). Upon exposure to heat, β-lg has the ability to self-assemble into a wide range of supramolecular structures. Notably, when incubated below its isoelectric point (pH 5.1), β-lg forms fine-stranded gels containing amyloid fibrils (Bromley et al., 2005; Gosal et al., 2002). Furthermore, β-lg serves as a key model protein for investigating the self-assembly mechanism of amyloid fibrils (Hamada et al.,2009; Bromley et al., 2005; Hamley, 2007). Despite extensive research on the formation kinetics and morphology of β-lg amyloid fibrils, the complete elucidation of the secondary structure of these fibrils is still pending.

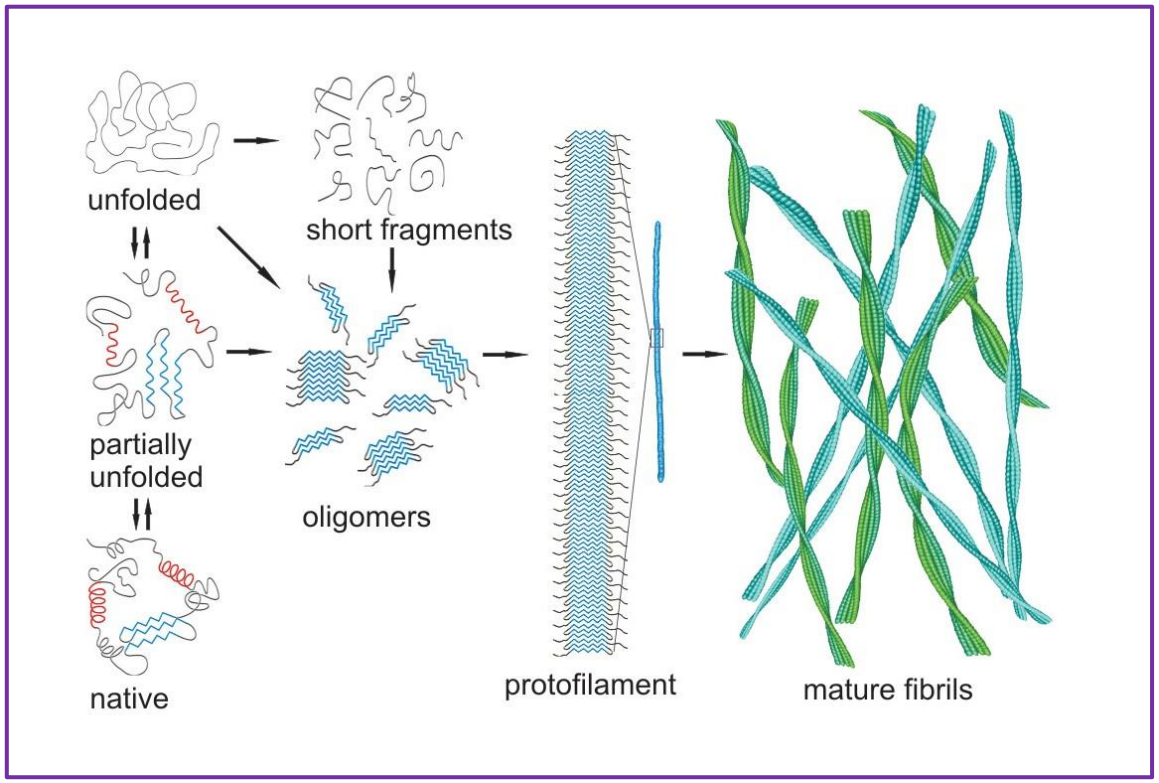

Figure 27: Schematic representation of the mechanism of conversion of globular protein into amyloid fibrils. (Adapted from Adamcik and Mezzenga, 2012).

1.12.15. Formation Mechanisms of Amyloid-Like Fibrils From β-lactoglobulin(β-lg)

The established model for amyloid fibril formation involves the assembly of oligomers into protofilaments, which can further aggregate into amyloid fibrils. Under normal conditions, native proteins like β-lg in solution exist in equilibrium with their partially unfolded state. This equilibrium can be shifted towards partially and completely unfolded states by altering conditions such as temperature and pH outside the physiological range. Partially unfolded proteins can refold into a cross-β-sheet secondary structure (Uversky and Fink, 2004), leading

to the linear growth of oligomers composed of hydrogen-bonded β-sheets orthogonal to the peptide backbone (Adamcik and Mezzenga, 2012). Additionally, oligomers can form through the hydrolysis of β-lg into short peptide fragments. Mass spectrometry has shown that β-lg fibrils formed at pH 2 upon heating are composed of peptide fragments, not intact β-lg monomers (Akkermans et al., 2008**)**. It has been demonstrated that this mechanism also applies to other proteins (Frare et al., 2004). The choice between partial unfolding or fragmentation appears to depend on the specific conditions used to promote fibrillation Figure 23 (Chiti and Dobson, 2006). After oligomers form in the nucleation step, the process of elongation into protofilaments occurs rapidly. Based on observations from atomic force microscopy (AFM) images, it has been suggested that short-range attractions, possibly of hydrophobic or Lennard-Jones type, drive the aggregation of protofilaments into mature fibrils (Bolisetty et al., 2011). Multi-stranded amyloid ribbons, consisting of 2 to 16 β-lg protofilaments, have been observed, all displaying a left-handed twist (Lara et al., 2011). The maximum conversion of monomers into amyloid fibrils upon heating β-lg at pH 2 ranges from 50% to 90%, depending on the protein concentration (vandenAkker et al., 2011).

1.12.16 Molecular Structure of Amyloid Fibrils of Bovine β-lactoglobulin (β-lg)

X-ray diffraction studies in the field of amyloid fibrils have provided valuable insights into their structural characteristics. It has been discovered that amyloid fibrils exhibit a distinctive cross-β core structure, characterized by the arrangement of β-strands. These β-strands are oriented perpendicular to the fibril axis, forming a continuous β-sheet along the axis. This structural arrangement is stabilized by extensive hydrogen bonding, as illustrated in Figure 24 (Chiti and Dobson, 2006; Fändrich et al., 2009; Tycko, 2004; Sawaya et al., 2007). It is noteworthy that the specific side-chain sequences play a crucial role in influencing the propensity of amyloid fibril formation (Wetzel et al., 2007).

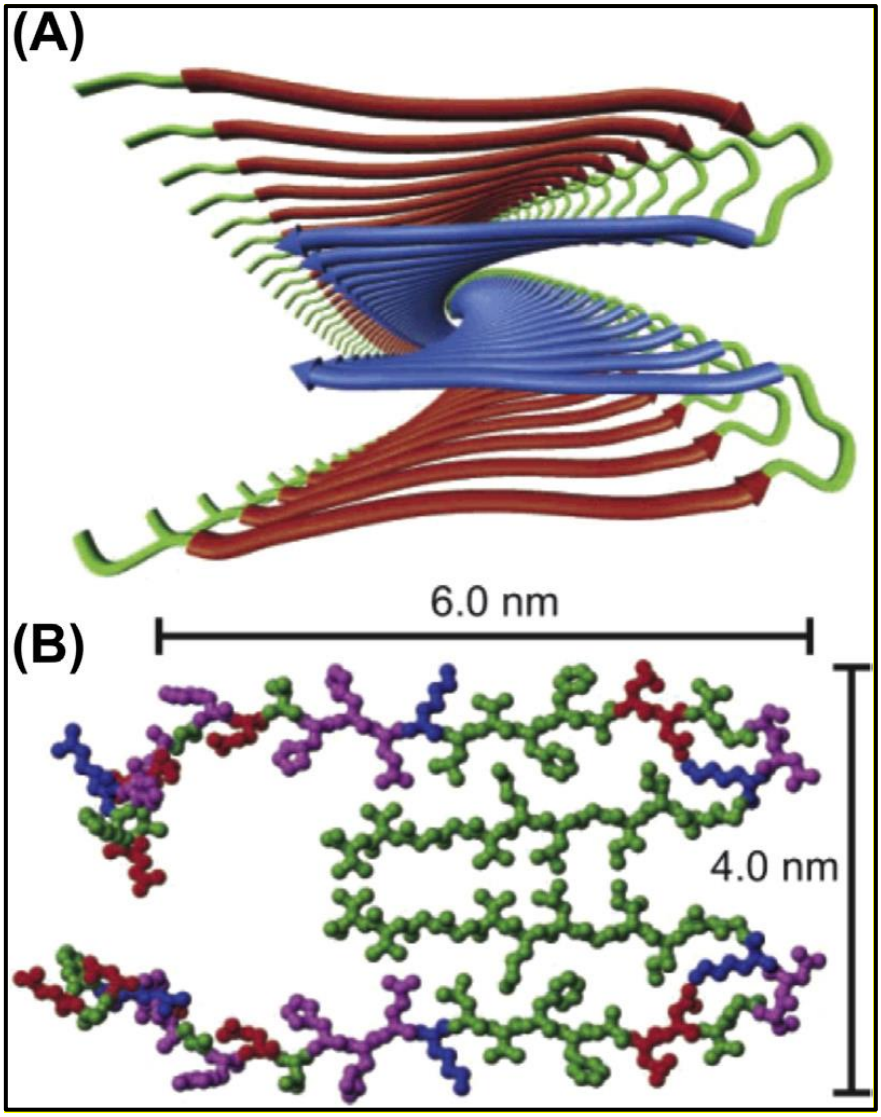

Figure 28: Structural model for Aβ1-40 protofilaments. (**A**) Ribbon representation viewed down the long axis of the protofilament. (**B)** Atomic representation with color coding to indicate residues with hydrophobic(green), polar (magenta), positively charged (blue) and negatively charged (red) side chains. (Adapted from Tycko,2003).

1.12.17. Polymorphism of Bovine β-lactoglobulin (β-lg) Amyloids: Rod-Like, Worm-Like, And Straight Fibrils

When beta-lactoglobulin (β-lg) monomers undergo partial unfolding or hydrolysis, they can give rise to diverse structural morphologies, the specifics of which depend on the experimental conditions employed. Due to the nanometric dimensions of these fibrils, they are typically analyzed using either atomic force microscopy (AFM) or electron microscopy (EM). It is important to note that the resulting amyloid fibrils are not uniform in their characteristics; their length, diameter, and persistence length exhibit significant variations among different fibrils

(Wetzel et al., 2007; Fändrich et al., 2009). Moreover, under certain experimental conditions, spherulites can also be formed, which consist of a central region composed of radially aligned amyloid fibrils (Jones et al., 2012; Krebs et al., 2008).

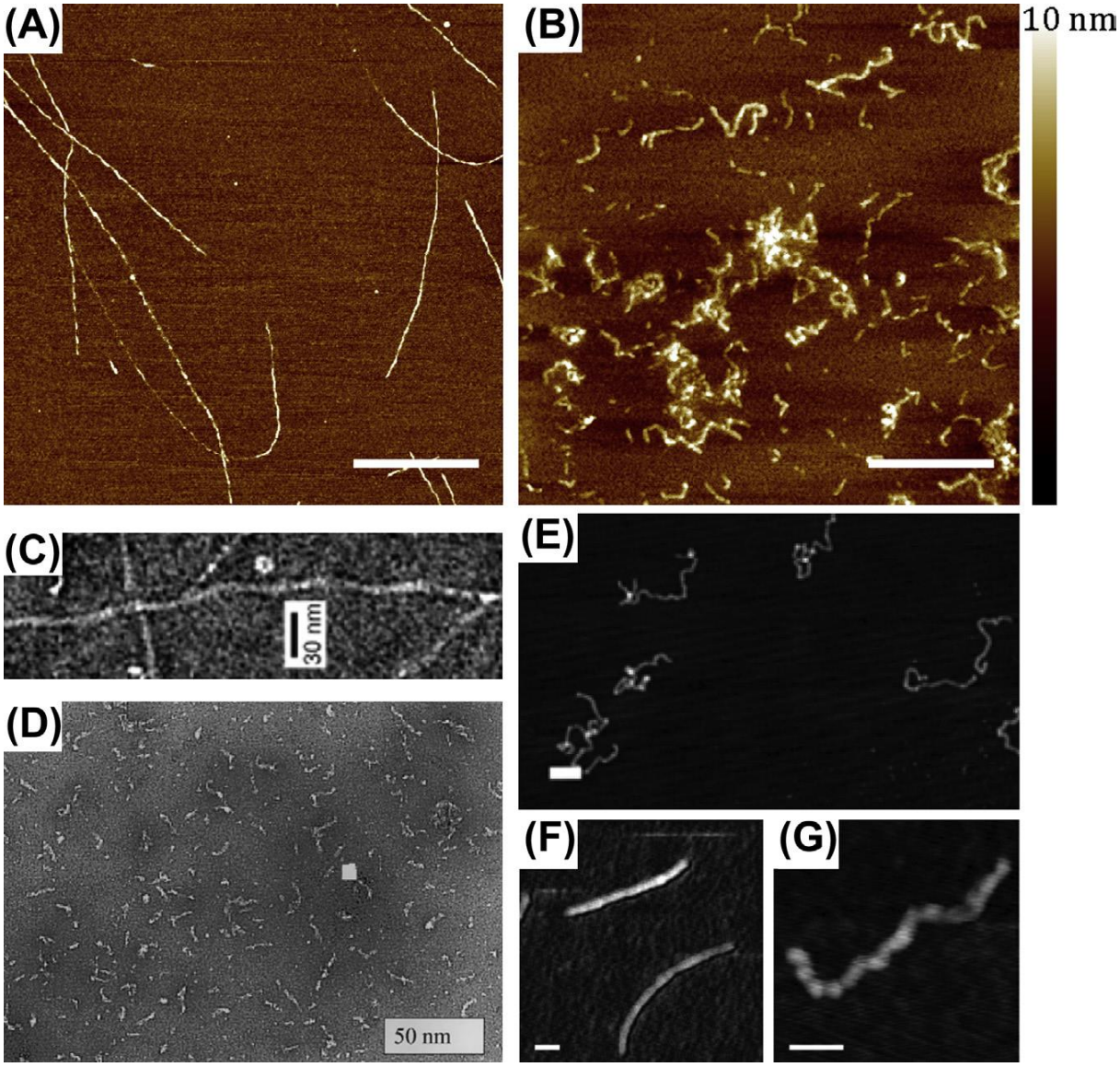

Figure 29: AFM height and TEM images of β-lg amyloid fibrils prepared under different conditions. (**A**) Incubation at pH 2 and 80°C for 16 hours at 30 mg/mL β-lg, and (**B**) 75 mg/mL β-lg. Scale bars are 500 nm. The color bar shows height calibration. (Adapted from vandenAkker et al., 2011**)**. (**C**) Incubation at pH 2.2 and 80°C for 6 hours at 10 mg/mL β-lg: fibril with wavy structure. The scalebar is 30 nm. (Adapted from Loveday et al., 2010). (**D**) Incubation at pH 3 and 80°C for 6 hours at 30 mg/mL β-lg. The scalebar is 50 nm. (Adapted from Kavanagh et al., 2000). (**E**) Incubation at pH 7 in 50% TFE (2,2,2-trifluoroethanol)-water mixtures at 40 mg/mL β-lg. The scalebar is 250 nm. Comparison of (**F**) heat-induced fibrils at

pH 2 and 80°C and (**G**) solvent-induced fibrils, 50% TFE–water mixture. Scale bars are 100 nm. (Adapted from Gosal et al., 2002**)**.

1.12.18. References

Abkevich, V.I., Gutin, A.M. and Shakhnovich, E.I., 1994. Free energy landscape for protein folding kinetics: intermediates, traps, and multiple pathways in theory and lattice model simulations. The Journal of Chemical Physics, 101(7), pp.6052-6062.

Acharya, N., Khandagale, P., Thakur, S., Sahu, J.K. and Utkalaja, B.G., 2020. Quaternary structural diversity in eukaryotic DNA polymerases: monomeric to multimeric form. Current genetics, 66, pp.635-655.

Adamcik, J. and Mezzenga, R., 2012. Proteins fibrils from a polymer physics perspective. Macromolecules, 45(3), pp.1137-1150.

Agashe, V. R.; Shastry, M. C. R.; Udgaonkar, J. B. Initial Hydrophobic Collapse in the Folding of Barstar. Nature. 1995, 377, 754−757.

Aggeli, A., Nyrkova, I.A., Bell, M., Harding, R., Carrick, L., McLeish, T.C., Semenov, A.N. and Boden, N., 2001. Hierarchical self-assembly of chiral rod-like molecules as a model for peptide β-sheet tapes, ribbons, fibrils, and fibers. Proceedings of the National Academy of Sciences, 98(21), pp.11857-11862.

Aguzzi, A. and O'Connor, T., 2010. Protein aggregation diseases: pathogenicity and therapeutic perspectives. Nature Reviews Drug Discovery, 9(3), pp.237-248.

Ahmad, B. and Lapidus, L.J., 2012. Curcumin prevents aggregation in α-synuclein by increasing reconfiguration rate. Journal of Biological Chemistry, 287(12), pp.9193-9199.

Ahmed, I.A.M., Al-Juhaimi, F.Y., Bhat, Z.F., Carne, A. and Bekhit, A.E.D.A., 2022. Non-traditional meat sources, production, nutritional and health aspects, consideration of safety aspects, and religious views. In Alternative Proteins (pp. 215-270). CRC Press.

Aich, R., Batabyal, S. and Joardar, S.N., 2014. Simple purification method for beta-lactoglobulin from buffalo milk. Adv. Anim. Vet. Sci, 2(2), pp.78-80.

Åkerström, B., Lögdberg, L., Berggård, T., Osmark, P. and Lindqvist, A., 2000. α1-Microglobulin: a yellow-brown lipocalin. Biochimica et Biophysica Acta (BBA)-Protein Structure and Molecular Enzymology, 1482(1-2), pp.172-184.

Akkermans, C., Venema, P., van der Goot, A.J., Gruppen, H., Bakx, E.J., Boom, R.M. and van der Linden, E., 2008. Peptides are building blocks of heat-induced fibrillar protein aggregates of β-lactoglobulin formed at pH 2. Biomacromolecules, 9(5), pp.1474-1479.

Alam, P., Siddiqi, K., Chaturvedi, S.K. and Khan, R.H., 2017. Protein aggregation: from background to inhibition strategies. International journal of biological macromolecules, 103, pp.208-219.

Allen, E., Henshaw, J. and Smith, P., 2001. A review of particle agglomeration (pp. 1-42). AEA Technology plc.

Alonso, D.O. and Dill, K.A., 1991. Solvent denaturation and stabilization of globular proteins. Biochemistry, 30(24), pp.5974-5985.

Anema, S.G. and McKenna, A.B., 1996. Reaction kinetics of thermal denaturation of whey proteins in heated reconstituted whole milk. Journal of Agricultural and Food Chemistry, 44(2), pp.422-428.

Anfinsen, C.B., 1972. The formation and stabilization of protein structure. Biochemical Journal, 128(4), p.737.

Anfinsen, C.B., 1973. Principles that govern the folding of protein chains. Science, 181(4096), pp.223-230.

Anuradha, S.N. and Prakash, V., 2008. Structural stabilization of bovine β-Lactoglobulin in presence of polyhydric alcohols.

Apenten, R.O., 1998. Protein stability function relations: β-lactoglobulin-A sulphydryl group reactivity and its relationship to protein unfolding stability. International journal of biological macromolecules, 23(1), pp.19-25.

Arai, K. and Iwaoka, M., 2019. Oxidative Protein Folding Using Trans-3, 4-Dihydroxyselenolane Oxide. Functional Disulphide Bonds: Methods and Protocols, pp.229-244.

Arai, K., Dedachi, K. and Iwaoka, M., 2011. Rapid and quantitative disulfide bond formation for a polypeptide chain using a cyclic selenoxide reagent in an aqueous medium. Chemistry–A European Journal, 17(2), pp.481-485.

Arai, K., Noguchi, M., Singh, B.G., Priyadarsini, K.I., Fujio, K., Kubo, Y., Takayama, K., Ando, S. and Iwaoka, M., 2013. A water-soluble selenoxide reagent as a useful probe for the reactivity and folding of polythiol peptides. FEBS Open Bio, 3, pp.55-64.

Arakawa, T., Kita, Y. and Timasheff, S.N., 2007. Protein precipitation and denaturation by dimethyl sulfoxide. Biophysical chemistry, 131(1-3), pp.62-70.

Armstrong, J.M., McKenzie, H.A. and Sawyer, W.H., 1967. On the fractionation of β-lactoglobulin and α-lactalbumin. Biochimica et Biophysica Acta (BBA)-Protein Structure, 147(1), pp.60-72.

Arnaudov, L.N., de Vries, R., Ippel, H. and van Mierlo, C.P., 2003. Multiple steps during the formation of β-lactoglobulin fibrils. Biomacromolecules, 4(6), pp.1614-1622.

Arolas, J.L., Aviles, F.X., Chang, J.Y. and Ventura, S., 2006. Folding of small disulfide-rich proteins: clarifying the puzzle. Trends in biochemical sciences, 31(5), pp.292-301.

Arosio, P., Knowles, T.P. and Linse, S., 2015. On the lag phase in amyloid fibril formation. Physical Chemistry Chemical Physics, 17(12), pp.7606-7618.

Aschaffenburg, R. and Drewry, J., 1955. Occurrence of different beta-lactoglobulins in cow's milk. Nature, 176(4474), pp.218-219.

Aschaffenburg, R. and Drewry, J., 1957. Improved method for the preparation of crystalline β-lactoglobulin and α-lactalbumin from cow's milk. Biochemical Journal, 65(2), p.273.

Aschaffenburg, R., Green, D.W. and Simmons, R.M., 1965. Crystal forms of β-lactoglobulin.

Ashrafian, H., Zadeh, E.H. and Khan, R.H., 2021. Review on Alzheimer's disease: inhibition of amyloid beta and tau tangle formation. International journal of biological macromolecules, 167, pp.382-394.

Astbury, W.T., Dickinson, S. and Bailey, K., 1935. The X-ray interpretation of denaturation and the structure of the seed globulins. Biochemical Journal, 29(10), p.2351.

Astwood, J.D., Leach, J.N. and Fuchs, R.L., 1996. Stability of food allergens to digestion in vitro. Nature Biotechnology, 14(10), pp.1269-1273.

Azevedo, E.P., Pereira, H.M., Garratt, R.C., Kelly, J.W., Foguel, D. and Palhano, F.L., 2011. Dissecting the structure, thermodynamic stability, and aggregation properties of the A25T transthyretin (A25T-TTR) variant involved in leptomeningeal amyloidosis: identifying protein partners that co-aggregate during A25T-TTR fibrillogenesis in cerebrospinal fluid. Biochemistry, 50(51), pp.11070-11083.

Babu, K.R., Moradian, A. and Douglas, D.J., 2001. The methanol-induced conformational transitions of β-lactoglobulin, cytochrome c, and ubiquitin at low pH: a study by electrospray ionization mass spectrometry. Journal of the American Society for Mass Spectrometry, 12(3), pp.317-328.

Balch, W.E., Morimoto, R.I., Dillin, A. and Kelly, J.W., 2008. Adapting proteostasis for disease intervention. science, 319(5865), pp.916-919.

Balchin, D., Hayer-Hartl, M. and Hartl, F.U., 2016. In vivo aspects of protein folding and quality control. Science, 353(6294), p.aac4354.

Baldwin, R.L. and Rose, G.D., 1999. Is protein folding hierarchic? I. Local structure and peptide folding. Trends in biochemical sciences, 24(1), pp.26-33.

Balistreri, A., Kahana, E., Janakiraman, S. and Chapman, M.R., 2020. Tuning functional amyloid formation through disulfide engineering. Frontiers in Microbiology, 11, p.944.

Bamdad, F., Bark, S., Kwon, C.H., Suh, J.W. and Sunwoo, H., 2017. Anti-inflammatory and antioxidant properties of peptides released from β-lactoglobulin by high hydrostatic pressure-assisted enzymatic hydrolysis. Molecules, 22(6), p.949.

Bashford, D., Cohen, F.E., Karplus, M., Kuntz, I.D. and Weaver, D.L., 1988. Diffusion-collision model for the folding kinetics of myoglobin. Proteins: Structure, Function, and Bioinformatics, 4(3), pp.211-227.

Baslé, E., Joubert, N. and Pucheault, M., 2010. Protein chemical modification on endogenous amino acids. Chemistry & biology, 17(3), pp.213-227.

Bates, G.P., Dorsey, R., Gusella, J.F., Hayden, M.R., Kay, C., Leavitt, B.R., Nance, M., Ross, C.A., Scahill, R.I., Wetzel, R. and Wild, E.J., 2015. Huntington's disease (Primer). Nature Reviews: Disease Primers, 1(1).

Beld, J., Woycechowsky, K.J. and Hilvert, D., 2007. Selenoglutathione: efficient oxidative protein folding by a diselenide. Biochemistry, 46(18), pp.5382-5390.

Bell, K., McKenzie, H.A. and Shaw, D.C., 1967. Amino acid composition and peptide maps of β-lactoglobulin variants.

Bellesia, G. and Shea, J.E., 2009. Diversity of kinetic pathways in amyloid fibril formation. The Journal of Chemical Physics, 131(11).

Bello, M., 2022. Structural mechanism of the Tanford transition of bovine β-lactoglobulin through microsecond molecular dynamics simulations. Journal of Biomolecular Structure and Dynamics, 40(7), pp.3011-3023.

Bello, M., Gutiérrez, G. and García-Hernández, E., 2012. Structure and dynamics of β-lactoglobulin in complex with dodecyl sulfate and laurate: a molecular dynamics study. Biophysical chemistry, 165, pp.79-86.

Bello, M., Pérez-Hernández, G., Fernández-Velasco, D.A., Arreguín-Espinosa, R. and García-Hernández, E., 2008. Energetics of protein homodimerization: effects of water sequestering on the formation of β-lactoglobulin dimer. Proteins: Structure, Function, and Bioinformatics, 70(4), pp.1475-1487.

Bernstein, S.L., Dupuis, N.F., Lazo, N.D., Wyttenbach, T., Condron, M.M., Bitan, G., Teplow, D.B., Shea, J.E., Ruotolo, B.T., Robinson, C.V. and Bowers, M.T., 2009. Amyloid-β protein oligomerization and the importance of tetramers and dodecamers in the etiology of Alzheimer's disease. Nature Chemistry, 1(4), pp.326-331.

Bewley, M.C., Qin, B.Y., Jameson, G.B., Sawyer, L. and Baker, E.N., 1997. Bovine β-lactoglobulin and its variants: a three-dimensional structural perspective.

Bhaduri, A. and Das, K.P., 1994. Adsorption Interaction of Native and Chemically Acetylated Beta Lactoglobulin at the Alumina-Water Interface. Journal Of Dispersion Science And Technology, 15(2), pp.165-188.

Bhak, G.B., Choe, Y.J. and Paik, S.R., 2009. Mechanism of amyloidogenesis: nucleation-dependent fibrillation versus double-concerted fibrillation. BMB reports, 42(9), pp.541-551.

Bhattacharjee, C., Saha, S., Biswas, A., Kundu, M., Ghosh, L. and Das, K.P., 2005. Structural changes of β-lactoglobulin during thermal unfolding and refolding–an FT-IR and circular dichroism study. The Protein Journal, 24(1), pp.27-35.

Bigi, A., Cascella, R., Chiti, F. and Cecchi, C., 2022. Amyloid fibrils act as a reservoir of soluble oligomers, the main culprits in protein deposition diseases. Bioessays, 44(11), p.2200086.

Bigman, L.S. and Levy, Y., 2020. Proteins: molecules defined by their trade-offs. Current opinion in structural biology, 60, pp.50-56.

Boczko, E.M. and Brooks III, C.L., 1995. First-principles calculation of the folding free energy of a three-helix bundle protein. Science, 269(5222), pp.393-396.

Boirie, Y., Dangin, M., Gachon, P., Vasson, M.P., Maubois, J.L. and Beaufrère, B., 1997. Slow and fast dietary proteins differently modulate postprandial protein accretion. Proceedings of the National Academy of Sciences, 94(26), pp.14930-14935.

Bolisetty, S., Adamcik, J. and Mezzenga, R., 2011. Snapshots of fibrillation and aggregation kinetics in multistranded amyloid β-lactoglobulin fibrils. Soft Matter, 7(2), pp.493-499.

Botelho, M.M., Valente-Mesquita, V.L., Oliveira, K.M., Polikarpov, I. and Ferreira, S.T., 2000. Pressure denaturation of β-lactoglobulin: Different stabilities of isoforms A and B, and an investigation of the Tanford transition. European Journal of Biochemistry, 267(8), pp.2235-2241.

Brehme, M., Voisine, C., Rolland, T., Wachi, S., Soper, J.H., Zhu, Y., Orton, K., Villella, A., Garza, D., Vidal, M. and Ge, H., 2014. A chaperone subnetwork safeguards proteostasis in aging and neurodegenerative disease. Cell reports, 9(3), pp.1135-1150.

Britten, M., Green, M.L., Boulet, M. and Paquin, P., 1988. Deposit formation on heated surfaces: effect of interface energetics. Journal of Dairy Research, 55(4), pp.551-562.

Bromley, E.H., Krebs, M.R. and Donald, A.M., 2005. Aggregation across the length-scales in β-lactoglobulin. Faraday Discussions, 128, pp.13-27.

Brownlow, S., Cabral, J.H.M., Cooper, R., Flower, D.R., Yewdall, S.J., Polikarpov, I., North, A.C. and Sawyer, L., 1997. Bovine β-lactoglobulin at 1.8 Å resolution—still an enigmatic lipocalin. Structure, 5(4), pp.481-495.

Bryngelson, J.D., Onuchic, J.N., Socci, N.D. and Wolynes, P.G., 1995. Funnels, pathways, and the energy landscape of protein folding: a synthesis. Proteins: Structure, Function, and Bioinformatics, 21(3), pp.167-195.

Bu, G., Luo, Y., Lu, J. and Zhang, Y., 2010. Reduced antigenicity of β-lactoglobulin by conjugation with glucose through controlled Maillard reaction conditions. Food and agricultural immunology, 21(2), pp.143-156.

Bucciantini, M., Giannoni, E., Chiti, F., Baroni, F., Formigli, L., Zurdo, J., Taddei, N., Ramponi, G., Dobson, C.M. and Stefani, M., 2002. Inherent toxicity of aggregates implies a common mechanism for protein misfolding diseases. nature, 416(6880), pp.507-511.

Bulaj, G., Kortemme, T. and Goldenberg, D.P., 1998. Ionization− reactivity relationships for cysteine thiols in polypeptides. Biochemistry, 37(25), pp.8965-8972.

Burova, T.V., Choiset, Y., Tran, V. and Haertlé, T., 1998. Role of free Cys121 in stabilization of bovine beta-lactoglobulin B. Protein Engineering, 11(11), pp.1065-1073.

Burr, R., Moore, C.H. and Hill, J.P., 1996. Evidence of multiple glycosylation of bovine β-lactoglobulin by electrospray ionization mass spectrometry.

Buyanbadrakh, B., 2014. Isolation of beta-lactoglobulin from cow milk. Research.

Caessens, P.W., Visser, S. and Gruppen, H., 1997. Method for the isolation of bovine β-lactoglobulin from a cheese whey protein fraction and physicochemical characterization of the purified product. International dairy journal, 7(4), pp.229-235.

Carrotta, R., Bauer, R., Waninge, R. and Rischel, C., 2001. Conformational characterization of oligomeric intermediates and aggregates in β-lactoglobulin heat aggregation. Protein Science, 10(7), pp.1312-1318.

Carulla, N., Caddy, G.L., Hall, D.R., Zurdo, J., Gairí, M., Feliz, M., Giralt, E., Robinson, C.V. and Dobson, C.M., 2005. Molecular recycling within amyloid fibrils. Nature, 436(7050), pp.554-558.

Carullo, D., Donsì, F. and Ferrari, G., 2020. Influence of high-pressure homogenization on structural properties and enzymatic hydrolysis of milk proteins. Lwt, 130, p.109657.

Castro, C.E., Dong, J., Boyce, M.C., Lindquist, S. and Lang, M.J., 2011. Physical properties of polymorphic yeast prion amyloid fibers. Biophysical Journal, 101(2), pp.439-448.

Cerbulis, J. and Farrell Jr, H.M., 1975. Composition of milk of dairy cattle. I. Protein, lactose, and fat contents and distribution of protein fraction. Journal of Dairy Science, 58(6), pp.817-827.

Chakraborty, J., Das, N., Das, K.P. and Halder, U.C., 2009. Loss of structural integrity and hydrophobic ligand binding capacity of acetylated and succinylated bovine β-lactoglobulin. International dairy journal, 19(1), pp.43-49.

Chamberlain, A.K. and Marqusee, S., 2000. Comparison of equilibrium and kinetic approaches for determining protein folding mechanisms. Advances in Protein Chemistry, 53, pp.283-328.

Chanasattru, W., Jones, O.G., Decker, E.A. and McClements, D.J., 2009. Impact of cosolvents on formation and properties of biopolymer nanoparticles formed by heat treatment of β-lactoglobulin–pectin complexes. Food Hydrocolloids, 23(8), pp.2450-2457.

Changani, S.D., Belmar-Beiny, M.T. and Fryer, P.J., 1997. Engineering and chemical factors associated with fouling and cleaning in milk processing. Experimental Thermal and Fluid Science, 14(4), pp.392-406.

Chattopadhyay, M., Durazo, A., Sohn, S.H., Strong, C.D., Gralla, E.B., Whitelegge, J.P. and Valentine, J.S., 2008. Initiation and elongation in fibrillation of ALS-linked superoxide dismutase. Proceedings of the National Academy of Sciences, 105(48), pp.18663-18668.

Chaturvedi, S.K., Siddiqi, M.K., Alam, P. and Khan, R.H., 2016. Protein misfolding and aggregation: Mechanism, factors, and detection. Process Biochemistry, 51(9), pp.1183-1192.

Chen, L. and Subirade, M., 2005. Chitosan/β-lactoglobulin core–shell nanoparticles as nutraceutical carriers. Biomaterials, 26(30), pp.6041-6053.

Cheng, B., Gong, H., Xiao, H., Petersen, R.B., Zheng, L. and Huang, K., 2013. Inhibiting toxic aggregation of amyloidogenic proteins: a therapeutic strategy for protein misfolding diseases. Biochimica et Biophysica Acta (BBA)-General Subjects, 1830(10), pp.4860-4871.

Chi, E.Y., Krishnan, S., Randolph, T.W. and Carpenter, J.F., 2003. Physical stability of proteins in aqueous solution: mechanism and driving forces in nonnative protein aggregation. Pharmaceutical research, 20, pp.1325-1336.

Chiancone, E. and Gattoni, M., 1991. Selective extraction of native β-lactoglobulin from whey. Journal of Chromatography A, 539(2), pp.455-463.

Chiti, F. and Dobson, C.M., 2006. Protein misfolding, functional amyloid, and human disease. Annu. Rev. Biochem., 75(1), pp.333-366.

Chiti, F. and Dobson, C.M., 2009. Amyloid formation by globular proteins under native conditions. Nature Chemical Biology, 5(1), pp.15-22.

Chiti, F. and Dobson, C.M., 2017. Protein misfolding, amyloid formation, and human disease: a summary of progress over the last decade. Annual review of biochemistry, 86(1), pp.27-68.

Chobert, J.M., 2012. Milk protein tailoring to improve functional and biological properties. Journal of BioScience & Biotechnology, 1(3).

Choe, Y.J., Park, S.H., Hassemer, T., Körner, R., Vincenz-Donnelly, L., Hayer-Hartl, M. and Hartl, F.U., 2016. Failure of RQC machinery causes protein aggregation and proteotoxic stress. Nature, 531(7593), pp.191-195.

Chopra, D., Gulati, M., Saluja, V., Pathak, P. and Bansal, P., 2008. Brain permeable nanoparticles. Recent Patents on CNS Drug Discovery (Discontinued), 3(3), pp.216-225.

Chou, K.C., Pottle, M., Némethy, G. and Scheraga, H.A., 1982. Structure of β-sheets: Origin of the right-handed twist and of the increased stability of antiparallel over parallel sheets. Journal of Molecular Biology, 162(1), pp.89-112.

Cohen, F.E. and Kelly, J.W., 2003. Therapeutic approaches to protein-misfolding diseases. Nature, 426(6968), pp.905-909.

Coles, M., Diercks, T., Muehlenweg, B., Bartsch, S., Zölzer, V., Tschesche, H. and Kessler, H., 1999. The solution structure and dynamics of human neutrophil gelatinase-associated lipocalin. Journal of molecular biology, 289(1), pp.139-157.

Compiani, M. and Capriotti, E., 2013. Computational and theoretical methods for protein folding. Biochemistry, 52(48), pp.8601-8624.

Conti, A., Godovac-Zimmermann, J., Liberatori, J., Braunitzer, G. And Minori, D., 1984. The primary structure of monomeric β-lactoglobulin I from horse colostrum (Equus caballus, Perissodactyla).

Conti, A., Godovac-Zimmermann, J., Pirchner, F., Liberatori, J. and Braunitzer, G., 1986. Pig β-lactoglobulin I (Sus scrofa domestica, Artiodactyla). The primary structure of the major component.

Cortez, L. and Sim, V., 2014. The therapeutic potential of chemical chaperones in protein folding diseases. Prion, 8(2), pp.197-202.

Cowan, S.W., Newcomer, M.E. and Jones, T.A., 1990. Crystallographic refinement of human serum retinol-binding protein at 2Å resolution. Proteins: Structure, Function, and Bioinformatics, 8(1), pp.44-61.

Crane, A. F., Chemical modification of proteins, Basic Prot. Pept. Protocols, 1994, 32, 311-320.

Creighton, T.E., 1990. Protein folding. Biochemical Journal, 270(1), p.1.

Croguennec, T., Bouhallab, S., Mollé, D., O'kennedy, B.T. and Mehra, R., 2003. Stable monomeric intermediate with exposed Cys-119 is formed during heat denaturation of β-lactoglobulin. Biochemical and Biophysical Research Communications, 301(2), pp.465-471.

Crowfoot, D. and Riley, D., 1938. Crystal Structures of the Proteins An X-Ray Study of Palmar's Lactoglobulin. Nature, 141(3568), pp.521-522.

Crowfoot, D., 1941. A Review of Some Recent X-ray Work on Protein Crystals. Chemical Reviews, 28(2), pp.215-228.

Crowther, J., 2017. Unraveling the mysteries of the milk protein β-lactoglobulin.

Crowther, J.M., Allison, J.R., Smolenski, G.A., Hodgkinson, A.J., Jameson, G.B. and Dobson, R.C., 2018. The self-association and thermal denaturation of caprine and bovine βlactoglobulin. European Biophysics Journal, 47(7), pp.739-750.

Cupo, J.F. and Pace, C.N., 1983. Conformational stability of mixed disulfide derivatives of. beta-lactoglobulin B. Biochemistry, 22(11), pp.2654-2658.

Daggett, V. and Fersht, A.R., 2003. Is there a unifying mechanism for protein folding?. Trends in biochemical sciences, 28(1), pp.18-25.

D'Alfonso, L., Collini, M. and Baldini, G., 2002. Does β-lactoglobulin denaturation occur via an intermediate state? Biochemistry, 41(1), pp.326-333.

D'Alfonso, L., Collini, M. and Baldini, G., 2003. Trehalose influence on beta-lactoglobulin stability and hydration by time-resolved fluorescence. European Journal of Biochemistry, 270(11), pp.2497-2504.

D'Alfonso, L., Collini, M., Ragona, L., Ugolini, R., Baldini, G. and Molinari, H., 2005. Porcine beta-lactoglobulin chemical unfolding: Identification of a non-native α-helical intermediate. Proteins: Structure, Function, and Bioinformatics, 58(1), pp.70-79.

Damon, A. J. H., Kresheck, G. C., Influence of surfactants on the conformation of β-lactoglobulin B using circular dichroism. Biopolymers, 1982, 21, 895-908.

Dar, T.A., Singh, L.R., Islam, A., Anjum, F., Moosavi-Movahedi, A.A. and Ahmad, F., 2007. Guanidinium chloride and urea denaturations of β-lactoglobulin A at pH 2.0 and 25 C: the equilibrium intermediate contains non-native structures (helix, tryptophan, and hydrophobic patches). Biophysical Chemistry, 127(3), pp.140-148.

Das, A., Gupta, A., Hong, Y., Carver, J.A. and Maiti, S., 2020. A spectroscopic marker for structural transitions associated with amyloid-β aggregation. Biochemistry, 59(19), pp.1813-1822.

Dasari, M., Espargaro, A., Sabate, R., Lopez del Amo, J.M., Fink, U., Grelle, G., Bieschke, J., Ventura, S. and Reif, B., 2011. Bacterial Inclusion Bodies of Alzheimer's Disease β-Amyloid Peptides Can Be Employed to Study Native-Like Aggregation Intermediate States. ChemBioChem, 12(3), pp.407-423.

Dasuri, K., Zhang, L. and Keller, J.N., 2013. Oxidative stress, neurodegeneration, and the balance of protein degradation and protein synthesis. Free Radical Biology and Medicine, 62, pp.170-185.

Davoodi, H., Esmaeili, S. and Mortazavian, A.M., 2013. Effects of milk and milk product consumption on cancer: a review. Comprehensive Reviews in Food Science and Food Safety, 12(3), pp.249-264.

Davoodi, S.H., Shahbazi, R., Esmaeili, S., Sohrabvandi, S., Mortazavian, A., Jazayeri, S. and Taslimi, A., 2016. Health-related aspects of milk proteins. Iranian Journal of Pharmaceutical Research: IJPR, 15(3), p.573.

De Jong, W.H. and Borm, P.J., 2008. Drug delivery and nanoparticles: applications and hazards. International journal of nanomedicine, 3(2), pp.133-149.

De Jongh, H.H.J., Gröneveld, T. and De Groot, J., 2001. Mild isolation procedure discloses new protein structural properties of β-lactoglobulin. Journal of Dairy Science, 84(3), pp.562-571.

de Oliveira, G.A., Marques, M.D.A., Cruzeiro-Silva, C., Cordeiro, Y., Schuabb, C., Moraes, A.H., Winter, R., Oschkinat, H., Foguel, D., Freitas, M.S. and Silva, J.L., 2016. Structural basis for the dissociation of α-synuclein fibrils triggered by pressure perturbation of the hydrophobic core. Scientific reports, 6(1), p.37990.

De Wit, J.N., 1990. Thermal stability and functionality of whey proteins. Journal of Dairy Science, 73(12), pp.3602-3612.

De Wit, J.N., 1998. Nutritional and functional characteristics of whey proteins in food products. Journal of Dairy Science, 81(3), pp.597-608.

Del Moral-Ramírez, E., DOMinguez-RAMirez, L.E.N.I.N., Cruz-Guerrero, A.E., Rodríguez-Serrano, G.M., García-Garibay, M., Gómez-Ruiz, L. and Jiménez-Guzmán, J., 2008. Role of Lysine ε-Amino Groups of β-Lactoglobulin on Its Activating Effect of Kluyveromyces lactis β-Galactosidase. Journal of Agricultural and Food Chemistry, 56(14), pp.5859-5863.

Dickinson, E. and Hong, S.T., 1994. surface Coverage of. beta-Lactoglobulin at the oil-water interface: Influence of protein heat treatment and various emulsifiers. Journal of Agricultural and Food Chemistry, 42(8), pp.1602-1606.

Dill, K.A. and MacCallum, J.L., 2012. The protein-folding problem, 50 years on. science, 338(6110), pp.1042-1046.

Dill, K.A., 1985. Theory for the folding and stability of globular proteins. Biochemistry, 24(6), pp.1501-1509.

Dill, K.A., 1990. Dominant forces in protein folding. Biochemistry, 29(31), pp.7133-7155.

Dobson, C.M., 2003. Protein folding and misfolding. Nature, 426(6968), pp.884-890.

Dobson, C.M., Šali, A. and Karplus, M., 1998. Protein folding: a perspective from theory and experiment. Angewandte Chemie International Edition, 37(7), pp.868-893.

Douglas, P.M. and Dillin, A., 2010. Protein homeostasis and aging in neurodegeneration. Journal of Cell Biology, 190(5), pp.719-729.

Dufour, E. and Haertl´, T., 1990. Alcohol-induced changes of β-lactoglobulin-retinol-binding stoichiometry. Protein Engineering, Design and Selection, 4(2), pp.185-190.

Dufour, E. and Haertle, T., 1990. Binding affinities of beta-ionone and related flavor compounds to beta-lactoglobulin: effects of chemical modifications. Journal of Agricultural and Food Chemistry, 38(8), pp.1691-1695.

Dufour, E., Bertrand-Harb, C. and Haertlé, T., 1993. Reversible effects of medium dielectric constant on structural transformation of β-lactoglobulin and its retinol binding. Biopolymers: Original Research on Biomolecules, 33(4), pp.589-598.

Dufour, E., Genot, C. and Haertlé, T., 1994. β-Lactoglobulin binding properties during its folding changes studied by fluorescence spectroscopy. Biochimica et Biophysica Acta (BBA)-Protein Structure and Molecular Enzymology, 1205(1), pp.105-112.

Edsall, J.T., 1995. Hsien Wu and the first theory of protein denaturation (1931). In Advances in protein chemistry (Vol. 46, pp. 1-5). Academic Press.

Edwards, P.J. and Jameson, G.B., 2020. Structure and stability of whey proteins. In Milk proteins (pp. 251-291). Academic Press.

Eisenberg, D.S. and Sawaya, M.R., 2017. Structural studies of amyloid proteins at the molecular level. Annual review of biochemistry, 86(1), pp.69-95.

Englander, S.W. and Mayne, L., 2014. The nature of protein folding pathways. Proceedings of the National Academy of Sciences, 111(45), pp.15873-15880.

Englander, S.W. and Mayne, L., 2017. The case for defined protein folding pathways. Proceedings of the National Academy of Sciences, 114(31), pp.8253-8258.

Etale, A., Onyianta, A.J., Turner, S.R. and Eichhorn, S.J., 2023. Cellulose: a review of water interactions, applications in composites, and water treatment. Chemical Reviews, 123(5), pp.2016-2048.

Evans, K.C., 1996. Conformational studies of the beta-amyloid protein and in vitro models for the effects of apolipoprotein E on fibril formation in Alzheimer's disease (Doctoral dissertation, Massachusetts Institute of Technology).

Expósito, I.L. and Recio, I., 2006. Antibacterial activity of peptides and folding variants from milk proteins. International Dairy Journal, 16(11), pp.1294-1305.

Fafournoux, P., Bruhat, A. and Jousse, C., 2000. Amino acid regulation of gene expression. Biochemical Journal, 351(1), pp.1-12.

Faisca, P.F., 2009. The nucleation mechanism of protein folding: a survey of computer simulation studies. Journal of Physics: Condensed Matter, 21(37), p.373102.

Falahati, M., Saboury, A.A., Shafiee, A., Sorkhabadi, S.M.R., Kachooei, E., Ma'Mani, L. and Haertlé, T., 2012. Highly efficient immobilization of beta-lactoglobulin in functionalized mesoporous nanoparticles: A simple and useful approach for enhancement of protein stability. Biophysical Chemistry, 165, pp.13-20.

Fändrich, M. and Dobson, C.M., 2002. The behavior of poly amino acids reveals an inverse side chain effect in amyloid structure formation. The EMBO journal, 21(21), pp.5682-5690.

Fändrich, M., Meinhardt, J. and Grigorieff, N., 2009. Structural polymorphism of Alzheimer Aβ and other amyloid fibrils. Prion, 3(2), pp.89-93.

Farrell Jr, H.M., Jimenez-Flores, R., Bleck, G.T., Brown, E.M., Butler, J.E., Creamer, L.K., Hicks, C.L., Hollar, C.M., Ng-Kwai-Hang, K.F. and Swaisgood, H.E., 2004. Nomenclature of the proteins of cows' milk—Sixth revision. Journal of Dairy Science, 87(6), pp.1641-1674.

Feeney, R.E., 1987. Chemical modification of proteins: comments and perspectives. International Journal of Peptide and Protein Research, 29(2), pp.145-161.

Fefilova, A.S., Fonin, A.V., Vishnyakov, I.E., Kuznetsova, I.M. and Turoverov, K.K., 2022. Stress-induced membrane-less organelles in eukaryotes and prokaryotes: bird's-eye view. International Journal of Molecular Sciences, 23(9), p.5010.

Felipe, X. and Law, A.J., 1997. Short Communications Preparative-scale fractionation of bovine, caprine, and ovine whey proteins by gel permeation chromatography. Journal of Dairy Research, 64(3), pp.459-464.

Feneberg, E., Gray, E., Ansorge, O., Talbot, K. and Turner, M.R., 2018. Towards a TDP-43-based biomarker for ALS and FTLD. Molecular neurobiology, 55, pp.7789-7801.

Ferrone, F., 1999. [17] Analysis of protein aggregation kinetics. In Methods in enzymology (Vol. 309, pp. 256-274). Academic Press.

Fersht, A.R. and Daggett, V., 2002. Protein folding and unfolding at atomic resolution. Cell, 108(4), pp.573-582.

Fersht, A.R., 1997. Nucleation mechanisms in protein folding. Current opinion in structural biology, 7(1), pp.3-9.

Finkelstein, A.V. and Ptitsyn, O.B., 1987. Why do globular proteins fit the limited set of folding patterns? Progress in biophysics and molecular biology, 50(3), pp.171-190.

Finkelstein, A.V., 2018. 50+ years of protein folding. Biochemistry (Moscow), 83, pp. S3-S18.

Fletcher, J.E., Spector, A.A. and Ashbrook, J.D., 1970. Analysis of macromolecule-ligand binding by determination of stepwise equilibrium constants. Biochemistry, 9(23), pp.4580-4587.

Fogolari, F., Moroni, E., Wojciechowski, M., Baginski, M., Ragona, L. and Molinari, H., 2005. MM/PBSA analysis of molecular dynamics simulations of bovine β-lactoglobulin: Free energy gradients in conformational transitions? Proteins: Structure, Function, and Bioinformatics, 59(1), pp.91-103.

Fox, K.K., Holsinger, V.H., Posati, L.P. and Pallansch, M.J., 1967. Separation of β-lactoglobulin from other milk serum proteins by trichloroacetic acid. Journal of Dairy Science, 50(9), pp.1363-1367.

Fox, P.F. and Mulvihill, D.M., 1982. Milk proteins: molecular, colloidal, and functional properties. Journal of Dairy Research, 49(4), pp.679-693.

Fox, P.F., Mcsweeney, P.L. and Paul, L.H., 1998. Dairy chemistry and biochemistry.

Frank, V.G. and Braunitzer, G., 1967. Primary structure of β-lactoglobulin.

Frare, E., De Laureto, P.P., Zurdo, J., Dobson, C.M. and Fontana, A., 2004. A highly amyloidogenic region of hen lysozyme. Journal of molecular biology, 340(5), pp.1153-1165.

Freibaum, B.D., Lu, Y., Lopez-Gonzalez, R., Kim, N.C., Almeida, S., Lee, K.H., Badders, N., Valentine, M., Miller, B.L., Wong, P.C. and Petrucelli, L., 2015. GGGGCC repeat expansion in C9orf72 compromises nucleocytoplasmic transport. Nature, 525(7567), pp.129-133.

Fugate, R.D. and Song, P.S., 1980. Spectroscopic characterization of beta-lactoglobulin-retinol complex. Biochimica et Biophysica Acta, 625(1), pp.28-42.

G. Reznikov, A. Baarsa and A. Delgado, Int. J. Food Sci.Technol., 2011,46, 2603. 57.

Galani, D. and Owusu Apenten, R.K., 1999. Heat-induced denaturation and aggregation of β-lactoglobulin: kinetics of formation of hydrophobic and disulphide-linked aggregates. International journal of food science & technology, 34(5-6), pp.467-476.

Gandhi, J., Antonelli, A.C., Afridi, A., Vatsia, S., Joshi, G., Romanov, V., Murray, I.V. and Khan, S.A., 2019. Protein misfolding and aggregation in neurodegenerative diseases: a review of pathogeneses, novel detection strategies, and potential therapeutics. Reviews in the Neurosciences, 30(4), pp.339-358.

Gautam, S., Karmakar, S., Bose, A. and Chowdhury, P.K., 2014. β-cyclodextrin and curcumin, a potent cocktail for disaggregating and/or inhibiting amyloids: a case study with α-synuclein. Biochemistry, 53(25), pp.4081-4083.

Gill, H.R.K. and Cross, M.L., 2000. Bovine milk: a unique source of immunomodulatory ingredients for functional foods In Buttriss J, Saltmarsh M.(eds.) Functional Foods II-claims and evidence.

Giurleo, J.T., He, X. and Talaga, D.S., 2008. β-lactoglobulin assembles into amyloid through sequential aggregated intermediates. Journal of molecular biology, 381(5), pp.1332-1348.

Glabe, C.G., 2006. Common mechanisms of amyloid oligomer pathogenesis in degenerative disease. Neurobiology of aging, 27(4), pp.570-575.

Gō, N., 1984. The consistency principle in protein structure and pathways of folding. Advances in biophysics, 18, pp.149-164.

Gordon, W.G., Basch, J.J. and Kalan, E.B., 1961. Amino acid composition of β-lactoglobulins A, B, and AB.

Gosal, W.S., Clark, A.H., Pudney, P.D. and Ross-Murphy, S.B., 2002. Novel amyloid fibrillar networks derived from a globular protein: β-lactoglobulin. Langmuir, 18(19), pp.7174-7181.

Green, D.W. and Aschaffenburg, R.J., 1959. Twofold symmetry of the β-lactoglobulin molecule in crystals.

Guo, Z. and Thirumalai, D., 1995. Kinetics of protein folding: nucleation mechanism, time scales, and pathways. Biopolymers: Original Research on Biomolecules, 36(1), pp.83-102.

Gutin, A.M., Abkevich, V.I. and Shakhnovich, E.I., 1995. Is burst hydrophobic collapse necessary for protein folding? Biochemistry, 34(9), pp.3066-3076.

Hall, W.L., Millward, D.J., Long, S.J. and Morgan, L.M., 2003. Casein and whey exert different effects on plasma amino acid profiles, gastrointestinal hormone secretion, and appetite. British Journal of Nutrition, 89(2), pp.239-248.

Halliday, J.A., Bell, K. and Shaw, D.C., 1991. The complete amino acid sequence of feline β-lactoglobulin II and a partial revision of the equine β-lactoglobulin II sequence. Biochimica et Biophysica Acta (BBA)-Protein Structure and Molecular Enzymology, 1077(1), pp.25-30.

Halpin, M.I. and Richardson, T., 1985. Selected functionality changes of β-Lactoglobulin upon esterification of side-chain carboxyl groups. Journal of Dairy Science, 68(12), pp.3189-3198.

Halttunen, M., Kämäräinen, M. and Koistinen, H., 2000. Glycodelin: a reproduction-related lipocalin. Biochimica et Biophysica Acta (BBA)-Protein Structure and Molecular Enzymology, 1482(1-2), pp.149-156.

Hamada, D. and Goto, Y., 1997. The equilibrium intermediate of β-lactoglobulin with non-native α-helical structure. Journal of molecular biology, 269(4), pp.479-487.

Hamada, D., Segawa, S.I. and Goto, Y., 1996. Non-native α-helical intermediate in the refolding of β-lactoglobulin, a predominantly β-sheet protein. Nature Structural Biology, 3(10), pp.868-873.

Hamada, D., Tanaka, T., Tartaglia, G.G., Pawar, A., Vendruscolo, M., Kawamura, M., Tamura, A., Tanaka, N. and Dobson, C.M., 2009. Competition between folding, native-state dimerization, and amyloid aggregation in β-lactoglobulin. Journal of molecular biology, 386(3), pp.878-890.

Hambling, S. G., McAlpine, A. S., Sawyer, L., Beta-Lactoglobulin. In: P. F. Fox, Editor. 1992, Advanced Dairy Chemistry - Volume 1: Proteins. Cambridge, UK: Elsevier Science Publishers, Ltd. p141.

Hamley, I.W., 2007. Peptide fibrillization. Angewandte Chemie International Edition, 46(43), pp.8128-8147.

Hansted, J.G., Wejse, P.L., Bertelsen, H. and Otzen, D.E., 2011. Effect of protein–surfactant interactions on aggregation of β-lactoglobulin. Biochimica et Biophysica Acta (BBA)-Proteins and Proteomics, 1814(5), pp.713-723.

Harper, J.D., Lieber, C.M. and Lansbury, P.T., 1997. Atomic force microscopic imaging of seeded fibril formation and fibril branching by the Alzheimer's disease amyloid-β protein. Chemistry & biology, 4(12), pp.951-959.

Hartl, F.U., 2017. Protein misfolding diseases. Annual review of biochemistry, 86(1), pp.21-26.

Hattori, M., Ametani, A., Katakura, Y., Shimizu, M. and Kaminogawa, S., 1993. Unfolding/refolding studies on bovine beta-lactoglobulin with monoclonal antibodies as probes. Does a renatured protein completely refold? Journal of Biological Chemistry, 268(30), pp.22414-22419.

Hattori, M., Numamoto, K.I., Kobayashi, K. and Takahashi, K., 2000. Functional changes in β-lactoglobulin by conjugation with cationic saccharides. Journal of Agricultural and Food Chemistry, 48(6), pp.2050-2056.

Heddleson, R.A., Allen, J.C., Wang, Q. and Swaisgood, H.E., 1997. Purity and yield of β-lactoglobulin isolated by an N-Retinyl-Celite bioaffinity column. Journal of Agricultural and Food Chemistry, 45(7), pp.2369-2373.

Hill, J.P., 1993. The relationship between β-lactoglobulin phenotypes and milk composition in New Zealand dairy cattle. Journal of Dairy Science, 76(1), pp.281-286.

Hinnenkamp, C.L., 2020. Blending of Procream with Functionally Enhanced Whey Protein Concentrate: A Structure-Function Approach to Whey Coproduct Utilization (Doctoral dissertation, University of Minnesota).

Hipp, M.S., Kasturi, P. and Hartl, F.U., 2019. The proteostasis network and its decline in aging. Nature reviews Molecular cell biology, 20(7), pp.421-435.

Hipp, M.S., Park, S.H. and Hartl, F.U., 2014. Proteostasis impairment in protein-misfolding and-aggregation diseases. Trends in cell biology, 24(9), pp.506-514.

Hodge, J.E., 1953. Chemistry of browning reactions in model systems.

Hoffmann, M.A. and van Mil, P.J., 1997. Heat-induced aggregation of β-lactoglobulin: role of the free thiol group and disulfide bonds. Journal of Agricultural and Food Chemistry, 45(8), pp.2942-2948.

Hoppenreijs, L.J., Overbeck, A., Brune, S.E., Biedendieck, R., Kwade, A., Krull, R., Boom, R.M. and Keppler, J.K., 2023. Amyloid-like aggregation of recombinant β-lactoglobulin at pH 3.5 and 7.0: Is disulfide bond removal the key to fibrillation? International Journal of Biological Macromolecules, 242, p.124855.

Hu, N.W., Smith, I.M., Walsh, D.M. and Rowan, M.J., 2008. Soluble amyloid-β peptides potently disrupt hippocampal synaptic plasticity in the absence of cerebrovascular dysfunction in vivo. Brain, 131(9), pp.2414-2424.

Huang, L., Liu, X., Cheng, B. and Huang, K., 2015. How our bodies fight amyloidosis: effects of physiological factors on pathogenic aggregation of amyloidogenic proteins. Archives of biochemistry and biophysics, 568, pp.46-55.

Hubbell, W.L., Cafiso, D.S. and Altenbach, C., 2000. Identifying conformational changes with site-directed spin labeling. Nature Structural Biology, 7(9), pp.735-739.

Impact of γ-radiation on antigenic properties of cow's milk β-lactoglobulin. Journal of Food Protection, 71(6), pp.1270-1272.

Invernizzi, G., Papaleo, E., Sabate, R. and Ventura, S., 2012. Protein aggregation: mechanisms and functional consequences. The International Journal of Biochemistry & Cell Biology, 44(9), pp.1541-1554.

Itzhaki, L.S., Otzen, D.E. and Fersht, A.R., 1995. The structure of the transition state for folding of chymotrypsin inhibitor 2 analyzed by protein engineering methods: evidence for a nucleation-condensation mechanism for protein folding. Journal of molecular biology, 254(2), pp.260-288.

Iwaoka, M., Kumakura, F., Yoneda, M., Nakahara, T., Henmi, K., Aonuma, H., Nakatani, H. and Tomoda, S., 2008. Direct observation of conformational folding coupled with disulfide rearrangement by using a water-soluble selenoxide reagent—A case of oxidative regeneration of ribonuclease A under weakly basic conditions. Journal of Biochemistry, 144(1), pp.121-130.

Jacob, S. W., Rosenbaum, E. E., Wood, D. C., Dimethyl Sulfoxide, vol. 1, Marcel Dekker, New York, 1971.

Jahn, T.R. and Radford, S.E., 2008. Folding versus aggregation: polypeptide conformations on competing pathways. Archives of biochemistry and biophysics, 469(1), pp.100-117.

Jarrett, J.T. and Lansbury Jr, P.T., 1993. Seeding "one-dimensional crystallization" of amyloid: a pathogenic mechanism in Alzheimer's disease and scrapie? Cell, 73(6), pp.1055-1058.

Jauhiainen, T. and Korpela, R., 2007. Milk Peptides and Blood Pressure1. the Journal of Nutrition, 137(3), pp.825S-829S.

Jayamani, J., Shanmugam, G. and Singam, E.R.A., 2014. Inhibition of insulin amyloid fibril formation by ferulic acid, a natural compound found in many vegetables and fruits. RSC advances, 4(107), pp.62326-62336.

Jensen, R.G., 1995. F. Miscellaneous Factors Affecting Composi. Handbook of milk composition, p.237.

Jeremy, J.Y., Gill, J., Fonseca, V., Dandona, P., Heeg, J.E., Gansevoort, R.T., De Jong, P.E. and De Zeeuw, D., 1990. ACE inhibitors and tissue binding. The Lancet, 336(8724), p.1189.

Jia, Y., Zhao, T., Zhao, N., Wei, H., Zhang, W. and Qiu, R., 2019. Effects of light irradiation on the complexes of cadmium and humic acids: The role of thiol groups. Chemosphere, 225, pp.174-181.

Jiang, C. and Chang, J.Y., 2007. Isomers of human α-synuclein stabilized by disulfide bonds exhibit distinct structural and aggregative properties. Biochemistry, 46(2), pp.602-609.

Jin, M., Shepardson, N., Yang, T., Chen, G., Walsh, D. and Selkoe, D.J., 2011. Soluble amyloid β-protein dimers isolated from Alzheimer's cortex directly induce Tau hyperphosphorylation and neuritic degeneration. Proceedings of the National Academy of Sciences, 108(14), pp.5819-5824.

Jones, M.N. and Wilkinson, A.L.A.N., 1976. The interaction between β-lactoglobulin and sodium n-dodecyl sulfate. Biochemical Journal, 153(3), pp.713-718.

Jones, O.G. and Mezzenga, R., 2012. Inhibiting, promoting, and preserving stability of functional protein fibrils. Soft Matter, 8(4), pp.876-895.

Jones, T.A., Newcomer, M.E. and Kraulis, P.J., 1986. The structure of β-lactoglobulin and its similarity to plasma retinol-binding protein. Nature, 324(6095), pp.383-385.

Judy, E. and Kishore, N., 2019. A look back at the molten globule state of proteins: Thermodynamic aspects. Biophysical Reviews, 11, pp.365-375.

Jung, J.M., Savin, G., Pouzot, M., Schmitt, C. and Mezzenga, R., 2008. Structure of heat-induced β-lactoglobulin aggregates and their complexes with sodium-dodecyl sulfate. Biomacromolecules, 9(9), pp.2477-2486.

Kaddouri, H., Mimoun, S., El-Mecherfi, K.E., Chekroun, A., Kheroua, O. and Saidi, D., 2008.

Karplus, M. and Weaver, D.L., 1979. Diffusion–collision model for protein folding. Biopolymers: Original Research on Biomolecules, 18(6), pp.1421-1437.

Kavanagh, G.M., Clark, A.H. and Ross-Murphy, S.B., 2000. Heat-induced gelation of globular proteins: part 3. Molecular studies on low pH β-lactoglobulin gels. International Journal of Biological Macromolecules, 28(1), pp.41-50.

Kella, N.K.D. and Kinsella, J.E., 1988. Structural stability of β-lactoglobulin in the presence of kosmotropic salts A kinetic and thermodynamic study. International Journal of Peptide and Protein Research, 32(5), pp.396-405.

Kerstens, S., Murray, B.S. and Dickinson, E., 2006. Microstructure of β-lactoglobulin-stabilized emulsions containing non-ionic surfactant and excess free protein: Influence of heating. Journal of Colloid and Interface Science, 296(1), pp.332-341.

Khan, S., Ipsen, R., Almdal, K., Svensson, B. and Harris, P., 2018. Revealing the Dimeric Crystal and Solution Structure of β-Lactoglobulin at pH 4 and Its pH and Salt Dependent Monomer–Dimer Equilibrium. Biomacromolecules, 19(7), pp.2905-2912.

Khoury, G.A., Smadbeck, J., Kieslich, C.A. and Floudas, C.A., 2014. Protein folding and de novo protein design for biotechnological applications. Trends in biotechnology, 32(2), pp.99-109.

Kim, P.S. and Baldwin, R.L., 1990. Intermediates in the folding reactions of small proteins. Annual review of biochemistry, 59(1), pp.631-660.

Kim, Y.E., Hosp, F., Frottin, F., Ge, H., Mann, M., Hayer-Hartl, M. and Hartl, F.U., 2016. Soluble oligomers of PolyQ-expanded huntingtin target a multiplicity of key cellular factors. Molecular cell, 63(6), pp.951-964., Y.E., Hosp, F., Frottin, F., Ge, H., Mann, M., Hayer-Hartl, M. and Hartl, F.U., 2016. Soluble oligomers of PolyQ-expanded huntingtin target a multiplicity of key cellular factors. Molecular cell, 63(6), pp.951-964.

Kitabatake, N., Cuq, J.L. and Cheftel, J.C., 1985. Covalent binding of glycosyl residues to. β -lactoglobulin: effects on solubility and heat stability. Journal of Agricultural and Food Chemistry, 33(1), pp.125-130.

Knekt, P., Järvinen, R., Seppänen, R., Pukkala, E. and Aromaa, A., 1996. Intake of dairy products and the risk of breast cancer. British Journal of Cancer, 73(5), pp.687-691.

Kobayashi, K., Hirano, A., Ohta, A., Yoshida, T., Takahashi, K. and Hattori, M., 2001. Reduced immunogenicity of β-lactoglobulin by conjugation with carboxymethyl dextran differing in molecular weight. Journal of Agricultural and Food Chemistry, 49(2), pp.823-831.

Kodali, R. and Wetzel, R., 2007. Polymorphism in the intermediates and products of amyloid assembly. Current opinion in structural biology, 17(1), pp.48-57.

Koistinen, H., Koistinen, R., Seppälä, M., Burova, T.V., Choiset, Y. and Haertlé, T., 1999. Glycodelin and β-lactoglobulin, lipocalins with a high structural similarity, differ in ligand binding properties. FEBS letters, 450(1-2), pp.158-162.

Kontopidis, G., Holt, C. and Sawyer, L., 2002. The ligand-binding site of bovine β-lactoglobulin: evidence for a function? Journal of molecular biology, 318(4), pp.1043-1055.

Kontopidis, G., Holt, C. and Sawyer, L., 2004. Invited review: β-lactoglobulin: binding properties, structure, and function. Journal of Dairy Science, 87(4), pp.785-796.

Kraulis, P.J., 1991. MOLSCRIPT: a program to produce both detailed and schematic plots of protein structures. Journal of Applied Crystallography, 24(5), pp.946-950.

Krebs, M.R., Devlin, G.L. and Donald, A.M., 2009. Amyloid fibril-like structure underlies the aggregate structure across the pH range for β-lactoglobulin. Biophysical journal, 96(12), pp.5013-5019.

Krebs, M.R., Domike, K.R., Cannon, D. and Donald, A.M., 2008. Common motifs in protein self-assembly. Faraday Discussions, 139, pp.265-274.

Kurouski, D., Washington, J., Ozbil, M., Prabhakar, R., Shekhtman, A. and Lednev, I.K., 2012. Disulfide bridges remain intact while native insulin converts into amyloid fibrils. PloS one, 7(6), p.e36989.

Kuwajima, K., Semisotnov, G.V., Finkelstein, A.V., Sugai, S. and Ptitsyn, O.B., 1993. Secondary structure of globular proteins at the early and the final stages in protein folding. FEBS letters, 334(3), pp.265-268.

Kuwajima, K., Yamaya, H., Miwa, S., Sugai, S. and Nagamura, T., 1987. Rapid formation of secondary structure framework in protein folding studied by stopped-flow circular dichroism. FEBS letters, 221(1), pp.115-118.

Kuwata, K., Hoshino, M., Forge, V., Era, S., Batt, C.A. and Goto, Y., 1999. Solution structure and dynamics of bovine β-lactoglobulin A. Protein Science, 8(11), pp.2541-2545.

L. Sawyer, Advanced dairy chem., 2003,1,319.

Labbadia, J. and Morimoto, R.I., 2015. The biology of proteostasis in aging and disease. Annual review of biochemistry, 84(1), pp.435-464.

Lamiot, E., Dufour, E. and Haertle, T., 1994. Insect Sex Pheromone Binding by Bovine. beta-Lactoglobulin. Journal of Agricultural and Food Chemistry, 42(3), pp.695-699.

Lara, C., Adamcik, J., Jordens, S. and Mezzenga, R., 2011. General self-assembly mechanism converting hydrolyzed globular proteins into giant multistranded amyloid ribbons. Biomacromolecules, 12(5), pp.1868-1875., C., Adamcik, J., Jordens, S. and Mezzenga, R., 2011. General self-assembly mechanism converting hydrolyzed globular proteins into giant multistranded amyloid ribbons. Biomacromolecules, 12(5), pp.1868-1875.

Larson, B.L., 1972. Methionine stimulation of milk protein synthesis in bovine mammary cell cultures. Journal of Dairy Science, 55(5), pp.629-631.

Lashuel, H.A., Overk, C.R., Oueslati, A. and Masliah, E., 2013. The many faces of α-synuclein: from structure and toxicity to therapeutic target. Nature Reviews Neuroscience, 14(1), pp.38-48.

Le Bon, C., Nicolai, T. and Durand, D., 1999. Kinetics of aggregation and gelation of globular proteins after heat-induced denaturation. Macromolecules, 32(19), pp.6120-6127.

Lee, H.J., McAuley, A., Schilke, K.F. and McGuire, J., 2011. Molecular origins of surfactant-mediated stabilization of protein drugs. Advanced drug delivery reviews, 63(13), pp.1160-1171.

Lees, W.J., 2008. Small-molecule catalysts of oxidative protein folding. Current Opinion in Chemical Biology, 12(6), pp.740-745.

Lefevre, T. and Subirade, M., 2000. Molecular differences in the formation and structure of fine-stranded and particulate β-lactoglobulin gels. Biopolymers: Original Research on Biomolecules, 54(7), pp.578-586.

Leonil, J., Mollé, D., Fauquant, J., Maubois, J.L., Pearce, R.J. and Bouhallab, S., 1997. Characterization by ionization mass spectrometry of lactosyl β-lactoglobulin conjugates formed during heat treatment of milk and whey and identification of one lactose-binding site. Journal of Dairy Science, 80(10), pp.2270-2281.

Levinthal, C., 1968. Are there pathways for protein folding? Journal de chimie physique, 65, pp.44-45.

Li, C., Xu, L., Zuo, Y.Y. and Yang, P., 2018. Tuning protein assembly pathways through superfast amyloid-like aggregation. Biomaterials science, 6(4), pp.836-841.

Li, Y., Gong, H., Sun, Y., Yan, J., Cheng, B., Zhang, X., Huang, J., Yu, M., Guo, Y., Zheng, L. and Huang, K., 2012. Dissecting the role of disulfide bonds on the amyloid formation of insulin. Biochemical and biophysical research communications, 423(2), pp.373-378.

Li, Y., Yang, C., Wang, S., Yang, D., Zhang, Y., Xu, L., Ma, L., Zheng, J., Petersen, R.B., Zheng, L. and Chen, H., 2020. Copper and iron ions accelerate the prion-like propagation of α-synuclein: a vicious cycle in Parkinson's disease. International journal of biological macromolecules, 163, pp.562-573.

Lim, W.K., Rösgen, J. and Englander, S.W., 2009. Urea, but not guanidinium, destabilizes proteins by forming hydrogen bonds to the peptide group. Proceedings of the National Academy of Sciences, 106(8), pp.2595-2600.

Lin, C.F., Yu, K.H., Jheng, C.P., Chung, R. and Lee, C.I., 2013. Curcumin reduces amyloid fibrillation of prion protein and decreases reactive oxidative stress. Pathogens, 2(3), pp.506-519.

Lindorff-Larsen, K., Piana, S., Dror, R.O. and Shaw, D.E., 2011. How fast-folding proteins fold. Science, 334(6055), pp.517-520.

Loveday, S.M., Wang, X.L., Rao, M.A., Anema, S.G., Creamer, L.K. and Singh, H., 2010. Tuning the properties of β-lactoglobulin nanofibrils with pH, NaCl, and CaCl2. International Dairy Journal, 20(9), pp.571-579.

Lozano, J.M., Giraldo, G.I. and Romero, C.M., 2008. An improved method for isolation of β-lactoglobulin. International Dairy Journal, 18(1), pp.55-63.

Lum, L.S., Dovč, P. and Medrano, J.F., 1997. Polymorphisms of bovine β-lactoglobulin promoter and differences in the binding affinity of activator protein-2 transcription factor. Journal of Dairy Science, 80(7), pp.1389-1397.

Lundén, A., Nilsson, M. and Janson, L., 1997. The marked effect of β-lactoglobulin polymorphism on the ratio of casein to total protein in milk. Journal of Dairy Science, 80(11), pp.2996-3005.

Ma, L., Yang, C., Zheng, J., Chen, Y., Xiao, Y. and Huang, K., 2020. Non-polyphenolic natural inhibitors of amyloid aggregation. European Journal of Medicinal Chemistry, 192, p.112197.

Ma, L., Zheng, J., Chen, H., Zeng, X., Wang, S., Yang, C., Li, X., Xiao, Y., Zheng, L., Chen, H. and Huang, K., 2021. A systematic screening of traditional Chinese medicine identifies two novel inhibitors against the cytotoxic aggregation of amyloid beta. Frontiers in Pharmacology, 12, p.637766.

Madar, D.J., Patel, A.S. and Lees, W.J., 2009. Comparison of the oxidative folding of lysozyme at a high protein concentration using aromatic thiols versus glutathione. Journal of Biotechnology, 142(3-4), pp.214-219.

Madureira, A.R., Pereira, C.I., Gomes, A.M., Pintado, M.E. and Malcata, F.X., 2007. Bovine whey proteins–Overview on their main biological properties. Food Research International, 40(10), pp.1197-1211.

Magdassi, S., Vinetsky, Y. and Relkin, P., 1996. Formation and structural heat-stability of β-lactoglobulin/surfactant complexes. Colloids and Surfaces B: Biointerfaces, 6(6), pp.353-362.

Maity, S., Sardar, S., Pal, S., Parvej, H., Chakraborty, J. and Halder, U.C., 2016. New insight into the alcohol-induced conformational change and aggregation of the alkaline unfolded state of bovine β-lactoglobulin. RSC advances, 6(78), pp.74409-74417.

Maity, S., Sepay, N., Pal, S., Sardar, S., Parvej, H., Pal, S., Chakraborty, J., Pradhan, A. and Halder, U.C., 2021. Modulation of amyloid fibrillation of bovine β-lactoglobulin by selective methionine oxidation. RSC advances, 11(19), pp.11192-11203.

Malhotra, P.; Udgaonkar, J. B. How Cooperative Are Protein Folding and Unfolding Transitions? Protein Sci. 2016, 25 (11), 1924−1941.

Manderson, G.A., Creamer, L.K. and Hardman, M.J., 1999. Effect of heat treatment on the circular dichroism spectra of bovine β-lactoglobulin A, B, and C. Journal of Agricultural and Food Chemistry, 47(11), pp.4557-4567.

Marcato, P.D. and Durán, N., 2008. New aspects of nanopharmaceutical delivery systems. Journal of nanoscience and nanotechnology, 8(5), pp.2216-2229.

Marinelli, P., Navarro, S., Graña-Montes, R., Bañó-Polo, M., Fernández, M.R., Papaleo, E. and Ventura, S., 2018. A single cysteine post-translational oxidation suffices to compromise globular proteins' kinetic stability and promote amyloid formation. Redox biology, 14, pp.566-575.

Master, P.B.Z. and Macedo, R.C.O., 2021. Effects of dietary supplementation in sport and exercise: A review of evidence on milk proteins and amino acids. Critical reviews in food science and nutrition, 61(7), pp.1225-1239.

Maté, J.I. and Krochta, J.M., 1994. β-Lactoglobulin separation from whey protein isolates on a large scale. Journal of Food Science, 59(5), pp.1111-1114.

Matheson Jr, R.R., and Scheraga, H.A., 1978. A method for predicting nucleation sites for protein folding based on hydrophobic contacts. Macromolecules, 11(4), pp.819-829.

Matthews, C.R., 1993. Pathways of protein folding. Annual review of biochemistry, 62, pp.653-683.

Maubois, J.L., Leonil, J., Bouhallab, S., Mollé, D. and Pearce, J.R., 1995. Characterization by ionization mass spectrometry of a lactosyl-bêta-lactoglobulin conjugate occurring during milk heating of whey. Journal of Dairy Science, 78(Suppl-1), p.133.

Maulik, S., Dutta, P., Chattoraj, D.K. and Moulik, S.P., 1998. Biopolymer–surfactant interactions: 5: Equilibrium studies on the binding of cetyltrimethylammonium bromide and sodium dodecyl sulfate with bovine serum albumin, β-lactoglobulin, haemoglobin, gelatin, lysozyme, and deoxyribonucleic acid. Colloids and Surfaces B: Biointerfaces, 11(1-2), pp.1-8.

Mayor, U., Guydosh, N.R., Johnson, C.M., Grossmann, J.G., Sato, S., Jas, G.S., Freund, S.M., Alonso, D.O., Daggett, V. and Fersht, A.R., 2003. The complete folding pathway of a protein from nanoseconds to microseconds. Nature, 421(6925), pp.863-867.

Mazaheri, M., Moosavi-Movahedi, A.A., Saboury, A.A., Khodagholi, F., Shaerzadeh, F. and Sheibani, N., 2015. Curcumin protects β-lactoglobulin fibril formation and fibril-induced neurotoxicity in PC12 cells. PLoS One, 10(7), p.e0133206.

McBain, S.C., Yiu, H.H. and Dobson, J., 2008. Magnetic nanoparticles for gene and drug delivery. International journal of nanomedicine, 3(2), pp.169-180.

McKenzie, H.A. and Sawyer, W.H., 1967. Effect of p H on β-Lactoglobulins. Nature, 214(5093), pp.1101-1104.

McLachlan, C.N.S., 2001. β-casein A1, ischaemic heart disease mortality, and other illnesses. Medical Hypotheses, 56(2), pp.262-272.

McMeekin, T.L., Groves, M.L. and Hipp, N.J., 1949. Apparent specific volume of α-casein and β-casein and the relationship of specific volume to amino acid composition. Journal of the American Chemical Society, 71(10), pp.3298-3300.

Meisel, H., 1998. Overview on milk protein-derived peptides. International Dairy Journal, 8(5-6), pp.363-373.

Mirny, L. and Shakhnovich, E., 2001. Protein folding theory: from lattice to all-atom models. Annual review of biophysics and biomolecular structure, 30(1), pp.361-396.

Mishra, P. and Jha, S.K., 2022. The native state conformational heterogeneity in the energy landscape of protein folding. Biophysical Chemistry, 283, p.106761.

Mitra, A. and Sarkar, N., 2022. The role of intra and inter-molecular disulfide bonds in modulating amyloidogenesis: A review. Archives of Biochemistry and Biophysics, 716, p.109113.

Monaco, H.L., Zanotti, G., Spadon, P., Bolognesi, M., Sawyer, L. and Eliopoulos, E.E., 1987. Crystal structure of the trigonal form of bovine beta-lactoglobulin and of its complex with retinol at 2.5 Å resolution. Journal of Molecular Biology, 197(4), pp.695-706.

Morell, M., Bravo, R., Espargaró, A., Sisquella, X., Avilés, F.X., Fernàndez-Busquets, X. and Ventura, S., 2008. Inclusion bodies: specificity in their aggregation process and amyloid-like structure. Biochimica et Biophysica Acta (BBA)-Molecular Cell Research, 1783(10), pp.1815-1825.

Morgan, F., Vénien, A., Bouhallab, S., Mollé, D., Léonil, J., Peltre, G. and Levieux, D., 1999. Modification of bovine β-lactoglobulin by glycation in a powdered state or in an aqueous solution: immunochemical characterization. Journal of Agricultural and Food Chemistry, 47(11), pp.4543-4548.

Morozova-Roche, L.A., Zurdo, J., Spencer, A., Noppe, W., Receveur, V., Archer, D.B., Joniau, M. and Dobson, C.M., 2000. Amyloid fibril formation and seeding by wild-type human lysozyme and its disease-related mutational variants. Journal of Structural Biology, 130(2-3), pp.339-351.

Mossine, V.V., Glinsky, G.V. and Feather, M.S., 1994. The preparation and characterization of some Amadori compounds (1-amino-1-deoxy-D-fructose derivatives) derived from a series of aliphatic ω-amino acids. Carbohydrate Research, 262(2), pp.257-270.

Mossuto, M.F., 2013. Disulfide bonding in neurodegenerative misfolding diseases. International Journal of Cell Biology, 2013(1), p.318319.

Mounsey, J.S. and O'kennedy, B.T., 2009. Stability of β-lactoglobulin/micellar casein mixtures on heating in simulated milk ultrafiltrate at pH 6.0. International journal of dairy technology, 62(4), pp.493-499.

Mulvihill, D. and Donovan, M., 1987. Whey proteins and their thermal denaturation review. Irish Journal of Food Science and Technology, 11(1), pp.43-75.

Münch, G., Schicktanz, D., Behme, A., Gerlach, M., Riederer, P., Palm, D. and Schinzel, R., 1999. Amino acid specificity of glycation and protein–AGE crosslinking reactivities determined with a dipeptide SPOT library. Nature Biotechnology, 17(10), pp.1006-1010.

Nader, E., Romana, M. and Connes, P., 2020. The red blood cell—inflammation vicious circle in sickle cell disease. Frontiers in immunology, 11, p.454.

Nakanishi, T., Yoshioka, M., Moriuchi, K., Yamamoto, D., Tsuji, M. and Takubo, T., 2010. S-sulfonation of transthyretin is an important trigger step in the formation of transthyretin-related amyloid fibril. Biochimica et Biophysica Acta (BBA)-Proteins and Proteomics, 1804(7), pp.1449-1456.

Naqvi, Z., Khan, R.H. and Saleemuddin, M., 2010. A procedure for the purification of beta-lactoglobulin from bovine milk using gel filtration chromatography at low pH. Preparative Biochemistry & Biotechnology, 40(4), pp.326-336.

Narayan, M. and Berliner, L.J., 1998. Mapping fatty acid binding to β-lactoglobulin: ligand binding is restricted by modification of Cys 121. Protein Science, 7(1), pp.150-157.

Narayan, M., 2020. Revisiting the formation of a native disulfide bond: consequences for protein regeneration and beyond. Molecules, 25(22), p.5337.

Narayan, M., Welker, E. and Scheraga, H.A., 2003. Native conformational tendencies in unfolded polypeptides: development of a novel method to assess native conformational tendencies in the reduced forms of multiple disulfide-bonded proteins. Journal of the American Chemical Society, 125(8), pp.2036-2037.

Narayan, M., Welker, E., Wanjalla, C., Xu, G. and Scheraga, H.A., 2003. Shifting the competition between the intramolecular reshuffling reaction and the direct oxidation

reaction during the oxidative folding of kinetically trapped disulfide-insecure intermediates. Biochemistry, 42(36), pp.10783-10789.

Narayan, M., Welker, E., Wedemeyer, W.J. and Scheraga, H.A., 2000. Oxidative folding of proteins. Accounts of chemical research, 33(11), pp.805-812.

Navarra, G., Tinti, A., Di Foggia, M., Leone, M., Militello, V. and Torreggiani, A., 2014. Metal ions modulate thermal aggregation of beta-lactoglobulin: A joint chemical and physical characterization. Journal of Inorganic Biochemistry, 137, pp.64-73.

Nelson, R., Sawaya, M.R., Balbirnie, M., Madsen, A.Ø., Riekel, C., Grothe, R. and Eisenberg, D., 2005. Structure of the cross-β spine of amyloid-like fibrils. Nature, 435(7043), pp.773-778.

Newcomer, M.E., Jones, T.A., Aqvist, J., Sundelin, J., Eriksson, U., Rask, L. and Peterson, P.A., 1984. The three-dimensional structure of retinol-binding protein. The EMBO journal, 3(7), pp.1451-1454.

Ng-Kwai-Hang, K.F., Hayes, J.F., Moxley, J.E. and Monardes, H.G., 1986. Relationships between milk protein polymorphisms and major milk constituents in Holstein-Friesian cows. Journal of Dairy Science, 69(1), pp.22-26.

Nie, S., Xing, Y., Kim, G.J. and Simons, J.W., 2007. Nanotechnology applications in cancer. Annu. Rev. Biomed. Eng., 9(1), pp.257-288.

Nielsen, L., Khurana, R., Coats, A., Frokjaer, S., Brange, J., Vyas, S., Uversky, V.N. and Fink, A.L., 2001. Effect of environmental factors on the kinetics of insulin fibril formation: elucidation of the molecular mechanism. Biochemistry, 40(20), pp.6036-6046.

Nieuwenhuizen, W.F., Dekker, H.L., Gröneveld, T., de Koster, C.G. and de Jong, G.A., 2004. Transglutaminase-mediated modification of glutamine and lysine residues in native bovine β-lactoglobulin. Biotechnology and Bioengineering, 85(3), pp.248-258.

Nilsson, M.R., 2004. Techniques to study amyloid fibril formation in vitro. Methods, 34(1), pp.151-160.

Oliveira, K.M., Valente-Mesquita, V.L., Botelho, M.M., Sawyer, L., Ferreira, S.T. and Polikarpov, I., 2001. Crystal structures of bovine β-lactoglobulin in the orthorhombic space group C2221: Structural differences between genetic variants A and B and

features of the Tanford transition. European Journal of Biochemistry, 268(2), pp.477-484.

Olzscha, H., Schermann, S.M., Woerner, A.C., Pinkert, S., Hecht, M.H., Tartaglia, G.G., Vendruscolo, M., Hayer-Hartl, M., Hartl, F.U. and Vabulas, R.M., 2011. Amyloid-like aggregates sequester numerous metastable proteins with essential cellular functions. Cell, 144(1), pp.67-78.

Oosawa, F. and Asakura, S., 1975. Thermodynamics of the Polymerization of Protein. Academic Press.

P.A., 1984. The three-dimensional structure of retinol-binding protein. The EMBO journal, 3(7), pp.1451-1454.

Pagel, O., Loroch, S., Sickmann, A. and Zahedi, R.P., 2015. Current strategies and findings in clinically relevant post-translational modification-specific proteomics. Expert review of proteomics, 12(3), pp.235-253.

Palmer, A.H., 1933. The preparation of a crystalline globulin from the albumin fraction of cow's milk.

Pan, Y., Lee, A., Wan, J., Coventry, M.J., Michalski, W.P., Shiell, B. and Roginski, H., 2006. Antiviral properties of milk proteins and peptides. International Dairy Journal, 16(11), pp.1252-1261.

Papiz, M.Z., Sawyer, L., Eliopoulos, E.E., North, A.C.T., Findlay, J.B.C., Sivaprasadarao, R., Jones, T.A., Newcomer, M.E. and Kraulis, P.J., 1986. The structure of β-lactoglobulin and its similarity to plasma retinol-binding protein. Nature, 324(6095), pp.383-385.

Park, S.H., Kukushkin, Y., Gupta, R., Chen, T., Konagai, A., Hipp, M.S., Hayer-Hartl, M. and Hartl, F.U., 2013. PolyQ proteins interfere with nuclear degradation of cytosolic proteins by sequestering the Sis1p chaperone. Cell, 154(1), pp.134-145.

Partschefeld, C., Richter, S., Schwarzenbolz, U. and Henle, T., 2007. Modification of β-lactoglobulin by microbial transglutaminase under high hydrostatic pressure: Localization of reactive glutamine residues. Biotechnology Journal: Healthcare Nutrition Technology, 2(4), pp.462-468.

Pedersen, K.O and Kekwick, R.A., 1936. Some physicochemical characteristics of the yellow respiratory enzyme. Biochemical Journal, 30(12), p.2201.

Pelczer, I. and Carter, B.G., 1997. Data processing in multidimensional NMR. Protein NMR techniques, pp.71-155.

Pennings, B., Boirie, Y., Senden, J.M., Gijsen, A.P., Kuipers, H. and van Loon, L.J., 2011. Whey protein stimulates postprandial muscle protein accretion more effectively than do casein and casein hydrolysate in older men. The American Journal of Clinical Nutrition, 93(5), pp.997-1005.

Perez, M.D., Sanchez, L., Aranda, P., Ena, J., Oria, R. and Calvo, M., 1992. Effect of β-lactoglobulin on the activity of pregastric lipase. A possible role for this protein in ruminant milk. Biochimica et Biophysica Acta (BBA)-Lipids and Lipid Metabolism, 1123(2), pp.151-155.

Perez, O.E. and Pilosof, A.M., 2004. Pulsed electric fields effects on the molecular structure and gelation of β-lactoglobulin concentrate and egg white. Food Research International, 37(1), pp.102-110.

Pérez, O.E., David-Birman, T., Kesselman, E., Levi-Tal, S. and Lesmes, U., 2014. Milk protein–vitamin interactions: Formation of beta-lactoglobulin/folic acid nano-complexes and their impact on in vitro gastro-duodenal proteolysis. Food Hydrocolloids, 38, pp.40-47.

Petit, J., Herbig, A.L., Moreau, A. and Delaplace, G., 2011. Influence of calcium on β-lactoglobulin denaturation kinetics: Implications in unfolding and aggregation mechanisms. Journal of Dairy Science, 94(12), pp.5794-5810.

Peydayesh, M., Vogt, J., Chen, X., Zhou, J., Donat, F., Bagnani, M., Müller, C.R. and Mezzenga, R., 2022. Amyloid-based carbon aerogels for water purification. Chemical Engineering Journal, 449, p.137703.

Philippe, J., 1991. Structure and pancreatic expression of the insulin and glucagon genes. Endocrine Reviews, 12(3), pp.252-271.

Pihlanto, A., 2011. Whey proteins and peptides: Emerging properties to promote health. Nutrafoods, 10, pp.29-42.

Potempa, M., Hafner, M. and Frech, C., 2010. Mechanism of gemini disulfide detergent mediated oxidative refolding of lysozyme in a new artificial chaperone system. The Protein Journal, 29, pp.457-465.

Prusiner, S.B., Scott, M.R., DeArmond, S.J. and Cohen, F.E., 1998. Prion protein biology. cell, 93(3), pp.337-348.

Ptitsyn, O.B., 1973. Stages in the mechanism of self-organization of protein molecules. Doklady Akademii Nauk SSSR, 210(5), pp.1213-1215.

Qi, X.L., Holt, C., Mcnulty, D., Clarke, D.T., Brownlow, S. And Jones, G.R., 1997. Effect of temperature on the secondary structure of β-lactoglobulin at pH 6.7, as determined by CD and IR spectroscopy: a test of the molten globule hypothesis. Biochemical Journal, 324(1), pp.341-346.

Qin, B.Y., Bewley, M.C., Creamer, L.K., Baker, E.N. and Jameson, G.B., 1999. Functional implications of structural differences between variants A and B of bovine βlactoglobulin. Protein Science, 8(1), pp.75-83.

Qin, B.Y., Bewley, M.C., Creamer, L.K., Baker, E.N. and Jameson, G.B., 1999. Functional implications of structural differences between variants A and B of bovine βlactoglobulin. Protein Science, 8(1), pp.75-83.

Qin, B.Y., Bewley, M.C., Creamer, L.K., Baker, H.M., Baker, E.N. and Jameson, G.B., 1998. Structural basis of the Tanford transition of bovine β-lactoglobulin. Biochemistry, 37(40), pp.14014-14023.

Quevedo, M., Jandt, U., Kulozik, U., Karbstein, H.P. and Emin, M.A., 2019. Investigation on the influence of high protein concentrations on the thermal reaction behavior of βlactoglobulin by experimental and numerical analyses. International dairy journal, 97, pp.99-110.

Rabbani, G. and Choi, I., 2018. Roles of osmolytes in protein folding and aggregation in cells and their biotechnological applications. International Journal of biological macromolecules, 109, pp.483-491.

Ragona, L., Fogolari, F., Romagnoli, S., Zetta, L., Maubois, J.L. and Molinari, H., 1999. Unfolding and refolding of bovine β-lactoglobulin monitored by hydrogen exchange measurements. Journal of molecular biology, 293(4), pp.953-969.

Rahaman, T., Vasiljevic, T. and Ramchandran, L., 2017. Digestibility and antigenicity of βlactoglobulin as affected by heat, pH, and applied shear. Food Chemistry, 217, pp.517523.

Ranjit Aich, R.A., Subhasis Batabyal, S.B. and Joardar, S.N., 2015. Isolation and purification of beta-lactoglobulin from cow milk.

Rao, I.M., 2009. Essential plant nutrients and their functions.

Ray, A., Chatterjee, R., Conformation of bio-polymers, Ramachandran, G. N. (Ed.), Academic Press, London, 1967, pp 235-251.

Reddy, I.M., Kella, N.K. and Kinsella, J.E., 1988. Structural and conformational basis of the resistance of. beta-lactoglobulin to peptic and chymotryptic digestion. Journal of Agricultural and Food Chemistry, 36(4), pp.737-741.

Redl, B. and Habeler, M., 2022. The diversity of lipocalin receptors. Biochimie, 192, pp.22-

Relkin, P. and Mulvihill, D.M., 1996. Thermal unfolding of β-lactoglobulin, α-lactalbumin, and bovine serum albumin. A thermodynamic approach. Critical Reviews in Food Science & Nutrition, 36(6), pp.565-601.

Renard, D., Lefebvre, J., Griffin, M.C.A. and Griffin, W.G., 1998. Effects of pH and salt environment on the association of β-lactoglobulin revealed by intrinsic fluorescence studies. International Journal of Biological Macromolecules, 22(1), pp.41-49.

Renard, D., Lefebvre, J., Robert, P., Llamas, G. and Dufour, E., 1999. Structural investigation of β-lactoglobulin gelation in ethanol/water solutions. International journal of biological macromolecules, 26(1), pp.35-44.

Robson, B. and Pain, R.H., 1971. Analysis of the code relating sequence to conformation in proteins: possible implications for the mechanism of formation of helical regions. Journal of molecular biology, 58(1), pp.237-257.

Rocha, T.L., Brownlow, S., Saddler, K.N., Fothergill-Gilmore, L.A. and Sawyer, L., 1996. The new crystal form of β-lactoglobulin. Journal of dairy research, 63(4), pp.575-584.

Roefs, S.P. and De Kruif, K.G., 1994. A model for the denaturation and aggregation of βlactoglobulin. European Journal of Biochemistry, 226(3), pp.883-889.

Rollins, G.C. and Dill, K.A., 2014. General mechanism of two-state protein folding kinetics. Journal of the American Chemical Society, 136(32), pp.11420-11427.

Ron, N., Zimet, P., Bargarum, J. and Livney, Y.D., 2010. Beta-lactoglobulin–polysaccharide complexes as nano vehicles for hydrophobic nutraceuticals in non-fat foods and clear beverages. International dairy journal, 20(10), pp.686-693.

Roos, R.A., 2010. Huntington's disease: a clinical review. Orphanet Journal of rare diseases, 5, pp.1-8.

Röper, H., Röper, S., Heyns, K. and Meyer, B., 1983. NMR spectroscopy of N-(1-deoxy-D-fructos-1-yl)-L-amino acids ("fructose-amino acids"). Carbohydrate Research, 116(2), pp.183-195.

Ross, C.A., Aylward, E.H., Wild, E.J., Langbehn, D.R., Long, J.D., Warner, J.H., Scahill, R.I., Leavitt, B.R., Stout, J.C., Paulsen, J.S. and Reilmann, R., 2014. Huntington disease: natural history, biomarkers and prospects for therapeutics. Nature Reviews Neurology, 10(4), pp.204-216.

Roth, S., Murray, B.S. and Dickinson, E., 2000. Interfacial shear rheology of aged and heat-treated β-lactoglobulin films: Displacement by nonionic surfactant. Journal of Agricultural and Food Chemistry, 48(5), pp.1491-1497.

Rothwarf, D.M. and Scheraga, H.A., 1993. Regeneration of bovine pancreatic ribonuclease A. 3. Dependence on the nature of the redox reagent. Biochemistry, 32(10), pp.2690-2697.

Sabaté, R. and Estelrich, J., 2005. Evidence of the existence of micelles in the fibrillogenesis of β-amyloid peptide. The Journal of Physical Chemistry B, 109(21), pp.11027-11032.

Sabaté, R., Baxa, U., Benkemoun, L., de Groot, N.S., Coulary-Salin, B., Maddelein, M.L., Malato, L., Ventura, S., Steven, A.C. and Saupe, S.J., 2007. Prion and non-prion amyloids of the HET-s prion forming domain. Journal of molecular biology, 370(4), pp.768-783.

Sabaté, R., Gallardo, M. and Estelrich, J., 2003. An autocatalytic reaction as a model for the kinetics of the aggregation of β-amyloid. Peptide Science, 71(2), pp.190-195.

Sahni, N., Yi, S., Taipale, M., Bass, J.I.F., Coulombe-Huntington, J., Yang, F., Peng, J., Weile, J., Karras, G.I., Wang, Y. and Kovács, I.A., 2015. Widespread macromolecular interaction perturbations in human genetic disorders. Cell, 161(3), pp.647-660.

Sakai, K., Sakurai, K., Sakai, M., Hoshino, M. and Goto, Y., 2000. Conformation and stability of thiol-modified bovine β lactoglobulin. Protein Science, 9(9), pp.1719-1729.

Sakurai, K. and Goto, Y., 2002. Manipulating monomer-dimer equilibrium of bovine β-lactoglobulin by amino acid substitution. Journal of Biological Chemistry, 277(28), pp.25735-25740.

Sakurai, K. and Goto, Y., 2006. Dynamics and mechanism of the Tanford transition of bovine β-lactoglobulin studied using heteronuclear NMR spectroscopy. Journal of molecular biology, 356(2), pp.483-496.

Sakurai, K., Oobatake, M. and Goto, Y., 2001. Salt-dependent monomer-dimer equilibrium of bovine β-lactoglobulin at pH 3. Protein Science, 10(11), pp.2325-2335.

Šali, A., Shakhnovich, E. and Karplus, M., 1994. Kinetics of protein folding: A lattice model study of the requirements for folding to the native state. Journal of molecular biology, 235(5), pp.1614-1636.

Sánchez, I.E. and Kiefhaber, T., 2003. Evidence for sequential barriers and obligatory intermediates in apparent two-state protein folding. Journal of molecular biology, 325(2), pp.367-376.

Sardar, S., Maity, S., Pal, S., Parvej, H., Das, N., Sepay, N., Sarkar, M. and Halder, U.C., 2016. Facile synthesis and characterization of β-lactoglobulin–copper nanocomposites having antibacterial applications. RSC advances, 6(88), pp.85340-85346.

Sardar, S., Pal, S., Maity, S., Chakraborty, J. and Halder, U.C., 2014. Amyloid fibril formation by β-lactoglobulin is inhibited by gold nanoparticles. International journal of biological macromolecules, 69, pp.137-145.

Sawaya, M.R., Sambashivan, S., Nelson, R., Ivanova, M.I., Sievers, S.A., Apostol, M.I., Thompson, M.J., Balbirnie, M., Wiltzius, J.J., McFarlane, H.T. and Madsen, A.Ø., 2007. Atomic structures of amyloid cross-β spines reveal varied steric zippers. Nature, 447(7143), pp.453-457.

Sawyer, L. and Kontopidis, G., 2000. The core lipocalin, bovine β-lactoglobulin. Biochimica et Biophysica Acta (BBA)-Protein Structure and Molecular Enzymology, 1482(1-2), pp.136-148.

Sawyer, L., Brownlow, S., Polikarpov, I. and Wu, S.Y., 1998. β-Lactoglobulin: structural studies, biological clues. International Dairy Journal, 8(2), pp.65-72.

Sawyer, L., Kontopidis, G. and Wu, S.Y., 1999. β-Lactoglobulin–a three-dimensional perspective. International journal of food science & technology, 34(5-6), pp.409-418.

Saxelin, M., Korpela, R. and Mäyrä-Mäkinen, A., 2003. Introduction: classifying functional dairy products.

Schmidt, A., Annamalai, K., Schmidt, M., Grigorieff, N. and Fändrich, M., 2016. Cryo-EM reveals the steric zipper structure of a light chain-derived amyloid fibril. Proceedings of the National Academy of Sciences, 113(22), pp.6200-6205.

Schmitt, C., Bovay, C., Rouvet, M., Shojaei-Rami, S. and Kolodziejczyk, E., 2007. Whey protein soluble aggregates from heating with NaCl: physicochemical, interfacial, and foaming properties. Langmuir, 23(8), pp.4155-4166.

Schokker, E.P., Singh, H., Pinder, D.N., Norris, G.E. and Creamer, L.K., 1999. Characterization of intermediates formed during heat-induced aggregation of β-lactoglobulin AB at neutral pH. International Dairy Journal, 9(11), pp.791-800.

Seebach, D., Hook, D.F. and Glättli, A., 2006. Helices and other secondary structures of β-and γ-peptides. Peptide Science: Original Research on Biomolecules, 84(1), pp.23-37.

Seo, J.A., Hédoux, A., Guinet, Y., Paccou, L., Affouard, F., Lerbret, A. and Descamps, M., 2010. Thermal denaturation of beta-lactoglobulin and stabilization mechanism by trehalose analyzed from Raman spectroscopy investigations. The Journal of Physical Chemistry B, 114(19), pp.6675-6684.

Séverin, S. and Wenshui, X., 2005. Milk biologically active components as nutraceuticals. Critical reviews in food science and nutrition, 45(7-8), pp.645-656.

Sgarbossa, A., Giacomazza, D. and Di Carlo, M., 2015. Ferulic acid: a hope for Alzheimer's disease therapy from plants. Nutrients, 7(7), pp.5764-5782.

Shah, N.P., 2000. Effects of milk-derived bioactives: an overview. British Journal of Nutrition, 84(S1), pp.3-10.

Shakya, A.K., Sami, H., Srivastava, A. and Kumar, A., 2010. Stability of responsive polymer–protein bioconjugates. Progress in Polymer Science, 35(4), pp.459-486.

Shang, L., Wang, Y., Jiang, J. and Dong, S., 2007. pH-dependent protein conformational changes in albumin: gold nanoparticle bioconjugates: a spectroscopic study. Langmuir, 23(5), pp.2714-2721.

Sharma, G.S., Krishna, S., Khan, S., Dar, T.A., Khan, K.A., and Singh, L.R., 2021. Protecting thermodynamic stability of protein: The basic paradigm against stress and unfolded protein response by osmolytes. International journal of biological macromolecules, 177, pp.229-240.

Shaw, E., 1970. Selective chemical modification of proteins. Physiological reviews, 50(2), pp.244-296.

Shi, T. and Rabenstein, D.L., 2000. Discovery of a highly selective and efficient reagent for the formation of intramolecular disulfide bonds in peptides. Journal of the American Chemical Society, 122(29), pp.6809-6815.

Shivaprasad, S. and Wetzel, R., 2004. An intersheet packing interaction in Aβ fibrils mapped by disulfide cross-linking. Biochemistry, 43(49), pp.15310-15317.

Shpigelman, A., Israeli, G. and Livney, Y.D., 2010. Thermally-induced protein–polyphenol co-assemblies: Beta lactoglobulin-based nanocomplexes as protective nanovehicles for EGCG. Food hydrocolloids, 24(8), pp.735-743.

Silva, S.V. and Malcata, F.X., 2005. Caseins as source of bioactive peptides. International dairy journal, 15(1), pp.1-15.

Simmons, M.J.H., Jayaraman, P. and Fryer, P.J., 2007. The effect of temperature and shear rate upon the aggregation of whey protein and its implications for milk fouling. Journal of Food Engineering, 79(2), pp.517-528.

Sitohy, M., Billaudel, S., Haertlé, T. and Chobert, J.M., 2007. Antiviral activity of esterified α-lactalbumin and β-lactoglobulin against herpes simplex virus type 1. Comparison with the effect of acyclovir and L-polylysines. Journal of Agricultural and Food Chemistry, 55(25), pp.10214-10220.

Sitohy, M., Chobert, J.M. and Haertle, T., 1995. Phosphorylation of β -Lactoglobulin under Mild Conditions. Journal of Agricultural and Food Chemistry, 43(1), pp.59-62.

Smethurst, P., Risse, E., Tyzack, G.E., Mitchell, J.S., Taha, D.M., Chen, Y.R., Newcombe, J., Collinge, J., Sidle, K. and Patani, R., 2020. Distinct responses of neurons and astrocytes to TDP-43 proteinopathy in amyotrophic lateral sclerosis. Brain, 143(2), pp.430-440.

Song, K.B. and Damodaran, S., 1991. Influence of electrostatic forces on the adsorption of succinylated. beta-lactoglobulin at the air-water interface. Langmuir, 7(11), pp.2737-2742.

Stanic-Vucinic, D., Prodic, I., Apostolovic, D., Nikolic, M. and Velickovic, T.C., 2013. Structure and antioxidant activity of β-lactoglobulin-glycoconjugates obtained by high-intensity-ultrasound-induced Maillard reaction in aqueous model systems under neutral conditions. Food Chemistry, 138(1), pp.590-599.

Stefani, M. and Dobson, C.M., 2003. Protein aggregation and aggregate toxicity: new insights into protein folding, misfolding diseases, and biological evolution. Journal of molecular medicine, 81, pp.678-699.

Stefani, M., 2007. Protein folding and misfolding, relevance to disease, and biological function. In Protein Misfolding in Neurodegenerative Diseases (pp. 25-92). CRC Press.

Stefani, M., 2010. Biochemical and biophysical features of both oligomer/fibril and cell membrane in amyloid cytotoxicity. The FEBS journal, 277(22), pp.4602-4613.

Steffensen, C.L., Andersen, M.L., Degn, P.E. and Nielsen, J.H., 2008. Cross-linking proteins by laccase-catalyzed oxidation: importance relative to other modifications. Journal of agricultural and food chemistry, 56(24), pp.12002-12010.

Stojadinovic, M., Burazer, L., Ercili-Cura, D., Sancho, A., Buchert, J., Velickovic, T.C. and Stanic-Vucinic, D., 2012. One-step method for isolation and purification of native β-lactoglobulin from bovine whey. Journal of the Science of Food and Agriculture, 92(7), pp.1432-1440.

Straub, J.E. and Thirumalai, D., 2011. Toward a molecular theory of early and late events in monomer to amyloid fibril formation. Annual review of physical chemistry, 62(1), pp.437-463.

Structural basis of the Tanford transition of bovine β-lactoglobulin. Biochemistry, 37(40), pp.14014-14023.

Sun, Y., Kakinen, A., Wan, X., Moriarty, N., Hunt, C.P., Li, Y., Andrikopoulos, N., Nandakumar, A., Davis, T.P., Parish, C.L. and Song, Y., 2021. Spontaneous formation of β-sheet nano-barrels during the early aggregation of Alzheimer's amyloid beta. Nano Today, 38, p.101125.

Surroca, Y., Haverkamp, J. and Heck, A.J.R., 2002. Towards the understanding of molecular mechanisms in the early stages of heat-induced aggregation of β-lactoglobulin AB. Journal of Chromatography A, 970(1-2), pp.275-285.

Svedberg, T., 1939. A discussion on the protein molecule. Proceedings of the Royal Society of London. Series A. Mathematical and Physical Sciences, 170(940), pp.40-79.

T. Matsumoto, Pediat. Allergy Immunol UK, 2011,22,235.

Tajc, S.G., Tolbert, B.S., Basavappa, R. and Miller, B.L., 2004. Direct determination of thiol pKa by isothermal titration microcalorimetry. Journal of the American Chemical Society, 126(34), pp.10508-10509.

Takagi, K., Teshima, R., Okunuki, H. and Sawada, J.I., 2003. Comparative study of in vitro digestibility of food proteins and effect of preheating on the digestion. Biological and Pharmaceutical Bulletin, 26(7), pp.969-973.

Tanaka, M., Collins, S.R., Toyama, B.H. and Weissman, J.S., 2006. The physical basis of how prion conformations determine strain phenotypes. Nature, 442(7102), pp.585-589.

Tanford, C. and Nozaki, Y., 1959. Physico-chemical comparison of β-lactoglobulins A and B.

Tanford, C., De, P.K. and Taggart, V.G., 1960. The Role of the α-Helix in the Structure of Proteins. Optical Rotatory Dispersion of β-Lactoglobulin1a. Journal of the American Chemical Society, 82(23), pp.6028-6034.

Tang, C.H. and Ma, C.Y., 2007. Modulation of the thermal stability of β-lactoglobulin by transglutaminase treatment. European Food Research and Technology, 225, pp.649652.

Taulier, N. and Chalikian, T.V., 2001. Characterization of pH-induced transitions of β-lactoglobulin: ultrasonic, densimetric, and spectroscopic studies. Journal of molecular biology, 314(4), pp.873-889.

Taylor, W.R., 1986. The classification of amino acid conservation. Journal of Theoretical Biology, 119(2), pp.205-218.

Thalmann, C. and Lötzbeyer, T., 2002. Enzymatic cross-linking of proteins with tyrosinase. European Food Research and Technology, 214, pp.276-281.

Therese, K.L., Jayanthi, U. and Madhavan, H.N., 2005. Application of nested polymerase chain reaction (nPCR) using MPB 64 gene primers to detect Mycobacterium tuberculosis DNA in clinical specimens from extrapulmonary tuberculosis patients. Indian Journal of Medical Research, 122(2), p.165.

Thirumalai, D., O'Brien, E.P., Morrison, G. and Hyeon, C., 2010. Theoretical perspectives on protein folding. Annual review of biophysics, 39(1), pp.159-183.

Timasheff, S.N. and Townend, R., 1961. Molecular Interactions in β-Lactoglobulin. VI. the Dissociation of the Genetic Species of β-Lactoglobulin at Acid pH's2. Journal of the American Chemical Society, 83(2), pp.470-473.

Tompa, P., Tusnády, G.E., Friedrich, P. and Simon, I., 2002. The role of dimerization in prion replication. Biophysical journal, 82(4), pp.1711-1718.

Towsend, R., Kumosisski, T.F. and Timasheff, S.N., 1967. The circular dichroism of variants of P-lactoglobulin. J. Biol. Chem, 242, pp.4538-4545.

Treece, J.M., Sheinson, R.S. and McMeekin, T.L., 1964. The solubilities of β-lactoglobulins a, B, and AB. Archives of Biochemistry and Biophysics, 108(1), pp.99-108.

Triulzi, R.C., Dai, Q., Zou, J., Leblanc, R.M., Gu, Q., Orbulescu, J. and Huo, Q., 2008. Photothermal ablation of amyloid aggregates by gold nanoparticles. Colloids and Surfaces B: Biointerfaces, 63(2), pp.200-208.

Tsong, T.Y., Baldwin, R.L., McPhie, P. and Elson, E.L., 1972. A sequential model of nucleation-dependent protein folding: kinetic studies of ribonuclease A. Journal of Molecular Biology, 63(3), pp.453-469.

Tycko, R., 2003. Insights into the amyloid folding problem from solid-state NMR. Biochemistry, 42(11), pp.3151-3159.

Tycko, R., 2004. Progress towards a molecular-level structural understanding of amyloid fibrils. Current opinion in structural biology, 14(1), pp.96-103.

Tycko, R., 2006. Molecular structure of amyloid fibrils: insights from solid-state NMR. Quarterly reviews of biophysics, 39(1), pp.1-55.

Tycko, R., 2011. Solid-state NMR studies of amyloid fibril structure. Annual review of physical chemistry, 62(1), pp.279-299.

Udgaonkar, J.B. and Baldwin, R.L., 1988. NMR evidence for an early framework intermediate on the folding pathway of ribonuclease A. Nature, 335(6192), pp.694-699.

Udgaonkar, J.B., 2008. Multiple routes and structural heterogeneity in protein folding. Annu. Rev. Biophys., 37(1), pp.489-510.

Udgaonkar, J.B., 2013. Polypeptide chain collapse and protein folding. Archives of biochemistry and biophysics, 531(1-2), pp.24-33.

Uhrínová, S., Smith, M.H., Jameson, G.B., Uhrín, D., Sawyer, L. and Barlow, P.N., 2000. Structural changes accompanying pH-induced dissociation of the β-lactoglobulin dimer. Biochemistry, 39(13), pp.3565-3574.

Uhrínová, S., Smith, M.H., Jameson, G.B., Uhrín, D., Sawyer, L. and Barlow, P.N., 2000. Structural changes accompanying pH-induced dissociation of the β-lactoglobulin dimer. Biochemistry, 39(13), pp.3565-3574.

Uversky, V.N. and Fink, A.L., 2004. Conformational constraints for amyloid fibrillation: the importance of being unfolded. Biochimica et Biophysica Acta (BBA)-Proteins and Proteomics, 1698(2), pp.131-153.

Uversky, V.N., 2010. Mysterious oligomerization of the amyloidogenic proteins. The FEBS journal, 277(14), pp.2940-2953.

Uversky, V.N., Narizhneva, N.V., Kirschstein, S.O., Winter, S. and Löber, G., 1997. Conformational transitions provoked by organic solvents in β-lactoglobulin: can a molten globule-like intermediate be induced by the decrease in dielectric constant? Folding and design, 2(3), pp.163-172.

Valastyan, J.S. and Lindquist, S., 2014. Mechanisms of protein-folding diseases at a glance. Disease models & mechanisms, 7(1), pp.9-14.

van Rooijen, B.D., Claessens, M.M. and Subramaniam, V., 2009. Lipid bilayer disruption by oligomeric α-synuclein depends on bilayer charge and accessibility of the hydrophobic core. Biochimica et Biophysica Acta (BBA)-Biomembranes, 1788(6), pp.1271-1278.

van Rooijen, B.D., Claessens, M.M. and Subramaniam, V., 2010. Membrane permeabilization by oligomeric α-synuclein: in search of the mechanism. PLoS One, 5(12), p.e14292.

vandenAkker, C.C., Engel, M.F., Velikov, K.P., Bonn, M. and Koenderink, G.H., 2011. Morphology and persistence length of amyloid fibrils are correlated to peptide molecular structure. Journal of the American Chemical Society, 133(45), pp.18030-18033.

Varley, P., Gronenborn, A.M., Christensen, H., Wingfield, P.T., Pain, R.H. and Clore, G.M., 1993. Kinetics of folding of the all-β sheet protein interleukin-1β. Science, 260(5111), pp.1110-1113.

Veitshans, T., Klimov, D. and Thirumalai, D., 1997. Protein folding kinetics: timescales, pathways and energy landscapes in terms of sequence-dependent properties. Folding and Design, 2(1), pp.1-22.

Verheul, M., Roefs, S.P. and de Kruif, K.G., 1998. Kinetics of heat-induced aggregation of β-lactoglobulin. Journal of Agricultural and Food Chemistry, 46(3), pp.896-903.

Vertegel, A.A., Siegel, R.W. and Dordick, J.S., 2004. Silica nanoparticle size influences the structure and enzymatic activity of adsorbed lysozyme. Langmuir, 20(16), pp.6800-6807.

Vetri, V. and Militello, V., 2005. Thermal-induced conformational changes involved in the aggregation pathways of beta-lactoglobulin. Biophysical chemistry, 113(1), pp.83-91.

Virtanen, T., 2001. Lipocalin allergens. Allergy, 56, pp.48-51.

Viseu, M.I., Carvalho, T.I. and Costa, S.M., 2004. Conformational transitions in β-lactoglobulin induced by cationic amphiphiles: equilibrium studies. Biophysical journal, 86(4), pp.2392-2402.

Viseu, M.I., Melo, E.P., Carvalho, T.I., Correia, R.F. and Costa, S.M., 2007. Unfolding kinetics of β-lactoglobulin induced by surfactant and denaturant: A stopped-flow/fluorescence study. Biophysical journal, 93(10), pp.3601-3612.

Wagner, V.A., Schild, T.A. and Geldermann, H., 1994. DNA variants within the 5′-flanking region of milk-protein-encoding genes II. The β-lactoglobulin-encoding gene. Theoretical and Applied Genetics, 89, pp.121-126.

Wahlgren, M.C. and Arnebrant, T., 1991. Interaction of cetyltrimethylammonium bromide and sodium dodecyl sulfate with β-lactoglobulin and lysozyme at solid surfaces. Journal of colloid and interface science, 142(2), pp.503-511.

Wang, L., Maji, S.K., Sawaya, M.R., Eisenberg, D. and Riek, R., 2008. Bacterial inclusion bodies contain amyloid-like structures. PLoS biology, 6(8), p.e195.

Wang, Q., Pan, M.H., Chiou, Y.S., Li, Z., Wei, S., Yin, X. and Ding, B., 2022. Insights from alpha-lactoalbumin and beta-Lactoglobulin into mechanisms of nanoliposome-whey protein interactions. Food hydrocolloids, 125, p.107436.

Wang, S., Zheng, J., Ma, L., Petersen, R.B., Xu, L. and Huang, K., 2022. Inhibiting protein aggregation with nanomaterials: the underlying mechanisms and impact factors. Biochimica et Biophysica Acta (BBA)-General Subjects, 1866(2), p.130061.

Waninge, R., Paulsson, M., Nylander, T., Ninham, B. and Sellers, P., 1998. Binding of sodium dodecyl sulfate and dodecyl trimethyl ammonium chloride to β-lactoglobulin: a calorimetric study. International Dairy Journal, 8(2), pp.141-148.

Wasmer, C., Lange, A., Van Melckebeke, H., Siemer, A.B., Riek, R. and Meier, B.H., 2008. Amyloid fibrils of the HET-s (218–289) prion form a β solenoid with a triangular hydrophobic core. Science, 319(5869), pp.1523-1526.

Westermark, P., Andersson, A. and Westermark, G.T., 2011. Islet amyloid polypeptide, islet amyloid, and diabetes mellitus. Physiological Reviews, 91(3), pp.795-826.

Wetlaufer, D.B., 1973. Nucleation, rapid folding, and globular intrachain regions in proteins. Proceedings of the National Academy of Sciences, 70(3), pp.697-701.

Wetzel, R., Shivaprasad, S. and Williams, A.D., 2007. Plasticity of amyloid fibrils. Biochemistry, 46(1), pp.1-10.

Woerner, A.C., Frottin, F., Hornburg, D., Feng, L.R., Meissner, F., Patra, M., Tatzelt, J., Mann, M., Winklhofer, K.F., Hartl, F.U. and Hipp, M.S., 2016. Cytoplasmic protein aggregates interfere with nucleocytoplasmic transport of protein and RNA. Science, 351(6269), pp.173-176.

Wolynes, P.G., Onuchic, J.N. and Thirumalai, D., 1995. Navigating the folding routes. Science, 267(5204), pp.1619-1620.

Woo, S.L. and Richardson, T., 1983. Functional properties of phosphorylated β-lactoglobulin. Journal of Dairy Science, 66(5), pp.984-987.

Woo, S.L., Creamer, L.K. and Richardson, T., 1982. Chemical phosphorylation of bovine β -lactoglobulin. Journal of Agricultural and Food Chemistry, 30(1), pp.65-70.

Wood, A. ed., 2016. Physiology, biophysics, and biomedical engineering. Taylor & Francis.

Wu, H. and Zhang, Y., 2014. Reversing DNA methylation: mechanisms, genomics, and biological functions. Cell, 156(1), pp.45-68.

Wu, X. and Narsimhan, G., 2008. Characterization of secondary and tertiary conformational changes of β-lactoglobulin adsorbed on silica nanoparticle surfaces. Langmuir, 24(9), pp.4989-4998.

Wu, X. and Narsimhan, G., 2008. Effect of surface concentration on secondary and tertiary conformational changes of lysozyme adsorbed on silica nanoparticles. Biochimica et Biophysica Acta (BBA)-Proteins and Proteomics, 1784(11), pp.1694-1701.

Xu, J., Hao, M., Sun, Q. and Tang, L., 2019. Comparative studies of the interaction of βlactoglobulin with three polyphenols. International journal of biological macromolecules, 136, pp.804-812.

Xue, W.F., Hellewell, A.L., Gosal, W.S., Homans, S.W., Hewitt, E.W. and Radford, S.E., 2009. Fibril Fragmentation Enhances Amyloid Cytotoxicity. Journal of Biological Chemistry, 284(49), pp.34272-34282.

Xue, W.F., Hellewell, A.L., Hewitt, E.W. and Radford, S.E., 2010. Fibril fragmentation in amyloid assembly and cytotoxicity: when size matters. Prion, 4(1), pp.20-25.

Yagi, M., Sakurai, K., Kalidas, C., Batt, C.A. and Goto, Y., 2003. Reversible unfolding of bovine β-lactoglobulin mutants without a free thiol group. Journal of Biological Chemistry, 278(47), pp.47009-47015.

Yalcin, A.S., 2006. Emerging therapeutic potential of whey proteins and peptides. Current pharmaceutical design, 12(13), pp.1637-1643.

Yan, W., Zhou, J., Sun, M., Chen, J., Hu, G. and Shen, B., 2014. The construction of an amino acid network for understanding protein structure and function. Amino acids, 46, pp.1419-1439.

Yancey, P.H. and Somero, G.N., 1979. Counteraction of urea destabilization of protein structure by methylamine osmoregulatory compounds of elasmobranch fishes. Biochemical Journal, 183(2), pp.317-323.

Yeates, T.O. and McPherson, A., 2019. The structure of bovine β-lactoglobulin in crystals grown at pH 3.8 exhibiting novel threefold twinning. Acta Crystallographica Section F: Structural Biology Communications, 75(10), pp.640-645.

Yonashiro, R., Tahara, E.B., Bengtson, M.H., Khokhrina, M., Lorenz, H., Chen, K.C., Kigoshi-Tansho, Y., Savas, J.N., Yates III, J.R., Kay, S.A. and Craig, E.A., 2016. The Rqc2/Tae2 subunit of the ribosome-associated quality control (RQC) complex marks ribosome-stalled nascent polypeptide chains for aggregation. Elife, 5, p.e11794.

Yong, W., Lomakin, A., Kirkitadze, M.D., Teplow, D.B., Chen, S.H. and Benedek, G.B., 2002. Structure determination of micelle-like intermediates in amyloid β-protein fibril assembly by using small angle neutron scattering. Proceedings of the National Academy of Sciences, 99(1), pp.150-154.

Yoshida, S., 1990. Isolation of β-lactoglobulin and α-lactalbumin by gel filtration using sephacryl S-200 and purification by diethylaminoethyl ion-exchange chromatography. Journal of Dairy Science, 73(9), pp.2292-2298.

Yoshikawa, M., Mizukami, T., Sasaki, R. and Chiba, H., 1978. Pre-β-lactoglobulin synthesis by mRNA from bovine mammary gland. Agricultural and Biological Chemistry, 42(11), pp.2185-2186.

Zaman, M., Khan, A.N., Zakariya, S.M. and Khan, R.H., 2019. Protein misfolding, aggregation and mechanism of amyloid cytotoxicity: An overview and therapeutic strategies to inhibit aggregation. International journal of biological macromolecules, 134, pp.1022-1037.

Zhang, Q., Cheng, Z., Chen, R., Wang, Y., Miao, S., Li, Z., Wang, S. and Fu, L., 2021. Covalent and non-covalent interactions of cyanidin-3-O-glucoside with milk proteins revealed modifications in protein conformational structures, digestibility, and allergenic characteristics. Food & Function, 12(20), pp.10107-10120.

Zhao, C., Chen, N. and Ashaolu, T.J., 2022. Whey proteins and peptides in health-promoting functions–A review. International Dairy Journal, 126, p.105269.

Zhao, D., Peng, Z., Fang, J., Fang, Z. and Zhang, J., 2023. Programmable and low-cost biohybrid membrane for efficient heavy metal removal from water. Separation and Purification Technology, 306, p.122751.

Zhou, H.X. and Pang, X., 2018. Electrostatic interactions in protein structure, folding, binding, and condensation. Chemical Reviews, 118(4), pp.1691-1741.

CHAPTER 2

Review Literature on Chalcones

2.1. General Overview of Chalcones

The production of a wide array of bioactive substances by living organisms has served as a rich source of inspiration for scientists in the ongoing quest to develop new medicinal agents. In the field of pharmaceutical and drug discovery studies, heterocycles stand out as essential pharmacophores (Guo et al., 2021; Atanasov et al., 2015; Butler, 2004). The historical records of ancient civilizations such as the Egyptians, Chinese, and Mesopotamians document a diverse range of plant-based medicines, some of which are still in use today (Cragg et al., 2009; Tay et al., 2020). However, the development of natural product drugs has been met with inherent challenges, prompting a shift in focus within the pharmaceutical industry towards the exploration of synthetic compound libraries and high-throughput screening (HTS) to identify potential pharmacological leads (Bernardini et al., 2018; David et al.,2015; Zheng et al., 2023). One noteworthy category of polyphenolic chemical substances is the (E)-1,3-diphenyl-2-propene-1-ones, commonly known as chalcones. These compounds are classified under the abundant class of natural substances referred to as flavonoids and isoflavonoids, which are prevalent in fruits, vegetables, teas, and soy products. Chalcones represent a highly diverse group of flavonoids, readily undergoing cyclization to yield the flavonoid structure—a pivotal isomeric process in the skeletal modification of chalcones. The chalcone scaffold is characterized by a unique structure consisting of two phenyl rings linked by a propenone bridge, forming an unsaturated carbonyl system with three carbons **(Fig.1)**. Illustrative of their chemical structure, chalcones exist in two distinct forms: the trans (E, 1) and cis (Z, 2) isomers. The trans isomers, or E isomers, are more commonly encountered due to their greater thermodynamic stability, whereas the cis isomers, or Z isomers, are comparatively less stable owing to steric hindrance arising from interactions between the carbonyl group and ring B (Aksöz and Ertan,2011; Gomes et al., 2017; Shalaby et al., 2023). Chalcones feature two aromatic rings and an electrophilic αβ-unsaturated carbonyl system that are continuously conjugated. This structural attribute may account for their low redox potential, stability, electron transfer reactions, and, most notably, their promising biological activities (Gaonkar and Vignesh, 2017). Consequently, chalcones represent a novel class of compounds with substantial therapeutic potential against various diseases. This rich complexity has contributed to decades of intensive research into chalcones and their diverse properties (Qiu et al., 2021;

Nowakowska, 2007). In higher plants, an enzyme known as chalcone synthase converts p-coumaroyl-CoA and malonyl-CoA into chalcones. L-phenylalanine is converted into p-coumaroyl-CoA through the phenylpropanoid pathway, which produces the chalcone aromatic B-ring and 3C bridge. Chalcone undergoes various metabolic pathways in plants, leading to the production of aurones, glycosyl conjugates, and naringenin. Chalcones play a crucial ecological role as signaling molecules in plant-microbe symbioses and as biochemical regulators of plant dispersal. Glycosyl-conjugated chalcones, which are also common in flowers, are essential for pollination (Rammohan et al., 2020; Díaz-Tielas et al., 2016; Martínez-Luis et al., 2007). The chalcone family has garnered significant attention due to its wide spectrum of biological activity, as well as from synthesis and biosynthesis perspectives. Plants and herbs have been used for thousands of years to create chalcones as remedies for various illnesses, such as cancer, diabetes, and inflammation (Zhuang et al., 2017; Rudrapal et al., 2021; Ammaji et al., 2022**)**. Chalcone compounds are classified according to their molecular structures, with the prevalent substances in plants often undergoing hydroxylation or methoxylation **(Fig.2)** (Rajendran et al., 2022). Several hydroxy chalcones possess medicinal and pharmaceutical potential, including anti-cancer (Asakura and Kitahora, 2018; Qin et al.,2008), antioxidant (Ammaji et al., 2022), anti-inflammatory (Abu et al.,2013; Feldman et al., 2010), antidiabetic (Padmavathi et al., 2017), antimicrobial, and neuroprotective properties (Wang, 2010; Park et al., 2014; Kil et al 2017). Notably, clinical trials have demonstrated positive results in the treatment of trunk or branch varicosity and chronic venous lymphatic insufficiency using hesperidin methylchalcone and hesperidin trimethylchalcone **(Fig. 3)**.

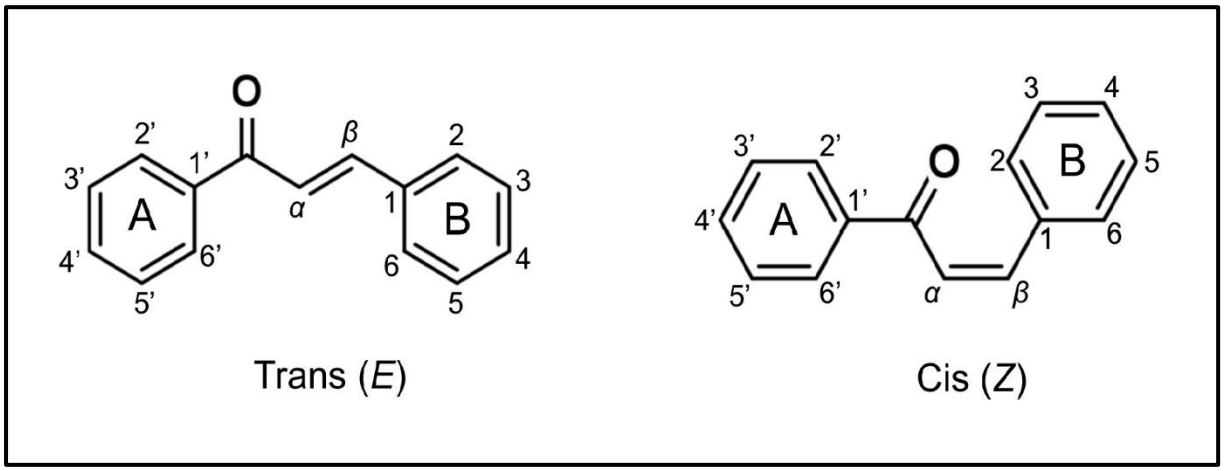

Figure 1: Structural and numerical representations of chalcone scaffold. (Adapted from Gomes et al., 2017).

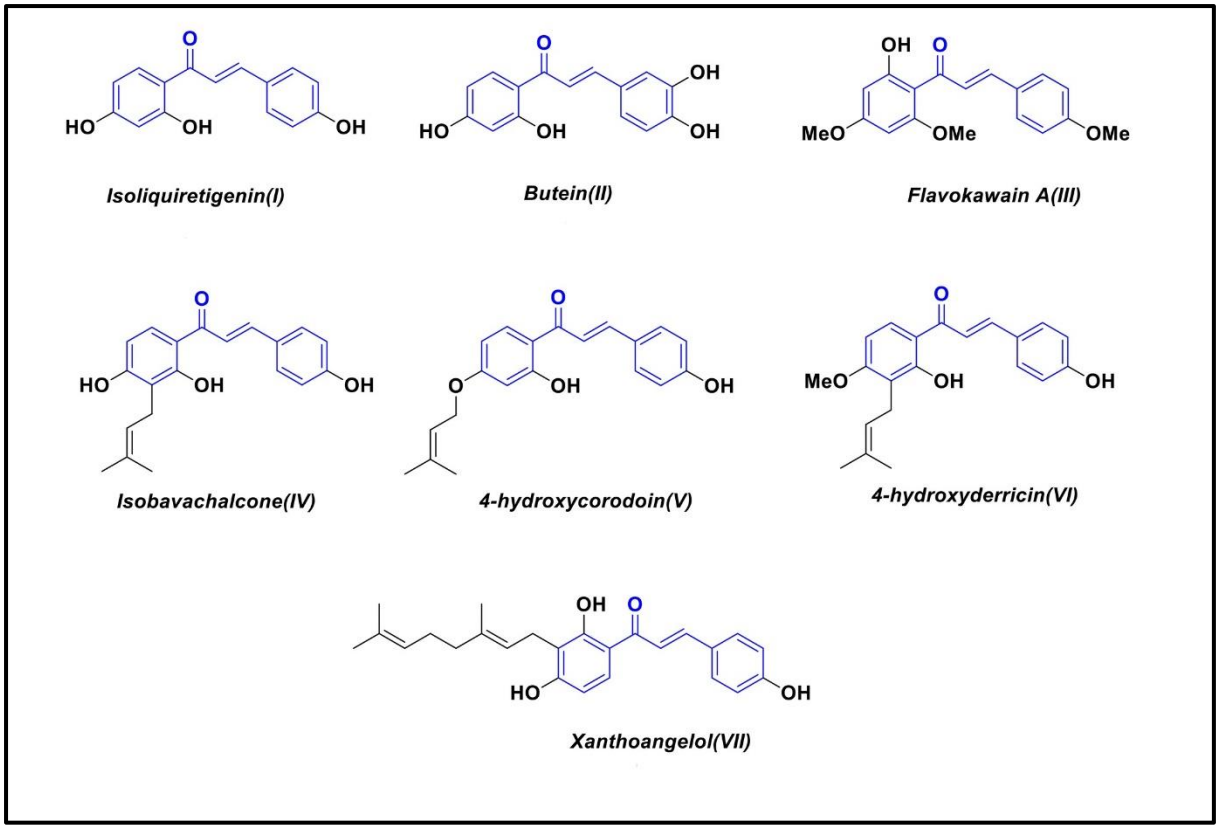

Figure 2: Analogues of chalcones with relevant biological applications. (Adapted from Shalaby et al., 2023).

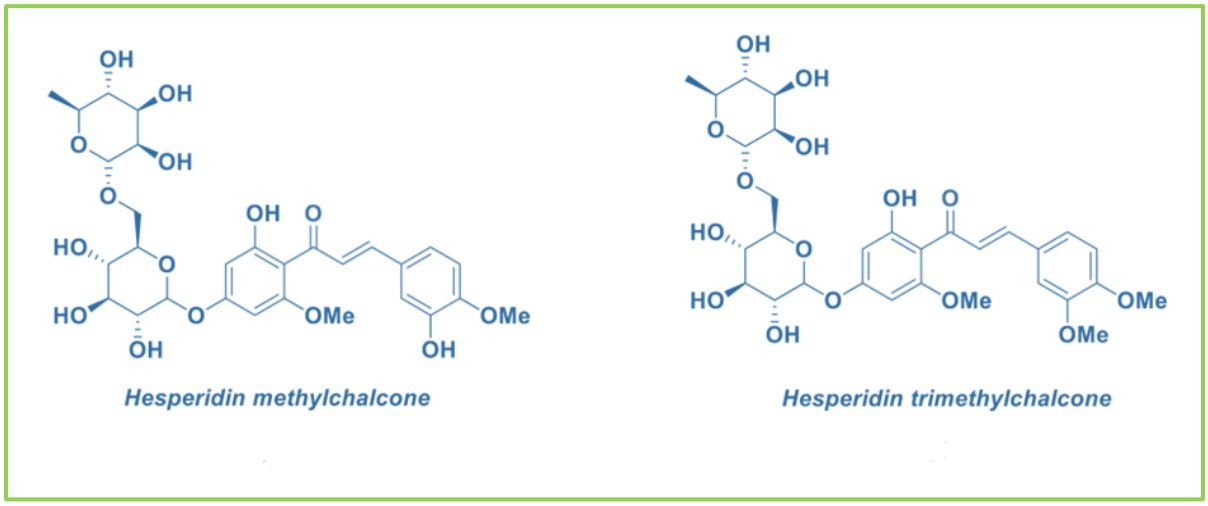

Figure 3: Chemical structures of naturally occurring chalcones approved for clinical use. (Adapted from Shalaby et al., 2023).

2.2. Nomenclature

The accepted IUPAC nomenclature for chalcone is 1,3-diphenyl-2-propen-1-one, also known as phenyl styryl ketone. It is notable that the numbering of positions within the chalcone nucleus is reversed compared to the structure of flavonoids. Within the chalcone, the aryl rings are denoted as rings A and B, with ring A utilizing primed numbers and ring B employing non-primed numbers, as illustrated in **(Fig.4)**. Generally, naturally occurring chalcones feature substitutions such as hydroxyls, methylation, and prenylation. They may also manifest as dihydrochalcones, dimers (bichalcones), and glycosides. Additionally, the numbering system serves to denote the positioning of fused ring prenyl substituents, including furano and pyrano groups, as illustrated in **(Fig. 4)**.

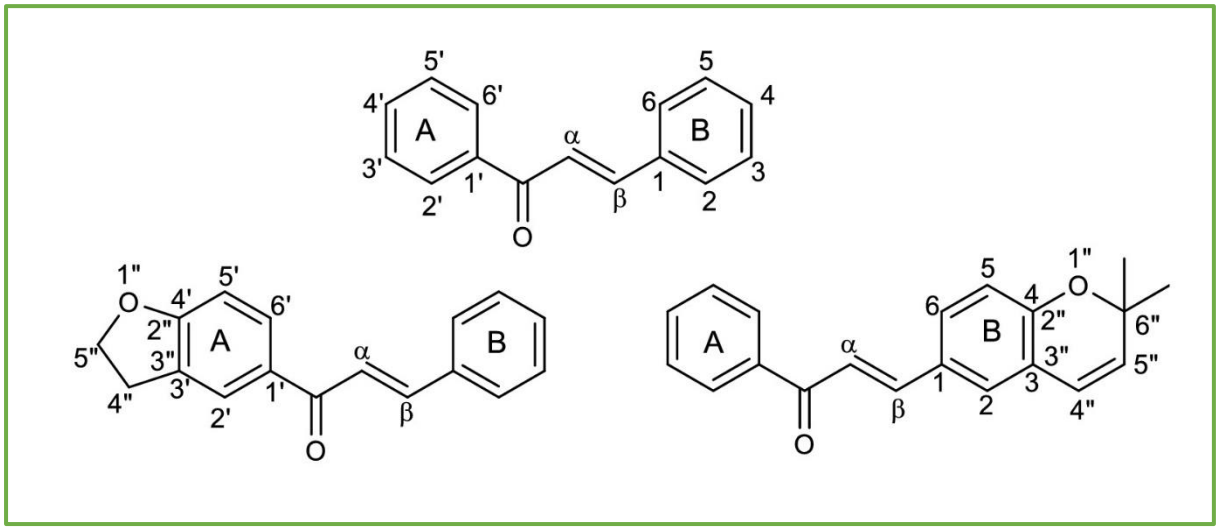

Figure 4: Systematic numbering of simple and fused ring prenyl substituted chalcones.

2.3. Biosynthesis of Chalcones

Numerous publications have elucidated the biosynthesis of chalcones. The dependable methodology expounded by Andersen and Markham (2006) is explicated herein. The biosynthesis of chalcones is a complex process that involves the convergence of two biogenesis pathways. Ring-A of chalcone is derived from the acetate pathway, specifically from phloroglucinol (a C6 unit), while the B-ring comes from the phenylpropanoid precursor (a C9 unit) synthesized through the shikimate pathway. This process includes the condensation of a phenylpropanoid CoA (p-coumaroyl CoA) with three molecules of melanoyl coenzyme A (melanoyl-CoA) to produce a tetraketide precursor. The tetraketide can undergo cyclization in two different ways: firstly, cyclization in the presence of chalcone synthase results in the formation of chalcone tri-oxygenation in ring A (Chalconaringenin), and secondly, reduction

in the presence of NADPH followed by cyclization in the presence of chalcone synthase produces 6'-deoxychalcone (Isoliquiritigenin). The presence of NADPH reductase of either tri or tetraketide serves as evidence for the formation of many 6'-deoxychalcones in Leguminosae.

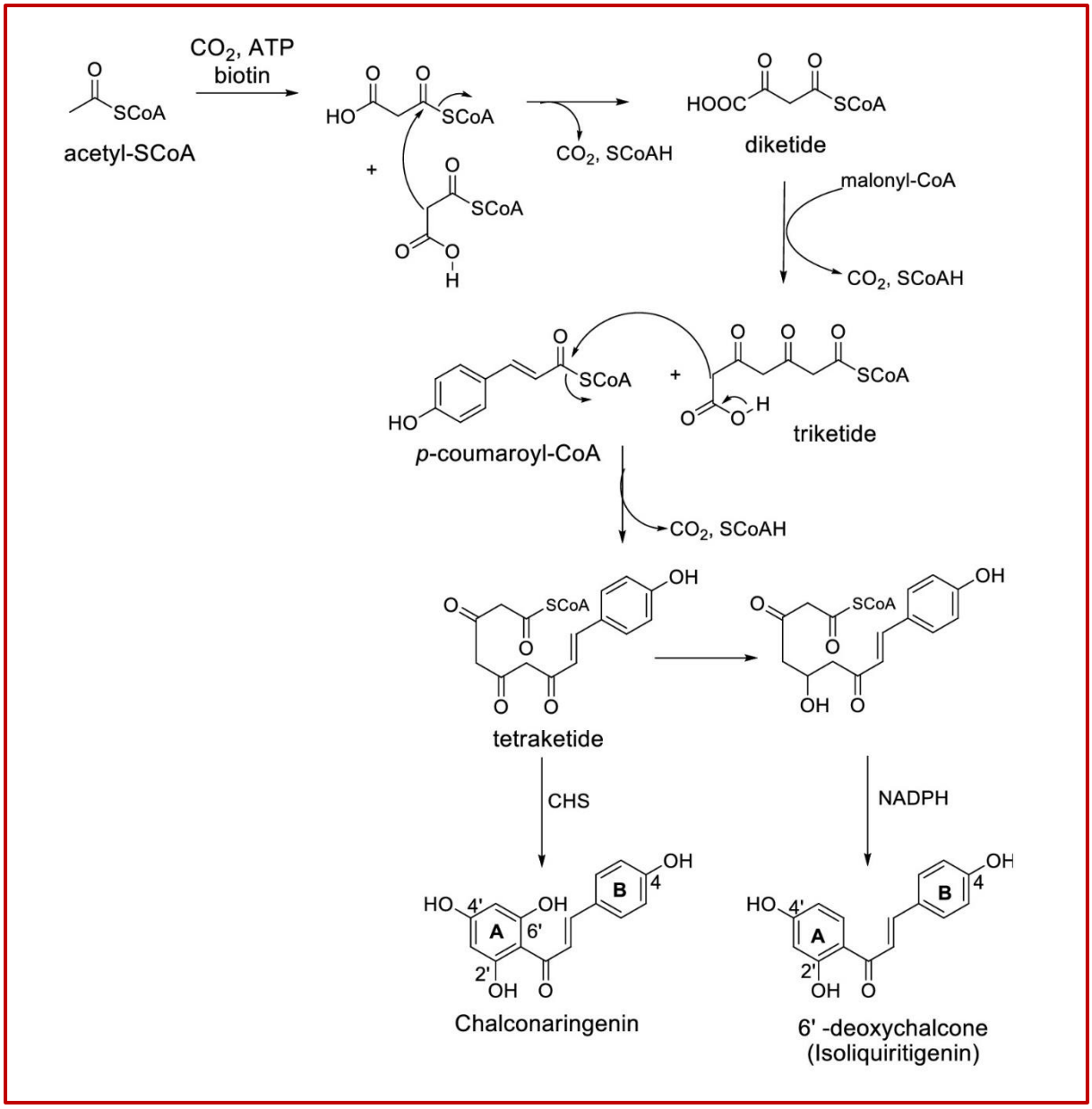

Figure 5: The biosynthesis of chalcones through tetraketide cyclization in the presence of chalcone synthase as well as reduction of tetraketide in the presence of NADPH reductase.

2.4. Physical and Chemical Properties

Chalcones are found not only in flowers but also in leaves, fruits, roots, stems, and all parts of the plant kingdom. Naturally occurring chalcones are typically crystalline solids and can have various colors such as yellow, orange, and brown. They are more stable than their related flavonoids and isoflavonoids. Chalcones are soluble in alcohols, aqueous acidic and alkaline

solutions, as well as organic solvents like acetone, chloroform, and dichloromethane. In alkaline solutions, they show deep red or orange-red colors. All chalcones test positive with the Wilson test, displaying a pink colorization with concentrated H_2SO_4. When treated with alcoholic ferric chloride solution, chalcones produce a violet colorization, indicating the presence of free phenolic hydroxyl groups. Chalcones undergo isomerization reactions to form flavonoids (Andersen and Markham, 2006; Harborne et al., 1975) as illustrated in **(Fig.6).**

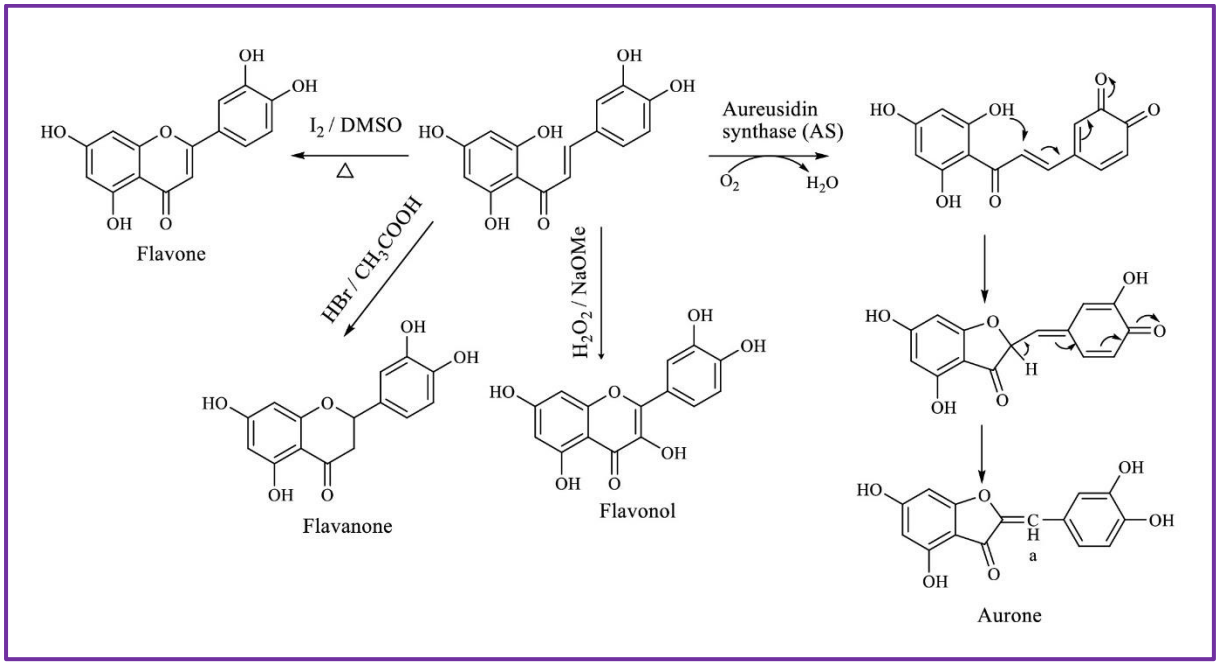

Figure 6: Possible isomerization reactions of chalcones as flavanone, flavonol, and aurone at different reaction pathways.

- When chalcones are heated with traces of iodine in dimethyl sulphoxide for 2 hours, they yield the corresponding flavones.
- Flavanones can be easily produced through the cyclization of chalcones when treated with hydrobromic acid in glacial acetic acid. In this isomerization reaction, partial demethylation and debenzylation may occur.
- Chalcones are converted into flavonols by oxidizing them using hydrogen peroxide in a methanolic sodium hydroxide solution.
- Another important isomerization reaction involves the formation of aurones from chalcone precursors in the presence of aureusidin synthase (Nakayama et al. 2001). The initial transformation of the o-dihydroxy groups of B-ring to an o-diquinone is a significant conversion because the presence of one or no hydroxyl groups in ring-B is currently unknown.

2.5. Fluorescent Properties of Chalcones

When a molecule is excited to a higher state, it emits electromagnetic radiation within a few nanoseconds, displaying the photoluminescence phenomenon known as fluorescence (Lakowicz,2006). Fluorophores, also known as fluorescent dyes, are compounds with fluorescence qualities, and their structural characteristics contribute to the fluorescence mechanism (Sapsford et al., 2006). The efficiency of fluorescence is measured by the Quantum yield (Φ_F), defined as the ratio of emitted photons to absorbed photons. A fluorescence quantum yield of 1.0 (100%) is reached when the number of absorbed photons equals the number of emitted photons, achieving the maximum (Φ_F) value. Additionally, excited 2′-hydroxychalcones have a broader range of reactivity than other chalcone derivatives, displaying exclusively cis/trans-isomerization and dimerization (Serdiuk et al., 2018; Leydet et al., 2013; Yaylı et al., 2005). The presence of the hydroxyl group at position 2' in the chalcone induces photoinduced cyclization, giving rise to the production of flavanone (Aksöz and Ertan, 2011; Fahim et al., 2021) and dark acid-base (Harborne, 2013). Additionally, phototautomers are formed due to intramolecular proton transfer (ESIPT) in the excited state, facilitated by hydrogen bonding between carbonyl and hydroxyl groups (Tokumura et al., 1998; Teshima et al., 2009). The fluorescence and nonlinear optical properties of chalcone and its derivatives, stemming from the π-conjugated planar structure, have garnered significant attention due to the delocalization of electronic charge distribution and overlapping π orbitals (Zhang et al., 2017). Chalcone and its derivatives are conventional luminogenic materials that exhibit strong luminescence in the solution state but diminish this property in high-concentration solutions or solids (Komarova et al., 2015). However, by introducing electron donors or acceptors into aromatic rings, their optical properties can be altered. Given the significance of chalcones and their structural modifiability, it is plausible to develop and manufacture chalcones that emit intense fluorescence in the solid state, thereby presenting potential value as chemical probes for mechanistic investigations and imaging/diagnosis.

The chalcone present in chalcone-based compounds functions as an optically active moiety and a recognition unit for the selective detection of target analytes. Upon interacting with the analytes, the photophysical properties of these compounds are disturbed, rendering them suitable for application as selective chemosensors in analytical contexts. Various methodologies, including photoinduced electron transfer (PET), intermolecular charge transfer (ICT), chelation-enhanced fluorescence (CHEF), and aggregation-induced emission (AIE), have been implemented in the development of chalcone-based chemosensors (D'Aléo et al.,

2015; Karuppusamy et al., 2017). Notably, a range of chalcones featuring appropriate substituents (electron-withdrawing functional groups) on both aryl rings have been identified to exhibit intrinsic fluorescence properties (Colucci-Guyon et al., 2019; Yu et al., 2017), as depicted in **(Fig.7)**.

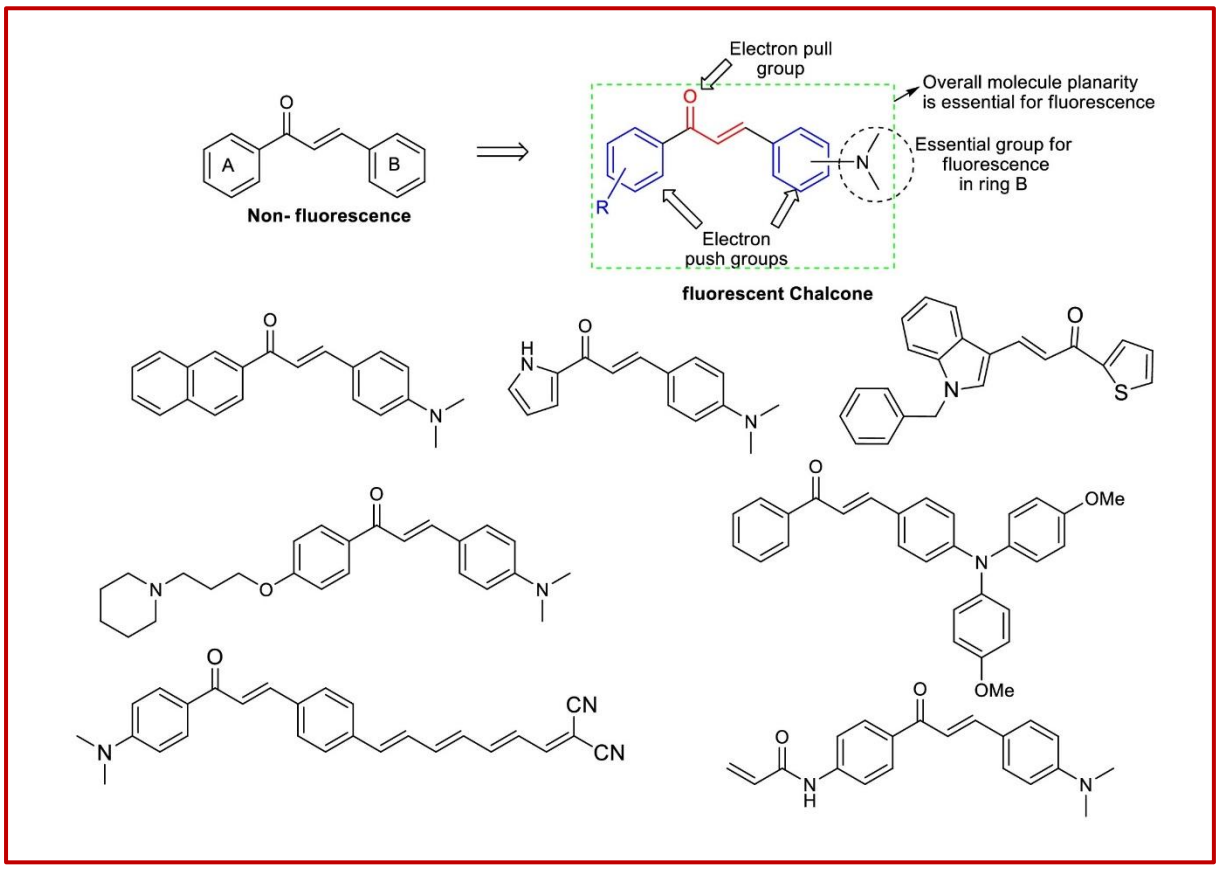

Figure 7: Several previously documented fluorescent chalcones and their corresponding structural analyses.

Fluorescent materials have garnered significant attention due to their potential applications in various fields such as chemical probes, electrochromic materials, fluorescent dyes, and sensors, as well as their use as additives in dye-sensitized solar cells. They also play a crucial role in the diagnosis for the development of new drugs (Da Costa et al.,2019; Krupadam, 2011; Tomasch et al., 2012; Watanabe et al., 2018; Yun et al.,2014; Zhou et al. 2016). Currently, fluorescent chalcones are being utilized to detect several diseases through emission color changes in living cells (Tomasch et al.,2012). These fluorescent chalcones offer new opportunities for using nonradioactive substitutes (Yun et al.,2014). Additionally, fluorescent chalcones are valuable for investigating cellular targets and as chemical probes for mechanistic investigations (Zhou et al. 2016). Watanabe et al., (2018) reported novel fluorescent chalcone analogues for inhibiting the formation of β-amyloid plaques, the current therapeutic approach used to treat

Alzheimer's disease (AD). In another study, heteroaryl chalcones with both electron donor and acceptor groups were reported (Pannipara et al., 2015) by altering the polarity of aprotic solvents, thereby enhancing the quantum yields and fluorescence intensity through intramolecular charge transfer (ICT). Pasricha et al., (2017) investigated the interaction of bovine serum albumin with napthylchalcone derivatives using the key parameter of fluorescence quenching.

Chalcones containing suitable substituents (electron-withdrawing functional groups) on both aryl rings have been reported to exhibit intrinsic fluorescence **(Fig.7)**. The fundamental parameters involved in the investigation of fluorescence include absorption (Abs_{nm}) and emission (Emi_{nm}) wavelengths, extinction coefficient (ε), and quantum yield (Φ). These physical parameters are contingent upon the electron density across the molecule, crucial for displaying intrinsic fluorescence. Based on prior experimental analysis, for a chalcone to qualify as a noteworthy fluorescent material, specific structural characteristics must be present.

- The molecule must exhibit planarity.
- In ring A, weak electron-donating groups such as methoxyl groups produce promising quantum yields, as opposed to electron-withdrawing groups like nitro and nitrile groups, which result in lower quantum yields.
- In-ring B, the presence of a disubstituted amino group such as dimethylamino, diethylamino, diaryl amino, or piperazine, piperidine groups holds great significance for achieving higher extinction coefficients, greater quantum yields, and fluorescence with a lower ionization potential.
- Moreover, an extension of the conjugation of the α, β-unsaturated system with additional bonds leads to reduced fluorescence and a resultant redshift of the maximum emission.

2.6. Spectral Properties of Chalcones

The technique of Ultraviolet and Visible absorption spectroscopy has long been recognized as essential for the identification of functional groups in flavonoids and chalcones. The UV spectrum of chalcones is characterized by two prominent absorption bands. The first band, known as band I, falls within the range of 340-390 nm, while the second, referred to as band II, occurs in the range of 200-270 nm. Generally, band II originates from the ring-A benzoyl system, whereas band I stems from the B-ring cinnamoyl system, as documented by Harborne et al., (2013) **(Fig.8)**. Notably, the chalcone band I occasionally manifests in the visible

spectrum, akin to anthocyanins, potentially contributing to their diverse solutions of colors, as posited by De Freitas and Mateus (2006). Furthermore, a less conspicuous, shoulder-like absorption peak is discernible in the UV spectrum of chalcones at 300-320 nm, a feature that often eludes detection.

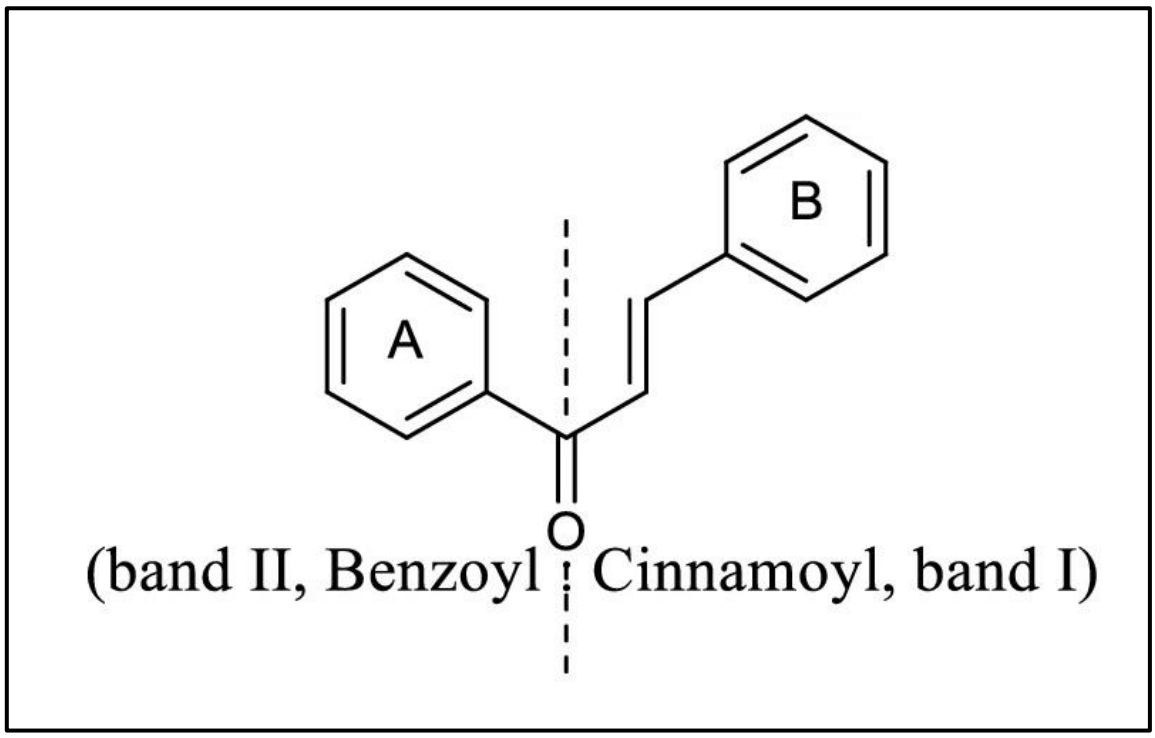

Figure 8: Classification of UV absorption bands in chalcones: Band I is attributed to the absorption of the cinnamoyl group, while Band II is attributed to the benzoyl chromophore of the chalcone

In chalcones, increasing the number of free hydroxyl groups leads to bathochromic shifts in both UV absorption bands, particularly in band I. If the 2'-hydroxyl group of chalcone is protected with a methyl, prenyl, or sugar moiety, a 15-20 nm hypochromic shift occurs in band II, while other positions show little effect. The positions of hydroxyl groups can be estimated significantly using shift reagents such as sodium methoxide (NaOMe), sodium acetate (NaOAc), sodium acetate/boric acid ($NaOAc/H_3BO_3$), aluminum chloride ($AlCl_3$), and aluminum chloride/hydrochloric acid ($AlCl_3$/HCl), as described by Mabry et al., (1970). The proton magnetic resonance (PMR) spectrum of chalcones displays two characteristic signals for H_α and H_β in the range of δ 6.7-7.4 and 7.3-7.7, respectively, as doublets (J =15-17 Hz) (Harborne et al., 2013). Additionally, the carbon nuclear magnetic resonance (^{13}C NMR) spectrum shows three characteristic signals for a chalcone: a typical signal for carbonyl in the range of δ188.6-194.4, and two other prominent signals for C_α and C_β in the ranges of 116.1-

128.1 and 136.9-145.4 ppm, respectively (Ward, 1990). These distinct UV and NMR patterns are valuable for detecting chalcones in natural product discovery.

2.7. Structural Diversity of Natural Chalcones

Chalcones featuring commonplace substituents such as hydroxyls, methoxyls, prenyls, and glycosides are abundant in natural settings. Conversely, chalcones with distinctive bonding and substitutions have been identified in botanical specimens. Illustrated in (Fig.9**)** are examples of these unique chalcones. Notably, two unusual β-OH chalcones have been discovered in natural sources. Galiposin (9A), a bis(methylenedioxy) chalcone, has been isolated from Galipea granulosa (Rutaceae), representing the initial instance documented in the literature (Lopez et al., 1998). Similarly, 2' β-hydroxy-4',6'-dimethoxy-3'-methyl chalcone (9B) has been sourced from the aerial parts of Leptospermum scoparium (Myrtaceae) (Mayer, 1993). Moreover, a bisdesmosidic triglycoside (9C) derived from the roots of Glycyrrhiza aspera (Leguminosae) stands out as a rare chalcone, characterized by the unusual bonding of three sugar moieties described in the literature to date (Kitagawa et al., 1998). Lastly, Rhuschalcone VI (9D), extracted from Rhus pyroides, constitutes a bichalcone formed through C-C linkage of two isoliquiritigenin units, a highly uncommon occurrence in nature (Masesane et al., 2000; Mdee et al., 2003). Azobechalcone (9E), an atypical oligomeric chalcone derived from Lophira alata (Ochnaceae), is formed through the condensation of six isoliquiritigenin (monomeric chalcone) molecules (Tih et al.,1999). The isolation and structural elucidation of this molecule poses significant challenges in the absence of thorough 2D NMR spectral characterization. Moreover, chalcones are notably relevant as dienophiles in Diels-Alder reactions and can manifest as Diels-Alder adducts in natural sources, particularly in plants within the Moraceae family. Sanggenon R (9F) stands as the initial documented instance of a Diels-Alder adduct derived from the roots of Morus species (Hano et al., 1995).

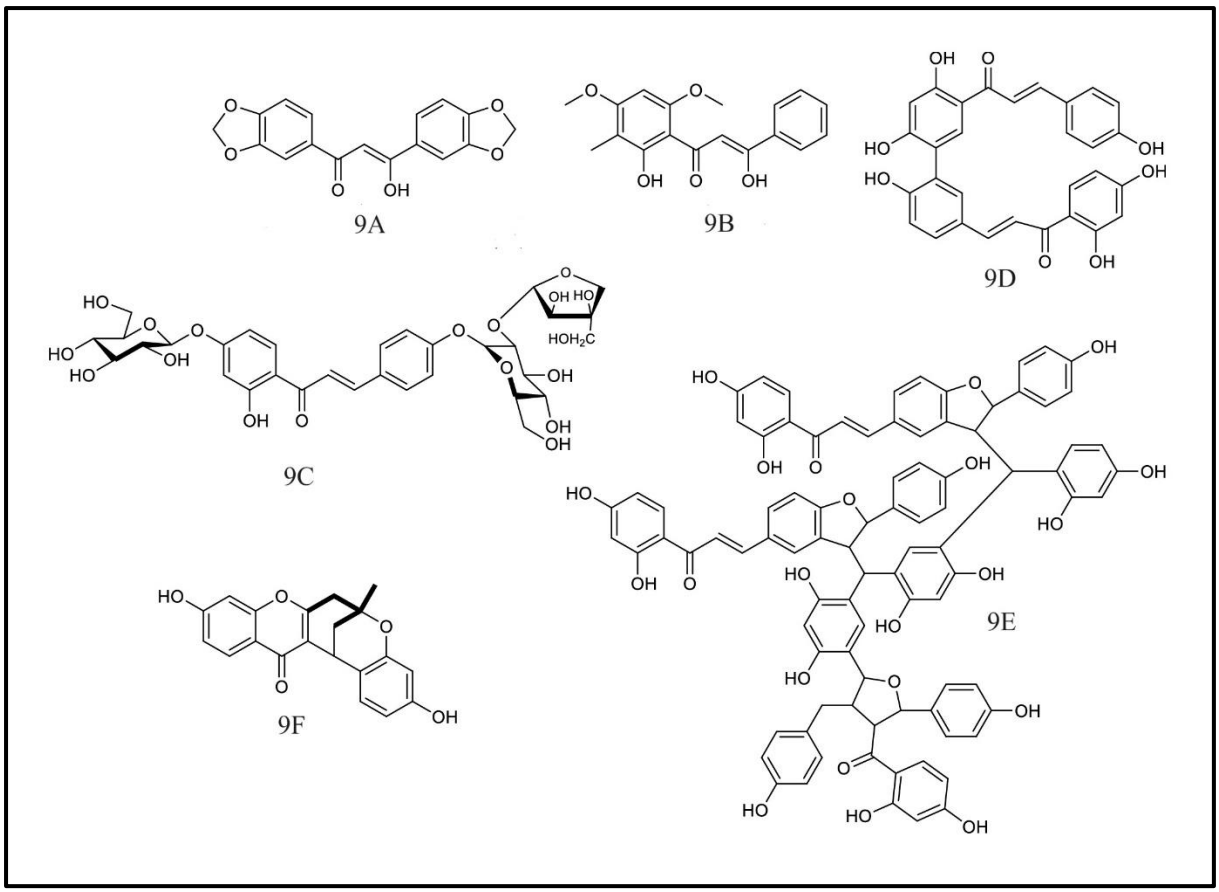

Figure 9: A series of uniquely structured chalcones with unconventional bonding and substitution patterns were methodically obtained from diverse plant sources. These chalcones have been meticulously documented and cataloged for future reference and analysis.

2.8. Synthesis of Chalcones

Chalcones are an important class of compounds with a distinct structural framework that is frequently used as a template in medicinal chemistry to facilitate the synthesis of a wide range of drugs. They are valued for their ability to undergo various substitutions and their relative ease of synthesis, which makes them valuable building blocks for drug discovery. The synthesis of chalcones is commonly achieved through condensation reactions, typically catalyzed by either acid or base. It is worth noting that a significant number of synthetic methods and procedures have been documented, showcasing the versatility and practicality of chalcones in biological applications. A comprehensive overview of the synthetic techniques, catalysts, reaction conditions, and general methodologies for the synthesis of chalcones will be presented below.

2.8.1. Claisen–Schmidt Condensation

The Claisen-Schmidt reaction is a well-known organic chemistry process used to prepare chalcone derivatives. This reaction involves the condensation of acetophenone and aldehyde derivatives in the presence of acid or base catalysts, typically in polar solvents at temperatures between 50-100ºC for several hours (Gaonkar and Vignesh 2017; Smith and Paulson 1954) **(Scheme 1)**. When a base is present, chalcone is formed from the aldol product via a dehydration of enolate mechanism, whereas in the case of acid catalysis, the product is produced from the enol mechanism. Commonly used base reagents for this condensation include NaOH, KOH, and NaH. However, this method has drawbacks, such as slow reaction rates, potential by-product formation, longer reaction times, and the possibility of unreacted starting materials remaining **(**Gaonkar and Vignesh 2017). The Claisen-Schmidt condensation is widely utilized for synthesizing chalcones due to its straightforward procedure and superior yields in comparison to other conventional methods. Burmaoglu et al., (2016) documented the successful synthesis of fluoro-substituted chalcones with high yields ranging from 80% to 90% by employing the Claisen condensation of trimethoxy acetophenone with respective fluoro-substituted aldehydes in an aqueous base solution. Furthermore, Passalacqua et al., (2015) described the preparation of novel prenylated chalcones through Claisen-Schmidt condensation in LiOH/MeOH, resulting in moderate yields.

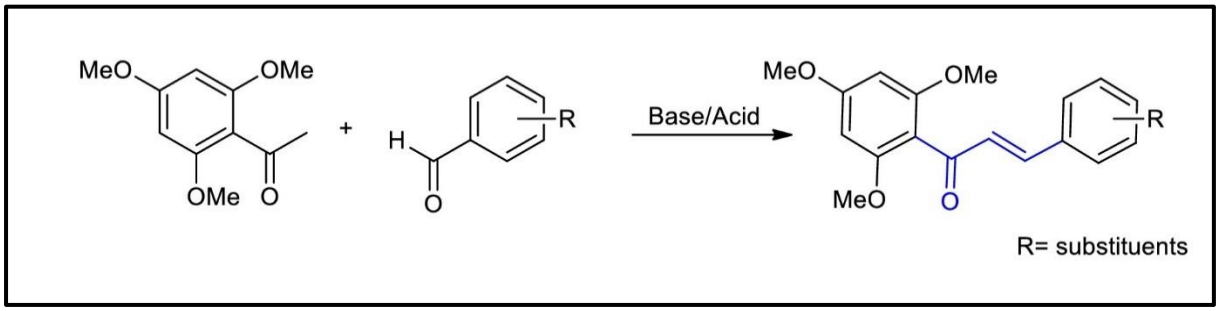

Scheme 1: Claisen-Schmidt reaction in the presence of base/acid catalyst.

The Claisen-Schmidt condensation reaction is typically conducted in the liquid phase; however, solid-phase condensations are also feasible in certain instances (Cheng et al., 2000; Watanabe and Imazawa, 1982). In this solid-phase condensation reaction, the acetophenone derivative is initially immobilized on the resin and subsequently treated with benzaldehyde derivatives. Ultimately, the chalcones are liberated from the resin through treatment with trifluoroacetic acid **(Scheme 2)**. The most suitable resins for solid-phase Claisen-Schmidt condensations are the complexes of Co (II) crosslinking 4-vinyl pyridine styrene and 2-chlorotritylchloride due

to the absence of byproducts in these resin-mediated reactions (Cheng et al., 2000; Watanabe and Imazawa, 1982).

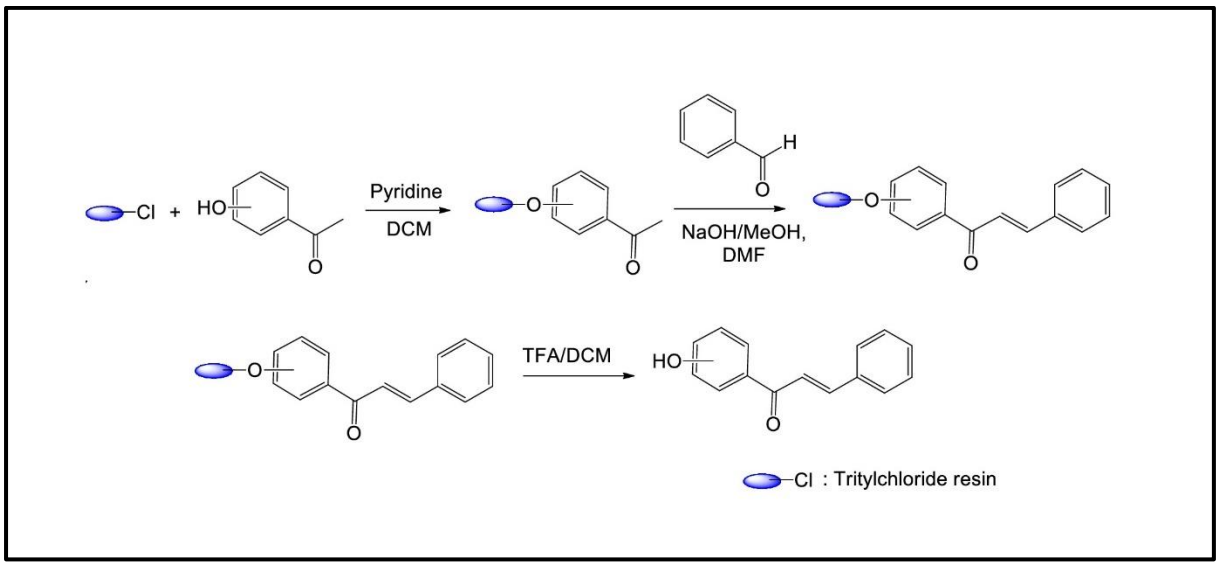

Scheme 2: Claisen-Schmidt reaction in solid phase medium.

In a similar fashion, it has been reported that zinc oxide-supported metal oxide effectively catalyzes the Claisen-Schmidt condensation of 2'-hydroxyacetophenone with aldehydes under solvent-free conditions, as outlined in **(Scheme 3)** (Saravanamurugan et al., 2005).

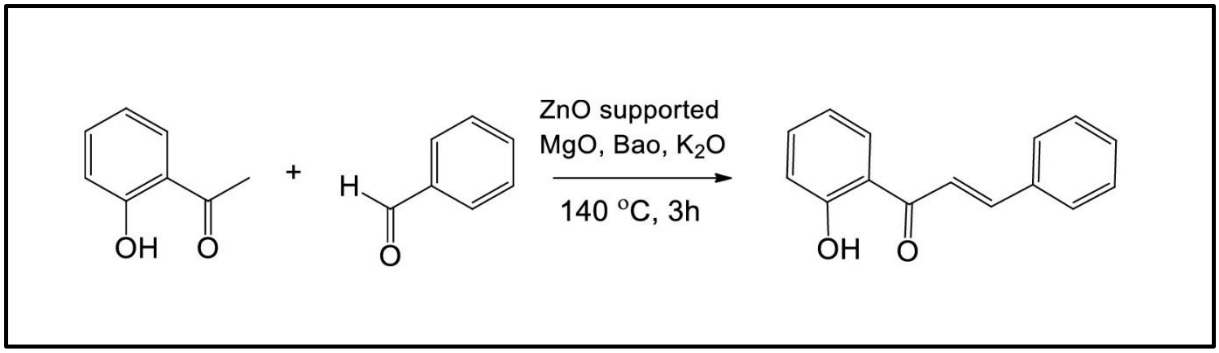

Scheme 3: Metal oxide catalyzed Claisen-Schmidt reaction under solvent-free condition.

The base-mediated Claisen-Schmidt condensation is a commonly employed method for the synthesis of chalcones, although alternative approaches utilizing Bronsted acids and Lewis's acids as acid catalysts have also been explored**.** Dhar (1981) conducted an acid-catalyzed Claisen-Schmidt condensation using HCl in ethanol, yielding poor results with only 10-40% yields. In contrast, the use of boron trifluoride-etherate (BF_3-Et_2O, **Scheme 4**) resulted in the successful synthesis of chalcones with appreciable yields ranging from 75-95% within a reaction time of less than 3 hours (Narender and Reddy, 2007).

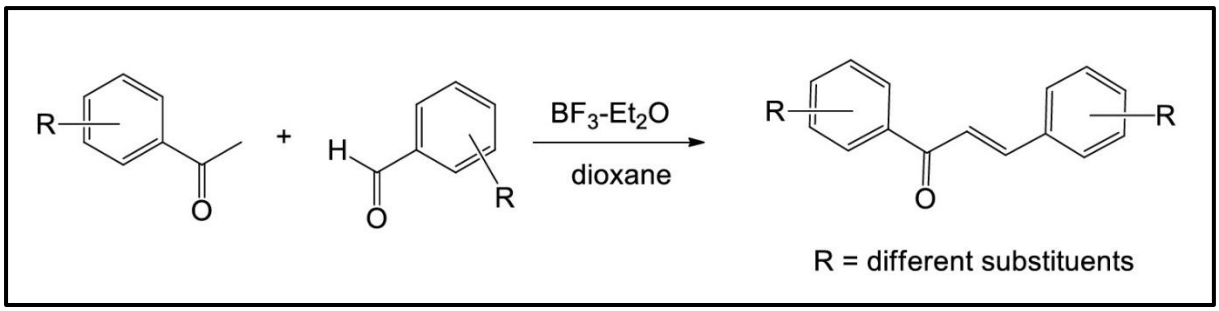

Scheme 4: Lewis's acids catalyzed Claisen-Schmidt reaction.

2.8.2. Grinding Method

The grinding method is a straightforward, eco-friendly, and solvent-free technique that results in rapid reactions and high yields. Rateb and Zohdi (2009) employed a simple, solvent-free, and environmentally friendly approach to synthesize chalcones at room temperature. This involved grinding a mixture of appropriate methyl ketones, aldehydes, and sodium hydroxide using a pestle in an open mortar to produce various chalcones. Radhakrishnan et al., (2016) also described the facile, solvent-free synthesis of Azachalcones by grinding the reactants. Additionally, Arslan et al., (2016) successfully prepared a new series of bischalcones through diazotization and diazo coupling using the grinding method, yielding good results (88-60%, **Scheme 5**).

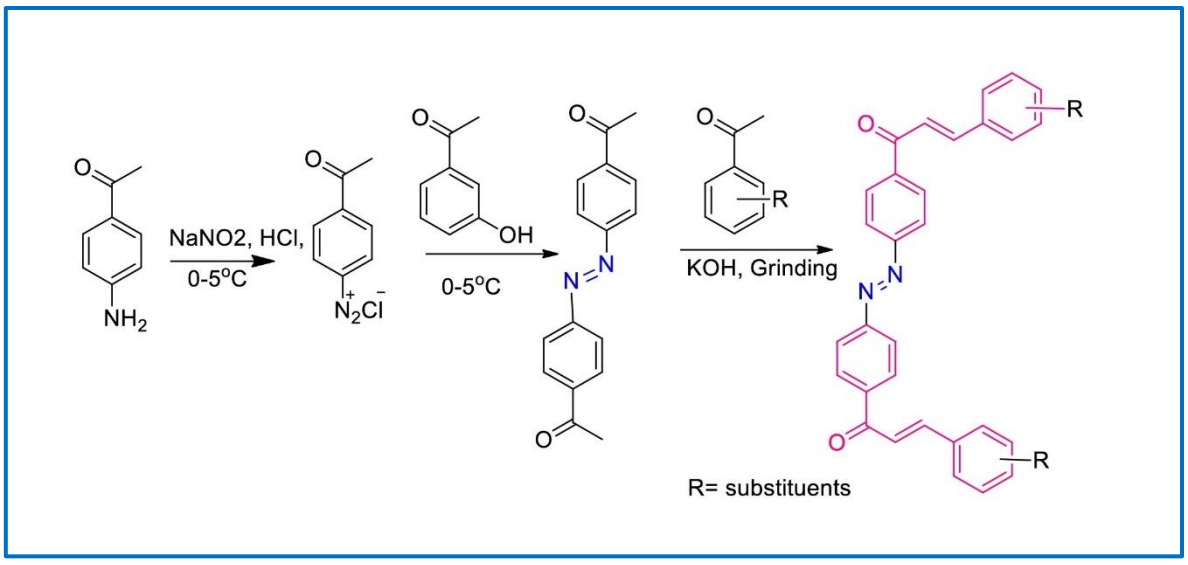

Scheme 5: Synthesis of chalcones using grinding method

2.8.3. Microwave Irradiation Condition

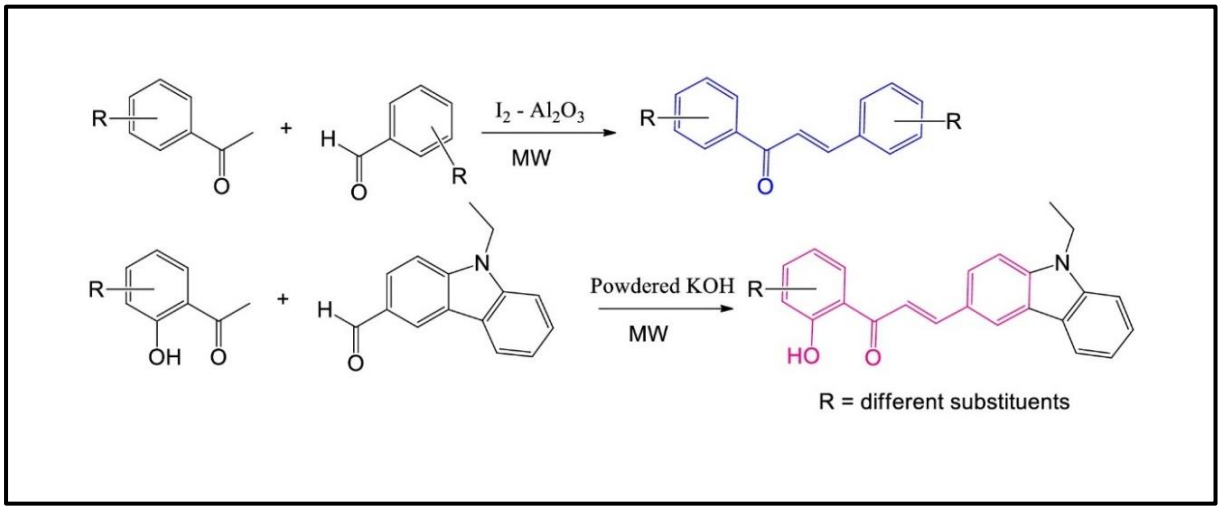

Scheme 6: Synthesis of chalcones through solvent-free microwave irradiation condition.

The use of microwave irradiation in organic synthesis has become well-established. This method offers significant advantages over conventional approaches by reducing reaction time, minimizing by-products, and eliminating the need for solvent evaporation. Notably, it also leads to enhanced yields (Gupta and Mahajan 2019). For instance, Kakati and Sarma (2011) reported on a solvent-free, molecular iodine impregnated alumina catalyzed microwave irradiation reaction of acetophenones with aldehydes. In this process, neutral alumina serves as a catalytic surface, while molecular iodine acts as a Lewis acid to activate the carbonyl group of aldehydes for nucleophilic attack with hydroxy aryl ketone **(Scheme 6)**. This method enables the preparation of polyhydroxy chalcones without the need for protecting groups. Similarly, Ashok et al., (2016) described the synthesis of a new class of carbazole-based chalcones using powdered KOH under solvent-free microwave conditions, resulting in enhanced products.

2.8.4. Ultrasound Irradiation Technique

The utilization of ultrasound irradiation represents an advantageous technique akin to microwave-assisted synthesis, attributable to its expeditious reaction time and elevated reaction yields. This approach operates on the principle of catalytic site activation through ultrasonic waves, potentially linked to an augmented vibrational state of the lattice, thereby expediting chemical reactions (Tran et al., 2015). Furthermore, the synthesis of chalcones can be undertaken via ultrasound irradiation in conjunction with heterogeneous catalysts, including K_2CO_3, basic Al_2O_3, Ba $(OH)_2$, KF-Al_2O_3, and aminografted zeolite (Chtourou et al., 2010; Fuentes et al., 1987; Li et al., 2002; Wei et al., 2005). Wei et al., (2005) documented the ultrasound-irradiated synthesis of chalcones with substantial yields in the presence of K_2CO_3

as a catalyst. Similarly, Chtourou et al., (2010) reported the solvent-free synthesis of chalcones with noteworthy yields (96-80 %) utilizing acidic clay (KSF) under ultrasonic irradiation **(Scheme 7).** Additionally, varied chalcones were prepared by employing KOH/EtOH (lacking a catalyst, yielding 52-97 %) and KF/MeOH (incorporating Al_2O_3, yielding 83-98 %) through ultrasonication **(**Calvino et al., 2006) under moderate temperature conditions.

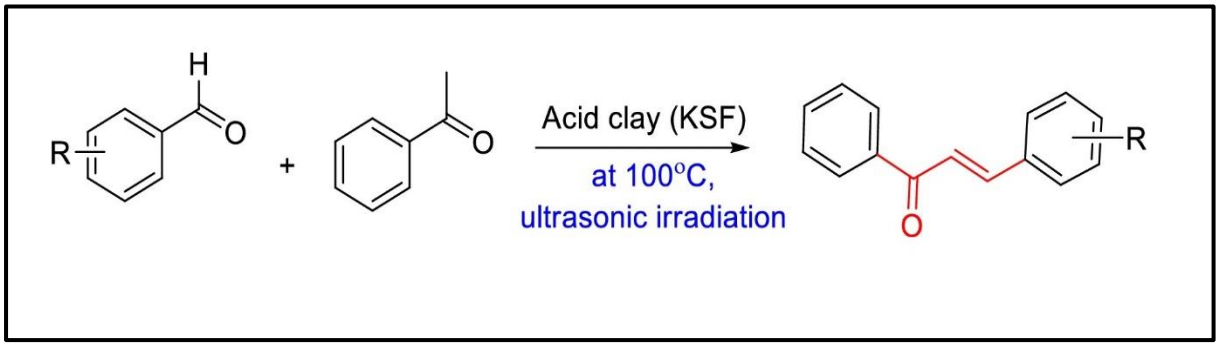

Scheme 7: Synthesis of chalcones under ultrasound irradiation.

2.8.5. Coupling Reactions

The conventional methods used for designing a new class of chalcones with various substituents often result in the production of undesired by-products alongside the intended products, making it difficult to separate them using chromatography. Consequently, researchers are now employing new strategies such as cross-couplings with transition metal catalysts like Julia-Kocienski olefination, Witting, and Friedel-Crafts acylation for the synthesis of potent pharmaceutical molecules, including chalcones (Diaz Sanchez et al. 2019; Guo et al. 2015; Zhuang et al. 2017). These newer methods offer more control over the synthesis process, leading to improved yields of the desired products and reducing the formation of undesired by-products.

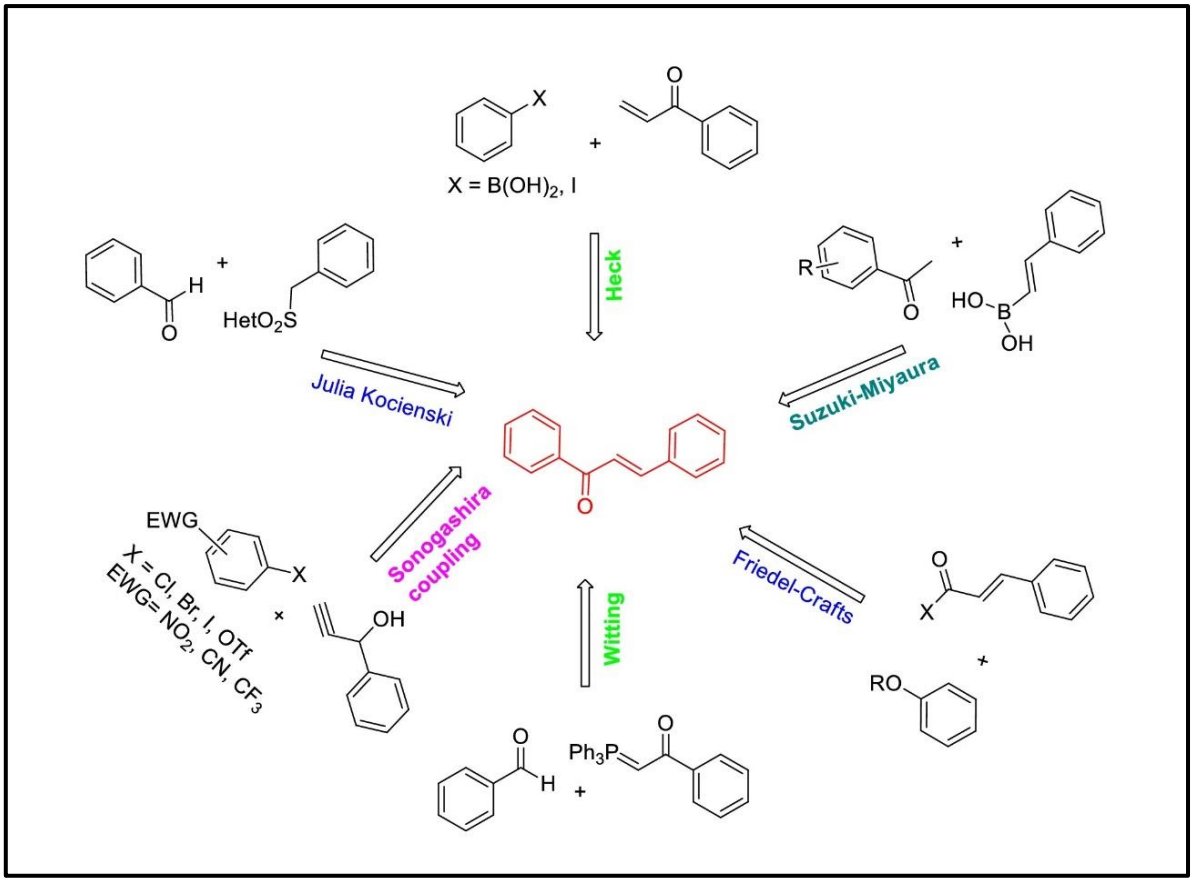

Figure 10: Various cross-coupling reactions are employed in the synthesis of chalcones.

2.8.5.1. Heck Coupling

The metal-catalyzed Heck coupling reactions are a highly efficient method for synthesizing chalcones. These reactions enable the coupling of aryl boronic acids and aryl vinyl ketones, resulting in the formation of robust carbon-carbon bonds. Notably, the coupling of aryl vinyl ketones with aryl iodides or aryl boronic acids consistently yields chalcone derivatives with exceptional yields, as demonstrated in the research by Hird et al.,1993. This process occurs under catalytic conditions using Pd $(OAc)_2$, Ph_3P, K_2CO_3, and DMF, as depicted in Scheme 8. Furthermore, an alternative method for chalcone synthesis involves the carbonylative vinylation of aryl halides with styrene in the presence of carbon monoxide, utilizing palladium catalysts, as reported by Guo et al., 2015.

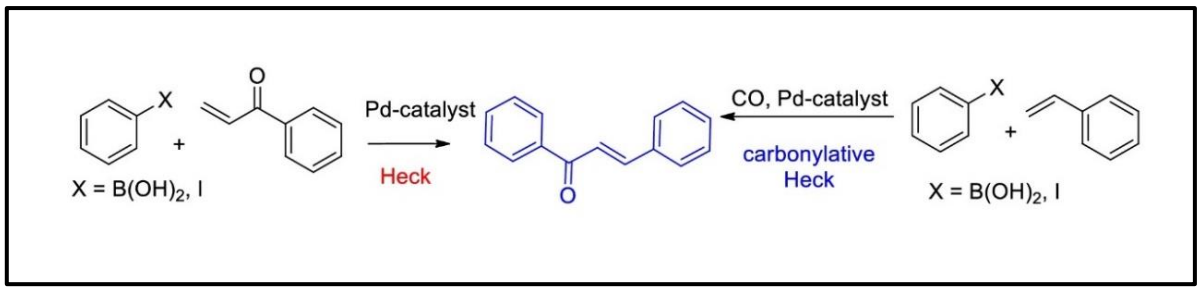

Scheme 8: Chalcone synthesis through Heck coupling.

2.8.5.2. Sonogashira Isomerization Coupling

The Sonogashira coupling is a widely utilized method for the cross-coupling of terminal alkynes with aryl halides. This reaction employs a palladium catalyst, often in combination with a co-catalytic amount of CuI, in a boiling mixture of trimethylamine and THF under inert gas conditions for a duration of 16-24 hours (**Scheme 9**; Muller et al., 2000). The process has proven effective for the synthesis of various chalcones, with yields ranging from moderate to excellent. However, this method is not without limitations, including prolonged reaction times, the necessity of an excess base, and the requirement for electron-deficient aryl halides. In response to these limitations, Schramm and Muller (2006) developed a novel approach known as microwave-assisted coupling isomerization reaction (MACIR) for the synthesis of chalcones. This innovative method has shown the ability to significantly reduce the reaction period to less than half an hour while still achieving notable yields.

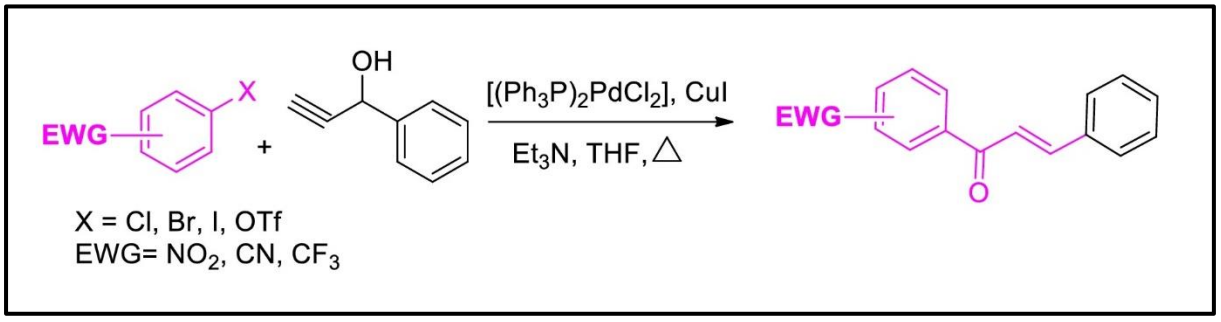

Scheme 9: Sonogashira isomerization coupling for the synthesis of chalcones (EWG: electron-withdrawing groups).

2.8.5.3. Suzuki-Miyaura Coupling

The Suzuki Coupling, introduced by Akira Suzuki in 1979, was later employed by Eddarir et al., (2003) for synthesizing chalcones, marking its inaugural application for this purpose. Additionally, the Suzuki-Miyaura coupling, an intriguing metal-catalyzed cross-coupling reaction, facilitates the formation of chalcones via the creation of a C-C bond between two

electronically divergent chemical fragments **(Scheme 10)**. Notably, a series of chalcones were synthesized by Haddach and McCarthy (1999) through the coupling of cinnamoyl chloride with various aryl boronic acids under specific conditions, yielding results of moderate efficacy. Conversely, under the same reaction specifications, the coupling of styryl-boronic acid with diverse benzoyl chlorides produced high yields (Haddach and McCarthy 1999). An inference drawn from these observations suggests that the absence of substitution patterns in benzoyl chlorides, which are present in aryl boronic acid, may impact the yields.

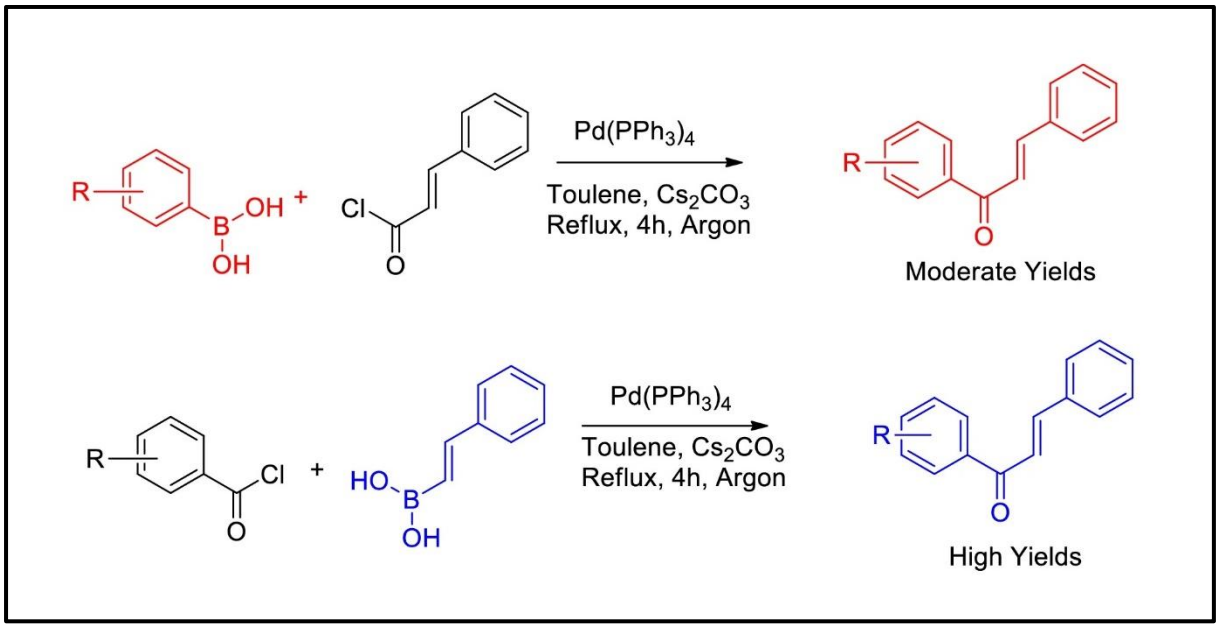

Scheme 10: Synthesis of chalcones using Suzuki Miyaura coupling

2.8.5.4. Julia–Kocienski Olefination

In a study conducted by Kumar et al., (2010), an innovative application of Julia Kocienski olefination **(Scheme 11)** was employed for the synthesis of chalcones with exceptionally high yields. Through a series of condensation reactions, utilizing a novel Julia coupling reagent, heteroaryl sulfonyl phenylethane, and aromatic aldehydes in a basic medium, a range of chalcones were successfully synthesized. The study identified 1,8- Diazabicyclo [5.4.0] undec-7-ene (DBU)and 2-(benzo[d]thiazol-2ylsulfonyl)-1-phenylethanone as the optimal base and Julia reagent pair for the efficient preparation of chalcones via Julia Kocienski olefination. It was observed that the choice of less polar solvents and an efficient base significantly influenced the synthesis of chalcones. Notably, even at low temperatures, the Julia Kocienski olefination consistently yielded E-chalcones as the predominant products.

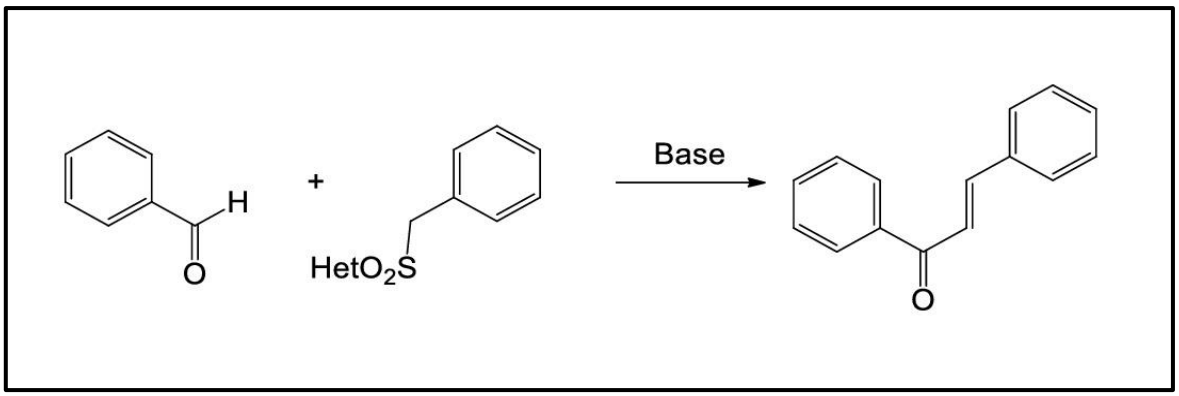

Scheme 11: Synthesis of chalcones using Julia Kocienski olefination.

2.8.5.5. Witting Reaction

Chalcones, which are α, β-unsaturated carbonyl derivatives, can be synthesized via Witting olefination. A method described by Ramirez and Dershowitz, 1957 involves the reaction of triphenylbenzoylmethylene phosphorane and benzaldehyde in THF over 30 hours at reflux or 3 days in benzene at reflux, resulting in moderate yields. In an alternative approach, Xu et al., (1995) reported a microwave-assisted synthesis of chalcones with remarkable yields using Witting olefination, with reaction times as short as 5-6 minutes. This innovative method significantly reduced the reaction time and enhanced the reaction rates, leading to excellent yields.

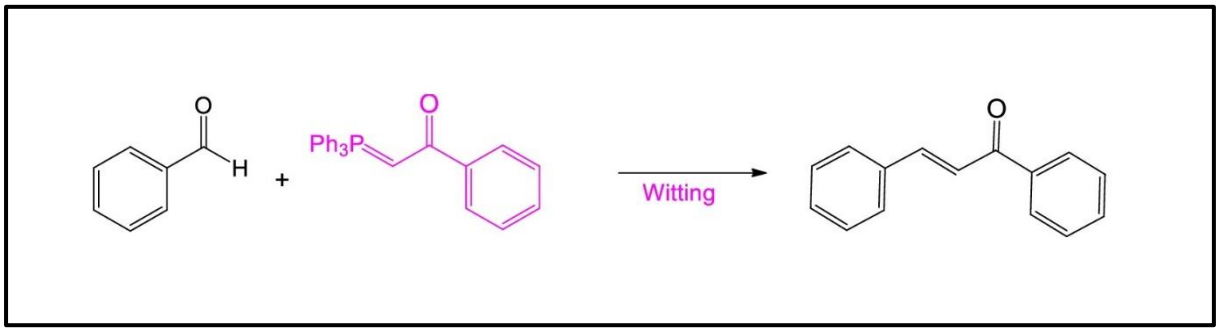

Scheme 12: Synthesis of chalcones using Witting olefination.

2.8.5.6. Friedel–Crafts acylation

Highly substituted chalcones have been prepared using the described technique, although its application is not widespread. In a study by Shotter et al., (1978), chalcones were synthesized through Friedel-Crafts acylation utilizing a Lewis acid catalyst. Specifically, the acylation of aromatic ethers with cinnamoyl chloride in the presence of the strong Lewis acid catalyst $AlCl_3$ yielded the desired chalcones, as illustrated in (Scheme 13).

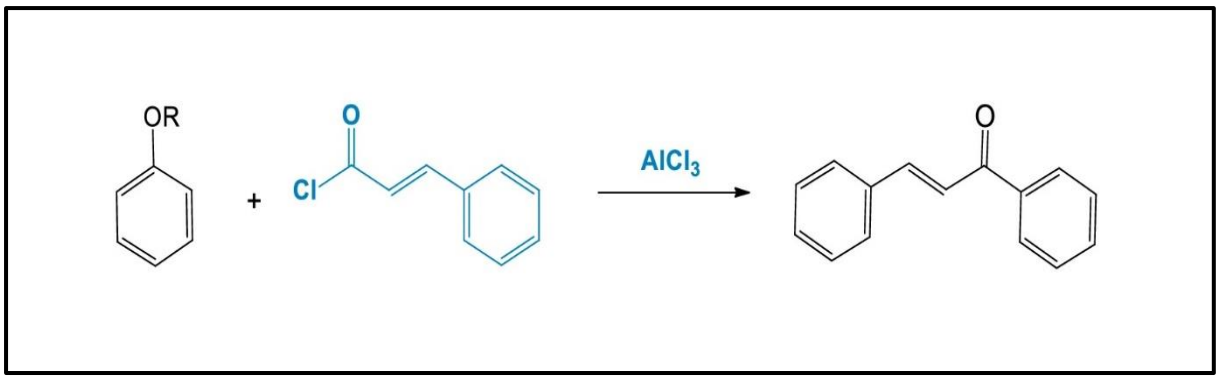

Scheme 13: Synthesis of chalcones using Friedel Crafts acylation.

2.8.5.7. Photo-Fries Rearrangement

The Photo-Fries rearrangement reactions yield ortho or para products based on the temperature and solvents employed. When phenyl cinnamates are subjected to a high-pressure mercury-arc lamp in benzene solvents under nitrogen, the result is a low yield of 2'-hydroxy chalcones (Obara et al., 1969, **Scheme 14**). In contrast, Ramakrishnan and Kagan (1970) reported an alternative Photo-Fries rearrangement reaction of chalcones in alcohols and chloroform, leading to improved yields of up to 50%. However, the limited use of these reactions is attributed to their low yields, protracted reaction times, and intricate handling procedures.

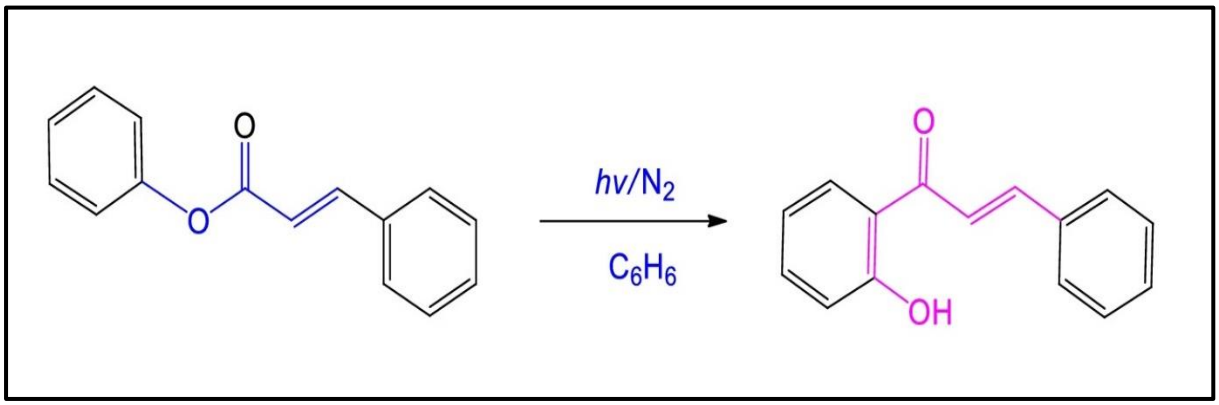

Scheme 14: Synthesis of chalcones via Photo Fries rearrangement

2.8.5.8. Synthesis of cis-Chalcones

The majority of reported chalcones, whether from natural sources or produced synthetically, exist in the trans-diastereomeric form due to the inherent instability of the cis form. Typically, the synthesis of cis-chalcones involves the photoisomerization of trans-chalcones, but this method yields low results. In 2006, Yoshizawa and Shioiri introduced a new method for synthesizing cis-chalcones using siloxypropynes **(Scheme 15)**. When aryl siloxypropynes are treated with a catalytic quantity of potassium tert-butoxide under mild conditions, they produce

siloxyallene intermediates. These intermediates are then subjected to concentrated H_2SO_4 in 1,2-dimethoxyethane, resulting in excellent yields of cis-chalcones with high enantioselectivity, achieving a cis/trans ratio of up to 99/1.

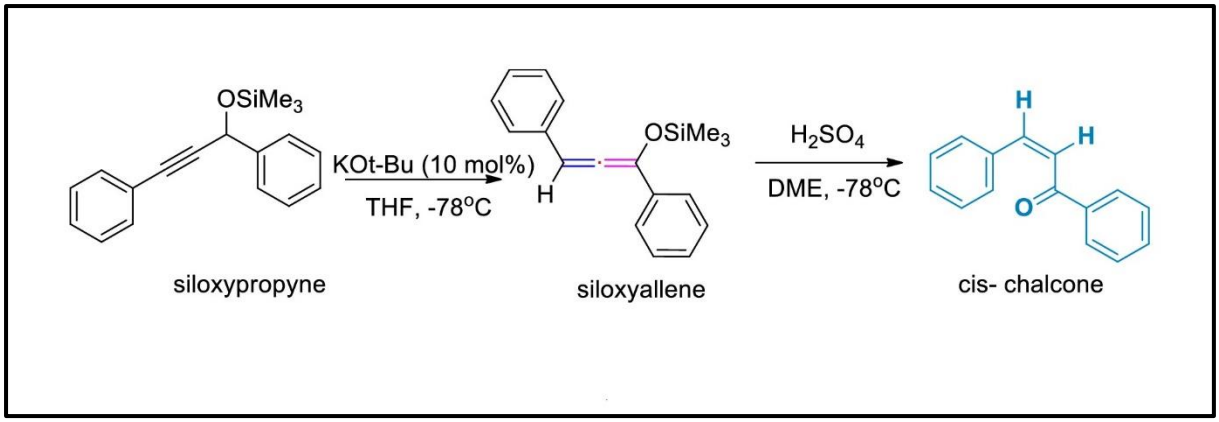

Scheme 15: Synthesis of chalcones cis-chalcones.

2.8.5.9. Hybrid Chalcones

Chalcones are highly versatile molecules that readily undergo cyclization to form a flavonoid structure, representing a crucial step in the biosynthetic pathway for skeletal modification. Due to their potential for structural modification, various synthetic attempts have been made to produce a new class of organic compounds, including azachalcones, isoxazoles, pyrazoles, chalcones with an indole base, and coumarinyl-quinolinyl chalcones **(Scheme 16)**. These compounds are known for their wide-ranging pharmacological potential.

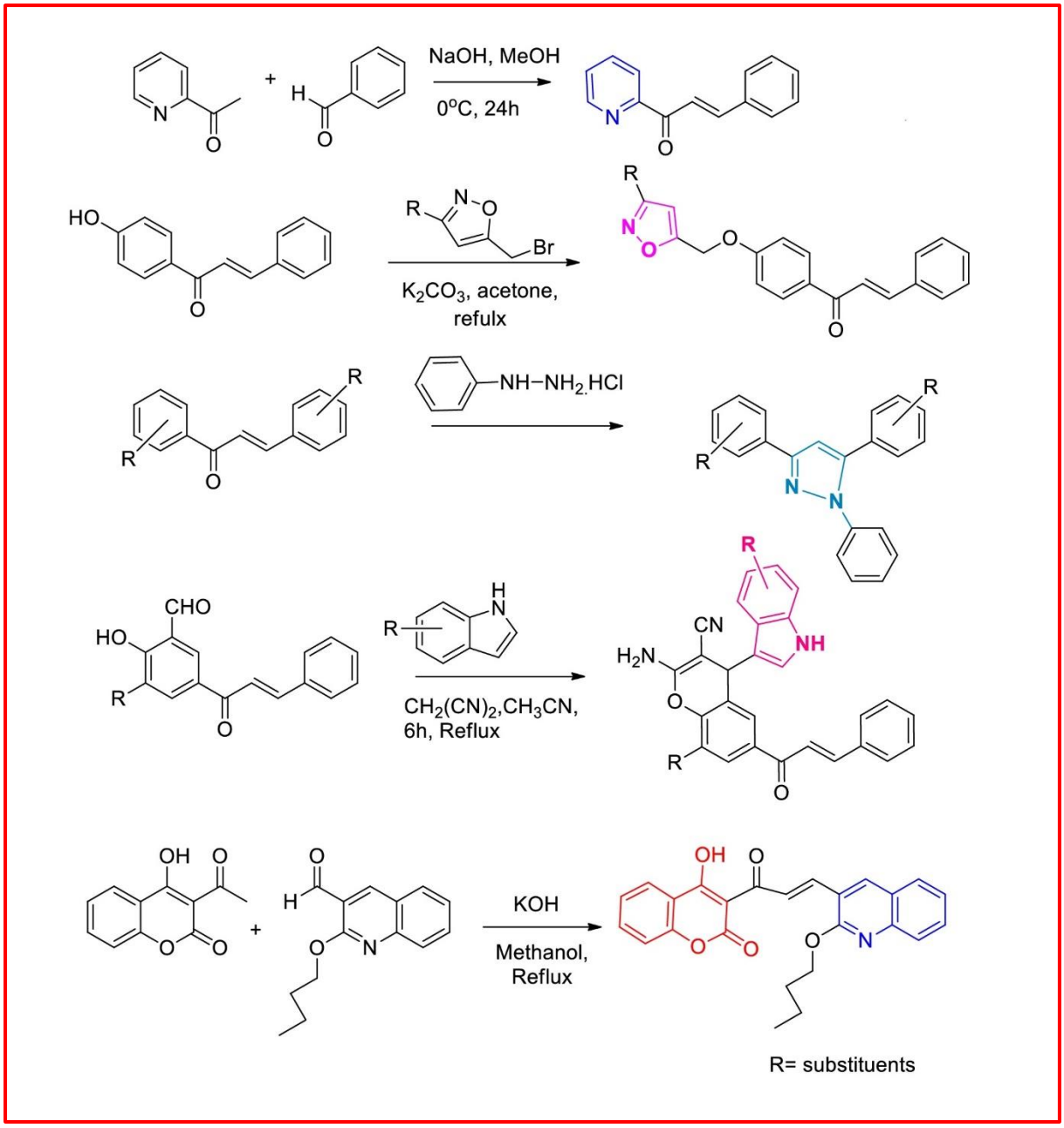

Scheme 16: Recent methodologies have been employed in the synthesis of hybrid chalcones across diverse reaction media.

Radhakrishnan et al., (2015) documented a series of azachalcones exhibiting inhibitory properties against the tyrosinase enzyme, particularly in the context of depigmentation. In a separate investigation, Niu et al., (2016) presented novel chalcones incorporating isoxazole moieties that demonstrated pronounced activation of the tyrosinase enzyme. Prasad et al., (2005) detailed the antidepressant activity of a pyrazoline derivative obtained through the condensation of a chalcone moiety with phenylhydrazine hydrochloride. Gupta et al., (2018) synthesized potent antiproliferative active indole chalcones via refluxing a mixture of chalcones, indole derivatives, and malononitrile in acetonitrile over a 6-hour reaction period,

showing promise for drug development against colorectal cancer. Finally, Abonia et al., (2018) described a new class of coumarinyl-quinolinyl chalcone hybrids, prepared through Claisen-Schmidt condensation of 3-acetyl-4-hydroxy-2H-chromene-2-one and 2-butoxyquinoline-3-carbaldehyde in methanol in the presence of a base.

2.8.6. Medicinal Applications of Chalcones

The chalcones and their derivatives hold significant importance in medicinal chemistry even in the 21st century due to their broad spectrum of therapeutic potential and pharmacological properties. Chalcone derivatives exhibit a wide range of biological activities, including anticancer, antibacterial, anticonvulsant, anti-HIV, antihyperglycemic, anti-inflammatory, antileishmanial, antimicrobial, antioxidant, antiprotozoal, antitubercular, antiviral, and anti-ulcerative properties. Below, we provide a concise overview of the biological importance of chalcones with examples.

2.8.6.1. Chalcones as Chemopreventors

Several chalcones were derived from natural sources, with some being identified as chemopreventive agents. (+)-Tephrosone (1) (Chang et al. 2000) and tephropurpurin (2) (Chang et al. 1997) were isolated from Tephrosia purpurea (Leguminosae) and established as chemopreventive agents through a cell-based quinone reductase induction assay. Munsericin (3) is another natural chemopreventive chalcone, isolated from Mundulea sericea (Leguminosae) **(**Luyengi et al., 1994). Xanthohumol (4) is a versatile chemopreventive agent (Stevens and Page 2004**)** with three key properties: (i) inhibition of metabolic activation of procarcinogens, (ii) induction of carcinogen-detoxifying enzymes, and (iii) early-stage inhibition of tumor growth.

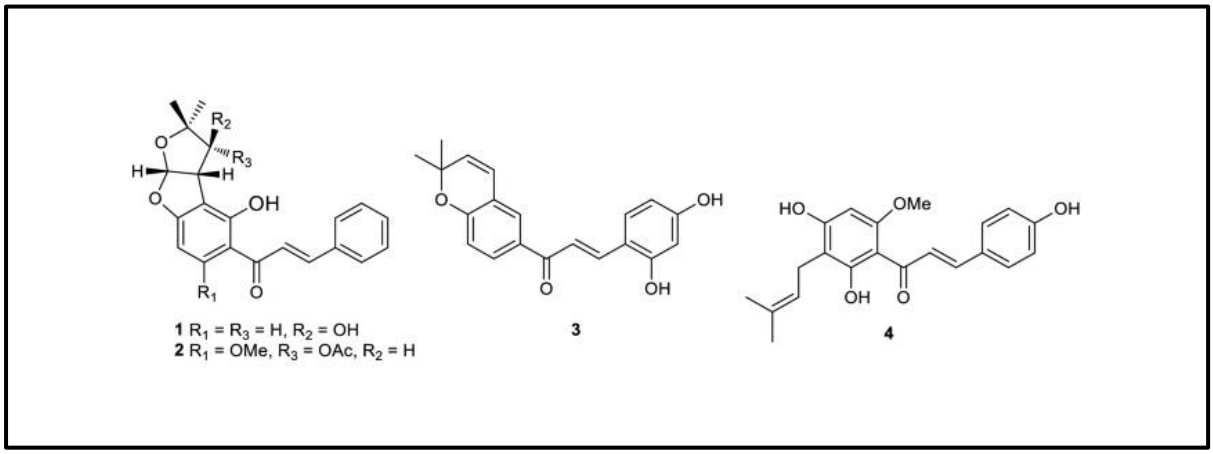

Figure 11: Some chalcones anticipated to have chemopreventive activities.

2.8.6.2. Anticancer Activity

Several chalcones, derived from both synthetic and natural sources, have exhibited promising anti-tumor properties in addition to demonstrating antioxidant activity through the inhibition of superoxide production and lipid peroxidation. Millepachine (5), an anticancer chalcone, was isolated from Millettia pachycarpa by Wu et al., in 2013. Licochalcone A (6), obtained from Glycyrrhiza inflate, demonstrated cytotoxic effects against L1210 leukemia and B16 melanoma cells (Shibata et al., 1991). A novel class of chalcone (7) has been postulated as an anti-mitotic agent, increasing the survival rate of mice inoculated with L1210 leukemia within a dosage range of 2.65-5.0 mg/kg (Edwards et al., 1990). Additionally, Butein (8), a natural chalcone, has been proven to suppress various human cancers, including breast cancer, colon carcinoma, osteosarcoma, and hepatic stellate cells in vitro (Wang et al., 2005; Yit and Das, 1994).

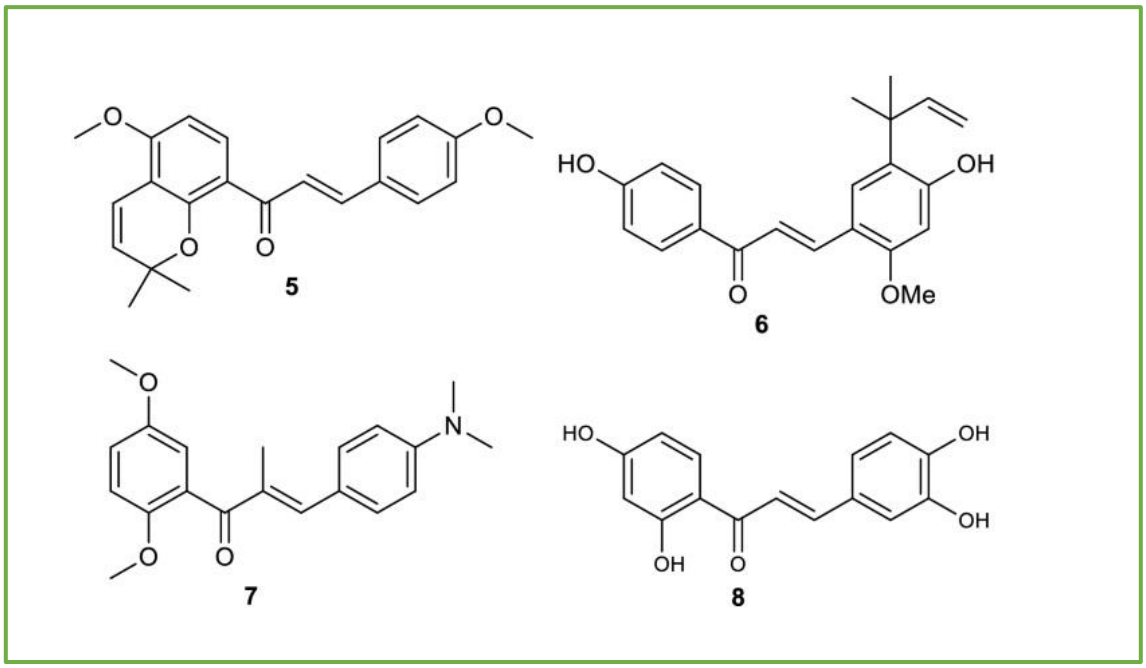

Figure 12: Some chalcones anticipated to have anticancer activities.

2.8.6.3. Antimicrobial Activity

The antimicrobial activity of chalcones is attributed to the presence of the α, β-unsaturated carbonyl function. Isobavachalcone (9) and bavachalcone (10) are two significant chalcones isolated from Psoralea corylifolia and identified as antibacterial agents from a natural source (Oh et al., 2010; Qiu et al. 2011). A synthetic compound, 3-(Carboxyalkyl) rhodanine (11), is an antimicrobial chalcone that exhibits potent inhibition at a low concentration (1 μg/mL) against human pathogens and is documented as both an antibacterial and antifungal agent (Yanbian University, 2012). Another chalcone **(**12), fused to a ring, is proposed as an

antimicrobial scaffold for the treatment of oral infections (Subramanyam et al., 2015). A hybrid chalcone containing the pharmacophore fluconazole (13) demonstrated potent inhibition with an IC50 concentration of 0.12 µg/mL against Candida albicans and is patented as an antifungal agent (Borate et al., 2016).

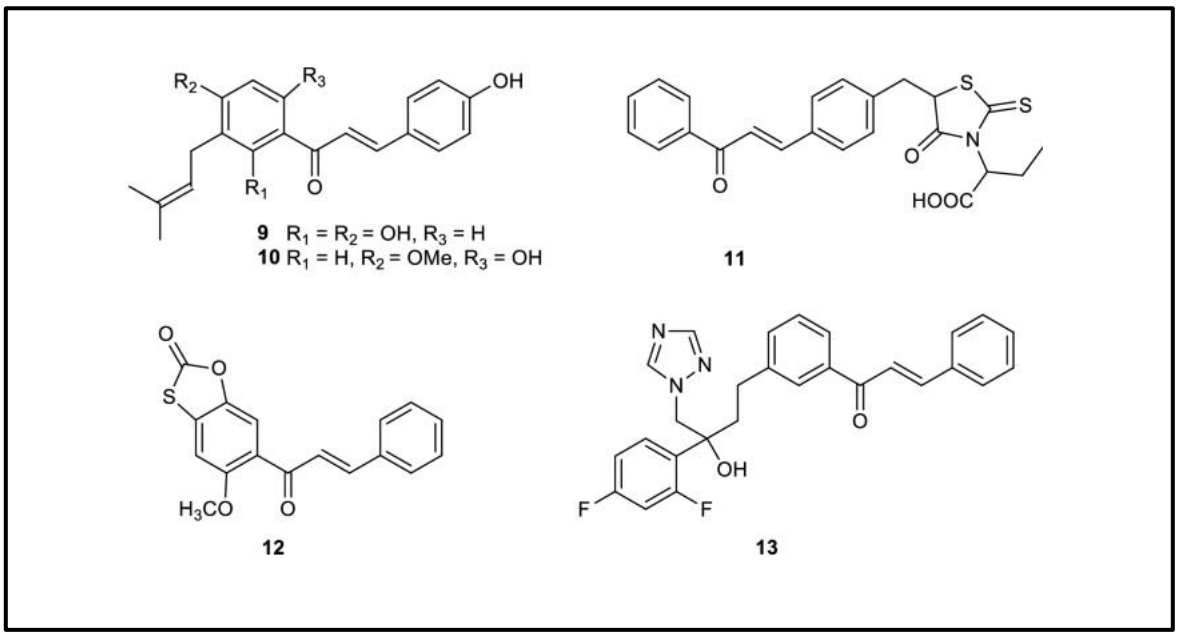

Figure 13: Chalcone analogs used for antimicrobial applications.

2.8.6.4. Anti-HIV

Numerous chalcones, a class of natural and synthetic compounds, have been identified for their potential to combat the Human Immunodeficiency Virus (HIV). One of these chalcones, known as xanthohumol (4), is obtained from Hops Humulus and has demonstrated anti-HIV properties (Wang et al., 2004). Researchers Nakagawa and Lee (2006) have isolated a unique β-hydroxy chalcone (14) from the genus Desmos, which exhibits notable anti-HIV activity. Furthermore, a chalcone (15) sourced from the leaves of Maclura tinctoria (Moraceae) has displayed inhibitory activity against Candida albicans and Cryptococcus neoformans, both of which are associated with AIDS (ElSohly et al., 2001). Additionally, an adamantly chalcone (16) was granted a patent for its observed activity against HIV (Xiamen University, 2014).

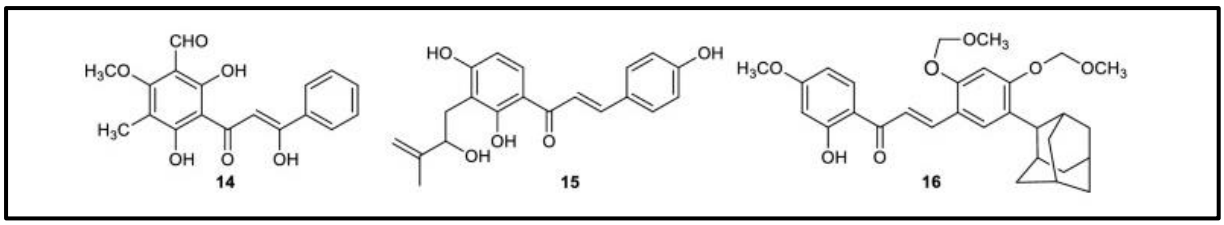

Figure 14: Chalcone analogs having some anti-HIV applications.

2.8.6.5. Antidiabetic Activity

Chalcones have been identified as potent inhibitors of α-glucosidase, dipeptidyl peptidase-4 (DPP4), peroxisome proliferator-activated receptors-γ (PPAR), and protein tyrosine phosphatase 1B (PTP1B), aldose reductase, making them significant agents for the treatment of diabetes mellitus (Mahapatra et al. 2015). Isoliquiritigenin (17), echinatin (18), licochalcone A (6), licochalcone C (19), and licochalcone E (20) have been isolated from Glycyrrhiza inflata, and their synthetic derivatives have been reported as PTP1B inhibitors, playing a vital role in the treatment of type II diabetes and obesity as negative regulators of the insulin and leptin signaling pathway (Yoon et al., 2009). Additionally, a novel chalcone, abyssinone-VI-4-O-methyl ether (21), isolated from the root bark of Erythrina mildbraedii has shown potent antidiabetic activity through the inhibition of PTP1B (Yang et al., 2006). Furthermore, Nakai et al., (2005) have reported new sulfonamide chalcones (22-29) as strong inhibitors of the α-glucosidase enzyme.

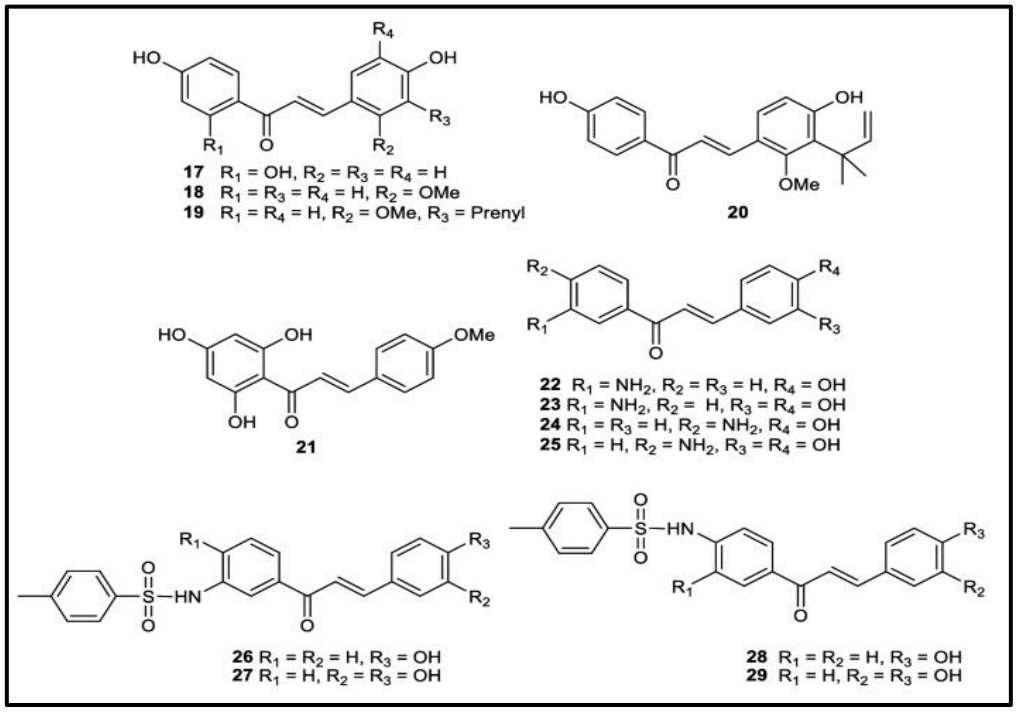

Figure 15: Synthetic chalcone analogs show potent antidiabetic activity.

2.8.6.6. Anti-inflammatory Activity

Naringenin-chalcone (30) is a widely recognized natural compound known for its anti-inflammatory properties, achieved through the inhibition of cytokine production, a key pro-inflammatory agent **(**Hirai et al., 2007). Isoliquiritigenin (31), derived from Nepalese propolis (Funakoshi et al., 2015), and butein (32), extracted from Rhus verniciflua (Yang et al., 1998), are other significant natural chalcones that demonstrate potent anti-inflammatory activity by inhibiting LPS-induced iNOS and COX-2 expression. Zhao et al. (2003) identified a reduced chalcone (33) as an anti-inflammatory agent due to its ability to inhibit the production of NO induced by LPS and INF- γ in murine macrophage-like cell lines. Additionally, a synthetic hetero chalcone (34) was reported as a potent cytokine inhibitor suitable for managing anti-inflammatory conditions (Piramal Life Sciences, 2011).

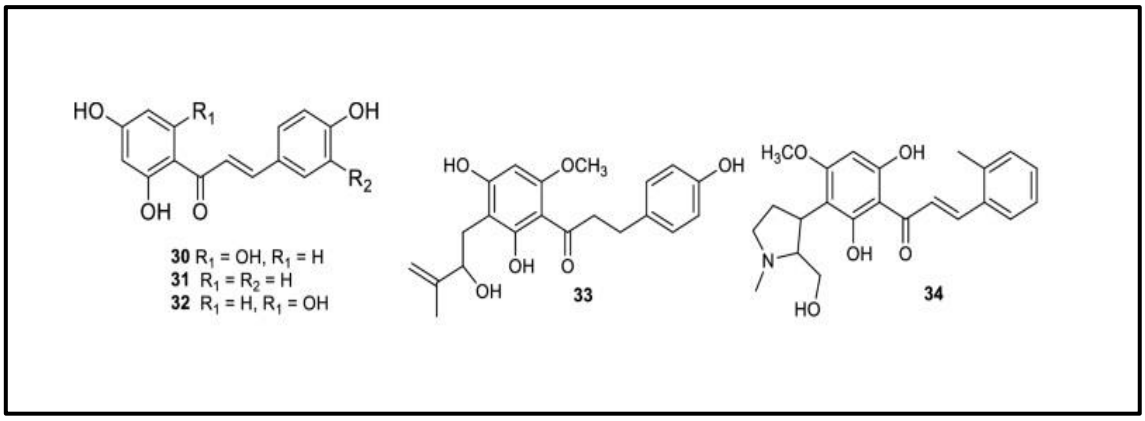

Figure 16: Chemical structures of synthetic chalcones as an anti-inflammatory agent.

2.8.6.7. Antileishmanial Activity

Licochalcone A (6) is a well-established natural antiparasitic agent utilized in the treatment of various abdominal spasmodic symptoms in Japan **(**Nagai et al., 2007). Kanzonol C (35), derived from licorice roots (Glycyrrhiza eurycarpa, Leguminosae), exhibited robust antileishmanial activity (Christensen et al.,1994). Another noteworthy chalcone, Crotaramosmin (36), isolated from Crotolaria rosmosissima, demonstrated potent antileishmanial activity (Narender et al., 2005). A dihydrochalcone (37) synthesized by Hermoso et al., (2003) displayed modest antileishmanial activity. Furthermore, Rashid et al., (2016**)** synthesized a novel class of dihydropyrimidine derivatives, and compound (38) exhibited antileishmanial activity against promastigotes of Leishmania major and L. donovani with inhibitory concentrations of 0.47 μg/mL and 1.5 μg/mL, respectively.

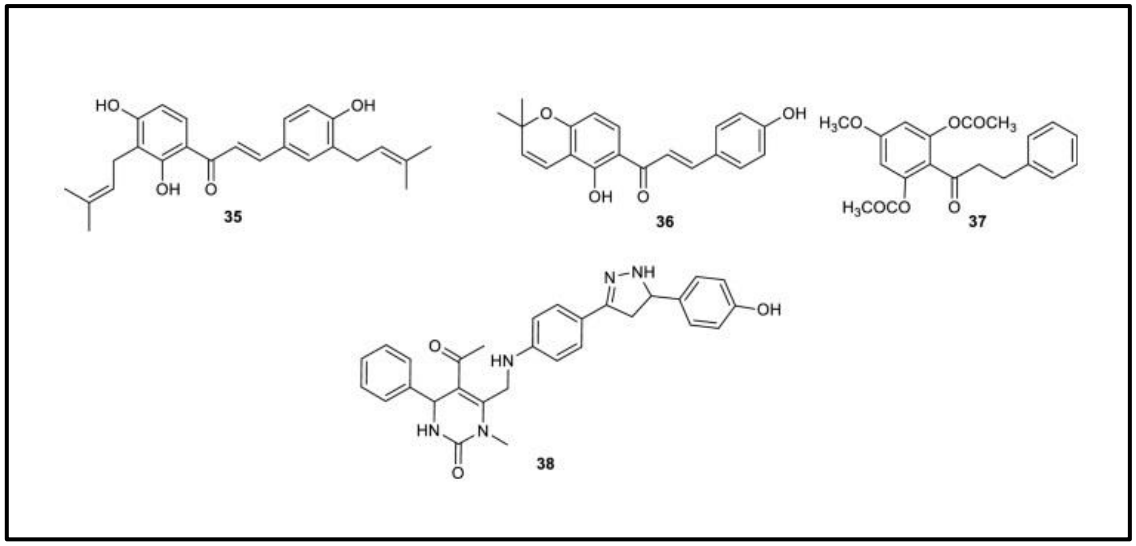

Figure 17: Some chalcones suitable for antileishmanial applications.

2.8.6.8. Antioxidant Activity

Abundant free radicals are produced within the human body during metabolic processes and have the potential to inflict damage upon biomolecules such as DNA, proteins, and lipids through oxidation, precipitating various oxidative damage-associated ailments such as cancer, non-inflammatory tumors, digestive ulcers, rheumatoid arthritis, and aging.

Hatano et al., (1997) documented the identification of a penta-oxygenated chalcone (39) isolated from Glycyrrhiza uralensis (Leguminosae) that exhibits robust DPPH radical activity and is utilized as traditional medicine in northeastern China. Cedredipronone (40), another chalcone isolated from the extracts of fruits and seeds of Cedrelopsis grevei (Ptaeroxylaceae), was found to possess potent superoxide scavenging properties (Koorbanally et al., 2003). The prenylated chalcone glycoside (41), isolated from the bark of Maclura tinctoria (Moraceae), demonstrated radical scavenging activity through various antioxidant mechanisms (Cioffi et al., 2003). Doan and Tran (2011) developed allylated chalcones (42-44) which exhibited superior antioxidant activity in comparison to non-allylated chalcones by inhibiting free radicals.

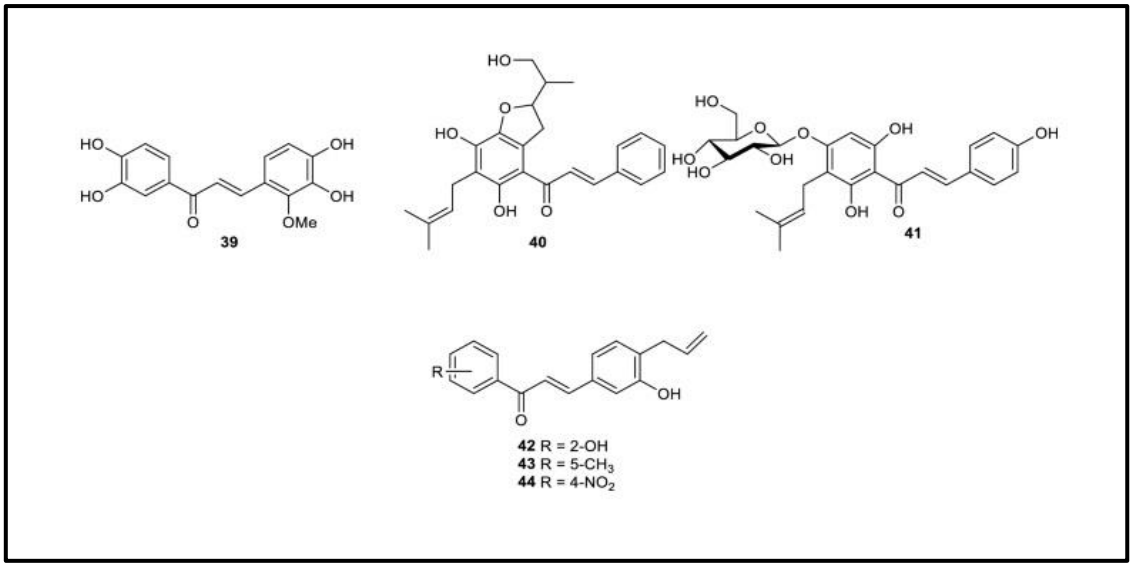

Figure 18: Chalcone analogs exhibiting potent antioxidant activity.

2.8.6.9. Antituberculosis Activity

Nardoaristolone A (45) is an intriguing terpenoid chalcone with a unique structure, which has been isolated from Nardostachys Chinensis. Studies have shown that this compound exhibited promising antituberculosis activity (Fang, 2013**)**. Furthermore, a fluorine-substituted synthetic chalcone (46) has been reported by Guantai et al., 2011 to possess antitubercular properties against Mycobacterium tuberculosis strains. These findings suggest the potential of these compounds as candidates for developing new antituberculosis agents.

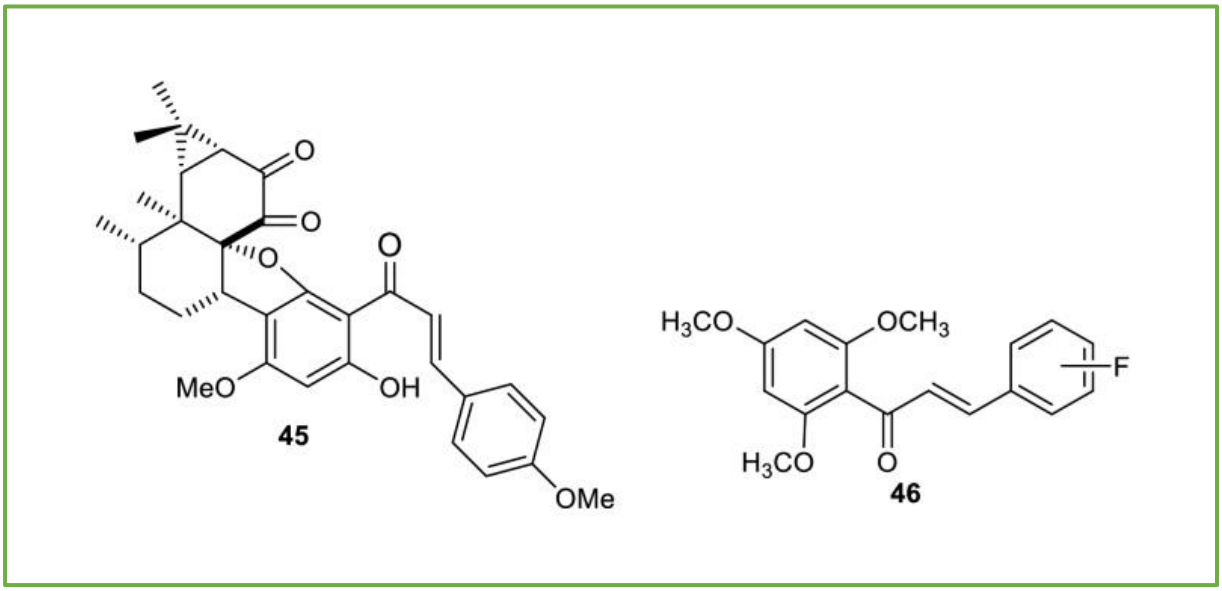

Figure 19: Chalcone analogs with potential antituberculosis activity.

2.8.6.10. Antiviral Activity

Naringenin-chalcone (30) is widely present in citrus fruits and is recognized for its antiviral properties (Kaul et al., 1985). Myrigalone G (47), a natural chalcone derived from Leptospermum recurvum (Myrtaceae), displays antiviral activity against the herpes simplex virus (Kjaergaard et al., 2003). Iryantherin K (48) and L (49) are two antiviral chalcones isolated from Iryantheria megistophulla, exhibiting significant inhibition against the potato virus and moderate inhibition against acetylcholinesterase (Kyogoku et al., 1979). Compounds 48 and 49 represent rare C-benzylated dihydrochalcone-lignan conjugate diastereoisomers, a rarity in the natural environment.

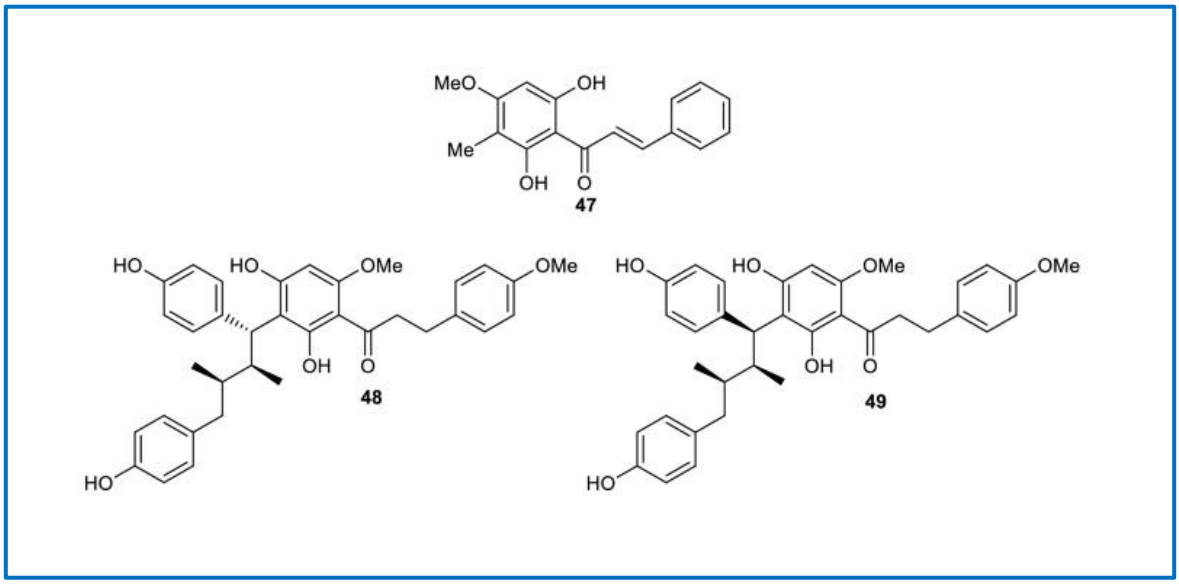

Figure 20: Some naturally occurring chalcone derivatives display antiviral activity.

2.8.6.11. Antiulcer Activity

Kanzonol C (35) occurs naturally and can also be synthesized. A synthetic derivative called chalcone (35) has shown potent antiulcer activity (Ming et al., 2002). Sophoradin (50) is a naturally prenylated chalcone, and its derivatives have demonstrated antiulcer activity (Sasajima et al., 1978). Synthetic analogs (51-53) of sophoradin have exhibited the highest antiulcer activity, with potency comparable to sophoradin.

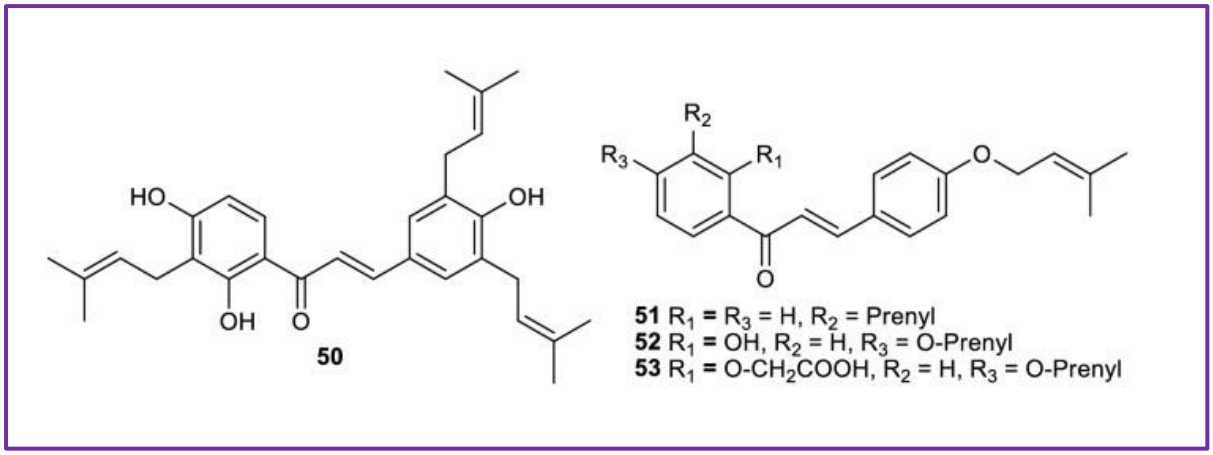

Figure 21: Derivatives of chalcones used for antiulcer applications.

2.8.6.12. Neuroprotective Activity

Alzheimer's disease, a prominent neurodegenerative disorder, originates from the aggregation of the beta-amyloid peptide and presents a significant global health challenge. The contemporary therapeutic interventions deployed to address neurodegenerative disorders encompass acetylcholinesterase inhibitors (AChE), butyrylcholinesterase inhibitors (BuChE), and memantine inhibitors, alongside synthesized compounds. Notably, the Thienylchalcone (54) compound, characterized by potent transglutaminase inhibition, holds promise for the prevention and treatment of Alzheimer's disease (Toray Industries, 2013). Furthermore, select nitro-substituted chalcones have demonstrated inhibitory activity against the catechol-O-methyltransferase enzyme, suggesting their potential efficacy in managing neurodegenerative disorders, including Parkinson's syndrome (ICM 2013). Exploration by Jeon et al., (2016) revealed the potent inhibitory action of synthetic chalcones **(**55) and (56) against μ-calpain and cathepsin B, offering potential therapeutic value for Alzheimer's-related conditions. Additionally, the coumarin chalcone hybrid (57), identified as a potent AChE inhibitor by Kang et al., (2018), holds promise as a treatment modality for neurodegenerative disorders.

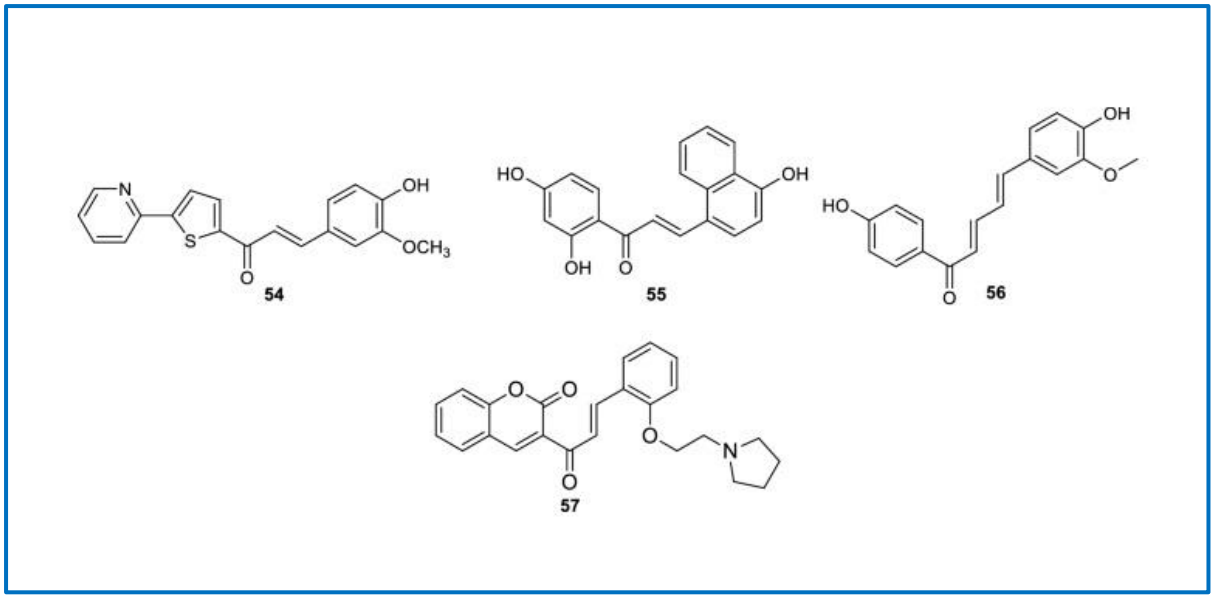

Figure 22: The potent inhibitory action of synthetic chalcone derivatives.

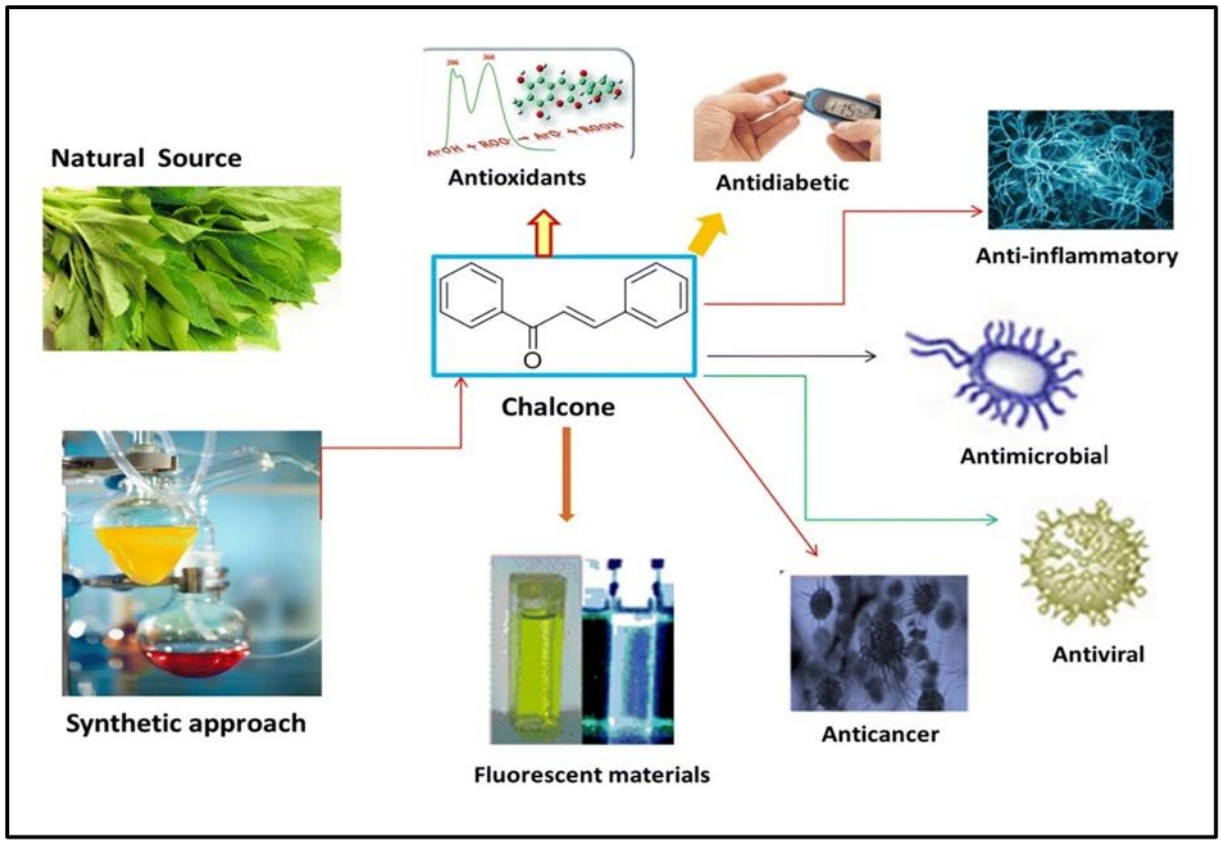

Figure 23: Represents the occurrence of chalcones in plants and through synthetic approaches, as well as their promising applications such as anticancer, antioxidants, antidiabetic, anti-inflammatory, antimicrobial, antiviral, and fluorescent materials. (Adapted from Rammohan et al., 2020).

2.8.7. Structure-Activity Relationship (SAR) Studies of Chalcones

In recent decades, numerous reports have been published on the structure-activity relationship (SAR) studies of chalcones, aiming to discern the structural attributes necessary for the design and development of new therapeutic molecules. Chalcones are known for their broad-spectrum pharmacological activities, believed to be attributed to the specific structural substitutions in rings A and B. Notably, Xu et al., (2019) presented a comprehensive review of the current developments in chalcones and their therapeutic applications as antibacterial agents. This review provides a succinct overview of the structural activity relationship of chalcone-based drugs against various bacterial infections.

Furthermore, the incorporation of two strong electron-withdrawing halogen groups at the 2, 4-positions of the aryl ring of chalcone **(Fig. 24)** may result in potent antibacterial activity, while the introduction of electron-donating groups, such as p-CH_3, 2,4-$(CH_3)_2$, p- or m-OCH_3 on aryl groups, diminishes the activity **(**Konduru et al., 2013). In a separate study, chalcones integrated with triazoles were synthesized and evaluated for their antibacterial activity against S. epidermidis, B. subtilis, E. coli, and P. aeruginosa (Chen et al., 2010). Strong electron withdrawing (-F, -NO_2) groups on the triazole ring of chalcone exerted a substantial influence on its antibacterial activity. Similarly, a novel class of potent antibacterial chalcones was developed by substituting one of the aryl rings with a ferrocene moiety. These ferrocene-based chalcone-linked triazoles coupled with organosilatranes exhibited promising antibacterial activities against E. faecalis and E. coli **(**Purser et al., 2008). Moreover, sulfone-linked chalcone hybrids demonstrated exceptional antibacterial activity against both Gram-positive and Gram-negative bacterial strains, encompassing both electron-withdrawing (Cl, Br, NO_2) and electron-donating (OMe) groups on aryl rings (Singh et al., 2019).

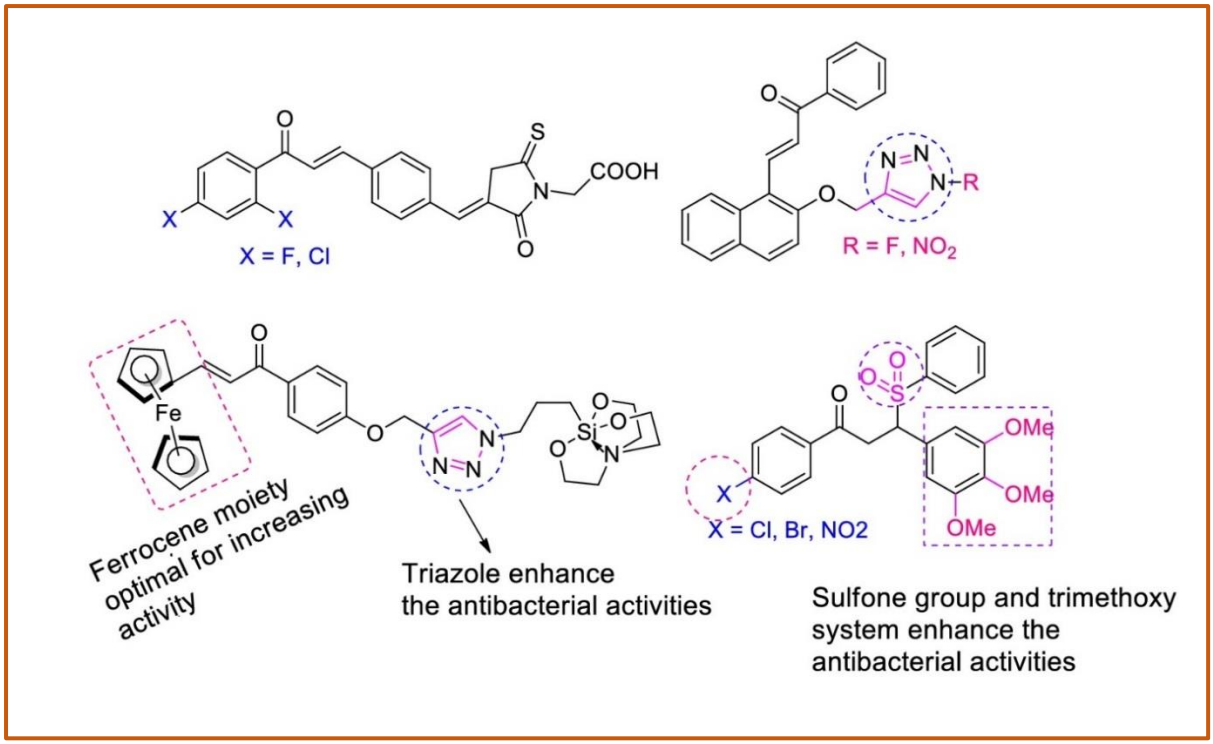

Figure 24: Investigation on the structure-activity relationship of antibacterial chalcones.

Diabetes Mellitus (DM) represents a significant metabolic disorder with global prevalence. The prevailing therapeutic approaches for diabetes target molecular entities such as aldose reductase (ALR), α-glucosidase, dipeptidyl peptidase-4 (DPP-4), peroxisome proliferator-activated receptor-γ (PPAR-γ), and protein tyrosine phosphatase 1B (PTP1B) enzyme inhibitors. However, these strategies are associated with various complications. Chalcones exhibit promising therapeutic potential in the management of diabetes owing to their distinct structural substitution pattern. Notably, the 2'-hydroxyl group serves as a pivotal feature of natural chalcones, conferring significant activity through the formation of hydrogen bonds and ensuring structural stability of the chalcone moiety **(Fig. 25)**.

Jung et al., (2006) have reported a novel series of 2'-hydroxy thiazolidinedione chalcone derivatives with ligand binding activities targeting peroxisome proliferator-activated receptor-γ (PPAR-γ). Chalcones possessing electron-releasing groups, such as dimethylamino, alkyl, and amino groups at the C-4 position of either ring A or ring B, have demonstrated more extensive activities than heteroaryl chalcones. Mahapatra et al., (2015) have expounded on the therapeutic approaches of chalcones and their structural implications in the context of diabetes. Chalcones bearing either 2'- and 4'-hydroxyl patterns or enhanced hydroxylation in ring B display potent antidiabetic activities. Structural features such as 2'-hydroxylation or 2'-, 3'-dihydroxylation, 2,3,4-trihydroxylation, and the presence of 4-dimethylamino groups in

chalcones are deemed crucial, endowing them with diverse pharmacological activities, including antioxidant and antibacterial properties (Avila et al.,2008; Prasad et al.,2007). Of particular note, 2'-hydroxylation in chelation with the carbonyl group demonstrates promising biological activities.

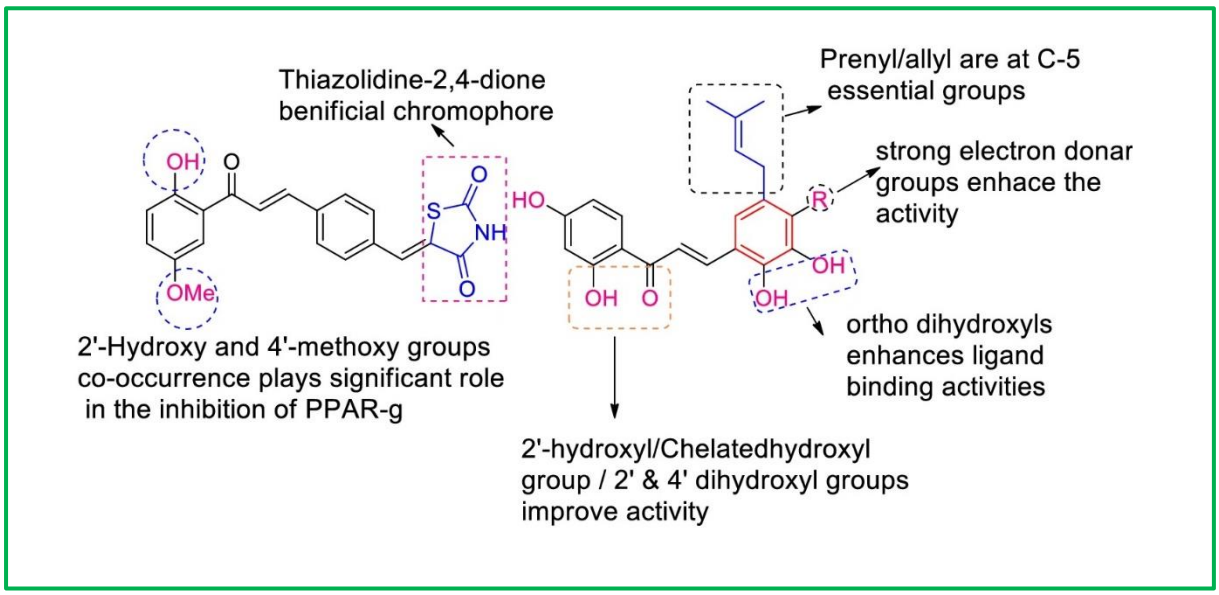

Figure 25: Exploration of Structure-activity relationship studies of antidiabetic chalcones.

Inflammation represents a significant health concern attributed to the oxidative damage of cellular biomolecules and the aberrant proliferation of tissue cells, culminating in inflammation-associated tumorigenesis. Numerous chalcones have been recognized as effective anti-inflammatory agents through the inhibition of nitric oxide synthase (NOX), lipoxygenase, and cyclooxygenase (COX-1 and COX-2) enzymes **(Fig.26)**. Chalcones containing mono- or poly-hydroxyl or methoxylated moieties have demonstrated notable anti-inflammatory activity by selectively inhibiting lipoxygenase (Kontogiorgis et al., 2008). Furthermore, the presence of potent electron-donating groups, such as dimethylamino substituents, has shown significant efficacy in NOX inhibition (Herencia et al., 2001). Notably, Broussochalcone A, a natural chalcone isolated from Broussonetia papyrifera, has exhibited pronounced anti-inflammatory properties through the potent inhibition of lipopolysaccharide (LPS)-induced iNOS protein (Cheng et al., 2001). The observed anti-inflammatory activity of Broussochalcone A is conjectured to be influenced by the presence of prenyl or orthodihydroxyl groups in ring B.

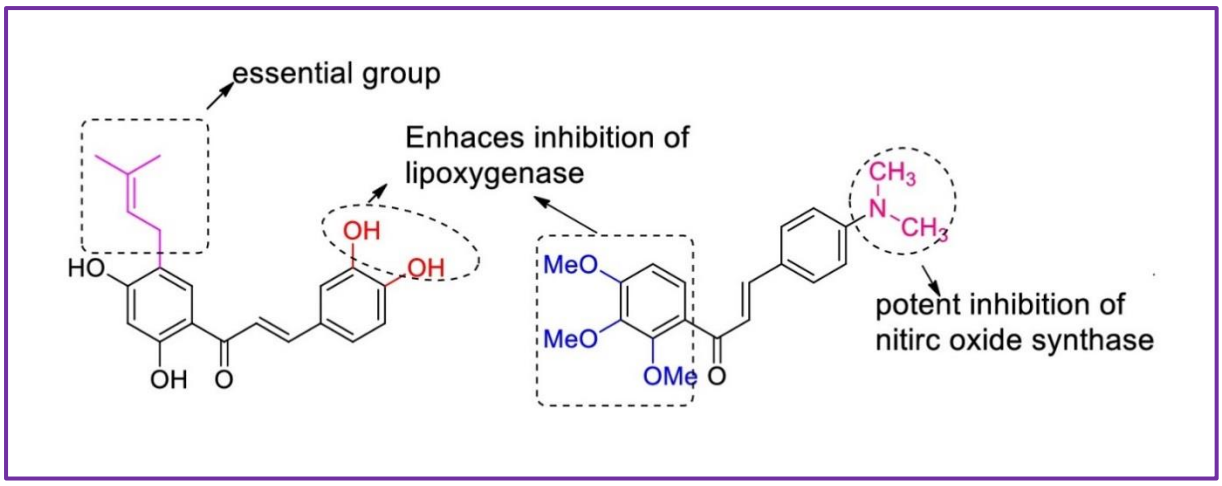

Figure 26: Illustration of the structure-activity relationship studies of anti-inflammatory chalcones and their structural significance.

2.8.8. Chalcones Analogs as Amyloid Inhibition

The amyloid cascade hypothesis, proposed in the early 1990s (Hardy and Allsop, 1991; Hardy and Selkoe, 2002), suggests that the imbalance in Aβ production and clearance leads to the development of Alzheimer's disease (AD). This imbalance results in the deposition of Aβ, leading to the formation of insoluble amyloid plaques and neurofibrillary tangles, which are believed to contribute to neuronal degeneration and cognitive decline. Aβ is generated from the amyloid precursor protein (APP) through the action of β- and γ-secretase proteases (Selkoe and Hardy, 2016). Depending on its processing by α- or β-secretase, APP can follow non-amyloidogenic or amyloidogenic metabolic pathways, respectively. In the pursuit of disease-modifying AD therapies, there has been a concerted effort to develop inhibitors targeting α- and β-secretase, as these enzymes play crucial roles in Aβ production. Notably, β-secretase (beta-site amyloid precursor protein cleaving enzyme 1; BACE-1) has garnered significant attention as a promising therapeutic target for AD, considering the substantial implications of α-secretase in Notch signaling and its associated severe toxicity. The beta-secretase (BACE-1) inhibitors are enzymes primarily present in neuronal cells. BACE-1 is an aspartyl protease that is bound to the cellular membrane and is responsible for cleaving the amyloid precursor protein (APP) at the beta site. This cleavage is considered the rate-limiting step in the generation of amyloid-beta (Aβ), a protein implicated in the pathogenesis of Alzheimer's disease. BACE-1 is predominantly located in the central nervous system (CNS), particularly in the brain and spinal cord. Originally, BACE-1 inhibitors were peptidomimetics designed based on the transition analog of APP. However, these compounds exhibited an inadequate pharmacokinetic (PK) profile, notably poor blood-brain barrier (BBB) permeability. Consequently, investigators

sought non-peptidomimetic compounds with sufficient size to accommodate the larger cavity of the BACE-1 active site, while also demonstrating a favorable PK profile and BBB permeability.

In a study conducted by Youn and Jun, it was reported that BACE-1 inhibition can be achieved by three flavonoids, namely a chalcone known as cardamonin sourced from Boesenbergia Rotunda (Youn and Jun, 2019). Additionally, Rampa et al. developed multiple chalcone derivatives inspired by natural compounds. Through in-house screening of small molecules, two compounds were identified as hits, encompassing a chalcone derivative(A) and benzophenone derivatives (B) (Fig 27). Computational modeling demonstrated the interaction between the N, N'-benzyl methylamine groups of the benzophenone derivative and the catalytic dyad of the BACE-1 enzyme (Rampa et al., 2016).

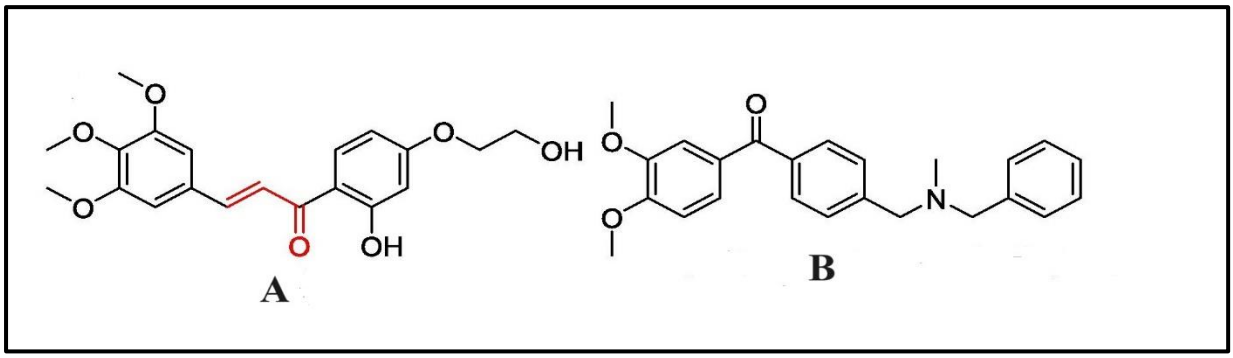

Figure 27: Naturally occurring BACE -1 Inhibitors (**A**: Chalcone derivatives and **B**: Benzophenone derivatives).

2.8.9. Chalcone as Amyloid Beta Aggregation Inhibitors

An alternative approach to impede the formation of amyloid plaque involves preventing the aggregation of Aβ into pathogenic oligomers and fibrils. This strategy is believed to be more advantageous than inhibiting the physiologically relevant Aβ production, as it may circumvent mechanism-based toxicity. Consequently, the development of disease-modifying Aβ aggregation inhibitors has emerged as an appealing area of Alzheimer's disease drug discovery (Estrada and Soto, 2007; Nie et al., 2011). However, the development of small molecules as inhibitors of Aβ aggregation presents challenges due to factors such as the larger size and geometry of the protein-protein interaction surface, and the absence of grooves or binding pockets for small molecules to accommodate (Whitty and Kumaravel, 2006).

In a study conducted by Cong et al., (2019), a series of hydroxylated chalcones was synthesized and subsequently tested for their dual inhibitory effects targeting Aβ aggregation and

ferroptosis. The researchers made an interesting observation that compounds, featuring trihydroxy substitution, displayed enhanced inhibitory effects on Aβ aggregation as compared to other compounds within the series. Their in vitro investigation further revealed that these trihydroxy-substituted chalcones exhibited superior neuroprotective properties against $A\beta_{1-42}$ induced neurotoxicity when compared to the well-known compounds EGCG and curcumin.

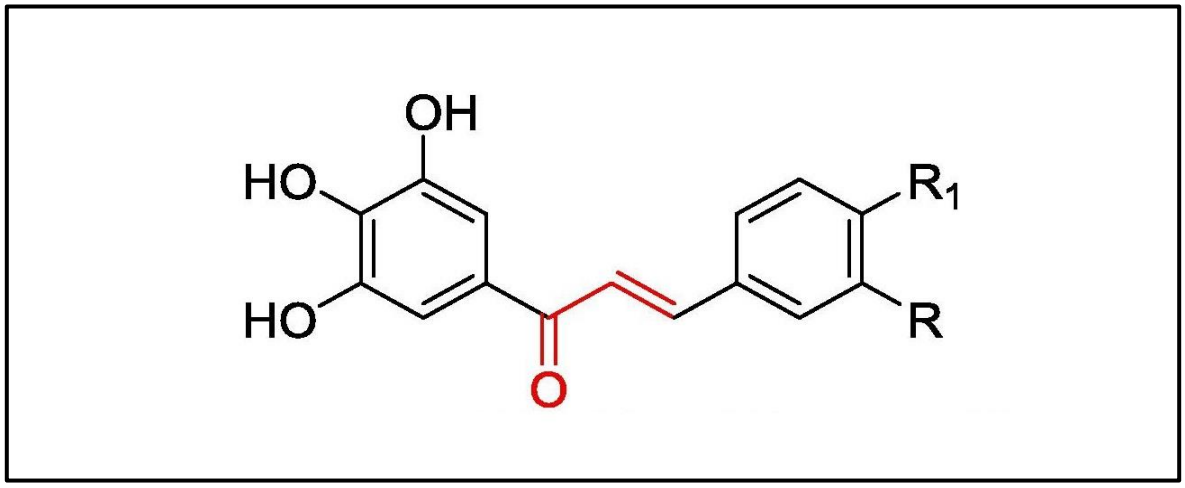

Figure 28: Aβ aggregation inhibitors by trihydroxy-substituted chalcones.

2.8.10. Conclusion

The literature extensively discusses the utilization of novel chalcones, which have been sourced from both natural origins and the realm of synthesis. This comprehensive review outlines the biosynthesis of chalcones, their structural significance as fluorescent materials, diverse synthetic approaches for their preparation, therapeutic applications, and their structure-activity relationship studies. Notably, chalcones are characterized by a privileged template featuring an α, β-unsaturated carbonyl system that readily allows for structural modifications. Consequently, researchers have devoted considerable attention to the skeletal modification of chalcones in the pursuit of designing new and innovative materials with varied applications. Therefore, chalcone serves as an innovative scaffold, playing a crucial role in the field of drug discovery.

2.8.11. References

Abonia, R., Gutiérrez, L., Quiroga, J. and Insuasty, B., 2018. (E)-3-[3-(2-Butoxyquinolin-3-yl) acryloyl]-2-hydroxy-4 H-chromen-4-one. Molbank, 2018(3), p.1001.

Abu, N., Ho, W.Y., Yeap, S.K., Akhtar, M.N., Abdullah, M.P., Omar, A.R. and Alitheen, N.B., 2013. The flavokawains: uprising medicinal chalcones. Cancer Cell International, 13, pp.1-7.

Aksöz, B.E. and Ertan, R., 2011. Chemical and structural properties of chalcones I. Fabad J Pharm Sci, 36, pp.223-242.

Ammaji, S., Masthanamma, S., Bhandare, R.R., Annadurai, S. and Shaik, A.B., 2022. Antitubercular and antioxidant activities of hydroxy and chloro substituted chalcone analogues: Synthesis, biological and computational studies. Arabian Journal of Chemistry, 15(2), p.103581.

Arslan, T., Celik, G., Celik, H., Şentürk, M., Yaylı, N. and Ekinci, D., 2016. Synthesis and biological evaluation of novel bischalcone derivatives as carbonic anhydrase inhibitors. Archiv der Pharmazie, 349(9), pp.741-748.

Asakura, H. and Kitahora, T., 2018. Polyphenols: prevention and treatment of human disease.

Ashok, D., Ravi, S., Ganesh, A., Lakshmi, B.V., Adam, S. and Murthy, S.D.S., 2016. Microwave-assisted synthesis and biological evaluation of carbazole-based chalcones, aurones, and flavones. Medicinal Chemistry Research, 25, pp.909-922.

Atanasov, A.G., Waltenberger, B., Pferschy-Wenzig, E.M., Linder, T., Wawrosch, C., Uhrin, P., Temml, V., Wang, L., Schwaiger, S., Heiss, E.H. and Rollinger, J.M., 2015. Discovery and resupply of pharmacologically active plant-derived natural products: A review. Biotechnology advances, 33(8), pp.1582-1614.

Ávila, H.P., Smânia, E.D.F.A., Delle Monache, F. and Júnior, A.S., 2008. Structure-activity relationship of antibacterial chalcones. Bioorganic & medicinal chemistry, 16(22), pp.9790-9794.

Bernardini, S., Tiezzi, A., Laghezza Masci, V. and Ovidi, E., 2018. Natural products for human health: A historical overview of the drug discovery approaches. Natural product research, 32(16), pp.1926-1950.

Burmaoglu, S., Algul, O., Anıl, D.A., Gobek, A., Duran, G.G., Ersan, R.H. and Duran, N., 2016. Synthesis and anti-proliferative activity of fluoro-substituted chalcones. Bioorganic & medicinal chemistry letters, 26(13), pp.3172-3176.

Butler, M.S., 2004. The role of natural product chemistry in drug discovery. Journal of natural products, 67(12), pp.2141-2153.

Calvino, V., Picallo, M., López-Peinado, A.J., Martín-Aranda, R.M. and Durán-Valle, C.J., 2006. Ultrasound accelerated Claisen–Schmidt condensation: A green route to chalcones. Applied Surface Science, 252(17), pp.6071-6074.

Chang, L.C., Chávez, D., Song, L.L., Farnsworth, N.R., Pezzuto, J.M. and Kinghorn, A.D., 2000. Absolute configuration of novel bioactive flavonoids from Tephrosia purpurea. Organic letters, 2(4), pp.515-518.

Chang, L.C., Gerhäuser, C., Song, L., Farnsworth, N.R., Pezzuto, J.M. and Kinghorn, A.D., 1997. Activity-guided isolation of constituents of Tephrosia purpurea with the potential to induce the phase II enzyme, quinone reductase. Journal of natural products, 60(9), pp.869-873.

Chen, Z.H., Zheng, C.J., Sun, L.P. and Piao, H.R., 2010. Synthesis of new chalcone derivatives containing a rhodanine-3-acetic acid moiety with potential anti-bacterial activity. European Journal of Medicinal Chemistry, 45(12), pp.5739-5743.

Cheng, M.S., Li, R.S. and Kenyon, G., 2000. A solid phase synthesis of chalcones by Claisen-Schmidt condensations. Chinese Chemical Letters, 11(10), pp.851-854.

Cheng, Z.J., Lin, C.N., Hwang, T.L. and Teng, C.M., 2001. Broussochalcone A, a potent antioxidant and effective suppressor of inducible nitric oxide synthase in lipopolysaccharide-activated macrophages. Biochemical Pharmacology, 61(8), pp.939-946.

Christensen, S.B., Ming, C., Andersen, L., Hjørne, U., Olsen, C.E., Cornett, C., Theander, T.G. and Kharazmi, A., 1994. An antileishmanial chalcone from Chinese licorice roots. Planta medica, 60(02), pp.121-123.

Chtourou, M., Abdelhédi, R., Frikha, M.H. and Trabelsi, M., 2010. Solvent free synthesis of 1, 3-diaryl-2-propenones catalyzed by commercial acid-clays under ultrasound irradiation. Ultrasonics sonochemistry, 17(1), pp.246-249.

Cioffi, G., Escobar, L.M., Braca, A. and De Tommasi, N., 2003. Antioxidant Chalcone Glycosides and Flavanones from Maclura (Chlorophora) tinctoria. Journal of Natural Products, 66(8), pp.1061-1064.

Colucci-Guyon, E., Batista, A.S., Oliveira, S.D., Blaud, M., Bellettini, I.C., Marteyn, B.S., Leblanc, K., Herbomel, P. and Duval, R., 2019. Ultraspecific live imaging of the dynamics of zebrafish neutrophil granules by a histopermeable fluorogenic benzochalcone probe. Chemical Science, 10(12), pp.3654-3670.

Cong, L., Dong, X., Wang, Y., Deng, Y., Li, B. and Dai, R., 2019. On the role of synthesized hydroxylated chalcones as dual functional amyloid-β aggregation and ferroptosis inhibitors for potential treatment of Alzheimer's disease. European Journal of Medicinal Chemistry, 166, pp.11-21.

Costa, R.G.D., Farias, F.R., Maqueira, L., Castanho, C., Carneiro, L.S., Almeida, J.M., Buarque, C.D., Aucélio, R.Q. and Limberger, J., 2019. Synthesis, photophysical, and electrochemical properties of novel D-π-D and D-π-A triphenylamino-chalcones and β-arylchalcones. Journal of the Brazilian Chemical Society, 30(1), pp.81-89.

Cragg, G.M., Grothaus, P.G. and Newman, D.J., 2009. Impact of natural products on developing new anti-cancer agents. Chemical Reviews, 109(7), pp.3012-3043.

D'Aléo, A., Karapetyan, A., Heresanu, V., Giorgi, M. and Fages, F., 2015. Tuning solid-state emission properties of pyrene-containing chalcone derivatives. Tetrahedron, 71(15), pp.2255-2259.

David, B., Wolfender, J.L. and Dias, D.A., 2015. The pharmaceutical industry and natural products: historical status and new trends. Phytochemistry Reviews, 14, pp.299-315.

de Freitas, V. and Mateus, N., 2006. Chemical transformations of anthocyanins yielding a variety of colors. Environmental Chemistry Letters, 4, pp.175-183.δ

Dhar, D.N., 1981. The chemistry of chalcones and related compounds. (No Title).

Díaz-Sánchez, M., Díaz-García, D., Prashar, S. and Gómez-Ruiz, S., 2019. Palladium nanoparticles supported on silica, alumina or titania: Greener alternatives for Suzuki–Miyaura and other C–C coupling reactions. Environmental Chemistry Letters, 17(4), pp.1585-1602.

Díaz-Tielas, C., Graña, E., Reigosa, M.J. and Sánchez-Moreiras, A.M., 2016. Biological activities and novel applications of chalcones. Planta Daninha, 34, pp.607-616.

Doan, T.N. and Tran, D.T., 2011. Synthesis, antioxidant, and antimicrobial activities of a novel series of chalcones, pyrazolic chalcones, and allylic chalcones. Pharmacology & Pharmacy, 2(04), pp.282-288.

Eddarir, S., Cotelle, N., Bakkour, Y. and Rolando, C., 2003. An efficient synthesis of chalcones based on the Suzuki reaction. Tetrahedron Letters, 44(28), pp.5359-5363.

Edwards, M.L., Stemerick, D.M. and Sunkara, P.S., 1990. Chalcones: a new class of antimitotic agents. Journal of medicinal chemistry, 33(7), pp.1948-1954.

ElSohly, H.N., Joshi, A.S., Nimrod, A.C., Walker, L.A. and Clark, A.M., 2001. Antifungal chalcones from Maclura tinctoria. Planta medica, 67(01), pp.87-89.

Estrada, L.D. and Soto, C., 2007. Disrupting β-amyloid aggregation for Alzheimer's disease treatment. Current topics in medicinal chemistry, 7(1), pp.115-126.

Fahim, A.M., Tolan, H.E., Awad, H. and Ismael, E.H., 2021. Synthesis, antimicrobial and antiproliferative activities, molecular docking, and computational studies of novel heterocycles. Journal of the Iranian Chemical Society, 18(11), pp.2965-2981.

Fang, Z., 2013. Application of nardoaristolone A in preparation of antitubercular drugs, CN103315991.

Feldman, M., Tanabe, S., Epifano, F., Genovese, S., Curini, M. and Grenier, D., 2011. Antibacterial and anti-inflammatory activities of 4-hydroxycordoin: potential therapeutic benefits. Journal of natural products, 74(1), pp.26-31.

Fuentes, A., Marinas, J.M. and Sinisterra, J.V., 1987. Catalyzed synthesis of chalcones under interfacial solid-liquid conditions with ultrasound. Tetrahedron Letters, 28(39), pp.4541-4544.

Funakoshi-Tago, M., Okamoto, K., Izumi, R., Tago, K., Yanagisawa, K., Narukawa, Y., Kiuchi, F., Kasahara, T. and Tamura, H., 2015. Anti-inflammatory activity of flavonoids in Nepalese propolis is attributed to inhibition of the IL-33 signaling pathway. International immunopharmacology, 25(1), pp.189-198.

Gaonkar, S.L. and Vignesh, U.N., 2017. Synthesis and pharmacological properties of chalcones: a review. Research on chemical intermediates, 43, pp.6043-6077.

Gomes, M.N., Muratov, E.N., Pereira, M., Peixoto, J.C., Rosseto, L.P., Cravo, P.V., Andrade, C.H. and Neves, B.J., 2017. Chalcone derivatives: promising starting points for drug design. Molecules, 22(8), p.1210.

Guantai, E.M., Ncokazi, K., Egan, T.J., Gut, J., Rosenthal, P.J., Bhampidipati, R., Kopinathan, A., Smith, P.J. and Chibale, K., 2011. Enone–and chalcone–chloroquinoline hybrid analogues: in silico guided design, synthesis, antiplasmodial activity, in vitro metabolism, and mechanistic studies. Journal of medicinal chemistry, 54(10), pp.3637-3649.

Guo, T., Jiang, Q., Yu, L. and Yu, Z., 2015. Synthesis of chalcones via domino dehydrochlorination/Pd (OAc) 2-catalyzed Heck reaction. Chinese Journal of Catalysis, 36(1), pp.78-85.

Guo, Y., Ding, L., Ghidinelli, S., Gotfredsen, C.H., de la Cruz, M., Mackenzie, T.A., Ramos, M.C., Sánchez, P., Vicente, F., Genilloud, O. and Coriani, S., 2021. Taxonomy-driven discovery of polyketides from Aspergillus californicus. Journal of Natural Products, 84(4), pp.979-985.

Gupta, P. and Mahajan, A., 2019. Sustainable approaches for steroid synthesis. Environmental Chemistry Letters, 17(2), pp.879-895.

Gupta, S., Maurya, P., Upadhyay, A., Kushwaha, P., Krishna, S., Siddiqi, M.I., Sashidhara, K.V. and Banerjee, D., 2018. Synthesis and bio-evaluation of indole-chalcone based benzopyrans as promising antiligase and antiproliferative agents. European Journal of Medicinal Chemistry, 143, pp.1981-1996.

Haddach, M. and McCarthy, J.R., 1999. A new method for the synthesis of ketones: The palladium-catalyzed cross-coupling of acid chlorides with aryl boronic acids. Tetrahedron Letters, 40(16), pp.3109-3112.

Hano, Y., Ichikawa, K., Okuyama, M. and Yamanaka, J., 1995. Sanggenons R, S, and T, Three New Isoprenylated Phenols from the Chinese Crude Drug. Heterocycles-Sendai Then Tokyo-, 40(2), pp.953-953.

Harborne, J.B., 2013. The flavonoids: advances in research since 1980.

Harborne, J.B., Marby, H. and Marby, T.J., 2013. The flavonoids. Springer.

Hardy, J. and Allsop, D., 1991. Amyloid deposition as the central event in the aetiology of Alzheimer's disease. Trends in pharmacological sciences, 12, pp.383-388.

Hardy, J. and Selkoe, D.J., 2002. The amyloid hypothesis of Alzheimer's disease: progress and problems on the road to therapeutics. science, 297(5580), pp.353-356.

Hatano, T., Takagi, M., Ito, H. and Yoshida, T., 1997. Phenolic constituents of liquorice. VII. A new chalcone with a potent radical scavenging activity and accompanying phenolics from liquorice. Chemical and Pharmaceutical Bulletin, 45(9), pp.1485-1492.

Herencia, F., Ferrándiz, M.L., Ubeda, A., Guillén, I., Dominguez, J.N., Charris, J.E., Lobo, G.M. and Alcaraz, M.J., 2001. 4-dimethylamino-3′, 4′-dimethoxychalcone downregulates iNOS expression and exerts anti-inflammatory effects. Free Radical Biology and Medicine, 30(1), pp.43-50.

Hermoso, A., Jiménez, I.A., Mamani, Z.A., Bazzocchi, I.L., Piñero, J.E., Ravelo, A.G. and Valladares, B., 2003. Antileishmanial activities of dihydrochalcones from Piper elongatum and synthetic related compounds. Structural requirements for activity. Bioorganic & medicinal chemistry, 11(18), pp.3975-3980.

Hirai, S., Kim, Y.I., Goto, T., Kang, M.S., Yoshimura, M., Obata, A., Yu, R. and Kawada, T., 2007. Inhibitory effect of naringenin chalcone on inflammatory changes in the interaction between adipocytes and macrophages. Life Sciences, 81(16), pp.1272-1279.

Hird, M., Toyne, K.J. and Gray, G.W., 1993. Palladium-catalyzed cross-coupling reactions in the synthesis of some high polarizability materials. Liquid Crystals, 14(3), pp.741-761.

Jeon, K.H., Lee, E., Jun, K.Y., Eom, J.E., Kwak, S.Y., Na, Y. and Kwon, Y., 2016. Neuroprotective effect of synthetic chalcone derivatives as competitive dual inhibitors against μ-calpain and cathepsin B through the downregulation of tau phosphorylation and insoluble Aβ peptide formation. European Journal of Medicinal Chemistry, 121, pp.433-444.

Jung, S.H., Park, S.Y., Kim-Pak, Y., Lee, H.K., Park, K.S., Shin, K.H., Ohuchi, K., Shin, H.K., Keum, S.R. and Lim, S.S., 2006. Synthesis and PPAR-γ ligand-binding activity of the new series of 2′-hydroxychalcone and thiazolidinedione derivatives. Chemical and Pharmaceutical Bulletin, 54(3), pp.368-371.

Kakati, D. and Sarma, J.C., 2011. Microwave-assisted solvent-free synthesis of 1, 3-diphenylpropenones. Chemistry Central Journal, 5, pp.1-5.

Kang, L., Gao, X.H., Liu, H.R., Men, X., Wu, H.N., Cui, P.W., Oldfield, E. and Yan, J.Y., 2018. Structure-activity relationship investigation of coumarin–chalcone hybrids with diverse side chains as acetylcholinesterase and butyrylcholinesterase inhibitors. Molecular diversity, 22, pp.893-906.

Karuppusamy, A., Vandana, T. and Kannan, P., 2017. Pyrene-based chalcone materials as solid state luminogens with aggregation-induced enhanced emission properties. Journal of Photochemistry and Photobiology A: Chemistry, 345, pp.11-20.

Kaul, T.N., Middleton Jr, E. and Ogra, P.L., 1985. Antiviral effect of flavonoids on human viruses. Journal of Medical Virology, 15(1), pp.71-79.

Kil, Y.S., Pham, S.T., Seo, E.K. and Jafari, M., 2017. Angelica keiskei, an emerging medicinal herb with various bioactive constituents and biological activities. Archives of pharmacal research, 40, pp.655-675.

Kitagawa, I., Chen, W.Z., Hori, K., Kobayashi, M. and Ren, J., 1998. Chemical studies of Chinese licorice roots. II. Five new flavonoid constituents from the roots of Glycyrrhiza aspera PALL. Collected in Xinjiang. Chemical and Pharmaceutical Bulletin, 46(10), pp.1511-1517.

Kjaergaard, H.G., Perry, N.B. and Weavers, R.T., 2003. Hydrogen-bonded rotamers of 2′, 4′, 6′-trihydroxy-3′-formyldihydrochalcone, an intermediate in the synthesis of a dihydrochalcone from Leptospermum recurvum. Tetrahedron, 59(32), pp.6113-6120.

Komarova, K.G., Sakipov, S.N., Plotnikov, V.G. and Alfimov, M.V., 2015. Luminescent properties of chalcone and its amino derivatives. Journal of Luminescence, 164, pp.57-63.

Konduru, N.K., Dey, S., Sajid, M., Owais, M. and Ahmed, N., 2013. Synthesis and antibacterial and antifungal evaluation of some chalcone-based sulfones and bisulfones. European Journal of Medicinal Chemistry, 59, pp.23-30.

Kontogiorgis, C., Mantzanidou, M. and Hadjipavlou-Litina, D., 2008. Chalcones and their potential role in inflammation. Mini reviews in medicinal chemistry, 8(12), pp.1224-1242.

Koorbanally, N.A., Randrianarivelojosia, M., Mulholland, D.A., van Ufford, L.Q. and van den Berg, A.J., 2003. Chalcones from the seed of Cedrelopsis grevei (Ptaeroxylaceae). Phytochemistry, 62(8), pp.1225-1229.

Krupadam, R.J., 2011. An efficient fluorescent polymer sensing material for detection of traces of benzo [a] pyrene in environmental samples. Environmental chemistry letters, 9, pp.389-395.

Kumar, A., Sharma, S., Tripathi, V.D. and Srivastava, S., 2010. Synthesis of chalcones and flavanones using Julia–Kocienski olefination. Tetrahedron, 66(48), pp.9445-9449.

Kyogoku, K., Hatayama, K., Yokomori, S., Saziki, R., Nakane, S., Sasajima, M., Sawada, J., Ohzeki, M. And Tanaka, I., 1979. Anti-ulcer effect of isoprenyl flavonoids. II. Synthesis and anti-ulcer activity of new chalcones related to sophoradin. Chemical and Pharmaceutical Bulletin, 27(12), pp.2943-2953.

Lakowicz, J.R. ed., 2006. Principles of fluorescence spectroscopy. Boston, MA: Springer US.

Leydet, Y., Batat, P., Jonusauskas, G., Denisov, S., Lima, J.C., Parola, A.J., McClenaghan, N.D. and Pina, F., 2013. Impact of water on the cis-trans photoisomerization of hydroxychalcones. The Journal of Physical Chemistry A, 117(20), pp.4167-4173.

Li, J.T., Yang, W.Z., Wang, S.X., Li, S.H. and Li, T.S., 2002. Improved synthesis of chalcones under ultrasound irradiation. Ultrasonics Sonochemistry, 9(5), pp.237-239.

López, J.A., Barillas, W., Gomez-Laurito, J., Martin, G.E., Lin, F.T., Al-Rehaily, A.J., Zemaitis, M.A. and Schiff, P.L., 1998. Galiposin: a new β-hydroxychalcone from Galipea granulosa. Planta medica, 64(01), pp.76-77.

Luyengi, L., Lee, I.S., Mar, W., Fong, H.H., Pezzuto, J.M. and Kinghorn, A.D., 1994. Rotenoids and chalcones from Mundulea sericea that inhibit phorbol ester-induced ornithine decarboxylase activity. Phytochemistry, 36(6), pp.1523-1526.

Mabry, T.J., Markham, K.R., Thomas, M.B., Mabry, T.J., Markham, K.R. and Thomas, M.B., 1970. The ultraviolet spectra of flavones and flavonols.

Mahapatra, D.K., Asati, V. and Bharti, S.K., 2015. Chalcones and their therapeutic targets for the management of diabetes: structural and pharmacological perspectives. European Journal of Medicinal Chemistry, 92, pp.839-865.

Martínez-Luis, S., Pérez-Vásquez, A. and Mata, R., 2007. Natural products with calmodulin inhibitor properties. Phytochemistry, 68(14), pp.1882-1903.

Masesane, I.B., Yeboah, S.O., Liebscher, J., Mügge, C. and Abegaz, B.M., 2000. A bichalcone from the twigs of Rhus pyroides. Phytochemistry, 53(8), pp.1005-1008.

Mata, R., 2007. Flavonoids, Chemistry, Biochemistry and Applications By ØM Andersen (University of Bergen) and KR Markham (Industrial Research Ltd.). CRC Press/Taylor & Francis, Boca Raton. 2006. xiv+ 1237 pp. 7× 101/4 in. $249.95. ISBN 0-8493-2021-6.

Mayer, R., 1993. A β-hydroxychalcone from Leptospermum scoparium. Planta medica, 59(03), pp.269-271.

Mdee, L.K., Yeboah, S.O. and Abegaz, B.M., 2003. Rhuschalcones II-VI, Five New Bichalcones from the Root Bark of Rhus pyroides. Journal of natural products, 66(5), pp.599-604.

Ming, D.S., López, A., Hillhouse, B.J., French, C.J., Hudson, J.B. and Towers, G.N., 2002. Bioactive Constituents from Iryanthera m egistophylla. Journal of natural products, 65(10), pp.1412-1416.

Müller, T. J., Markus Ansorge, and Daniel Aktah. "An Unexpected Coupling-Isomerization Sequence as an Entry to Novel Three-Component-Pyrazoline Syntheses This work was supported by the Deutsche Forschungsgemeinschaft and the Fonds der Chemischen Industrie. We thank Prof. Dr. H. Mayr for his generous support." Angewandte Chemie (International ed. in English) 39, no. 7 (2000): 1253-1256.

Nagai, H., He, J.X., Tani, T. and Akao, T., 2007. Antispasmodic activity of licochalcone A, a species-specific ingredient of Glycyrrhiza inflata roots. Journal of Pharmacy and Pharmacology, 59(10), pp.1421-1426.

Nakagawa-Goto, K. and Lee, K.H., 2006. Anti-AIDS agents 68. The first total synthesis of a unique potent anti-HIV chalcone from genus Desmos. Tetrahedron Letters, 47(47), pp.8263-8266.

Nakai, H., Okuyama, M., Kim, Y.M., Saburi, W., Wongchawalit, J., Mori, H., Chiba, S. and Kimura, A., 2005. Molecular analysis of α-glucosidase belonging to GH-family 31. Biologia, 60(Suppl. 16), pp.131-135.

Nakayama, T., Sato, T., Fukui, Y., Yonekura-Sakakibara, K., Hayashi, H., Tanaka, Y., Kusumi, T. and Nishino, T., 2001. Specificity analysis and mechanism of aurone synthesis catalyzed by aureusidin synthase, a polyphenol oxidase homolog responsible for flower coloration. FEBS letters, 499(1-2), pp.107-111.

Narender, T. and Reddy, K.P., 2007. A simple and highly efficient method for the synthesis of chalcones by using boron trifluoride-etherate. Tetrahedron Letters, 48(18), pp.3177-3180.

Narender, T., Tanvir, K., Rao, M.S., Srivastava, K. and Puri, S.K., 2005. Prenylated chalcones isolated from Crotalaria genus inhibits in vitro growth of the human malaria parasite Plasmodium falciparum. Bioorganic & medicinal chemistry letters, 15(10), pp.2453-2455.

Nie, Q., Du, X.G. and Geng, M.Y., 2011. Small molecule inhibitors of amyloid β peptide aggregation as a potential therapeutic strategy for Alzheimer's disease. Acta Pharmacologica Sinica, 32(5), pp.545-551.

Niu, C., Yin, L., Nie, L.F., Dou, J., Zhao, J.Y., Li, G. and Aisa, H.A., 2016. Synthesis and bioactivity of novel isoxazole chalcone derivatives on tyrosinase and melanin synthesis in murine B16 cells for the treatment of vitiligo. Bioorganic & medicinal chemistry, 24(21), pp.5440-5448.

Nowakowska, Z., 2007. A review of anti-infective and anti-inflammatory chalcones. *European Journal of Medicinal Chemistry*, *42*(2), pp.125-137.

Obara, H., Takahashi, H. and Hirano, H., 1969. The photo-Fries rearrangement of hydroxyphenyl cinnamates. Bulletin of the Chemical Society of Japan, 42(2), pp.560-561.

Oh, K.Y., Lee, J.H., Curtis-Long, M.J., Cho, J.K., Kim, J.Y., Lee, W.S. and Park, K.H., 2010. Glycosidase inhibitory phenolic compounds from the seed of Psoralea corylifolia. Food Chemistry, 121(4), pp.940-945.

Padmavathi, G., Roy, N.K., Bordoloi, D., Arfuso, F., Mishra, S., Sethi, G., Bishayee, A. and Kunnumakkara, A.B., 2017. Butein in health and disease: A comprehensive review. Phytomedicine, 25, pp.118-127.

Pannipara, Mehboobali, Abdullah M. Asiri, Khalid A. Alamry, Muhammad N. Arshad, and Samy A. El-Daly. "Synthesis, spectral behaviour and photophysics of donor–acceptor kind of chalcones: excited-state intramolecular charge transfer and fluorescence quenching studies." Spectrochimica Acta Part A: Molecular and Biomolecular Spectroscopy 136 (2015): 1893-1902.

Park, J., Yun, J., Kim, J., Jang, D.J., Park, C.H. and Lee, K., 2014. Brønsted Acid-Catalyzed Meyer–Schuster rearrangement for the synthesis of α, β-unsaturated carbonyl compounds. Synthetic Communications, 44(13), pp.1924-1929.

Pasricha, S., Sharma, D., Ojha, H., Gahlot, P., Pathak, M., Basu, M., Chawla, R., Singhal, S., Singh, A., Goel, R. and Kukreti, S., 2017. Luminescence, circular dichroism, and in silico studies of binding interaction of synthesized naphthylchalconeε derivatives with bovine serum albumin. Luminescence, 32(7), pp.1252-1262.

Passalacqua, T.G., Dutra, L.A., De Almeida, L., Velásquez, A.M.A., Torres, F.A.E., Yamasaki, P.R., dos Santos, M.B., Regasini, L.O., Michels, P.A., da Silva Bolzani, V. and Graminha, M.A., 2015. Synthesis and evaluation of novel prenylated chalcone derivatives as anti-leishmanial and anti-trypanosomal compounds. Bioorganic & Medicinal Chemistry Letters, 25(16), pp.3342-3345.

Prasad, R.Y., Kumar, R.P., Rao, L.A. and Viswanadh, K.R., 2007. In vitro antioxidant activity and scavenging effect effects of some new 1, 3, 5-Triphenyl-2-pyrazolines and 3-(2 {sup-} Hydroxy Naphthalen-1 {sup-} YL)-1, 5-Diphenyl-2-Pyrazolines. Saudi Pharmaceutical Journal, 15.

Purser, S., Moore, P.R., Swallow, S. and Gouverneur, V., 2008. Fluorine in medicinal chemistry. Chemical Society Reviews, 37(2), pp.320-330.

Qin, C.X., Chen, X., Hughes, R.A., Williams, S.J. and Woodman, O.L., 2008. Understanding the cardioprotective effects of flavonols: discovery of relaxant flavonols without antioxidant activity. Journal of Medicinal Chemistry, 51(6), pp.1874-1884.

Qiu, R.L., Li, L., Zhu, M.H. and Liu, J., 2011. Study on the chemical constituents of Psoralea corylifolia. Zhong yao cai= Zhongyaocai= Journal of Chinese medicinal materials, 34(8), pp.1211-1213.

Qiu, X., Zhu, L., Wang, H., Tan, Y., Yang, Z., Yang, L. and Wan, L., 2021. From natural products to HDAC inhibitors: An overview of drug discovery and design strategy. *Bioorganic & Medicinal Chemistry*, *52*, p.116510.

Radhakrishnan, S.K., Shimmon, R.G., Conn, C. and Baker, A.T., 2016. Inhibitory Kinetics of Azachalcones and their Oximes on Mushroom Tyrosinase: A Facile Solid-state Synthesis. Chemistry & Biodiversity, 13(5), pp.531-538.

Radhakrishnan, S.K., Shimmon, R.G., Conn, C. and Baker, A.T., 2015. Azachalcones: A new class of potent polyphenol oxidase inhibitors. Bioorganic & Medicinal Chemistry Letters, 25(8), pp.1753-1756.

Rajendra Prasad, Y., Lakshmana Rao, A., Prasoona, L., Murali, K. and Ravi Kumar, P., 2005. Synthesis and antidepressant activity of some 1, 3, 5-triphenyl-2-pyrazolines and 3-(2-hydroxy naphthalen-1-yl)-1, 5-diphenyl-2-pyrazolines. Bioorganic & medicinal chemistry letters (Print), 15(22), pp.5030-5034.

Rajendran, G., Bhanu, D., Aruchamy, B., Ramani, P., Pandurangan, N., Bobba, K.N., Oh, E.J., Chung, H.Y., Gangadaran, P. and Ahn, B.C., 2022. Chalcone: a promising bioactive scaffold in medicinal chemistry. Pharmaceuticals, 15(10), p.1250.

Ramakrishnan, V.T. and Kagan, J., 1970. Photochemical synthesis of 2'-hydroxychalcones from phenyl cinnamates. The Journal of Organic Chemistry, 35(9), pp.2901-2904.

Ramirez, F. and Dershowitz, S., 1957. Phosphinemethylenes. 1 II. Triphenylphosphine acylmethylenes. The Journal of Organic Chemistry, 22(1), pp.41-45.

Rammohan, A., Reddy, J.S., Sravya, G., Rao, C.N. and Zyryanov, G.V., 2020. Chalcone synthesis, properties, and medicinal applications: a review. Environmental Chemistry Letters, 18, pp.433-458.

Rampa, A., Tarozzi, A., Mancini, F., Pruccoli, L., Di Martino, R.M.C., Gobbi, S., Bisi, A., De Simone, A., Palomba, F., Zaccheroni, N. and Belluti, F., 2016. Naturally inspired molecules as multifunctional agents for Alzheimer's disease treatment. Molecules, 21(5), p.643.

Rashid, U., Sultana, R., Shaheen, N., Hassan, S.F., Yaqoob, F., Ahmad, M.J., Iftikhar, F., Sultana, N., Asghar, S., Yasinzai, M. and Ansari, F.L., 2016. Structure based medicinal

chemistry-driven strategy to design substituted dihydropyrimidines as potential antileishmanial agents. European Journal of Medicinal Chemistry, 115, pp.230-244.

Rateb, N.M. and Zohdi, H.F., 2009. Atom-efficient, solvent-free, green synthesis of chalcones by grinding. Synthetic Communications®, 39(15), pp.2789-2794.

Rudrapal, M., Khan, J., Dukhyil, A.A.B., Alarousy, R.M.I.I., Attah, E.I., Sharma, T., Khairnar, S.J. and Bendale, A.R., 2021. Chalcone scaffolds, bio precursors of flavonoids: Chemistry, bioactivities, and pharmacokinetics. Molecules, 26(23), p.7177.

Sapsford, K.E., Berti, L. and Medintz, I.L., 2006. Materials for fluorescence resonance energy transfer analysis: beyond traditional donor-acceptor combinations. Angewandte Chemie International Edition, 45(28), pp.4562-4589.

Saravanamurugan, S., Palanichamy, M., Arabindoo, B. and Murugesan, V., 2005. Solvent free synthesis of chalcone and flavanone over zinc oxide supported metal oxide catalysts. Catalysis Communications, 6(6), pp.399-403.

Sasajima, M., Nakane, S., Saziki, R., Saotome, H., Hatayama, K., Kyogoku, K. and Tanaka, I., 1978. Studies on the anti-ulcer effects of isoprenyl flavonoids (1). The anti-ulcer effects of isoprenyl chalcone extracted from Sophora subprostrata (author's transl). Nihon yakurigaku zasshi. Folia pharmacologica Japonica, 74(8), pp.897-905.

Schramm, O.G. and Mueller, T.J., 2006. Microwave-Accelerated Coupling-Isomerization Reaction (MACIR)–A General Coupling-Isomerization Synthesis of 1, 3-Diarylprop-2-en-1-ones. Advanced Synthesis & Catalysis, 348(18), pp.2565-2570.

Selkoe, D.J. and Hardy, J., 2016. The amyloid hypothesis of Alzheimer's disease at 25 years. EMBO molecular medicine, 8(6), pp.595-608.

Serdiuk, I.E., Wera, M. and Roshal, A.D., 2018. Structural and spectral features of 4′-substituted 2′-hydroxychalcones in solutions and crystals: Spectroscopic and theoretical investigations. The Journal of Physical Chemistry A, 122(8), pp.2030-2038.

Shalaby, M.A., Fahim, A.M. and Rizk, S.A., 2023. Microwave-assisted synthesis, antioxidant activity, docking simulation, and DFT analysis of different heterocyclic compounds. Scientific Reports, 13(1), p.4999.

Shalaby, M.A., Rizk, S.A. and Fahim, A.M., 2023. Synthesis, reactions, and application of chalcones: A systematic review. Organic & Biomolecular Chemistry, 21(26), pp.5317-5346.

Shibata, S., Inoue, H., Iwata, S., Ma, R., Yu, L., Ueyama, H., Takayasu, J., Hasegawa, T., Tokuda, H., Nishino, A. and Nishino, H., 1991. Inhibitory effects of licochalcone A isolated from Glycyrrhiza inflata root on inflammatory ear edema and tumor promotion in mice. Planta medica, 57(03), pp.221-224.

Shotter, R.G., Johnston, K.M. and Jones, J.F., 1978. Reactions of unsaturated acid halides—IV: Competitive Friedel-crafts acylations and alkylations of monohalogenobenzenes by the bifunctional cinnamoyl chloride. Tetrahedron, 34(6), pp.741-746.

Singh, G., Arora, A., Kalra, P., Maurya, I.K., Ruizc, C.E., Estebanc, M.A., Sinha, S., Goyal, K. and Sehgal, R., 2019. A strategic approach to the synthesis of ferrocene appended chalcone linked triazole allied organosilatranes: Antibacterial, antifungal, antiparasitic and antioxidant studies. Bioorganic & Medicinal Chemistry, 27(1), pp.188-195.

Smith, H.E. and Paulson, M.C., 1954. The Preparation of Chalcones from Hydroxy and Methoxy Aldehydes and Ketones1. Journal of the American Chemical Society, 76(17), pp.4486-4487.

Stevens, J.F. and Page, J.E., 2004. Xanthohumol and related prenylflavonoids from hops and beer: to your good health! Phytochemistry, 65(10), pp.1317-1330.

Subramanyam, R., Du-Thumm, L., Qazi, G.N., Khan, I.A., Suri, K.A., Satti, N.K., Ali, F. and Kalia, N.P., Council of Scientific, Industrial Research CSIR and Colgate Palmolive Co, 2015. Chalcones as enhancer of antimicrobial agents. U.S. Patent 9,192,589.

Tay, W.S., Li, Y., Lu, Y., Pullarkat, S.A. and Leung, P.H., 2020. Chemoselective Synthesis and Evaluation of β-Oxovinylarsines as an Arsenic Synthetic Precursor. Organometallics, 39(2), pp.271-278.

Teshima, T., Takeishi, M. and Arai, T., 2009. Red fluorescence from tautomers of 2′-hydroxychalcones induced by intramolecular hydrogen atom transfer. New Journal of Chemistry, 33(6), pp.1393-1401.

Tih, A.E., Tih, R.G., Sondengam, B.L., Martin, M.T. and Bodo, B., 1999. A novel hexafla vonoid from Lophira alata. Tetrahedron Letters, 40(25), pp.4721-4724.

Tokumura, K., Nagaosa, K., Ohta, Y. and Matsushima, R., 1998. Temperature-dependent tautomer fluorescence spectra of 3′, 4′-benzo-2′-hydroxychalcone: Direct evidence for photoenolization followed by Z→ E isomerization in the singlet manifold. Chemical Physics Letters, 295(5-6), pp.516-524.

Tomasch, M., Schwed, J.S., Weizel, L. and Stark, H., 2012. Novel chalcone-based fluorescent human histamine H3 receptor ligands as pharmacological tools. Frontiers in systems neuroscience, 6, p.14.

Tran, N., Drogui, P. and Brar, S.K., 2015. Sonochemical techniques to degrade pharmaceutical organic pollutants. Environmental chemistry letters, 13, pp.251-268.

Wang, H., 2010. Comprehensive Organic Name Reactions (Vol. 2, pp. 11-20). New York, NY, USA: Wiley.

Wang, Q., Ding, Z.H., Liu, J.K. and Zheng, Y.T., 2004. Xanthohumol, a novel anti-HIV-1 agent purified from Hops Humulus lupulus. Antiviral Research, 64(3), pp.189-194.

Wang, Y., Chan, F.L., Chen, S. and Leung, L.K., 2005. The plant polyphenol butein inhibits testosterone-induced proliferation in breast cancer cells expressing aromatase. Life Sciences, 77(1), pp.39-51.

Ward, R.S., 1990. Carbon-13 NMR of flavonoids (studies in organic chemistry series, no. 39). PK Agrawal (Ed.). Elsevier, Amsterdam, 1989.

Watanabe, H., Saji, H. and Ono, M., 2018. Novel fluorescence probes based on the chalcone scaffold for in vitro staining of β-amyloid plaques. Bioorganic & Medicinal Chemistry Letters, 28(19), pp.3242-3246.

Watanabe, K.I. and Imazawa, A., 1982. Aldol condensations catalyzed by Co (II) complexes of pyridine-containing copolymers. Bulletin of the Chemical Society of Japan, 55(10), pp.3208-3211.

Wei, W., Qunrong, W., Liqin, D., Aiqing, Z. and Duoyuan, W., 2005. Synthesis of dinitrochalcones by using ultrasonic irradiation in the presence of potassium carbonate. Ultrasonics sonochemistry, 12(6), pp.411-414.

Whitty, A. and Kumaravel, G., 2006. Between a rock and a hard place? Nature Chemical Biology, 2(3), pp.112-118.

Wu, W., Ye, H., Wan, L., Han, X., Wang, G., Hu, J., Tang, M., Duan, X., Fan, Y., He, S. and Huang, L., 2013. Millepachine, a novel chalcone, induces G 2/M arrest by inhibiting CDK1 activity and causing apoptosis via ROS-mitochondrial apoptotic pathway in human hepatocarcinoma cells in vitro and in vivo. Carcinogenesis, 34(7), pp.1636-1643.

Xu, C., Chen, G. and Huang, X., 1995. Chalcones by the Wittig reaction of a stable ylide with aldehydes under microwave irradiation. Organic preparations and procedures international, 27(5), pp.559-561.

Xu, M., Wu, P., Shen, F., Ji, J. and Rakesh, K.P., 2019. Chalcone derivatives and their antibacterial activities: Current development. Bioorganic Chemistry, 91, p.103133.

Yang, E.B., Zhang, K., Cheng, L.Y. and Mack, P., 1998. Butein, a specific protein tyrosine kinase inhibitor. Biochemical and biophysical research communications, 245(2), pp.435-438.

Yang, S., Min Kyun, N., Jang, J.P., Kim, K.A., Kim, B.Y., Sung, N.J., Oh, W.K. and Ahn, J.S., 2006. Inhibition of protein tyrosine phosphatase 1B by lignans from Myristica fragrans. Phytotherapy Research: An International Journal Devoted to Pharmacological and Toxicological Evaluation of Natural Product Derivatives, 20(8), pp.680-682.

Yaylı, N. and Gök, Y., 2005. O. Uç üncü, A. Yasar, Ç. Atasoy, E. Sahinbas, M. Küç ük. J. Chem. Res, pp.155-159.

Yit, C.C. and Das, N.P., 1994. Cytotoxic effect of butein on human colon adenocarcinoma cell proliferation. Cancer Letters, 82(1), pp.65-72.

Yoon, G., Lee, W., Kim, S.N., and Cheon, S.H., 2009. Inhibitory effect of chalcones and their derivatives from Glycyrrhiza inflata on protein tyrosine phosphatase 1B. Bioorganic & medicinal chemistry letters, 19(17), pp.5155-5157.

Yoshizawa, K. and Shioiri, T., 2006. Convenient stereoselective synthesis of (Z)-chalcone derivatives from 1, 3-diaryl-2-propynyl silyl ethers. Tetrahedron Letters, 47(28), pp.4943-4945.

Youn, K. and Jun, M., 2019. Biological evaluation and docking analysis of potent BACE1 inhibitors from Boesenbergia rotunda. Nutrients, 11(3), p.662.

Yu, F., Wang, M., Sun, H., Shan, Y., Du, M., Khan, A., Usman, R., Zhang, W., Shan, H. and Xu, C., 2017. Tuning the solid-state fluorescence of chalcone crystals via molecular coplanarity and J-aggregate formation. RSC advances, 7(14), pp.8491-8503.

Yun, S.W., Kang, N.Y., Park, S.J., Ha, H.H., Kim, Y.K., Lee, J.S. and Chang, Y.T., 2014. Diversity-oriented fluorescence library approach (DOFLA) for live cell imaging probe development. Accounts of chemical research, 47(4), pp.1277-1286.

Zhang, L., Liu, J., Gao, J., Lu, R. and Liu, F., 2017. Adjustment of the solid fluorescence of a chalcone derivative through controlling steric hindrance. RSC advances, 7(73), pp.46354-46357.

Zhao, F., Nozawa, H., Daikonnya, A., Kondo, K. and Kitanaka, S., 2003. Inhibitors of nitric oxide production from hops (Humulus lupulus L.). Biological and Pharmaceutical Bulletin, 26(1), pp.61-65.

Zheng, M., Huang, C., Yan, J.Z., Xie, S.L., Ke, S.J., Xia, H.D. and Duan, Y.N., 2023. In Situ Hypoiodite-Catalyzed Oxidative Rearrangement of Chalcones: Scope and Mechanistic Investigation. The Journal of Organic Chemistry, 88(3), pp.1504-1514.

Zhou, B., Jiang, P., Lu, J. and Xing, C., 2016. Characterization of the fluorescence properties of 4-dialkylaminochalcones and investigation of the cytotoxic mechanism of chalcones. Archiv der Pharmazie, 349(7), pp.539-552.

Zhuang, C., Zhang, W., Sheng, C., Zhang, W., Xing, C. and Miao, Z., 2017. Chalcone: a privileged structure in medicinal chemistry. Chemical Reviews, 117(12), pp.7762-7810.

CHAPTER 3

Electronic effect of (E)-1-(2-hydroxyphenyl)-3-phenylprop-2-en-1-one derivatives on the promotion and modulation of the aggregation of bovine beta-lactoglobulin.

3.1. Introduction

Proteins are vital components in the functioning of biological systems, with their biological roles heavily reliant on their intricate three-dimensional structures (Alberts, 2002). Any deviations in the structural integrity of proteins can lead to misfolding and subsequent aggregation, resulting in the loss of original biological function and the generation of harmful compounds within the body. For instance, the aggregation of proteins like $A\beta_{42}$ peptide, α-synuclein, prion protein, and insulin has been linked to various neurodegenerative disorders such as Alzheimer's disease (AD), Parkinson's disease (PD), prion disease, and type II diabetes, respectively (Kelly, 1998; Dobson, 2001; Stefani and Dobson, 2003; Bader et al., 2006; Serpell et al., 2000; Dobson, 2003; Englander et al., 2007; Rambaran and Serpell, 2008; Harper et al., 1999; Spires-Jones et al., 2017; M Ashraf et al., 2014). Under conditions of stress, it has been observed that diverse proteins aggregate to form amyloid fibrils, implying that amyloid formation may be an inherent genetic trait of all peptides. Numerous factors, including pH, temperature, and ionic strength of the medium, as well as the protein's primary structure, types and distribution of amino acid residues, their charge, hydrophobicity, and beta-sheet propensity, collectively influence the protein's capacity to undergo amyloid formation (Liu et al., 1994; Maity et al.,2016; Patel et al., 2005). During the process of protein aggregation, extensive structural modifications occur, leading to the dominance of a β-sheet structural motif (Pal et al., 2016), which ultimately transforms into amyloid fibrils. Structural studies have demonstrated that amyloid fibrils primarily manifest a stable cross-β conformation, rendering them resilient to proteolysis and thermodynamically stable, despite being formed by structurally and functionally diverse proteins associated with different disorders (Dobson, 2002; Arora et al., 2004; Dirix et al., 2005; Nordstedt et al., 1994; Surmacz-Chwedoruk et al., 2012). The exact mechanism by which a diverse array of proteins aggregates to form a common structure continues to be a subject of ongoing investigation and represents an active area of research.

Organic small molecules or biologically active compounds have the ability to engage with protein molecules, forming bonds with various structural motifs of the protein. This interaction has a significant impact on the process of protein aggregation, potentially either slowing it down or accelerating it, leading to the production of toxic amyloid fibrils (Parvej et al., 2022; Majid et al., 2023). As a result, the prevention of soluble aggregate formation could offer a means of controlling several neurodegenerative diseases (Parvej et al., 2022; Majid et al., 2023; Soto and Pritzkow, 2018). Additionally, exploring the influence of biologically active compounds on protein aggregation can provide valuable insights into the origins and preventive measures for these diseases.

Hydroxychalcones are a group of chemical compounds that serve as a structural foundation for many naturally occurring substances. They can be found in a wide variety of plant tissues, including vegetables, teas, fruits, and other plants worldwide (Singh et al., 2014; K Sahu et al., 2012; Gomes et al., 2017). These compounds share a common structural feature known as chalconoid, specifically 1,3-diphenyl-2E-propene-1-one, which consists of two benzene rings and an α, β-unsaturated ketone functional group. Due to this unique structure, hydroxychalcones are utilized as a valuable template in the field of drug discovery (Simmler et al., 2017). These compounds have a long history of use in traditional medicine, with derivatives of hydroxychalcone being employed to treat a range of medical ailments such as diabetes, inflammation, tuberculosis, and cancer. Some hydroxychalcone-based compounds, like sofalcone, metochalcone, and hesperidin methyl chalcone, have been previously utilized as antiulcer and neuroprotective drugs, choleretic drugs, and vascular protective agents, respectively (Rahman, 2011). One of the key factors contributing to the interest in hydroxychalcone derivatives for drug discovery is their ease of optimization in terms of lipophilicity, low molecular weight, and straightforward synthesis procedures. As a result, hydroxychalcones have garnered significant attention in the realm of drug discovery, particularly in the context of central nervous system (CNS) diseases, including Alzheimer's disease (AD).

The whey protein β-lactoglobulin, a prominent protein in whey, has garnered attention due to its numerous therapeutic applications, nutraceutical values, and notable transport properties (Papiz et al., 1986; Kontopidis et al., 2004; Mansouri et al., 1998; Ouwehand et al., 1997; Gomez et al., 2002; Teng et al., 2015). Bovine β-lactoglobulin (β-lg), present in the milk of various mammalian species, has a molecular weight of 18400 Da. It primarily consists of approximately 50% β-sheet, 15% α-helix, and 15–20% reverse turn. Upon exposure to thermal

incubation, significant structural modifications occur in β-lg, leading to the exposure of buried hydrophobic residues and the thiol (–SH) group of Cys-121. This process results in the formation of a beta barrel-like structure comprised of eight antiparallel β-sheet structures (Creamer et al., 1983; Sawyer et al., 1999). At a thermal incubation temperature of 70ºC, β-lg undergoes partial denaturation and subsequent aggregation, ultimately leading to the formation of soluble aggregates. When the temperature rises above 75°C, the non-covalent interactions become increasingly important, leading to the exchange of disulfide bonds and hydrophobic contacts, which then take over the aggregation process. As a result, the protein β-lg forms amyloid fibrils when exposed to these high temperatures. These amyloid fibrils closely resemble the disease-related amyloid fibrils, making the β-lg protein an ideal model for studying the aggregation pathways of disease-related proteins (Maity et al., 2018). In this particular study, chalcones with attached electron-donating and withdrawing groups were specifically created to investigate how they influence the structure of β-lg. Furthermore, the study delved into the impact of the structural changes in the protein due to the attachment of these synthesized molecules on protein-protein interactions under thermal aggregation conditions.

3.2. Experimental Section

3.2.1. Synthesis of Chalcone Analogs

In a round bottom flask equipped with a magnetic stir bar, a solution was prepared by combining 1mM of 2-hydroxy acetophenone and 1mM of benzaldehyde and its derivatives in a 10% aqueous-ethanolic (1:1) NaOH solution. The resulting mixture was stirred for 1 hour, leading to the formation of bright yellow to red precipitates of compounds (SC1 – SC4) after the solution was neutralized at room temperature. The crude product was then subjected to filtration and crystallization using a combination of ethyl acetate and petroleum ether (20%) (Elkanzi et al., 2022). The resulting crystallized compounds were further filtered, dried, and characterized using 1H NMR spectroscopy.

(E)-3-(4-(dimethylamino) phenyl)-1-(2-hydroxyphenyl) prop-2-en-1-one (**SC1**): Light yellow solid: Mp. 180 °C; Yield: 82 %; 1H NMR (600 MHz, CDCl3) δ: 3.05 (s, 6H, N-(CH3)2), 6.72 (d, 1H, J = 6.0 Hz, Ar-H), 6.95 (d, 1H, J = 15.6 Hz, CH = CH), 7.01 (d, 2H, J = 6 Hz, Ar-H), 7.46 (dd, 1H, J = 2.4 Hz, Ar-H), 7.46 (d, 1H, J = 1.8 Hz, Ar-H), 7.50 (d, 1H, J= 2.8 Hz, Ar-H), 7.58 (d, 1H, J = 6.0 Hz, Ar-H), 7.95 (d, 1H, J = 15.6 Hz, CH = CH), 13.18 (s, 1H, OH).

(E)-1-(2-hydroxyphenyl)-3-(4-methoxyphenyl) prop-2-en-1-one (**SC2**). Yellow solid (75%); 1H NMR (300 MHz, CDCl3) δ 3.62 (s, 3H, -CH3), 6.96 (d, 1H, J = 7.2 Hz, Ar-H), 7.64 (d, 2H, J = 7.1 Hz, Ar-H), 7.61(d, J = 15 Hz, 1H, CH = CH), 7.46 (m, 2H, Ar-H), 7.72 (d, J = 7.1 Hz, 2H, Ar-H), 8.03 (d, J = 15 Hz, 1H, CH = CH), 8.09 (d, J = 7.2 Hz, 1H, Ar-H), 13.6 (s, 1H, OH).

(E)-1-(2-hydroxyphenyl)-3-phenylprop-2-en-1-one (**SC3**). Yellow solid (71%); 1H NMR (300 MHz, CDCl3) δ 6.82 (d, J = 7.2 Hz, 1H, Ar-H), 7.33-7.54 (m, 7H, Ar-H), 7.60 (d, J = 15 Hz, 1H, CH = CH), 8.02 (d, J = 15 Hz, 1H, CH = CH), 8.07 (d, J = 7.2 Hz, 1H, Ar-H), 13.4 (s, 1H, OH).

(E)-1-(2-hydroxyphenyl)-3-(3-nitrophenyl) prop-2-en-1-one (**SC4**). Yellow solid (75%); 1H NMR (300 MHz, CDCl3) δ 6.9 (d, J = 7.2 Hz, 1H, Ar-H), 7.46 (d, J = 7.1 Hz, 2H, Ar-H), 7.69 (d, J = 7.2 Hz, 1H, Ar-H), 7.91 (d, J = 15 Hz, 1H, CH = CH), 7.99 (m, 1H, Ar-H), 8.03 (d, J = 7.2 Hz, 1H, Ar-H), 8.19 (d, J = 15 Hz, 1H, CH = CH), 8.16 (d, J = 7.1 Hz, 1H), 8.33 (d, J = 7.2 Hz, 1H), 13.6 (s, 1H, OH).

3.2.2. Isolation, Purification, and Preparation of β–lactoglobulin (β-lg) Solution

The bovine β-lactoglobulin (β-lg) was extracted and purified from cow's milk using the Aschaffenburg and Drewry method (Aschaffenburg and Drewry, 1957). After dialysis, the final product, which contained a high concentration of ion-free water, was freeze-dried using an Eyela Lyophilizer, resulting in a solid powder that was stored at 4°C. For our research, a 10 mg protein sample was dissolved in a 10 mM sodium phosphate buffer solution with 2% ethanol at a pH of 7.4 (Giamblanco et al., 2018). The extinction coefficient of β-lg at 280 nm (0.959 mg^{-1} mL^{-1} cm^{-1} at 280 nm) was utilized to prepare 20 mM β-lg samples by diluting the stock solution of 5 mg/mL using a UV-vis Spectrophotometer. Subsequently, for spectroscopic measurements, the stock solution of β-lg was further diluted with a sodium-phosphate buffer solution at pH 7.4 containing 2% ethanol.

3.2.3. UV-VIS Spectroscopy Studies

Utilizing the JASCO UV-visible spectrophotometer (Serial no: B184461798, Model: V-730) in conjunction with the JASCO Spectra Manager Software, we conducted absorption spectroscopy on samples comprising native β-lg, thermally incubated β-lg in the presence and absence of the SC3 derivative at room temperature (25°C). Our measurements employed two Quartz cells, each with a path length of 1cm, for the sample and reference solutions. The

reference cell contained phosphate buffer (10mM) with a pH of 7.4 and 2% ethanol, while the sample solution maintained a β-lg concentration of 20µm.

3.2.4. Intrinsic Fluorescence Measurements

In order to explore the changes in the tertiary structure or the micro-environment surrounding the fluorophores of the native β-lactoglobulin (β-lg) protein, we performed intrinsic fluorescence measurements. This involved analyzing the native form of β-lg as well as β-lg that had been subjected to heat incubation at 75 ºC for 1 hour at pH 7.4, both in the presence and absence of SC3 derivatives. To carry out this investigation, we utilized a Horiba Fluorometer (Serial No: 1734D-4018-FM, Model: Fluoromax-4C). As part of the experimental procedure, we prepared sample solutions containing β-lg at a concentration of 20µM in a quartz cuvette with a path length of 1cm. The protein was excited at a wavelength of λmax 295 nm (Horvath and Wittung-Stafshede, 2016), with both the excitation and emission slits set at 5 nm. Subsequently, we recorded the emission spectra within the range of 300-400 nm to capture a comprehensive understanding of the fluorescence changes.

3.2.5. ANS Study to monitor the hydrophobicity changes

The yellow-colored fluorescent dye 8-Anilinonaphthalene-1-sulfonic acid (ANS) is utilized to assess the surface hydrophobicity of protein molecules. To prepare the ANS sample, a stock solution of 1 mg/mL was created using Milli-Q water. In our research, we added 30 µM of ANS solution to each sample solution to ensure a 50-molar excess of ANS compared to the protein concentration (Semisotnov et al., 1991). The ANS-fluorescence was measured using a Horiba Fluorometer (Serial No: 1734D-4018-FM, Model: Fluoromax-4C) after exciting each sample at λmax 385 nm in a four-side transparent rectangular quartz cell of 1 cm pathlength. The emission and excitation slits were set at 5 nm, and the ANS-fluorescence emission spectra were recorded in the wavelength range of 395 to 600 nm using the Fluoromax Software (Khan et al., 2013).

3.2.6. Thioflavin T (ThT) fluorescence for quantitative measurements of β-lg aggregates

Thioflavin T (ThT) is a vibrant yellow-colored organic dye renowned for its ability to selectively bind to the beta-sheeted structure of protein aggregates, resulting in a significant increase in fluorescence emission at around 485 nm (Nilsson, 2004). This unique characteristic allows for the quantification and comparative analysis of aggregate formation in a given solution through the ThT binding assay. The process commenced with the meticulous

preparation of a 5mM stock solution of ThT by dissolving the dye in a 10mM sodium phosphate buffer. Subsequently, 20 µL of this prepared stock solution was meticulously introduced into each β-lg sample solution—comprising naïve samples, those subjected to thermal incubation at 75 ºC for 1 hour at pH 7.4 in the presence and absence of SC3 compounds and thoroughly mixed to ensure a consistent 30 µM ThT concentration in each sample. Following this, the sample solutions underwent a 30-minute incubation period at a room temperature of 25°C. Leveraging the capabilities of a Horiba Fluorometer (Serial No: 1734D-4018-FM, Model: Fluoromax-4C), the ThT fluorescence assay was conducted by exciting each sample at λmax 450 nm in a transparent rectangular quartz cuvette with a 1 cm pathlength (Banerjee and Das, 2012). To capture the emission spectra, both the excitation and emission slits were meticulously set at 5 nm, and data were recorded within the wavelength range of 460-600 nm.

3.2.7. Transmission Electron Microscopy Study

A high-resolution transmission electron microscopy (HR TEM) study was conducted to examine the behavior of β-lg in the presence and absence of ZnO nanoparticles. The imaging was performed using a JEOL HRTEM-2011 instrument from Tokyo, Japan, at various magnifications (Hoppenreijs et al., 2022). Prior to the study, the sample solutions were centrifuged, diluted, and carefully drop-cast onto a carbon-coated copper grid with a mesh size of 300C. After removing the excess solution, a 2% uranyl acetate solution from Sigma was added to stain the sample, and the grids were air-dried overnight in a desiccator. Following this process, the grids were ready for TEM imaging at a specific magnification.

3.2.8. Rayleigh light scattering (RLS) Study

The thermal behavior of β-lactoglobulin (β-lg) in the presence and absence of the synthesized SC compounds was studied using Resonance Light Scattering (RLS) experiments in a Shimadzu spectrofluorometer (Model: Shimadzu 5301 PC). The fluorescence intensities were recorded at 350 nm after exciting the sample solutions at the same wavelength (Sardar et al., 2014). The experiments were conducted in a quartz cell with a path length of 1 cm using NaH_2PO_4 buffer (10 mM) at pH 7.4. Both the emission and excitation slits were set at 5 nm. These experiments were replicated three times for accuracy.

3.2.9. Dynamic light scattering (DLS) measurements

When tiny particles are dispersed in a solution, they cause fluctuations in the intensity of scattered light. Dynamic light scattering (DLS) is used to detect these fluctuations using an

auto-correlator on a microsecond time scale, enabling the analysis of molecular distribution. In this study, DLS measurements were carried out using a Zetasizer Nano (Malvern Instrument, UK) on native β-lg solutions and heated β-lg solutions with and without various SC derivatives. The solutions were incubated at 75 ºC for 1 hour at pH 7.4 and then illuminated with a 633 nm laser (Yu et al., 2007). The measurements were conducted using a 2 mL transparent rectangular quartz cuvette with a path length of 10mm, using sample solutions containing a 20μM β-lg concentration at room temperature. The time-dependent autocorrelation function was obtained with 12 acquisitions for every run, and the reported data represents the mean of three consecutive sets of data.

3.2.10. Fourier-Transform Infrared (FT-IR) measurements

The Amide I band at 1600-17000 cm^{-1} and the Amide II band in the range of 1480-1570 cm^{-1} are recognized as crucial diagnostic indicators in FT-IR spectra for characterizing the secondary structures of both native and incubated β-lg with SC compounds. Hence, these bands serve as pivotal tools for discerning the structural alterations in β-lg in the presence of various SC derivatives. Our analysis involved using a Spectrum 100 FT-IR spectrometer (Perkin-Elmer) to ascertain the infrared absorption spectra of the samples at a temperature of 25°C, with a nominal resolution of 2 cm^{-1}. For each sample, a β-lg concentration of 500 μm was upheld, with data being recorded within the 1500-1700 cm^{-1} range (Yang et al., 2015).

3.2.11. AFM Study

In preparation for conducting an experiment, it was essential to prepare AFM grid slides. A solution containing various samples, each comprising 5 mg mL^{-1} of β-lg, was carefully drop-casted onto a glass slide. Following this, the sample was evenly spread and allowed to dry overnight to facilitate optimal observation. Subsequently, images of β-lg, heat-treated β-lg, and β-lg that had been exposed to different chalcone (SC) compounds at 75°C were meticulously captured using a VEECO DICP II auto probe (Model AP 0100) and an AFM microscope. The acquisition of these images was executed with meticulous attention to detail to ensure the precision and accuracy of the results (Hoppenreijs et al., 2022).

3.2.12. Molecular Docking Study

A detailed molecular docking model was meticulously crafted to investigate the intricate interactions and binding mechanisms of β-lg molecules with the synthesized SC3 compounds (Morris et al., 2009). This intricate model leveraged the powerful AutoDock 4.2 software,

enabling precise visualization of the molecular interactions. Furthermore, the energy of the SC3 derivatives was carefully minimized through sophisticated Gaussian 0.9w DFT optimization techniques. Notably, the molecular docking process incorporated a substantial 126x126x126 grid box and harnessed the Lamarckian genetic algorithm (LGA) to meticulously explore the binding characteristics.

3.3. Results and Discussion

3.3.1. Design and Synthesis of Hydroxychalcones

The electronic effect, which refers to the influence of substituents attached to a molecule on its interactions with other molecules, plays a significant role in determining the behavior of hydroxychalcone compounds. These compounds, with their varying electron densities, have the potential to interact with proteins in unique ways. To explore this, we have deliberately chosen hydroxychalcone variants with high electron-rich, moderate electron-rich, neutral, and moderate electron-deficient properties. In order to address issues related to solubility, we specifically opted for hydroxychalcone. The synthesis of the hydroxychalcone derivatives was achieved using the classical Claisen-Schmidt reaction. One of our main challenges was to select appropriate starting materials, determining which phenyl ring of the resulting compounds would contain a hydroxyl group, while allowing for variation in the other ring. To mitigate potential synthetic difficulties, we made the decision to place the hydroxyl group on the phenyl ring containing the ketone, while introducing variations in the functional groups on the second ring. This approach enabled us to generate hydroxychalcone compounds with the specific electron density characteristics we sought to study.

In the presence of 10% NaOH, the reaction between 2-hydroxy acetophenone (1) and substituted benzaldehyde (2) in a 1:1 aqueous ethanol mixture produces derivatives of (E)-1-(2-hydroxyphenyl)-3-phenylprop-2-en-1-one (SC). The reaction process is illustrated in **Scheme 1**, resulting in the synthesis of four compounds with high yields. When 2-hydroxy acetophenone reacts with para-N, N-dimethylbenzaldehyde, it yields the electron-rich and highly polar SC1, attributed to extended conjugation. Conversely, by employing 4-methoxy benzaldehyde, the electron density and polarity of the SC can be diminished, culminating in the production of SC2. SC1, derived from the reaction between 2-hydroxyacetophenone and benzaldehyde, serves as the neutral reference compound. Replacing the tertiary amino group with a nitro group results in the formation of SC4, which exhibits increased polarity and electron deficiency compared to other compounds. This study introduces substituents with

distinct electronic and steric effects on the SC3 nucleus. The resultant molecules' polarity and hydrophobicity, influenced by this substitution, can elicit varied interactions with proteins, potentially influencing the protein conformation and thereby either promoting or inhibiting the protein aggregation process.

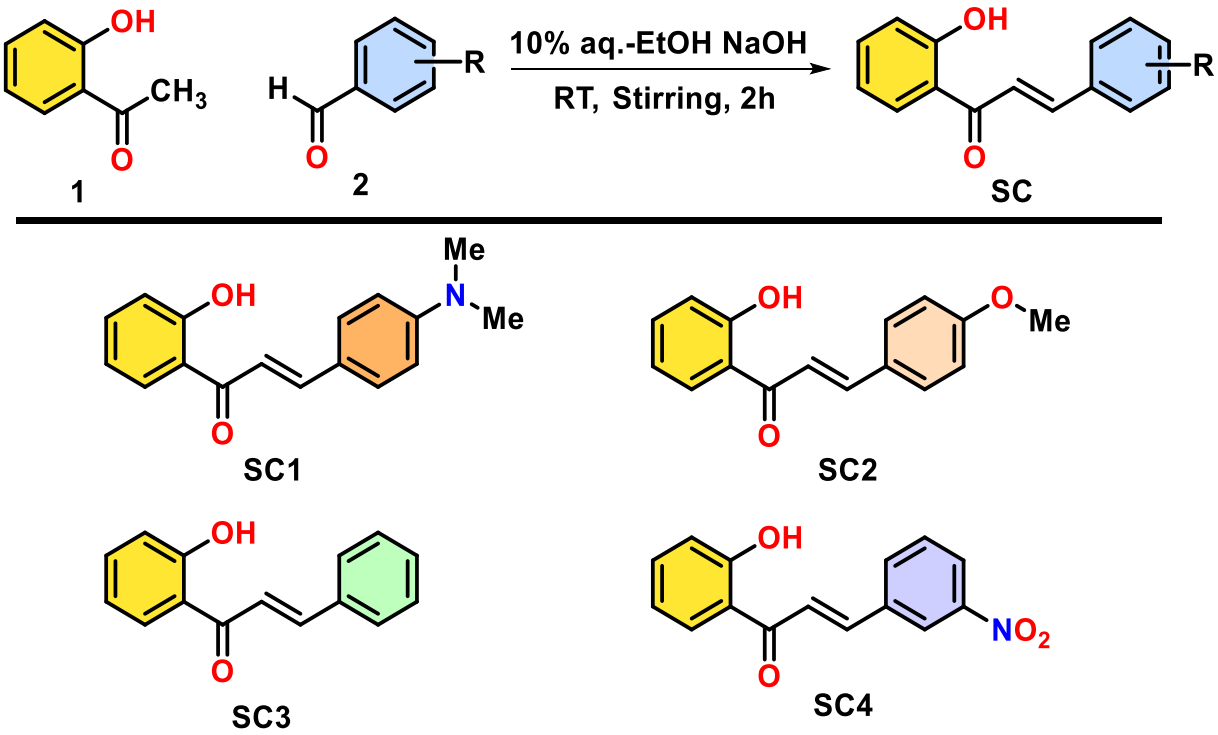

Scheme 1: Synthesis of SC1-SC4 compounds.

3.3.2. ^{1}H NMR analysis of the SC1-SC4 compounds

(E)-3-(4-(dimethylamino) phenyl)-1-(2-hydroxyphenyl) prop-2-en-1-one (**SC1**): Light yellow solid: Mp. 180 °C; Yield: 82 %; 1H NMR (600 MHz, CDCl3) δ: 3.05 (s, 6H, N-(CH3)2), 6.72 (d, 1H, J = 6.0 Hz, Ar-H), 6.95 (d, 1H, J = 15.6 Hz, CH = CH), 7.01 (d, 2H, J = 6 Hz, Ar-H), 7.46 (dd, 1H, J = 2.4 Hz, Ar-H), 7.46 (d, 1H, J = 1.8 Hz, Ar-H), 7.50 (d, 1H, J= 2.8 Hz, Ar-H), 7.58 (d, 1H, J = 6.0 Hz, Ar-H), 7.95 (d, 1H, J = 15.6 Hz, CH = CH), 13.18 (s, 1H, OH).

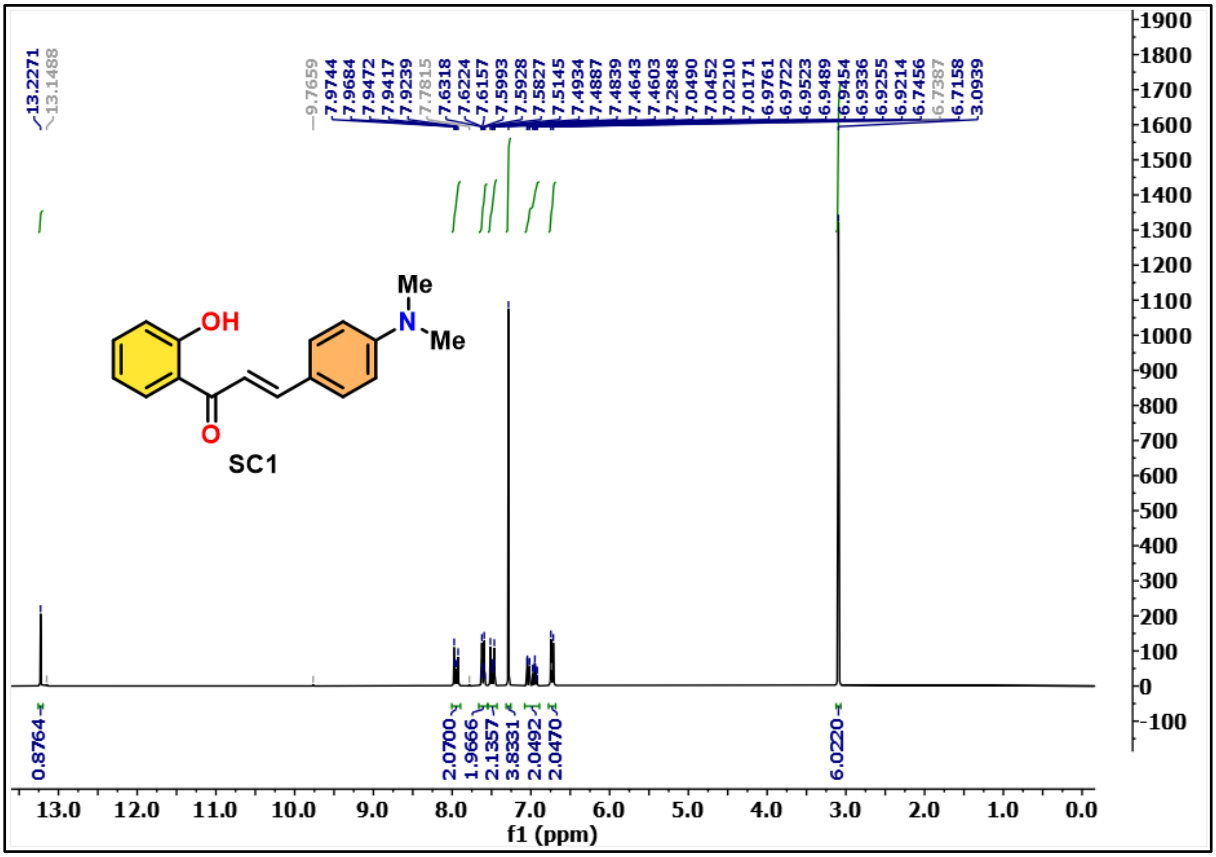

Figure 1: ^{1}H NMR spectrum of SC1 Compound.

(E)-1-(2-hydroxyphenyl)-3-(4-methoxyphenyl) prop-2-en-1-one (**SC2**). Yellow solid (75%); 1H NMR (300 MHz, CDCl3) δ 3.62 (s, 3H, -CH3), 6.96 (d, 1H, J = 7.2 Hz, Ar-H), 7.64 (d, 2H, J = 7.1 Hz, Ar-H), 7.61(d, J = 15 Hz, 1H, CH = CH), 7.46 (m, 2H, Ar-H), 7.72 (d, J = 7.1 Hz, 2H, Ar-H), 8.03 (d, J = 15 Hz, 1H, CH = CH), 8.09 (d, J = 7.2 Hz, 1H, Ar-H), 13.6 (s, 1H, OH).

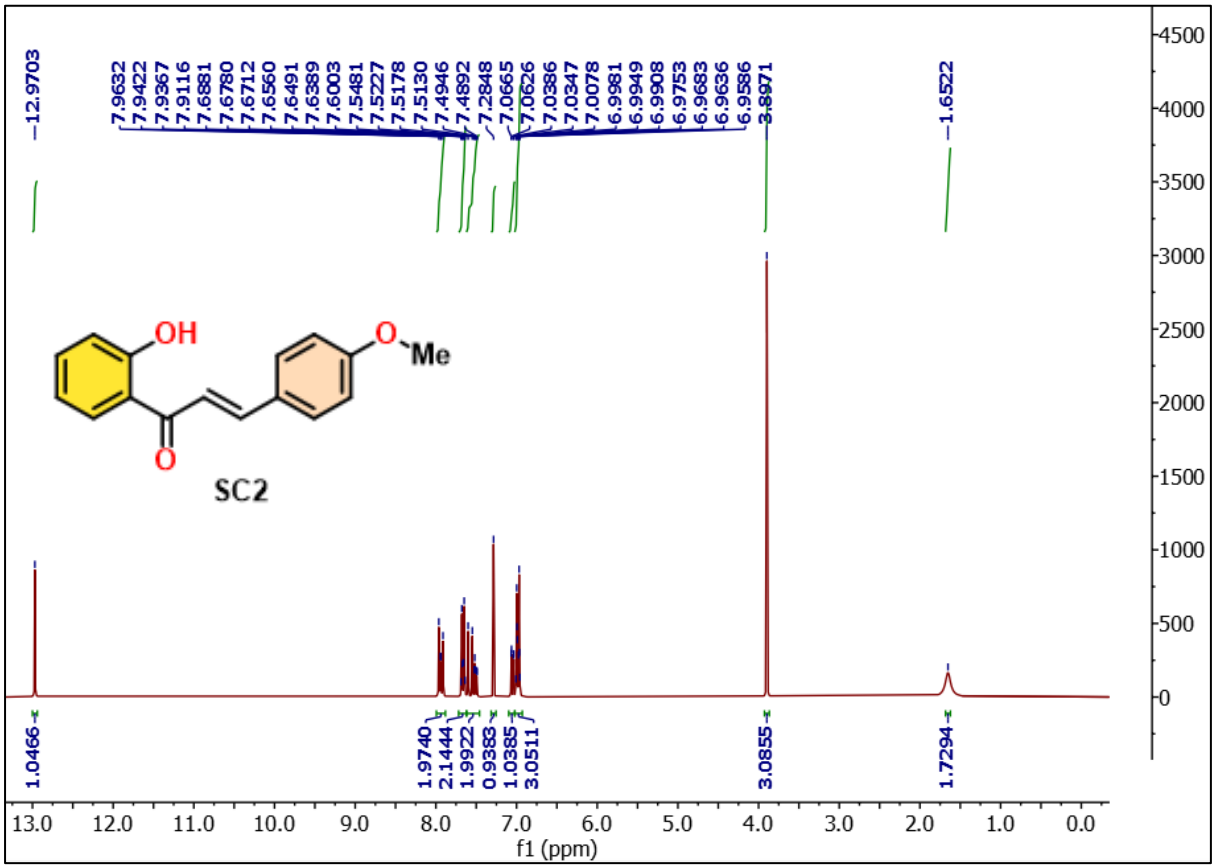

Figure 2: ^{1}H NMR spectrum of SC2 Compound.

(E)-1-(2-hydroxyphenyl)-3-phenylprop-2-en-1-one (**SC3**). Yellow solid (71%); 1H NMR (300 MHz, CDCl3) δ 6.82 (d, J = 7.2 Hz, 1H, Ar-H), 7.33-7.54 (m, 7H, Ar-H), 7.60 (d, J = 15 Hz, 1H, CH = CH), 8.02 (d, J = 15 Hz, 1H, CH = CH), 8.07 (d, J = 7.2 Hz, 1H, Ar-H), 13.4 (s, 1H, OH).

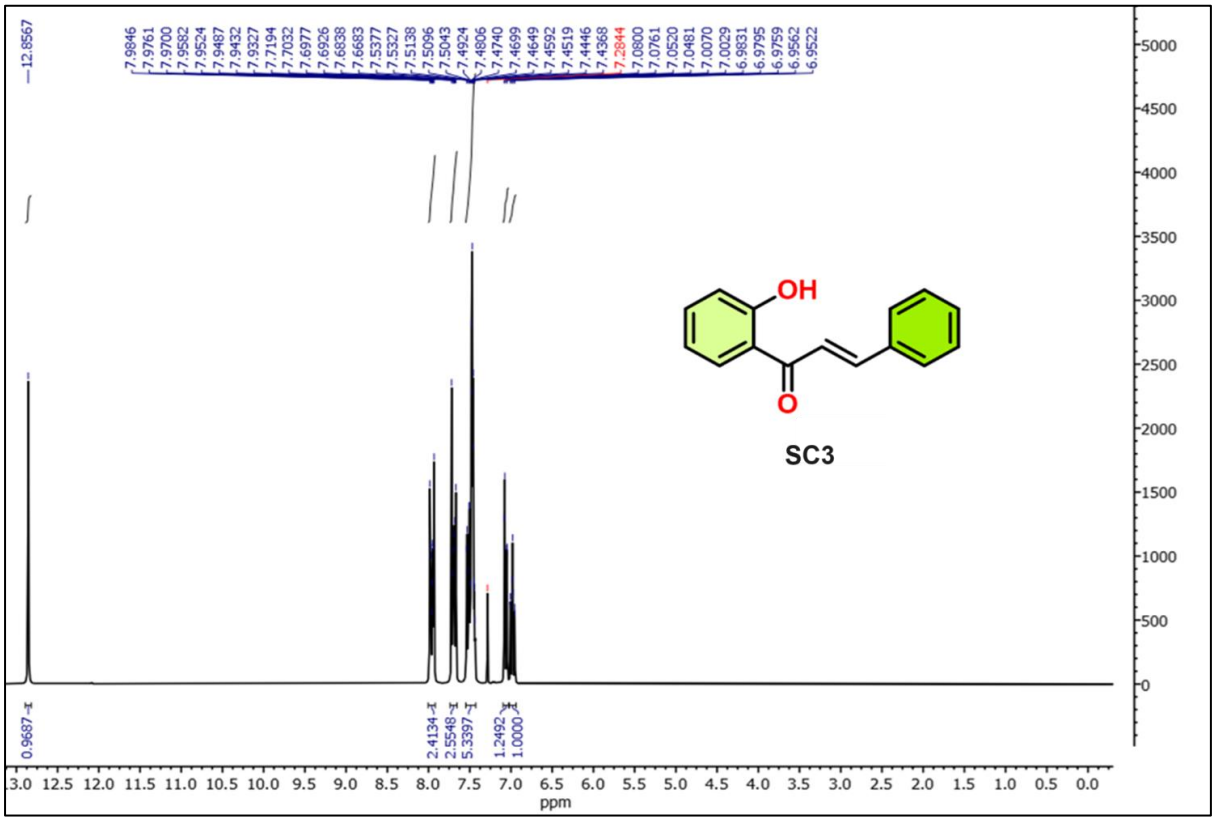

Figure 3: ^{1}H NMR spectrum of SC3 Compound.

E-1-(2-hydroxyphenyl)-3-(3-nitrophenyl) prop-2-en-1-one (**SC4**). Yellow solid (75%); 1H NMR (300 MHz, CDCl3) δ 6.9 (d, J = 7.2 Hz, 1H, Ar-H), 7.46 (d, J = 7.1 Hz, 2H, Ar-H), 7.69 (d, J = 7.2 Hz, 1H, Ar-H), 7.91 (d, J = 15 Hz, 1H, CH = CH), 7.99 (m, 1H, Ar-H), 8.03 (d, J = 7.2 Hz, 1H, Ar-H), 8.19 (d, J = 15 Hz, 1H, CH = CH), 8.16 (d, J = 7.1 Hz, 1H), 8.33 (d, J = 7.2 Hz, 1H), 13.6 (s, 1H, OH).

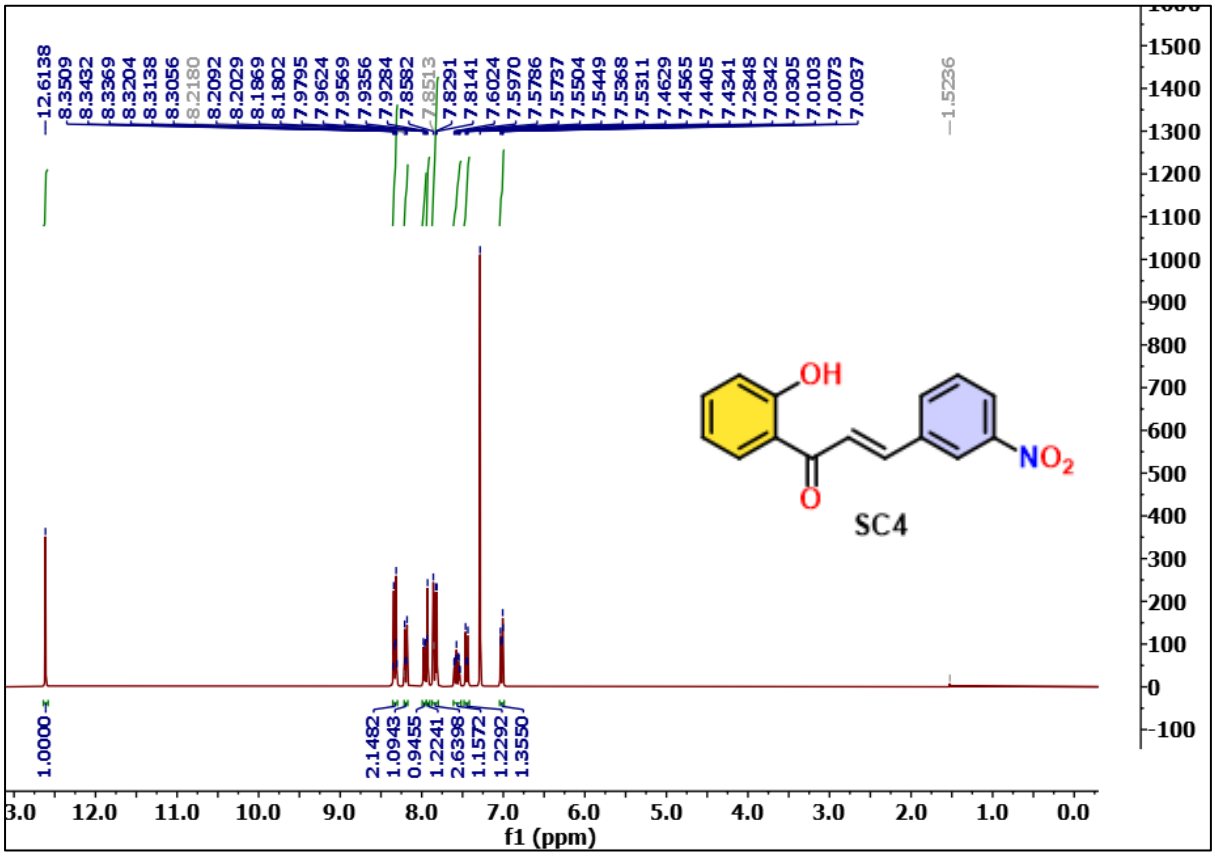

Figure 4: 1H NMR spectrum of SC4 Compound.

To inve stigate the influence of substituents on the B ring of hydroxychalcones, researchers can turn to 1H NMR analysis. Let's start by examining compound SC3, the unsubstituted hydroxychalcone, which features five protons on the B ring with chemical shifts of δ = 7.54 (C2 and C6), 7.35 (C3 and C5), and 7.33 (C4) ppm. Moving on to compound SC1, which includes an NMe2 substitution at C4, we notice that the proton appears in the upfield region due to electron donation to the B ring. The chemical shifts of the protons in this case were found to be δ = 7.46 (C2), 7.50 (C6), and 7.01 (C3 and C5) ppm. It's worth noting that the ortho positions of the NMe2 group at C3 and C5 experience significant upfield shifts due to the highest shielding by resonance. Now, let's focus on compound SC2, where we anticipate that the electron-donating (-) effect of the OMe group will cause the C3 and C5 protons to appear slightly downfield compared to those in SC1. Interestingly, they appeared more downfield than in both SC1 and SC3, with chemical shifts of δ = 7.64 (C2 and C6) and 7.61

(C3 and C5) ppm. This can be attributed to the -I effect of the OMe. Notably, the chemical shift of C2 and C6 was higher than that of C3 and C5, indicating that the -OMe has a slight (-) effect in addition to the -I effect.

Finally, in the case of compound SC4, the -I and -R effects dominate at the B ring, as evidenced by the chemical shifts (δ = 8.03 (C2), 7.64 (C3), 8.16 (C4), and 8.33 (C6) ppm). This provides a comprehensive understanding of the electronic effects of different substituents on the B ring of hydroxychalcones.

Table 1: ^{1}H NMR assignment of the B ring of hydroxychalcones.

Compounds	**For B-ring (Toad color)**
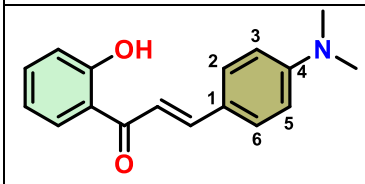 **SC1**	δ = 7.46 (C2), 7.50 (C6) and 7.01 (C3 and C5)
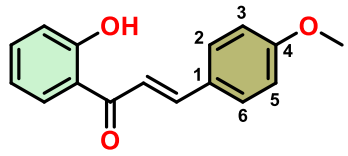 **SC2**	δ = 7.64 (C2 and C6) and 7.61 (C3 and C5)
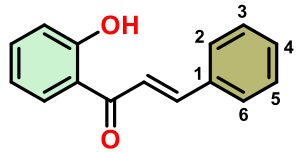 **SC3**	δ = 7.54 (C2 and C6), 7.35 (C3 and C5), and 7.33 (C4)
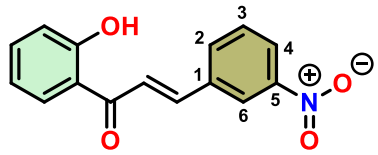 **SC4**	δ = 8.03 (C2), 7.64 (C3), 8.16 (C4), and 8.33 (C6)

3.3.3. UV-VIS Spectral Characterization

All four compounds were analyzed using UV-vis spectroscopy, and their maximum absorbance peaks were observed at different wavelengths **(Fig.5a)**. SC1 displayed a maximum absorbance (λmax) at 450 nm, while SC2 had a λmax at 380 nm. The base compound SC3 exhibited a

λmax at 305 nm, which was the lowest value among all compounds, and SC4 had a λmax at 330 nm.

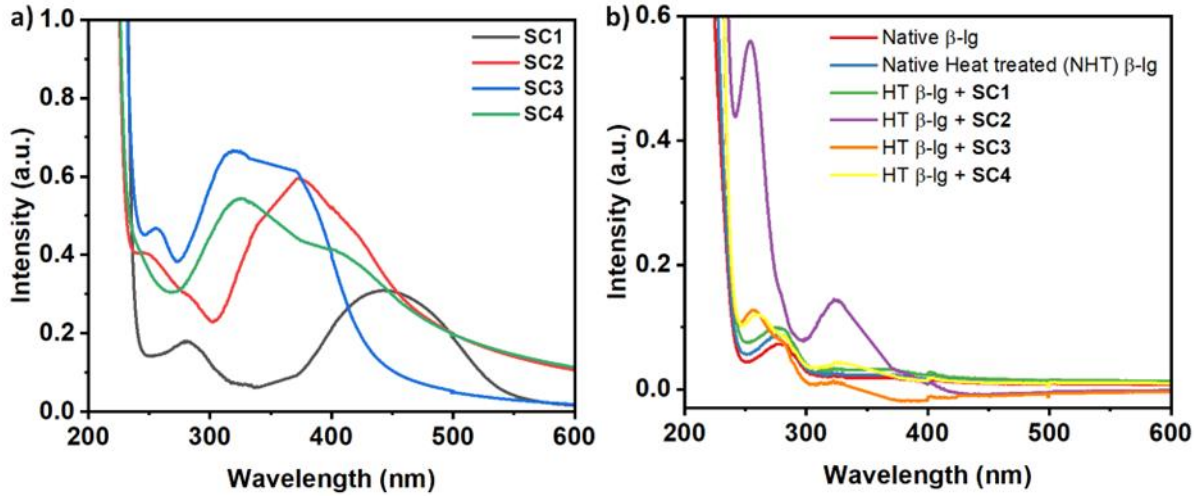

Figure 5: a) Normalised UV-vis absorption spectra of SC1-SC4, b) Normalised UV-vis absorption spectra of native β-lg and β-lg incubated at 75°C for 1 h in the presence and absence of different synthesized compound SC1-SC4. The concentration of β-lg was 15 μM where the concentrations of synthesized compounds (SC1-SC4) were kept at 10 μM**.**

The β-Lactoglobulin (β-lg) demonstrates specific characteristics in its UV-visible spectra attributable to the presence of chromophores with aromatic nuclei conjugated with groups that impart distinct electronic effects. As shown in **(Fig.5b)**, the native β-lg exhibits a λmax at 280 nm, a characteristic band for proteins containing tryptophan residues. Any deviation in the UV-visible spectrum of the native β-lg serves as an indicator of the micro-environmental alterations surrounding the chromophores (Zhong et al., 2012). Following thermal incubation, the peak absorbance intensity of the heat-treated β-lg moderately increases with a marginal blue shift of the peak. Incubation with SC1 also leads to an increase in the absorbance intensity of the β-lg peak. However, a notable abrupt change in the β-lg peak at 280 nm is observed in the presence of the synthesized compound SC2. Further, distinct blue shifts of the protein peak are evident for SC3 and SC4. These observations unmistakably signify the micro-environmental alterations of the β-lg in the presence of the SC derivatives. Consequently, all synthesized SC molecules under investigation demonstrate the capacity to interact with the β-lg to varying degrees, as a result of the substituents imparting diverse electronic effects, thereby inducing changes in the microenvironments around Trp and Tyr residues of the protein and reflecting alterations in the UV-absorbance of the β-lg.

3.3.4. Intrinsic Fluorescence Studies

The fluorescence exhibited by β-lg primarily arises from the presence of two tryptophan fluorophores within the protein. These fluorophores, Trp19 and Trp61, offer a convenient means of spectroscopic evaluation for determining the protein's conformational state. Notably, in its native state, Trp61 experiences quenching due to its proximity to the neighboring disulfide bridge, Cys160-66. Concurrently, Trp19 is situated within the hydrophobic calyx at the center of the protein. Consequently, Trp19 predominantly serves as the probe for tryptophan fluorescence in bovine β-lg, with a minor contribution from tyrosine.

It's important to note the following details: Any conformational change in the protein can result in an increase or decrease in its intrinsic fluorescence intensity. The observed changes in the fluorescence signal primarily indicate structural alterations at the protein's tertiary structure due to the interaction of the synthesized SCs with β-lg. The native β-lg displays a fluorescence emission peak at 335 nm when excited at 285 nm. Upon heating, the exposure of fluorophores causes a decrease in the fluorescence intensity of the heat-treated β-lg compared to the native protein **(Fig.6)** (Croguennec et al., 2004). In the presence of SC3, the emission intensity is higher than that of the aforementioned heat-treated protein, showing slight shifts in the peak towards longer wavelengths. For all other synthesized SCs, the fluorescence intensities of the heat-induced β-lg samples were observed to be higher than the native β-lg with slight shifts toward longer wavelengths. However, the intensities of these samples were lower than the heat-treated β-lg in the absence of the SC sample. This change in fluorescence intensity is attributed to the alteration of the tertiary structure of the protein molecule as the compounds interact with the protein molecules.

In accordance with our research, it has been observed that compound SC3 exhibits a pronounced capacity for fluorophore exposure attributed to a structural modification that induces protein aggregation. Conversely, SC2 and SC4 manifest minimal impact and demonstrate superficial interaction with the protein. The effects pertaining to SC1 are comparatively modest. Notably, the hierarchical order of influence is delineated as SC3 > SC1 > SC4 > SC2. Subsequent trials were conducted to corroborate this observation. Results indicate that the binding of these compounds to the protein elicits a conformational change, thereby prompting self-assembly and protein aggregation.

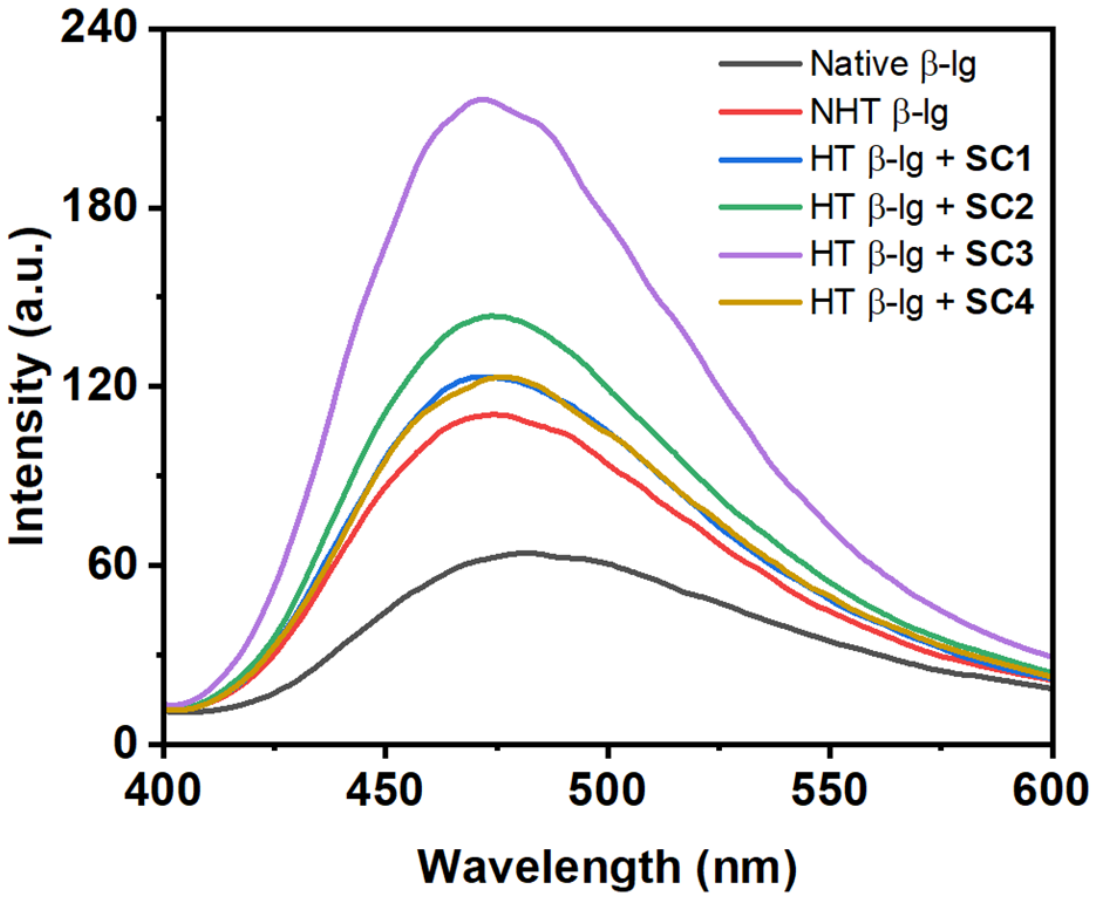

Figure 6: ANS-fluorescence emission spectra of native β-lg and thermally incubated β-lg (at 78°C for 1 h) in the absence and presence of SC1-SC4 (10 μM) in 10 mM phosphate buffer, pH 7.4. The excitation was done at 390 nm and emissions were measured between 400 nm and 600 nm. Both the excitation and emission slits were set at 5 nm. The concentration of β-lg was 13.6 μM throughout the experiment. The results were the mean of three different experiments.

3.3.5. Raleigh Light Scattering

The measurement of Raleigh Light Scattering (RLS) is a valuable tool for examining protein aggregation. This method involves measuring the scattering of light, which increases in the presence of colloidal particles in the medium. Larger protein aggregates scatter light more effectively than smaller ones. In our study, we collected RLS data after subjecting β-lg solutions to thermal incubation at 75°C for 1 hour, both with and without SC1-SC4. The native β-lg exhibited the lowest scattering intensity, containing only pure soluble native β-lg. However, following thermal incubation, the exposed hydrophobic groups led to aggregate formation, resulting in increased RLS intensity in the absence of the synthesized compounds **(Fig.7**). Furthermore, when the compounds (SC1-SC4) interacted with β-lg, heightened RLS intensities indicated the formation of larger β-lg aggregates. Each SC compound demonstrated higher RLS

intensities than the heat-incubated β-lg alone **(Fig.7)**, thereby confirming the formation of larger aggregates when β-lg was thermally exposed in the presence of the synthesized molecules (SC1-SC4). Additionally, the synthesized compounds' effectiveness in promoting β-lg aggregation followed the order SC3 > SC2 > SC1 > SC4.

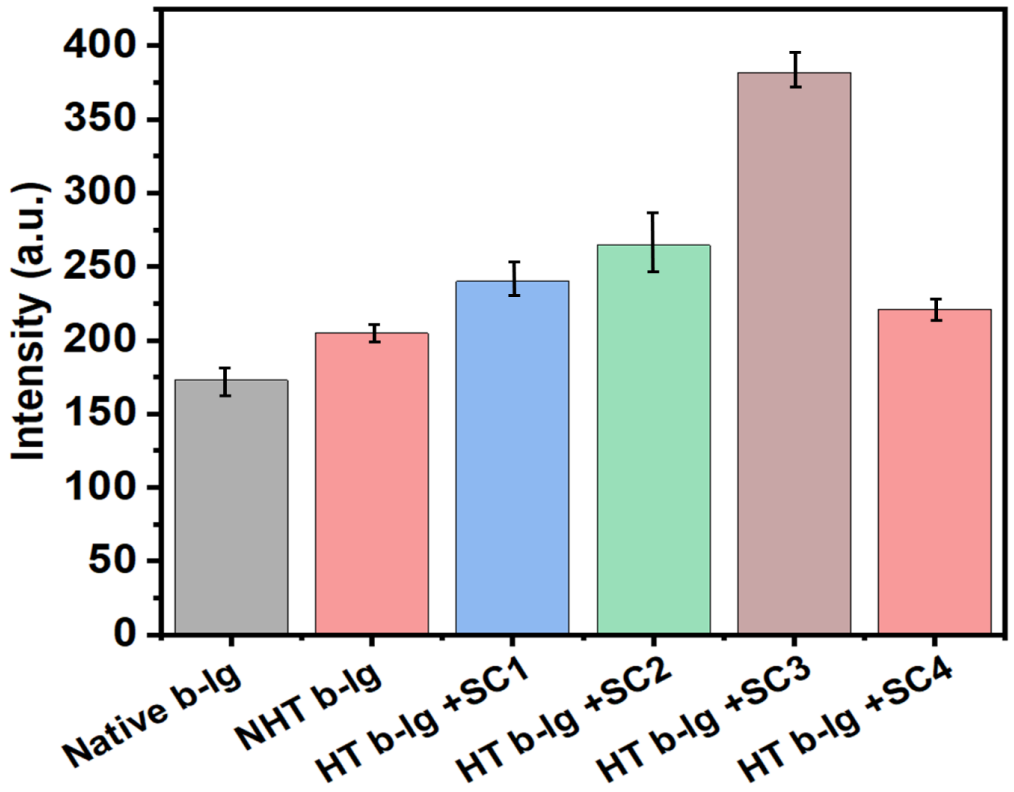

Figure 7: RLS spectra of native β-lg and β-lg incubated at 75°C for 1 h in the absence and presence of different synthesized compounds (SC1-SC4). The concentration of β-lg was 15 µM where the concentrations of synthesized compounds (SC1-SC4) were kept at 10 µM. Sample No. 1 represents: native β-lg, Sample No. 2 represents: heat incubated β-lg in the absence of SC, Sample No. 3 represents: heat incubated β-lg in the presence of SC1, Sample No.4 represents: heat incubated β-lg in the presence of SC2, Sample No.5 represents: heat incubated β-lg in presence of SC3 and Sample No. 6 represents: heat incubated β-lg in presence of SC4.

3.3.6. TEM Study

Based on the fluorescence data from Th-T analysis, it was observed that there is only a minimal increase in fluorescence intensity when the protein is combined with chalcones. This may indicate that the protein either does not aggregate at all or if it does, it does not lead to significant fibril formation under the specific thermal conditions used in the study. To further investigate this, we made the decision to utilize imaging techniques such as transmission electron microscopy (TEM) and other relevant studies.

In the TEM study conducted to analyze the structure and characteristics of the protein in the presence and absence of compounds (SC1-SC4), several significant findings were observed. The native state of the protein showed small fragments, as depicted in **(Fig.8a).** Upon subjecting the native protein to heat, some level of protein aggregation was observed, as indicated by the presence of larger non-fibrillar protein aggregates **(Fig. 8b).**

Furthermore, the introduction of chalcones resulted in a notable increase in both the size and quantity of protein aggregates, as illustrated in **(Fig. 8c-f).** Specifically, the protein aggregates formed in the presence of SC1 appeared globular and larger than those formed from heat-treated protein alone **(Fig.8c)**. Additionally, the presence of SC2 led to even larger protein aggregates compared to other systems **(Fig. 8d).** The highest level of aggregation and particle size was observed in the presence of SC3 **(Fig. 8e)**. However, the size of the protein aggregates decreased to an intermediate level between SC1 and heat-treated protein for SC4 **(Fig. 8f)**. In summary, the order of protein aggregate size is as follows: SC3 > SC2 > SC1 > SC4 > heat-treated β-lg. Notably, these results are consistent with the aggregation order observed in Th-T and other studies.

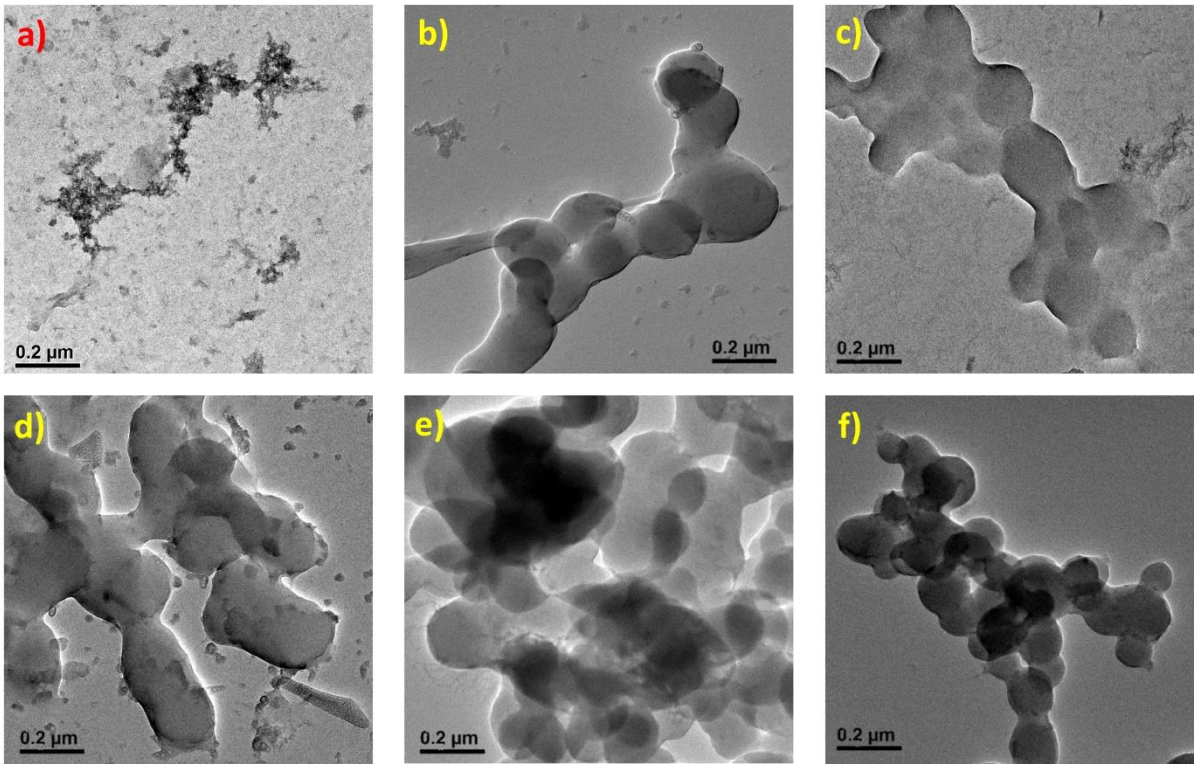

Figure 8: TEM image of (a) native β-lg, (b) β-lg after thermal incubation (75°C for 1 h); β-lg after thermal incubation in the presence of the SC derivatives (c) SC1, (d) SC2, (e) SC3, and (f) SC4 75°C for 1 h.

3.3.7. Influence of the SC derivatives on the propensity of β-lg self-assembly formation

The benzothiazole dye, Thioflavin T, is utilized to detect protein aggregates formed through fibrillation. This dye predominantly binds to the β-sheets of fibrillar aggregates of the protein and emits strong fluorescence at 485 nm when excited at 440 nm. It is commonly employed to identify the cross beta-structure of the protein aggregates and assess the extent of amyloid formation (Nilsson, 2004). Consequently, a higher ThT emission intensity signifies a greater extent of protein aggregation. Upon thermal incubation at 75°C for 1 hour, the formation of β-lg aggregates can be quantified through the ThT emission intensity. The results demonstrate that native β-lg exhibits weak interaction with the ThT probe and subsequently displays the lowest ThT intensity. Subsequent to thermal incubation, the aggregates form due to loss of structural stability and exposure of hydrophobic sites on the β-lg molecule, resulting in comparatively higher ThT emission intensity **(Fig.9).** All other heat-treated β-lg samples in the presence of various SC derivatives exhibit a proportional relationship between the ThT emission intensities and the number of aggregates formed in each protein solution. The β-lg sample incubated in the presence of SC3 displayed the highest ThT fluorescence intensity, confirming that SC3 has the greatest ability to interact with β-lg and promote the self-assembly formation of β-lg.

The fluorescence of Thioflavin T (Th-T) in all derivatives of SC3 indicates a greater binding with the aggregates in comparison to native and heat-treated native β-lactoglobulin (β-lg). This suggests that all the synthesized compounds have the ability to promote the aggregation of β-lg in the order of SC3 > SC2 > SC1 > SC4, indicating that they are effective fibrillating agents. The increase in Th-T fluorescence intensity in the presence and absence of SC derivatives is moderate under thermal incubation conditions. To validate the results of Th-T fluorescence, we have conducted AFM (atomic force microscopy) imaging experiments. The AFM imaging of different β-lg aggregates correlated with the findings from the Th-T fluorescence experiments.

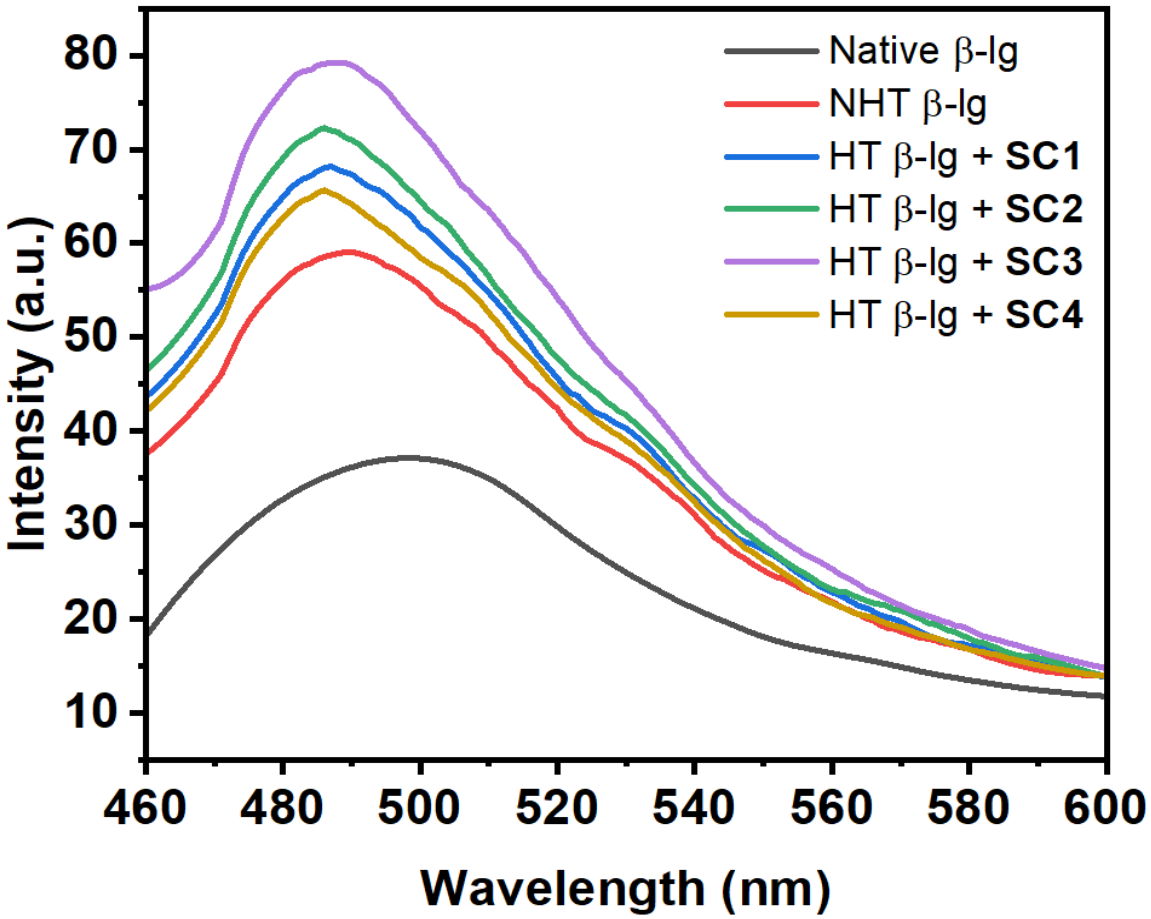

Figure 9: Th T-fluorescence emission spectra of native β-lg and thermally incubated β-lg (at 75°C for 1 h) in the absence and presence of SC1-SC4 (10 µM) in 10 mM phosphate buffer, pH 7.4. The excitation was done at 440 nm and emissions were measured between 460 nm and 600 nm. Both the excitation and emission slits were set at 5 nm. The concentration of β-lg was 13.6 µM through the experiment. The results were the mean of three different experiments.

3.3.8. FT-IR Spectroscopic measurements for monitoring the secondary structural changes

FT-IR spectroscopy is frequently used to examine the secondary structural changes of proteins under varying experimental conditions. This method enables the study of alterations in the shape and frequency of the amide C=O (amide I) stretching and coupled N-H bending and C-N (amide II) stretching bands, which serve as indicators of the structural transitions and behavior of a β-lg during self-assembly or fibrillar structure formation of a protein (Eissa et al., 2006). In our research, we employed this technique to investigate the secondary structural changes of β-lg during thermal incubation (at 75°C for 1 hour) in the presence and absence of our synthesized compounds (SC1-SC4). At room temperature, the native β-lg molecule exhibits

the amide-I band at approximately 1633cm^{-1} **(Fig.10)**, signifying the protein's predominant β-sheet structure, which is characteristic of β-lg. The FT-IR spectrum of β-lg subsequent to thermal incubation at 75 °C in the absence of any SC derivative indicates a transition of the band from 1633 cm-1 to 1644 cm-1. This shift suggests an escalation in β-sheet structural components compared to the native β-lg due to the formation of self-assembled structures. The peak for SC1 was detected at 1641 cm-1 with a marginally higher transmittance level compared to heat-treated β-lg alone, corroborating the formation of protein aggregates with enhanced β-sheet content. In the presence of SC3, the amide I band shifted to 1643 cm-1 and exhibited the highest transmittance level compared to heat-treated β-lg alone or in the presence of other SC derivatives. Consequently, the compound SC3 is identified as the most influential in inducing the alteration in the secondary structure of β-lg during its amyloid fibril formation. With SC2 and SC4, the amide I band of β-lg appeared at 1642 and 1643 cm-1, respectively, with a greater transmittance level observed in the case of SC2. Hence, all the SC compounds (SC1-SC4) reveal the capacity to modify the secondary structure of β-lg and facilitate self-assembly formation in the order of SC3 > SC2 > SC1 > SC4.

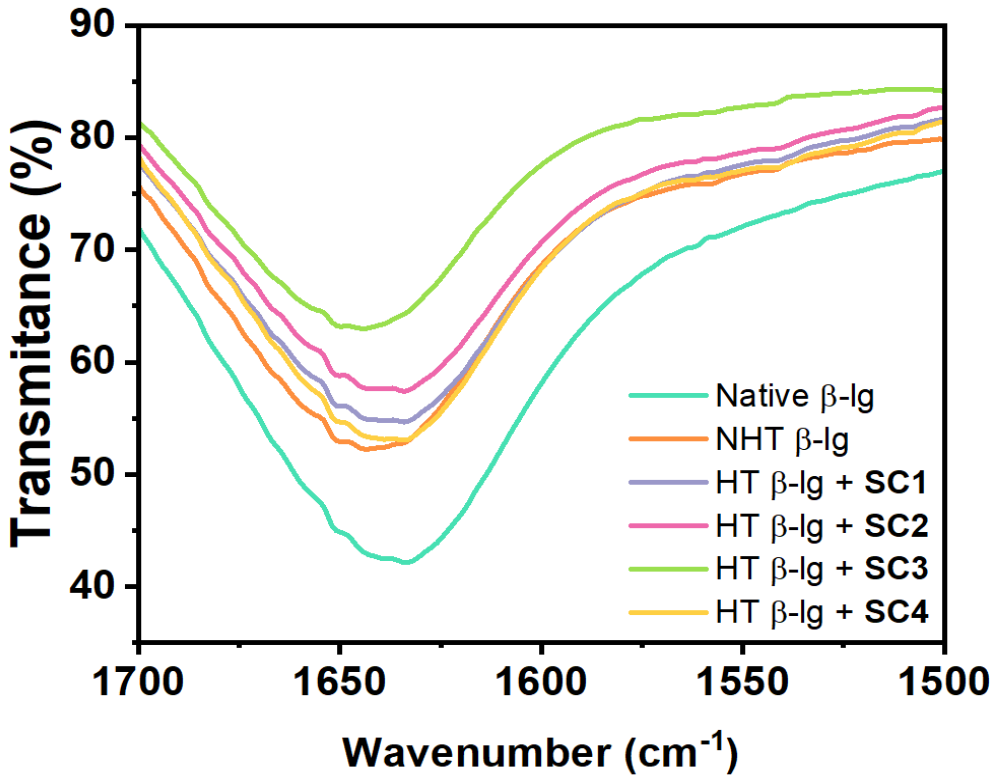

Figure 10: FT-IR spectra in the wavelength region 1500-1700 cm-1 of native β-lg and β-lg incubated at 75°C for 1 h in the absence and presence of different synthesized compounds (SC1-SC4). The concentration of β-lg was 15 μM where the concentrations of synthesized compounds (SC1-SC4) were kept at 10 μM.

3.3.9. Dynamic Light Scattering Measurements

Dynamic Light Scattering (DLS) is a method used to monitor the temporal behavior of scattered light intensity. It is a rapid, label-free, and non-destructive approach for analyzing the size of various macromolecules and biomolecules such as peptides, proteins, viruses, and nucleic acids. DLS examines the changes in the intensity of scattered light from a sample (Zhong et al., 2012). By observing how quickly the scattered light intensity changes over time, DLS can offer valuable insights into the size of particles in the solution. The swift movement of tiny particles causes rapid changes in light intensity, while the slower movement of larger particles results in slower changes. DLS has the capability to detect even extremely rare aggregates in a sample due to the intense light scattering from larger particles.

In our research, we conducted an analysis of the influence of a specific SC molecule on the hydrodynamic radius of β-lg protein during thermal incubation. The findings, as depicted in **(Fig.11)**, revealed that the native β-lg protein demonstrated the smallest hydrodynamic radius, whereas the heat-incubated β-lg exhibited an increased radius of approximately 160 nm. Upon introduction of the synthesized derivatives (SC1-SC4), a substantial escalation in the hydrodynamic radius (200-550 nm) was observed, indicating the formation of larger protein aggregates. Notably, the presence of SC led to the generation of protein aggregates with larger sizes in comparison to those without the compound (150 nm). Particularly, the size of the aggregates was observed to increase to 250 nm in the case of SC4. It is noteworthy that the thermal incubation of β-lg with SC1 yielded protein aggregates with a radius of 300 nm, while the introduction of SC2 resulted in an increase to approximately 350 nm. Most significantly, the largest β-lg aggregates, with the highest hydrodynamic radii (350-540 nm), were produced when the protein was subjected to SC3. Consequently, it can be inferred that all four SC derivatives exert an impact on the self-assembly formation of β-lg during thermal incubation, with the sequence of promoting aggregation being SC3>SC2>SC1>SC4. This sequencing aligns with the outcomes derived from the Th T and ANS-fluorescence, FTIR, and RLS data.

Thus, the association of these SC derivatives with the protein results in a modification of the protein conformation through an increased exposure of hydrophobic residues, thereby destabilizing the protein in an aqueous medium and leading to the formation of protein aggregates.

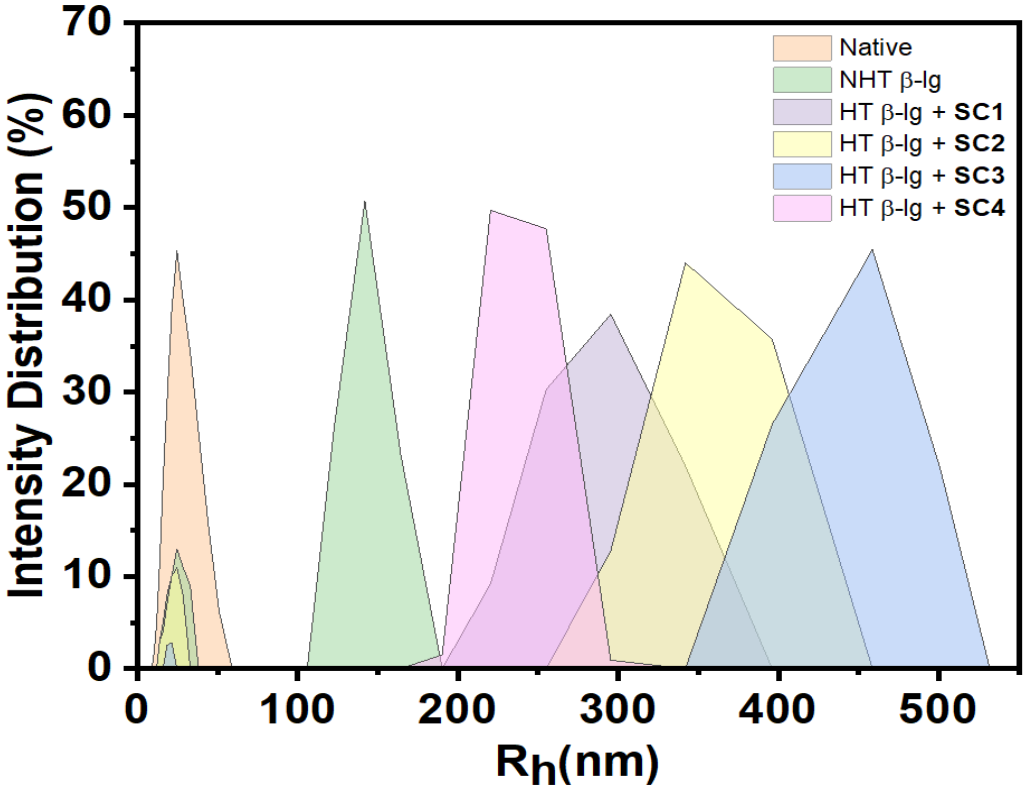

Figure 11: DLS plot of mean intensity versus hydrodynamic radius of spectra of native β-lg and β-lg incubated at 75°C for 1 h in the absence and presence of different synthesized SC1-SC4. The concentration of β-lg was 50 μM where the concentrations of synthesized compounds (SC1-SC4) were kept at 10 μM. Every spectrum is a mean of 48 scans.

3.3.10. Morphological Studies with Atomic Force Microscopy (AFM)

Atomic force microscopy (AFM) offers several advantages over other techniques. Firstly, AFM provides high-resolution images and nanoscale topographic data, allowing us to study materials at the atomic scale. Secondly, AFM is a non-destructive technique, meaning that it does not require sample preparation or alteration, making it suitable for studying delicate or sensitive samples. Lastly, AFM offers a wide range of scanning modes, such as contact and non-contact modes, which enable the study of a wide range of samples, including biological samples.

Using atomic force microscopy (AFM) to study protein aggregates provides detailed information about their structure, size, and topography. AFM provides a non-invasive approach, allowing for the study of protein aggregates in their native environment without altering the sample. This allows for a better understanding of the composition and arrangement of the aggregates, which is crucial in studying diseases related to protein misfolding and aggregation, such as Alzheimer's and Parkinson's disease.

The protein's morphology, including its shape, size, and structure, was investigated through atomic force microscopy (AFM) under various conditions, with and without the presence of compounds SC1-SC4. The AFM study revealed the morphology of the β-lg aggregates, displaying globular structures rather than fibrillary ones. Specifically, the 3D micrograph of native β-lg depicted small random particles **(Fig.12a)**, while thermal incubation resulted in larger particles, signifying a loss of structure and the formation of aggregates due to the exposure of hydrophobic residues **(Fig.12b)**, consistent with prior experiments.

Upon thermal incubation in the presence of SC3, sizable strip-like or flake-like protein aggregates were observed **(Fig.12e)**, aligning with findings from Th-T and DLS studies. Additionally, smaller particles were observed with SC2 compared to SC3, accompanied by visible sheet-like protein aggregates **(Fig.12d)**. Following incubation with SC1, smaller protein aggregates resembling broken sheets were noted compared to those observed with β-lg-SC2 **(Fig.12c)**. Furthermore, in the case of SC4, the morphology of the protein aggregates fell between those obtained from heat-treated β-lg and heat-treated β-lg-SC1 **(Fig.12f)**. Importantly, the AFM study results complemented the observations from RLS, ThT, and DLS studies.

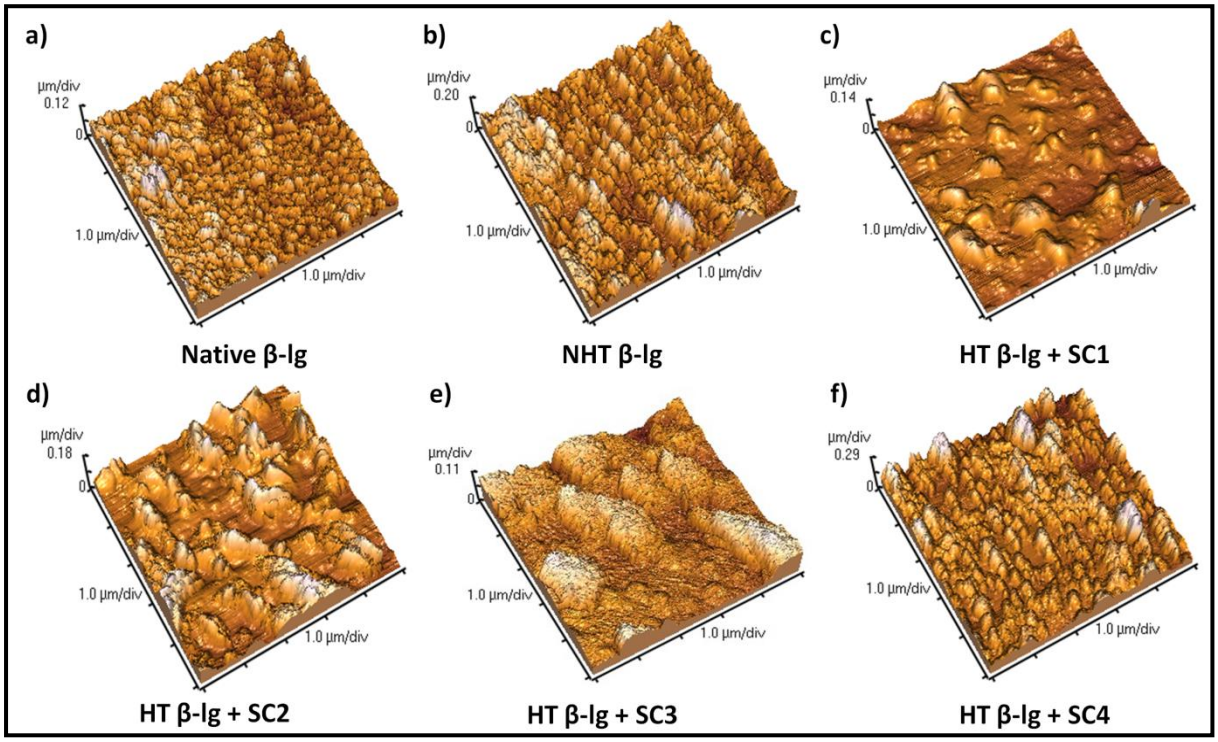

Figure12: AFM image of (a) native β-lg, (b) β-lg after thermal incubation (75°C for 1 h); β-lg after thermal incubation in the presence of the SC derivatives (c) SC1, (d) SC2, (e) SC3, and (f) SC4 at 75°C for 1 h.

3.3.11. Molecular Docking

Molecular docking studies involve the analysis of interactions between a ligand, such as a small molecule or a protein, and a receptor. These studies aid in predicting binding modes, determining binding energies, and identifying key interactions contributing to affinity and selectivity. They are valuable in drug discovery, providing insights into the mode of action of drugs and assisting in the design and evaluation of potential drug candidates.

In our research, we conducted molecular docking to understand the binding mechanism of SC derivatives (SC1-SC4) to the β-lg protein. The protein comprises eight anti-parallel β-sheets forming a barrel, known as a calyx, which serves as a natural hydrophobic binding pocket. Our molecular docking results revealed that all four molecules bind at the calyx **(Fig.13a)**, suggesting that their hydrophobic nature is responsible for this binding. Notably, the binding energies of the compounds varied, with the binding energies (ΔG°) of SC1, SC2, SC3, and SC4 measured at -7.16, -6.88, -6.42, and -7.54 kcal/mol, respectively. This data indicates that the electron-withdrawing and electron-donating groups in the SC compounds can strongly interact with the protein, leading to a decrease in the exposure of the protein's hydrophobic residues. As a result, these molecules influence a reduced protein aggregation, aligning with the observations of our study.

The investigation delved deeper into the protein interaction mechanism to gain insight into the nature of the interaction between the protein and SC derivatives. In the case of SC3, the molecules exhibited interactions with the V41, V43, L46, I56, V92, F105, and M107 amino acid residues of the calyx **(Fig.13b)**. These amino acids are characterized by hydrophobic residues. Conversely, SC1 displayed interactions with V41, I56, L58, K69, I71, and M107 amino acids primarily through hydrophobic interactions **(Fig.13c)**. A single H-bond between the hydroxyl oxygen and the side chain ammonium hydrogen of K69 may account for their robust binding. Moreover, amino acid residues L39, V41, K60, I71, and M107 interacted with SC4 through the formation of an H-bond (K60) and hydrophobic interactions **(Fig.13d)**. Consequently, the hydrophobic interactions between the SC molecules and the protein significantly contribute to conformational changes and the exposure of hydrophobic residues to the solvent, thereby influencing protein aggregation. The degree of aggregation is contingent upon the strong binding capacity of the molecules.

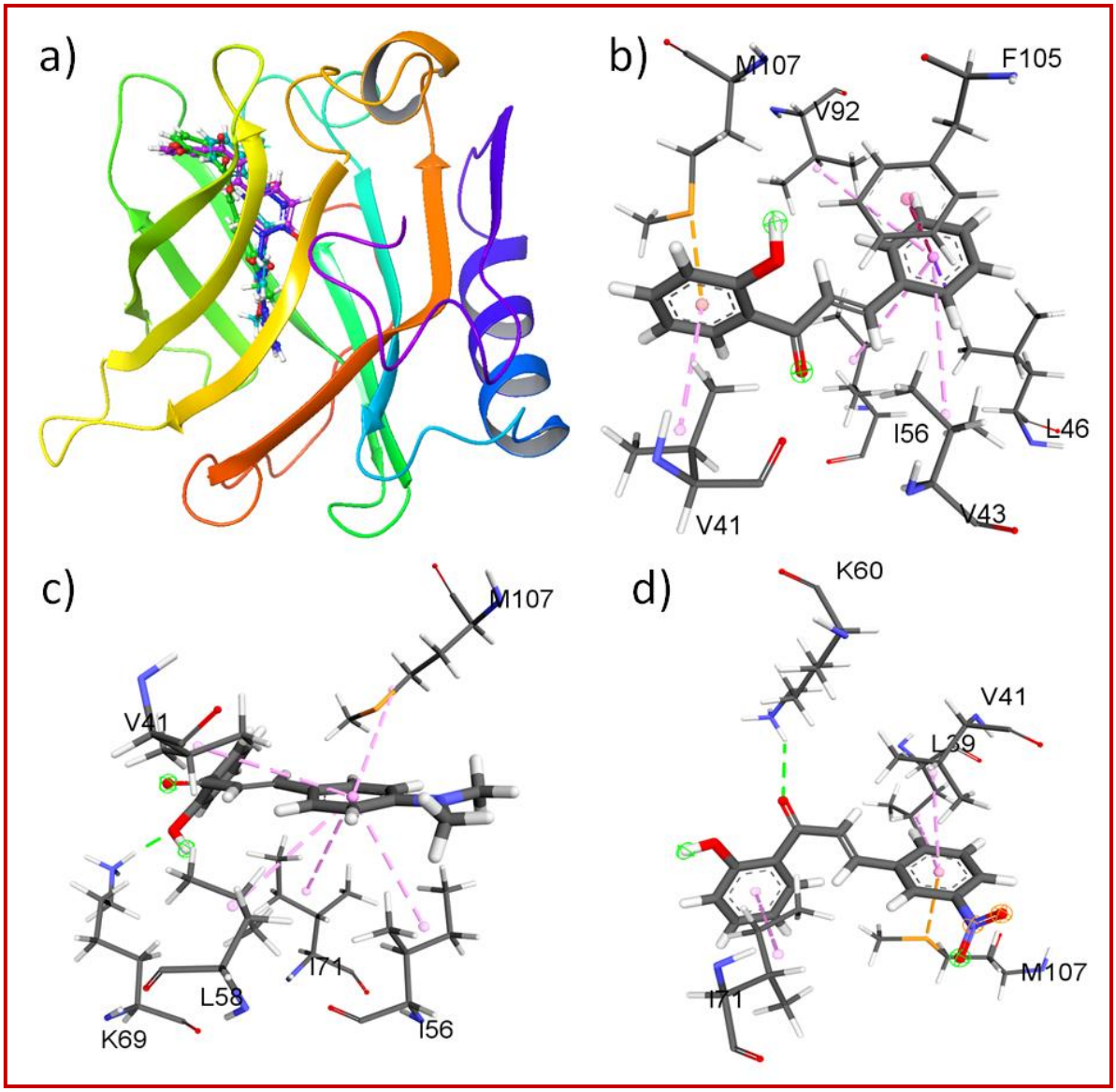

Figure 13: (a) Overlay of all the docking poses of SC molecules and protein; different non-covalent interactions between amino acid residues of protein and (b) SC3, (c) SC1, and (d) SC4.

3.4. Conclusion

In summary, our research involved the synthesis of various derivatives of SC, each with unique substituents placed at different positions with distinct polarity and electronic features. We conducted an in-depth investigation into how these substituents affect the aggregation of the model protein, beta-lactoglobulin (β-lg). Our study demonstrated that all the synthesized compounds exerted an influence on the aggregation of β-lg and produced alterations in the morphology of the resulting aggregates. Notably, our findings revealed that the compound (E)-1-(2-hydroxyphenyl)-3-phenylprop-2-en-1-one (known as SC3) exhibited the most substantial

capacity to accelerate the aggregation of β-lg. We also observed that both electron-withdrawing and donating groups attached to the SC nucleus had a notable impact on the kinetics of β-lg aggregation. Furthermore, we found that a specifically designed compound has the potential to modulate protein-protein interactions through hydrogen bonds and hydrophobic interactions. Additionally, our study suggests that other synthesized SC compounds displayed comparatively lower effectiveness in promoting the thermal aggregation of β-lg.

3.5. References

Alberts, B., 2002. Molecular Biology of the Cell 4th edition.

Arora, A., Ha, C. and Park, C.B., 2004. Insulin amyloid fibrillation at above 100 C: new insights into protein folding under extreme temperatures. Protein Science, 13(9), pp.2429-2436.

Aschaffenburg, R. and Drewry, J., 1957. Improved method for the preparation of crystalline β-lactoglobulin and α-lactalbumin from cow's milk. Biochemical Journal, 65(2), p.273.

Bader, R., Bamford, R., Zurdo, J., Luisi, B.F. and Dobson, C.M., 2006. Probing the mechanism of amyloidogenesis through a tandem repeat of the PI3-SH3 domain suggests a generic model for protein aggregation and fibril formation. Journal of molecular biology, 356(1), pp.189-208.

Banerjee, V. and Das, K.P., 2012. Modulation of pathway of insulin fibrillation by a small molecule helix inducer 2, 2, 2-trifluoroethanol. Colloids and Surfaces B: Biointerfaces, 92, pp.142-150.

Creamer, L.K., Parry, D.A.D. and Malcolm, G.N., 1983. Secondary structure of bovine β-lactoglobulin B. Archives of Biochemistry and Biophysics, 227(1), pp.98-105.

Croguennec, T., Mollé, D., Mehra, R. and Bouhallab, S., 2004. Spectroscopic characterization of heat-induced nonnative β-lactoglobulin monomers. Protein Science, 13(5), pp.1340-1346.

Dirix, C., Meersman, F., MacPhee, C.E., Dobson, C.M. and Heremans, K., 2005. High hydrostatic pressure dissociates early aggregates of TTR105–115, but not the mature amyloid fibrils. Journal of molecular biology, 347(5), pp.903-909.

Dobson, C.M., 2001. The structural basis of protein folding and its links with human disease. Philosophical Transactions of the Royal Society of London. Series B: Biological Sciences, 356(1406), pp.133-145.

Dobson, C.M., 2002. Protein-misfolding diseases: Getting out of shape. Nature, 418(6899), pp.729-730.

Dobson, C.M., 2003. Protein folding and misfolding. Nature, 426(6968), pp.884-890.

Eissa, A.S., Puhl, C., Kadla, J.F. and Khan, S.A., 2006. Enzymatic cross-linking of β-lactoglobulin: Conformational properties using FTIR spectroscopy. Biomacromolecules, 7(6), pp.1707-1713.

Elkanzi, N.A., Hrichi, H., Alolayan, R.A., Derafa, W., Zahou, F.M. and Bakr, R.B., 2022. Synthesis of chalcones derivatives and their biological activities: a review. ACS omega, 7(32), pp.27769-27786.

Englander, S.W., Mayne, L. and Krishna, M.M., 2007. Protein folding and misfolding: mechanism and principles. Quarterly reviews of biophysics, 40(4), pp.1-41.

Giamblanco, N., Coglitore, D., Gubbiotti, A., Ma, T., Balanzat, E., Janot, J.M., Chinappi, M. and Balme, S., 2018. Amyloid growth, inhibition, and real-time enzymatic degradation revealed with single conical nanopore. Analytical chemistry, 90(21), pp.12900-12908.

Gomes, M.N., Muratov, E.N., Pereira, M., Peixoto, J.C., Rosseto, L.P., Cravo, P.V., Andrade, C.H. and Neves, B.J., 2017. Chalcone derivatives: promising starting points for drug design. Molecules, 22(8), p.1210.

Gomez, H.F., Ochoa, T.J., Herrera-Insua, I., Carlin, L.G. and Cleary, T.G., 2002. Lactoferrin protects rabbits from Shigella flexneri-induced inflammatory enteritis. Infection and immunity, 70(12), pp.7050-7053.

Harper, J.D., Wong, S.S., Lieber, C.M. and Lansbury, P.T., 1999. Assembly of Aβ amyloid protofibrils: an in vitro model for a possible early event in Alzheimer's disease. Biochemistry, 38(28), pp.8972-8980.

Hoppenreijs, L.J.G., Fitzner, L., Ruhmlieb, T., Heyn, T.R., Schild, K., Van Der Goot, A.J., Boom, R.M., Steffen-Heins, A., Schwarz, K. and Keppler, J.K., 2022. Engineering amyloid and amyloid-like morphologies of β-lactoglobulin. Food Hydrocolloids, 124, p.107301.

Horvath, I. and Wittung-Stafshede, P., 2016. Cross-talk between amyloidogenic proteins in type-2 diabetes and Parkinson's disease. Proceedings of the National Academy of Sciences, 113(44), pp.12473-12477.

K Sahu, N., S Balbhadra, S., Choudhary, J. and v Kohli, D., 2012. Exploring pharmacological significance of chalcone scaffold: a review. Current medicinal chemistry, 19(2), pp.209-225.

Kelly, J.W., 1998. The alternative conformations of amyloidogenic proteins and their multi-step assembly pathways. Current opinion in structural biology, 8(1), pp.101-106.

Khan, J.M., Qadeer, A., Ahmad, E., Ashraf, R., Bhushan, B., Chaturvedi, S.K., Rabbani, G. and Khan, R.H., 2013. Monomeric banana lectin at acidic pH overrules conformational stability of its native dimeric form. PloS one, 8(4), p.e62428.

Kontopidis, G., Holt, C. and Sawyer, L., 2004. Invited review: β-lactoglobulin: binding properties, structure, and function. Journal of Dairy Science, 87(4), pp.785-796.

Liu, T.X., Relkin, P. and Launay, B., 1994. Thermal denaturation and heat-induced gelation properties of β-lactoglobulin. Effects of some chemical parameters. Thermochimica acta, 246(2), pp.387-403.

M Ashraf, G., H Greig, N., A Khan, T., Hassan, I., Tabrez, S., Shakil, S., A Sheikh, I., K Zaidi, S., Akram, M., R Jabir, N. and K Firoz, C., 2014. Protein misfolding and aggregation in Alzheimer's disease and type 2 diabetes mellitus. CNS & Neurological Disorders-Drug Targets (Formerly Current Drug Targets-CNS & Neurological Disorders), 13(7), pp.1280-1293.

Maity, S., Pal, S., Sardar, S., Sepay, N., Parvej, H., Begum, S., Dalui, R., Das, N., Pradhan, A. and Halder, U.C., 2018. Inhibition of amyloid fibril formation of β-lactoglobulin by natural and synthetic curcuminoids. New Journal of Chemistry, 42(23), pp.19260-19271.

Maity, S., Sardar, S., Pal, S., Parvej, H., Chakraborty, J. and Halder, U.C., 2016. New insight into the alcohol induced conformational change and aggregation of the alkaline unfolded state of bovine β-lactoglobulin. RSC advances, 6(78), pp.74409-74417.

Majid, N., Siddiqi, M.K., Hassan, M.N., Malik, S., Khan, S. and Khan, R.H., 2023. Inhibition of primary and secondary nucleation along with disruption of amyloid fibrils and

alleviation of associated cytotoxicity: A biophysical insight of a novel property of Chlorpropamide (an anti-diabetic drug). Biomaterials Advances, 151, p.213450.

Mansouri, A., Guéant, J.L., Capiaumont, J., Pelosi, P., Nabet, P. and Haertlé, T., 1998. Plasma membrane receptor for beta-lactoglobulin and retinol-binding protein in murine hybridomas. Biofactors, 7(4), pp.287-298.

Morris, G.M., Huey, R., Lindstrom, W., Sanner, M.F., Belew, R.K., Goodsell, D.S. and Olson, A.J., 2009. AutoDock4 and AutoDockTools4: Automated docking with selective receptor flexibility. Journal of computational chemistry, 30(16), pp.2785-2791.

Nilsson, M.R., 2004. Techniques to study amyloid fibril formation in vitro. Methods, 34(1), pp.151-160.

Nordstedt, C., Näslund, J., Tjernberg, L.O., Karlström, A.R., Thyberg, J. and Terenius, L., 1994. The Alzheimer A beta peptide develops protease resistance in association with its polymerization into fibrils. Journal of Biological Chemistry, 269(49), pp.30773-30776.

Ouwehand, A.C., Salminen, S.J., Skurnik, M. and Conway, P.L., 1997. Inhibition of pathogen adhesion by β-lactoglobulin. International Dairy Journal, 7(11), pp.685-692.

Pal, S., Maity, S., Sardar, S., Chakraborty, J. and Halder, U.C., 2016. Insight into the co-solvent induced conformational changes and aggregation of bovine β-lactoglobulin. International journal of biological macromolecules, 84, pp.121-134.

Papiz, M.Z., Sawyer, L., Eliopoulos, E.E., North, A.C.T., Findlay, J.B.C., Sivaprasadarao, R., Jones, T.A., Newcomer, M.E. and Kraulis, P.J., 1986. The structure of β-lactoglobulin and its similarity to plasma retinol-binding protein. Nature, 324(6095), pp.383-385.

Parvej, H., Begum, S., Dalui, R., Paul, S., Mondal, B., Sardar, S., Sepay, N., Maiti, G. and Halder, U.C., 2022. Coumarin derivatives inhibit the aggregation of β-lactoglobulin. RSC advances, 12(27), pp.17020-17028.

Patel, H.A., Singh, H., Havea, P., Considine, T. and Creamer, L.K., 2005. Pressure-induced unfolding and aggregation of the proteins in whey protein concentrate solutions. Journal of Agricultural and Food Chemistry, 53(24), pp.9590-9601.

Rahman, M.A., 2011. Chalcone: a valuable insight into the recent advances and potential pharmacological activities. Chem Sci J CSJ-29: 1–16.

Rambaran, R.N. and Serpell, L.C., 2008. Amyloid fibrils: abnormal protein assembly. Prion, 2(3), pp.112-117.

Sardar, S., Pal, S., Maity, S., Chakraborty, J. and Halder, U.C., 2014. Amyloid fibril formation by β-lactoglobulin is inhibited by gold nanoparticles. International journal of biological macromolecules, 69, pp.137-145.

Sawyer, L., Kontopidis, G. and Wu, S.Y., 1999. β-Lactoglobulin–a three-dimensional perspective. International journal of food science & technology, 34(5-6), pp.409-418.

Semisotnov, G.V., Rodionova, N.A., Razgulyaev, O.I., Uversky, V.N., Gripas', A.F. and Gilmanshin, R.I., 1991. Study of the "molten globule" intermediate state in protein folding by a hydrophobic fluorescent probe. Biopolymers: Original Research on Biomolecules, 31(1), pp.119-128.

Serpell, L.C., Sunde, M., Benson, M.D., Tennent, G.A., Pepys, M.B. and Fraser, P.E., 2000. The protofilament substructure of amyloid fibrils. Journal of molecular biology, 300(5), pp.1033-1039.

Simmler, C., Lankin, D.C., Nikolić, D., van Breemen, R.B. and Pauli, G.F., 2017. Isolation and structural characterization of dihydrobenzofuran congeners of licochalcone A. Fitoterapia, 121, pp.6-15.

Singh, P., Anand, A. and Kumar, V., 2014. Recent developments in biological activities of chalcones: A mini review. European Journal of Medicinal Chemistry, 85, pp.758-777.

Soto, C. and Pritzkow, S., 2018. Protein misfolding, aggregation, and conformational strains in neurodegenerative diseases. Nature Neuroscience, 21(10), pp.1332-1340.

Spires-Jones, T.L., Attems, J. and Thal, D.R., 2017. Interactions of pathological proteins in neurodegenerative diseases. Acta neuropathologica, 134, pp.187-205.

Stefani, M. and Dobson, C.M., 2003. Protein aggregation and aggregate toxicity: new insights into protein folding, misfolding diseases, and biological evolution. Journal of molecular medicine, 81, pp.678-699.

Surmacz-Chwedoruk, W., Nieznańska, H., Wójcik, S. and Dzwolak, W., 2012. Cross-seeding of fibrils from two types of insulin induces new amyloid strains. Biochemistry, 51(47), pp.9460-9469.

Teng, Z., Xu, R. and Wang, Q., 2015. Beta-lactoglobulin-based encapsulating systems as emerging bioavailability enhancers for nutraceuticals: a review. RSC Advances, 5(44), pp.35138-35154.

Yang, H., Yang, S., Kong, J., Dong, A. and Yu, S., 2015. Obtaining information about protein secondary structures in aqueous solution using Fourier transform IR spectroscopy. Nature Protocols, 10(3), pp.382-396.

Yu, W.W., Chang, E., Falkner, J.C., Zhang, J., Al-Somali, A.M., Sayes, C.M., Johns, J., Drezek, R. and Colvin, V.L., 2007. Forming biocompatible and nonaggregated nanocrystals in water using amphiphilic polymers. Journal of the American Chemical Society, 129(10), pp.2871-2879.

Zhong, J.Z., Liu, W., Liu, C.M., Wang, Q.H., Li, T., Tu, Z.C., Luo, S.J., Cai, X.F. and Xu, Y.J., 2012. Aggregation and conformational changes of bovine β-lactoglobulin subjected to dynamic high-pressure microfluidization in relation to antigenicity. Journal of dairy science, 95(8), pp.4237-4245.

CHAPTER 4

Literature Review on Nanoparticles and Nanotechnology

4.1. General Introduction to Nanoparticles and Nanotechnology

Nanotechnology is an interdisciplinary field of science that has garnered considerable attention in recent years. It pertains to the study of matter at the scale of 1 billionth of a meter (1 nm $=10^{-9}$ m) and the manipulation of matter at the atomic and molecular scale. The fundamental component in nanostructure fabrication is a nanoparticle, which is significantly smaller than everyday objects governed by Newton's laws of motion, but larger than an atom or a simple molecule subject to the laws of quantum mechanics. The study of nanoparticles has become increasingly important due to their unique properties, which differ significantly from their bulk counterparts. This has led to a plethora of applications in a wide range of fields, including medicine, electronics, energy, and materials science. Human dreams and imagination have often led to the development of new science and technology. Nanotechnology, a frontier of the 21st century, emerged from such dreams. Nanotechnology is defined as the understanding and control of matter at dimensions between 1 and 100 nanometers, where unique phenomena enable novel applications. Although human exposure to nanoparticles has been happening throughout history, it significantly increased during the Industrial Revolution. The study of nanoparticles is not a recent development. The concept of a ‘nanometer’ was first proposed by Richard Zsigmondy, the 1925 Nobel Prize Laureate in chemistry. He coined the term ‘nanometer’ explicitly for characterizing particle size and was the first to measure the size of particles such as gold colloids using a microscope.

Modern nanotechnology was the brainchild of Richard Feynman, the 1965 Nobel Prize Laureate in physics. During the 1959 American Physical Society meeting at Caltech, he presented a lecture titled "There's Plenty of Room at the Bottom", in which he introduced the concept of manipulating matter at the atomic level. This novel idea demonstrated new ways of thinking, and Feynman's hypotheses have since been proven correct. It is for these reasons that he is considered the father of modern nanotechnology (Feynman,2018). Almost 15 years after Feynman’s lecture, a Japanese scientist, Norio Taniguchi, was the first to use ‘nanotechnology’ to describe semiconductor processes that occurred on the order of a nanometer. He advocated that nanotechnology consisted of the processing, separation, consolidation, and deformation of materials by one atom or one molecule (Taniguchi, 1974). The golden era of nanotechnology began in the 1980s when Kroto, Smalley, and Curl discovered fullerenes and Eric Drexler of

the Massachusetts Institute of Technology (MIT) used ideas from Feynman's "There is Plenty of Room at the Bottom" and Taniguchi's term nanotechnology in his 1986 book titled "Engines of Creation: The Coming Era of Nanotechnology." Drexler proposed the idea of a nanoscale 'assembler' that would be able to build a copy of itself and other items of arbitrary complexity. Drexler's vision of nanotechnology is often called 'molecular nanotechnology' (Drexler, 1987). The science of nanotechnology was advanced further when Iijima, another Japanese scientist, developed carbon nanotubes (Iijima,1991). The invention of scanning tunneling microscopy (STM) by Gerd Binning and Heinrich Rohrer in the same year aided in a better understanding of the nanoworld and earned them the Nobel Prize in Physics in 1986(Binnig et al., 1982). In 1985, the discovery of fullerene, a football-shaped molecule made up of sixty carbon atoms, by Professor Harold Kroto, Richard Smalley, and Robert Curl won them the Nobel Prize in Chemistry in 1996(Curl and Smalley, 1988). This was followed by the discovery of carbon nanotubes, which are hollow tubes of several nanometers derived from graphite sheets.

Nanotechnology has advanced as a significant scientific achievement in the 21st century. This field encompasses the synthesis, management, and application of materials with a size smaller than 100 nm, and it falls under the interdisciplinary umbrella. Nanoparticles have wide-ranging applications in various sectors including the environment, agriculture, food, biotechnology, and biomedical sciences. For example, they are used in the treatment of wastewater (Zahra et al., 2020), environmental monitoring (Rassaei et al., 2011), as functional food additives (Chen et al., 2023), and as antimicrobial agents (Islam et al., 2022). The unique properties of nanoparticles, such as their nature, biocompatibility, anti-inflammatory and antibacterial activity, effective drug delivery, bioactivity, bioavailability, tumor targeting, and bio-absorption, have increased their use in biotechnological and applied microbiological applications. Nanoparticles, particles of matter with a diameter within one to one hundred nanometers (nm), possess distinct size-dependent features attributable to their diminutive size and substantial surface area. As particles approach the nano-scale, the periodic boundary conditions of the crystalline particle are disrupted as the characteristic length scale becomes comparable to or smaller than the de Broglie wavelength or the wavelength of light (Guo et al., 2013). This prompts significant deviations in the physical characteristics of nanoparticles in comparison to bulk materials, consequently giving rise to a spectrum of innovative applications (Hasan, 2015). Nanotechnologies involve the creation and manipulation of materials at the nanometer scale, either by scaling up from single groups of atoms or by refining or reducing bulk materials. Scientific focus on nanosized objects emerged far back in the early 1200-1300

B.C., and its recurrence has led to mounting inventions in the field of nanotechnology. Decades ago, interest in metal nanoparticles was limited to applications, such as the Damascus steel, which was used to make swords, and the glass Lycurgus cup, which has unique colors. However, after the development of modern devices to analyze nanometer-scale material, nano-materials became very attractive as possible machines that can travel through the body, hence they are able to repair damaged tissues and deliver therapeutic drugs and genes. In 1857, Faraday reported the synthesis of colloidal gold (and other metals such as Cu, Zn, Fe, and Sn) and its interaction with light (Katti and Sharon, 2019). Another example of interest is the case of magnetic NPs which illustrated the role that magnetic materials play in biology and medicine. In the field of magnetic NPs, a noteworthy pioneering work was published by Blakemore in 1975, where biochemically precipitated magnetite (Fe_3O_4) was found in the tissues of various organisms, including bacteria, algae, insects, birds, and mammals. The field of colloid science has developed enormously and has been used to produce many materials, including metals, oxides, and organic products. One of the first and most easily prepared magnetic colloidal systems was developed by Stephen Papell of the National Aeronautics and Space Administration in the early 1960s (Papell,1960). To prevent particle-particle agglomeration or sedimentation, Papell added oleic acid as a dispersing agent. Subsequently, similar magnetic suspensions have also been synthesized with different nanometer-sized particles of pure elements, such as iron, nickel, and cobalt, in a wide range of carrier liquids.

4.2. Definition of Nanoscience and Nanotechnology

The term ‘nano’ is of Greek origin and means ‘dwarf’ or something very small. It is used to refer to one billionth of a meter (10^{-9}m). It's important to make a distinction between nanoscience and nanotechnology. Nanoscience encompasses the study of structures and molecules on a scale ranging from 1 to 100 nanometers, while nanotechnology involves the practical application of this knowledge in devices and other technologies (Mansoori. et.al**.,** 2005). To put it into context, consider that a single human hair is approximately 60,000 nanometers thick, while the DNA double helix has a radius of about 1 nanometer **(Fig.1)** (Gnach. et.al.,2015). The roots of nanoscience can be traced back to the ancient Greeks and Democritus in the 5th century B.C. when the concept of atoms as small, indivisible, and indestructible particles started to emerge as a fundamental aspect of matter.

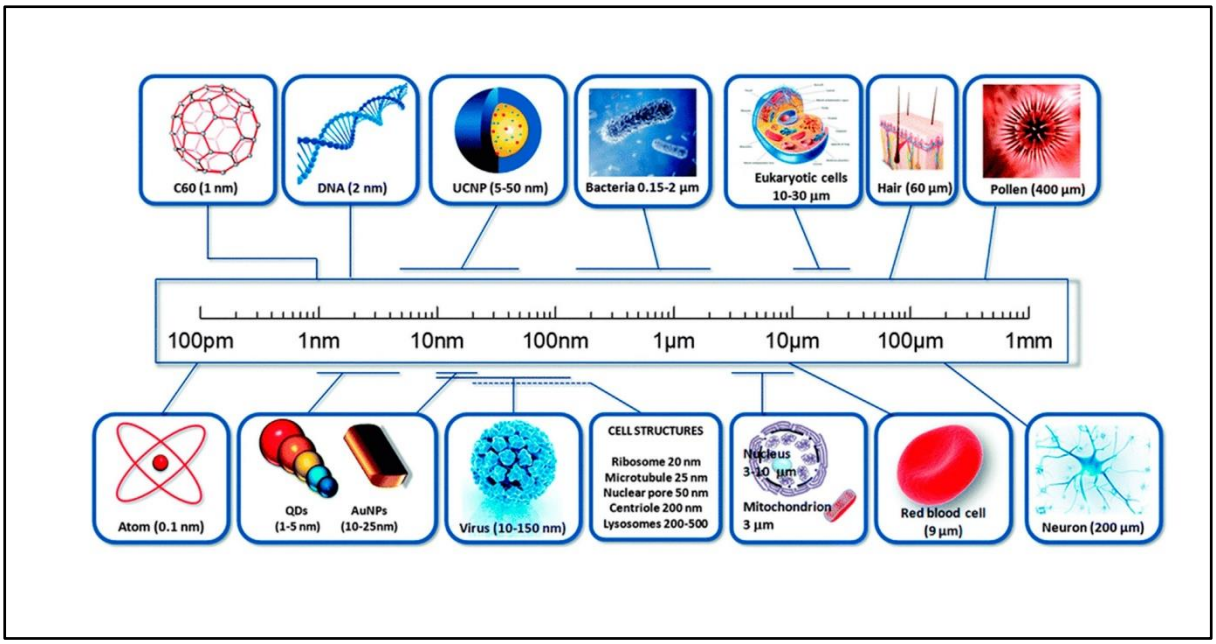

Figure 1: A comparison of sizes of nanomaterial (Adapted from Gnach. et.al.,2015).

Nanotechnology represents one of the most promising technological advancements of the 21st century. It encompasses the translation of nanoscience theory into practical applications through the observation, measurement, manipulation, assembly, control, and manufacturing of matter at the nanometer scale. The National Nanotechnology Initiative (NNI) in the United States defines nanotechnology as "a science, engineering, and technology conducted at the nanoscale (1 to 100 nm), where unique phenomena enable novel applications in a wide range of fields, from chemistry, physics, and biology to medicine, engineering, and electronics". This definition underscores the necessity for nanotechnology to operate within the nanometer scale while leveraging distinct properties inherent to this scale.

Table 1: Definitions of nanoparticles and nanomaterials by various organizations. (Adapted from Horikoshi et al., 2013).

Organization	Nanoparticle	Nanomaterial
International Organization for Standardization (ISO)	A particle spanning 1–100 nm (diameter)	–
The American Society of Testing and Materials (ASTM)	An ultrafine particle whose length in 2 or 3 places is 1–100 nm	–
National Institute of Occupational Safety and Health (NIOSH)	A particle with a diameter between 1 and 100 nm, or a fiber spanning the range 1–100 nm.	–
Scientific Committee on Consumer Products (SCCP)	At least one side is in the nanoscale range.	**Material for which at least one side or internal structure is in the nanoscale**
British Standards Institution (BSI)	All the fields or diameters are in the nanoscale range.	**Material for which at least one side or internal structure is in the nanoscale**
Bundesanstalt für Arbeitsschutz und Arbeitsmedizin (BAuA).	All the fields or diameters are in the nanoscale range.	**Material consisting of a nanostructure or a nanosubstance**

In general, the size of a nanoparticle spans the range between 1 and 100 nm. Metallic nanoparticles have different physical and chemical properties from bulk metals (e.g., lower melting points, higher specific surface areas, specific optical properties, mechanical strengths, and specific magnetizations), properties that might prove attractive in various industrial applications. However, how a nanoparticle is viewed and defined depends very much on the specific application. In this regard, **Table 1** summarizes the definition of nanoparticles and nanomaterials by various organizations of particular importance, the optical property is one of the fundamental attractions and a characteristic of a nanoparticle. For example, a 20-nm gold nanoparticle has a characteristic wine-red color. A silver nanoparticle is yellowish-gray.

Platinum and palladium nanoparticles are black. Not surprisingly, the optical characteristics of nanoparticles have been used from time immemorial in sculptures and paintings even before the 4th century AD. The most famous example is the Lycurgus cup (fourth century AD) illustrated in **(Fig.2)**. This extraordinary cup is the only complete historical example of a very special type of glass, known as dichroic glass, that changes color when held up to the light. The opaque green cup turns to a glowing translucent red when light is shone through it internally (i.e., light is incident on the cup at 90° to the viewing direction). Analysis of the glass revealed that it contains a very small quantity of tiny (~ 70 nm) metal crystals of Ag and Au in an approximate molar ratio of 14: 1, which gives it these unusual optical properties. It is the presence of these nanocrystals that gives the Lycurgus Cup its special color display. The reader can marvel at the cup now in the British Museum **(https://www.britishmuseum.org/)**.

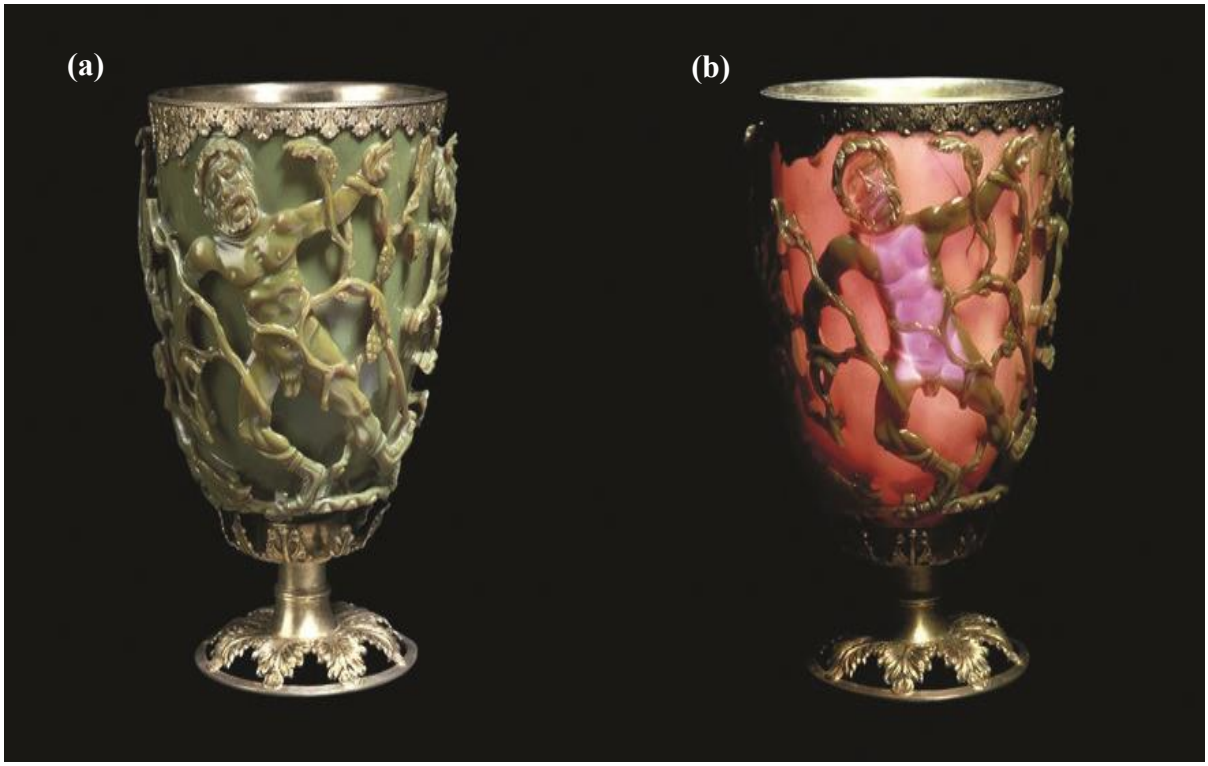

Figure 2: Photographs of the famous Lycurgus cup which displays a different color depending on whether it is illuminated externally (a) or internally (b). For details, please consult the website of the British Museum (https://www.britishmuseum.org/).

Table 2: Chronological Table of Nanotechnology

Year	Remarks	Country/ People
1200–1300 BC	Discovery of soluble gold	Egypt and China
290–325 AD	Lycurgus cup	Alexandria or Rome
1618	The first book on colloidal gold	F. Antonii
1676	Book published on drinkable gold that contains metallic gold in neutral media	J. von Löwenstern-Kunckel (German
1718	Publication of a complete treatise on colloidal gold	Hans Heinrich Helcher
1857	Synthesis of colloidal gold	M. Faraday (The Royal Institution of Great Britain)
1902	Surface plasmon resonance (SPR)	R. W. Wood (Johns Hopkins University, USA)
1908	Scattering and absorption of electromagnetic fields by a nanosphere	G. Mie (University of Göttingen, Germany)
1931	Transmission electron microscope (TEM)	M. Knoll and E. Ruska (Technical University of Berlin, Germany)
1959	Feynman's Lecture on "There' s Plenty of Room at the Bottom"	R. P. Feynman (California Institute of Technology, Pasadena, CA, USA)
1960	Microelectromechanical systems (MEMS)	I. Igarashi (Toyota Central R&D Labs, Japan)
1960	Successful oscillation of a laser	T. H. Maiman (Hughes Research Laboratories, USA)
1962	The Kubo effect	R. Kubo (University of Tokyo, Japan)
1965	Moore's Law	G. Moore (Fairchild Semiconductor Inc., USA)
1969	The Honda–Fujishima effect	A. Fujishima and K. Honda (University of Tokyo, Japan)
1972	Amorphous heterostructure photodiode created with bottom-up process	E. Maruyama (Hitachi Co. Ltd., Japan)

1974	Concept of nanotechnology proposed	N. Taniguchi (Tokyo University of Science, Japan)
1976	Carbon nanofiber	M. Endo (Shinshu University, Japan)
1976	Amorphous silicon solar cells	D. E. Carlson and C. R. Wronski (RCA, USA)
1980	Quantum hall effect (Nobel Prize)	K. von Klitzing (University of Würzburg, Germany)
1982	Scanning tunnelling microscope (STM) (Nobel Prize)	G. Binnig and H. Rohrer (IBM Zurich Research Lab., Switzerland)
1986	Atomic force microscope (AFM)	G. Binnig (IBM Zurich Research Lab., Switzerland)
1986	Three-dimensional space manipulation of atoms demonstrated (Nobel Prize)	S. Chu (Bell Lab., USA)
1987	Gold nanoparticle catalysis	M. Haruta (Industrial Research Institute of Osaka, Japan)
1990	Atoms controlled with a scanning tunnelling microscope (STM)	D. M. Eigler (IBM, USA)
1991	Carbon nanotubes discovered	S. Iijima (NEC Co., Japan)
1992	Japan's National Project on Ultimate Manipulation Begins of Atoms and Molecules	Japan
1995	Nano-imprinting	S. Y. Chou (University of Minnesota, USA)
1996	Nano sheets	T. Sasaki (National Institute for Research in Inorganic Materials, Japan)
2000	National Nanotechnology Initiative (NNI)	USA
2003	21st Century Nanotechnology Research and Development Act	USA
2005	Nanosciences and Nanotechnologies: An Action Plan	Europe

4.3. Classification of Nanoparticles (NPs)

Nanoparticles (NPs) may be categorized into distinct classes based on their specific attributes, such as shape, size, and chemical properties.

4.3.1. Carbon-based NPs

Fullerenes and carbon nanotubes (CNTs) are both important subcategories of carbon-based nanoparticles. Fullerenes are hollow, cage-like structures made of carbon atoms arranged in pentagonal and hexagonal shapes, exhibiting sp^2 hybridization. These carbon structures, also known as buckyballs, possess unique properties such as high electrical conductivity, strength, and adaptability, making them economically valuable. On the other hand, carbon nanotubes (CNTs) are elongated cylindrical structures with diameters typically ranging from 1 to 2 nanometers. They are composed of rolled-up graphene sheets, resembling graphite rolled into a tube. The number of walls defines their categorization as single-walled (SWNTs), double-walled (DWNTs), or multi-walled carbon nanotubes (MWNTs). This classification is based on the arrangement of carbon atoms within the tubular structures. These nanomaterials have garnered significant attention due to their unique properties and potential applications in various fields (Elliott et al., 2013; Astefanei et al., 2015). Fullerenes and carbon nanotubes (CNTs) are significant classes of carbon-based nanoparticles. Fullerenes are comprised of hollow, spherical carbon structures that have generated considerable commercial interest due to their exceptional electrical conductivity, high strength, structural attributes, electron affinity, and versatility (Astefanei et al., 2015). They are composed of arranged pentagonal and hexagonal carbon units, with each carbon being sp^2 hybridized. Notable fullerenes include C60 and C70, with respective diameters of 7.114 and 7.648 nm, as depicted in **(Fig.3)**. CNTs, conversely, are elongated tubular structures with diameters ranging from 1 to 2 nm (Ibrahim, 2013). They may exhibit metallic or semiconducting properties contingent upon their diameter (Aqel et al., 2012). Structurally, CNTs resemble a rolled-up graphite sheet, as illustrated in **(Fig. 4)**. They may exist as single-walled (SWNTs), double-walled (DWNTs), or multi-walled (MWNTs) structures, based on the number of walls. Commonly, they are synthesized through the deposition of carbon precursors, particularly atomic carbons, vaporized from graphite by laser or electric arc onto metal particles, and more recently, via chemical vapor deposition (CVD) **(**Elliott et al., 2013).

Considering their unique physical, chemical, and mechanical characteristics, fullerenes and CNTs are not only utilized in their pristine forms but are also incorporated into nanocomposites

for diverse commercial applications, including deployment as fillers (Saeed and Khan, 2016, 2014**),** efficient gas adsorbents for environmental remediation (Ngoy et al., 2014), and as supporting matrices for various inorganic and organic catalysts (Mabena et al., 2011).

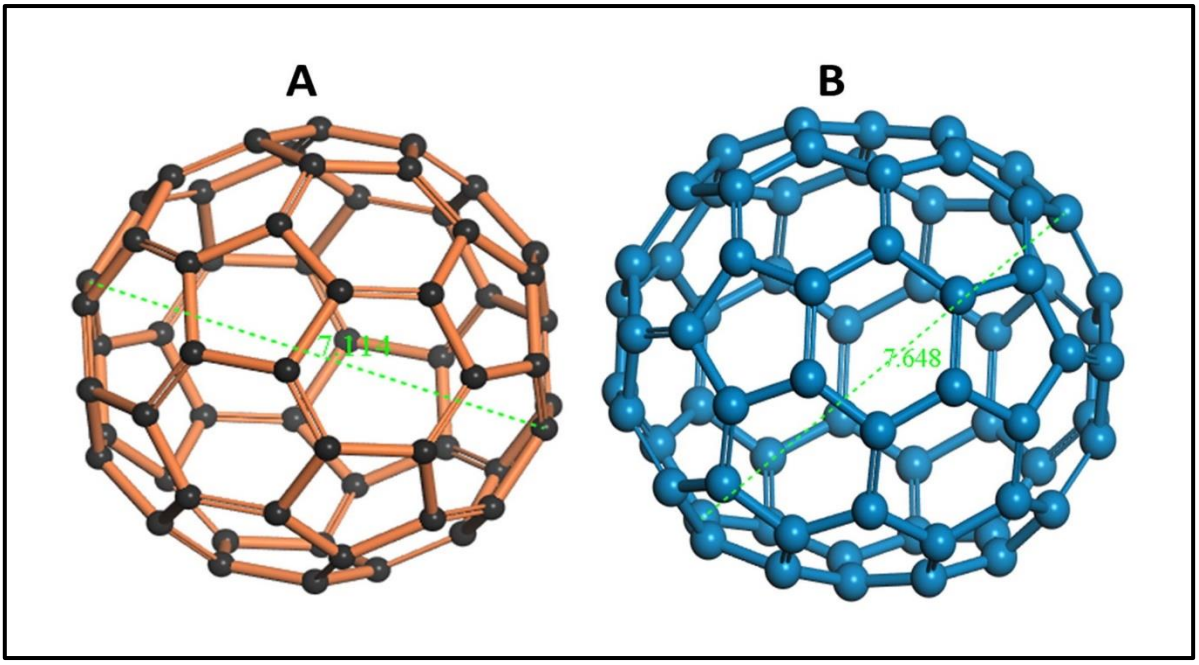

Figure 3: Different forms of Fullerenes/buck balls (A) C60 and (B) C70. (Adapted from Astefanei et al., 2015).

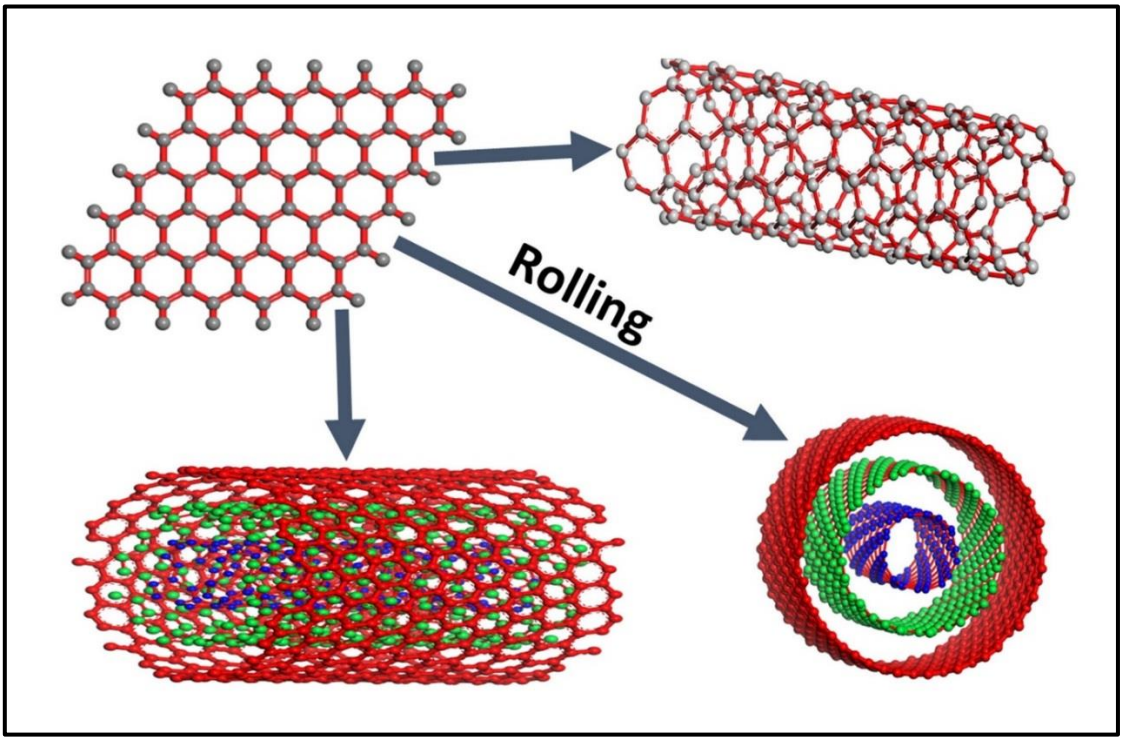

Figure 4: Rolling of graphite layer into single-walled and multi-walled CNTs. (Adapted from Aqel et al., 2012).

4.3.2. Metal nanoparticles (NPs)

Metal nanoparticles (NPs) consist solely of metal precursors and possess distinct optoelectronic properties due to their well-established localized surface plasmon resonance (LSPR) characteristics. Notably, NPs of alkali and noble metals such as Cu, Ag, and Au exhibit a broad absorption band in the visible electromagnetic solar spectrum. The precise synthesis of metal NPs, including control over facets, sizes, and shapes, holds significant relevance in contemporary materials research (Dreaden et al., 2012). Given their sophisticated optical attributes, metal NPs find widespread applications across various research domains. In particular, gold NP coating is extensively employed in scanning electron microscopy (SEM) for sample enhancement, ultimately leading to the acquisition of high-fidelity SEM images **(Fig. 5)**.

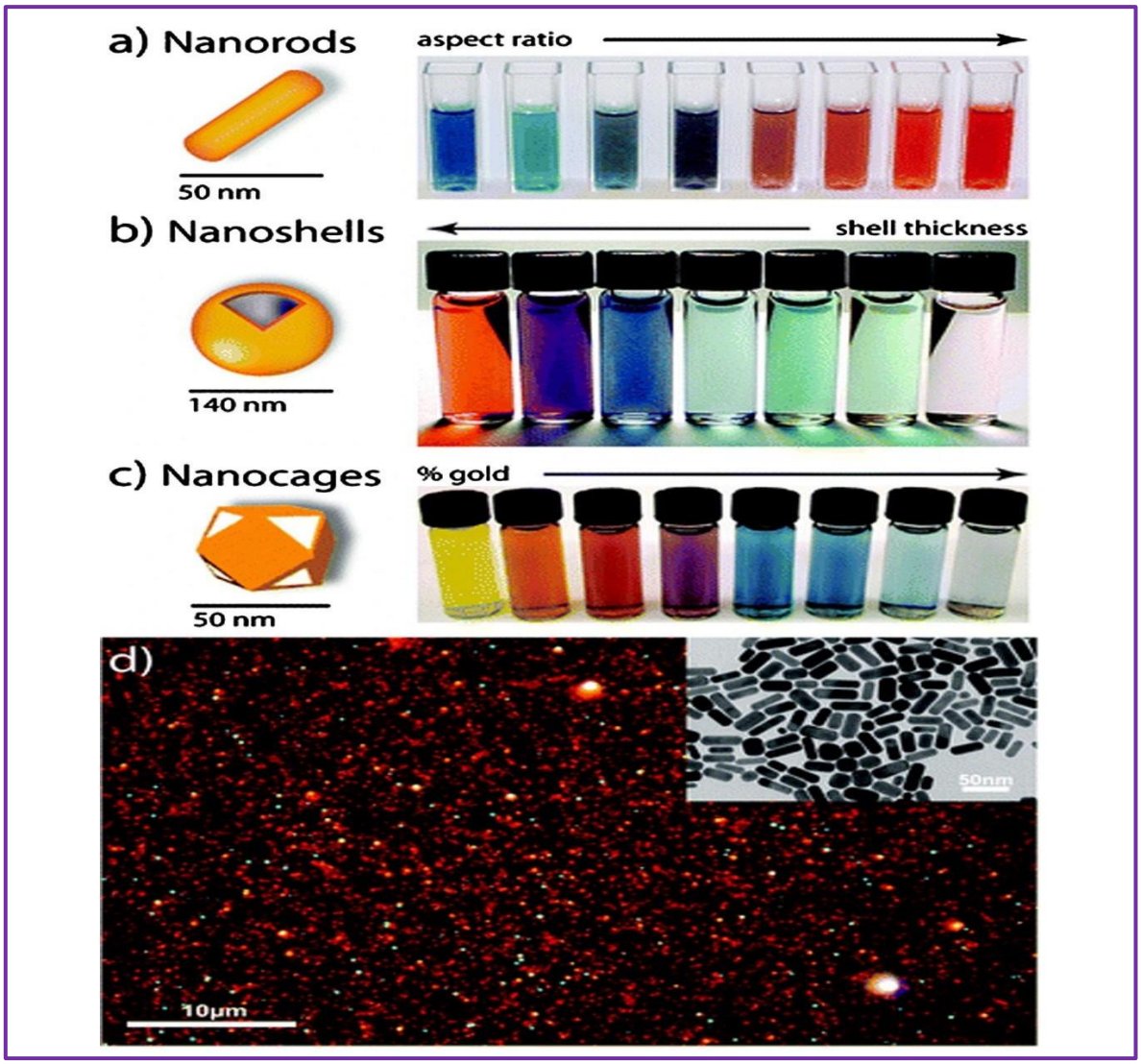

Figure 5: Color dependence of AuNPs on size and shape. (Adapted from Dreaden et al., 2012)

4.3.3. Ceramics NPs

Ceramic nanoparticles (NPs) are a category of inorganic nonmetallic solids synthesized through controlled heating and subsequent cooling processes. These nanoparticles exhibit varied structural characteristics, encompassing both amorphous and polycrystalline forms, as well as dense, porous, and hollow morphologies (Sigmund et al., 2006). The unique properties of ceramic nanoparticles have garnered substantial attention from researchers due to their potential utility in diverse applications such as catalysis, photocatalysis, dye photodegradation, and imaging (Thomas et al., 2015).

4.3.4. Semiconductor NPs

Semiconductor materials display a unique set of properties that position them at the interface between metals and nonmetals, imparting them with a diverse range of applications across various fields (Ali et al., 2017; Khan et al., 2017a). One notable category within this domain is semiconductor nanoparticles (NPs), which possess wide bandgaps, leading to significant modifications in their characteristics through bandgap tuning. This property makes them particularly important in areas such as photocatalysis, photo optics, and electronic devices (Sun, 2000). For example, a wide array of semiconductor NPs have demonstrated exceptional proficiency in applications such as water splitting, harnessing their well-suited bandgap and band edge positions for efficient performance (Hisatomi et al., 2014).

4.3.5. Polymeric NPs

These nanoparticles are typically organic-based. In the literature, they are collectively referred to as polymer nanoparticles (PNPs). They are primarily nanospheres or nanocapsules (Mansha et al., 2017). The former are solid matrix particles with other molecules adsorbed at the outer boundary of the spherical surface, while in the latter case, the solid mass is completely encapsulated within the particle (Rao et al.,2011). PNPs are easily functionalized and have numerous applications in the literature (Abd Ellah et al., 2016; Abouelmagd et al., 2016).

4.3.6. Lipid-based NPs

The described nanoparticles (NPs) are composed of lipid components and are widely utilized in a multitude of biomedical applications. Typically, a lipid NP is characterized by its spherical shape with a diameter ranging from 10 to 1000 nm. Similar to polymeric NPs, lipid NPs consist of a solid core made of lipids and a matrix containing soluble lipophilic molecules. The external core of these NPs is stabilized by surfactants or emulsifiers (Rawat et al., 2011). Lipid

nanotechnology (Mashaghi et al., 2013) is a specialized field focusing on the design and synthesis of lipid NPs for diverse applications such as drug carriers and delivery (Puri et al., 2009), and RNA release in cancer therapy (Gujrati et al., 2014).

4.3.7. Protein-based Nanoparticles (PNPs)

Proteins and enzymes represent versatile biomaterials with diverse applications in the field of medicine due to their notable specificity for receptors and substrates, high degradability, low toxicity, and overall strong biocompatibility. The formation of protein nanoparticles occurs as a result of the arrangement of numerous native or modified proteins into nanometer-sized assemblies. Proteins constitute well-defined biopolymers, composed of a linear peptide chain that undergoes folding to attain a sophisticated three-dimensional structure (D. J. Dietzen 2018**)**. The assembly of proteins into nanometer-sized particles can address the limitations of single proteins, such as prolonged circulation time, improved cellular uptake, and spatial proximity for cascade reactions. Nature's toolkit offers a plethora of protein nanoparticles that form highly organized structures through supramolecular assembly processes (Edwardson et al.,2022). Three prominent categories of natural protein assemblies utilized for drug delivery include virus-like particles, ferritin complexes, and bacterial protein cages **(Fig.6)**.

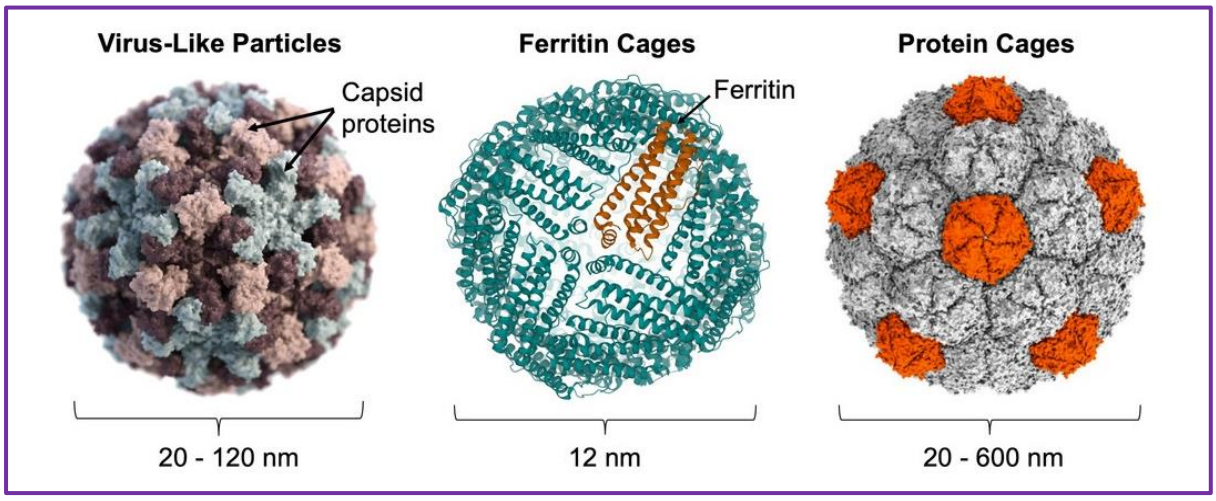

Figure 6: Illustrates the formation of protein nanoparticles through the self-assembly of protein subunits. This process gives rise to various classes of nanoparticles such as virus-like particles, ferritin cages, and bacterial protein cages. (Adapted from Jones et al.,2021).

4.3.8. Magnetic Nanoparticles (MNPs)

In the past decade, magnetic nanoparticles (MNPs) have garnered significant attention within scientific and academic circles due to their extensive applicability in various specialized fields

such as medicine, cancer theranostics, biosensing, catalysis, agriculture, and environmental science **(Fig.7)**. The precise manipulation of MNP surface properties is of utmost importance in the development of multifunctional MNPs tailored to specific applications. MNPs have demonstrated remarkable efficacy as thermoelectric materials, imaging agents, drug delivery vehicles, and biosensors. Their multifaceted nature and potential implications across a range of disciplines position them as an area of keen scholarly interest warranting further exploration and research. Magnetic nanoparticles (MNPs) are composed of various metal elements, either individually or in composites, along with their corresponding oxides, exhibiting magnetic properties (Kefeni et al., 2017). Particularly, superparamagnetic magnetite (Fe_3O_4) is widely utilized as an iron oxide due to its excellent biocompatibility and minimal toxicity (Assa et al., 2016; Farjadian et al., 2017). Iron oxide MNPs have recently garnered considerable attention for their potential applications in diverse fields (Bansal et al., 2017). The surface chemistry of superparamagnetic iron oxide MNPs can be modulated by adjusting their physicochemical properties and can find applications in various domains such as hyperthermia, magnetic resonance imaging (MRI), immunoassays, drug delivery, and cell separation (Weissleder et al., 1995; Kumar et al., 2011).

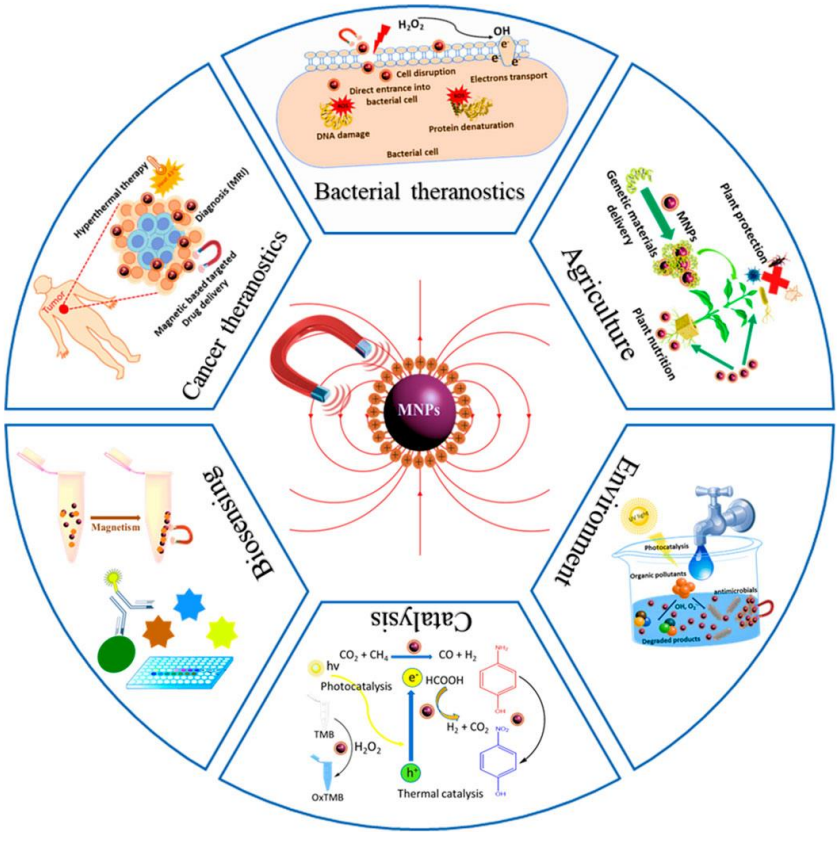

Figure 7: Schematic illustration of the magnetic nanoparticles (MNPs) with different perspectives. (Adapted from Ali et al.,2021).

4.4. Types of different metal-based and metal oxide-based NPs

Metal nanoparticles (NPs) are exclusively composed of metal precursors. These NPs exhibit distinct optoelectrical properties due to their well-documented localized surface plasmon resonance (LSPR) characteristics. Alkali and noble metal NPs, such as Cu, Ag, and Au, demonstrate a wide absorption band within the visible region of the solar electromagnetic spectrum. The controlled synthesis of metal NPs, encompassing facet, size, and shape, holds critical significance in contemporary advanced materials (Dreaden et al., 2012; Khan et al., 2019). Metal-oxide nanomaterials (MONs) have recently attracted a lot of interest in the development of flexible and wearable sensors. This is due to their adjustable band gap, low cost, large surface area, and easy manufacturability. Moreover, there is a high demand for MONs in various applications such as gas leakage detection, environmental protection, health monitoring, and integration with smart devices. Metal-oxide nanomaterials (MONs)are promising candidates in diverse areas of chemistry, materials science, physics, and biotechnology (Vorokhta et.al., 2018).

4.4.1. Silver nanoparticles (AgNPs)

Silver nanoparticles (AgNPs) are defined as particles comprised of silver within the size range of 1–100 nanometers. Their distinct physical and chemical properties stem from their small size, high surface area-to-volume ratio, and capacity to absorb and scatter light within the visible and near-infrared spectrum. Owing to their reduced dimensions and increased surface-to-volume ratios, AgNPs may exhibit additional antimicrobial capabilities not inherent in ionic silver (Shenashen et al., 2014). Furthermore, the characteristics of AgNPs depend on their size and forms, which are contingent upon the specific manufacturing process. Chemical reduction stands as the predominant technique for synthesizing AgNPs. Nanosilver demonstrates a broad spectrum of antimicrobial activity, effectively inhibiting the growth of both Gram-positive and Gram-negative bacteria, such as Escherichia coli, Pseudomonas aeruginosa, and Staphylococcus aureus (Birla et al., 2009; Li et al., 2010).

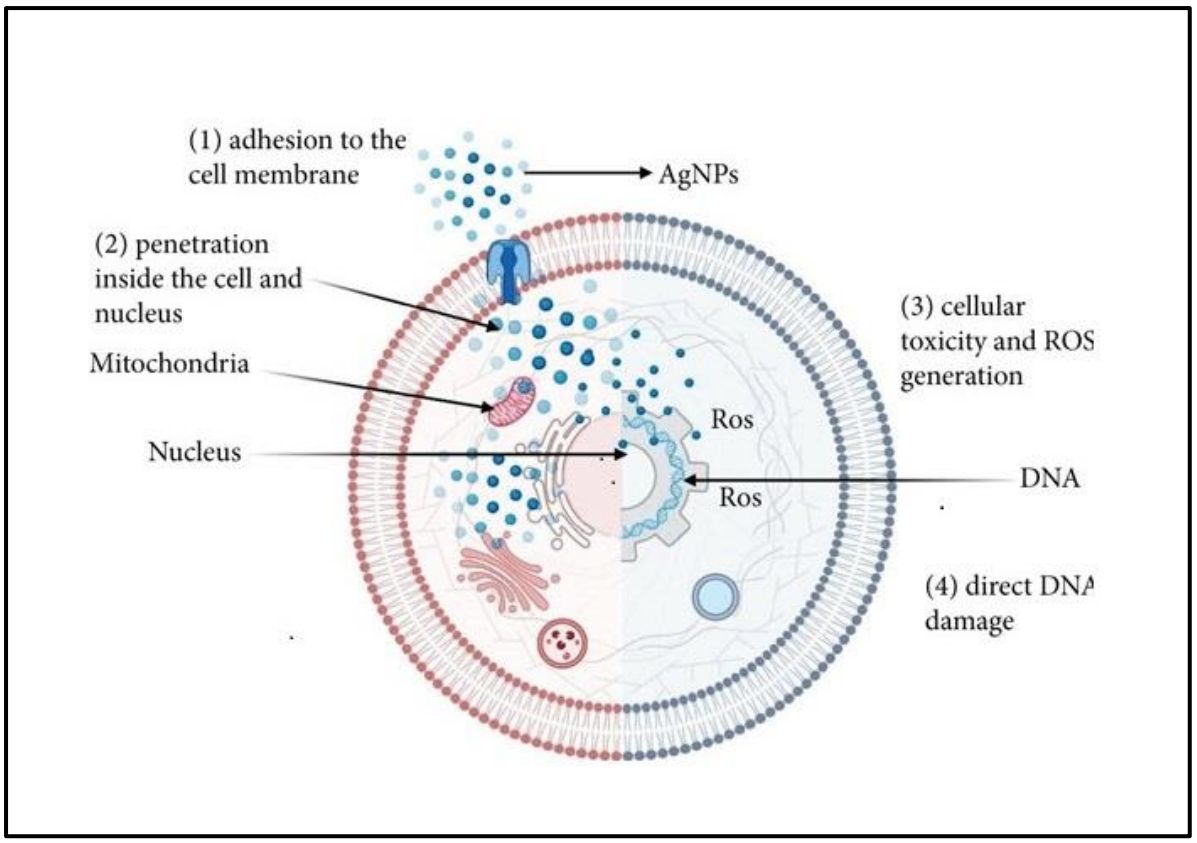

Figure 8: The proposed antimicrobial mechanism of action of AgNPs involves: (**1**) Adherence to microbial cell surfaces, causing membrane damage and altered transport activity, (**2**) Penetration into microbial cells and interaction with cellular organelles, (**3**) Induction of increased ROS levels inside microbial cells, leading to cell damage and (**4**) Direct DNA damage and disruption of cellular signaling. (Generated from https://biorender.com/.)

4.4.2. Gold nanoparticles (AuNPs)

Gold nanoparticles (AuNPs) are minute particles consisting of gold, characterized by unique physical and chemical properties that enable them to interact with and disperse light within the visible and near-infrared spectrum (Rad et al., 2011; Compostella et al., 2017). In the early 20th century, scientists observed that AuNPs exhibit anisotropic qualities, contrary to the assumption of spherical morphology when their size is 40 nm or smaller. Moreover, anisotropic gold particles displaying diverse colors were identified (Li et al., 2014). Zsigmondy's seminal contributions culminated in his reception of the Nobel Prize in 1925 for elucidating the heterogeneous nature of colloidal solutions and for inventing the ultramicroscope, which enabled the visualization of Au particle forms. Notably, Zsigmondy documented the frequent crystallization of gold into a hexagonal leaf shape (Li et al., 2014). AuNPs are the subject of extensive research due to their optical, electrical, and molecular recognition capabilities,

presenting numerous potential applications across a wide array of disciplines including electron microscopy, electronics, nanotechnology, materials science, and biomedicine (Rad et al., 2011).

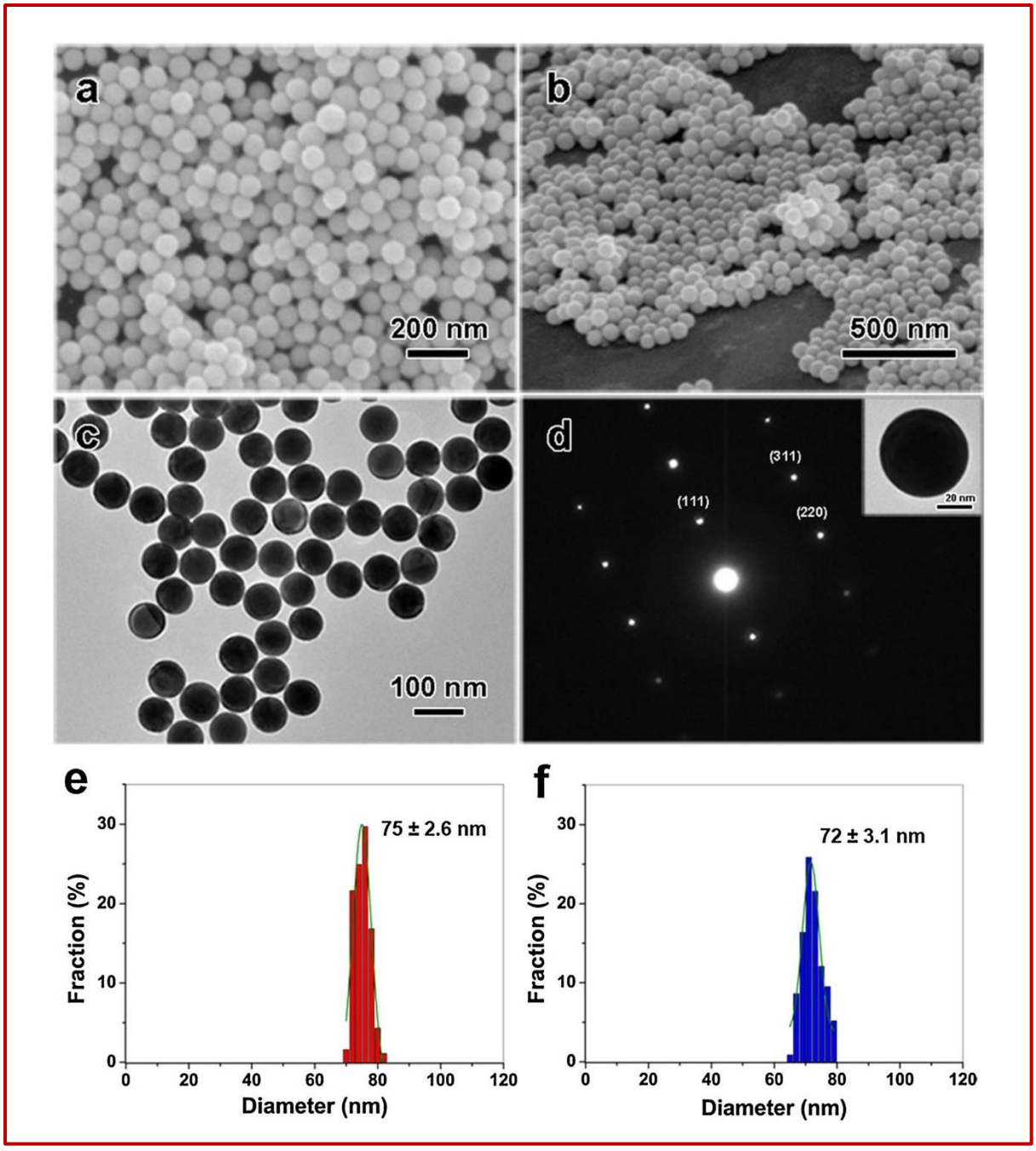

Figure 9: SEM depicts Au nanospheres in three perspectives: (a) top view, (b) tilted view, and (c) TEM image. Additionally, it includes the SAED pattern, with a TEM image of a single Au particle as an inset, and the size distribution spectra of spherical and octahedral AuNPs (Liu et al., 2015a, 2015b).

4.4.3. Zinc oxide nanoparticles (ZnONPs)

Zinc nanoparticles (ZnONPs) are tiny particles ranging in size from 1 to 100 nanometers and are comprised of zinc. Zinc oxide (ZnONPs), characterized by a wide band gap semiconductor, possesses a room temperature energy gap of 3.37 eV. Their catalytic, electrical, optoelectronic, and photochemical capabilities have rendered them immensely valuable in various applications (Kumar S.S. et al., 2013). Furthermore, ZnO nanostructures demonstrate exceptional suitability for catalyzing various reaction processes (Chen and Tang, 2007). The antibacterial properties of ZnONPs have shown promise for various antimicrobial applications (Sawai, 2003). Additionally, it is anticipated that the high photocatalytic activity and chemical stability of ZnO nanocomposites will greatly facilitate their practical application in the removal of organic pollutants from wastewater (Zhang et al.,2012).

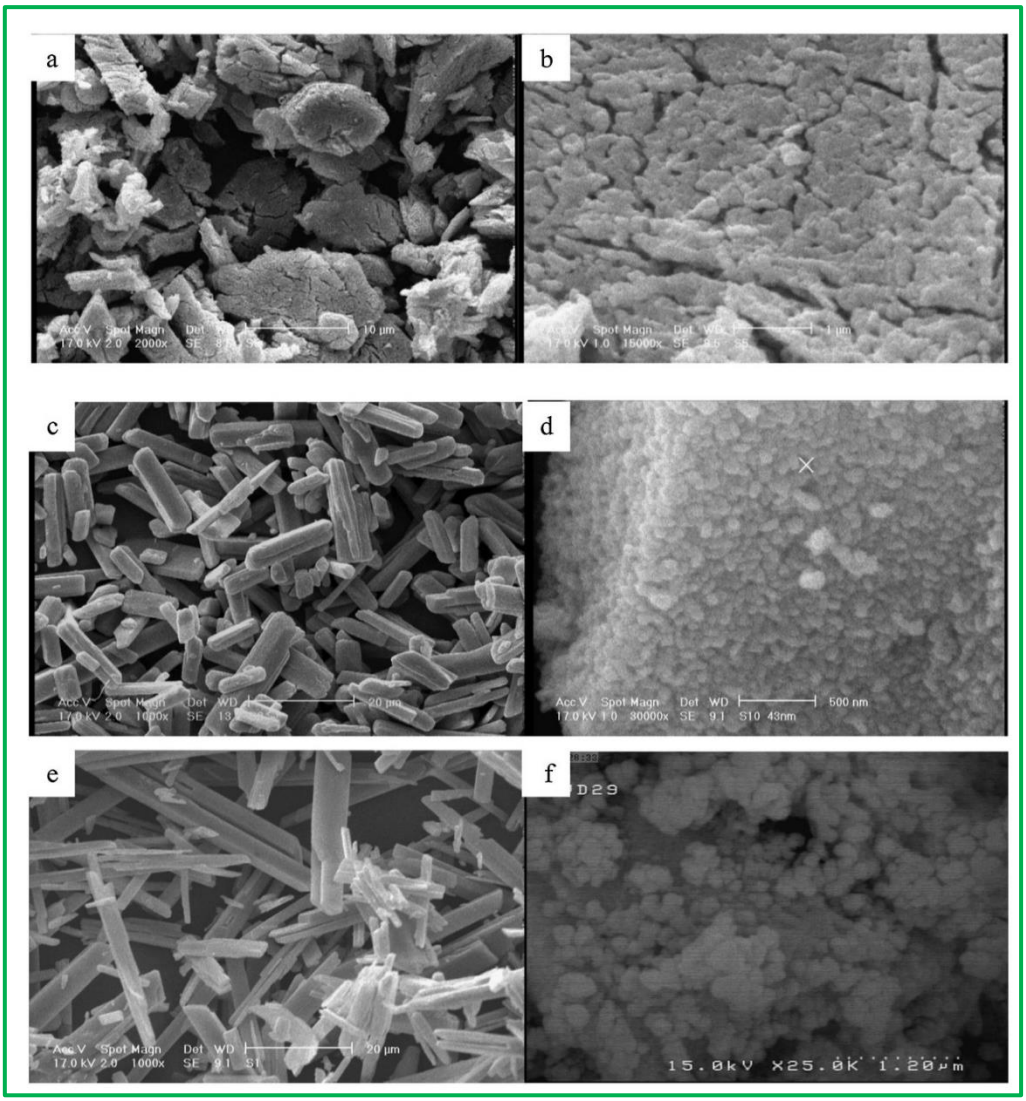

Figure 10: SEM images of ZnO-modified MOFs at different temperatures. Adapted from (Mirzadeh et al., 2016).

4.4.4. Copper nanoparticles (CuNPs)

Copper nanoparticles (CuNPs) encompass copper-based particles within the size range of 1 to 100 nm (Khan et al., 2019). Both copper (Cu) and gold (Au) metals demonstrate fluorescence properties. Upon excitation at 488 nm, a fluorescence peak centered on the interband absorption edge of the metals is evident. Copper nanoparticles (CuNPs) have piqued the interest of the public due to their impressive mechanical, electrical, magnetic, and thermal properties. These tiny particles have found applications in water treatment processes, heat transfer systems, and antimicrobial coatings for surgical tools **(**Mohamed et al.,2020; Chandraker et al.,2020**).** Copper is an indispensable element involved in vital metabolic processes in both humans and animals (Bhattacharya et al., 2016). The use of copper nanoparticles (CuNPs) as additives in lubricants, polymers, and inks has been documented (Adeleye et al., 2014; Conway et al., 2015). Given their small size and capacity to release ions under acidic conditions, CuNPs exhibit antimicrobial properties, rendering them prospective additives for conventional wastewater treatment (Chen et al., 2006).

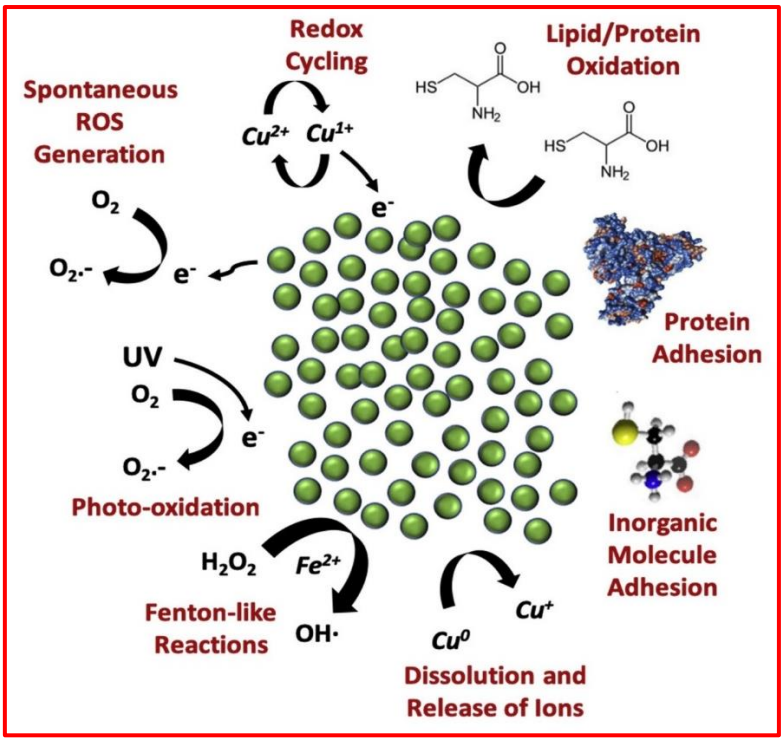

Figure 11: The chemical and biochemical reactions exhibited by copper nanoparticles in aqueous suspensions encompass a range of processes. These include the oxidation of lipid or protein biomolecules, the conjugation with proteins or inorganic molecules, the dissolution into cupric ions, the induction of Fenton-like reactions, photo-oxidation, the generation of reactive oxygen species (ROS), and the Redox cycling between Cu^{2+} and Cu^{1+}. (Adapted from Ameh et al., 2019).

4.4.5. Copper oxide nanoparticles (CuONPs)

Copper oxide (CuO), also referred to as copper (II) oxide or cupric oxide, is a semiconducting compound characterized by a monoclinic structure. CuO has garnered significant scientific interest due to its status as the most rudimentary member of the copper compound family, and its manifestation of a diverse array of potentially advantageous physical properties, inclusive of high-temperature superconductivity, electron correlation effects, and spin dynamics (Cava, 1990; Tranquada et al.,1995). CuO, serving as an important p-type semiconductor, finds diverse applications in gas sensors, catalysis, batteries, high-temperature superconductors, solar energy conversion, and field emission emitters. In the realm of energy conservation, fluids containing nano CuO particles can enhance fluid viscosity and thermal conductivity **(**Kwak et al., 2005). The crystal structures of CuO possess a narrow bandgap, offering valuable photocatalytic, photovoltaic, and photoconductive properties (Xu et al.,1999). Although information on the potential antimicrobial activity of nano CuO is limited, its cost-effectiveness compared to silver, ease of mixing with polymers, and relative stability in terms of chemical and physical properties make it a promising option. Highly ionic nanoparticulate metal oxides like CuO may prove to be particularly beneficial as antimicrobial agents due to their capacity to be prepared with exceptionally high surface areas and unique crystal morphologies **(**Stoimenov et al.,2002).

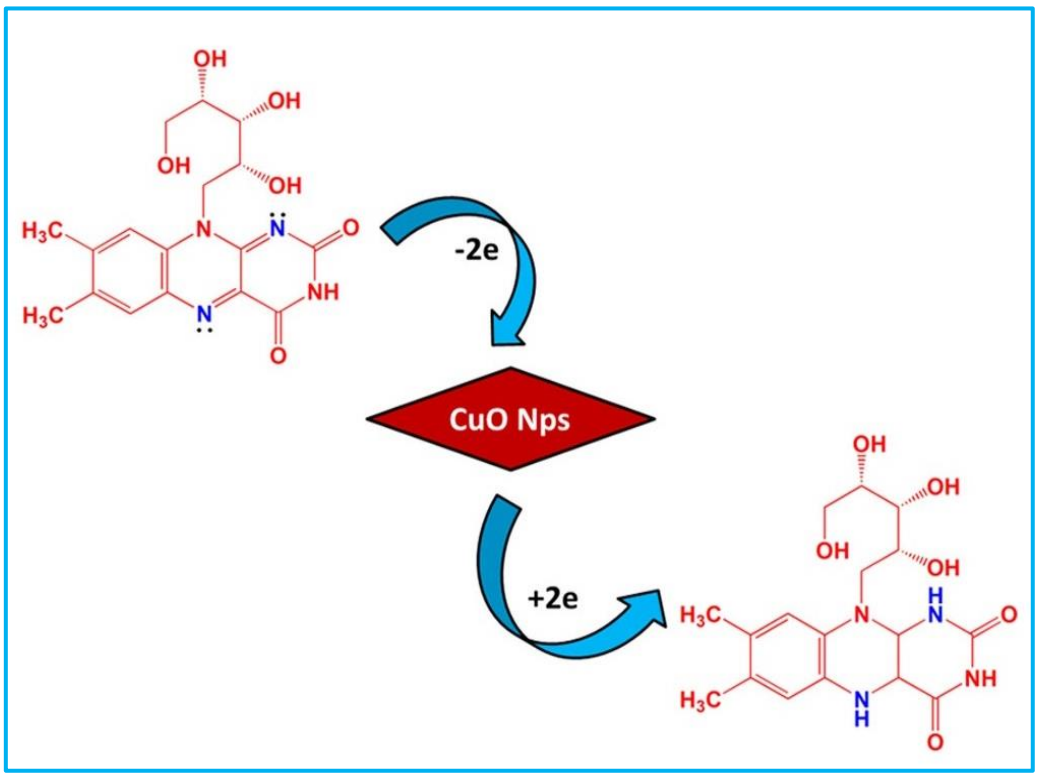

Figure 12: Potential redox mechanism depicting the interaction of Riboflavin [vitamin B2 (VB2)] with the CuONPs modified electrode. Adapted from (Sukumar et al., 2020)

4.5. Approaches for the Synthesis of Metal NPs

In the field of nanoparticle (NP) synthesis, different approaches are employed, primarily encompassing physical, chemical, and biological methods. The physical approach, often referred to as the top-down method, involves the breaking down of larger structures into nanoparticles. Conversely, the chemical and biological approaches, collectively termed the bottom-up method, involve the assembly of nanoparticles from molecular or atomic components. Notably, the biological approach is also recognized as a green system of NPs, indicating its environmentally friendly nature. It is important to note that these approaches are further categorized based on the specific methods and techniques utilized in NP synthesis. For a comprehensive understanding, **(Fig.13)** depicts the diverse methodologies reported for NP synthesis within each approach. These approaches can be further divided into various subclasses based on the operation, reaction conditions, and adopted protocols.

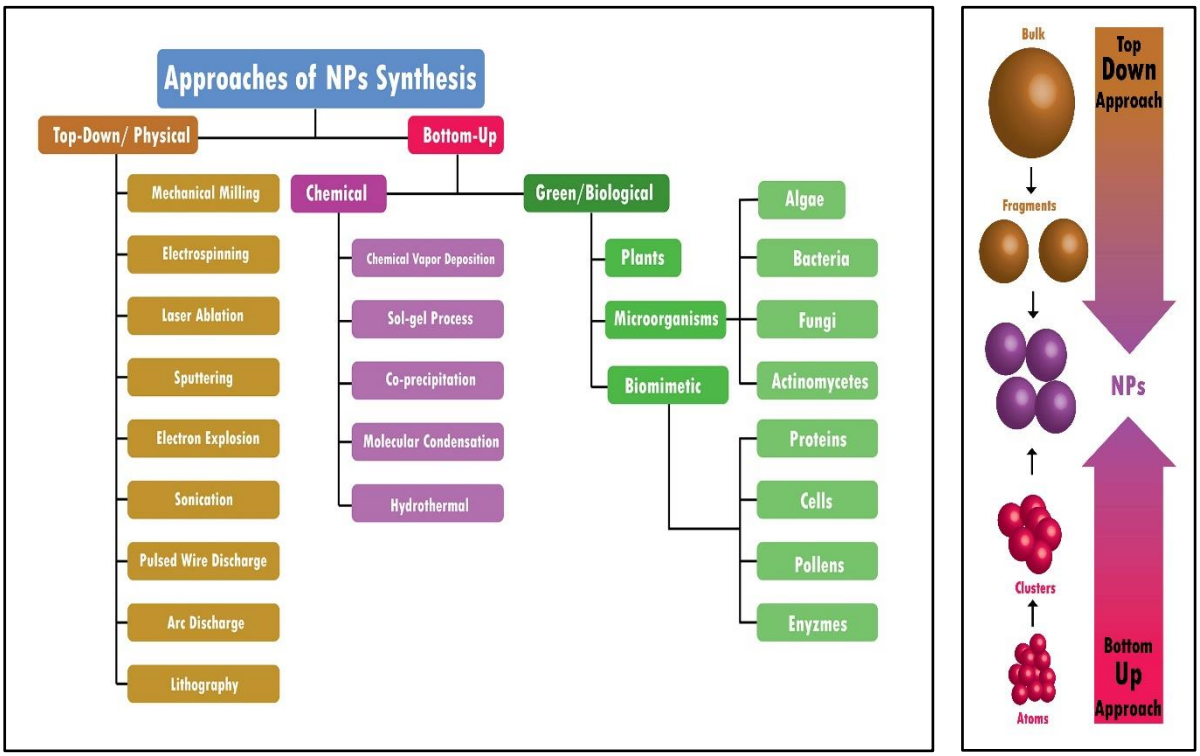

Figure 13: Approaches of NPs synthesis: Top-down and Bottom-up approaches and the difference between top-down and bottom-up approaches. (Adapted from Altammar, 2023).

4.5.1. Top-Down/Physical Approach

Bulk materials are mechanically broken down into smaller components using top-down methods to create nano-structured materials, as illustrated in Figure 13. These methods, also

known as physical approaches according to (Baig et al.,2021), involve the use of specific techniques to achieve a top-down approach, such as:

4.5.1.1. Mechanical Milling

The process of mechanical milling involves the use of balls inside containers and is typically conducted in various types of mills, including planetary and shaker mills. This method is characterized by high-energy impact (Gorrasi and Sorrentino in 2015). Mechanical milling offers a practical approach to transforming bulk materials into nanoscale materials. It can be applied to create aluminum alloys that are strengthened with oxide and carbide, as well as wear-resistant spray coatings, nanoalloys based on aluminum, nickel, magnesium, and copper, and a wide variety of other nanocomposite materials. One particularly noteworthy group of nanoparticles is ball-milled carbon nanomaterials, which have demonstrated potential for meeting the requirements of energy storage, energy conversion, and environmental remediation (Yadav et al., 2012; Lyu et al., 2017).

4.5.1.2. Electrospinning

Electrospinning is commonly employed to fabricate nanofibers using various materials, predominantly polymers (Ostermann et al., 2011). This process entails the drawing of charged threads from polymer melts or solutions, resulting in the production of fibers with diameters measured in the range of a few hundred nanometers (Chronakis, 2010). Coaxial electrospinning constitutes a notable progression in the realm of electrospinning. It employs a spinneret composed of two coaxial capillaries. Within these capillaries, core-shell nanoarchitectures can be generated by utilizing two viscous liquids, whereby the shell consists of a viscous liquid and the core encompasses a non-viscous liquid (Du et al., 2012). This technique has been instrumental in the development of core-shell and hollow polymer, inorganic, organic, and hybrid materials (Kumar et al., 2013).

4.5.1.3. Laser Ablation

A microfeature can be generated through the utilization of a laser beam to vaporize a singular substance (Tran and Wen, 2014). The process of laser ablation synthesis facilitates the production of nanoparticles by subjecting the target material to an intense laser beam. The substantial intensity of the laser irradiation employed in the laser ablation procedure causes the evaporation of the source material or precursor, resulting in the formation of nanoparticles (Amendola and Meneghetti, 2009). Laser ablation represents an environmentally sustainable

approach to the creation of noble metal nanoparticles (Baig et al., 2021). This method is conducive to the fabrication of an extensive range of nanomaterials, encompassing metal nanoparticles, carbon nanomaterials, oxide composites, and ceramics (Su and Chang, 2018; Baig et al., 2021).

4.5.1.4. Sputtering

Microparticles of a solid material are ejected from its surface during the phenomenon known as sputtering, which occurs when the solid substance is bombarded by intense plasma or gas particles (Behrisch, 1981). Energetic gaseous ions, depending on their energy, physically expel tiny atom clusters from the target surface during the sputtering deposition process (Muñoz-García et al., 2009). The sputtering method is of particular interest due to its cost-effectiveness compared to electron-beam lithography, and the resulting nanomaterials maintain a composition similar to the target material with fewer contaminants (Baig et al., 2021).

4.5.1.5. Electron Explosion

In this method, a slender metal wire is subjected to a high-current pulse, inducing an explosion, evaporation, and ionization. Consequently, the metal transforms into vapor and ions, undergoing expansion and subsequent cooling through interaction with the adjacent gas or liquid medium. Ultimately, the condensed vapor gives rise to the formation of nanoparticles (Joh et al., 2013). The nomenclature "electron explosion method" denotes the generation of plasma from the electrical explosion of a metallic wire, facilitating nanoparticle creation from a Pt solution without using of a reducing agent (Joh et al., 2013).

4.5.1.6. Sonication

The key step in the production of nanofluids is sonication. Following magnetic stirring in a magnetic stirrer, the mixture undergoes sonication using an ultrasonication bath, ultrasonic vibrator, and mechanical homogenizer. Sonicators have emerged as the standard for probe sonication, offering superior power and effectiveness compared to ultrasonic cleaner baths for nanoparticle applications. Probe sonication is highly effective in processing various nanomaterials including carbon nanotubes, graphene, inks, and metal oxides (Zheng et al., 2010).

4.5.1.7. Pulsed Wire Discharge Method

The preferred technique for producing metal nanoparticles involves using a pulsating current to vaporize a metal wire. The resulting vapor is then cooled by an ambient gas, leading to the formation of nanoparticles. This approach is known for its ability to rapidly generate substantial amounts of energy (Patil et al., 2021).

4.5.1.8. Arc Discharge Method

In the process of Arc Discharge, two graphite rods are positioned in a chamber with a constant helium pressure. It is imperative to fill the chamber with helium since the presence of oxygen or moisture impedes the synthesis of fullerenes. Through the arc discharge between the ends of the graphite rods, carbon vaporization occurs. The conditions surrounding the occurrence of arc discharge play a crucial role in the generation of novel nanoparticle types. This method demonstrates the capability to synthesize various nanostructured materials (Berkman et al., 2014). It is acknowledged for its efficacy in producing carbon-based materials including fullerenes, carbon nano horns (CNHs), carbon nanotubes (Shi et al., 2000), few-layer graphene, and amorphous spherical carbon nanoparticles (Kumar R et al., 2013).

4.5.1.9. Lithography

Lithography conventionally employs a focused beam of light or electrons to fabricate nanoparticles, representing a valuable technique (Pimpin and Srituravanich, 2012). Masked and maskless lithography constitute the two principal categories. In maskless lithography, freeform nanoscale pattern printing is achieved without the need for a mask. Furthermore, this method is cost-effective and straightforward to implement (Brady et al., 2019).

4.5.2. Bottom-Up Approach

In bottom-up approaches, tiny atoms and molecules are combined to create nano-structured particles, as illustrated in **(Fig. 13)** (Baig et al., 2021). These methods encompass both chemical and biological approaches.

4.5.2.1. Chemical Vapor Deposition (CVD)

During Chemical Vapor Deposition (CVD), a thin coating is formed on the substrate surface through a chemical process involving vapor-phase precursors (Dikusar et al., 2009). The suitability of precursors for CVD depends on factors such as volatility, chemical purity, evaporation stability, cost-effectiveness, non-hazardous nature, and shelf life. Moreover, the

breakdown of precursors should not result in any contaminants. Variants of CVD include vapor phase epitaxy, metal-organic CVD, atomic layer epitaxy, and plasma-enhanced CVD. The advantages of this method include the production of highly pure, stiff, homogeneous, and robust nanoparticles (Ago, 2015), making it an excellent approach for generating high-quality nanomaterials (Machac et al., 2020). Additionally, CVD is renowned for its capability to produce two-dimensional nanoparticles (Baig et al., 2021).

4.5.2.2. Sol-Gel Process

The sol-gel method, a widely used wet-chemical approach, is utilized for creating nanomaterials (Das and Srivastava, 2016; Baig et al., 2021). In this method, metal alkoxides or metal precursors in solution are condensed, hydrolyzed, and thermally decomposed, resulting in a stable solution or sol. The gel gains greater viscosity due to hydrolysis or condensation. By adjusting the precursor concentration, temperature, and pH levels, the particle size can be controlled. It may take a few days for the solvent to be removed, for Ostwald ripening to occur, and for the phase to change during the mature stage, which is necessary for enabling the growth of solid mass. Unstable chemical ingredients are separated to create nanoparticles, resulting in an environmentally friendly material with numerous benefits due to the sol-gel technique (Patil et al., 2021). The sol-gel technique offers advantages such as uniform quality of the generated material, low processing temperature, and ease in producing composites and complex nanostructures (Parashar et al., 2020).

4.5.2.3. Co-Precipitation

The described technique is based on solvent displacement and represents a wet chemical procedure. Solvents such as ethanol, acetone, hexane, and non-solvent polymers are commonly employed in this context. It is noteworthy that polymer phases may be of synthetic or natural origin. When the polymer solution is amalgamated, rapid diffusion of the polymer-solvent into the non-solvent phase of the polymer occurs, resulting in the creation of nanoparticles due to interfacial stress at the interface of both phases (Das and Srivastava, 2016). One of the noteworthy advantages of this method is its innate capacity to generate substantial quantities of water-soluble nanoparticles through a straightforward process. Moreover, this process is widely utilized for the development of various commercial iron oxide NP-based MRI contrast agents, such as Feridex, Resovist, and Combidex (Baig et al., 2021; Patil et al., 2021).

4.5.2.4 Inert Gas Condensation/Molecular Condensation

Production of metal nanoparticles on a large scale is achieved through the utilization of the inert gas condensation method. This prevalent approach involves the vaporization of a metallic source within an inert gas environment, such as argon, helium, or neon, at a controlled temperature, resulting in manageable metal evaporation rates. For instance, producing copper metal nanoparticles entails vaporizing copper within a vessel containing argon, helium, or neon. Subsequently, the vaporized metal atoms are rapidly cooled using liquid nitrogen, leading to the generation of nanoparticles within the range of 2–100 nm (Pérez-Tijerina et al., 2008; Patil et al., 2021).

4.5.2.5. Hydrothermal

In the production of nanoparticles using hydrothermal synthesis, a wide temperature range is employed, from ambient temperature to extremely high temperatures. This method offers several advantages compared to physical and biological approaches. However, it's worth noting that at higher temperature ranges, the nanomaterials produced by hydrothermal synthesis could become unstable (Banerjee et al., 2008; Patil et al., 2021).

4.5.3. Green/Biological Synthesis

The process of producing a variety of metal nanoparticles using organic agents such as plant materials, microbes, and biowastes such as vegetable waste, fruit peels, eggshells, and agricultural waste is known as "green" or "biological" nanoparticle synthesis (Kumari et al., 2021). It is imperative to develop reliable and sustainable green synthesis technologies to mitigate the formation of undesired or hazardous byproducts **(Fig.14)**. Green synthesis of nanoparticles presents several advantages, including simplicity, cost-effectiveness, high stability of the generated nanoparticles, rapid production, generation of non-toxic byproducts, and the potential for seamless scalability for large-scale synthesis (Malhotra and Alghuthaymi, 2022).

4.5.3.1. Biological Synthesis using Microorganisms

Microbes employ metal capture, enzymatic reduction, and capping mechanisms to create nanoparticles. Initially, metal ions are trapped on the surface or inside microbial cells before being transformed into nanoparticles by enzymes (Ghosh et al., 2021). The utilization of microorganisms, particularly marine microbes, for the synthesis of metallic nanoparticles, is not only environmentally friendly but also a rapid and cost-effective process (Patil and Kim, 2018). Various microorganisms are utilized in the synthesis of metal nanoparticles, including:

Biosynthesis of NPs by Bacteria: Bacterial cells are considered a potential biofactory for the production of gold, silver, and cadmium sulfide nanoparticles. It is well-documented that bacteria can generate inorganic compounds internally or externally within their cellular environment (Hulkoti and Taranath, 2014). Desulforibrio caledoiensis (Qi et al., 2013), Enterococcus sp. (Rajeshkumar et al., 2014), Escherichia coli VM1 (Maharani et al., 2016), and Ochrobactrum anhtropi (Thomas et al., 2014) have been previously documented for their potential photocatalytic properties (Qi et al., 2013), antimicrobial activity (Rajeshkumar et al., 2014), and anticancer activity (Maharani et al., 2016) based on metal nanoparticles.

Extracellular Synthesis of NPs by Bacteria:

The extracellular reductase enzymes of microorganisms play a crucial role in the reduction of silver ions to the nanoscale range. Protein analysis of microorganisms has elucidated that the NADH-dependent reductase enzyme is responsible for the bioreduction of silver ions to AgNPs. During this bioreduction process, the enzyme utilizes electrons from NADH, leading to its conversion to NAD+. It is important to note that the enzyme undergoes oxidation concurrently with the reduction of silver ions to nanosilver. Additionally, it has been observed that nitrate-dependent reductase can sporadically initiate bioreduction. This reduction process happens rapidly within a few minutes (Mathew et al., 2010). Notably, in an experimental setting with R. capsulata bacteria at pH 7, gold nanoparticles ranging from 10-20 nm in size were synthesized. Upon altering the pH to four, the production of numerous nanoplates and spherical gold nanoparticles was observed (Sriram et al., 2012). Furthermore, the shape of the gold nanoparticles can be modulated by adjusting the pH levels. The release of cofactor NADH and NADH-dependent enzymes by the bacteria R. capsulata may lead to the bioreduction of Au (3+) to Au (0) and the consequent generation of gold nanoparticles. Employing NADH-dependent reductase as an electron carrier facilitates the initiation of the reduction of gold ions (Sriram et al., 2012).

Intracellular Synthesis of NPs by Bacteria:

The intracellular synthesis of nanoparticles (NPs) involves three key processes: trapping, bioreduction, and capping. This process relies significantly on the cell walls of microorganisms and the presence of charged ions. It involves specific ion transportation in the presence of enzymes, coenzymes, and other molecules within microbial cells. Microbes possess a variety of polysaccharides and proteins in their cell walls, which act as active sites for binding metal ions (Slavin et al., 2017). It is important to note that not all bacteria have the ability to produce metal and metal oxide nanoparticles. Heavy metal ions pose a significant threat to

microorganisms; in response to this threat, microorganisms react by capturing or trapping the ions on the cell wall through electrostatic interactions. This occurs due to the attraction of metal ions to the cell wall's carboxylate groups, along with cysteine, polypeptides, and specific enzymes with a negative charge (Zhang et al., 2011). Additionally, electron transfers from

NADH via NADH-dependent reductases, located within the plasma membrane, result in the reduction of trapped ions into elemental atoms. These atoms eventually develop into NPs and accumulate in the cytoplasm or the periplasmic space. Furthermore, the stability of NPs is maintained by proteins, peptides, and amino acids present inside cells, including cysteine, tyrosine, and tryptophan (Mohd Yusof et al., 2019).

Biosynthesis of NPs by Fungi:

The use of fungi for the biosynthesis of nanoparticles offers the advantage of generating monodisperse nanoparticles with distinct dimensions, diverse chemical compositions, and various sizes. This approach is facilitated by the presence of numerous enzymes in fungal cells and the ease of handling. Fungi, therefore, represent promising candidates for the production of both metal and metal sulfide nanoparticles (Mohanpuria et al., 2008). Notably, the synthesis of nanoparticles occurs on the mycelia's surface. Upon analysis and observation of the solution, it was determined that electrostatic interactions between gold ions and negatively charged carboxylate groups initially capture Ag+ ions on the surface of fungal cells. This process, facilitated by enzymes in the mycelia's cell wall, subsequently leads to the reduction of silver ions and the formation of silver nuclei. The growth of these nuclei is further enhanced as more Ag ions are reduced and accumulate on them.

The TEM data reveals the presence of silver nanoparticles both on and inside the cytoplasmic membrane. The findings suggest that enzymes within the cytoplasm and on the cytoplasmic membrane decrease the permeation of Ag ions through the cell wall. It is also plausible that some silver nanoparticles diffuse through the cell wall and become trapped in the cytoplasm (Mukherjee et al., 2001; Hulkoti and Taranath, 2014).

The shape of the synthesized gold nanoparticles was found to be independent of the age of the culture, although a decrease in the number of particles was observed when older cells were used. Various pH levels were noted to yield different shapes of gold nanoparticles, underscoring the pivotal role of pH in determining their shape. Moreover, the incubation temperature was found to significantly impact the accumulation of gold nanoparticles, with a faster particle growth rate at higher temperatures (Mukherjee et al., 2001; Ahmad et al., 2003). Additionally, it was observed that Verticillium luteoalbum can synthesize gold nanoparticles

ranging from 20 to 40 nm in size (Erasmus et al., 2014). Aspergillus terreus and Penicillium brevicompactum KCCM 60390-based metal NPs have been reported for their antimicrobial (Li G. et al., 2011) and cytotoxic activities (Mishra et al., 2011), respectively.

Biosynthesis of NPs using Actinomycetes:

Actinomycetes are classified as prokaryotes due to their significant similarities with fungi and are sometimes known as ray fungi (Mathew et al., 2010). The process of producing nanoparticles (NPs) from actinomycetes is similar to that of fungi (Sowani et al., 2016). For instance, a newly discovered extremophilic actinomycete species, Thermomonospora sp., has been found to produce extracellular, monodispersed, spherical gold nanoparticles with an average size of 8 nm (Narayanan and Sakthivel, 2010). Additionally, metal NPs synthesized by Rhodococcus sp. (Ahmad et al., 2003) and Streptomyces sp. Al-Dhabi-87 (Al-Dhabi et al., 2018) are known for their antimicrobial activities.

Biosynthesis of NPs using Algae:

Algae possess a high concentration of polymeric molecules, enabling them to hyper-accumulate heavy metal ions and convert them into malleable forms through the reduction process. Algal extracts are known to contain pigments, carbohydrates, proteins, minerals, polyunsaturated fatty acids, and other bioactive compounds, such as antioxidants, utilized as stabilizing, capping, and reducing agents (Khanna et al., 2019). Furthermore, nanoparticles demonstrate a heightened photosynthesis rate in comparison to their biosynthetic counterparts. Algae, in both live and deceased states, are employed as model organisms in the environmentally sound production of bionanomaterials, including metallic nanoparticles (Hasan, 2015). Silver (Ag) and gold (Au) have emerged as the most extensively studied noble metals for nanoparticle synthesis by algae, whether through intracellular or extracellular pathways (Dahoumane et al., 2017).

Intracellular synthesis of NPs using Algae:

To facilitate the production of intracellular nanoparticles, an initial step involves the gathering of algal biomass, which must be meticulously cleansed with distilled water. Subsequently, the living algae biomass is subjected to treatment using metallic solutions, such as AgNO3. Following this, the amalgamation undergoes an incubation process at a specified pH and temperature for a predetermined duration. Finally, the resulting mixture is subjected to centrifugation and sonication to yield the extracted stable nanoparticles (Uzair et al., 2020).

Extracellular synthesis of NPs using Algae:

In the process of synthesizing nanoparticles (NPs) from algal biomass, the first step involves collecting the biomass and thoroughly cleaning it with distilled water (Uzair et al., 2020). Subsequently, the following three techniques are commonly employed:(i) Drying the algal biomass for a specific period, followed by treating the dried powder with distilled water and filtering it. (ii) Subjecting the algal biomass to sonication with distilled water to obtain a cell-free extract. (iii) Rinsing the algal biomass with distilled water, allowing it to incubate for a period of 8 to 16 hours, and then filtering the resultant product.

4.5.3.2. Biological Synthesis using Plant Extracts

The active ingredient extracted from plant tissue for an intended purpose is commonly known as a plant extract (Jadoun et al., 2021). Plant extracts are combined with a metal salt solution at ambient temperature to synthesize nanoparticles, with the process culminating within minutes. This technique has been successfully employed in the production of silver, gold, and various other metallic nanoparticles (Li X. et al., 2011). The biosynthesis of nanoparticles is achieved through the utilization of diverse plant species. It is well-established that the type and concentration of the plant extract, the metal salt concentration, pH, temperature, and the duration of contact time collectively influence the kinetics, yield, and other characteristics of the resulting nanoparticles (Mittal and Chisti, 2013). Notably, a leaf extract derived from Polyalthia longifolia was utilized in the synthesis of silver nanoparticles, yielding particles with an average size of approximately 58 nm (Kumar and Yadav, 2009; Kumar et al., 2016).

4.5.3.3. Biological Synthesis using Biomimetic

The term "biomimetic synthesis" refers to the replication of biological synthesis processes carried out by living organisms through chemical means (Dahoumane et al., 2017). In this approach, proteins, enzymes, cells, viruses, pollen, and waste biomass are utilized to create nanoparticles (NPs). Biomimetic synthesis can be categorized into two types:

1. Functional Biomimetic Synthesis: This type involves using a variety of materials and methods to replicate specific characteristics of natural materials, structures, and systems (Zan and Wu, 2016).

2. Process Biomimetic Synthesis: This technique aims to replicate the synthesis pathways, processes, or procedures of natural chemicals and materials/structures to create different desirable nanomaterials and structures. For example, in vitro, unique nano-superstructures such as satellite structures, dendrimer-like structures, pyramids, cubes, 2D nanoparticle arrays, 3D

AuNP tubes, etc., have been assembled by simulating the protein manufacturing process (Zan and Wu, 2016).

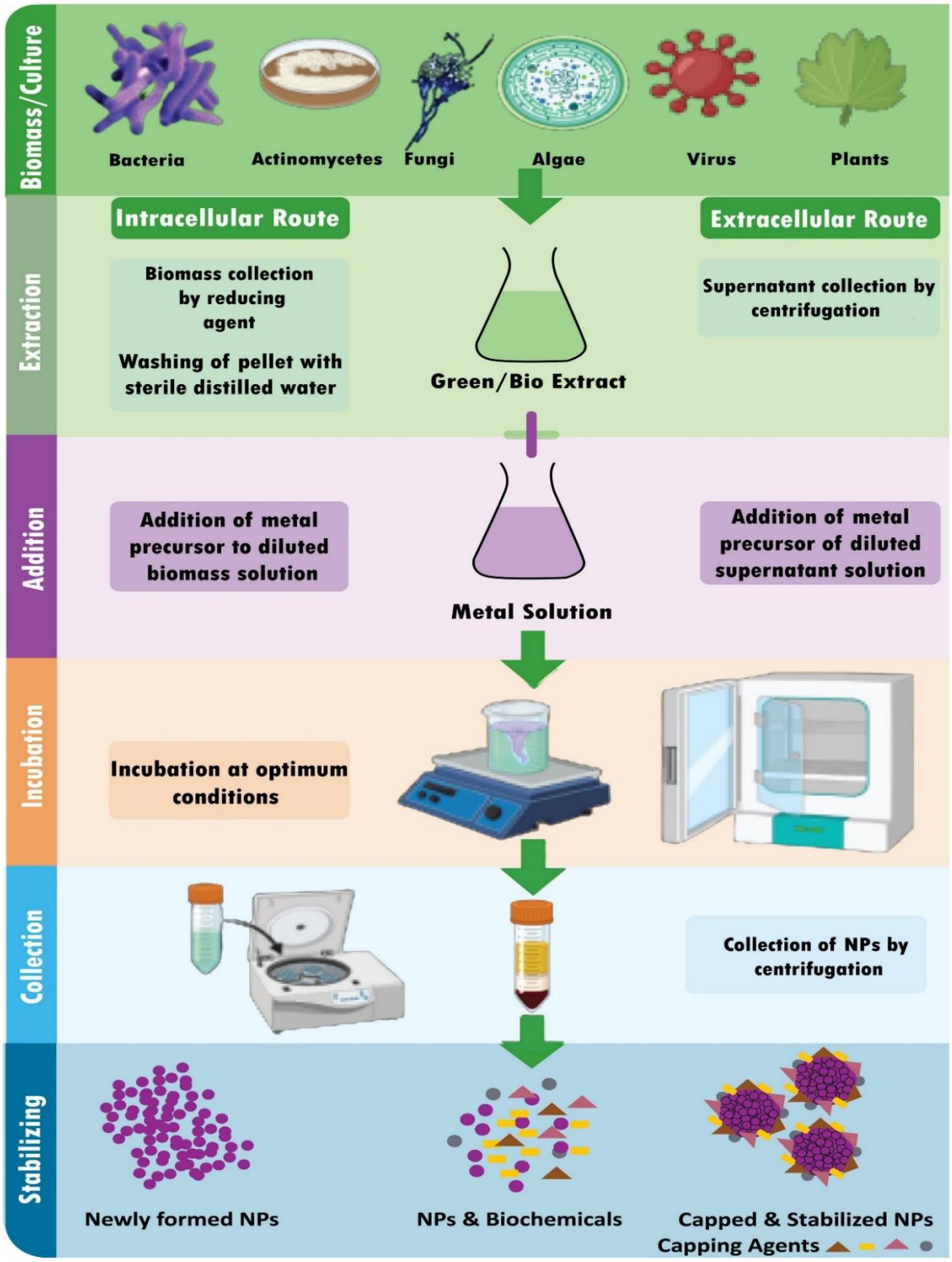

Figure 14: Schematic representation of the biosynthetic pathway for the production of NPs (Adapted from Altammar, 2023).

Table 2: Various Analytical Techniques and Their Applications in the Study of Nanoparticles.

Analytical technique	Purpose	Reference
Centrifugation	To separate the synthesized NPs from the reaction solution.	(Patil and Kim, 2018)
Transmission electron microscopy (TEM)	Get High-Resolution Pictures than a light microscope. Used to study the structure and presence of NPs.	(Kohl and Reimer, 2008; Patil and Kim, 2018)
Scanning electron microscope (SEM)	Get a three-dimensional appearance 3D based on the interaction of the electron beam with the specimen surface.	(Delvallée et al., 2015)
Scanning tunneling microscopy (STM)	To study the local electronic structure of metal NPs as well as the structure and presence of NPs.	(Wiesendanger and Güntherodt, 2013)
Ultraviolet-visible spectroscopy (UV-Vis)	Used for the optical study of the materials and to determine the synthesis of NPs.	(Patil and Kim, 2018; Rocha et al., 2018)
Fourier transform infrared spectroscopy (FTIR)	To study the surface chemistry of metal NPs. Used for the identification of organic, inorganic, and polymeric materials utilizing infrared light for scanning the samples. Used to identify functional groups in the material.	(Titus et al., 2019; Praseptiangga et al., 2020)
X-ray diffraction (XRD)	Used for characterization of nanopowders of any size. Provide useful information and also help correlate microscopic observations with the bulk sample.	(Kahle et al., 2002; Holder and Schaak, 2019)
X-ray photoelectron spectroscopy (XPS)	Used to identify the elemental composition and chemical states of the elements present at the surface of a material.	(Haasch, 2014; Greczynski and Hultman, 2020)

Dynamic light scattering (DLS)	Used to measure the size of particles and analyze complex colloidal systems.	(Hoo et al., 2008; Patil and Kim, 2018)
Zeta potential instruments/zeta potential	Measure of the electrical charge at the surface of a particle suspended in a liquid. To study the stability of metal NPs in solution.	(Salopek et al., 1992; Bhattacharjee, 2016)
Small-angle X-ray scattering (SAXS)	Used to measure the intensities of X-rays scattered by a sample as a function of the scattering angle.	(Li et al., 2016)
Energy dispersive X-ray spectrometry (EDS), Wavelength dispersive X-ray spectrometry (WDS), X-ray fluorescence spectroscopy (XRF)	Used to identify the elemental composition of a sample.	(Newbury and Ritchie, 2013; Giurlani et al., 2018)
Field emission scanning electron microscope (FESEM)	Used to capture the microstructure image of the materials.	(Lewczuk and Szyry´nska, 2021)
Atomic force microscopy (AFM) (Cadene et al., 2005; Delvallée et al., 2015)	Analyze complex colloidal systems and obtain information by touching the sample's surface with a probe used to obtain high-resolution images.	To study the size, shape, and surface roughness of metal NPs.
Particle tracking velocimetry (PTV)	Track individual particles in fluidic systems.	(Kreizer et al., 2010)
Dynamic light scattering (DLS)	Measure the hydrodynamic diameter of nanoparticles in solution.	(De La Calle et al., 2018; Falke and Betzel, 2019)

Nanoparticle tracking analysis (NTA)	Used to obtain the nanoparticle size distribution of samples in liquid suspension. Analyses many particles individually and simultaneously (particle-by-particle).	(Dragovic et al., 2011; Patois et al., 2012)
Raman spectroscopy	Study the vibrational modes of bonds in metal NPs.	(Lyon et al., 1998)
Nuclear magnetic resonance (NMR) spectroscopy	To study the chemical structure and bonding of metal NPs.	(Jayaraman et al., 2014)
Auger electron spectroscopy (AES)	Study the chemical states and bonding of metal NPs.	(Haasch, 2014)
Thermogravimetric analysis (TGA)	Study the thermal stability and decomposition of metal NPs.	(Saldarriaga et al., 2015)
Liquid chromatography	Used to separate and purify compounds that are dissolved in a liquid.	(Chen and Zhu, 2016)

4.6. Physicochemical Properties of NPs

Nanoparticles (NPs) possess distinctive physical and chemical properties not present in larger forms of the same materials, making them suitable for a wide array of applications. The upcoming sections will provide an overview of the key physicochemical properties that undergo significant changes at the nanoscale.

4.6.1. Electronic and Optical Properties

The properties of nanoparticles (NPs) are intricately linked, with noble metal NPs demonstrating size-dependent optical properties and a unique UV-visible extinction band absent in bulk metals. This band results from the excitation of conduction electrons, known as localized surface plasmon resonance (LSPR) when the photon frequency matches. LSPR excitation leads to selective absorption of specific wavelengths with extremely high molar excitation coefficients and resonance Rayleigh light scattering with efficiency equal to that of ten fluorophores. Additionally, LSPR creates enhanced local electromagnetic fields near the NP surface, resulting in enhanced spectroscopies. The peak wavelength of the LSPR spectrum depends on the size, shape, and interparticle spacing of the NPs, and their dielectric properties, as well as those of their local environment including the substrate, solvents, and adsorbates

(Eustis and El-Sayed, 2006). The discoloration observed in stained glass door and window panels is attributed to the presence of gold colloidal nanoparticles, manifesting as rusty hues, and silver nanoparticles, which typically exhibit a yellow appearance. Notably, the surface electrons of these nanoparticles (specifically, the d electrons in silver and gold) are capable of facile movement within the nanomaterial. The average distance traveled by these electrons (mean free path) in silver and gold is approximately 50 nm, surpassing the dimensions of the nanoparticles in question. Consequently, negligible scattering is anticipated from the bulk material upon illumination; instead, the nanoparticles assume a state of standing resonance, thus engendering localized surface plasmon resonance (LSPR) within these nanoparticles as depicted in **(Fig. 15)** (Khlebtsov and Dykman, 2010a, 2010b).

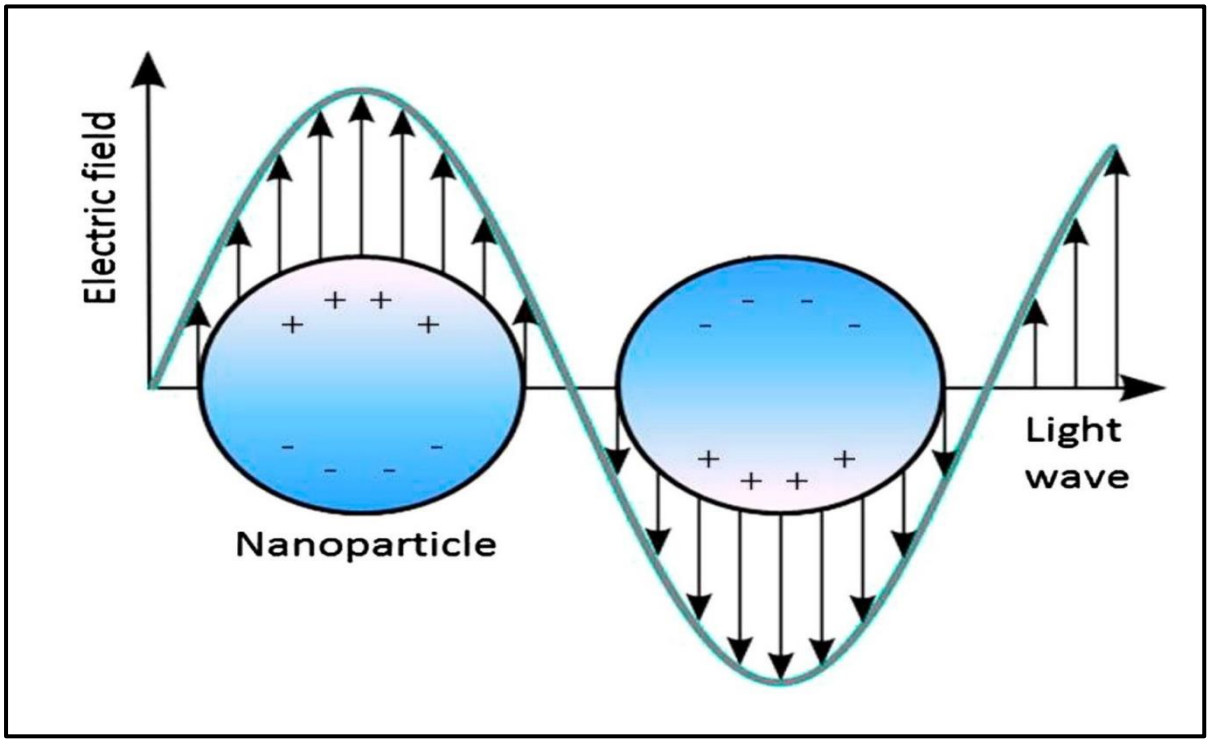

Figure 15: Graphical illustration exemplifying the localized surface plasmon (LSPR) on nanoparticle outer surface (Adapted from Khlebtsov and Dykman, 2010a, 2010b).

4.6.2. Magnetic Properties

Magnetic nanoparticles (NPs) have garnered significant attention from researchers spanning diverse disciplines, encompassing heterogenous and homogenous catalysis, biomedicine, magnetic fluids, data storage, magnetic resonance imaging (MRI), and environmental remediation, particularly in water decontamination. Literature has demonstrated that NPs exhibit optimal performance when their size falls below a critical threshold, typically 10–20 nm (Reiss and Hütten, 2005). At this scale, the magnetic properties of NPs become predominant, imbuing them with immense value for multifaceted applications (Faivre and

Bennet, 2016; Priyadarshana et al., 2015; Reiss and Hütten, 2005; Zhu et al., 1994). The non-uniform distribution of electrons in NPs underlies their magnetic attributes, which are contingent upon the synthetic protocol. Various synthetic methods, such as solvothermal (Qi et al., 2016), coprecipitation, micro-emulsion, thermal decomposition, and flame spray synthesis, are employed for the preparation of magnetic NPs (Wu et al., 2008).

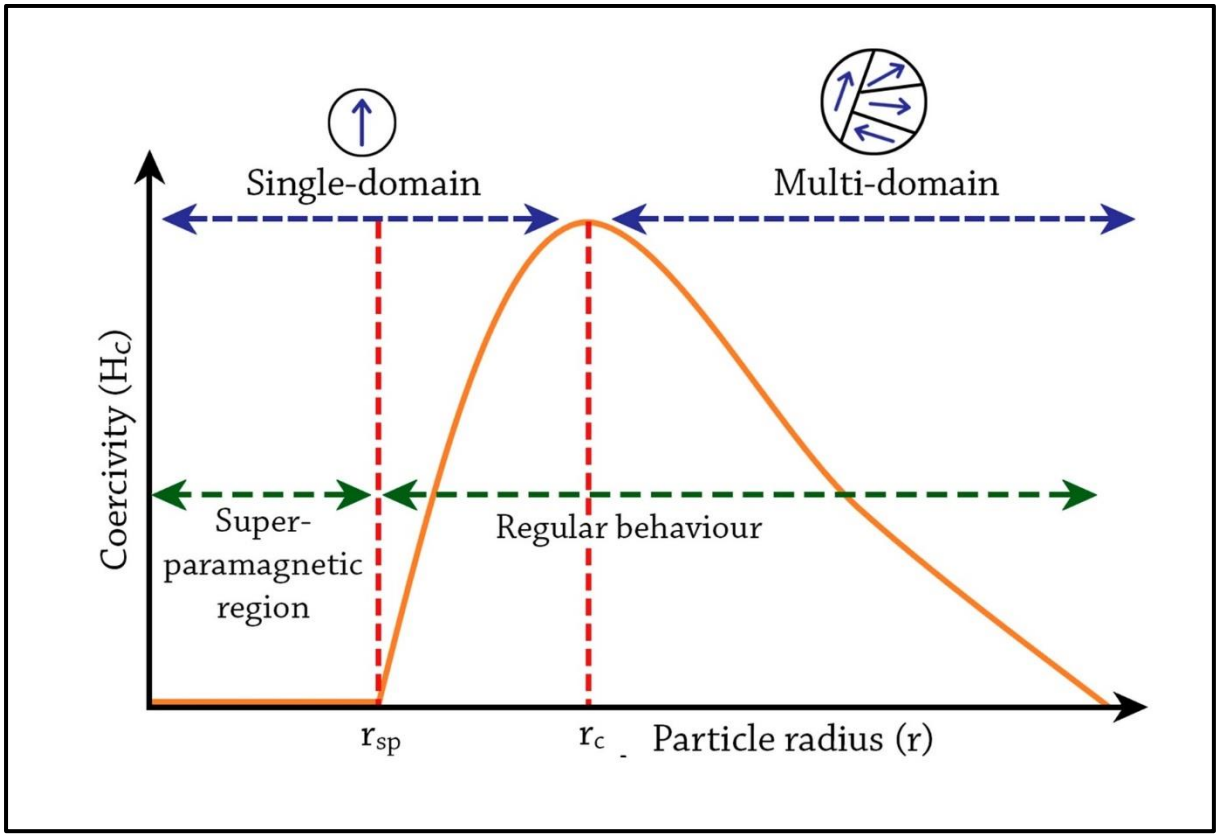

Figure 16: The change in magnetic coercivity of NPs as a function of particle radius. (Adapted from Kalubowilage et al., 2019). Where r_c critical radius and r_{sp} threshold radius for superparamagnetism.

4.6.3. Mechanical Properties

The mechanical properties of nanoparticles (NPs) are diverse and present opportunities for novel applications in various important fields such as tribology, surface engineering, nanofabrication, and nanomanufacturing. Researchers can explore different mechanical parameters including elastic modulus, hardness, stress and strain, adhesion, and friction to gain an in-depth understanding of the mechanical behavior of NPs. Surface coating, coagulation, and lubrication also play significant roles in influencing the mechanical properties of NPs (Guo et al., 2014). When compared to microparticles and bulk materials, NPs display distinct mechanical properties. In lubricated or greased contacts, the disparity in stiffness between NPs and the external surface dictates whether the NPs indent into the plane surface or deform under

significant pressure. This knowledge is crucial for understanding the performance of NPs in contact situations. Precise control over the mechanical characteristics of NPs and their interactions with different surfaces is essential for enhancing surface quality and material removal processes. Achieving significant advancements in these fields necessitates a comprehensive understanding of the fundamental mechanical properties of NPs, such as elastic modulus, hardness, movement law, friction, interfacial adhesion, and their size-dependent characteristics (Guo et al., 2014).

4.6.4. Thermal properties

It is a widely acknowledged fact that metal nanoparticles (NPs) possess thermal conductivities higher than those of fluids in the solid state. For instance, at room temperature, the thermal conductivity of copper is approximately 700 times greater than that of water and about 3000 times greater than that of engine oil. Notably, even oxides such as alumina (Al_2O_3) demonstrate higher thermal conductivity than water. Consequently, it is anticipated that fluids containing suspended solid particles will manifest significantly enhanced thermal conductivities relative to those of traditional heat transfer fluids. Nanofluids are formulated through the dispersion of nanoscale solid particles into liquids such as water, ethylene glycol, or oils. Notably, nanofluids are expected to display superior properties relative to those of conventional heat transfer fluids and fluids containing microscopic-sized particles. Given that heat transfer occurs at the particle surface, the utilization of particles with a large total surface area is desirable. Moreover, the substantial total surface area contributes to enhanced suspension stability (Lee et al., 1999). Recent studies have substantiated that nanofluids comprising CuO or Al_2O_3 NPs in water or ethylene glycol exhibit enhanced thermal conductivity (Cao, 2002).

4.6.5. Catalytic Properties

Nanoparticle (NP) catalysis, which involves using nanoparticles as catalysts, represents a rapidly advancing area within chemical catalysis. NPs offer significantly enhanced or entirely new catalytic properties, including reactivity and selectivity, compared to larger-scale catalysts. These enhanced properties are influenced by several factors such as the size, shape, composition, interparticle spacing, oxidation state, and the support of the NPs (Cuenya,2010). It's well-documented that the catalytic activity of NPs is inversely related to their size, meaning that smaller NPs exhibit higher catalytic activity. Moreover, studies have revealed that the use of NP alloys can improve catalytic activity by producing changes in electronic properties, reducing poisoning effects, and offering distinct selectivities. However, it's important to consider the potential impact of alloying on specific reactions; for instance, the combination of Pt with Fe, Ru, and Pd may lead to reduced reactivity in methanol decomposition (Croy et al.,

2008). This reduced reactivity is attributed to the potential occupation of the NP surface by additional metal atoms, as pure Fe, Ru, and Pd clusters demonstrate lower reactivity for methanol decomposition when compared to similarly-sized pure Pt clusters. Overall, altering the composition of NPs leads to changes in the electronic structure of metal surfaces, primarily through the formation of bimetallic bonds and modifications in metal-metal bond lengths.

4.7. Applications of nanoparticles (NPs)

4.7.1. Applications of NPs in the Environmental Industry

Nanoparticles (NPs) are extensively utilized in a wide range of applications owing to their distinctive and optimized physicochemical properties. These applications span across diverse fields and are constantly being explored for potential applications in research and development. Some specific examples of these versatile and promising applications are elaborated hereby. The **(Fig.17)** provides a visual representation of the properties and advantages associated with nanoparticles.

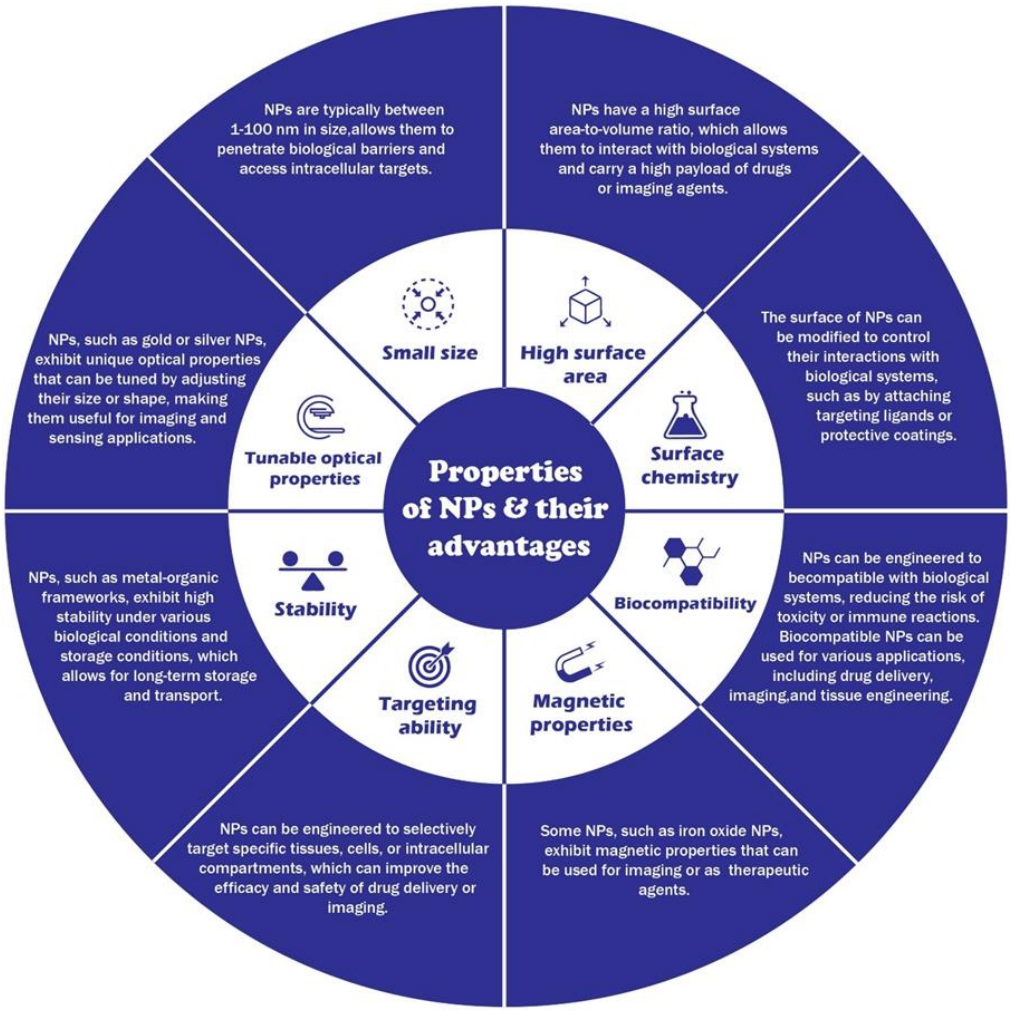

Figure 17: Properties of nanoparticles and their advantages.

4.7.1.1. Bioremediation

Nanoparticles (NPs) exhibit the capacity to eliminate environmental pollutants, including heavy metals from water and organic contaminants from soil (Zhuang and Gentry, 2011). Notably, silver nanoparticles (AgNPs) demonstrate efficacy in the degradation of specific pollutants, such as organic dyes and compounds present in wastewater. Various nanomaterials, namely nanoscale zeolites, metal oxides, and carbon nanotubes and fibers, have been under consideration for employment in remediation activities (Zhuang and Gentry, 2011).

Utilized in remediation processes, nanoscale particles can infiltrate areas inaccessible to larger particles. Furthermore, they can be coated to facilitate transportation and prevent interaction with surrounding soil matrices prior to engaging with contaminants. Notably, Nanoscale zerovalent iron (nZVI) stands as a prevalent nanomaterial employed for remediation, having seen application at numerous hazardous waste sites for the purification of groundwater contaminated by chlorinated solvents (Elliott et al., 2013). The removal of heavy metals such as mercury, lead, thallium, cadmium, and arsenic from natural water sources has garnered considerable attention due to their deleterious impact on both the environment and human health. The application of superparamagnetic iron oxide NPs has proven effective as a sorbent material for the aforementioned toxic substances. Nevertheless, the absence of analytical methodologies capable of quantifying trace concentrations of engineered NPs has precluded the assessment of their presence in the environment (Elliott et al., 2013).

4.7.1.2. Sensors in Environment

Nanotechnology and nanoparticles (NPs) are currently being used to enhance water quality and aid in environmental cleanup efforts (Pradeep, 2009). Their potential use as environmental sensors to monitor pollutants is also becoming increasingly feasible. NPs can act as sensors to identify the presence of certain compounds in the environment, such as heavy metals or pollutants. The small size and broad detection range of nano-sensors offer great flexibility in practical applications. Studies have shown that nanoscale sensors can be used to detect microbial pathogens and biological compounds, such as toxins, in aqueous environments (Yadav et al., 2010). NPs can be designed to selectively bind to specific types of pollutants, allowing for their detection even at low concentrations. For instance, gold nanoparticles (AuNPs) have been utilized as sensors for the detection of mercury in water (Theron et al., 2010).

4.7.1.3. Catalysts in Environment

Nanoparticles (NPs) serve as catalysts in diverse chemical reactions, playing a crucial role in processes such as the production of biofuels and the remediation of environmental contaminants. Furthermore, they exhibit the ability to catalyze the conversion of biomass into fuels, notably ethanol and biodiesel. Notably, platinum nanoparticles (PtNPs) have been the subject of extensive research due to their efficacy in facilitating the conversion of biomass into fuels (Lam and Luong, 2014). Additionally, PtNPs have displayed notable sensing properties, as demonstrated by their capacity to quantify Hg ions within the range of 50–500 nM in various samples, including MilliQ, tap, and groundwater. The limit of quantification for Hg ions has been measured at 16.9, 26, and 47.3 nM, respectively. Utilizing a biogenic PtNPs-based probe has proven effective in the detection and quantification of Hg ions (Kora and Rastogi, 2018). In conclusion, nanoparticles hold significant promise for environmental applications and are the subject of ongoing research in various fields.

4.7.2. Applications of NPs in Medicine Industry

Nanoparticles (NPs) exhibit distinctive physical and chemical properties owing to their diminutive size, rendering them appealing for a broad spectrum of applications, particularly within the medical sector. Noteworthy potential applications of NPs in the field of medicine encompass:

4.7.2.1. Drug Delivery

The remarkable optical properties, ease of synthesis, and chemical stability of AuNPs have sparked substantial interest in their technological applications. These nanoparticles have found widespread use in various biomedical fields, including cancer treatment (Sun et al., 2014), biological imaging (Abdulle and Chow, 2019), chemical sensing, and drug delivery (Sun et al., 2014) extensively discussed two methods of controlled drug release associated with NPs: sustained (i.e., diffusion-controlled and erosion-controlled) and stimuli-responsive (i.e., pH-sensitive, enzyme-sensitive, thermoresponsive, and photosensitive). Figure 18 illustrates how NPs serve as targeted delivery systems for medicines to treat cancer cells (Figure 19A) and deliver therapeutic genes to synthesize proteins of interest in targeted cells (Figure 19B). NPs facilitate the targeted delivery of drugs to specific body areas, allowing for more effective and precise treatment (Siddique and Chow, 2020). For instance, AgNPs have been investigated for use in drug delivery due to their stability and ability to accumulate in certain types of cancerous tumors (Siddique and Chow, 2020). Similarly, ZnONPs have been explored for drug delivery

due to their capacity to selectively target cancer cells (Anjum et al., 2021), while CuNPs have demonstrated antimicrobial properties and are being investigated for drug delivery to treat bacterial infections (Yuan et al., 2018). With their unique optical, electrical, and catalytic properties, AuNPs are also under exploration for drug delivery, owing to their ability to accumulate in specific cancerous tumors. Furthermore, Silver NPs (AgNPs) have been integrated into wound dressings, bone cement, and implants (Schröfel et al., 2014).

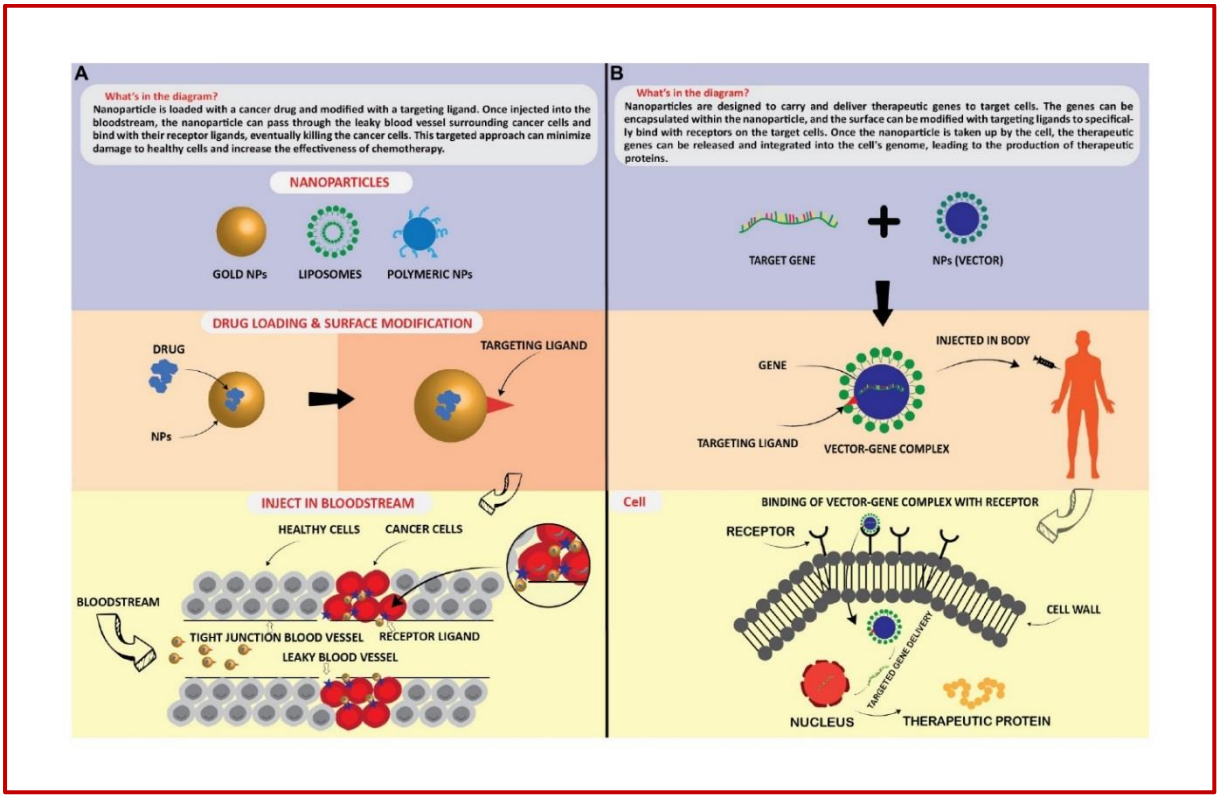

Figure 18: Application of nanoparticles as; targeted drug delivery (A), and therapeutic protein generation in targeted cells (B).

4.7.2.2. Diagnostics

Nanoparticles (NPs) can serve as imaging agents to visualize specific areas of the body. For example, iron oxide nanoparticles (Fe_3O_4 NPs) have been used as contrast agents for magnetic resonance imaging (MRI) to visualize tissues and organs (Nguyen et al., 2013). AuNPs have unique optical, electrical, and catalytic properties and are being explored for diagnostics due to their ability to accumulate in certain cancerous tumors (Siddique and Chow, 2020).

4.7.2.3. Tissue Engineering

Nanoparticles, or NPs, are promising agents for stimulating tissue and organ growth and repair. A specific example is the investigation of titanium dioxide nanoparticles (TiO_2NPs) for

application in tissue engineering due to their capacity to enhance the proliferation and activity of bone cells (Kim et al., 2014). This research suggests that TiO_2NPs could potentially be utilized to facilitate the regeneration and repair of bone tissue and hold significant promise in the field of regenerative medicine**.**

4.7.2.4. Antimicrobials

Certain nanoparticles (NPs), such as silver nanoparticles (AgNPs) and copper nanoparticles (CuNPs), exhibit potent antimicrobial properties and are under scrutiny for potential integration into a range of medical products, including wound dressings and medical devices (Hoseinzadeh et al., 2017). NPs hold significant promise for medical industry applications and are actively under investigation for diverse uses. However, it is imperative to thoroughly assess the potential hazards and advantages of employing NPs in medicine and to ensure their safe and responsible utilization.

4.7.3. Applications of NPs in Agriculture Industry

Nanoparticles (NPs) hold great promise for revolutionizing the agricultural sector through a variety of potential applications. These applications could lead to significant advancements and improvements within the agricultural industry.

4.7.3.1. Pesticides and Herbicides

Nanoparticles (NPs) offer the potential to deliver pesticides and herbicides in a targeted manner, thereby reducing the requisite quantity of chemicals and mitigating the risk of environmental contamination (Khan et al., 2019). Both Silver nanoparticles (AgNPs) and Copper nanoparticles (CuNPs) demonstrate antimicrobial properties, rendering them potentially valuable for pest and disease management in agricultural crops. Furthermore, NPs can function as carriers for active ingredients, facilitating precise application and diminishing the likelihood of environmental contamination (Hoseinzadeh et al., 2017; Dangi and Verma, 2021). It is imperative to acknowledge that the application of metal NPs in pesticides and herbicides remains at a nascent stage. Consequently, further research is imperative to discern their potential implications on human health and the environment (Dangi and Verma, 2021).

4.7.3.2. Fertilizers and Plant Growth

Nano fertilizers have the potential to significantly improve plant mineral nutrition. According to some studies, nanomaterials may outperform conventional fertilizers by controlling the

release of nutrients, thus increasing plant uptake efficiency and potentially reducing adverse environmental impacts linked to nutrient loss. However, other studies have found that nanomaterials might be equally or even less effective than conventional fertilizers. Nanoparticles (NPs) are employed to deliver fertilizers to plants more efficiently, reducing the required amount of fertilizer and diminishing the risk of nutrient runoff (Kopittke et al., 2019). NPs based on Ag (Jaskulski et al., 2022), Zn (Song and Kim, 2020), Cu, Au, Al, and Fe (Kopittke et al., 2019) have demonstrated fertilizing and plant growth-promoting properties, potentially providing essential nutrients to plants and enhancing plant growth and yield. It's important to note that the use of NPs in fertilizers is still in the early stages of development, requiring further research to understand their potential impacts on human health and the environment.

4.7.4. Food Safety

Nanoparticles (NPs) are extremely small particles that can effectively detect and eliminate harmful pathogens present in food products, thereby significantly improving food safety and reducing the likelihood of foodborne illness (Zhuang and Gentry 2011). This innovative approach holds great promise for enhancing the overall safety and quality of our food supply.

4.7.5. Water Purification

Nanoparticles (NPs) have the potential to play a significant role in agricultural practices. By being utilized to purify irrigation water, they offer the benefit of reducing the risk of crop contamination and simultaneously improving crop yield (Zhuang and Gentry, 2011). When incorporated into agriculture, NPs have the capacity to not only enhance crop yields but also to minimize the environmental impact of agricultural activities. Furthermore, their application can lead to an overall improvement in the safety and quality of food products, thereby benefiting both producers and consumers alike.

4.7.6. Applications of NPs in Food Industry

Nanoparticles (NPs) have a wide range of potential applications within the food sector, including but not limited to improving the shelf life of food products, enhancing nutritional properties, enabling targeted delivery of bioactive compounds, and providing alternative food packaging solutions.

4.7.6.1. Food Processing and Food Preservation/Food Packaging

Nanoparticles (NPs) play a crucial role in enhancing the efficiency and effectiveness of food processing procedures, including grinding, mixing, and drying. Notably, AgNPs have been harnessed as a natural antimicrobial agent within food processing operations, effectively curbing the proliferation of bacteria and other microorganisms (Dangi and Verma, 2021). Furthermore, the application of NPs extends to elevating the performance of materials utilized in food packaging, rendering them more resilient against environmental pollutants such as moisture and gases.

4.7.6.2. Food Fortification

Nanoparticles (NPs) offer a promising approach for enhancing the delivery of crucial nutrients to food products. For instance, nanoscale forms of iron (Fe_2O_3) and copper (CuNPs) have demonstrated potential in fortifying food items with essential nutrients. Copper is particularly important for the metabolism of iron and other vital nutrients. This is significant because iron deficiency is a common issue in many people's diets, especially in developing nations (Kopittke et al., 2019).

4.7.7. Sensors

Nanoparticles (NPs) are being utilized to advance the precision and selectivity of food sensors. This application allows for the detection of a more extensive variety of substances or signals **(**Yadav et al., 2010). The integration of NPs into the food industry has the potential to significantly enhance the performance, safety, and nutritional value of various food products and processes. This includes but is not limited to improving the shelf life of perishable foods, enhancing the detection of contaminants, and fortifying the nutritional content of food items.

4.7.8. Applications of NPs in Electronics Industry and Automotive Industry

In numerous ways, nanoparticles (NPs) have the potential to bring about significant changes in the electronics sector. NPs possess unique properties that make them suitable for various electrical applications, such as:

4.7.8.1 Display Technologies/Storage Devices

Nanoparticles (NPs) can significantly enhance the performance of displays, such as LCD and OLED displays, by improving brightness, color, and contrast. They have been explored for their potential to enhance the conductivity of the displays, with silver NPs and gold NPs being

the subject of particular interest (Gwynne, 2020). Additionally, NPs play a crucial role in improving the performance and longevity of energy storage devices, such as batteries and supercapacitors, by boosting energy density and charging speed. This is exemplified by the potential use of zinc oxide nanoparticles (ZnO NPs) in such devices due to their energy storage capabilities (Singh et al., 2011).

4.7.8.2. Data Storage

Nanoparticles (NPs) possess the potential to enhance the capacity and speed of data storage devices, such as hard drives and flash drives. Magnetic NPs, exemplified by iron oxide NPs, are currently being explored for integration into data storage devices owing to their capability to encode and retrieve data through magnetism. Typically consisting of a magnetic metal, such as iron, cobalt, or nickel, these NPs can undergo magnetization and demagnetization processes, thus enabling data storage and retrieval (Ahmad et al., 2021). Overall, the incorporation of NPs in electronic systems holds promise for augmenting the performance and efficiency of a wide spectrum of electronic applications.

4.7.9. Applications of NPs in the Chemical Industry

Nanoparticles (NPs) have the potential to fundamentally transform the chemical industry across a variety of domains. The ensuing implications outline potential avenues for the utilization of NPs in the chemical industry (Salem and Fouda, 2021).

4.7.9.1. Chemical Processing/Catalysis

Nanoparticles (NPs) are utilized as catalysts in various chemical reactions, facilitating enhanced efficiency and reduced operating temperatures. Notable examples of metal NPs serving as catalysts within the chemical industry encompass PtNPs, leveraged in fuel cell reactions (Bhavani et al., 2021), hydrogenation reactions, and oxidation reactions (Lara and Philippot, 2014); PdNPs, employed in hydrogenation reactions and cross-coupling reactions (Pérez-Lorenzo, 2012); FeNPs, applied in hydrolysis reactions (Jiang and Xu, 2011) and oxygen reduction reactions; and NiNPs, utilized in hydrogenation and hydrolysis reactions (Salem and Fouda, 2021).

4.7.9.2. Separation and Purification

Nanoparticles (NPs) are employed for the separation and purification of chemicals, gases, and liquids based on their size-dependent properties (Hollamby et al., 2010). Various types of metal

nanoparticles have been researched for their applicability in the separation and purification processes within the chemical industry. For instance, Fe_2O_3 NPs are utilized for the separation and purification of gases, liquids, and chemicals, as well as for the removal of contaminants from water (Pradeep, 2009; Siddique and Chow, 2020). AgNPs are utilized for water purification, removal of contaminants, such as bacteria and viruses, and extraction of heavy metals from water and other substances (Pradeep, 2009; Zhuang and Gentry, 2011). Similarly, AuNPs are employed for water purification, removal of contaminants, and separation of gases and liquids (Siddique and Chow, 2020; Zhuang and Gentry, 2011). Furthermore, AlNPs have demonstrated efficacy in the removal of contaminants from water, oils, and fuels, as well as in the purification of gases (Zhuang and Gentry, 2011).

4.7.10. Applications of NPs in the Defence Industry

Nanoparticles, or NPs, have shown promising potential in enhancing the efficiency and performance of chemical processing operations, especially in the areas of refining and synthesizing chemicals (Schröfel et al., 2014). Their unique properties enable them to play a crucial role in improving reaction kinetics, catalysis, and selectivity in chemical processes. Additionally, NPs have garnered significant interest in the defense industry due to their capability to enhance the performance of materials for armor, sensors, and detection systems. Furthermore, their potential use in nanoelectronics and energy storage technologies holds promise for enhancing defense capabilities in the future.

4.7.10.1. Sensors

The integration of nanoparticles (NPs) into sensor technology has been found to significantly enhance the sensitivity and specificity of defense systems. These advancements have notably improved the detection capabilities for chemical, biological, and radiological threats (Zheng et al., 2010).

4.7.10.2. Protective Coatings

Nanoparticles (NPs) have the potential to significantly enhance the performance and durability of protective coatings applied to defense equipment, making them more resistant to chemical or biological agents. For instance, the addition of metal NPs such as aluminum or zinc can improve the mechanical properties and longevity of the coating, while nickel or chromium-based NPs can enhance its wear resistance (Rangel-Olivares et al., 2021).

4.7.10.3. Weapons

Nanoparticles (NPs) are employed as agents against viruses, bacteria, etc. (Ye et al., 2020), and also in the development of armor and protective materials. There have been reports of the potential use of NPs in military and defense applications, particularly in the development of armor and protective materials. For instance, incorporating nanoparticles, such as ceramic or metal NPs, into polymers or other materials can enhance their mechanical properties and make them more resistant to damage. Additionally, there have been reports of the use of NPs in the development of sensors and detection systems for defense purposes.

4.7.10.4. Manufacturing

Nanoparticles (NPs) play a crucial role in enhancing the performance and durability of materials used in defense equipment, such as armor and structural materials. Metal NPs can be incorporated into materials as fillers or reinforcements in polymers. For example, integrating metal NPs like aluminum (Al), copper (Cu), or nickel (Ni) into polymers can enhance the mechanical properties, thermal stability, and electrical conductivity of the resulting composite material (Khan et al., 2019). Moreover, metal NPs can be utilized to create functional materials, including catalysts and sensors. For instance, metals like gold (Au) and platinum (Pt) can act as catalysts in various chemical reactions owing to their high surface area and ability to adsorb reactants (Zheng et al., 2010).

4.7.10.5. Energy Storage

Nanoparticles (NPs) have the potential to enhance the performance and efficiency of energy storage systems used in defense applications, such as batteries or fuel cells (Morsi et al., 2022). In the context of batteries, nanoparticles can be utilized as cathode materials to enhance the battery's energy density, rate capability, and cycling stability. For example, lithium cobalt oxide ($LiCoO_2$) nanoparticles are being used as cathode materials in lithium-ion batteries due to their high capacity and excellent rate performance. Moreover, nanoparticles of transition metal oxides, such as iron oxide (Fe_2O_3) and manganese oxide (MnO_2), have demonstrated promise as cathode materials in rechargeable lithium batteries due to their high capacity and good rate performance. In the case of supercapacitors, nanoparticles can serve as the active material in the electrodes, leading to an increase in the device's capacitance due to the augmented specific surface area (Morsi et al., 2022). The integration of NPs in the defense industry has the potential to bolster the performance, efficiency, and safety of defense systems.

Recent studies have alerted us to the limitations and scarcity of fossil fuels in the coming years due to their nonrenewable nature. As a result, scientists are redirecting their research efforts

toward generating renewable energies using easily accessible resources at a low cost. They have found that nanoparticles (NPs) are ideal for this purpose due to their large surface area, optical behavior, and catalytic nature. NPs are widely utilized in photocatalytic applications to produce energy through photoelectrochemical (PEC) and electrochemical water splitting (Avasare et al., 2015; Mueller and Nowack, 2008; Ning et al., 2016). In addition to water splitting, NPs are also used for electrochemical CO2 reduction to fuel precursors, solar cells, and piezoelectric generators, offering advanced options for energy generation (Fang et al., 2013; Gawande et al., 2016; Lei et al., 2015; Li et al., 2016; Nagarajan et al., 2014; Sagadevan, 2015; Young et al., 2012; Zhou et al., 2016). **Fig.19** illustrates energy-generating devices that employ nanoparticles.

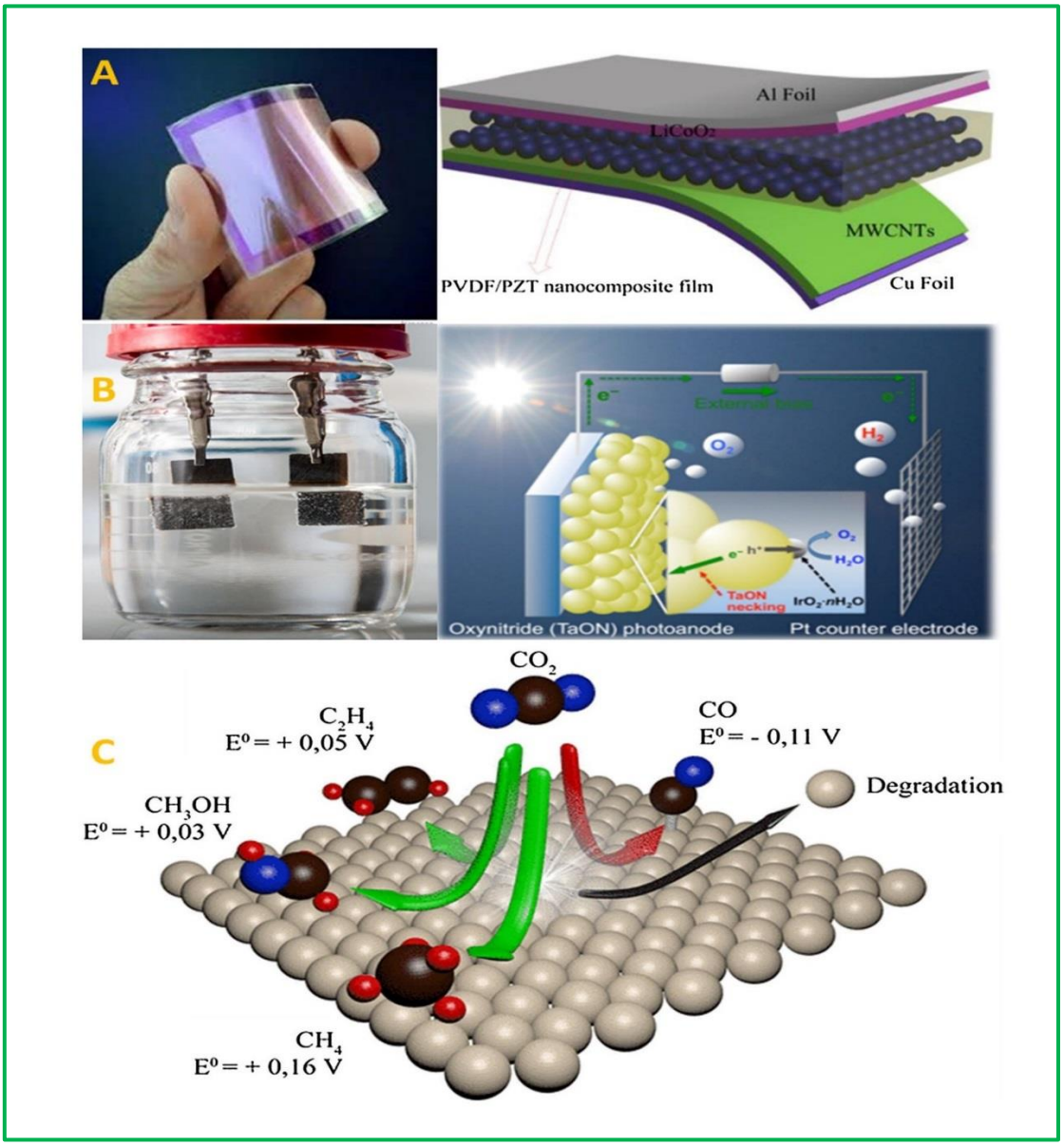

Figure 19: Energy generation approaches from (A) Piezoelectrics actuators (B) Water splitting (C) CO2 reduction. (Adapted from Khan et al., 2019).

4.8. Toxicity of NPs

Apart from their numerous industrial and medical applications, NPs and other nanomaterials are associated with specific toxicities (Bahadar et al., 2016; Ibrahim, 2013; Khlebtsov and Dykman, 2011, 2010b) that require a basic understanding to address effectively. NPs can enter the environment through water, soil, and air due to various human activities. Additionally, the intentional introduction or disposal of engineered NPs into soil or aquatic systems for environmental treatment has raised significant concerns among stakeholders. The advantageous characteristics of magnetic NPs, including their small size, high reactivity, and large capacity, can potentially lead to adverse cellular toxic and harmful effects, which differ from those of larger particles. Studies have shown that NPs can enter organisms through ingestion or inhalation and move within the body to various organs and tissues, where they may induce toxic effects. While some research has examined the toxicological effects of NPs on animal and plant cells, studies on the toxicological effects of magnetic NPs on plants remain limited. The utilization of silver nanoparticles (Ag NPs) in a wide array of consumer products results in their release into the aquatic environment, where they serve as a source of dissolved silver, thus eliciting detrimental effects on various aquatic organisms, including bacteria, algae, fish, and daphnia (Navarro et al., 2008). Notably, the respiratory system presents a distinct target for the potential toxicity of nanoparticles due to its role as both the portal of entry for inhaled particles and the recipient of the entire cardiac output (Ferreira et al., 2013).

Nanoparticles (NPs) are widely utilized in various bio applications. Despite the rapid progress and early acceptance of nanobiotechnology, the potential adverse health effects of prolonged NP exposure at different concentration levels in humans and the environment have not been firmly established. However, it is anticipated that the environmental impact of NPs will increase in the future. One of the concerns regarding NPs is their potential toxicity due to their ability to interact with proteins. This ability depends on particle size, curvature, shape, surface charge, functionalized groups, and free energy. These interactions can lead to adverse biological outcomes such as protein unfolding, fibrillation, thiol crosslinking, and loss of enzymatic activity. Another issue of concern is the release of toxic ions when the thermodynamic properties of materials favor particle dissolution in a suspending medium or biological environment (Xia et al., 2008)**.** Nanoparticles (NPs) tend to aggregate in hard water and seawater and are significantly influenced by the specific type of organic matter or other natural particles (colloids) present in freshwater. The dispersion of NPs can alter their ecotoxicity, but many abiotic factors affecting this, such as pH, salinity, and the presence of

organic matter, still require systematic investigation as part of ecotoxicological studies (Handy et al., 2008).

4.9. Future Perspectives

Metal nanoparticles (NPs) exhibit significant potential for diverse applications across electronics, energy storage, catalysis, and medicine. However, the utilization of metal NPs is encumbered by various challenges and offers prospective future directions. An eminent challenge pertains to the precision in synthesizing and processing metal NPs with regard to size and shape control. Numerous synthesis methods entail high temperatures and stringent chemical conditions, posing scalability issues for large-scale production. Furthermore, the properties and potential applications of metal NPs are profoundly influenced by their size and shape, necessitating precise control in synthesis.

Another noteworthy challenge revolves around the environmental implications of metal NPs. Certain variants, such as silver NPs, possess toxicity to aquatic life and may entail environmental ramifications. It is imperative to undertake extensive research pertaining to the environmental impact of metal NPs and develop environmentally sustainable synthesis and processing modalities. Looking ahead, an auspicious realm entails leveraging metal NPs for energy storage, conversion, and environmental safeguarding. For instance, metal NPs hold the potential to enhance battery performance and advance solar cell efficiency. Furthermore, their application in catalysis stands to bolster the efficacy of chemical reactions. Ongoing research is also probing the potential of metal NPs in medical applications, encompassing drug delivery and cancer therapy.

4.10. References

Abd Ellah, N.H. and Abouelmagd, S.A., 2017. Surface functionalization of polymeric nanoparticles for tumor drug delivery: approaches and challenges. Expert opinion on drug delivery, 14(2), pp.201-214.

Abdulle, A. and Chow, J.C., 2019. Contrast enhancement for portal imaging in nanoparticle-enhanced radiotherapy: A Monte Carlo phantom evaluation using flattening-filter-free photon beams. Nanomaterials, 9(7), p.920.

Abouelmagd, S.A., Meng, F., Kim, B.K., Hyun, H. and Yeo, Y., 2016. Tannic acid-mediated surface functionalization of polymeric nanoparticles. ACS biomaterials science & engineering, 2(12), pp.2294-2303.

Adeleye, A.S., Conway, J.R., Perez, T., Rutten, P. and Keller, A.A., 2014. Influence of extracellular polymeric substances on the long-term fate, dissolution, and speciation of copper-based nanoparticles. Environmental science & technology, 48(21), pp.12561-12568.

Adeleye, A.S., Stevenson, L.M., Su, Y., Nisbet, R.M., Zhang, Y. and Keller, A.A., 2016. Influence of phytoplankton on fate and effects of modified zerovalent iron nanoparticles. Environmental science & technology, 50(11), pp.5597-5605.

Ago, H., 2015. CVD growth of high-quality single-layer graphene. Frontiers of Graphene and Carbon Nanotubes: Devices and Applications, pp.3-20.

Ahmad, A., Senapati, S., Khan, M.I., Kumar, R., Ramani, R., Srinivas, V. and Sastry, M., 2003. Intracellular synthesis of gold nanoparticles by a novel alkalotolerant actinomycete, Rhodococcus species. Nanotechnology, 14(7), p.824.

Ahmad, A.A., Alsaad, A.M., Al-Bataineh, Q.M., Al-Akhras, M.A.H., Albataineh, Z., Alizzy, K.A. and Daoud, N.S., 2021. Synthesis and characterization of ZnO NPs-doped PMMA-BDK-MR polymer-coated thin films with UV curing for optical data storage applications. Polymer Bulletin, 78, pp.1189-1211.

Al-Dhabi, N.A., Mohammed Ghilan, A.K. and Arasu, M.V., 2018. Characterization of silver nanomaterials derived from marine Streptomyces sp. al-dhabi-87 and its in vitro application against multidrug-resistant and extended-spectrum beta-lactamase clinical pathogens. Nanomaterials, 8(5), p.279.

Ali, S., Khan, I., Khan, S.A., Sohail, M., Ahmed, R., ur Rehman, A., Ansari, M.S. and Morsy, M.A., 2017. Electrocatalytic performance of Ni@ Pt core–shell nanoparticles supported on carbon nanotubes for methanol oxidation reaction. Journal of Electroanalytical Chemistry, 795, pp.17-25.

Altammar, K.A., 2023. A review on nanoparticles: characteristics, synthesis, applications, and challenges. Frontiers in microbiology, 14, p.1155622.

Ameh, T. and Sayes, C.M., 2019. The potential exposure and hazards of copper nanoparticles: A review. Environmental Toxicology and Pharmacology, 71, p.103220.

Amendola, V. and Meneghetti, M., 2009. Laser ablation synthesis in solution and size manipulation of noble metal nanoparticles. Physical chemistry chemical physics, 11(20), pp.3805-3821 and applications. J. Phys. D 47:013001.

Anjum, S., Hashim, M., Malik, S.A., Khan, M., Lorenzo, J.M., Abbasi, B.H. and Hano, C., 2021. Recent advances in zinc oxide nanoparticles (ZnO NPs) for cancer diagnosis, target drug delivery, and treatment. Cancers, 13(18), p.4570.

Aqel, A., Abou El-Nour, K.M., Ammar, R.A. and Al-Warthan, A., 2012. Carbon nanotubes, science and technology part (I) structure, synthesis, and characterization. Arabian Journal of Chemistry, 5(1), pp.1-23.

Assa, F., Jafarizadeh-Malmiri, H., Ajamein, H., Anarjan, N., Vaghari, H., Sayyar, Z. and Berenjian, A., 2016. A biotechnological perspective on the application of iron oxide nanoparticles. Nano Research, 9, pp.2203-2225.

Astefanei, A., Núñez, O. and Galceran, M.T., 2015. Characterization and determination of fullerenes: a critical review. Analytica chimica acta, 882, pp.1-21.

Avasare, V., Zhang, Z., Avasare, D., Khan, I. and Qurashi, A., 2015. Room-temperature synthesis of TiO2 nanospheres and their solar-driven photoelectrochemical hydrogen production. International Journal of Energy Research, 39(12), pp.1714-1719.

Bahadar, H., Maqbool, F., Niaz, K. and Abdollahi, M., 2016. Toxicity of nanoparticles and an overview of current experimental models. Iranian Biomedical Journal, 20(1), p.1.

Baig, N., Kammakakam, I. and Falath, W., 2021. Nanomaterials: A review of synthesis methods, properties, recent progress, and challenges. Materials advances, 2(6), pp.1821-1871.

Banerjee, A.N., Krishna, R. and Das, B., 2008. Size-controlled deposition of Cu and Si nano-clusters by an ultra-high vacuum sputtering gas aggregation technique. Applied Physics A, 90, pp.299-303.

Bansal, R., Nagórniewicz, B., Storm, G. and Prakash, J., 2017. Relaxin-coated superparamagnetic iron-oxide nanoparticles as a novel theranostic approach for the diagnosis and treatment of liver fibrosis. Journal of Hepatology, 1(66), p.S43.

Behrisch, R. ed., 1981. Sputtering by particle bombardment (Vol. 1, pp. 9-64). New York: Springer-Verlag.

Berkman, A.J., Jagannatham, M., Priyanka, S. and Haridoss, P., 2014. Synthesis of branched, nano channeled, ultrafine, and nano carbon tubes from PET wastes using the arc discharge method. Waste management, 34(11), pp.2139-2145.

Bhattacharjee, S., 2016. DLS and zeta potential–what they are and what they are not? Journal of controlled release, 235, pp.337-351.

Bhattacharya, P.T., Misra, S.R. and Hussain, M., 2016. Nutritional aspects of essential trace elements in oral health and disease: an extensive review. Scientifica, 2016(1), p.5464373.

Bhavani, K.S., Anusha, T. and Brahman, P.K., 2021. Platinum nanoparticles decorated on graphitic carbon nitride-ZIF-67 composite support: An electrocatalyst for the oxidation of butanol in fuel cell applications. International Journal of Hydrogen Energy, 46(13), pp.9199-9214.

Binnig, G., Rohrer, H., Gerber, C. and Weibel, E., 1982. Surface studies by scanning tunneling microscopy. Physical review letters, 49(1), p.57.

Birla, S.S., Tiwari, V.V., Gade, A.K., Ingle, A.P., Yadav, A.P. and Rai, M.K., 2009. Fabrication of silver nanoparticles by Phoma glomerata and its combined effect against Escherichia coli, Pseudomonas aeruginosa, and Staphylococcus aureus. Letters in Applied Microbiology, 48(2), pp.173-179.

Brady, B., Wang, P.H., Steinhoff, V. and Brolo, A.G., 2019. Nanostructuring solar cells using metallic nanoparticles. In Metal nanostructures for photonics (pp. 197-221). Elsevier.

C Thomas, S., Kumar Mishra, P. and Talegaonkar, S., 2015. Ceramic nanoparticles: fabrication methods and applications in drug delivery. Current pharmaceutical design, 21(42), pp.6165-6188.88.

Cadene, A., Durand-Vidal, S., Turq, P. and Brendle, J., 2005. Study of individual Na-montmorillonite particles size, morphology, and apparent charge. Journal of Colloid and Interface Science, 285(2), pp.719-730.

Cao, Y.C., Jin, R. and Mirkin, C.A., 2002. Nanoparticles with Raman spectroscopic fingerprints for DNA and RNA detection. Science, 297(5586), pp.1536-1540.

Cava, R.J., 1990. Structural chemistry and the local charge picture of copper oxide superconductors. Science, 247(4943), pp.656-662.

Chandraker, S.K., Lal, M., Ghosh, M.K., Tiwari, V., Ghorai, T.K. and Shukla, R., 2020. Green synthesis of copper nanoparticles using leaf extract of Ageratum houstonianum Mill. and study of their photocatalytic and antibacterial activities. Nano Express, 1(1), p.010033.

Chen, J. and Zhu, X., 2016. Magnetic solid phase extraction using ionic liquid-coated core–shell magnetic nanoparticles followed by high-performance liquid chromatography for determination of Rhodamine B in food samples. Food Chemistry, 200, pp.10-15.

Chen, J., Guo, Y., Zhang, X., Liu, J., Gong, P., Su, Z., Fan, L. and Li, G., 2023. Emerging nanoparticles in food: Sources, application, and safety. Journal of Agricultural and Food Chemistry, 71(8), pp.3564-3582.

Chen, J.C. and Tang, C.T., 2007. Preparation and application of granular ZnO/Al2O3 catalyst for the removal of hazardous trichloroethylene. Journal of hazardous materials, 142(1-2), pp.88-96.

Chen, Z., Meng, H., Xing, G., Chen, C., Zhao, Y., Jia, G., Wang, T., Yuan, H., Ye, C., Zhao, F. and Chai, Z., 2006. Acute toxicological effects of copper nanoparticles in vivo. Toxicology letters, 163(2), pp.109-120.

Chen, Z., Meng, H., Xing, G., Yuan, H., Zhao, F., Liu, R., Chang, X., Gao, X., Wang, T., Jia, G. and Ye, C., 2008. Age-related differences in pulmonary and cardiovascular responses to SiO2 nanoparticle inhalation: nanotoxicity has a susceptible population. Environmental science & technology, 42(23), pp.8985-8992.286.

Chronakis, I.S., 2010. Micro-/nano-fibers by electrospinning technology: processing, properties, and applications. Micromanufacturing engineering and technology, 2010, pp.264-

Compostella, F., Pitirollo, O., Silvestri, A. and Polito, L., 2017. Glyco-gold nanoparticles: synthesis and applications. Beilstein Journal of Organic Chemistry, 13(1), pp.1008-1021.

Conway, J.R., Adeleye, A.S., Gardea-Torresdey, J. and Keller, A.A., 2015. Aggregation, dissolution, and transformation of copper nanoparticles in natural waters. Environmental science & technology, 49(5), pp.2749-2756.

Croy, J.R., Mostafa, S., Hickman, L., Heinrich, H. and Cuenya, B.R., 2008. Bimetallic Pt-Metal catalysts for the decomposition of methanol: Effect of secondary metal on the oxidation state, activity, and selectivity of Pt. Applied Catalysis A: General, 350(2), pp.207-216.

Cuenya, B.R., 2010. Synthesis and catalytic properties of metal nanoparticles: Size, shape, support, composition, and oxidation state effects. Thin Solid Films, 518(12), pp.3127-3150.

Curl, R.F. and Smalley, R.E., 1988. Probing C60. Science, 242(4881), pp.1017-1022.

D. J. Dietzen in Principles and Applications of MolecularDiagnostics (Eds.: N. Rifai, A. R. Horvath, C. T. Wittwer), Elsevier, Amsterdam, 2018, p. 345.

Dahoumane, S.A., Mechouet, M., Wijesekera, K., Filipe, C.D., Sicard, C., Bazylinski, D.A. and Jeffryes, C., 2017. Algae-mediated biosynthesis of inorganic nanomaterials as a promising route in nanobiotechnology–a review. Green Chemistry, 19(3), pp.552-587.

Dangi, K. and Verma, A.K., 2021. Efficient & eco-friendly smart nano-pesticides: Emerging prospects for agriculture. Materials Today: Proceedings, 45, pp.3819-3824.

Das, S. and Srivasatava, V.C., 2016. Synthesis and characterization of ZnO–MgO nanocomposite by co-precipitation method. Smart Science, 4(4), pp.190-195.

Delvallée, A., Feltin, N., Ducourtieux, S., Trabelsi, M. and Hochepied, J.F., 2015. Direct comparison of AFM and SEM measurements on the same set of nanoparticles. Measurement Science and Technology, 26(8), p.085601.

Dikusar, A.I., Globa, P.G., Belevskii, S.S. and Sidel'nikova, S.P., 2009. On limiting rate of dimensional electrodeposition at meso-and nanomaterial manufacturing by template synthesis. Surface Engineering and Applied Electrochemistry, 45, pp.171-179.

Ding, R.G., Lu, G.Q., Yan, Z.F. and Wilson, M.A., 2001. Recent advances in the preparation and utilization of carbon nanotubes for hydrogen storage. Journal of Nanoscience and Nanotechnology, 1(1), pp.7-29.

Dragovic, R.A., Gardiner, C., Brooks, A.S., Tannetta, D.S., Ferguson, D.J., Hole, P., Carr, B., Redman, C.W., Harris, A.L., Dobson, P.J. and Harrison, P., 2011. Sizing and phenotyping of cellular vesicles using Nanoparticle Tracking Analysis. Nanomedicine: Nanotechnology, Biology and Medicine, 7(6), pp.780-788.

Dreaden, E.C., Alkilany, A.M., Huang, X., Murphy, C.J. and El-Sayed, M.A., 2012. The golden age: gold nanoparticles for biomedicine. Chemical Society Reviews, 41(7), pp.2740-2779.

Drexler, E., 1987. Engines of creation: The coming era of nanotechnology. Anchor.

Du, P., Song, L., Xiong, J., Li, N., Xi, Z., Wang, L., Jin, D., Guo, S. and Yuan, Y., 2012. Coaxial electrospun TiO2/ZnO core–sheath nanofibers film: Novel structure for photoanode of dye-sensitized solar cells. Electrochimica Acta, 78, pp.392-397.

Edwardson, T.G., Levasseur, M.D., Tetter, S., Steinauer, A., Hori, M. and Hilvert, D., 2022. Protein cages: from fundamentals to advanced applications. Chemical Reviews, 122(9), pp.9145-9197.

Elliott, J.A., Shibuta, Y., Amara, H., Bichara, C. and Neyts, E.C., 2013. Atomistic modeling of CVD synthesis of carbon nanotubes and graphene. Nanoscale, 5(15), pp.6662-6676.

Erasmus, M., Cason, E.D., van Marwijk, J., Botes, E., Gericke, M. and van Heerden, E., 2014. Gold nanoparticle synthesis using the thermophilic bacterium Thermus scotoductus SA-01 and the purification and characterization of its unusual gold-reducing protein. Gold Bulletin, 47, pp.245-253.

Eustis, S. and El-Sayed, M.A., 2006. Why gold nanoparticles are more precious than pretty gold: noble metal surface plasmon resonance and its enhancement of the radiative and nonradiative properties of nanocrystals of different shapes. Chemical Society reviews, 35(3), pp.209-217.

Faivre, D. and Bennet, M., 2016. Magnetic nanoparticles line up. Nature, 535(7611), pp.235-236.

Fang, X.Q., Liu, J.X. and Gupta, V., 2013. Fundamental formulations and recent achievements in piezoelectric nanostructures: a review. Nanoscale, 5(5), pp.1716-1726.

Farjadian, F., Moradi, S. and Hosseini, M., 2017. Thin chitosan films containing super-paramagnetic nanoparticles with contrasting capability in magnetic resonance imaging. Journal of Materials Science: Materials in Medicine, 28, pp.1-10.

Ferreira, A.J., Cemlyn-Jones, J. and Cordeiro, C.R., 2013. Nanoparticles, nanotechnology and pulmonary nanotoxicology. Revista Portuguesa de Pneumologia (English Edition), 19(1), pp.28-37.

Feynman, R., 2018. There's plenty of room at the bottom. In Feynman and Computation (pp. 63-76). CRC Press.

For details about the British Museum see the website: http://www. britishmuseum.org/explore/highlight_ image. asp? image = k741.jpg&retpage = 20945.

Gawande, M.B., Goswami, A., Felpin, F.X., Asefa, T., Huang, X., Silva, R., Zou, X., Zboril, R. and Varma, R.S., 2016. Cu and Cu-based nanoparticles: synthesis and applications in catalysis. Chemical Reviews, 116(6), pp.3722-3811.

Ghosh, S., Ahmad, R., Zeyaullah, M. and Khare, S.K., 2021. Microbial nano-factories: synthesis and biomedical applications. Frontiers in Chemistry, 9, p.626834.

Giurlani, W., Innocenti, M. and Lavacchi, A., 2018. X-ray microanalysis of precious metal thin films: thickness and composition determination. Coatings, 8(2), p.84.

Gorrasi, G. and Sorrentino, A., 2015. Mechanical milling as a technology to produce structural and functional bio-nanocomposites. Green Chemistry, 17(5), pp.2610-2625.

Greczynski, G. and Hultman, L., 2020. X-ray photoelectron spectroscopy: towards reliable binding energy referencing. Progress in Materials Science, 107, p.100591.

Guo, D., Xie, G. and Luo, J., 2013. Mechanical properties of nanoparticles: basics and applications. Journal of Physics D: applied physics, 47(1), p.013001.

Gwynne, K.M., 2020. Enhancement of the photostability of blue phosphorescence using plasmonic surfaces (Master's thesis, Rutgers State University of New Jersey, School of Graduate Studies).

Haasch, R.T., 2014. X-ray photoelectron spectroscopy (XPS) and auger electron spectroscopy (AES). In Practical Materials Characterization (pp. 93-132). New York, NY: Springer New York.

Handy, R.D., Von der Kammer, F., Lead, J.R., Hassellöv, M., Owen, R. and Crane, M., 2008. The ecotoxicology and chemistry of manufactured nanoparticles. Ecotoxicology, 17, pp.287-314.

Hasan, S., 2015. A review on nanoparticles: their synthesis and types. Res. J. Recent Sci, 2277, p.2502.

Hisatomi, T., Kubota, J. and Domen, K., 2014. Recent advances in semiconductors for photocatalytic and photoelectrochemical water splitting. Chemical Society Reviews, 43(22), pp.7520-7535.

Holder, C.F. and Schaak, R.E., 2019. Tutorial on powder X-ray diffraction for characterizing nanoscale materials. Acs Nano, 13(7), pp.7359-7365.

Hollamby, M.J., Eastoe, J., Chemelli, A., Glatter, O., Rogers, S., Heenan, R.K. and Grillo, I., 2010. Separation and purification of nanoparticles in a single step. Langmuir, 26(10), pp.6989-6994.

Hoo, C.M., Starostin, N., West, P. and Mecartney, M.L., 2008. A comparison of atomic force microscopy (AFM) and dynamic light scattering (DLS) methods to characterize nanoparticle size distributions. Journal of Nanoparticle Research, 10, pp.89-96.

Hoseinzadeh, E., Makhdoumi, P., Taha, P., Hossini, H., Stelling, J., Amjad Kamal, M. and Md Ashraf, G., 2017. A review on nano-antimicrobials: metal nanoparticles, methods and mechanisms. Current drug metabolism, 18(2), pp.120-128.

Hulkoti, N.I. and Taranath, T.C., 2014. Biosynthesis of nanoparticles using microbes—a review. Colloids and surfaces B: Biointerfaces, 121, pp.474-483.

Ibrahim, K.S., 2013. Carbon nanotubes? properties and applications: A review. Carbon letters, 14(3), pp.131-144.

Iijima, S., 1991. Helical microtubules of graphitic carbon. nature, 354(6348), pp.56-58.

Islam, F., Shohag, S., Uddin, M.J., Islam, M.R., Nafady, M.H., Akter, A., Mitra, S., Roy, A., Emran, T.B. and Cavalu, S., 2022. Exploring the journey of zinc oxide nanoparticles (ZnO-NPs) toward biomedical applications. Materials, 15(6), p.2160.

Jadoun, S., Arif, R., Jangid, N.K. and Meena, R.K., 2021. Green synthesis of nanoparticles using plant extracts: A review. Environmental Chemistry Letters, 19(1), pp.355-374.

Jaskulski, D., Jaskulska, I., Majewska, J., Radziemska, M., Bilgin, A. and Brtnicky, M., 2022. Silver nanoparticles (AgNPs) in urea solution in laboratory tests and field experiments with crops and vegetables. Materials, 15(3), p.870.

Jayaraman, V., Ghosh, S., Sengupta, A., Srivastava, S., Sonawat, H.M. and Narayan, P.K., 2014. Identification of biochemical differences between different forms of male

infertility by nuclear magnetic resonance (NMR) spectroscopy. Journal of assisted reproduction and genetics, 31(9), pp.1195-1204.

Jiang, H.L. and Xu, Q., 2011. Catalytic hydrolysis of ammonia borane for chemical hydrogen storage. Catalysis Today, 170(1), pp.56-63.

Joh, D.W., Jung, T.K., Lee, H.S. and Kim, D.H., 2013. Synthesis of nanoparticles using electrical explosion of Ni wire in Pt solution. Journal of nanoscience and nanotechnology, 13(9), pp.6092-6094.

Jones, J.A. and Giessen, T.W., 2021. Advances in encapsulin nanocompartment biology and engineering. Biotechnology and Bioengineering, 118(1), pp.491-505.

Kahle, M., Kleber, M. and Jahn, R., 2002. Review of XRD-based quantitative analyses of clay minerals in soils: the suitability of mineral intensity factors. Geoderma, 109(3-4), pp.191-205.

Kalubowilage, M., Janik, K. and Bossmann, S.H., 2019. Magnetic nanomaterials for magnetically-aided drug delivery and hyperthermia. Applied Sciences, 9(14), p.2927.

Katti, A.K.S. and Sharon, M., 2019. European Nano knowledge that led to Faraday's understanding of gold nanoparticles. History of Nanotechnology: From Pre-Historic to Modern Times, pp.141-212.

Kefeni, K.K., Msagati, T.A. and Mamba, B.B., 2017. Ferrite nanoparticles: synthesis, characterization, and applications in the electronic device. Materials Science and Engineering: B, 215, pp.37-55.

Khan, I., Ibrahim, A.A., Sohail, M. and Qurashi, A., 2017. Sonochemical assisted synthesis of RGO/ZnO nanowire arrays for photoelectrochemical water splitting. Ultrasonics sonochemistry, 37, pp.669-675.

Khan, I., Saeed, K., and Khan, I., 2019. Nanoparticles: Properties, applications, and toxicities. Arabian Journal of Chemistry, 12(7), pp.908-931.

Khanna, P., Kaur, A. and Goyal, D., 2019. Algae-based metallic nanoparticles: Synthesis, characterization, and applications. Journal of microbiological methods, 163, p.105656.

Khlebtsov, N. and Dykman, L., 2011. Biodistribution and toxicity of engineered gold nanoparticles: a review of in vitro and in vivo studies. Chemical Society Reviews, 40(3), pp.1647-1671.

Khlebtsov, N., Dykman, L., 2010. Plasmonic nanoparticles. pp. 37–85. http://dx.doi.org/10.1201/9781439806296-c2.

Khlebtsov, N.G. and Dykman, L.A., 2010. Optical properties and biomedical applications of plasmonic nanoparticles. Journal of Quantitative Spectroscopy and Radiative Transfer, 111(1), pp.1-35.

Kim, J.H., Sheikh, F.A., Ju, H.W., Park, H.J., Moon, B.M., Lee, O.J. and Park, C.H., 2014. 3D silk fibroin scaffold incorporating titanium dioxide (TiO2) nanoparticles (NPs) for tissue engineering. International journal of biological macromolecules, 68, pp.158-168.

Kohl, H., and Reimer, L. (2008). Transmission Electron Microscopy. Berlin: Springer Series in Optical Sciences, 36.

Kopittke, P. M., Lombi, E., Wang, P., Schjoerring, J. K., and Husted, S. (2019). Nanomaterials as fertilizers for improving plant mineral nutrition and environmental outcomes. Environ. Sci. 6, 3513–3524. doi: 10.3390/biology10111123.

Kora, A.J. and Rastogi, L., 2018. Peroxidase activity of biogenic platinum nanoparticles: A colorimetric probe towards selective detection of mercuric ions in water samples. Sensors and Actuators B: Chemical, 254, pp.690-700.

Kumar, C.S. and Mohammad, F., 2011. Magnetic nanomaterials for hyperthermia-based therapy and controlled drug delivery. Advanced drug delivery reviews, 63(9), pp.789-808.

Kumar, M., Xiong, X., Wan, Z., Sun, Y., Tsang, D.C., Gupta, J., Gao, B., Cao, X., Tang, J. and Ok, Y.S., 2020. Ball milling as a mechanochemical technology for fabrication of novel biochar nanomaterials. Bioresource technology, 312, p.123613.

Kumar, R., Singh, R.K., Dubey, P.K., Kumar, P., Tiwari, R.S. and Oh, I.K., 2013. Pressure-dependent synthesis of high-quality few-layer graphene by plasma-enhanced arc discharge and their thermal stability. Journal of nanoparticle research, 15, pp.1-10.

Kumar, S.S., Venkateswarlu, P., Rao, V.R. and Rao, G.N., 2013. Synthesis, characterization, and optical properties of zinc oxide nanoparticles. International Nano Letters, 3, pp.1-6.

Kumar, V. and Yadav, S.K., 2009. Plant-mediated synthesis of silver and gold nanoparticles and their applications. Journal of Chemical Technology & Biotechnology: International Research in Process, Environmental & Clean Technology, 84(2), pp.151-157.

Kumar, V., Bano, D., Mohan, S., Singh, D.K. and Hasan, S.H., 2016. Sunlight-induced green synthesis of silver nanoparticles using aqueous leaf extract of Polyalthia longifolia and its antioxidant activity. Materials Letters, 181, pp.371-377.

Kumari, S. C., Dhand, V., and Padma, P. N. (2021). Green synthesis of metallic nanoparticles: a review. Nanomaterials 2021, 259–281.

Kwak, K. and Kim, C., 2005. Viscosity and thermal conductivity of copper oxide nanofluid dispersed in ethylene glycol. Korea-Australia Rheology Journal, 17(2), pp.35-40.

Lam, E. and Luong, J.H., 2014. Carbon materials as catalyst supports and catalysts in the transformation of biomass to fuels and chemicals. ACS catalysis, 4(10), pp.3393-3410.

Lara, P., and Philippot, K. (2014). The hydrogenation of nitroarenes mediated by platinum nanoparticles: an overview. Catal. Sci. Technol. 4, 2445–2465.Pérez-Lorenzo, M., 2012. Palladium nanoparticles as efficient catalysts for Suzuki cross-coupling reactions. The Journal of Physical Chemistry Letters, 3(2), pp.167-174.

Lee, S., Choi, S.S., Li, S.A. and Eastman, J.A., 1999. Measuring thermal conductivity of fluids containing oxide nanoparticles.

Lei, Y.M., Huang, W.X., Zhao, M., Chai, Y.Q., Yuan, R. and Zhuo, Y., 2015. Electrochemiluminescence resonance energy transfer system: mechanism and application in ratiometric aptasensor for lead ion. Analytical chemistry, 87(15), pp.7787-7794.

Lewczuk, B. and Szyryńska, N., 2021. Field-emission scanning electron microscope as a tool for large-area and large-volume ultrastructural studies. Animals, 11(12), p.3390.

Li, D., Baydoun, H., Verani, C.N. and Brock, S.L., 2016. Efficient water oxidation using CoMnP nanoparticles. Journal of the American Chemical Society, 138(12), pp.4006-4009.

Li, G., He, D., Qian, Y., Guan, B., Gao, S., Cui, Y., Yokoyama, K. and Wang, L., 2011. Fungus-mediated green synthesis of silver nanoparticles using Aspergillus terreus. International journal of molecular sciences, 13(1), pp.466-476.

Li, N., Zhao, P. and Astruc, D., 2014. Anisotropic gold nanoparticles: synthesis, properties, applications, and toxicity. Angewandte Chemie International Edition, 53(7), pp.1756-1789.

Li, T., Senesi, A.J. and Lee, B., 2016. Small angle X-ray scattering for nanoparticle research. Chemical Reviews, 116(18), pp.11128-11180.

Li, W.R., Xie, X.B., Shi, Q.S., Duan, S.S., Ouyang, Y.S. and Chen, Y.B., 2011. Antibacterial effect of silver nanoparticles on Staphylococcus aureus. Biometals, 24, pp.135-141.

Li, X., Xu, H., Chen, Z.S. and Chen, G., 2011. Biosynthesis of nanoparticles by microorganisms and their applications. Journal of nanomaterials, 2011(1), p.270974.

Liu, D., Li, C., Zhou, F., Zhang, T., Zhang, H., Li, X., Duan, G., Cai, W. and Li, Y., 2015. Rapid synthesis of monodisperse Au nanospheres through a laser irradiation-induced shape conversion, self-assembly, and their electromagnetic coupling SERS enhancement. Scientific reports, 5(1), p.7686.

Liu, J., Liu, Y., Liu, N., Han, Y., Zhang, X., Huang, H., Lifshitz, Y., Lee, S.T., Zhong, J. and Kang, Z., 2015. Metal-free efficient photocatalyst for stable visible water splitting via a two-electron pathway. Science, 347(6225), pp.970-974.

Lyon, L.A., Keating, C.D., Fox, A.P., Baker, B.E., He, L., Nicewarner, S.R., Mulvaney, S.P. and Natan, M.J., 1998. Raman spectroscopy. Analytical Chemistry, 70(12), pp.341-362.

Mabena, L.F., Sinha Ray, S., Mhlanga, S.D. and Coville, N.J., 2011. Nitrogen-doped carbon nanotubes as a metal catalyst support. Applied Nanoscience, 1, pp.67-77.

Malhotra, S.P.K. and Alghuthaymi, M.A., 2022. Biomolecule-assisted biogenic synthesis of metallic nanoparticles. Agri-Waste and Microbes for Production of Sustainable Nanomaterials, pp.139-163.

Mansoori, G.A. and Soelaiman, T.F., 2005. Nanotechnology--An introduction for the standards community. Chicago: ASTM International.

Mathew, L., Chandrasekaran, N. and Mukherjee, A., 2010. Biomimetic synthesis of nanoparticles: science, technology & applicability. Biomimetics learning from nature.

Menon, J.U., Jadeja, P., Tambe, P., Vu, K., Yuan, B. and Nguyen, K.T., 2013. Nanomaterials for photo-based diagnostic and therapeutic applications. Theranostics, 3(3), p.152.

Mirzadeh, E. and Akhbari, K., 2016. Synthesis of nanomaterials with desirable morphologies from metal-organic frameworks for various applications. CrystEngComm, 18(39), pp.7410-7424.

Mishra, A., Tripathy, S.K., Wahab, R., Jeong, S.H., Hwang, I., Yang, Y.B., Kim, Y.S., Shin, H.S. and Yun, S.I., 2011. Microbial synthesis of gold nanoparticles using the fungus Penicillium brevicompactum and their cytotoxic effects against mouse mayo blast cancer C 2 C 12 cells. Applied microbiology and biotechnology, 92, pp.617-630.

Mittal, A.K., Chisti, Y. and Banerjee, U.C., 2013. Synthesis of metallic nanoparticles using plant extracts. Biotechnology advances, 31(2), pp.346-356.

Mohamed, E.A., 2020. Green synthesis of copper & copper oxide nanoparticles using the extract of seedless dates. Heliyon, 6(1).

Mohanpuria, P., Rana, N.K. and Yadav, S.K., 2008. Biosynthesis of nanoparticles: technological concepts and future applications. Journal of nanoparticle research, 10, pp.507-517.

Mohd Yusof, H., Mohamad, R., Zaidan, U.H. and Abdul Rahman, N.A., 2019. Microbial synthesis of zinc oxide nanoparticles and their potential application as an antimicrobial agent and a feed supplement in animal industry: a review. Journal of Animal Science and Biotechnology, 10, pp.1-22.

Morsi, M.A., Abdelrazek, E.M., Ramadan, R.M., Elashmawi, I.S. and Rajeh, A., 2022. Structural, optical, mechanical, and dielectric properties studies of carboxymethyl cellulose/polyacrylamide/lithium titanate nanocomposites films as an application in energy storage devices. Polymer Testing, 114, p.107705.

Mueller, N.C. and Nowack, B., 2008. Exposure modeling of engineered nanoparticles in the environment. Environmental science & technology, 42(12), pp.4447-4453.

Mukherjee, P., Ahmad, A., Mandal, D., Senapati, S., Sainkar, S.R., Khan, M.I., Parishcha, R., Ajaykumar, P.V., Alam, M., Kumar, R. and Sastry, M., 2001. Fungus-mediated

synthesis of silver nanoparticles and their immobilization in the mycelial matrix: a novel biological approach to nanoparticle synthesis. Nano letters, 1(10), pp.515-519.

Muñoz-García, J., Vázquez, L., Cuerno, R., Sánchez-García, J.A., Castro, M. and Gago, R., 2009. Self-organized surface nanopatterning by ion beam sputtering. Toward Functional Nanomaterials, pp.323-398.

Nagarajan, P.K., Subramani, J., Suyambazhahan, S. and Sathyamurthy, R., 2014. Nanofluids for solar collector applications: a review. Energy Procedia, 61, pp.2416-2434.

Narayanan, K.B. and Sakthivel, N., 2010. Biological synthesis of metal nanoparticles by microbes. Advances in colloid and interface science, 156(1-2), pp.1-13.

Navarro, E., Piccapietra, F., Wagner, B., Marconi, F., Kaegi, R., Odzak, N., Sigg, L. and Behra, R., 2008. Toxicity of silver nanoparticles to Chlamydomonas reinhardtii. Environmental science & technology, 42(23), pp.8959-8964.

Newbury*, D.E. and Ritchie, N.W., 2013. Is scanning electron microscopy/energy dispersive X-ray spectrometry (SEM/EDS) quantitative? Scanning, 35(3), pp.141-168.

Ngoy, J.M., Wagner, N., Riboldi, L. and Bolland, O., 2014. A CO2 capture technology using multi-walled carbon nanotubes with polyaspartamide surfactant. Energy Procedia, 63, pp.2230-2248.

Ning, F., Shao, M., Xu, S., Fu, Y., Zhang, R., Wei, M., Evans, D.G. and Duan, X., 2016. TiO 2/graphene/NiFe-layered double hydroxide nanorod array photoanodes for efficient photoelectrochemical water splitting. Energy & Environmental Science, 9(8), pp.2633-2643.

Ostermann, R., Cravillon, J., Weidmann, C., Wiebcke, M. and Smarsly, B.M., 2011. Metal-organic framework nanofibers via electrospinning. Chemical Communications, 47(1), pp.442-444.

Papell, S.S., 1960. Effect on gaseous film cooling of coolant injection through angled slots and normal holes (Vol. 299). National Aeronautics and Space Administration.

Parashar, M., Shukla, V.K. and Singh, R., 2020. Metal oxide nanoparticles via sol-gel method: a review on synthesis, characterization, and applications. Journal of Materials Science: Materials in Electronics, 31(5), pp.3729-3749.

Patil, M.P. and Kim, G.D., 2018. Marine microorganisms for synthesis of metallic nanoparticles and their biomedical applications. Colloids and Surfaces B: Biointerfaces, 172, pp.487-495.

Patil, N., Bhaskar, R., Vyavhare, V., Dhadge, R., Khaire, V. and Patil, Y., 2021. Overview on methods of synthesis of nanoparticles. International Journal of Current Pharmaceutical Research, 13(2), pp.11-16.

Patois, E., Capelle, M.A.H., Palais, C., Gurny, R. and Arvinte, T., 2012. Evaluation of nanoparticle tracking analysis (NTA) in the characterization of therapeutic antibodies and seasonal influenza vaccines: pros and cons. Journal of drug delivery science and technology, 22(5), pp.427-433.

Pérez-Tijerina, E., Pinilla, M.G., Mejía-Rosales, S., Ortiz-Méndez, U., Torres, A. and José-Yacamán, M., 2008. Highly size-controlled synthesis of Au/Pd nanoparticles by inert-gas condensation. Faraday discussions, 138, pp.353-362.

Pérez-Tijerina, E., Pinilla, M.G., Mejía-Rosales, S., Ortiz-Méndez, U., Torres, A. and José-Yacamán, M., 2008. Highly size-controlled synthesis of Au/Pd nanoparticles by inert-gas condensation. Faraday discussions, 138, pp.353-362.

Pimpin, A. and Srituravanich, W., 2012. Review on micro-and nanolithography techniques and their applications. Engineering Journal, 16(1), pp.37-56.

Pradeep, T., 2009. Noble metal nanoparticles for water purification: a critical review. Thin solid films, 517(24), pp.6441-6478.

Praseptiangga, D., Zahara, H.L., Widjanarko, P.I., Joni, I. and Panatarani, C., 2020, May. Preparation and FTIR spectroscopic studies of SiO2-ZnO nanoparticles suspension for the development of carrageenan-based bio-nanocomposite film. In AIP Conference Proceedings (Vol. 2219, No. 1). AIP Publishing.

Priyadarshana, G., Kottegoda, N., Senaratne, A., de Alwis, A. and Karunaratne, V., 2015. Synthesis of magnetite nanoparticles by top-down approach from a high-purity ore. Journal of Nanomaterials, 2015(1), p.317312.

Qi, M., Zhang, K., Li, S., Wu, J., Pham-Huy, C., Diao, X., Xiao, D. and He, H., 2016. Superparamagnetic Fe 3 O 4 nanoparticles: synthesis by a solvothermal process and

functionalization for a magnetic targeted curcumin delivery system. New Journal of Chemistry, 40(5), pp.4480-4491.

Qi, P., Zhang, D. and Wan, Y., 2013. Sulfate-reducing bacteria detection based on the photocatalytic property of microbial synthesized ZnS nanoparticles. Analytica Chimica Acta, 800, pp.65-70.

Rad, A.G., Abbasi, H. and Afzali, M.H., 2011. Gold nanoparticles: synthesizing, characterizing, and reviewing novel applications in recent years. Physics Procedia, 22, pp.203-208.

Rajeshkumar, S., Ponnanikajamideen, M., Malarkodi, C., Malini, M. and Annadurai, G., 2014. Microbe-mediated synthesis of antimicrobial semiconductor nanoparticles by marine bacteria. Journal of Nanostructure in Chemistry, 4, pp.1-7.

Rangel-Olivares, F.R., Arce-Estrada, E.M. and Cabrera-Sierra, R., 2021. Synthesis and characterization of polyaniline-based polymer nanocomposites as anti-corrosion coatings. Coatings, 11(6), p.653.

Rao, J.P. and Geckeler, K.E., 2011. Polymer nanoparticles: Preparation techniques and size-control parameters. Progress in polymer science, 36(7), pp.887-913.

Rassaei, L., Marken, F., Sillanpää, M., Amiri, M., Cirtiu, C.M. and Sillanpää, M., 2011. Nanoparticles in electrochemical sensors for environmental monitoring. TrAC Trends in Analytical Chemistry, 30(11), pp.1704-1715.

Reiss, G. and Hütten, A., 2005. Applications beyond data storage. Nature Materials, 4(10), pp.725-726.

Rocha, F.S., Gomes, A.J., Lunardi, C.N., Kaliaguine, S. and Patience, G.S., 2018. Experimental methods in chemical engineering: Ultraviolet-visible spectroscopy—UV-Vis. The Canadian Journal of Chemical Engineering, 96(12), pp.2512-2517.

Saeed, K. and Khan, I., 2014. Preparation and properties of single-walled carbon nanotubes/poly (butylene terephthalate) nanocomposites. Iranian Polymer Journal, 23, pp.53-58.

Saeed, K. and Khan, I., 2016. Preparation and characterization of single-walled carbon nanotube/nylon 6, 6 nanocomposites. Instrumentation Science & Technology, 44(4), pp.435-444.

Sagadevan, S., 2015. A review on role of nanofluids for solar energy applications. American Journal of Nano Research and Applications, 8(2), pp.53-61.

Saldarriaga, J.F., Aguado, R., Pablos, A., Amutio, M., Olazar, M. and Bilbao, J., 2015. Fast characterization of biomass fuels by thermogravimetric analysis (TGA). Fuel, 140, pp.744-751.

Salem, S.S. and Fouda, A., 2021. Green synthesis of metallic nanoparticles and their prospective biotechnological applications: an overview. Biological trace element research, 199(1), pp.344-370.

Salopek, B., Krasic, D. and Filipovic, S., 1992. Measurement and application of zeta-potential. Rudarsko-geolosko-naftni zbornik, 4(1), p.147.

Sawai, J., 2003. Quantitative evaluation of antibacterial activities of metallic oxide powders (ZnO, MgO, and CaO) by conductimetric assay. Journal of microbiological methods, 54(2), pp.177-182.

Schröfel, A., Kratošová, G., Šafařík, I., Šafaříková, M., Raška, I. and Shor, L.M., 2014. Applications of biosynthesized metallic nanoparticles–a review. Acta biomaterialia, 10(10), pp.4023-4042.

Siddique, S. and Chow, J.C., 2020. Gold nanoparticles for drug delivery and cancer therapy. Applied Sciences, 10(11), p.3824.

Sigmund, W., Yuh, J., Park, H., Maneeratana, V., Pyrgiotakis, G., Daga, A., Taylor, J. and Nino, J.C., 2006. Processing and structure relationships in electrospinning of ceramic fiber systems. Journal of the American Ceramic Society, 89(2), pp.395-407.

Singh, R.P., Shukla, V.K., Yadav, R.S., Sharma, P.K., Singh, P.K. and Pandey, A.C., 2011. Biological approach of zinc oxide nanoparticles formation and its characterization. Adv. Mater. Lett, 2(4), pp.313-317.

Slavin, Y.N., Asnis, J., Hńfeli, U.O. and Bach, H., 2017. Metal nanoparticles: understanding the mechanisms behind antibacterial activity. Journal of Nanobiotechnology, 15, pp.1-20.

Song, U. and Kim, J., 2020. Zinc oxide nanoparticles: a potential micronutrient fertilizer for horticultural crops with little toxicity. Horticulture, Environment, and Biotechnology, 61(3), pp.625-631.

Sowani, H., Mohite, P., Munot, H., Shouche, Y., Bapat, T., Kumar, A.R., Kulkarni, M. and Zinjarde, S., 2016. Green synthesis of gold and silver nanoparticles by an actinomycete Gordonia amicalis HS-11: mechanistic aspects and biological application. Process Biochemistry, 51(3), pp.374-383.

Sriram, M.I., Kalishwaralal, K., Barathmanikanth, S. and Gurunathani, S., 2012. Size-based cytotoxicity of silver nanoparticles in bovine retinal endothelial cells. Nanoscience Methods, 1(1), pp.56-77.

Stoimenov, P.K., Klinger, R.L., Marchin, G.L. and Klabunde, K.J., 2002. Metal oxide nanoparticles as bactericidal agents. Langmuir, 18(17), pp.6679-6686.

Su, S.S. and Chang, I., 2018. Review of production routes of nanomaterials. Commercialization of nanotechnologies–a case study approach, pp.15-29.

Sukumar, S., Rudrasenan, A. and Padmanabhan Nambiar, D., 2020. Green-synthesized rice-shaped copper oxide nanoparticles using Caesalpinia bonducella seed extract and their applications. ACS omega, 5(2), pp.1040-1051.

Sun, T., Zhang, Y.S., Pang, B., Hyun, D.C., Yang, M. and Xia, Y., 2021. Engineered nanoparticles for drug delivery in cancer therapy. Nanomaterials and Neoplasms, pp.31-142.

Taniguchi, N., 1974. On the basic concept of nanotechnology. In Proc. Intl. Conf. Prod. Eng. Tokyo, Part II, 1974. Japan Society of Precision Engineering.

Theron, J., Eugene Cloete, T. and de Kwaadsteniet, M., 2010. Current molecular and emerging nanobiotechnology approaches for the detection of microbial pathogens. Critical reviews in microbiology, 36(4), pp.318-339.

Thomas, R., Janardhanan, A., Varghese, R.T., Soniya, E.V., Mathew, J. and Radhakrishnan, E.K., 2014. Antibacterial properties of silver nanoparticles synthesized by marine Ochrobactrum sp. Brazilian Journal of Microbiology, 45, pp.1221-1227.

Titus, D., Samuel, E.J.J. and Roopan, S.M., 2019. Nanoparticle characterization techniques. In Green synthesis, characterization and applications of nanoparticles (pp. 303-319). Elsevier.

Tran, V. and Wen, X., 2014. Rapid prototyping technologies for tissue regeneration. Rapid prototyping of biomaterials, pp.97-155.

Tranquada, J.M., Sternlieb, B.J., Axe, J.D., Nakamura, Y. and Uchida, S.I., 1995. Evidence for stripe correlations of spins and holes in copper oxide superconductors. nature, 375(6532), pp.561-563.

Uzair, B., Liaqat, A., Iqbal, H., Menaa, B., Razzaq, A., Thiripuranathar, G., Fatima Rana, N. and Menaa, F., 2020. Green and cost-effective synthesis of metallic nanoparticles by algae: Safe methods for translational medicine. Bioengineering, 7(4), p.129.

Viswanathan, M., Arumugam, S. and Thangavel, B., 2016. In vitro anticancer activity of silver nanoparticles synthesized by Escherichia coli VM1 isolated from marine sediments of encore southeast coast of India. Enzyme and Microbial Technology, 95, pp.146-154.

Vorokhta, M., Khalakhan, I., Vondráček, M., Tomeček, D., Marešová, E., Nováková, J., Vlček, J., Fitl, P., Novotný, M., Hozák, P. and Lančok, J., 2018. Investigation of gas sensing mechanism of SnO2-based chemiresistor using near ambient pressure XPS. Surface Science, 677, pp.284-290.

Weissleder, R., Bogdanov, A., Neuwelt, E.A. and Papisov, M., 1995. Long-circulating iron oxides for MR imaging. Advanced Drug Delivery Reviews, 16(2-3), pp.321-334.

Wiesendanger, R. and Güntherodt, H.J. eds., 2013. Scanning tunneling microscopy III: Theory of STM and related scanning probe methods (Vol. 29). Springer Science & Business Media.

Wu, W., He, Q. and Jiang, C., 2008. Magnetic iron oxide nanoparticles: synthesis and surface functionalization strategies. Nanoscale research letters, 3, pp.397-415.

Xia, T., Kovochich, M., Liong, M., Madler, L., Gilbert, B., Shi, H., Yeh, J.I., Zink, J.I. and Nel, A.E., 2008. Comparison of the mechanism of toxicity of zinc oxide and cerium oxide nanoparticles based on dissolution and oxidative stress properties. ACS nano, 2(10), pp.2121-2134.

Xu, J.F., Ji, W., Shen, Z.X., Tang, S.H., Ye, X.R., Jia, D.Z. and Xin, X.Q., 1999. Preparation and characterization of CuO nanocrystals. Journal of Solid-State Chemistry, 147(2), pp.516-519.

Yadav, R., Dwivedi, S., Kumar, S. and Chaudhury, A., 2010. Trends and perspectives of biosensors for food and environmental virology. Food and Environmental Virology, 2, pp.53-63.

Yadav, T.P., Yadav, R.M. and Singh, D.P., 2012. Mechanical milling: a top-down approach for the synthesis of nanomaterials and nanocomposites. Nanoscience and Nanotechnology, 2(3), pp.22-48.

Ye, Q., Chen, W., Huang, H., Tang, Y., Wang, W., Meng, F., Wang, H. and Zheng, Y., 2020. Iron and zinc ions, potent weapons against multidrug-resistant bacteria. Applied Microbiology and Biotechnology, 104, pp.5213-5227.

Young, K.J., Martini, L.A., Milot, R.L., Snoeberger III, R.C., Batista, V.S., Schmuttenmaer, C.A., Crabtree, R.H. and Brudvig, G.W., 2012. Light-driven water oxidation for solar fuels. Coordination chemistry reviews, 256(21-22), pp.2503-2520.

Yuan, P., Ding, X., Yang, Y.Y. and Xu, Q.H., 2018. Metal nanoparticles for diagnosis and therapy of bacterial infection. Advanced Healthcare Materials, 7(13), p.1701392.

Zahra, Z., Habib, Z., Chung, S. and Badshah, M.A., 2020. Exposure route of TiO2 NPs from industrial applications to wastewater treatment and their impacts on the agro-environment. Nanomaterials, 10(8), p.1469.

Zan, G. and Wu, Q., 2016. Biomimetic and bioinspired synthesis of nanomaterials/nanostructures. Advanced Materials, 28(11), pp.2099-214.

Zhang, X., Shao, C., Zhang, Z., Li, J., Zhang, P., Zhang, M., Mu, J., Guo, Z., Liang, P. and Liu, Y., 2012. In situ generation of well-dispersed ZnO quantum dots on electrospun silica nanotubes with high photocatalytic activity. ACS Applied Materials & Interfaces, 4(2), pp.785-790.

Zhang, X., Yan, S., Tyagi, R.D. and Surampalli, R.Y., 2011. Synthesis of nanoparticles by microorganisms and their application in enhancing microbiological reaction rates. Chemosphere, 82(4), pp.489-494.

Zheng, Z., Zhang, X., Carbo, D., Clark, C., Nathan, C.A. and Lvov, Y., 2010. Sonication-assisted synthesis of polyelectrolyte-coated curcumin nanoparticles. Langmuir, 26(11), pp.7679-7681.

Zhou, Y., Dong, C.K., Han, L.L., Yang, J. and Du, X.W., 2016. Top-down preparation of active cobalt oxide catalyst. ACS Catalysis, 6(10), pp.6699-6703.

Zhu, Y.U.A.N., Goodridge, A.G. and Stapleton, S.R., 1994. Zinc, vanadate, and selenate inhibit the tri-iodothyronine-induced expression of fatty acid synthase and malic enzyme in chick-embryo hepatocytes in culture. Biochemical Journal, 303(1), pp.213-216.

Zhuang, J., and Gentry, R. W. (2011). "Environmental application and risks of nanotechnology: a balanced view," in Biotechnology and Nanotechnology Risk Assessment: Minding and Managing the Potential Threats around Us, eds S. Ripp and T. Henry (Washington, DC: ACS Publications), 41–67. doi: 10.3390/ijerph16234848.

CHAPTER 5

Zinc Oxide nanoparticle assisted refolding of alkali denatured bovine β-lactoglobulin: A useful technique for protein renaturation.

5.1. Introduction

Proteins are widely utilized as crucial components in various food and drug industries. Extensive research has focused on the processing and stabilization of proteins in solutions (Clark, 2001; Fu et al., 2000). While proteins naturally maintain their functional and soluble state under physiological conditions, they exhibit a propensity to aggregate in diverse environmental contexts. In vivo, protein aggregation is associated with several neurodegenerative diseases and metabolic disorders, with aggregated proteins assuming the structure of amyloid fibrils (Hartl, 2017; Stefani and Dobson, 2003). The intricate process of protein folding within biological cells occurs within a crowded molecular environment and is facilitated by molecular chaperones. In living organisms, molecular chaperones play a critical role in regulating the folding and unfolding of proteins, helping them attain their natural structures from partially folded states. By interacting with hydrophobic residues and balancing internal charges, these chaperones not only capture the initially formed unfolded protein structure but also prevent the irreversible aggregation of proteins during refolding (Ellis, 1987; Hartl et al., 2011). Therefore, studying the folding pathways in vitro to understand the refolding mechanism is of great interest. Identifying and characterizing intermediates in the folding pathway are crucial steps in understanding the folding, stabilization, and function of a protein. Various techniques, such as removing denaturants from the protein solution (Kohyama et al., 2010), controlling physical parameters like pH, temperature, or ionic strength of the solution, or adding refolding agents to the denatured protein solutions (Sakamoto et al., 2004; Singh and Flowers, 2010), are used for renaturing proteins from their solutions.

Bovine beta-lactoglobulin (β-lg), a well-studied globular whey protein commonly found in ruminant milk with a molecular weight of 18.3 kDa, serves as a significant carrier protein for oxidation-sensitive hydrophobic drugs and nutraceuticals owing to its distinct resistance to acidic pH and potential encapsulating properties (Liu et al.,1998). Exposure to elevated temperatures induces a conformational change in the protein, leading to the exposure of its hydrophobic residues and the thiol (SH) group of the Cys121 residue (Yagi et al., 2003).

Consequently, β-lg is commonly utilized as a model protein for investigating the aggregation and folding/unfolding phenomenon of proteins. Furthermore, it is soluble in water, comprising nine anti-parallel β-strands and one α-helix segment, with its hydrophobic chains predominantly buried (Brownlow et al., 1997).

Different methods such as temperature (Jones et al., 1998), a combination of heat and pressure (Zhong et al., 2011), high-intensity ultrasound (Stanic-Vucinic et al., 2012), microwave radiation (Grar et al., 2009), and enzymatic hydrolysis (Ena et al., 1995) have been found to be capable of destroying or altering the epitopes in β-lg. The pH level of the medium significantly influences the structure of β-lg. Specifically, at pH 3, bovine β-lg undergoes dimerization, resulting in a slight alteration of its structure (Kontopidis et al., 2002). Additionally, below pH 3.0, the dimer dissociates into monomers while maintaining their native structure (Eigel et al., 1984). Notably, within the pH range of 4.0 to 5.0, β-lg undergoes a transition from dimers to octamers, as determined by optical rotatory dispersion (ORD) measurements (Pessen et al., 1985). It is worth noting that structural changes occurring between pH 2.0 and pH 9.0 do not result in any appreciable alterations in the native-like β-barrel conformation of β-lg (Blanch et al., 1999). However, above pH 9, β-lg experiences irreversible, base-induced unfolding, leading to significant disruptions in both secondary and tertiary structures (Waissbluth and Grieger., 1974). The relaxation of the globular structure under alkaline pH impacts the accessibility of β-lg to tyrosinase-induced oxidation and subsequent cross-linking. This loss of native structure resulting from any external influence leads to the formation of amorphous or fibril-like aggregates.

In recent years, there has been remarkable progress in the study of nanomaterials, driven by their exceptional properties and diverse potential applications. These applications encompass biosensing (Sudhagar et al., 2011), biolabeling (Lin et al., 2007), therapy (Brannon-Peppas and Blanchette, 2004), and tissue engineering (Goldberg et al., 2007). Within this context, a range of synthetic chaperones has been developed, including polymers (Ma et al., 2017), metallic nanoparticles (NPs) (De and Rotello, 2008), silica NPs (Wang et al., 2007), and self-assembled nanostructures (Takahashi et al., 2011; Kameta et al., 2012). Notably, porous nanoparticles have exhibited great promise in delivering biomolecules such as proteins (Han et al., 2014) and plasmid DNA (Kim et al., 2011) to target cells due to their expansive surface area, adjustable pore size, and customizable surface modifications. Excitingly, there has been a growing focus on leveraging multifunctional synthetic nano-chaperones for peptide folding and facilitating intracellular delivery (Park et al., 2022). The changes in protein structure and function depend

significantly on both the nature of the adsorbed protein and the physicochemical properties of the solid surfaces. For example, ribonuclease A unfolds and loses stability when adsorbed on silica nanoparticle surfaces (Shang et al., 2007), while no significant change in the structure and stability of cytochrome-C has been observed when it interacts with zinc oxide nanoparticles (Šimšíková and Antalík, 2013). Recent reports indicate that certain nanomaterials can induce the formation of protein-based aggregates or catalyze the formation of protein fibrils by modifying the protein structure and leading to the growth of extended assemblies (Linse et al., 2007; Zhang et al., 2009). It has been observed that proteins at the nanoparticle surface are partially unfolded. These nanoparticle-induced unfolded proteins likely catalyze the observed aggregate formation and growth. Our research group has reported the stabilizing effect of negatively charged gold nanoparticles (NP) on the monomeric structure of bovine β-lg, thereby inhibiting its thermal unfolding and aggregation (Sardar et al., 2014). Additionally, our fluorescence and dynamic light scattering (DLS) studies have demonstrated the refolding of thermally unfolded GFP at 100°C by ZnO nanoparticles (Pandurangan et al., 2016). Furthermore, our investigation revealed that thermally inactivated α-amylase regained 65% of its residual activity upon incubation with unmodified TiO2 NPs (Ahmad et al., 2013). Certain NPs, such as a combination of ZnO with gold and silver NPs, are recognized for their low toxicity and high biocompatibility, making them suitable for various biomedical and pharmaceutical applications (Rasmussen et al., 2010). However, limited research has been conducted on the alkaline unfolded states of bovine β-lg around pH 11-12, where the tyrosine residues of the protein remain deprotonated. Given this, our current study focuses on examining the interaction between ZnO nanoparticles and bovine β-lg. Additionally, we are investigating the potential application of ZnO nanoparticles as artificial chaperones in the refolding of β-lg stressed under alkaline conditions.

5.2. Materials And Methods

5.2.1. Reagents and Chemicals Required

Sodium dihydrogen phosphate, zinc acetate, potassium hydroxide (KOH), and methanol were sourced from Merck in Mumbai, India. Acrylamide, bisacrylamide, N, N, N', N'-tetramethylethylenediamine (TEMED), ammonium persulfate (APS), sodium dodecyl sulfate (SDS), bromophenol blue, and Coomassie brilliant blue were purchased from Sigma-Aldrich. Various fluorescent probes, including 8-anilinonaphthalene-1-sulfonic acid ammonium salt (ANS), Congo red (CR), and Thioflavin T (ThT), were acquired from Sigma Chemical Co. in

St. Louis, USA, and used without further purification. All other chemicals used were of the highest available purity. All buffer solutions were filtered through a 0.22 mm syringe filter from Millipore in the USA.

5.2.2. Isolation and purification of bovine beta-lactoglobulin (β-lg).

Bovine beta-lactoglobulin (β-lg) was extracted and purified from cow's milk using the method outlined by Aschaffenburg and Drewry (Aschaffenburg and Drewry, 1957). The final product was freeze-dried and stored at 4°C. To prepare the spectroscopic samples, β-lg was weighed and dissolved in a 0.01 M sodium phosphate buffer solution at pH 7.4. Protein stock solutions were then prepared using the same phosphate buffer at pH 7.4. Different concentrations of protein samples were created by dissolving β-lg in Milli-Q water and measuring the optical density at 280 nm, taking into account the known extinction coefficient of β-lg (0.96 mg^{-1} mL^{-1} cm^{-1} at 280 nm).

5.2.3. Preparation of zinc oxide nanoparticles (ZnO NPs)

Zinc oxide (ZnO) nanoparticles (NPs) were successfully synthesized in accordance with a previously reported method (Pourrahimi et al., 2014). The glassware utilized in this synthesis underwent a meticulous cleaning process involving aqua regia (nitric acid: hydrochloric acid 1:3) followed by thorough rinsing with milli-Q water and subsequent drying in an oven. The primary objective of this study was to meticulously investigate the synthesis and optical characterization of Zinc Oxide (ZnO) nanoparticles using a precise combination of Zinc acetate, potassium hydroxide (KOH), and methanol as chemical reagents. The synthesis procedure commenced by dissolving 0.8977g of KOH into 100 mL of methanol, a process that involved heating the solution to 60°C to ensure the attainment of a uniform mixture. Subsequently, a specific solution of 2.107 g of zinc acetate dihydrate in 60 mL of deionized water was meticulously prepared. The introduction of the Zn solution into the KOH solution, coupled with vigorous stirring at 60°C for a duration of 90 minutes, yielded a well-dissolved solution. The resulting solution was then carefully divided into three equitably-sized portions for further investigation.

The properties of the ZnO particles were determined using the first part as a reference. The second and third parts underwent a modified Meulekamp washing method, which utilized methanol as the dispersing agent and a centrifuge to remove byproducts (Alvarado et al., 2013). This washing and redispersion process was repeated three times to obtain pure ZnO NPs. A meticulous process was followed to comprehensively characterize the product. At each stage,

the solvent was carefully removed by heating it to 60°C until a white, dry powder containing the ZnO nanoparticles was obtained. The product was then subjected to thorough analysis using powder diffraction, with a D8 diffractometer utilized for crystal phase identification. Scherrer's formula was used to precisely estimate the average crystalline sizes. The purity of the ZnO NPs was confirmed through the repeated washing and redispersion method.

The UV-visible spectroscopic characterization of ZnO NPs was conducted at room temperature. The optical absorption spectra in the wavelength range of 200-600 nm were acquired in the presence and absence of the β-lg sample using a Shimadzu-TCC 240 A UV-Vis spectrophotometer. The characteristic signal of ZnO NPs was detected at 365 nm, thereby confirming the formation of ZnO NPs with a diameter of 30 nm. This finding was further validated by the XRD study. Moreover, the absorption band of ZnO NPs exhibited a notable shift in the presence of β-lg **(**Alvarado et al., 2013).

5.2.4. Electrophoresis measurement

The sodium dodecyl sulfate-polyacrylamide gel electrophoresis (SDS-PAGE) was conducted under non-reducing conditions using a 15% acrylamide resolving gel as per Laemmli's method (Laemmli,1970). Samples of β-lg solution (2.5 mg/ml) in 10 mM sodium phosphate buffer at pH 7.4, and at pH 11.0, were separately treated in the presence and absence of ZnO NPs. The resulting solutions underwent filtration using a syringe filter with a 0.2mm membrane. Subsequently, 20 µl aliquots of heat-treated β-lg solution with and without ZnO NPs were loaded into the wells, along with 30 µl of native β-lg solution (2.5 mg ml-1) in a separate well. Electrophoretic separations were conducted using a maximum 100-volt application for 1 hour. Post separation, the gel was stained with Coomassie Brilliant Blue R-250 and destained using a solution containing methanol and acetic acid.

5.2.5. UV-visible spectroscopy

The UV-visible JASCO spectrophotometer (Model V-730, Serial No. B184461798) and JASCO Spectra Manager Software were employed to acquire absorption spectra for the evaluation of binding affinity and binding constant at a standard temperature of 25°C. This experiment utilized two PerkinElmer quartz cells with a 1 cm path length for both the reference and samples. The absorbance measurements captured the intensity vs. wavelength spectra over the 200-600 nm range. A 10 mm phosphate buffer at pH 7.4 served as the reference, and the sample solutions exhibited a concentration of 13 µM.

5.2.6. ANS fluorescence study to monitor the change in hydrophobicity

8-Anilinonaphthalene-1-sulfonic acid (ANS) is utilized to gauge the surface hydrophobicity of protein molecules. A stock solution of 1 mg/ml ANS sample was prepared using Milli-Q water. In our study, to maintain a 50-molar excess of ANS compared to the protein concentration, 30 µl of ANS solution was added to each sample. ANS Fluorescence Measurements were carried out using a Horiba Fluorometer (Serial No: 1734D-4018-FM, Model: Fluoromax-4C). The samples were excited at 385 nm in a 1 cm pathlength four-sided transparent rectangular quartz cell. The emission and excitation slit widths were 5 nm, and the ANS fluorescence emission spectra were recorded from 395 nm to 600 nm using the Fluoromax Software. Each spectrum was blank-corrected, and the data points represented the average of triplicate measurements (Cattoni et al., 2009).

5.2.7. Dynamic light scattering (DLS) measurements

In solution, the diffusion of minute particles results in variations in the intensity of scattered light. Dynamic Light Scattering (DLS) leverages an autocorrelator on a microsecond time scale to discern these variations and analyze molecular distribution. Utilizing the Zetasizer Nano (Malvern Instrument, UK), DLS assessments were executed on native β-lg solutions under differing ZnO NPs presence states, achieved by exposing samples to a 633-nm laser (Yu et al., 2007). Sample solutions, with a 20 µM β-lg concentration at room temperature, were contained within a 2 mL transparent rectangular quartz cuvette with a path length of 10 mm. The acquisition of the time-dependent autocorrelation function was derived from 12 acquisitions per run, and the reported data represents the mean of three consecutive observations.

5.2.8 Transmission Electron Microscopy

High-resolution transmission electron microscopy (HR TEM) imaging was performed to analyze the behavior of β-lg in the presence and absence of ZnO nanoparticles. The imaging was carried out using a JEOL HRTEM-2011 instrument from Tokyo, Japan, at various magnifications (Hoppenreijs et al., 2022). Prior to the study, the sample solutions were centrifuged and diluted. These diluted solutions were then carefully drop-cast onto a carbon-coated copper grid with a mesh size of 300C from Pro Sci Tech. After 20 seconds, excess solution was removed by gently shocking the grid on a filter paper. Subsequently, a 2% uranyl acetate solution from Sigma was added to stain the sample, and the grids were left to air-dry overnight in a desiccator. Once dried, the grids were ready for TEM imaging at a specific magnification.

5.2.9. Circular dichroism (CD) spectroscopy

To investigate the potential impact of zinc oxide nanoparticles (ZnO NPs) on the structure of β-lg, we conducted circular dichroism measurements using a Jasco Spectropolarimeter (J-815) at 20 °C in the far-UV range (200–260 nm) with rectangular cells of 1mm and 10 mm path length. The tests were performed on native β-lg solutions at pH 7.4 with concentrations of 0.25 mg ml-1, both in the presence and absence of ZnO NPs, as well as at pH 11.0. All spectra were the averages of three scans, and the final spectrum was obtained after subtracting the corresponding solvent spectrum. The far UV-CD curves were analyzed using the CDNN 2.1 curve-fitting program to determine the percentages of secondary structures present in β-lg under different conditions.

5.2.10. Field emission scanning electron microscopy (FESEM)

The physical characteristics of the synthesized ZnO NPs, specifically their shape and size, were investigated using a Hitachi S-4800 field emission scanning electron microscope (FESEM) at an operating voltage of 20 kV. To prepare the samples for analysis, each solution was thinned with ethanol to create a thin film on carbon tape. The prepared samples were then placed in a vacuum desiccator to allow for evaporation. Finally, the dried samples underwent a gold-coating process before being subjected to FESEM analysis.

5.2.11 Fourier-Transform Infrared (FT-IR) measurements

The vibration bands known as Amide I at 1600-1700 cm^{-1} and Amide II in the range of 1480-1570 cm^{-1} are essential for characterizing the secondary structures of native β-lg when in the presence of ZnO NPs, as observed in FT-IR spectra. These bands are valuable for identifying any changes in the structure of β-lg influenced by the presence of ZnO NPs. We conducted our analysis using a Spectrum 100 FT-IR spectrometer (Perkin-Elmer) and measured the infrared absorption spectra of the samples at room temperature (25°C) with a resolution of 2 cm^{-1}. Throughout our study, we consistently maintained β-lg concentrations at 500 μM in each sample and recorded the data in the range of 1500-1700 cm^{-1} (Banerjee and Das, 2012).

5.3. Results And Discussion

5.3.1. UV-Visible Spectroscopy

The ZnO nanoparticles underwent thorough analysis of their optical characteristics using UV-Vis spectroscopy at room temperature, as illustrated in **(Fig.1)**. The obtained results showcased

a prominent absorption feature within the ultraviolet range, spanning from 200 to 400 nm. Notably, the absorption peak, centered around 365 nm, revealed the excitonic behavior of ZnO at room temperature. This observation aligns with prior research on the optical properties of ZnO nanoparticles, underscoring the significance of understanding their features for diverse applications in the realm of nanotechnology (Singh et al., 2011). Furthermore, the confirmation of the synthesized ZnO nanoparticles was achieved through meticulous SEM and TEM studies.

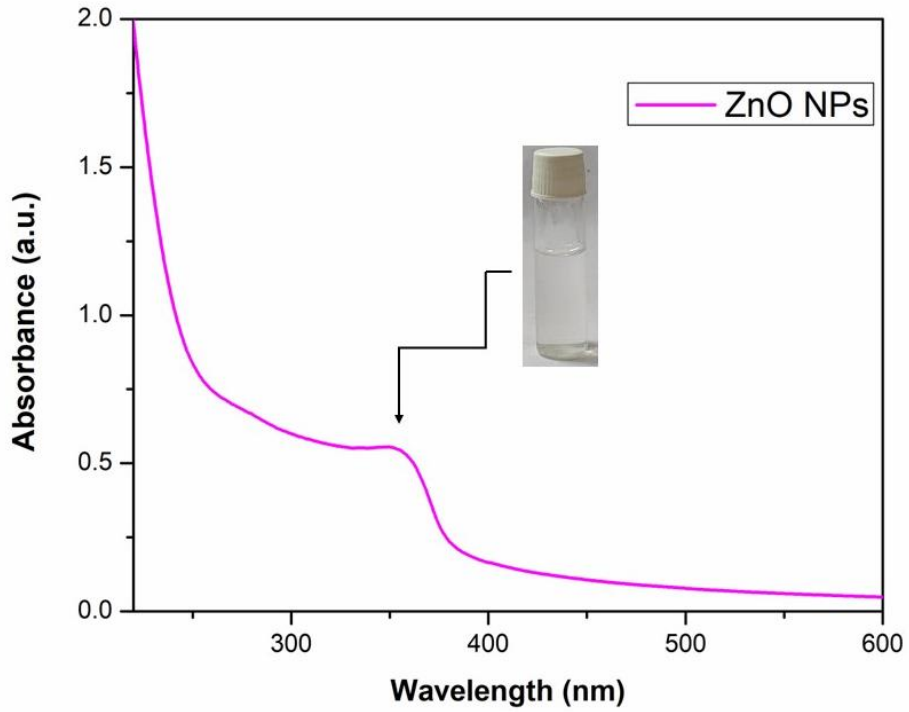

Figure 1: UV-VIS absorption spectrum of synthesized ZnO NPs.

Beta-lactoglobulin (β-Lg) is known for its unique UV-visible spectra, which can be attributed to the presence of chromophores with an aromatic nucleus conjugated with groups having varying electronic effects. The native β-Lg displays a characteristic protein band due to tryptophan residues, with a maximum wavelength (λmax) of 280 nm, as depicted in **(Fig.2)**. Any changes in the UV-visible spectrum of native β-Lg can signify alterations in the micro-environment surrounding the chromophores, as reported in the literature (Yu et al., 2007). These findings suggest that the micro-environment of β-lactoglobulin changes in the presence of ZnO nanoparticles. ZnO nanoparticles interact with β-lactoglobulin to different extents, leading to modifications in the micro-environment of the protein around its tryptophan (Trp) and tyrosine (Tyr) residues. These resultant structural modifications of the protein manifest in the UV-absorbance of β-lactoglobulin.

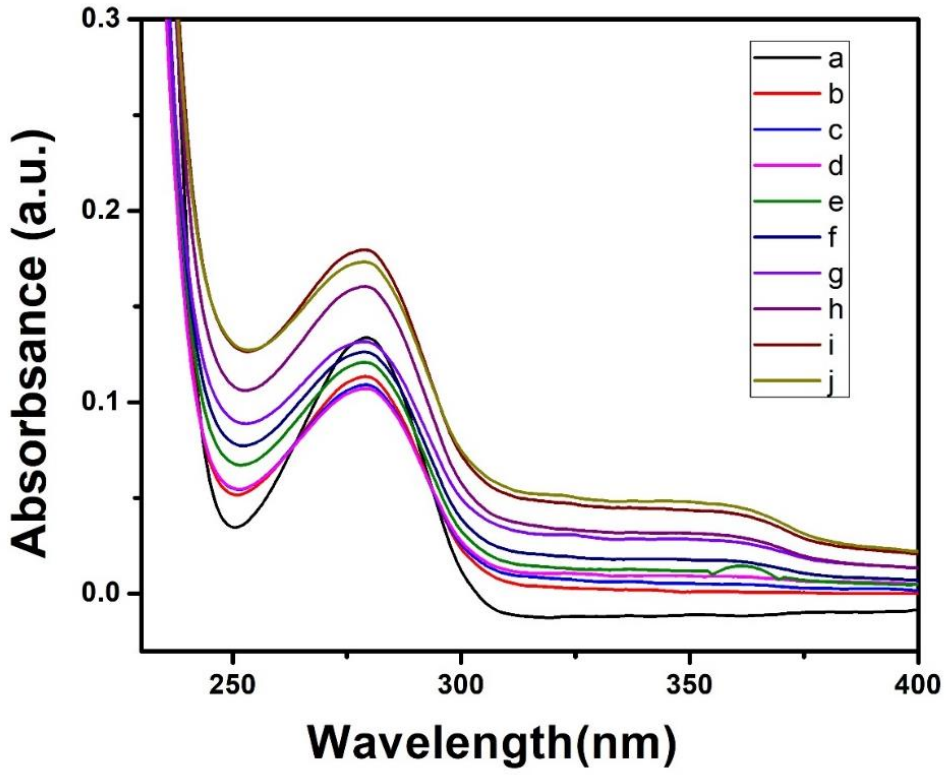

Figure 2: The UV-VIS spectrum of native β-lg at physiological pH (a), as well as at pH 11 (b), and with ZnO nanoparticle treatment at pH 11 (c-j), was measured. The concentration of the nanoparticles gradually increased from 10 μM to 150 μM. The concentration of β-lg was kept constant at 0.25 mg/ml throughout the UV-VIS measurement.

5.3.2. Powdered XRD Spectra

The X-ray diffraction (XRD) pattern gathered from the sample clearly indicates the presence of well-defined crystalline ZnO nanoparticles. The XRD spectra exhibit prominent diffraction peaks at 31, 34, 36, 47, 56, 62, 66, 67, and 68 degrees of 2θ, corresponding to the (100), (002), (101), (102), (110), (103), (200), (112), and (201) crystal planes, respectively **(Fig.3)**. These findings are consistent with the JCPDS file 36145, suggesting a hexagonal wurtzite structure of ZnO with space group P63 mc. The lattice parameters are determined to be a = b = 3.249 Å and c = 5.206 Å (Singh et al., 2011).

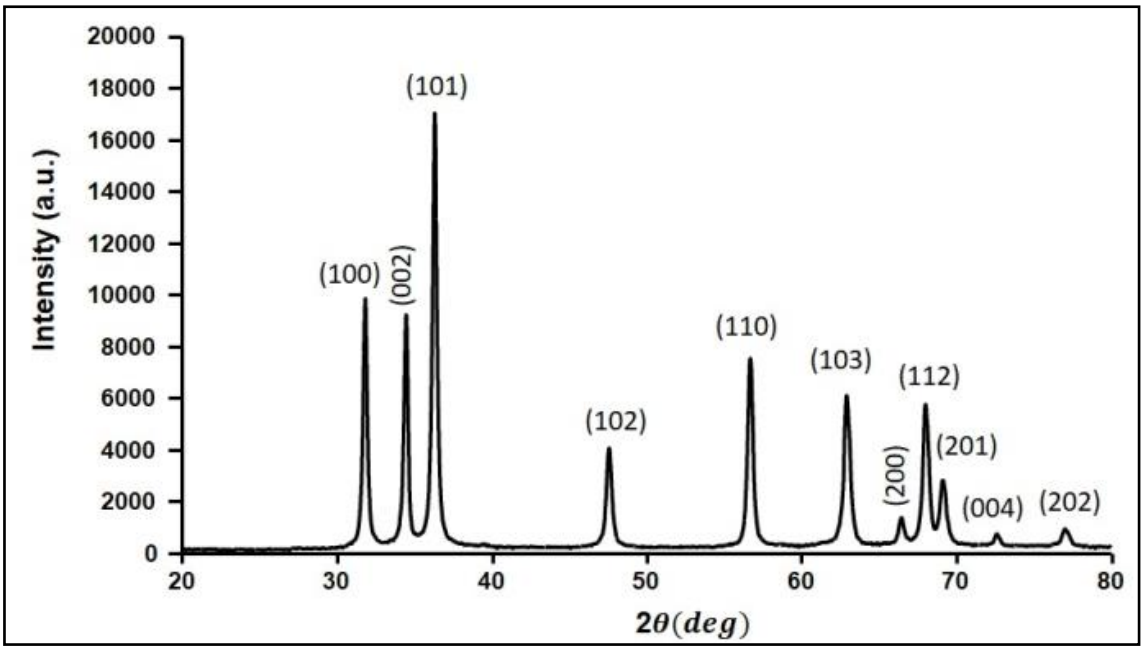

Figure 3: XRD pattern of synthesized ZnO nanoparticles.

5.3.3. Scanning Electron Microscopy (SEM)

The Scanning Electron Microscopy (SEM) image depicted in **(Fig.4)** illustrates the distinctive spherical and granular morphology of the particles, characterized by dimensions within the nanoscale range. This observation provides valuable insights into the intricate structural composition of the particles and their potential implications for material properties and applications.

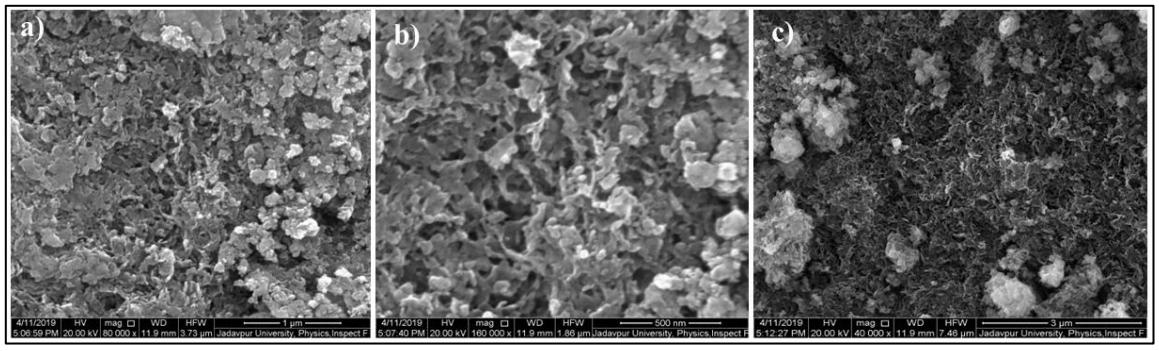

Figure 4: SEM picture of synthesized ZnO NPs.

5.3.4. ANS Fluorescence Study

The current research is focused on investigating the molten globule state of β-lg by employing ANS binding to the protein's hydrophobic region. When the protein is under physiological pH, there is a noticeable increase in fluorescence intensity, as indicated by the black line in **(Fig.5)**. Conversely, at pH 11, the fluorescence of the native protein experiences a significant decrease,

which suggests a substantial reduction in the availability of hydrophobic patches for ANS binding, as demonstrated by the red line in **(Fig.5)**. Additionally, as ZnO nanoparticles are gradually introduced to the native model protein at pH 11, at concentrations ranging from 25µM to 150µM, there is a progressive increase in fluorescence intensities. This observation suggests a greater availability of hydrophobic patches for ANS binding, illustrated by the blue(sky), green, pink, deep blue, and brown lines in **(Fig.5)**. Notably, the ZnO nanoparticles demonstrate the ability to promote the refolding of the protein in a concentration-dependent manner, as evidenced by the gradual increase in fluorescence intensity.

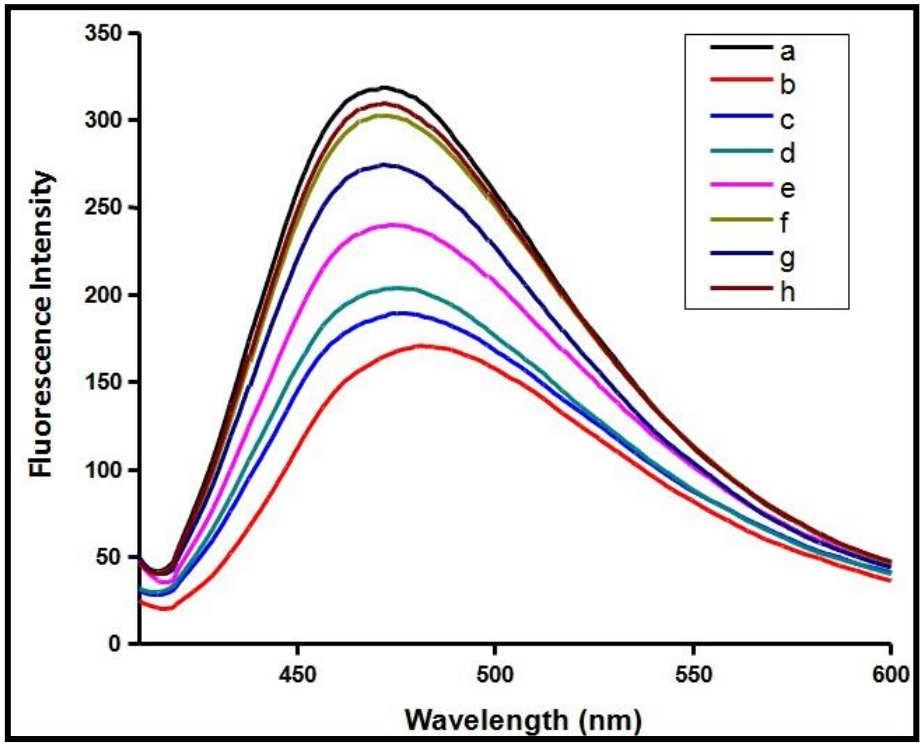

Figure 5: The ANS fluorescence of native β-lg was measured in 10 mM phosphate buffer with a pH of 7.4 and 11(a and b). The excitation was done at a specific wavelength of 380nm and emissions were measured in the range of 400nm-600nm. The fluorescence of ZnO nanoparticles treated with native β-lg of pH11 was represented in Fig.4 (c-h). The concentration of ZnO nanoparticles was varied from 25µM to 150µM. The concentration of protein was maintained at 0.25mg/ml throughout the ANS measurement.

5.3.5. Secondary structural change monitored by Circular Dichroism (CD)

This study is conducted to investigate the variations in the secondary structure of the native protein β-lg under diverse conditions, specifically in 10mM phosphate buffer at physiological pH, pH 11, and pH 11 following treatment with ZnO nanoparticles at room temperature. At physiological pH, the native β-lg protein exhibits a negative MRE value on the CD plot at

wavelength maxima of 214nm-216nm, indicative of a predominance of beta-sheet structure. Contrastingly, at pH 11, the native β-lg demonstrates a more negative MRE value with wavelength maxima of 212nm-216nm, signifying an augmentation in beta-sheet structures and a diminution in alpha-helices and beta-turn structures. This escalation in beta-sheet structure is ascribed to the reduction of alpha-helices, identifiable when β-lg is subjected to ZnO nanoparticle treatment.

The findings indicate that the introduction of zinc oxide (ZnO) nanoparticles significantly impacts the physicochemical characteristics of β-lactoglobulin (β-lg). This revelation holds substantial potential for the advancement of novel nanomaterials intended for use in food and biotechnology domains.

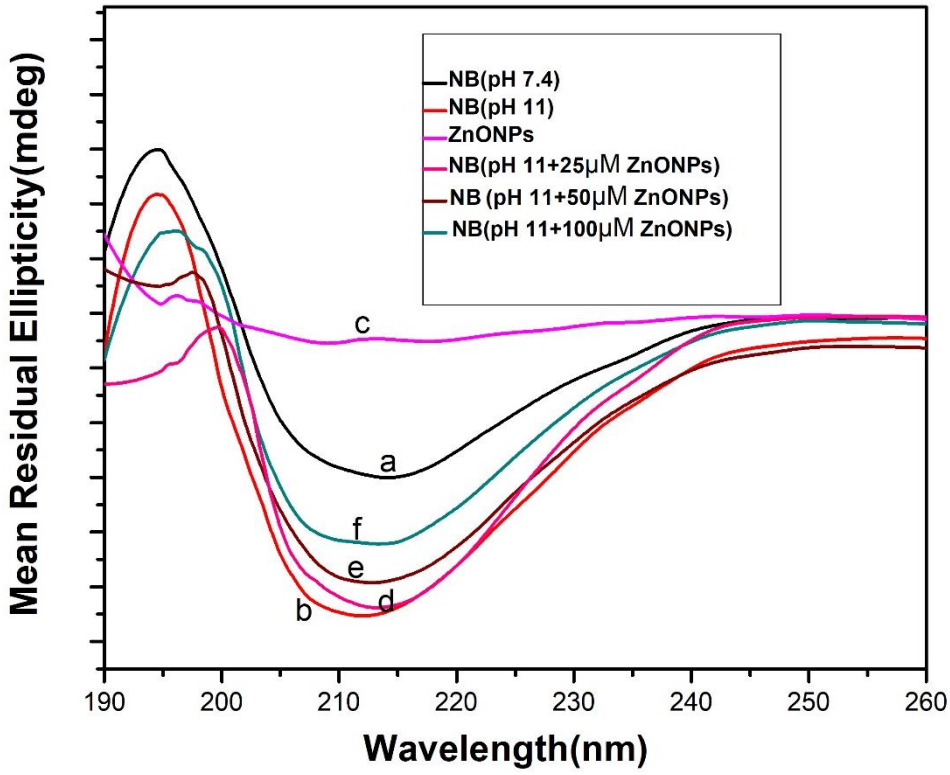

Figure 6: Far UV-CD spectra of native β-lg at physiological pH (a), as well as at pH11(b), with ZnO nanoparticle treatment at pH11(d-f). The concentration of the nanoparticles gradually increased from 25μM to 100μM. The CD plot of only 200μM ZnO nanoparticles is indicated by the pink line (i). The concentration of β-lg was kept constant throughout the CD measurement at 0.25mg/ml.

5.3.6 Fourier Transform Infrared Spectroscopy (FTIR)

The FT-IR spectra analysis revealed the acquisition of ZnO nanoparticles, with prominent absorption bands representing asymmetric and symmetric C=O bands at 1380 cm^{-1} and 1600 cm^{-1}, respectively. The examination of the amide I band in the FTIR spectra, spanning 1500-1700cm^{-1}, provided significant insights into the secondary structures of proteins. Within this context, the FTIR spectra of β-lg samples (both native and in the absence and presence of ZnO NPs) in the D2O buffer were carefully studied. As a protein-rich in beta-sheets, β-lg displayed a distinct peak at approximately 1634 cm^{-1} in its amide I contour, signifying the existence of intramolecular beta-sheet structures (Yu et al., 2007). Additionally, an added peak at around 1634 cm^{-1} in the amide I contour further indicated a shift in the β-sheet band in the protein FTIR spectra, hinting at the presence of intermolecular beta-sheet structures as opposed to intramolecular ones.

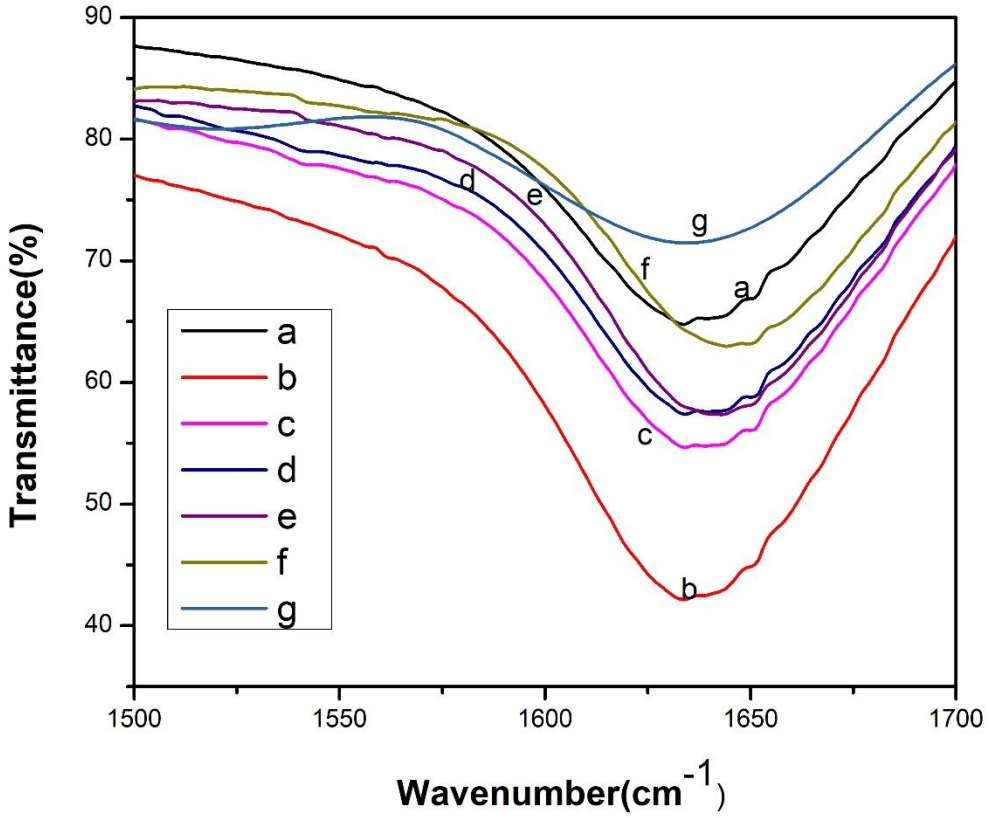

Figure 7: FTIR spectra were obtained for native β-lg under physiological pH (a), as well as at pH 11 (b), and following treatment with ZnO nanoparticles at pH 11 (c-f). The concentration of the nanoparticles ranged from 25 μM to 100 μM. The spectra were recorded in the amide-I region, specifically from 1500 to 1700 cm^{-1}, and each spectrum represents an average of 32 scans in D2O solvent at 25°C.

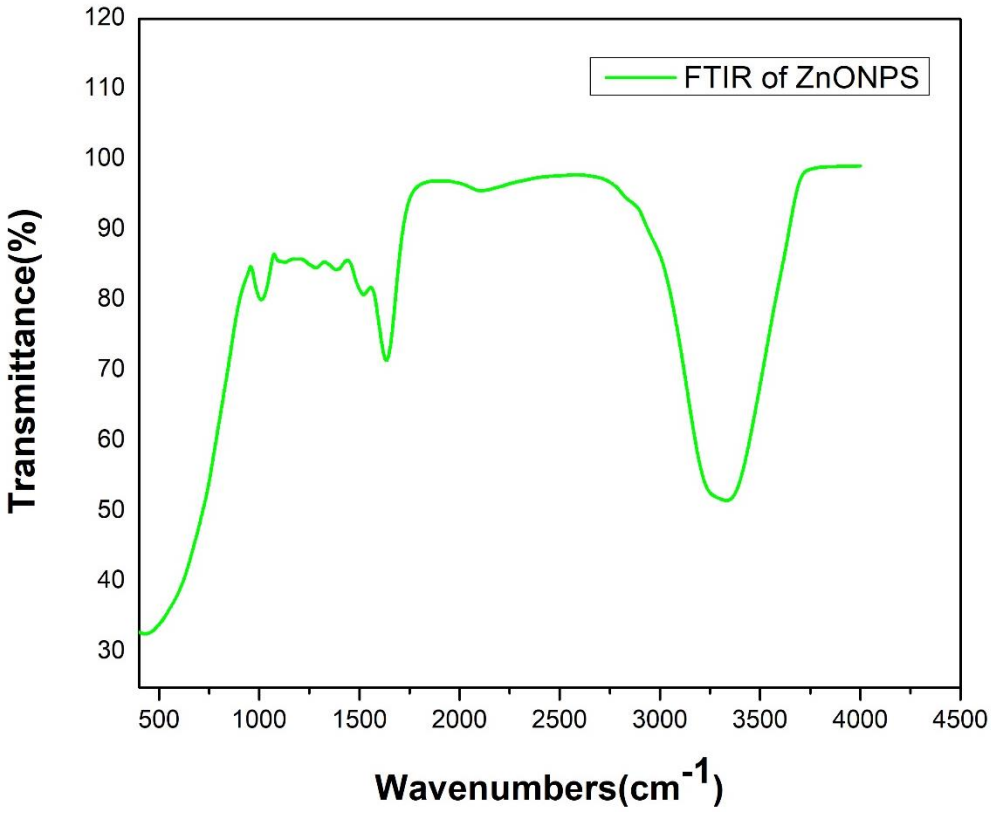

Figure 8: FTIR spectrum of synthesized zinc oxide nanoparticles (ZnO NPs).

5.3.7 SDS- Polyacrylamide Gel Electrophoresis Measurement

The SDS page technique was utilized to analyze the size and aggregation state of the β-lg protein. The first two lanes served as a reference for determining the size, while the subsequent lanes were utilized to assess the state of the β-lg protein under varying conditions. Lanes 3 and 4 displayed a distinct single band under non-reducing conditions at pH 7.4, indicating the presence of the native β-lg protein in a monomeric state with a molecular weight of approximately 18.4 kDa. This observation was made by comparing the band in these lanes with the reference marker proteins in lanes 1 and 2. The pH was then adjusted to 11, and lane 5 revealed a series of bands, suggesting the formation of oligomers under non-reducing conditions. These observed oligomers could potentially be attributed to the formation of disulfide bonds between the β-lg proteins **(Fig.9)**.

To examine the impact of ZnO nanoparticles on β-lg aggregation, we treated the protein with ZnO nanoparticles at concentrations of 25μM and 50μM, at pH 11. The resulting samples were loaded onto lanes 6 and 7, respectively. Analysis via the SDS page revealed a decrease in higher aggregates when ZnO nanoparticles were present, suggesting their potential effectiveness in inhibiting further aggregation.

Overall, the study offers a comprehensive understanding of the state of β-lg protein under varying conditions and underscores the potential of ZnO nanoparticles as a viable solution for preventing protein aggregation.

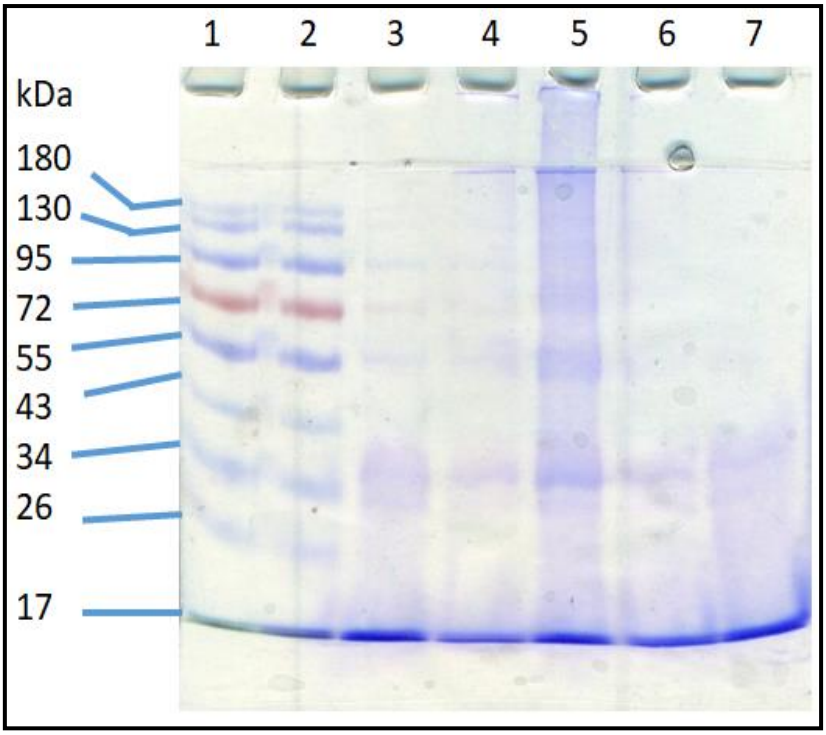

Figure 9: The SDS-PAGE (12%) patterns of the marker protein are shown in lanes 1 and 2. Lanes 3 and 4 represent native beta-lactoglobulin at physiological pH 7.4. Lane 5 shows beta-lactoglobulin at elevated pH 11. In lanes 6 and 7, beta-lactoglobulin is present in the presence of ZnO NPs at concentrations of 25µM and 50µM respectively.

5.3.8. Dynamic Light Scattering (DLS) Study

We employed dynamic light scattering (DLS) as a highly informative and versatile technique to thoroughly analyze the structure and stability of colloidal solutions. This sophisticated method provided a comprehensive understanding of the size, shape, and distribution of aggregates in the solution, offering crucial insights into the behavior of the studied materials. Our research focused on the application of DLS to investigate the hydrodynamic diameter of both synthesized ZnO nanoparticles and beta-lactoglobulin (β-lg) under a variety of different conditions. By utilizing DLS, we were able to gather detailed data on the size distribution of the nanoparticles, shedding light on their potential applications in various fields.

The DLS study revealed that the hydrodynamic diameter of the synthesized ZnO nanoparticles exhibited a range from 10 nm to 60 nm, as visually depicted in **(Fig.10a)**. This comprehensive

understanding of the nanoparticle size distribution is of utmost significance in evaluating their potential utility in diverse applications, laying the groundwork for further exploration and application within various scientific and industrial contexts.

Additionally, we observed a significant increase in the hydrodynamic diameter of β-lg at pH 11, (as depicted in **Fig.10b**), compared to the diameter at physiological pH, as shown in **(Figure 10c**). This increase suggests the formation of larger aggregates of the model protein due to the exposure of hydrophobic patches. These findings deepen our understanding of the protein's aggregation behavior and stability. Furthermore, we investigated the impact of ZnO nanoparticles on the larger aggregates of β-lg. The results revealed that treatment with ZnO nanoparticles at pH 11 resulted in a substantial reduction in the hydrodynamic diameter of β-lg. This decrease indicates the ability of ZnO nanoparticles to decrease the larger protein aggregates, a crucial factor for their potential application in drug delivery systems.

In summary, our study provides an in-depth analysis of the hydrodynamic diameter of nanoparticles and proteins using DLS measurement. It offers insights into the stability, shape, and size distribution of aggregates, which are essential for understanding the behavior of colloidal solutions in various applications.

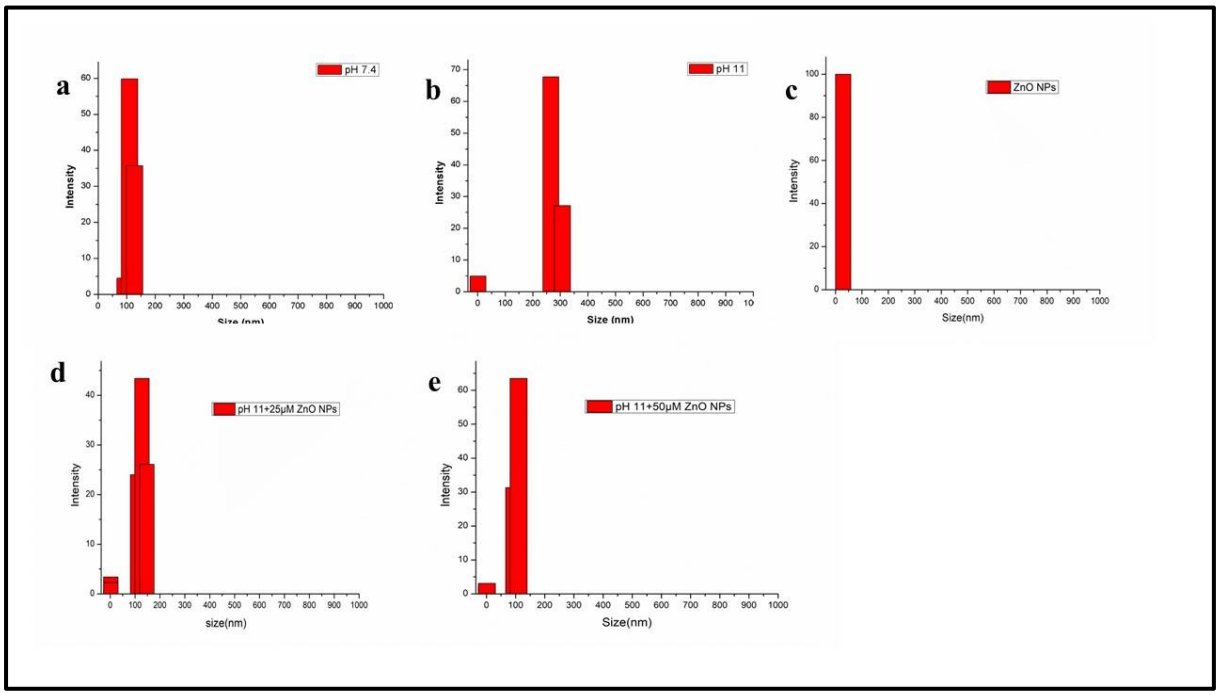

Figure 10: The dynamic light scattering of ZnO nanoparticles (Fig.10c), beta-lactoglobulin (β-lg) at physiological pH (Fig.10a), pH 11 (Fig.10b), and beta-lactoglobulin(β-lg) of pH 11 with ZnO nanoparticles (Fig.10d and 10 e).

5.3.9. Transmission Electron Microscopy (TEM) analysis

The study utilized transmission electron microscopy (TEM) to examine the fibrillar aggregates of native β-lg at pH 11 (as shown in Fig. 11a) and their interaction with ZnO nanoparticles. The results indicated a noticeable decrease in the formation of these aggregates when ZnO nanoparticles were present alongside β-lg at the same pH (as illustrated in Fig.11b). Additionally, TEM analysis revealed the generation of larger aggregates and oligomers at pH 11 of the model protein β-lg. Notably, significant morphological changes were observed in the presence of 25μM ZnO nanoparticles with β-lg, while maintaining the same pH and temperature (25°C), providing compelling evidence of the morphological change of β-lg in the absence and presence of ZnO nanoparticles.

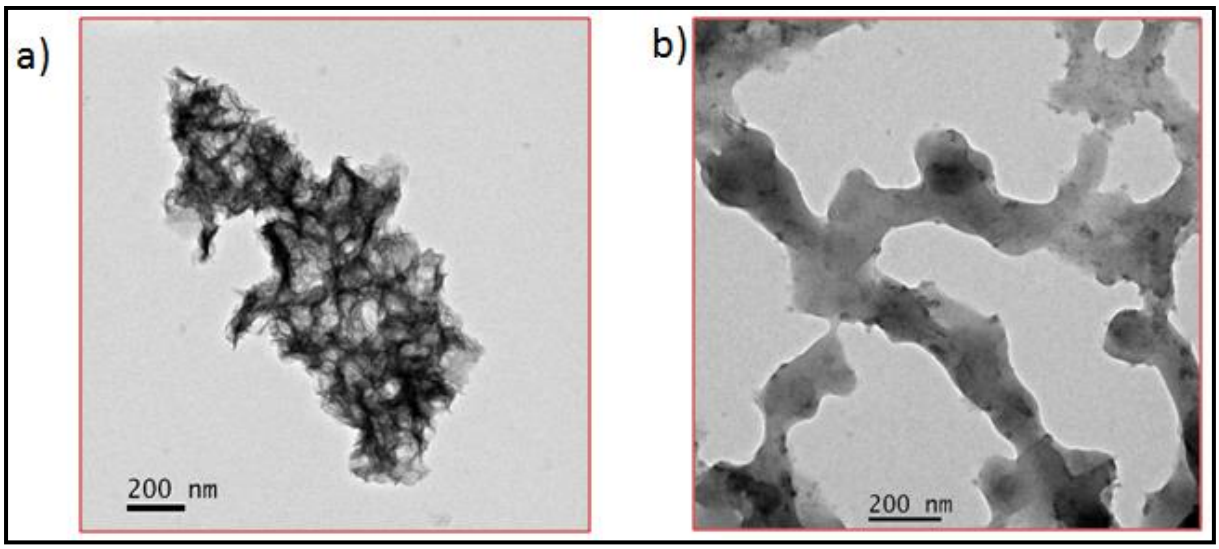

Figure 10: TEM images of native β-lg - at pH11 (a) and 25μM ZnO nanoparticles treated β-lg at the same pH (b) at respectively at 25°C in 10 mM phosphate buffer.

5.4. Conclusion

The main objective of our present research endeavors is to engage in the intricate process of synthesizing and characterizing zinc oxide (ZnO) nanoparticles through the application of highly advanced analytical techniques including UV spectroscopy, X-ray diffraction (XRD), and field emission scanning electron microscopy (FESEM). These sophisticated methods allow us to deeply analyze the structural and optical properties of the ZnO nanoparticles and gain a comprehensive understanding of their characteristics. Our extensive study has unveiled the truly remarkable chaperone-like activity exhibited by these nanoparticles. This intrinsic property allows them to effectively act as molecular chaperones, facilitating the restoration of alkali-unfolded β-lactoglobulin protein to its native conformation. The discovery of this unique

chaperone-like activity sets ZnO nanoparticles apart and positions them as highly versatile and valuable materials in various applications.

Furthermore, our findings have revealed that ZnO nanoparticles retain their chaperone-like function even under extremely high pH conditions. This exceptional resilience makes them an ideal candidate for a diverse range of industrial and biomedical applications. The ability to maintain their chaperone-like activity in such challenging conditions makes these nanoparticles highly desirable for applications where stability and effectiveness at extreme pH levels are essential. The results of our comprehensive study strongly advocate for the significant potential of ZnO nanoparticles in the critical fields of protein refolding and stabilization. These findings pave the way for the exploration of innovative therapeutic agents and advancements in the development of cutting-edge biomedical applications.

5.5. References

Ahmad, R., Khatoon, N. and Sardar, M., 2013. Biosynthesis, characterization, and application of TIO.

Alvarado, J.A., Maldonado, A., Juarez, H. and Pacio, M., 2013. Synthesis of colloidal ZnO nanoparticles and deposit of thin films by spin coating technique. Journal of Nanomaterials, 2013(1), p.903191.

Aschaffenburg, R. and Drewry, J., 1957. Improved method for the preparation of crystalline β-lactoglobulin and α-lactalbumin from cow's milk. Biochemical Journal, 65(2), p.273.

Banerjee, V. and Das, K.P., 2012. Modulation of the pathway of insulin fibrillation by a small molecule helix inducer 2, 2, 2-trifluoroethanol. Colloids and Surfaces B: Biointerfaces, 92, pp.142-150.

Blanch, E.W., Hecht, L. and Barron, L.D., 1999. New insight into the pH-dependent conformational changes in bovine β-lactoglobulin from Raman optical activity. Protein Science, 8(6), pp.1362-1367.

Brannon-Peppas, L. and Blanchette, J.O., 2004. Nanoparticle and targeted systems for cancer therapy. Advanced drug delivery reviews, 56(11), pp.1649-1659.

Brownlow, S., Cabral, J.H.M., Cooper, R., Flower, D.R., Yewdall, S.J., Polikarpov, I., North, A.C. and Sawyer, L., 1997. Bovine β-lactoglobulin at 1.8 Å resolution—still an enigmatic lipocalin. Structure, 5(4), pp.481-495.

Cattoni, D.I., Kaufman, S.B. and Flecha, F.L.G., 2009. Kinetics and thermodynamics of the interaction of 1-anilino-naphthalene-8-sulfonate with proteins. Biochimica et Biophysica Acta (BBA)-Proteins and Proteomics, 1794(11), pp.1700-1708.

Clark, E.D.B., 2001. Protein refolding for industrial processes. Current opinion in biotechnology, 12(2), pp.202-207.

De, M. and Rotello, V.M., 2008. Synthetic "chaperones": nanoparticle-mediated refolding of thermally denatured proteins. Chemical communications, (30), pp.3504-3506.

Eigel, W.N., Butler, J.E., Ernstrom, C.A., Farrell Jr, H.M., Harwalkar, V.R., Jenness, R. and Whitney, R.M., 1984. Nomenclature of proteins of cow's milk: fifth revision. Journal of Dairy Science, 67(8), pp.1599-1631.

Ellis, J., 1987. Proteins as molecular chaperones. Nature, 328(6129), pp.378-379.

Ena, J.M., Van Beresteijn, E.C.H., Robben, A.J.P.M. and Schmidt, D.G., 1995. Whey protein antigenicity reduction by fungal proteinases and a pepsin/pancreatin combination. Journal of food science, 60(1), pp.104-110.

Fu, K., Klibanov, A.M. and Langer, R., 2000. Protein stability in controlled-release systems. Nature Biotechnology, 18(1), pp.24-25.

Goldberg, M., Langer, R. and Jia, X., 2007. Nanostructured materials for applications in drug delivery and tissue engineering. Journal of Biomaterials Science, Polymer Edition, 18(3), pp.241-268.

Grar, H., Kaddouri, H., Gourine, H., Negaoui, H., Kheroua, O. and Saïdi, D., 2009. Microwave irradiation under different pH conditions induced a decrease in β-lactoglobulin antigenicity. European Food Research and Technology, 229, pp.779-783.

Han, D.H., Na, H.K., Choi, W.H., Lee, J.H., Kim, Y.K., Won, C., Lee, S.H., Kim, K.P., Kuret, J., Min, D.H. and Lee, M.J., 2014. Direct cellular delivery of human proteasomes to delay tau aggregation. Nature communications, 5(1), p.5633.

Hartl, F.U., 2017. Protein misfolding diseases. Annual review of biochemistry, 86(1), pp.21-26.

Hartl, F.U., Bracher, A. and Hayer-Hartl, M., 2011. Molecular chaperones in protein folding and proteostasis. Nature, 475(7356), pp.324-332.

Hoppenreijs, L.J.G., Fitzner, L., Ruhmlieb, T., Heyn, T.R., Schild, K., Van Der Goot, A.J., Boom, R.M., Steffen-Heins, A., Schwarz, K. and Keppler, J.K., 2022. Engineering amyloid and amyloid-like morphologies of β-lactoglobulin. Food Hydrocolloids, 124, p.107301.

Jones, N.S., Carney, A.S. and Davis, A., 1998. The prevalence of allergic rhinosinusitis: a review. The Journal of Laryngology & Otology, 112(11), pp.1019-1030.

Kameta, N., Masuda, M. and Shimizu, T., 2012. Soft nanotube hydrogels functioning as artificial chaperones. ACS nano, 6(6), pp.5249-5258.

Kim, M.H., Na, H.K., Kim, Y.K., Ryoo, S.R., Cho, H.S., Lee, K.E., Jeon, H., Ryoo, R. and Min, D.H., 2011. Facile synthesis of monodispersed mesoporous silica nanoparticles with ultra-large pores and their application in gene delivery. ACS nano, 5(5), pp.3568-3576.

Kohyama, K., Matsumoto, T. and Imoto, T., 2010. Refolding of an unstable lysozyme by gradient removal of a solubilizer and gradient addition of a stabilizer. Journal of Biochemistry, 147(3), pp.427-431.

Kontopidis, G., Holt, C. and Sawyer, L., 2002. The ligand-binding site of bovine β-lactoglobulin: evidence for a function? Journal of molecular biology, 318(4), pp.1043-1055.

Laemmli, U.K., 1970. Cleavage of structural proteins during the assembly of the head of bacteriophage T4. nature, 227(5259), pp.680-685.

Lin, C.A.J., Liedl, T., Sperling, R.A., Fernández-Argüelles, M.T., Costa-Fernandez, J.M., Pereiro, R., Sanz-Medel, A., Chang, W.H. and Parak, W.J., 2007. Bioanalytics and biolabeling with semiconductor nanoparticles (quantum dots). Journal of Materials Chemistry, 17(14), pp.1343-1346.

Linse, S., Cabaleiro-Lago, C., Xue, W.F., Lynch, I., Lindman, S., Thulin, E., Radford, S.E. and Dawson, K.A., 2007. Nucleation of protein fibrillation by nanoparticles. Proceedings of the National Academy of Sciences, 104(21), pp.8691-8696.

Liu, J.L., Lu, K.V., Eris, T., Katta, V., Westcott, K.R., Narhi, L.O. and Lu, H.S., 1998. In vitro methionine oxidation of recombinant human leptin. Pharmaceutical research, 15, pp.632-640.

Ma, F.H., An, Y., Wang, J., Song, Y., Liu, Y. and Shi, L., 2017. Synthetic nano chaperones facilitate refolding of denatured proteins. Acs Nano, 11(10), pp.10549-10557.

Pandurangan, M., Zamany, A.J. and Kim, D.H., 2016. ZnO nanoparticles assist in the refolding of denatured green fluorescent protein. Journal of Molecular Recognition, 29(4), pp.170-173.

Park, I.S., Kim, S., Yim, Y., Park, G., Choi, J., Won, C. and Min, D.H., 2022. Multifunctional synthetic nano-chaperone for peptide folding and intracellular delivery. Nature Communications, 13(1), p.4568.

Pessen, Helmut, James M. Purcell, and Harold M. Farrell Jr. "Proton relaxation rates of water in dilute solutions of β-lactoglobulin. Determination of cross-relaxation and correlation with structural changes by the use of two genetic variants of a self-associating globular protein." Biochimica et Biophysica Acta (BBA)-Protein Structure and Molecular Enzymology 828, no. 1 (1985): 1-12.

Pourrahimi, A.M., Liu, D., Pallon, L.K., Andersson, R.L., Abad, A.M., Lagarón, J.M., Hedenqvist, M.S., Ström, V., Gedde, U.W. and Olsson, R.T., 2014. Water-based synthesis and cleaning methods for high purity ZnO nanoparticles–comparing acetate, chloride, sulfate, and nitrate zinc salt precursors. RSC Advances, 4(67), pp.35568-35577.

Rasmussen, J.W., Martinez, E., Louka, P. and Wingett, D.G., 2010. Zinc oxide nanoparticles for selective destruction of tumor cells and potential for drug delivery applications. Expert opinion on drug delivery, 7(9), pp.1063-1077.

Sakamoto, R., Nishikori, S. and Shiraki, K., 2004. High temperature increases the refolding yield of reduced lysozyme: implication for the productive process for folding. Biotechnology progress, 20(4), pp.1128-1133.

Sardar, S., Pal, S., Maity, S., Chakraborty, J. and Halder, U.C., 2014. Amyloid fibril formation by β-lactoglobulin is inhibited by gold nanoparticles. International journal of biological macromolecules, 69, pp.137-145.

Shang, W., Nuffer, J.H., Dordick, J.S. and Siegel, R.W., 2007. Unfolding of ribonuclease A on silica nanoparticle surfaces. Nano letters, 7(7), pp.1991-1995.

Šimšíková, M. and Antalík, M., 2013. Interaction of cytochrome c with zinc oxide nanoparticles. Colloids and Surfaces B: Biointerfaces, 103, pp.630-634.

Singh, R. and Flowers, R.A., 2010. Efficient protein renaturation using tunable hemifluorinated anionic surfactants as additives. Chemical Communications, 46(2), pp.276-278.

Singh, R.P., Shukla, V.K., Yadav, R.S., Sharma, P.K., Singh, P.K. and Pandey, A.C., 2011. Biological approach of zinc oxide nanoparticles formation and its characterization. Adv. Mater. Lett, 2(4), pp.313-317.

Stanic-Vucinic, D., Stojadinovic, M., Atanaskovic-Markovic, M., Ognjenovic, J., Grönlund, H., van Hage, M., Lantto, R., Sancho, A.I. and Velickovic, T.C., 2012. Structural changes and allergenic properties of β-lactoglobulin upon exposure to high-intensity ultrasound. Molecular nutrition & food research, 56(12), pp.1894-1905.

Stefani, M. and Dobson, C.M., 2003. Protein aggregation and aggregate toxicity: new insights into protein folding, misfolding diseases, and biological evolution. Journal of molecular medicine, 81, pp.678-699.

Sudhagar, S., Sathya, S., Pandian, K. and Lakshmi, B.S., 2011. Targeting and sensing cancer cells with ZnO nanoprobes in vitro. Biotechnology letters, 33, pp.1891-1896.

Takahashi, H., Sawada, S.I. and Akiyoshi, K., 2011. Amphiphilic polysaccharide nanoballs: a new building block for nanogel biomedical engineering and artificial chaperones. ACS nano, 5(1), pp.337-345.

Waissbluth, M.D. and Grieger, R.A., 1974. Alkaline denaturation of β-lactoglobulins. Activation parameters and effect on dye binding site. Biochemistry, 13(6), pp.1285-1288.

Wang, X., Lu, D., Austin, R., Agarwal, A., Mueller, L.J., Liu, Z., Wu, J. and Feng, P., 2007. Protein refolding assisted by periodic mesoporous organosilicas. Langmuir, 23(10), pp.5735-5739.

Yagi, M., Sakurai, K., Kalidas, C., Batt, C.A. and Goto, Y., 2003. Reversible unfolding of bovine β-lactoglobulin mutants without a free thiol group. Journal of Biological Chemistry, 278(47), pp.47009-47015.

Yu, W.W., Chang, E., Falkner, J.C., Zhang, J., Al-Somali, A.M., Sayes, C.M., Johns, J., Drezek, R. and Colvin, V.L., 2007. Forming biocompatible and nonaggregated nanocrystals in water using amphiphilic polymers. Journal of the American Chemical Society, 129(10), pp.2871-2879.

Zhang, D., Neumann, O., Wang, H., Yuwono, V.M., Barhoumi, A., Perham, M., Hartgerink, J.D., Wittung-Stafshede, P. and Halas, N.J., 2009. Gold nanoparticles can induce the formation of protein-based aggregates at physiological pH. Nano letters, 9(2), pp.666-671.

Zhong, J., Liu, C., Liu, W., Cai, X., Tu, Z. and Wan, J., 2011. Effect of dynamic high-pressure microfluidization at different temperatures on the antigenic response of bovine β-lactoglobulin. European Food Research and Technology, 233, pp.95-102.

CHAPTER 6

Formation of amyloid aggregates of bovine beta-lactoglobulin is inhibited by highly dispersed copper oxide nanoparticles prepared by a quick-precipitation method: An approach to therapeutics for protein misfolding diseases.

6.1. Introduction

The misfolding of proteins, the growth of amyloids, and their subsequent deposition are implicated in a spectrum of severe disorders, including Alzheimer's disease (Verma et al., 2015), Parkinson's disease (Polymeropoulos et al., 1997), Huntington's disease (Melkani et al., 2013), type II diabetes (Cooper et al., 1987), and lysozyme amyloidosis (Pepys et al., 1993). A distinctive feature of amyloid fibrils is the formation of a cross-β sheet structure, leading to self-assembly into long fibrils (Sunde et al., 1997). These amyloid fibrils can arise from the mutation and misfolding of diverse proteins, such as α-synuclein (Conway et al., 1998), insulin (Gupta et al., 2015), lysozyme (Jean et al., 2014), and huntingtin (Melkani et al., 2013), thereby contributing to the development of amyloid-related diseases. Numerous strategies have been explored as preventive measures against amyloid formation, encompassing small peptides (Sciarretta et al., 2006), chaperones (Muchowski et al., 2000), various drugs (Nowacek et al., 2009; Gilgun-Sherki et al., 2006), gene therapy techniques (Murphy et al., 2013), and chemical osmolytes (Choudhary et al., 2015). However, a primary concern associated with existing therapies is their limited capability to target and traverse the blood-brain barrier (BBB), as well as apprehensions regarding the stability of the components within the biological system.

Typically, amyloid structures exhibit a cross-β sheet pattern with fibril axes oriented perpendicularly (Nelson and Eisenberg, 2006). Amyloid fibrillation is recognized as a two-phase process. During the lag phase, the protein undergoes a loss of its native conformation and develops β-sheet-intermediate structures. These intermediates then transition to proto-fibrils, fibrils, and soluble oligomers in the elongation phase (Kumar and Udgaonkar, 2010). The ultimate outcome, whether it be amorphous aggregates, amyloid fibrils, or oligomers, is influenced by the protein's amino acid sequence and environmental factors (Fink, 1998). The partial unfolding of several naturally folded proteins can lead to the formation of amyloid fibrils under specific conditions such as pH (McParland et al., 2000), (Zurdo et al., 2001), metal ions

(Pandey et al.,2010), (Stirpe et al., 2011), salts (Raman et al., 2005), (Pedersen et al., 2006), temperature (Litvinovich et al.,1998), (Fändrich et al.,2001), pressure (Ferrao-Gonzales et al.,2001), and cosolvents (Chiti et al., 1999). In some cases, the addition of surfactants has proven effective in stabilizing non-native conformations or intermediates that occur during protein folding pathways (Chamani et al., 2006), (Chamani and Moosavi-Movahedi, 2006). To date, only a limited number of small molecules, peptides, and chaperones have been reported to inhibit amyloid fibrillation (Muchowski et al., 2000), (Sharma and Ghosh, 2019).

The unique properties of nanomaterials, such as their resemblance in size to biomolecules, high surface-to-volume ratio, and ease of surface functionalization, make them ideal for a wide range of biomedical applications. Nanoparticles have shown promise in inhibiting amyloid fibrillation. For instance, Fe_2O_3 nanoparticles (Skaat et al., 2009), fullerene (Xie et al., 2014), gold nanoparticles (Sharma et al.,2020), and silver nanoparticles (AgNPs) (Ban and Paul,2019), (Sen et al., 2016), (Barbalinardo et al., 2020) have demonstrated their capability to suppress protein fibrillation. Furthermore, surface functionalization of nanoparticles using curcumin, or incorporating it into nanostructures, has increased their effectiveness against amyloid fibrillation (Mathew et al., 2012), (Palmal et al., 2014), (Taylor et al., 2011).

On the other hand, nanoparticles (NPs) with sizes smaller than 100 nm and adjustable surface properties are currently being explored as potential therapeutic agents and drug carriers for various diseases (De Jong et al., 2008; Arvizo et al., 2010; Cho et al., 2008). However, their impact on protein misfolding, particularly amyloid formation, requires further investigation. Several in vitro studies with different amyloidogenic proteins have indicated that nanoparticles such as cerium oxide, copolymers, carbon nanotubes, quantum dots (Linse et al., 2007), and titanium dioxide (Wu et al., 2008) can shorten amyloid nucleation time and enhance amyloid fibril growth. Conversely, other reports have shown that gold, CdTe quantum dots (Hsieh et al., 2013; Palmal et al., 2014; Xiao et al., 2010), and iron oxide nanoparticles (Bellova et al., 2010) inhibit amyloid growth. An antibacterial Cu-β-lg nanocomposite is synthesized through the interaction between the free thiol groups of β-lactoglobulin (β-lg) and copper ions. This interaction leads to the N-H bending of the amide II region of the protein (Sardar et al., 2016). When β-lg is treated with gold nanoparticles (AuNPs) at 75°C, it results in the formation of smaller, irregular aggregates. The findings suggest that AuNPs have the capacity to inhibit the formation of amyloid fibrillar aggregates of β-lg in a concentration-dependent manner, potentially aiding the refolding of the protein into a native-like structure. Consequently, AuNPs

act as nano-chaperones that help suppress protein aggregation (Sardar et al., 2014). Conversely, silver nanoparticles (AgNPs) strongly bind to the aggregation-prone regions of β-lg, altering its aggregation pathway and leading to the formation of rod-shaped aggregates (Sardar et al., 2019).The interaction between NPs and proteins occurs through interfacial interaction, and the surface properties of both the proteins and NPs significantly influence any effects on the dynamics of the fibrillation process. The nature and extent of these effects largely depend on the core material and surface functionalization of NPs, as well as the type of proteins they interact with, and these parameters should be thoroughly studied. Furthermore, the administration time and dosage of NPs may influence the dynamics of fibrillation, leading to different stages of amyloid growth.

As particles are reduced from a micrometer to a nanometer size, their properties can undergo significant changes. For instance, electrical conductivity, hardness, active surface area, chemical reactivity, and biological activity are all known to be affected. The bactericidal effectiveness of metal nanoparticles is believed to stem from both their size and high surface-to-volume ratio. These characteristics enable them to closely interact with bacterial membranes, rather than the effect solely arising from the release of metal ions (Morones et al., 2005). Copper oxide (CuO), also known as copper (II) oxide or cupric oxide, is a semiconductor with a monoclinic structure that has attracted considerable attention due to its fundamental position in the family of copper compounds and its diverse range of potentially advantageous physical properties. These properties include high-temperature superconductivity, electron correlation effects, and spin dynamics (Cava,1990; Tranquada et al.,1995). As a crucial p-type semiconductor, CuO boasts varied applications in gas sensors, catalysis, batteries, high-temperature superconductors, solar energy conversion, and field emission emitters. In the realm of energy conservation, the incorporation of nano CuO particles into energy-transferring fluids has shown promising results in enhancing fluid viscosity and improving thermal conductivity (Kwak and Kim, 2005). The crystal structures of CuO feature a narrow band gap, which gives rise to valuable photocatalytic or photovoltaic properties, as well as photoconductive functionalities (Xu et al., 1999). Despite limited available information about the potential antimicrobial activity of nano CuO, its cost-effectiveness compared to silver, ease of incorporation into polymers, and relative stability in terms of both chemical and physical properties make it an attractive option. Highly ionic nanoparticulate metal oxides such as CuO may hold particular value as antimicrobial agents due to their ability to be prepared with extremely high surface areas and unique crystal morphologies (Stoimenov et al., 2002).

Bovine β-lg is a well-known globular whey protein weighing 18.4kD and having a pI of 5.2. It is composed of 162 amino acid residues and is mainly a β-sheet protein. It is believed that β-lg acts as a transporter for certain hydrophobic molecules, such as retinol and long-chain fatty acids, across the intestinal membrane. When heated above 60°C, the native structure of β-lg begins to change, leading to a decrease in ordered zones and an increase in the exposure of tryptophan and free thiol groups (Mills et al.,1976; Halder et al., 2012). At acidic pH, β-lg is readily converted into amyloid fibrils (Schokker et al., 2000; Giurleo et al., 2009). At pH 7.0, the protein exists as a reversible dimer, and the extent of dimerization depends on pH, temperature, protein concentration, and ionic strength of the medium. Additionally, β-lg forms soluble aggregates of polymerized protein after being heated to 80°C for 1 hour at pH 7.0. Results from reducing and non-reducing SDS-PAGE indicated that both covalent and non-covalent interactions are responsible for aggregate formation (Zúñiga et al., 2010; Krebs et al., 2009).

In our recent study, we synthesized and utilized copper oxide nanoparticles (CuONPs) of specific dimensions, opting for non-functionalized variants. Our focus was on exploring the interaction between copper oxide nanoparticles and the model amyloidogenic protein β-lg. This involved a detailed investigation of the self-assembly behavior of thermally perturbed unfolded β-lg in the presence and absence of 8 nm diameter copper oxide nanoparticles across varying concentrations. Additionally, we meticulously characterized the resulting aggregates, size distribution, and morphological features of the species formed during the thermal exposure of β-lg at 75°C for 1 hour, maintaining a pH level of approximately 7.4. Our analysis employed a range of techniques including Rayleigh Scattering, the thioflavin T (Th T) assay, dynamic light scattering (DLS), and transmission electron microscopy (TEM). Our findings conclusively demonstrate the capacity of copper oxide nanoparticles (CuONPs) to impede the self-assembly process of β-lg, revealing noteworthy insights into the interactions between copper oxide nanoparticles and amyloidogenic proteins.

6.2. Materials And Methods

6.2.1. Reagents and Chemicals Required

Sodium dihydrogen phosphate, copper acetate monohydrate (Cu $(CH_3COO)_2$ H2O), acetic acid glacial, Sodium hydroxide NaOH (pellets), and methanol were purchased from Merck (Mumbai, India). Acrylamide, bis acryl amide, N, N, N, N-tetramethylethylenediamine

(TEMED), ammonium persulfate (APS), sodium dodecyl sulfate (SDS), bromophenol blue and Coomassie brilliant blue were obtained from Sigma-Aldrich. Different fluorescent probes, viz., 8-anilinonaphthalene-1-sulfonic acid ammonium salt (ANS), Congo red (CR), and Thioflavin T (ThT), were purchased from Sigma Chemical Co. (St. Louis, USA) and used as received without further purification. The other chemicals used were of the highest purity available. Deionized water was used throughout the experiment, and buffer solutions were filtered through a 0.22 μm syringe filter (Millipore, USA).

6.2.2. Isolation and purification of beta-lactoglobulin(β-lg)

Bovine β-lg was isolated and purified from cow milk as described by Aschaffenburg and Drewry (Aschaffenburg and Drewry,1957). The final product was lyophilized and stored at 4oC. For spectroscopic sample preparation, β-lg was weighed and dissolved in 0.01 M Na-phosphate buffer pH 7.4 solution. Protein stock solutions were prepared using phosphate buffer pH-7.4. Since the extinction coefficient of β-lg (0.96 mg-1 mL-1 cm-1 at 280 nm) is known, different concentrations of protein samples were prepared by dissolving β-lg samples in Milli-Q-water and then measuring the O.D. at 280 nm.

6.2.3. Synthesis of Copper oxide nanoparticles (CuO NPs)

CuO NPs were synthesized following a previously reported method (Zhu et al., 2008). Glasswares used in this preparation were thoroughly cleaned in aqua regia (nitric acid: sulphuric acid 1:3), rinsed in milli-Q-water, and then dried in an oven. This study investigated the synthesis and optical characterization of copper oxide (CuO) nanoparticles. An aqueous solution of copper acetate (0.02 mol) is prepared in a round-bottom flask. Subsequently, 1 ml of glacial acetic acid is introduced to the aforementioned solution, followed by heating to 100°C with continuous stirring. Approximately 0.4 g of NaOH is carefully added to the heated solution until reaching a pH level of 6-7, leading to the immediate formation of a substantial black precipitate. This precipitate is subsequently subjected to centrifugation and washed 3-4 times with deionized water. Finally, the resulting precipitate is air-dried for 24 hours.

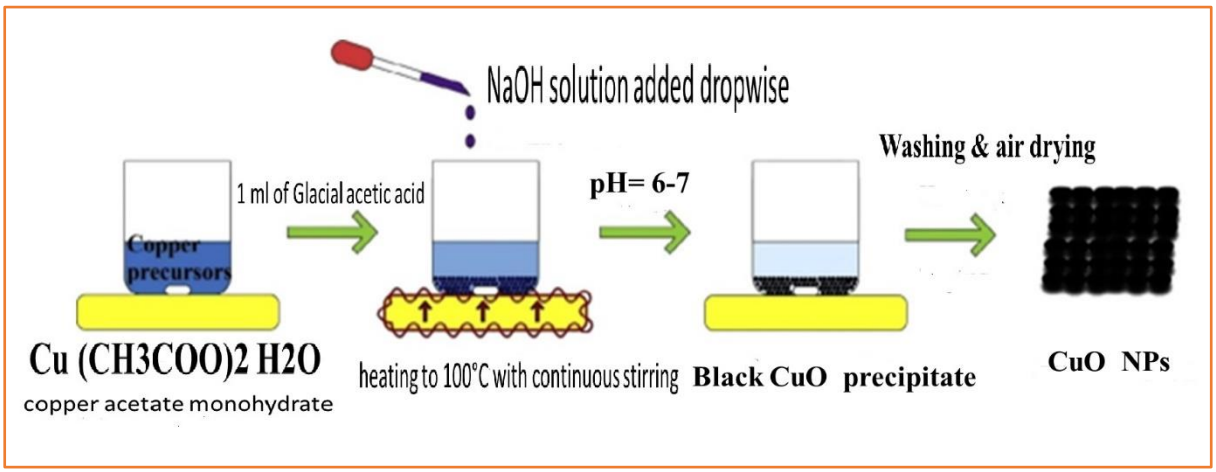

Scheme 1: Schematic of a typical chemical precipitation synthetic process for CuO nanoparticles.

6.2.4. Electrophoresis measurement

The sodium dodecyl sulfate-polyacrylamide gel electrophoresis (SDS-PAGE) was conducted under non-reducing conditions utilizing a 12% acrylamide resolving gel according to Laemmli's method (Laemmli,1970)). Samples of β-lg solution (2.5 mg/ml) in 10 mM sodium phosphate buffer at pH 7.4 were subjected to heating at 75°C for 1 hour in the presence and absence of CuO NPs separately. The resulting solutions were then filtered using a syringe filter with a 0.2 µm membrane filter. Subsequently, aliquots of 30 µl heat-treated β-lg solution in the presence and absence of CuO NPs were loaded into the wells. Similarly, 30 µl of native β-lg solution (2.5 mg/ml) was loaded into another well. Electrophoretic separations were performed by applying a maximum voltage of 100 volts for 1 hour. Following this, the gel was stained with Coomassie Brilliant Blue R-250 and destained using a solution customarily containing methanol and acetic acid.

6.2.5. UV-visible spectroscopy

To investigate the binding affinity at room temperature (25°C), we conducted a UV-visible spectroscopy experiment using a JASCO V-730 spectrophotometer with the serial number B184461798 and JASCO Spectra Manager Software. The experiment involved the use of two PerkinElmer quartz cells with a path length of 1 cm for both the reference and sample solutions. We recorded the absorbance measurements over a wavelength range of 200 - 600 nm. The reference solution used was a 10 mm phosphate buffer with a pH of 7.4, and the concentration of the sample solutions was 13.6µM.

6.2.6. ANS Fluorescence Study to monitor the change in Hydrophobicity

8-Anilinonaphthalene-1-sulfonic acid (ANS), also known as 8-(Phenylamino) naphthalene-1-sulfonic acid, is a fluorescent molecule utilized to assess the surface hydrophobicity of protein molecules. To prepare the ANS sample, a stock solution of 1 mg/ml was created using Milli-Q water. In our study, to ensure a 50-molar excess of ANS compared to the protein concentration, 20 µl of the ANS solution was added to each sample.

For the ANS Fluorescence measurements, we utilized a Horiba Fluorometer (Serial No: 1734D-4018-FM, Model: Fluoromax-4C). Each sample was excited at λmax 385 nm in a four-sided transparent rectangular quartz cell with a 1 cm path length. The emission and excitation slit widths were set to 5 nm. The Fluoromax Software was employed to record ANS fluorescence emission spectra ranging from 395 nm to 600 nm. It's important to note that each spectrum was blank-corrected. Furthermore, the data points presented in our study represent the average of triplicate measurements (Cattoni et al., 2009).

6.2.7. Thioflavin T (ThT) fluorescence for quantitative measurements of β-lg aggregates

Thioflavin T (Th T) is a yellow-colored organic dye that binds with the beta-sheeted structure of the aggregates and shows enhanced fluorescence around 485 nm (Nilsson, 2004). Hence the amount of aggregate formed in a solution can be measured and compared by this Th-T binding assay. At first 5mM stock solution of ThT was prepared by dissolving ThT in 10mM sodium phosphate buffer. Then, 20 µL of this stock solution was added to each β-lg sample solution (native and thermally incubated at 75 ºC for 1 hour at pH 7.4 in the presence and absence of CuO nanoparticles) and mixed thoroughly to maintain 30 µM Th T solution in each sample solution. Next, the sample solutions were incubated for 30 minutes at a room temperature of 25°C. Employing a Horiba Fluorometer (Serial No: 1734D-4018-FM, Model: Fluoromax-4C) ThT fluorescence assay was performed by exciting each sample at λmax 450 nm in a transparent rectangular quartz cuvette of 1 cm pathlength (Banerjee and Das, 2012). Both excitation and emission slits were maintained at 5 nm and the emission spectra were recorded in the wavelength range of 460-600 nm.

6.2.8. Rayleigh light scattering (RLS) Study

The thermal aggregations of β-lg in the presence and absence of the synthesized SC compounds were monitored by RLS experiments in a Shimadzu spectrofluorometer (Model: Shimadzu 5301 PC). The fluorescence intensities were measured at 350 nm after excitation of the sample

solutions at the same wavelength (Sardar et al., 2014). A quartz cell of 1 cm path length was used for the experiment, and all sample solutions were made in NaH2PO4 buffer (10 mM) at pH 7.4. Slits for emission and excitation were kept at 5 nm. These tests were carried out three times.

6.2.9. Transmission Electron Microscopy

High-resolution Transmission Electron Microscopy (HR TEM) imaging of β-lg in the presence and absence of CuO NPs was performed using a JEOL HRTEM-2011 instrument in Tokyo, Japan, at various magnifications (Hoppenreijs et al., 2022).To prepare the samples, all solutions were centrifuged and subsequently diluted. These diluted solutions were drop-cast onto a carbon-coated copper grid with a mesh size of 300C (Pro Sci Tech). After 20 seconds, the droplet was blotted on a filter paper using the mesh grid and removed. Subsequently, a droplet of 2% uranyl acetate (Sigma) was added to stain the grid. The grids were then air-dried overnight in a desiccator. Following a brief incubation period, the grids were utilized for TEM imaging at a specific magnification.

6.2.10. Circular dichroism (CD) spectroscopy

We conducted circular dichroism measurements using a Jasco Spectropolarimeter (J-815) to investigate the effects of copper oxide nanoparticles (CuO NPs) on the structural and conformational changes of β-lactoglobulin (β-lg). The measurements were performed at 20°C in the far-UV range (200–260 nm) using rectangular cells with path lengths of 1mm and 10mm. The solutions of heat-treated β-lg, both with and without the presence of CuO NPs, had concentrations of 0.25 mg ml-1 for the far-UV CD measurements. The presented spectra are averages of three scans, and the final spectrum was obtained after subtracting the corresponding solvent spectrum. After obtaining the far UV-CD curves, we employed a curve-fitting program, CDNN 2.1, to determine the percentage of secondary structures present in β-lg under different conditions.

6.3. Results And Discussion

6.3.1. UV-Visible Spectroscopy

The optical properties of the CuO nanoparticles were investigated using UV-Vis spectroscopy at room temperature, as shown in **(Fig.1**). The analysis revealed a clear absorption feature in the ultraviolet range, specifically spanning from 200 to 400 nm. Notably, the absorption peak,

centered at approximately 300 nm, indicated the presence of excitonic behavior in CuO at room temperature. This discovery is consistent with previous research on the optical characteristics of CuO nanoparticles, highlighting the importance of understanding their properties for a variety of nanotechnology applications (Singh et al., 2011). Furthermore, the synthesized CuO nanoparticles were confirmed through extensive SEM and TEM studies.

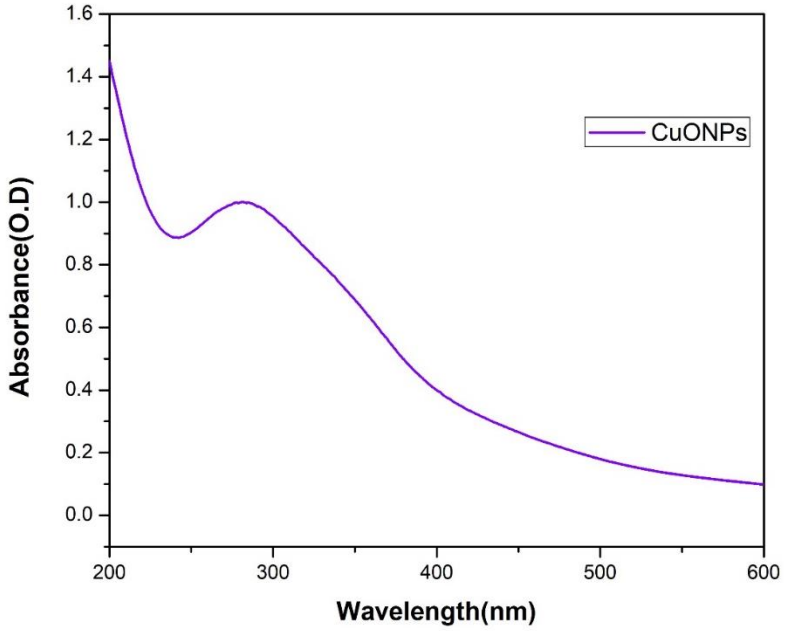

Figure 1: UV-VIS absorption spectrum of synthesized CuO NPs.

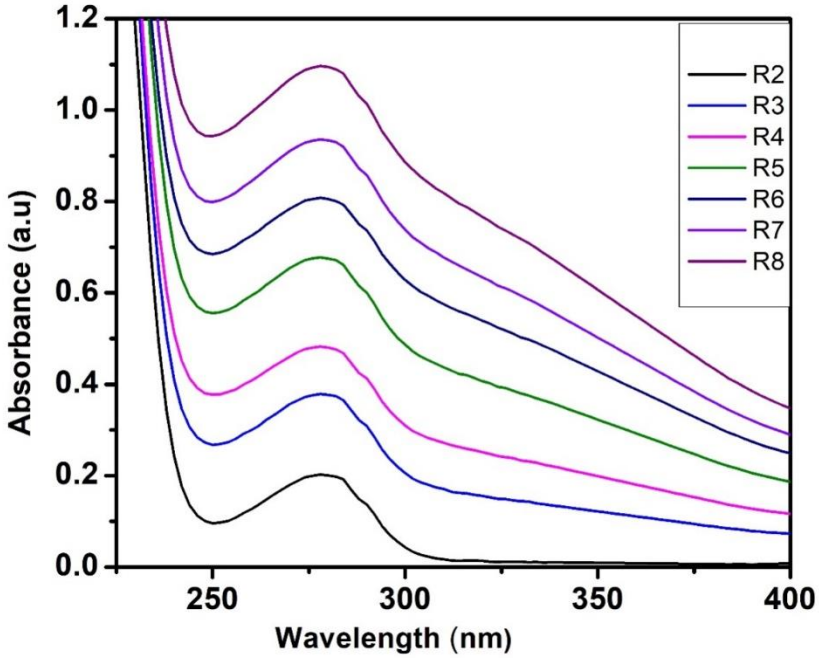

Figure 2: The UV-VIS spectrum of native β-lg at physiological pH (R2), R3 denotes β-lg under thermal conditions and with CuO nanoparticle treatment at the same pH (R4-R8), was

measured. The concentration of the nanoparticles gradually increased from 10 μM to 100 μM. The concentration of β-lg was kept constant at 0.25 mg/ml throughout the UV-VIS measurement.

Beta-lactoglobulin (β-Lg) is recognized for exhibiting distinct UV-visible spectra, owing to the presence of chromophores with an aromatic nucleus conjugated with groups that have varying electronic effects. The native β-Lg displays a characteristic protein band associated with tryptophan residues, with a peak wavelength (λmax) of 280 nm **(Fig.2)**. Any modification in the UV-visible spectrum of native β-Lg can provide valuable insights into the changes occurring in the micro-environment surrounding the chromophores, as evidenced in existing literature (Yu et al., 2007). These observations suggest that the micro-environment of β-lactoglobulin undergoes alterations in the presence of CuO nanoparticles. It is evident that CuO nanoparticles interact with β-lactoglobulin, inducing changes in the micro-environment of the protein surrounding its tryptophan (Trp) and tyrosine (Tyr) residues. These structural modifications are reflected in the UV-absorbance of β-lactoglobulin.

6.3.2. Powdered XRD Spectra

The X-ray diffraction (XRD) pattern of the CuO nanoparticles prepared is depicted in **(Fig.3)**. The average crystallite size (t) was determined using Scherrer's equation: $t = 0.9l/B\cos\theta$, where l represents the X-ray wavelength and B is the full width at half maximum (FWHM). The analysis confirms a single-phase with a monoclinic structure. Additionally, the lattice parameters are reported as: a = 4.84 Å, b = 3.47 Å, and c = 5.33 Å. The intensities and positions of the peaks closely match the values in the JCPDS file No. 05-661(Lanje et al., 2010). Importantly, no impurity peaks were detected in the XRD pattern. The observed broadening of the peaks is attributed to the nano-size effect. The broadening of the peaks in the data suggests the small size of the products. Our findings indicate that the addition temperature of NaOH significantly influences the shape and size of CuO nanocrystals. Additionally, the size of the rod-like crystallites corresponds to the calculated values from the XRD patterns. According to the Scherrer formula, the average crystallite size of the CuO nanoparticles was calculated to be 8 nm.

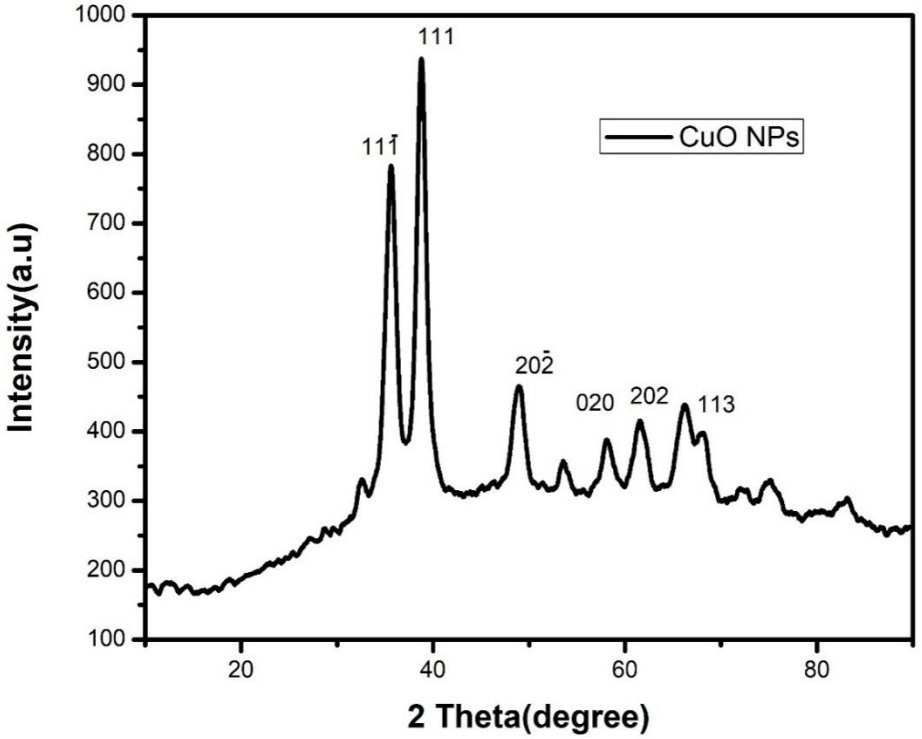

Figure 3: XRD pattern of synthesized CuO nanoparticles.

6.3.3. ANS-fluorescence study to monitor the hydrophobicity change of Beta-lactoglobulin (β -lg)

The alterations in the hydrophobicity of β-lg during thermal aggregation, with and without the presence of CuO nanoparticles, were tracked by capturing the ANS emission spectra. It is evident that ANS, a fluorescent hydrophobic probe, attaches to the molten globule state of proteins and demonstrates fluorescence intensity (Matulis et al., 1999). The interaction of ANS with β-lg may be attributed to both electrostatic and hydrophobic interactions (Collini et al., 2003).

(In Fig. 4), the ANS fluorescence spectra of heat-treated β-lg in sodium phosphate buffer at pH 7.4 are displayed. It is evident that heat-induced β-lg exhibited a significant ANS fluorescence signal at around 485 nm at pH 7.4 **(profile b, Fig. 4)**, with a notably higher ANS intensity compared to native β-lg **(profile a, Fig. 4)**. This marked increase in fluorescence intensity could be attributed to the heightened penetration of ANS into the hydrophobic loops present in thermally exposed β-lg as opposed to native β-lg. Consequently, this amplification in hydrophobic loops leads to enhanced protein-protein interactions, ultimately resulting in an augmented thermal aggregation of β-lg (Sardar et al., 2014). When β-lg was subjected to incubation at 75°C for 1 hour in the presence of varying concentrations of CuO NPs (ranging

from 10µM to 100µM) as outlined in **(Fig.4)**, we observed notable discrepancies in the results. The fluorescence intensity of β-lg exhibited a substantial decrease, indicating a decreased exposure of hydrophobic loops in β-lg. This suggests that CuO NPs effectively impeded the formation of amyloid fibrils in β-lg. Our assertion is strongly corroborated by the ThT data presented below.

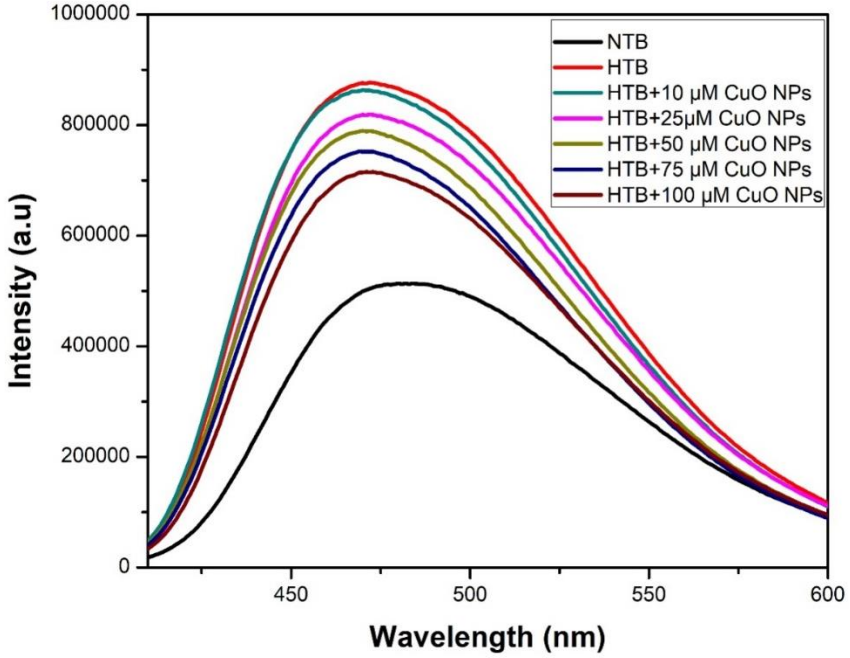

Figure 4: The fluorescence of native β-lactoglobulin (β-lg) in the presence of 10 mM phosphate buffer at a pH of 7.4 was measured using 380nm excitation, with emissions recorded in the 400nm-600nm range. Subsequently, the fluorescence of β-lg-treated CuO nanoparticles at pH 7.4 was examined under thermal conditions, as illustrated in **(Fig.4)**. The concentration of CuO nanoparticles varied from 10µM to 100µM, while the protein concentration was consistently maintained at 0.25 mg/ml throughout the ANS measurement.

6.3.4. Thioflavin T (ThT) fluorescence for quantitative measurements of β-lg aggregates

In assessing the inhibitory effect of CuO nanoparticles on the temperature-induced β-lg amyloid fibrillation, we utilized Thioflavin T (ThT) dye. This dye serves as a non-covalent indicator of amyloid aggregates and is commonly employed to observe protein aggregation. Typically, ThT binds to amyloid aggregates, resulting in a pronounced increase in fluorescence emission (Biancalana and Koide, 2010). It has been reported that the bolstering of ThT fluorescence intensity at its peak wavelength (485 nm) is attributed to the formation of a hydrogen bond between ThT and amyloid fibrils (Khurana et al., 2005). **Fig.5** illustrates the

ThT fluorescence intensities of various β-lg samples. A substantial increase in ThT emission intensity at 485 nm was observed in thermally incubated β-lg, indicative of amyloid fibrils. Though the interaction between ThT and amyloid fibrils is not fully understood, literature reports (Jayamani et al.; Bramanti et al., 2013) suggest its dependence on the amyloidogenic protein and binding pattern (Kuznetsova et al.,2012). Additionally, the heightened fluorescence intensity at 485 nm confirms the presence of β-lg amyloid fibrils. The ThT intensity of β-lg consistently decreased with varying CuO nanoparticle concentration, suggesting an efficient concentration-dependent inhibitory effect of CuO nanoparticles on β-lg fibril formation.

Thus, CuO nanoparticles played a significant role in protecting against β-lg fibrillation, as supported by TEM imaging of the different β-lg fibrils.

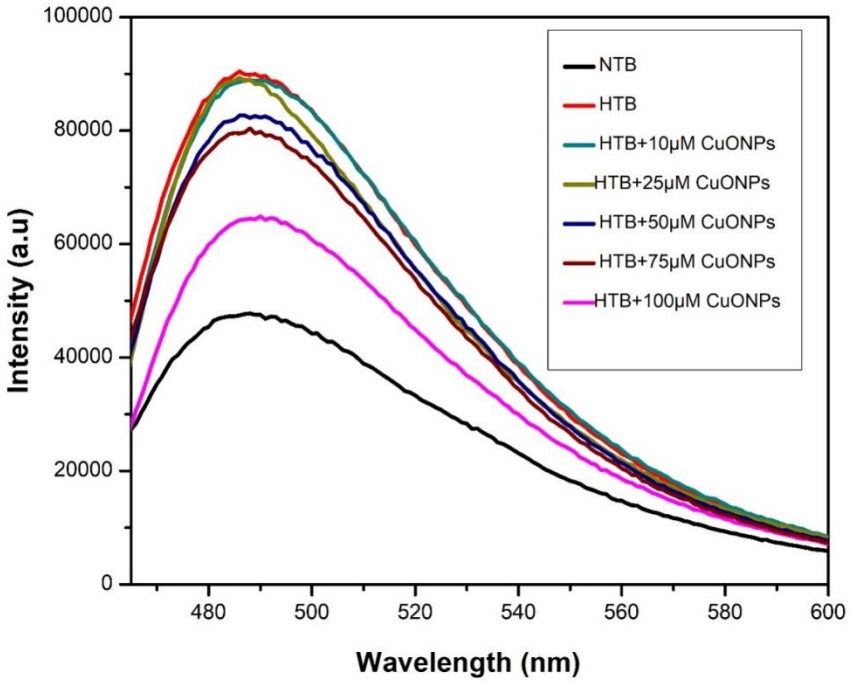

Figure 5: The ThT assay was performed to investigate the aggregation of heat-stressed (75°C for 1 hour) β-lg in both the presence and absence of CuO NPs. Fluorescence emissions were detected within the 460–600 nm wavelength range following excitation at 450 nm. The black profile in **(Fig.5)** represents native β-lg at physiological pH, while the red profile indicates β-lg that was thermally incubated at approximately 75°C for 1 hour. The additional profiles depict β-lg thermally incubated with varying concentrations of copper oxide nanoparticles (CuO NPs).

6.3.5. Rayleigh light scattering (RLS) Study

Rayleigh light scattering (RLS) is a widely used experiment to investigate protein aggregation. In this study, the scattering of light is measured to detect the presence of colloidal particles in the medium. Larger protein aggregates scatter light more effectively than smaller ones. Therefore, an increase in RLS intensity in a protein solution is an indication of aggregation, whereas a decrease in intensity can signal protein disaggregation or disassembly. **Fig.6** illustrates the changes in scattering intensity measured at 350 nm after exciting heat-treated beta-lactoglobulin solution at 350 nm in the absence and presence of varying concentrations of the copper oxide nanoparticles (CuO NPs) at pH 7.4. In our study, we collected RLS data following the thermal incubation of β-lg solutions at 75°C for 1 hour, both with and without the presence of CuO NPs. The native β-lg exhibited minimal scattering intensity, indicating the presence of pure soluble native β-lg. After thermal incubation, the exposed hydrophobic groups led to aggregate formation, resulting in higher RLS intensity for the heat-incubated β-lg without CuO NPs **(Fig.6)**. Upon exposure to varying concentrations of synthesized copper oxide nanoparticles (CuO NPs), thermally incubated β-lg exhibited reduced RLS intensities, suggesting the formation of smaller β-lg aggregates. The decrease in RLS intensities was observed to diminish in a concentration-dependent manner, thereby affirming the formation of considerably smaller aggregates subsequent to the thermal exposure of β-lg in the presence of the synthesized CuO NPs.

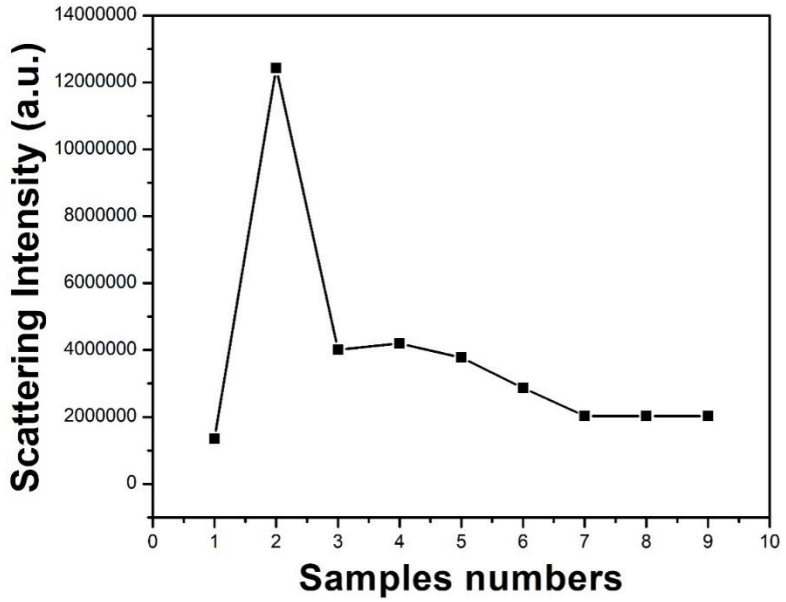

Figure 6: Rayleigh light scattering data was collected for native β -lg (sample no.1) and β -lg incubated at 75°C for 1 hour (sample no.2). This was performed in the absence and presence

of copper oxide nanoparticles (CuO NPs) at concentrations including samples no. 3, 4, 5, 6, 7, 8, and 9. The samples were excited at 350 nm and emitted at the same wavelength.

6.3.6. Secondary Structural change monitored by Circular Dichroism (CD)

The investigation utilized the Far-UV CD technique to explore the potential impact of copper oxide nanoparticles (CuO NPs) on the secondary structural transformation of β -lg. The protein was subjected to incubation, both with and without CuO NPs, at 75°C for a duration of 1 hour in 10 mM phosphate buffer, pH 7.4. Subsequently, CD spectroscopy was employed to assess the presence of β-sheet structures. Scanning the CD spectra within the 190–260 nm spectral region at varying concentrations of CuO NPs enabled the examination of potential alterations in the protein structure associated with amyloid fibrils. The findings from the far UV-CD studies are illustrated in **(Fig.7)**.

The CD spectra of native β-lg show two negative bands at 207 and 216 nm, indicating the presence of ordered secondary structural content containing α-helix and β-sheet (Bhattacharjee et al., 2005). The negative signal at 216 nm is characteristic of the protein's β-sheet structure. However, the heat-stressed β-lg **(Fig. 7, profile b)** exhibits an increase in negative ellipticity at 216 nm, suggesting the retention of the native secondary structure with the potential formation of cross-linked β-sheet structures. Thermal denaturation exposes the buried Cys121, leading to the formation of disulfide-linked oligomers. The higher non-covalent oligomer formation at this elevated temperature is the reason behind the formation of these cross-linked β-sheet structures.

The circular dichroism (CD) spectra of β -β-lactoglobulin (β-lg) subjected to heat stress in the presence of varied concentrations of CuO nanoparticles reveal a notable alteration in their patterns. Incubation of β-lg at 75°C in the presence of CuO nanoparticles results in a transformation of the secondary structure. Specifically, the diminished intensity of the minimum at 216 nm implies a loss of β-sheet structure, concomitant with an increase in α-helical structure, as demonstrated by heightened ellipticity at 205 nm and 207 nm in each instance. Notably, at higher concentrations of CuO nanoparticles, the CD spectra of β-lg exhibit more negative mean residue ellipticity (MRE) values within the 206-207 nm range and the disappearance of the 216 nm band. These characteristics signify structural transitions culminating in the disaggregation of the fibrillar structure. The β -lg sample underwent thermal stress at 75°C in the presence of varying concentrations of CuO NPs, resulting in observed

transitions from β to α -helical and random coil structures. Analysis of the individual secondary structural elements utilizing CDNN 2.1 software is delineated in Table 1 to further elucidate AuNP-induced β to a-helical transitions. These findings postulate that CuO NPs possess the capability to impede the formation of cross-linked β-sheet structures while concurrently fostering the emergence of α -helical structural content.

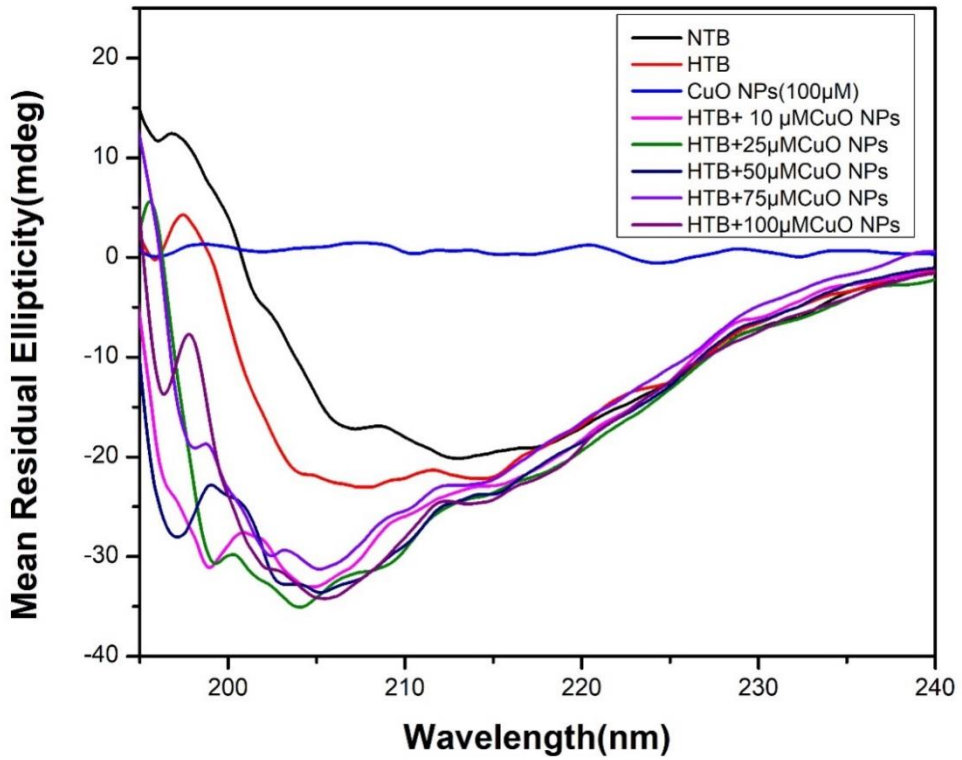

Figure 7: The far ultraviolet-circular dichroism (UV-CD) spectra of native β-lactoglobulin and β-lactoglobulin subjected to heat stress at 75°C for 1 hour were examined. The analysis was conducted in both the absence and presence of copper oxide (CuO) nanoparticles in a 10 mM phosphate buffer at pH 7.4. The concentration of the nanoparticles gradually increased from 10μM to 100μM. The concentration of β-lg was kept constant throughout the CD measurement at 0.25mg/ml.

Table 1: The secondary structure composition of the β-lactoglobulin (β-lg) sample was analyzed after a 1-hour incubation at 75°C in a 10 mM phosphate buffer with a pH of 7.4, both in the absence and in the presence of CuO NPs.

Samples	α-Helix (%)	β -Structure (%)	β -turn (%)	Random coil(%)
Native β-lg	22.3	39.7	11.4	26.6
Heat treated β-lg (HTB)	20.8	35.6	11.9	31.7
HTB+ 10μM CuO NPs	21.9	33.4	12.5	32.2
HTB+ 25μM CuO NPs	22.3	31.6	13.1	33.0
HTB+ 50μM CuO NPs	22.9	30.2	13.6	33.3
HTB+ 75μM CuO NPs	23.2	29.0	14.1	33.7
HTB+ 100μM CuO NPs	23.5	27.3	14.3	34.9

6.3.7. SDS- Polyacrylamide Gel Electrophoresis measurement

The SDS-PAGE analysis serves as a convenient method for examining protein aggregation under non-reducing conditions. In the course of this study, the native β--lg was observed as a singular band (Lane 2) in the gel at approximately 18.3 kDa, indicative of its monomeric state. Subsequent to an incubation period at 75°C in 10 mM phosphate buffer at pH 7.4 for 1 hour, the β--lg sample in **(Fig.8)** revealed an array of protein bands (Lane 3), implying the formation of densely packed aggregates. This analytical technique facilitated the isolation of non-covalently bonded aggregates into monomers while preserving the integrity of disulphide-linked aggregates. The thiol group of Cys121 of β-lg forms S–S linkages upon incubation at 75–80°C, resulting in the generation of dimers and other covalently bound 'intermediates' during the process of aggregation (Manderson et al., 1998; Croguennec et al., 2004). This mechanism entails the reconfiguration of disulfide bonds, encompassing the establishment of new intramolecular and intermolecular disulfide bridges, as well as the rearrangement of existing intramolecular disulfide bridges (Mousavi et al., 2008).

When beta-lactoglobulin (β -lg) was subjected to incubation at 75°C for a duration of 1-hour, distinct bands manifested in the gel, signifying the emergence of self-assemblies of β -lg (Lane 3) alongside a less pronounced band aligning with the monomer. Notably, the application of SDS-PAGE analysis to β -lg subjected to heat treatment in the presence of CuO NPs under non-reducing conditions resulted in markedly disparate outcomes. The bands corresponding to β -lg oligomers with lower electrophoretic mobilities and the larger aggregates, which do not enter the gel, are noticeably absent in lanes 4, 5, 6, and 7. Hence, CuO NPs demonstrate the capacity

to impede the aggregation of β -lg under conditions of thermal stress. The immobilization of β -lg on the surface of CuO NPs, facilitated by the free thiol (Cys121) on β-lg, stands as the primary factor responsible for reducing the likelihood of random protein-protein interactions, consequently leading to the inhibition of protein aggregation. Lane 1 depicts the SDS-PAGE pattern of a marker protein with a known molecular weight (PageRulerTM, Prestained Protein Ladder, comprising bands at 10, 17, 26, 34, 43, 55, 72, 95, 130, and 170 kDa, sourced from Fermentus Life Science, reference #SM0671), run in parallel.

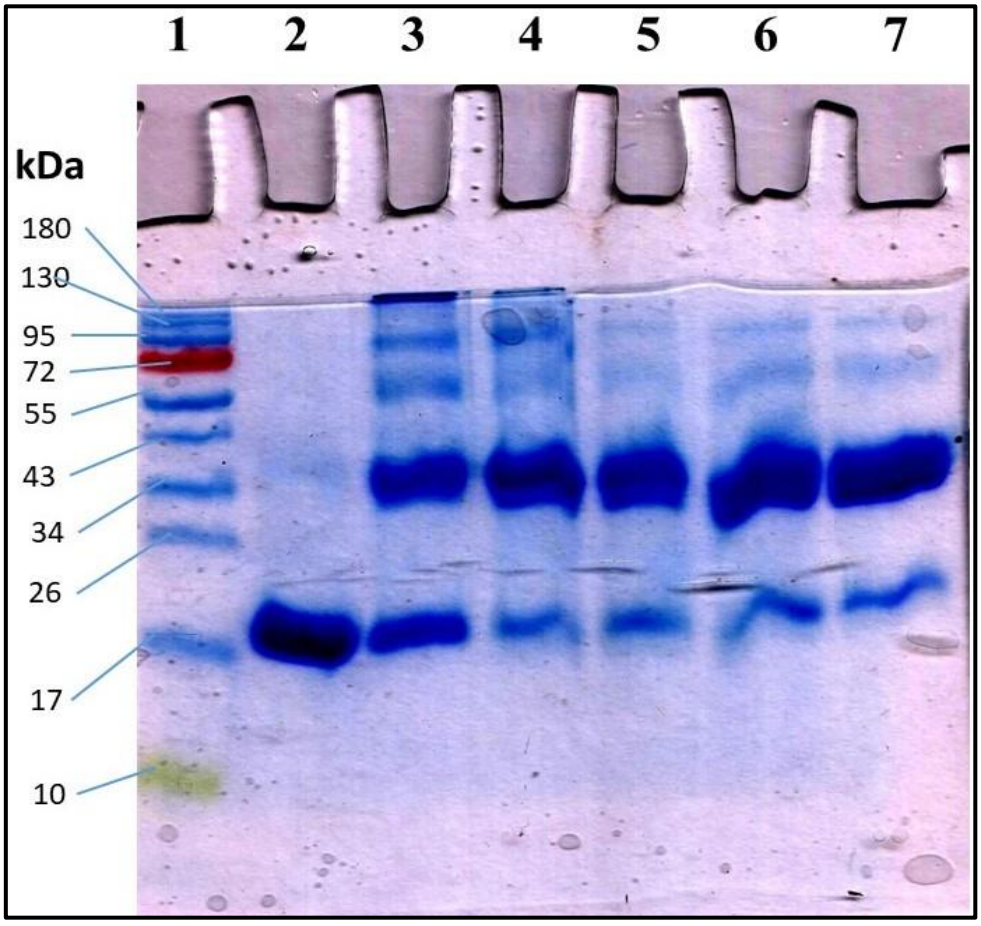

Figure 8: The SDS-PAGE (12%) profiles show the native β-lactoglobulin (β-lg) in lane 2, heat-stressed β-lg at 75°C for 1 hour without CuO NPs in lane 3, and with CuO NPs at concentrations of 10 µM, 25 µM, 50 µM, and 75 µM in lanes 4, 5, 6, and 7, respectively. Lane 1 displays the SDS-PAGE profile of a marker protein with known molecular weights (PageRulerTM, Prestained Protein Ladder, with bands at 10, 17, 26, 34, 43, 55, 72, 95, 130, and 170 kDa, obtained from Fermentus Life Science, #SM0671) run alongside the other samples.

6.3.8. Transmission electron microscopy (TEM) analysis

In order to confirm the results obtained from previous sections, we conducted morphological studies using TEM to examine the end-point products resulting from the heat-induced aggregation of β-lg in the absence and presence of CuO NPs. In the images, the bare CuO nanoparticles are depicted as spherical black particles with a diameter of approximately 8 nm. **(Fig. 9, profile c)**. Without CuO NPs, β-lg formed long, smooth fibrillar aggregates **(Fig.9 profile b)** after incubation at 75°C for 1 hour. However, when incubated with 25 μM CuO NPs, β-lg formed aggregates with different morphological characteristics **(Fig.9, profile d)**. The number of well-defined fibrils decreased, and some fibrils became fragmented. Additionally, we observed some spherical oligomers along with the formation of amorphous aggregates. The reduction of amyloid fibrillation was notably observed when the beta-lactoglobulin was subjected to treatment with 100 μM CuO NPs under thermal conditions **(Fig.9, profile e)**. The CuO nanoparticles demonstrated a notable protective effect on the aggregation of bovine β-lg. Our in vitro observations establish that CuO nanoparticles exhibit potent anti-fibrillogenic activity on the aggregation of bovine β-lg.

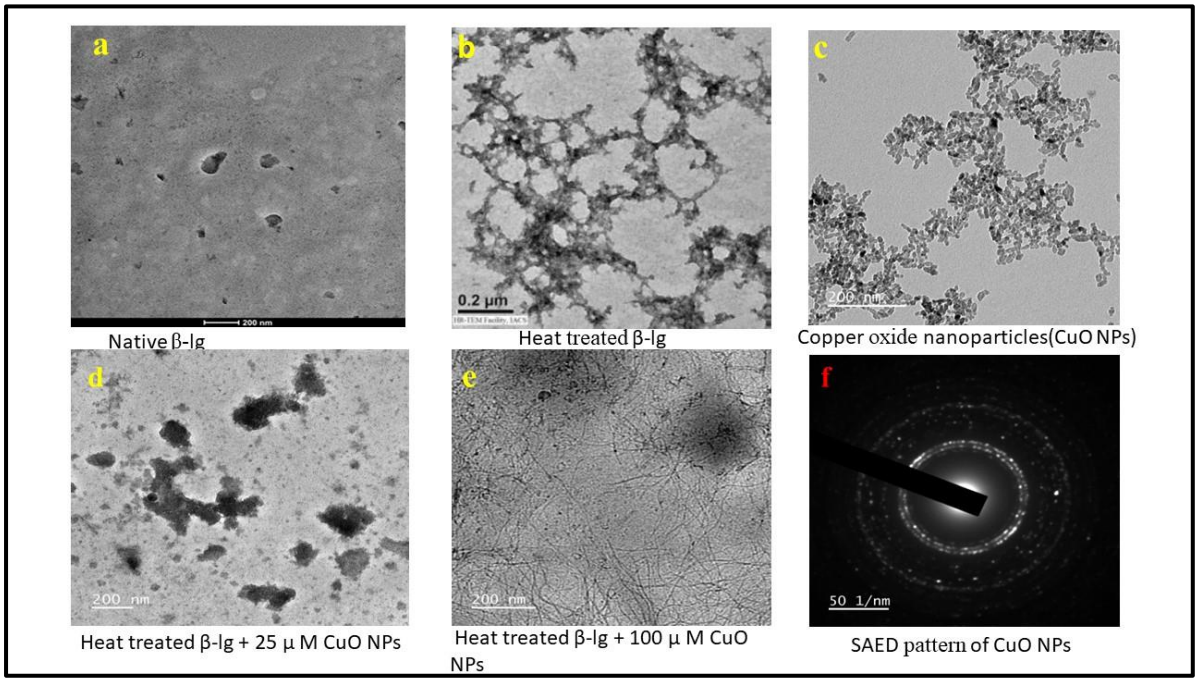

Figure 9: Selected TEM images of CuO nanoparticles (profile c) and heat-stressed β-lactoglobulin at 75°C for 1 hour in the absence (profile b) and presence (profile d and e) of CuO nanoparticles in a 10 mM phosphate buffer at pH 7.4. Throughout the incubations, the concentrations of beta-lactoglobulin and CuO nanoparticles were maintained at 2.5 mg/ml, 25

μM, and 100 μM, respectively. Profile a and f represent native β-lg at physiological pH and SAED pattern of synthesized CuO NPs respectively.

The observed particle size in the TEM image falls within the range of 7-8 nm, which aligns well with the size calculated using the Scherrer formula based on X-ray diffraction (XRD) data. Furthermore, **(Fig.9, profile e)** showcases the selected area electron diffraction (SAED) pattern of the as-prepared CuO nanoparticles. This pattern indicates that the particles possess a well-crystallized structure. Additionally, the diffraction rings observed in the SAED image correspond to the peaks in the XRD pattern, further confirming the monoclinic structure of the as-prepared CuO nanoparticles (Wang et al., 2002).

6.4. Conclusion

Protein misfolding diseases constitute a group of disorders characterized by the accumulation of misfolded proteins, potentially resulting in the formation of toxic protein aggregates. Nanoparticles have demonstrated promise in mitigating protein aggregation owing to their distinctive properties. Our primary objective is to diligently assess the influence of copper oxide nanoparticles on protein aggregation and to elucidate the mechanisms through which nanoparticles disrupt this process. Our focus is on the fundamental factors influencing protein-nanoparticle interactions, including size, charge, concentration, surface modification, and morphology, in order to achieve the desired impact of nanoparticles on protein aggregation. Our ultimate goal is to provide comprehensive insights into these interactions and to propose a systematic approach to nanoparticle design capable of inhibiting protein aggregation in protein misfolding diseases.

6.5. References

Arvizo, R., Bhattacharya, R. and Mukherjee, P., 2010. Gold nanoparticles: opportunities and challenges in nanomedicine. Expert opinion on drug delivery, 7(6), pp.753-763.

Aschaffenburg, R. and Drewry, J., 1957. Improved method for the preparation of crystalline β-lactoglobulin and α-lactalbumin from cow's milk. Biochemical Journal, 65(2), p.273.

Ban, D.K. and Paul, S., 2019. Functionalized gold and silver nanoparticles modulate amyloid fibrillation, defibrillation, and cytotoxicity of lysozyme via altering protein surface character. Applied Surface Science, 473, pp.373-385.

Banerjee, V. and Das, K.P., 2012. Modulation of pathway of insulin fibrillation by a small molecule helix inducer 2, 2, 2-trifluoroethanol. Colloids and Surfaces B: Biointerfaces, 92, pp.142-150.

Barbalinardo, M., Antosova, A., Gambucci, M., Bednarikova, Z., Albonetti, C., Valle, F., Sassi, P., Latterini, L., Gazova, Z. and Bystrenova, E., 2020. Effect of metallic nanoparticles on amyloid fibrils and their influence to neural cell toxicity. Nano Research, 13, pp.1081-1089.

Bellova, A., Bystrenova, E., Koneracka, M., Kopcansky, P., Valle, F., Tomasovicova, N., Timko, M., Bagelova, J., Biscarini, F. and Gazova, Z., 2010. Effect of Fe3O4 magnetic nanoparticles on lysozyme amyloid aggregation. Nanotechnology, 21(6), p.065103.

Bhattacharjee, C., Saha, S., Biswas, A., Kundu, M., Ghosh, L. and Das, K.P., 2005. Structural changes of β-lactoglobulin during thermal unfolding and refolding–an FT-IR and circular dichroism study. The Protein Journal, 24(1), pp.27-35.

Biancalana, M. and Koide, S., 2010. Molecular mechanism of Thioflavin-T binding to amyloid fibrils. Biochimica et Biophysica Acta (BBA)-Proteins and Proteomics, 1804(7), pp.1405-1412.

Bramanti, E., Fulgentini, L., Bizzarri, R., Lenci, F. and Sgarbossa, A., 2013. β-Amyloid amorphous aggregates induced by the small natural molecule ferulic acid. The Journal of Physical Chemistry B, 117(44), pp.13816-13821.

Cattoni, D.I., Kaufman, S.B. and Flecha, F.L.G., 2009. Kinetics and thermodynamics of the interaction of 1-anilino-naphthalene-8-sulfonate with proteins. Biochimica et Biophysica Acta (BBA)-Proteins and Proteomics, 1794(11), pp.1700-1708.

Cava, R.J., 1990. Structural chemistry and the local charge picture of copper oxide superconductors. Science, 247(4943), pp.656-662.

Chamani, J. and Moosavi-Movahedi, A.A., 2006. Effect of n-alkyl trimethylammonium bromides on folding and stability of alkaline and acid-denatured cytochrome c: a spectroscopic approach. Journal of colloid and interface science, 297(2), pp.561-569.

Chamani, J., Moosavi-Movahedi, A.A., Rajabi, O., Gharanfoli, M., Momen-Heravi, M., Hakimelahi, G.H., Neamati-Baghsiah, A. and Varasteh, A.R., 2006. Cooperative α-

helix formation of β-lactoglobulin induced by sodium n-alkyl sulfates. Journal of colloid and interface science, 293(1), pp.52-60.

Chiti, F., Webster, P., Taddei, N., Clark, A., Stefani, M., Ramponi, G. and Dobson, C.M., 1999. Designing conditions for in vitro formation of amyloid protofilaments and fibrils. Proceedings of the National Academy of Sciences, 96(7), pp.3590-3594.

Cho, K., Wang, X.U., Nie, S., Chen, Z. and Shin, D.M., 2008. Therapeutic nanoparticles for drug delivery in cancer. Clinical cancer research, 14(5), pp.1310-1316.

Choudhary, S., Kishore, N. and Hosur, R.V., 2015. Inhibition of insulin fibrillation by osmolytes: Mechanistic Insights. Scientific reports, 5(1), p.17599.

Collini, M., D'Alfonso, L., Molinari, H., Ragona, L., Catalano, M. and Baldini, G., 2003. Competitive binding of fatty acids and the fluorescent probe 1-8-anilinonaphthalene sulfonate to bovine β-lactoglobulin. Protein Science, 12(8), pp.1596-1603.

Conway, K.A., Harper, J.D. and Lansbury, P.T., 1998. Accelerated in vitro fibril formation by a mutant α-synuclein linked to early-onset Parkinson disease. Nature medicine, 4(11), pp.1318-1320.

Cooper, G.J., Willis, A.C., Clark, A., Turner, R.C., Sim, R.B. and Reid, K.B., 1987. Purification and characterization of a peptide from amyloid-rich pancreases of type 2 diabetic patients. Proceedings of the National Academy of Sciences, 84(23), pp.8628-8632.

Croguennec, T, T. O'Kennedy, B. and Mehra, R., 2004. Heat-induced denaturation/aggregation of β-lactoglobulin A and B: kinetics of the first intermediates formed. International Dairy Journal, 14(5), pp.399-409.

De Jong, W.H. and Borm, P.J., 2008. Drug delivery and nanoparticles: applications and hazards. International journal of nanomedicine, 3(2), pp.133-149.

Fändrich, M., Fletcher, M.A. and Dobson, C.M., 2001. Amyloid fibrils from muscle myoglobin. Nature, 410(6825), pp.165-166.

Ferrao-Gonzales, A.D., Souto, S.O., Silva, J.L. and Foguel, D., 2000. The pre-aggregated state of an amyloidogenic protein: hydrostatic pressure converts native transthyretin into the amyloidogenic state. Proceedings of the National Academy of Sciences, 97(12), pp.6445-6450.

Fink, A.L., 1998. Protein aggregation: folding aggregates, inclusion bodies, and amyloid. Folding and design, 3(1), pp. R9-R23.

Gilgun-Sherki, Y., Melamed, E. and Offen, D., 2006. Anti-inflammatory drugs in the treatment of neurodegenerative diseases: current state. Current pharmaceutical design, 12(27), pp.3509-3519.

Giurleo, J.T., He, X. and Talaga, D.S., 2009. Erratum to" β-Lactoglobulin Assembles into Amyloid through Sequential Aggregated Intermediates"[J. Mol. Biol. 381 (2008) 1332-1348. Journal of Molecular Biology, 388(1), p.208.

Gupta, Y., Singla, G. and Singla, R., 2015. Insulin-derived amyloidosis. Indian journal of endocrinology and metabolism, 19(1), pp.174-177.

Halder, U.C., Chakraborty, J., Das, N. and Bose, S., 2012. Tryptophan dynamics in the exploration of micro-conformational changes of refolded β-lactoglobulin after thermal exposure: A steady-state and time-resolved fluorescence approach. Journal of Photochemistry and Photobiology B: Biology, 109, pp.50-57.

Hoppenreijs, L.J.G., Fitzner, L., Ruhmlieb, T., Heyn, T.R., Schild, K., Van Der Goot, A.J., Boom, R.M., Steffen-Heins, A., Schwarz, K. and Keppler, J.K., 2022. Engineering amyloid and amyloid-like morphologies of β-lactoglobulin. Food Hydrocolloids, 124, p.107301.

Hsieh, S., Chang, C.W. and Chou, H.H., 2013. Gold nanoparticles as amyloid-like fibrillogenesis inhibitors. Colloids and Surfaces B: Biointerfaces, 112, pp.525-529.

Jayamani, J., Shanmugam, G. and Singam, E.R.A., 2014. Inhibition of insulin amyloid fibril formation by ferulic acid, a natural compound found in many vegetables and fruits. RSC advances, 4(107), pp.62326-62336.

Jean, E., Ebbo, M., Valleix, S., Benarous, L., Heyries, L., Grados, A., Bernit, E., Grateau, G., Papo, T., Granel, B. and Daniel, L., 2014. A new family with hereditary lysozyme amyloidosis with gastritis and inflammatory bowel disease as prevailing symptoms. BMC Gastroenterology, 14, pp.1-6.

Khurana, R., Coleman, C., Ionescu-Zanetti, C., Carter, S.A., Krishna, V., Grover, R.K., Roy, R. and Singh, S., 2005. Mechanism of thioflavin T binding to amyloid fibrils. Journal of Structural Biology, 151(3), pp.229-238.

Krebs, M.R., Devlin, G.L. and Donald, A.M., 2009. Amyloid fibril-like structure underlies the aggregate structure across the pH range for β-lactoglobulin. Biophysical journal, 96(12), pp.5013-5019.

Kumar, S. and Udgaonkar, J.B., 2010. Mechanisms of amyloid fibril formation by proteins. Current Science, pp.639-656.

Kuznetsova, I.M., Sulatskaya, A.I., Uversky, V.N. and Turoverov, K.K., 2012. A new trend in the experimental methodology for the analysis of the thioflavin T binding to amyloid fibrils. Molecular neurobiology, 45, pp.488-498.

Kwak, K. and Kim, C., 2005. Viscosity and thermal conductivity of copper oxide nanofluid dispersed in ethylene glycol. Korea-Australia Rheology Journal, 17(2), pp.35-40.

Laemmli, U.K., 1970. Cleavage of structural proteins during the assembly of the head of bacteriophage T4. nature, 227(5259), pp.680-685.

Lanje, A.S., Sharma, S.J., Pode, R.B. and Ningthoujam, R.S., 2010. Synthesis and optical characterization of copper oxide nanoparticles. Adv Appl Sci Res, 1(2), pp.36-40.

Linse, S., Cabaleiro-Lago, C., Xue, W.F., Lynch, I., Lindman, S., Thulin, E., Radford, S.E. and Dawson, K.A., 2007. Nucleation of protein fibrillation by nanoparticles. Proceedings of the National Academy of Sciences, 104(21), pp.8691-8696.

Litvinovich, S.V., Brew, S.A., Aota, S., Akiyama, S.K., Haudenschild, C. and Ingham, K.C., 1998. Formation of amyloid-like fibrils by self-association of a partially unfolded fibronectin type III module. Journal of molecular biology, 280(2), pp.245-258.

Maity, S., Pal, S., Parvej, H., Das, N., Sepay, N., Sarkar, M. and Halder, U.C., 2016. Facile synthesis and characterization of beta lactoglobulin–copper nanocomposites having antibacterial applications. RSC advances, 6(88), pp.85340-85346.

Manderson, G.A., Hardman, M.J. and Creamer, L.K., 1998. Effect of heat treatment on the conformation and aggregation of β-lactoglobulin A, B, and C. Journal of Agricultural and Food Chemistry, 46(12), pp.5052-5061.

Mathew, A., Fukuda, T., Nagaoka, Y., Hasumura, T., Morimoto, H., Yoshida, Y., Maekawa, T., Venugopal, K. and Kumar, D.S., 2012. Curcumin loaded-PLGA nanoparticles

conjugated with Tet-1 peptide for potential use in Alzheimer's disease. PLoS one, 7(3), p.e32616.

Matulis, D., Baumann, C.G., Bloomfield, V.A. and Lovrien, R.E., 1999. 1-Anilino-8-naphthalene sulfonate as a protein conformational tightening agent. Biopolymers: Original Research on Biomolecules, 49(6), pp.451-458.

McParland, V.J., Kad, N.M., Kalverda, A.P., Brown, A., Kirwin-Jones, P., Hunter, M.G., Sunde, M. and Radford, S.E., 2000. Partially unfolded states of β2-microglobulin and amyloid formation in vitro. Biochemistry, 39(30), pp.8735-8746.

Melkani, G.C., Trujillo, A.S., Ramos, R., Bodmer, R., Bernstein, S.I. and Ocorr, K., 2013. Huntington's disease induced cardiac amyloidosis is reversed by modulating protein folding and oxidative stress pathways in the Drosophila heart. PLoS genetics, 9(12), p.e1004024.

Mills, O.E., 1976. Effect of temperature on tryptophan fluorescence of β-lactoglobulin B. Biochimica et Biophysica Acta (BBA)-Protein Structure, 434(2), pp.324-332.

Morones, J.R., Elechiguerra, J.L., Camacho, A., Holt, K., Kouri, J.B., Ramírez, J.T. and Yacaman, M.J., 2005. The bactericidal effect of silver nanoparticles. Nanotechnology, 16(10), p.2346.

Mousavi, S.H.A., Bordbar, A.K. and Haertlé, T., 2008. Changes in structure and in interactions of heat-treated bovine β-lactoglobulin. Protein and Peptide Letters, 15(8), pp.818-825.

Muchowski, P.J., Schaffar, G., Sittler, A., Wanker, E.E., Hayer-Hartl, M.K. and Hartl, F.U., 2000. Hsp70 and hsp40 chaperones can inhibit the self-assembly of polyglutamine proteins into amyloid-like fibrils. Proceedings of the National Academy of Sciences, 97(14), pp.7841-7846.

Muchowski, P.J., Schaffar, G., Sittler, A., Wanker, E.E., Hayer-Hartl, M.K. and Hartl, F.U., 2000. Hsp70 and hsp40 chaperones can inhibit self-assembly of polyglutamine proteins into amyloid-like fibrils. Proceedings of the National Academy of Sciences, 97(14), pp.7841-7846.

Murphy, S.R., Chang, C.C., Dogbevia, G., Bryleva, E.Y., Bowen, Z., Hasan, M.T. and Chang, T.Y., 2013. Acat1 knockdown gene therapy decreases amyloid-β in a mouse model of Alzheimer's disease. Molecular Therapy, 21(8), pp.1497-1506.

Nelson, R. and Eisenberg, D., 2006. Recent atomic models of amyloid fibril structure. Current opinion in structural biology, 16(2), pp.260-265.

Nilsson, M.R., 2004. Techniques to study amyloid fibril formation in vitro. Methods, 34(1), pp.151-160.

Nowacek, A., Kosloski, L.M. and Gendelman, H.E., 2009. Neurodegenerative disorders and nanoformulated drug development. Nanomedicine, 4(5), pp.541-555.

Palmal, S., Jana, N.R. and Jana, N.R., 2014. Inhibition of amyloid fibril growth by nanoparticle coated with histidine-based polymer. The Journal of Physical Chemistry C, 118(37), pp.21630-21638.

Palmal, S., Maity, A.R., Singh, B.K., Basu, S., Jana, N.R. and Jana, N.R., 2014. Inhibition of amyloid fibril growth and dissolution of amyloid fibrils by curcumin–gold nanoparticles. Chemistry–A European Journal, 20(20), pp.6184-6191.

Pandey, N.K., Ghosh, S. and Dasgupta, S., 2010. Fibrillation in human serum albumin is enhanced in the presence of copper (II). The Journal of Physical Chemistry B, 114(31), pp.10228-10233.

Pedersen, J.S., Flink, J.M., Dikov, D. and Otzen, D.E., 2006. Sulfates dramatically stabilize a salt-dependent type of glucagon fibrils. Biophysical journal, 90(11), pp.4181-4194.

Pepys, M.B., Hawkins, P.N., Booth, D.R., Vigushin, D.M., Tennent, G.A., Soutar, A.K., Totty, N., Nguyen, O., Blake, C.C.F., Terry, C.J. and Feest, T.G., 1993. Human lysozyme gene mutations cause hereditary systemic amyloidosis. Nature, 362(6420), pp.553-557.

Polymeropoulos, M.H., Lavedan, C., Leroy, E., Ide, S.E., Dehejia, A., Dutra, A., Pike, B., Root, H., Rubenstein, J., Boyer, R. and Stenroos, E.S., 1997. Mutation in the α-synuclein gene identified in families with Parkinson's disease. science, 276(5321), pp.2045-2047.

Raman, B., Chatani, E., Kihara, M., Ban, T., Sakai, M., Hasegawa, K., Naiki, H., Rao, C.M. and Goto, Y., 2005. Critical balance of electrostatic and hydrophobic interactions is required for β2-microglobulin amyloid fibril growth and stability. Biochemistry, 44(4), pp.1288-1299.

Sardar, S., Anas, M., Maity, S., Pal, S., Parvej, H., Begum, S., Dalui, R., Sepay, N. and Halder, U.C., 2019. Silver nanoparticle modulates the aggregation of beta-lactoglobulin and

induces to form rod-like aggregates. International journal of biological macromolecules, 125, pp.596-604.

Sardar, S., Pal, S., Maity, S., Chakraborty, J. and Halder, U.C., 2014. Amyloid fibril formation by β-lactoglobulin is inhibited by gold nanoparticles. International journal of biological macromolecules, 69, pp.137-145.

Schokker, E.P., Singh, H., Pinder, D.N. and Creamer, L.K., 2000. Heat-induced aggregation of β-lactoglobulin AB at pH 2.5 as influenced by ionic strength and protein concentration. International Dairy Journal, 10(4), pp.233-240.

Sciarretta, K.L., Gordon, D.J. and Meredith, S.C., 2006. Peptide-based inhibitors of amyloid assembly. Methods in enzymology, 413, pp.273-312.

Sen, S., Konar, S., Das, B., Pathak, A., Dhara, S., Dasgupta, S. and Dasgupta, S., 2016. Inhibition of fibrillation of human serum albumin through interaction with chitosan-based biocompatible silver nanoparticles. RSC advances, 6(49), pp.43104-43115.

Sharma, V. and Ghosh, K.S., 2019. Inhibition of amyloid fibrillation by small molecules and nanomaterials: strategic development of pharmaceuticals against amyloidosis. Protein and Peptide Letters, 26(5), pp.315-323.

Sharma, V., Sharma, S., Rana, S. and Ghosh, K.S., 2020. Inhibition of amyloid fibrillation of human γD-crystallin by gold nanoparticles: Studies at molecular level. Spectrochimica Acta Part A: Molecular and Biomolecular Spectroscopy, 233, p.118199.

Skaat, H., Belfort, G. and Margel, S., 2009. Synthesis and characterization of fluorinated magnetic core-shell nanoparticles for inhibition of insulin amyloid fibril formation. Nanotechnology, 20(22), p.225106.

Stirpe, A., Pantusa, M., Rizzuti, B., Sportelli, L., Bartucci, R. and Guzzi, R., 2011. Early-stage aggregation of human serum albumin in the presence of metal ions. International journal of biological macromolecules, 49(3), pp.337-342.

Stoimenov, P.K., Klinger, R.L., Marchin, G.L. and Klabunde, K.J., 2002. Metal oxide nanoparticles as bactericidal agents. Langmuir, 18(17), pp.6679-6686.

Sunde, M., Serpell, L.C., Bartlam, M., Fraser, P.E., Pepys, M.B. and Blake, C.C., 1997. Common core structure of amyloid fibrils by synchrotron X-ray diffraction. Journal of molecular biology, 273(3), pp.729-739.

Taylor, M., Moore, S., Mourtas, S., Niarakis, A., Re, F., Zona, C., La Ferla, B., Nicotra, F., Masserini, M., Antimisiaris, S.G. and Gregori, M., 2011. Effect of curcumin-associated and lipid ligand-functionalized nanoliposomes on aggregation of the Alzheimer's Aβ peptide. Nanomedicine: Nanotechnology, Biology and Medicine, 7(5), pp.541-550.

Tranquada, J.M., Sternlieb, B.J., Axe, J.D., Nakamura, Y. and Uchida, S.I., 1995. Evidence for stripe correlations of spins and holes in copper oxide superconductors. nature, 375(6532), pp.561-563.

Verma, M., Vats, A. and Taneja, V., 2015. Toxic species in amyloid disorders: Oligomers or mature fibrils. Annals of Indian Academy of Neurology, 18(2), pp.138-145.

Wang, H., Xu, J.Z., Zhu, J.J. and Chen, H.Y., 2002. Preparation of CuO nanoparticles by microwave irradiation. Journal of crystal growth, 244(1), pp.88-94.

Wu, W.H., Sun, X., Yu, Y.P., Hu, J., Zhao, L., Liu, Q., Zhao, Y.F. and Li, Y.M., 2008. TiO2 nanoparticles promote β-amyloid fibrillation in vitro. Biochemical and biophysical research communications, 373(2), pp.315-318.

Xiao, L., Zhao, D., Chan, W.H., Choi, M.M. and Li, H.W., 2010. Inhibition of beta 1–40 amyloid fibrillation with N-acetyl-l-cysteine capped quantum dots. Biomaterials, 31(1), pp.91-98.

Xie, L., Luo, Y., Lin, D., Xi, W., Yang, X. and Wei, G., 2014. The molecular mechanism of fullerene-inhibited aggregation of Alzheimer's β-amyloid peptide fragment. Nanoscale, 6(16), pp.9752-9762.

Xu, J.F., Ji, W., Shen, Z.X., Tang, S.H., Ye, X.R., Jia, D.Z. and Xin, X.Q., 1999. Preparation and characterization of CuO nanocrystals. Journal of Solid-State Chemistry, 147(2), pp.516-519.

Yu, W.W., Chang, E., Falkner, J.C., Zhang, J., Al-Somali, A.M., Sayes, C.M., Johns, J., Drezek, R. and Colvin, V.L., 2007. Forming biocompatible and nonaggregated nanocrystals in water using amphiphilic polymers. Journal of the American Chemical Society, 129(10), pp.2871-2879.

Zhu, J., Bi, H., Wang, Y., Wang, X., Yang, X. and Lu, L., 2008. CuO nanocrystals with controllable shapes grown from solution without any surfactants. Materials Chemistry and Physics, 109(1), pp.34-38.

Zúñiga, R.N., Tolkach, A., Kulozik, U. and Aguilera, J.M., 2010. Kinetics of formation and physicochemical characterization of thermally-induced β-lactoglobulin aggregates. Journal of Food Science, 75(5), pp. E261-E268.

Zurdo, J., Guijarro, J.I., Jiménez, J.L., Saibil, H.R. and Dobson, C.M., 2001. Dependence on solution conditions of aggregation and amyloid formation by an SH3 domain. Journal of molecular biology, 311(2), pp.325-340.

CHAPTER 7

Self‑assembly formation and acceleration of thermal aggregation of bovine β‑lactoglobulin in the presence of synthesized zinc oxide nanoparticles.

7.1. Introduction

Proteins possess the capacity to undergo conformational changes and engage in diverse self-assembly processes, resulting in the generation of distinct aggregates under varying environmental circumstances. Notably, protein aggregation is frequently linked with a partially unfolded intermediate state of the protein. Elevated protein concentrations under stress conditions, such as acidic pH and high temperature, can induce partial unfolding and subsequent self-assembly into amyloid fibrils. This phenomenon is implicated in the pathogenesis of a range of serious disorders, including Alzheimer's disease (Verma et al., 2015), Parkinson's disease (Polymeropoulos et al., 1997), Huntington's disease (Melkani et al., 2013), type II diabetes (Cooper et al., 1987), and lysozyme amyloidosis (Pepys et al., 1993). A defining characteristic of amyloid fibrils is the adoption of a cross-β sheet structure, leading to their self-assembly into elongated fibrillar structures (Sunde et al., 1997). Amyloid fibrils can originate from the misfolding and mutation of diverse proteins, including α-synuclein (Conway et al., 1998), insulin (Gupta et al., 2015), lysozyme (Jean et al., 2014), and huntingtin (Melkani et al., 2013), thereby contributing to the onset of amyloid-related diseases. Numerous strategies have been investigated as preventive measures against amyloid formation. These approaches encompass small peptides (Sciarretta et al., 2006), chaperones (Muchowski et al., 2000), various drugs (Nowacek et al., 2009; Gilgun-Sherki et al., 2006), gene therapy techniques (Murphy et al., 2013), and chemical osmolytes (Choudhary et al., 2015). However, a primary concern associated with current therapies is their limited ability to target and penetrate the blood-brain barrier (BBB), as well as concerns about the stability of the components within the biological system.

Additionally, aggregation can significantly reduce protein expression yields (Song et al., 2001). However, when carefully controlled, protein aggregation has often resulted in the creation of novel materials with diverse potential uses (Zhang, 2001). Therefore, the study of protein aggregation is considered to be one of the most promising areas of current scientific research. The process of amyloid aggregation, which is implicated in numerous diseases, has been the

subject of extensive research (Alam et al., 2016). It is important to note that under varying stress conditions, proteins manifest structures beyond amyloid fibrils (Krebs et al., 2009a).

For instance, β-lactoglobulin (β-lg) has been found to form amyloid fibrils resembling those present in several neurodegenerative diseases when the pH deviates significantly from its isoelectric point. Additionally, at the isoelectric point pI, β-lactoglobulin (β-lg) forms spherical aggregates (Krebs et al., 2009b). Furthermore, it has been observed by Krebs et al. that many other proteins exhibit similar properties to β-lactoglobulin (β-lg) (Krebs et al., 2007). Consequently, it is believed that protein particulate represents an additional prevalent form of protein aggregation. Amyloid fibrils are distinguishable by their capacity to bind amyloid-specific dyes such as ThT and Congo red, as well as by their characteristic X-ray diffraction patterns resulting from the cross-β structure (Hill et al., 2011). These unique features enable the differentiation of amyloid fibril aggregates from amorphous (disordered) protein aggregates. The pathological features of Alzheimer's disease (AD) involve the formation of amyloid-beta (Aβ) fibrils, which are rich in cross β-sheet structures due to the misfolding of Aβ peptide (Jakob-Roetne and Jacobsen, 2009; Siddiqi et al., 2016). These fibrils are formed through a process known as nucleation and growth (Harper and Lansbury Jr, 1997). As the disease progresses, monomers transform into oligomers, which then act as nuclei for fibril formation, followed by the elongation of the fibrils through the addition of more monomers (Roychaudhuri et al., 2009). β-Lactoglobulin (β-lg) has been extensively used in research on protein folding and aggregation.

β-Lactoglobulin (β-lg) is a fascinating protein with a predominantly beta-sheet structure containing 162 amino acid residues and a molecular weight of 18.4 kDa. This well-known globular whey protein has a pI of 5.2. Its structural composition includes a beta-barrel with 8 strands (A to H), followed by three turn alpha-helix and a final beta-strand (strand I) (Papiz et al., 1986). At pH 7.0, the protein exists as a reversible dimer, and the degree of dimerization is influenced by several factors such as pH, temperature, protein concentration, and ionic strength of the medium. When exposed to 75°C for 1 hour at pH 7.0, β-lg forms soluble aggregates of polymerized protein (Krebs et al., 2009a). β-lg is typically found in a dimeric state at room temperature and neutral pH, but it separates into monomers under acidic conditions (pH < 3) due to electrostatic repulsions between the subunits. It is noteworthy that β-lg contains two disulfide bonds (Cys66-Cys160 and Cys109-Cys119) along with a free thiol group (Cys121) (Sakurai et al., 2009). The presence of the free thiol Cys121 and disulfide linkage in β-lg is known to contribute to the formation of amyloid fibrillar aggregates of this protein under heat-

treated conditions. Research indicates that β-lg can rapidly form amyloid-like fibrils at low pH and high temperatures, or in the presence of denaturants at neutral pH (Giurleo et al., 2008). β-lg also forms amyloid-like aggregates in the presence of urea, low ionic strength, and acidic pH (Hamada and Dobson, 2002). Additionally, it forms nanofibrils at low pH through conventional and microwave heating (Hill et al., 2006; Hettiarachchi et al., 2012), or at neutral pH in the presence of co-solvents, dyes, and metal ions (Pal et al., 2016; Al-Shabib et al., 2018; Navarra et al., 2009). During the formation of these aggregates, the β-lg monomer goes through the development of aggregation-prone unfolding intermediates. The unfolding of the β-lg structure at temperatures above 60°C involves sulfhydryl-disulfide exchange reactions (Prabakaran and Damodaran, 1997; Yagi et al., 2003). A recent study shows that TFE can stabilize the alkaline unfolded intermediate of β-lg at low concentrations, but it leads to the formation of aggregates with different morphologies (Maity et al., 2016).

The misfolding of proteins, the subsequent growth of amyloids, and their deposition are associated with a spectrum of severe disorders, including Alzheimer's disease (Verma et al., 2015), Parkinson's disease (Polymeropoulos et al., 1997), Huntington's disease (Melkani et al., 2013), type II diabetes (Cooper et al., 1987), and lysozyme amyloidosis (Pepys et al., 1993). A distinguishing feature of amyloid fibrils is the formation of a cross-β sheet structure, leading to self-assembly into extended fibrils (Sunde et al., 1997). These amyloid fibrils can arise from the mutation and misfolding of various proteins, such as α-synuclein (Conway et al., 1998), insulin (Gupta et al., 2015), lysozyme (Jean et al., 2014), and huntingtin (Melkani et al., 2013), thereby contributing to the development of amyloid-related diseases.

Nanoparticles (NPs) smaller than 100 nm with adjustable surface properties are currently under investigation as potential therapeutic agents and drug carriers for various diseases (De Jong et al., 2008; Arvizo et al., 2010; Cho et al., 2008). However, further research is needed to understand their impact on protein misfolding, particularly amyloid formation. In vitro studies with different amyloidogenic proteins have shown that nanoparticles such as cerium oxide, copolymers, carbon nanotubes, quantum dots (Linse et al., 2007), and titanium dioxide (Wu et al., 2008) can accelerate amyloid nucleation time and enhance amyloid fibril growth. Conversely, other reports have indicated that gold, CdTe quantum dots (Hsieh et al., 2013; Palmal et al., 2014; Xiao et al., 2010), and iron oxide nanoparticles (Bellova et al., 2010) inhibit amyloid growth. Upon adsorption onto silica nanoparticles, lysozyme experiences a reduction in both alpha-helical content and enzymatic activity, with a more pronounced effect observed with larger nanoparticles (NPs) (Vertegel et al., 2004). This process of protein adsorption is

also effective for surface coating, thereby contributing to the stabilization of the nanoparticles and the mitigation of their cytotoxicity. Linse et al. demonstrated that a variety of nanoparticles (including copolymer, ceria, carbon nanotubes, and quantum dots) have the capability to prompt fibrillation of β2-microglobulin by enhancing protein localization on the nanoparticle surface, resulting in the formation of oligomers (Linse et al., 2007). This interaction with the nanoparticle surface can also introduce thermodynamic instability to the adsorbed protein molecules, rendering them susceptible to chemical denaturation. Moreover, ZnO nanoparticles were observed to induce unfolding of the periplasmic domain of the ToxR protein of Vibrio cholera, thereby rendering the protein vulnerable to denaturation by chaotropic agents (Chatterjee et al., 2010). Ribonuclease A experiences decreased stability upon adsorption on silica nanoparticle surfaces (Shang et al., 2007). In contrast, the structure and stability of cytochrome-C remain largely unaffected by interaction with zinc oxide nanoparticles (Šimšíková and Antalík, 2013). Recent findings suggest that certain nanomaterials have the capacity to prompt the formation of protein-based aggregates or act as catalysts in the creation of protein fibrils by altering the protein structure, thereby promoting the growth of extended assemblies (Linse et al., 2007; Zhang et al., 2009). An antibacterial Cu-β-lg nanocomposite is synthesized through the interaction of the free thiol of β-lg and copper ions, leading to the N-H bending of amide II of this protein (Sardar et al., 2016). Treatment of β-lg with AuNPs at 75°C produces smaller irregular aggregates. The findings indicate that AuNPs possess the capacity to impede the formation of amyloid fibrillar aggregates of β-lg in a concentration-dependent manner, potentially facilitating the refolding into a native-like structure. Consequently, AuNPs serve as nano-chaperones to suppress protein aggregation (Sardar et al., 2014). AgNPs strongly bind to the aggregation-prone regions of β-lg, thereby modifying its aggregation pathway and resulting in the formation of rod-shaped aggregates (Sardar et al., 2019). The interaction between NPs and proteins occurs through interfacial interaction, and the surface properties of both the proteins and NPs significantly influence any effects on the dynamics of the fibrillation process. The nature and extent of these effects depend largely on the core material and surface functionalization of NPs, as well as the type of proteins they interact with. These parameters should be thoroughly studied. Furthermore, the dynamics of fibrillation may be influenced by the administration time and dosage of NPs, leading to different stages of amyloid growth.

In particular, synthesized zinc oxide nanoparticles (ZnO NPs) have garnered attention due to their unique properties. Their small size and large surface area offer enhanced reactivity, while

their strong UV absorption and inherent antimicrobial properties make them especially valuable in medical applications. Furthermore, these nanoparticles show potential in cancer therapy and exhibit photocatalytic properties that position them as an invaluable resource in environmental remediation efforts (Radad et al.,2012; Maurer-Jones et al., 2013).

Our study focused on the interaction between β-lg and ZnO nanoparticles (NPs) under thermal conditions. Typically, when β-lg is exposed to heat, it forms amyloidal aggregates with a fibrillar structure. However, we observed that when β-lg is treated with ZnO NPs at 75°C, pH 7.5, using 10 mM sodium dihydrogen phosphate buffer, it forms rod-shaped fibrillar aggregates. This can be attributed to the large surface area of the ZnO NPs, allowing them to bind to β-lg through an adsorption process. As a result, the protein molecules come into proximity, leading to a specific ordered arrangement. Conformational changes cause buried portions of the protein to open up and bind to each other through non-covalent interactions such as hydrophobic interactions and hydrogen bonding.

7.2. Materials And Methods

7.2.1. Reagents and Chemicals Required

Sodium dihydrogen phosphate, zinc acetate, potassium hydroxide (KOH), and methanol were sourced from Merck in Mumbai, India. Acrylamide, bisacrylamide, N, N, N', N'-tetramethylethylenediamine (TEMED), ammonium persulfate (APS), sodium dodecyl sulfate (SDS), bromophenol blue, and Coomassie brilliant blue were purchased from Sigma-Aldrich. Various fluorescent probes, including 8-anilinonaphthalene-1-sulfonic acid ammonium salt (ANS), Congo red (CR), and Thioflavin T (ThT), were acquired from Sigma Chemical Co. in St. Louis, USA, and used without further purification. All other chemicals used were of the highest available purity. All buffer solutions were filtered through a 0.22 mm syringe filter from Millipore in the USA.

7.2.2. Isolation and purification of bovine beta-lactoglobulin (β-lg)

Bovine beta-lactoglobulin (β-lg) was extracted and purified from cow's milk using the method outlined by Aschaffenburg and Drewry (Aschaffenburg and Drewry, 1957). The final product was freeze-dried and stored at 4°C. To prepare the spectroscopic samples, β-lg was weighed and dissolved in a 0.01 M sodium phosphate buffer solution at pH 7.4. Protein stock solutions were then prepared using the same phosphate buffer at pH 7.4. Different concentrations of protein samples were created by dissolving β-lg in Milli-Q water and measuring the optical

density at 280 nm, taking into account the known extinction coefficient of β-lg (0.96 mg-1 mL-1 cm-1 at 280 nm).

7.2.3. Preparation of zinc oxide nanoparticles (ZnO NPs)

Zinc oxide (ZnO) nanoparticles (NPs) were successfully synthesized in accordance with a previously reported method (Pourrahimi et al., 2014). The glassware utilized in this synthesis underwent a meticulous cleaning process involving aqua regia (nitric acid: hydrochloric acid 1:3) followed by thorough rinsing with milli-Q water and subsequent drying in an oven. The primary objective of this study was to meticulously investigate the synthesis and optical characterization of Zinc Oxide (ZnO) nanoparticles using a precise combination of Zinc acetate, potassium hydroxide (KOH), and methanol as chemical reagents. The synthesis procedure commenced by dissolving 0.8977g of KOH into 100 mL of methanol, a process that involved heating the solution to 60°C to ensure the attainment of a uniform mixture. Subsequently, a specific solution of 2.107 g of zinc acetate dihydrate in 60 mL of deionized water was meticulously prepared. The introduction of the Zn solution into the KOH solution, coupled with vigorous stirring at 60°C for a duration of 90 minutes, yielded a well-dissolved solution. The resulting solution was then carefully divided into three equitably-sized portions for further investigation.

The properties of the ZnO particles were determined using the first part as a reference. The second and third parts underwent a modified Meulekamp washing method, which utilized methanol as the dispersing agent and a centrifuge to remove byproducts (Alvarado et al., 2013). This washing and redispersion process was repeated three times to obtain pure ZnO NPs. A meticulous process was followed to comprehensively characterize the product. At each stage, the solvent was carefully removed by heating it to 60°C until a white, dry powder containing the ZnO nanoparticles was obtained. The product was then subjected to thorough analysis using powder diffraction, with a D8 diffractometer utilized for crystal phase identification. Scherrer's formula was used to precisely estimate the average crystalline sizes. The purity of the ZnO NPs was confirmed through the repeated washing and redispersion method.

The UV-visible spectroscopic characterization of ZnO NPs was conducted at room temperature. The optical absorption spectra in the wavelength range of 200-600 nm were acquired in the presence and absence of the β-lg sample using a Shimadzu-TCC 240 A UV-Vis spectrophotometer. The characteristic signal of ZnO NPs was detected at 365 nm, thereby confirming the formation of ZnO NPs with a diameter of 30 nm. This finding was further

validated by the XRD study. Moreover, the absorption band of ZnO NPs exhibited a notable shift in the presence of β-lg (Alvarado et al., 2013).

7.2.4. Electrophoresis measurement

The sodium dodecyl sulfate-polyacrylamide gel electrophoresis (SDS-PAGE) was conducted under non-reducing conditions using a 15% acrylamide resolving gel as per Laemmli's method (Laemmli,1970). Samples of β-lg solution (2.5 mg/ml) in 10 mM sodium phosphate buffer at pH 7.4, and at pH 11.0, were separately treated in the presence and absence of ZnONPs. The resulting solutions underwent filtration using a syringe filter with a 0.2μm membrane. Subsequently, 20 μl aliquots of heat-treated β-lg solution with and without ZnONPs were loaded into the wells, along with 30 μl of native β-lg solution (2.5 mg ml-1) in a separate well. Electrophoretic separations were conducted using a maximum 100-volt application for 1 hour. Post-separation, the gel was stained with Coomassie Brilliant Blue R-250 and destained using a solution containing methanol and acetic acid.

7.2.5. UV-visible spectroscopy

The UV-visible JASCO spectrophotometer (Model V-730, Serial No. B184461798) and JASCO Spectra Manager Software were employed to acquire absorption spectra for the evaluation of binding affinity and binding constant at a standard temperature of 25°C. This experiment utilized two PerkinElmer quartz cells with a 1 cm path length for both the reference and samples. The absorbance measurements captured the intensity vs. wavelength spectra over the 200-600 nm range. A 10 mm phosphate buffer at pH 7.4 served as the reference, and the sample solutions exhibited a concentration of 13 μM.

7.2.6. ANS fluorescence study to monitor the change in hydrophobicity

8-Anilinonaphthalene-1-sulfonic acid (ANS) is utilized to gauge the surface hydrophobicity of protein molecules. A stock solution of 1 mg/ml ANS sample was prepared using Milli-Q water. In our study, to maintain a 50-molar excess of ANS compared to the protein concentration, 30 μl of ANS solution was added to each sample. ANS Fluorescence Measurements were carried out using a Horiba Fluorometer (Serial No: 1734D-4018-FM, Model: Fluoromax-4C). The samples were excited at 385 nm in a 1 cm pathlength four-sided transparent rectangular quartz cell. The emission and excitation slit widths were 5 nm, and the ANS fluorescence emission spectra were recorded from 395 nm to 600 nm using Fluoromax Software. Each spectrum was

blank-corrected, and the data points represented the average of triplicate measurements (Cattoni et al., 2009).

7.2.7. Congo Red Assay

In order to examine the formation of aggregates in the presence of ZnO NPs, an investigation was conducted by measuring the shift in absorbance of Congo red within the range of 400–650 nm. To carry out the experiment, 60 µl of protein solutions (at a concentration of 5 mg/ml) were withdrawn and mixed with 500 µl of a solution containing 100 µM Congo red in a 10-mM sodium phosphate buffer at pH 7.4. The final volume of the solution was then adjusted to 2.0 ml (Hudson et al., 2009). The concentration of the protein was 27.2 µM, while the concentration of Congo red was maintained at 40 µM

7.2.8. Transmission Electron Microscopy

High-resolution transmission electron microscopy (HR TEM) imaging was performed to analyze the behavior of β-lg in the presence and absence of ZnO nanoparticles. The imaging was carried out using a JEOL HRTEM-2011 instrument from Tokyo, Japan, at various magnifications (Hoppenreijs et al., 2022). Prior to the study, the sample solutions were centrifuged and diluted. These diluted solutions were then carefully drop-cast onto a carbon-coated copper grid with a mesh size of 300C from Pro Sci Tech. After 20 seconds, the excess solution was removed by gently shocking the grid on a filter paper. Subsequently, a 2% uranyl acetate solution from Sigma was added to stain the sample, and the grids were left to air-dry overnight in a desiccator. Once dried, the grids were ready for TEM imaging at a specific magnification.

7.2.9. Circular dichroism (CD) spectroscopy

To investigate the potential impact of zinc oxide nanoparticles (ZnO NPs) on the structure of β-lg, we conducted circular dichroism measurements using a Jasco Spectropolarimeter (J-815) at 20 °C in the far-UV range (200–260 nm) with rectangular cells of 1mm and 10 mm path length. The tests were performed on native β-lg solutions at pH 7.4 with concentrations of 0.25 mg ml-1, both in the presence and absence of ZnO NPs, as well as at pH 11.0. All spectra were the averages of three scans, and the final spectrum was obtained after subtracting the corresponding solvent spectrum. The far UV-CD curves were analyzed using the CDNN 2.1 curve-fitting program to determine the percentages of secondary structures present in β-lg under different conditions.

7.3. Results And Discussion

7.3.1. UV-Visible Spectroscopy

The ZnO nanoparticles underwent thorough analysis of their optical characteristics using UV-Vis spectroscopy at room temperature, as illustrated in **(Fig.1**). The obtained results showcased a prominent absorption feature within the ultraviolet range, spanning from 200 to 400 nm. Notably, the absorption peak, centered around 365 nm, revealed the excitonic behavior of ZnO at room temperature. This observation aligns with prior research on the optical properties of ZnO nanoparticles, underscoring the significance of understanding their features for diverse applications in the realm of nanotechnology (Singh et al., 2011). Furthermore, the confirmation of the synthesized ZnO nanoparticles was achieved through meticulous SEM and TEM studies.

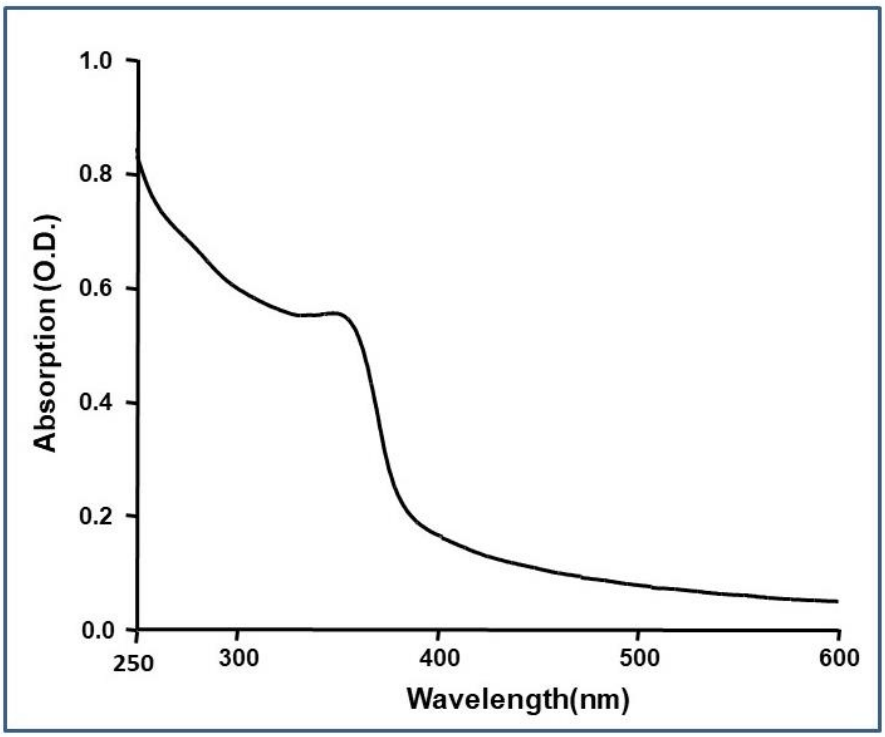

Figure 1: UV-VIS absorption spectrum of synthesized ZnO NPs.

Beta-lactoglobulin (β-lg) is known for its unique UV-visible spectra, which can be attributed to the presence of chromophores with an aromatic nucleus conjugated with groups having varying electronic effects. The native β-lg displays a characteristic protein band due to tryptophan residues, with a maximum wavelength (λmax) of 280 nm, as depicted in (Fig.2). Any changes in the UV-visible spectrum of native β-lg can signify alterations in the micro-environment surrounding the chromophores, as reported in the literature (Yu et al., 2007). These findings suggest that the micro-environment of β-lactoglobulin changes in the presence

of ZnO nanoparticles. ZnO nanoparticles interact with β-lactoglobulin to different extents, leading to modifications in the micro-environment of the protein around its tryptophan (Trp) and tyrosine (Tyr) residues. These resultant structural modifications of the protein manifest in the UV-absorbance of β-lactoglobulin.

7.3.2. Powdered XRD Spectra

The X-ray diffraction (XRD) pattern gathered from the sample clearly indicates the presence of well-defined crystalline ZnO nanoparticles. The XRD spectra exhibit prominent diffraction peaks at 31, 34, 36, 47, 56, 62, 66, 67, and 68 degrees of 2θ, corresponding to the (100), (002), (101), (102), (110), (103), (200), (112), and (201) crystal planes, respectively **(Fig.2)**. These findings are consistent with the JCPDS file 36145, suggesting a hexagonal wurtzite structure of ZnO with space group P63 mc. The lattice parameters are determined to be a = b = 3.249 Å and c = 5.206 Å (Singh et al., 2011).

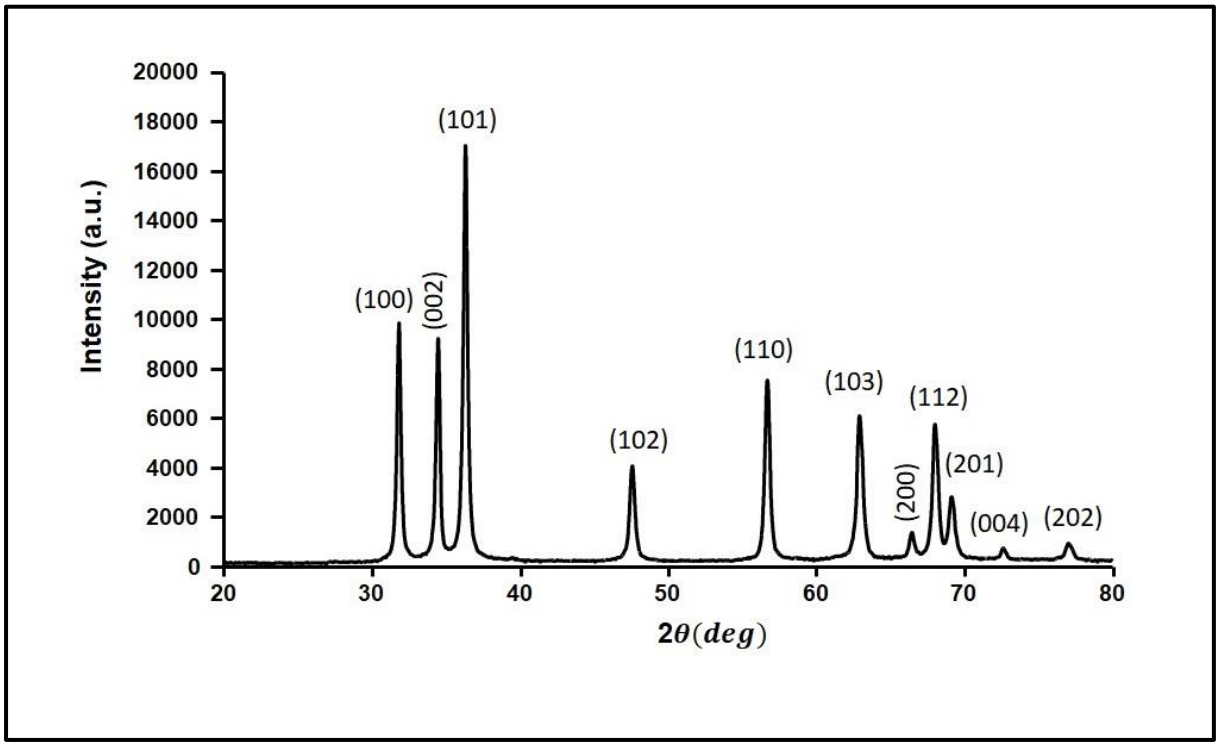

Figure 2: XRD pattern of synthesized ZnO nanoparticles.

7.3.3. Scanning Electron Microscopy (SEM)

The Scanning Electron Microscopy (SEM) image depicted in **(Fig.3)** illustrates the distinctive spherical and granular morphology of the particles, characterized by dimensions within the nanoscale range. This observation provides valuable insights into the intricate structural composition of the particles and their potential implications for material properties and

applications. This image provides a magnified view of zinc oxide prepared using zinc acetate as the initial material, captured with a Scanning Electron Microscope (SEM). At lower magnification, we observe that the particles display some degree of agglomeration, indicating a lack of optimal particle separation. Additionally, it is evident that the weak physical forces are responsible for keeping these particles together.

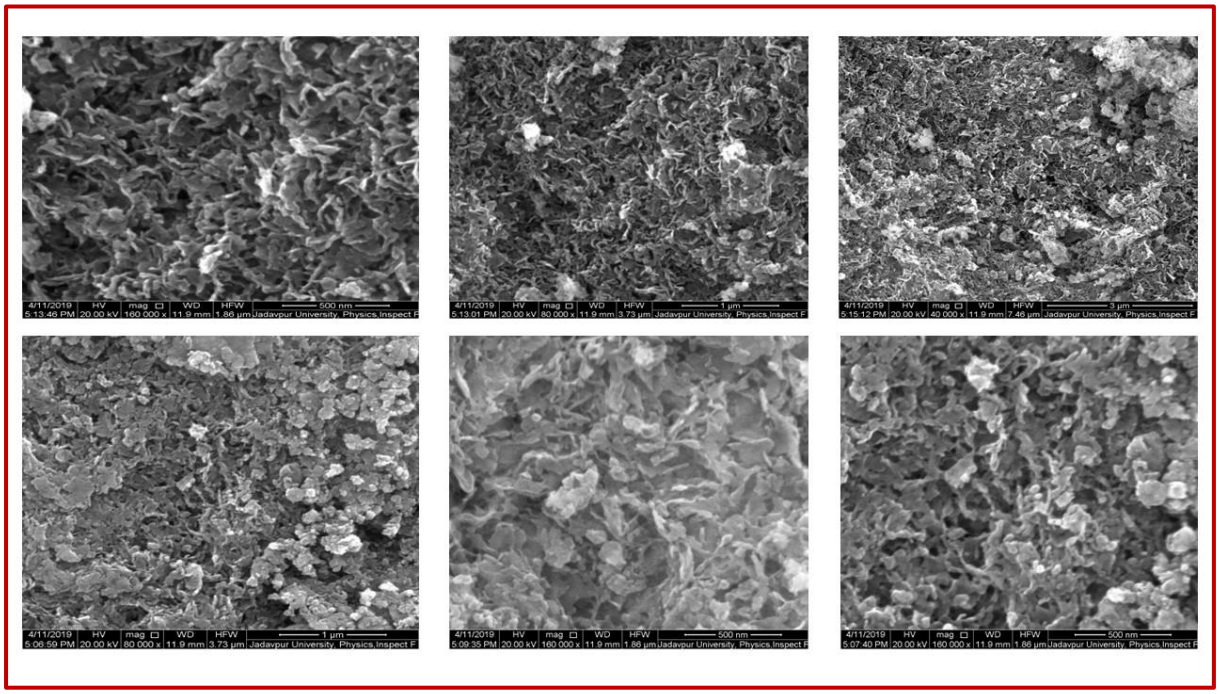

Figure 3: SEM pictures of synthesized ZnO NPs.

7.3.4. ANS-fluorescence measurement to monitor the hydrophobicity change

The changes induced by heating β-lg were further confirmed through ANS fluorescence studies. When proteins undergo partial unfolding, ANS binds to their hydrophobic regions, resulting in an increase in fluorescence intensity (Matulis et al.,1999). **Fig.4** illustrates the ANS fluorescence spectra of heat-exposed β-lg with and without ZnO NPs. In the absence of ZnO NPs, the lowest ANS fluorescence intensity at 480 nm was observed for heat-exposed β-lg at pH 7.4. The increased fluorescence intensity indicates that more ANS was able to bind to the exposed hydrophobic areas of the protein following thermal denaturation. These hydrophobic areas promote protein-protein interactions, leading to the thermal aggregation of β-lg (Cattoni et al.,2009). However, the presence of ZnO NPs significantly increased ANS fluorescence during the thermal exposure of β-lg, suggesting the enhancement of ANS binding sites. The gradual increase in ANS fluorescence intensity and minor shift in emission maximum when β-lg was exposed to heat in the presence of varying amounts of ZnO NPs imply the formation of

more hydrophobic areas in β-lg under thermal stress at 75 °C. As a result, ZnO NPs have the capacity to enhance β-lg aggregation in a concentration-dependent manner.

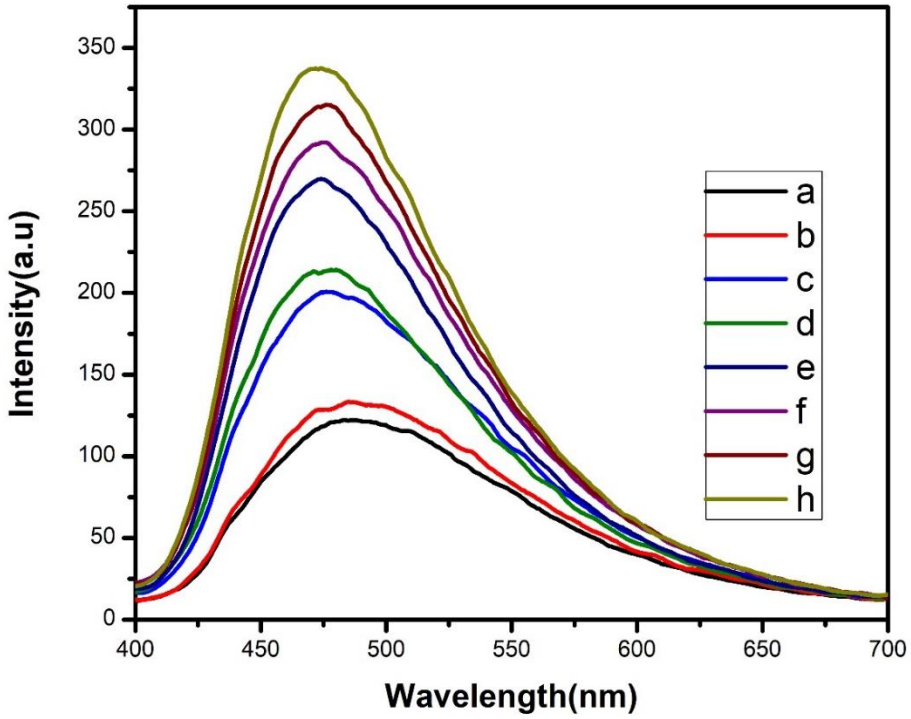

Figure 4: The ANS fluorescence of β-lg after being heat stressed at 75°C for 1 hour was measured in the presence and absence of ZnO NPs. This was carried out in a 10 mM phosphate buffer at pH 7.4, with excitation at 380nm and emissions measured within the 400–700 nm wavelength range. The protein concentration during ANS fluorescence measurements was 0.25 mg mL^{-1}.

7.3.5. Thioflavin T (Th T) assay

The cationic benzothiazole dye ThT exhibits heightened fluorescence upon binding to protein assemblies in vitro. Its binding specifically targets the intermolecular beta-sheet structure found within the aggregates (Naeem et al., 2004). Thus, assembly of β-lg molecules into aggregates was confirmed using the ThT assay. The increased fluorescence intensity when ThT binds to the protein assembly indicates aggregate formation. The native β-lg undergoes thermal aggregation in the absence of ZnO NPs, displaying minimal ThT intensity upon binding **(Fig.5, profile a)**. The fluorescence intensity gradually increases, reaching its maximum after the thermal exposure of the protein with varying concentrations of ZnO NPs (10 µM to 125 µM). This ThT assay result demonstrates that amyloid fibril formation of β-lg increases in the presence of ZnO NPs under thermal conditions (Khurana et al., 2005).

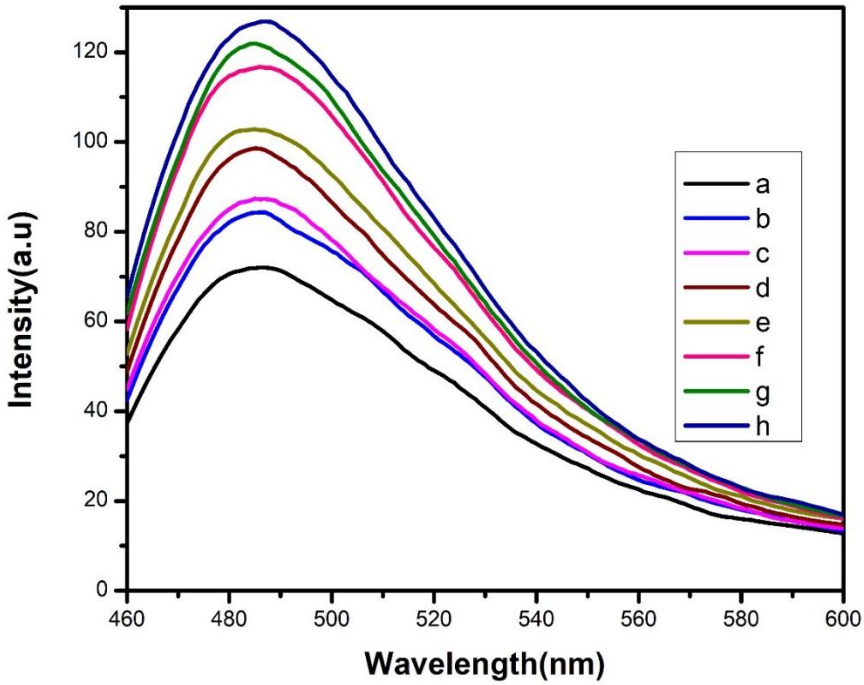

Figure 5: Th T assay to study the aggregation of heat exposed β-lg at 75°Cat pH7.4. Profile a represents β-lg at its native state whereas profile (b-h) represents the heat exposed β-lg in the absence and the presence of ZnO NPs (10 µM to 125 µM) respectively. Fluorescence emissions were monitored in the wavelength range 460–600 nm after excitation at 450 nm.

7.3.6. Circular dichroism (CD) spectroscopy

In the process of protein fibrillation, the molecules initially undergo unfolding processes, leading to the exposure of β-sheet structures. Subsequently, intermolecular β-sheets extend over the length of the fibril and arrange perpendicularly to the fibril axis, thus resulting in the formation of protofibrils (Alam et al., 2017; Giurleo et al., 2008). As such, the β-sheet structures play crucial roles in the formation of amyloid-like aggregation, as demonstrated in prior research (Zhao et al., 2018). We conducted an investigation to examine the secondary structural changes of β-lg during aggregation in the presence of ZnO NPs. Far UV-CD spectra of β-lg were assessed at pH 7.4 in the absence and presence of ZnO NPs during the aggregation process. The far-UV CD spectra of β-lg samples at pH 7.4, in the absence of ZnO NPs, exhibited a negative band at 216 nm, indicative of a β-sheet-rich conformation. Notably, β-lg maintained its predominantly β–sheet structure even at low pH. However, following a 1-hour incubation at 75°C, a major negative peak at 210 nm and a negative shoulder around 218 nm were observed, suggesting the formation of amyloid fibrils. In the presence of 10-100 µM ZnO NPs, the far-UV CD spectra of β-lg samples at pH 7.4 also displayed a negative band at 216 nm. However, distinct peaks at 205 nm and 220 nm were observed following a 1-hour

incubation. These findings indicate that the secondary structure of β-lg in amyloid aggregates differed from that in spherical aggregates.

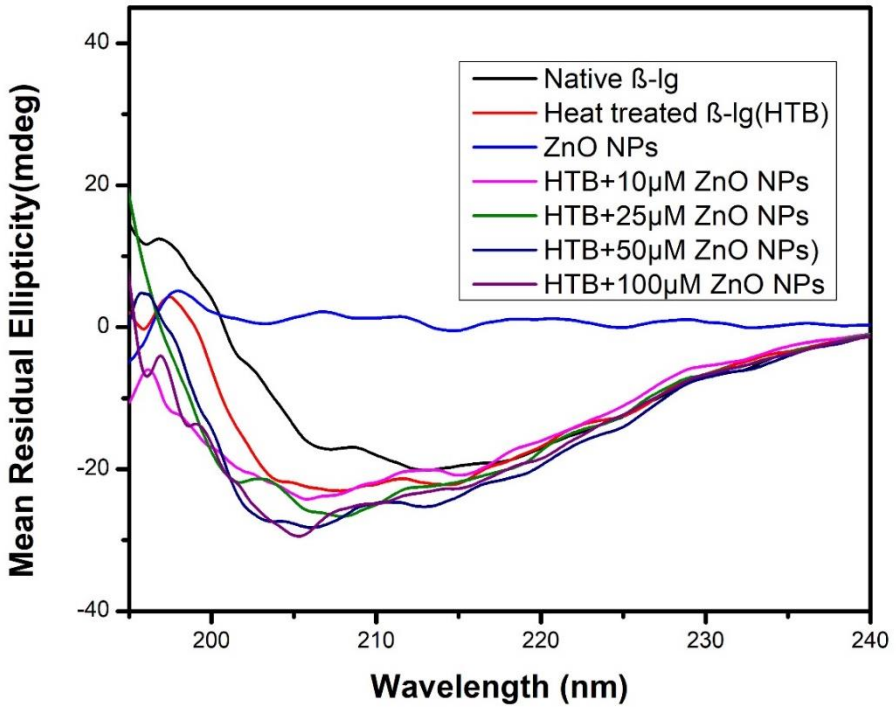

Figure 6: The far-UV CD spectra of β-lg were measured after the protein was incubated at 75°C for 1 hour. The analysis was conducted in both the absence and presence of zinc oxide nanoparticles (ZnO NPs) in a 10 mM phosphate buffer at pH 7.4. The concentration of the nanoparticles gradually increased from 10 μM to 100 μM, while the concentration of β-lg was maintained at 0.25 mg/ml throughout the CD measurement.

Table 1: The secondary structure composition of the β-lactoglobulin (β-lg) sample was analyzed after a 1-hour incubation at 75°C in a 10 mM phosphate buffer with a pH of 7.4, both in the absence and in the presence of ZnO NPs.

Samples	**α**-Helix (%)	**β** -Structure (%)	**β** -turn (%)	Random coil(%)
Native β-lg	22.3	39.7	11.4	26.6
Heat treated β-lg	20.8	35.6	11.9	31.7
HTB+ 10μM ZnO NPs	19.8	34.8	12.1	33.3
HTB+ 25μM ZnO NPs	19.3	34.1	12.3	34.3
HTB+ 50μM ZnO NPs	18.7	33.2	13.1	35.0
HTB+ 100μM ZnO NPs	17.9	32.5	14.0	35.6

7.3.7. Congo Red (CR) Assay

The Congo red assay can be utilized to confirm the partial unfolding and subsequent aggregation of beta-lactoglobulin (β-lg). Congo red (CR), a dye that exhibits preferential binding to beta-sheet structures within the aggregates but not to the native protein, is analogous to ThT and is commonly deployed for the identification of protein aggregates. The interaction between CR and the aggregates results in a distinctive increase in the absorption maxima from 480 nm to 490 nm **(Fig.7).** To scrutinize the formation of such aggregates, the CR absorption spectra of β-lg were documented in the absence and presence of various concentrations of zinc oxide nanoparticles (ZnO NPs). The native β -lg displayed absorption maxima at 495 nm. Subsequent to the gradual addition of the ZnO NPs there was a discernible enhancement in CR absorption intensities precipitated by the partial unfolding of the β-lg molecule.

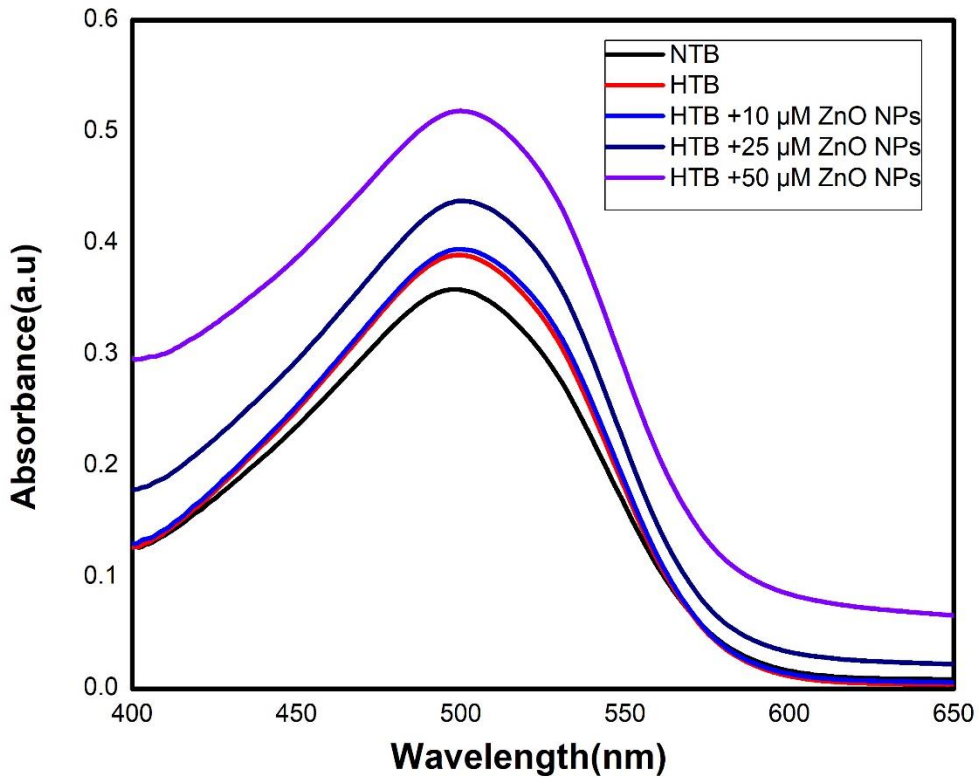

Figure 7: Depicts the Congo red absorption spectra of native β-lg in 10 mM sodium phosphate buffer at pH 7.4. Absorbance was scanned in the wavelength range of 400 nm to 650 nm using a UV-Vis spectrophotometer. Results are the mean of three different experiments. The protein concentration was maintained at 27.2 μM.

To corroborate the findings of the ThT assay, the Congo red (CR) binding assay was implemented to validate the inhibition of beta-lactoglobulin (β-lg) aggregation. CR binding to the extensive beta-sheet structures is anticipated to induce an augmentation in absorption, accompanied by a characteristic shift in its absorption spectrum from around 490 nm when unbound to 500 nm when bound, contingent upon the state of protein aggregation. The CR spectral shift assay presents the potential for quantifying amyloid fibrils, where substances with coloration may impede ThT fluorescence (Hudson et al.,2009). Notably, under neutral pH conditions, beta-lactoglobulin exhibited absorption maxima at 493 nm **(Fig.7)**, while thermally incubated beta-lactoglobulin demonstrated absorption maxima at 500 nm, concomitant with an expansion of the areas of absorbance. The broadening observed can be ascribed to the captivity of the CR dye within the clusters of the beta-sheet peptide backbones of the aggregates.

7.3.8. The Sodium Dodecyl Sulfate-Polyacrylamide Gel Electrophoresis (SDS-PAGE)

The SDS-PAGE analysis under non-reducing conditions **(Fig.8)** reveals that the native β-lg manifests as a single band (lanes 2 and 3) indicative of its monomeric state. In contrast, the β-lg solution exposed to heat (heated at 75 °C for 1 hour) exhibits a series of protein bands in SDS-PAGE, suggesting the formation of β-lg oligomers (lane 4). This analytical method effectively separates non-covalently bonded aggregates into monomers while preserving the integrity of disulfide-linked aggregates. Upon heating to 75 °C, the Cys-121 of β-lg undergoes S-S linkage, resulting in the formation of dimers and other covalently bound intermediates during the aggregation process. This thermal treatment induces the reorganization of disulfide bonds, leading to the creation of new intramolecular and intermolecular disulfide bridges and the rearrangement of existing intramolecular disulfide bonds (Croguennec et al., 2004 and Mousavi et al., 2008).

When subjected to a temperature of 75°C, the intensity of the band representing the monomer decreases, accompanied by a subsequent rise in the intensities of the bands corresponding to various oligomers and higher aggregates. However, the SDS-PAGE analysis of heat-treated β-lg in the presence of ZnO NPs under non-reducing conditions yields a distinct outcome. In the presence of ZnO NPs, the heat-stressed β-lg (lanes 5,6 and 7) exhibits a decline in the intensity of the monomer and an increase in the intensities of the dimer and other higher aggregates, indicating a substantial acceleration in the aggregation of this protein in the presence of ZnO NPs. Lane 1 demonstrates the SDS-PAGE pattern of known molecular weight marker proteins

(Page Ruler TM, Prestained Protein Ladder, 10, 17, 34, 43, 55, 72, 95, 130, and 170 kDa, respectively, Fermentus Life Science, #SM0671) run in parallel.

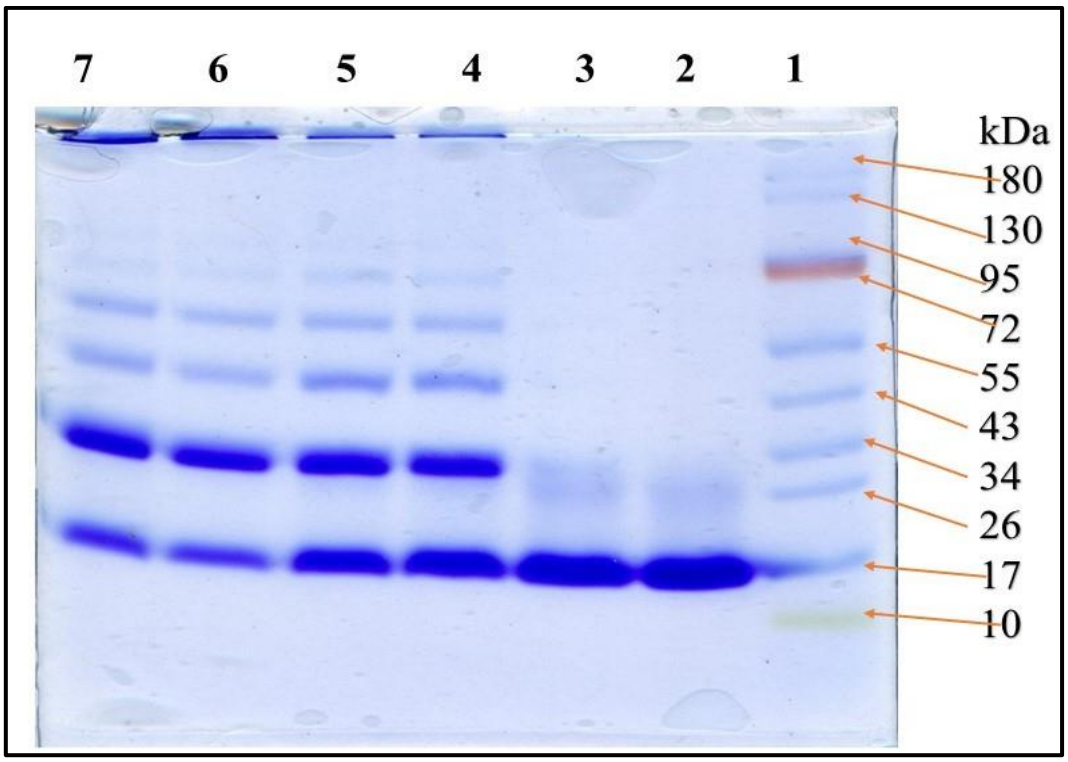

Figure 8: The SDS-PAGE (12%) patterns of native β-lg were observed in lanes 2 and 3. Additionally, heat-stressed β-lg at 75 °C for 1 hour in the absence (lane 4) and in the presence of 10, 25, and 50 μM of ZnO NPs (lanes 5, 6, and 7 respectively) were displayed. Lane 1 illustrates the SDS-PAGE pattern of a marker protein with known molecular weights (PageRulerTM, Prestained Protein Ladder, with bands at 10, 17, 26, 34, 43, 55, 72, 95, 130, and 180 kDa, respectively; Fermentus Life Science, #SM0671) run simultaneously.

7.3.9. Morphological Study by Transmission Electron Microscopy (TEM)

To corroborate previous findings such as ANS and ThT, we utilized TEM to conduct morphological studies of the end products formed during the heat-induced aggregation of β-lg, with and without the presence of ZnO NPs. The internal structure of the ZnO nanoparticles was also investigated using TEM, and the resulting images (**Fig.9c**) depicted homogeneously aggregated spherical ZnO nanoparticles with a typical size of 30-35 nm, consistent with the XRD result.

In the absence of ZnO NPs, heat-treated β-lg formed a network of spherical aggregates after incubation at 75 °C for 1 hour (**Fig.9b**). Conversely, incubation at the same temperature in the presence of ZnO NPs yielded an enhancement of amorphous aggregates (**Fig.9e** and **Fig.9f**).

This was attributed to the orderly adsorption of a substantial amount of β-lg on the extensive surface of ZnO NPs, resulting in a change in the secondary conformation of β-lg (α-helical and β-sheet structure). The sequential arrangement of β-lg molecules provided an ideal platform for interaction with neighboring β-lg already adsorbed on the ZnO NPs, culminating in the formation of spherical aggregates.

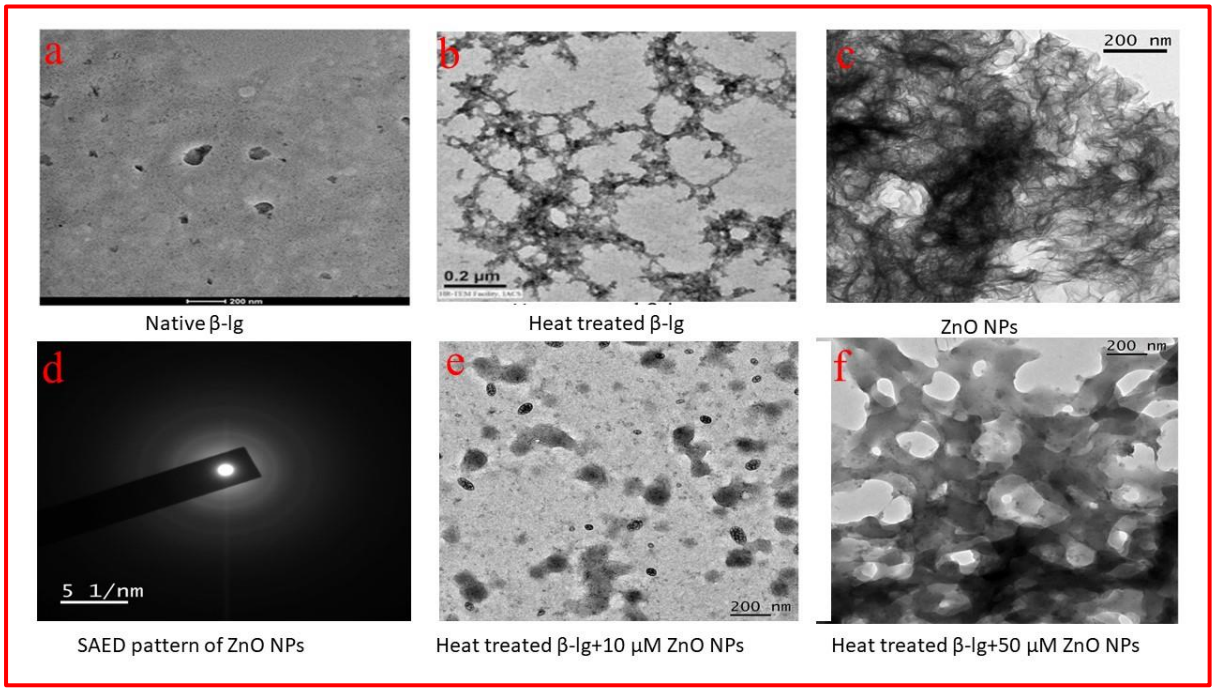

Figure 9: Transmission Electron Microscopy (TEM) images are provided for comparison. Images (profile e and profile f) show the TEM images of heat-treated β-lg in the presence of ZnO NPs, while Image (profile b) depicts the heat-treated β-lg in the absence of ZnO NPs for reference. In the provided images, profiles a, c, and d depict native β-lg, whereas only the ZnO NPs and the SAED pattern of the synthesized nanoparticles are presented, respectively.

7.4. Conclusion

In our study, we observed that the use of ThT fluorescence and CR binding enhanced the formation of amyloid aggregates of β-lg. However, upon examination using TEM, we noted the formation of spherical aggregates under these conditions. It seems that these spherical aggregates share some characteristics with amyloid fibrils.

Numerous scientific studies have provided evidence that the net charge of proteins is influenced by intermolecular interactions, consequently dictating the ultimate structure of protein aggregates. It has been increasingly recognized that electrostatic effects play a pivotal role in shaping the morphology of protein aggregation (Greenwald and Riek.,2010). These findings

indicate that the formation of spherical particles may be ascribed to alterations in β-lg surface electrostatic interactions. Furthermore, the results corroborate that electrostatic interactions govern the ultimate morphology of aggregates (Foderà et al., 2013).

The multifaceted, dynamic, and transient short-lived characteristics of the various forms of lactoglobulin can assume complicate the study of its physico-chemical and biochemical properties. Moving forward, we envision that further studies into the behavior of lactoglobulin may provide additional molecular insights into the workings of this multifunctional protein.

7.5. References

Alam, P., Chaturvedi, S.K., Siddiqi, M.K., Rajpoot, R.K., Ajmal, M.R., Zaman, M. and Khan, R.H., 2016. Vitamin k3 inhibits protein aggregation: implication in the treatment of amyloid diseases. Scientific reports, 6(1), p.26759.

Alam, P., Siddiqi, M.K., Chaturvedi, S.K., Zaman, M. and Khan, R.H., 2017. Vitamin B12 offers neuronal cell protection by inhibiting Aβ-42 amyloid fibrillation. International journal of biological macromolecules, 99, pp.477-482.

Al-Shabib, N.A., Khan, J.M., Malik, A., Alsenaidy, A.M., Alsenaidy, M.A., Husain, F.M., Shamsi, M.B., Hidayathulla, S. and Khan, R.H., 2018. Negatively charged food additive dye "Allura Red" rapidly induces SDS-soluble amyloid fibril in beta-lactoglobulin protein. International journal of biological macromolecules, 107, pp.1706-1716.

Alvarado, J.A., Maldonado, A., Juarez, H. and Pacio, M., 2013. Synthesis of colloidal ZnO nanoparticles and deposit of thin films by spin coating technique. Journal of Nanomaterials, 2013(1), p.903191.

Arvizo, R., Bhattacharya, R. and Mukherjee, P., 2010. Gold nanoparticles: opportunities and challenges in nanomedicine. Expert opinion on drug delivery, 7(6), pp.753-763.

Aschaffenburg, R. and Drewry, J., 1957. Improved method for the preparation of crystalline β-lactoglobulin and α-lactalbumin from cow's milk. Biochemical Journal, 65(2), p.273.

Bellova, A., Bystrenova, E., Koneracka, M., Kopcansky, P., Valle, F., Tomasovicova, N., Timko, M., Bagelova, J., Biscarini, F. and Gazova, Z., 2010. Effect of Fe3O4 magnetic nanoparticles on lysozyme amyloid aggregation. Nanotechnology, 21(6), p.065103.

Cattoni, D.I., Kaufman, S.B. and Flecha, F.L.G., 2009. Kinetics and thermodynamics of the interaction of 1-anilino-naphthalene-8-sulfonate with proteins. Biochimica et Biophysica Acta (BBA)-Proteins and Proteomics, 1794(11), pp.1700-1708.

Chatterjee, T., Chakraborti, S., Joshi, P., Singh, S.P., Gupta, V. and Chakrabarti, P., 2010. The effect of zinc oxide nanoparticles on the structure of the periplasmic domain of the Vibrio cholerae ToxR protein. *The FEBS journal*, *277*(20), pp.4184-4194.

Cho, K., Wang, X.U., Nie, S., Chen, Z. and Shin, D.M., 2008. Therapeutic nanoparticles for drug delivery in cancer. Clinical cancer research, 14(5), pp.1310-1316.

Choudhary, S., Kishore, N. and Hosur, R.V., 2015. Inhibition of insulin fibrillation by osmolytes: Mechanistic Insights. Scientific reports, 5(1), p.17599.

Conway, K.A., Harper, J.D. and Lansbury, P.T., 1998. Accelerated in vitro fibril formation by a mutant α-synuclein linked to early-onset Parkinson disease. Nature medicine, 4(11), pp.1318-1320.

Cooper, G.J., Willis, A.C., Clark, A., Turner, R.C., Sim, R.B. and Reid, K.B., 1987. Purification and characterization of a peptide from amyloid-rich pancreases of type 2 diabetic patients. Proceedings of the National Academy of Sciences, 84(23), pp.8628-8632.

Croguennec, T., T O'Kennedy, B. and Mehra, R., 2004. Heat-induced denaturation/aggregation of β-lactoglobulin A and B: kinetics of the first intermediates formed. International Dairy Journal, 14(5), pp.399-409.

De Jong, W.H. and Borm, P.J., 2008. Drug delivery and nanoparticles: applications and hazards. International journal of nanomedicine, 3(2), pp.133-149.

Fodera, V., Zaccone, A., Lattuada, M. and Donald, A.M., 2013. Electrostatics controls the formation of amyloid superstructures in protein aggregation. Physical review letters, 111(10), p.108105.

Gilgun-Sherki, Y., Melamed, E. and Offen, D., 2006. Anti-inflammatory drugs in the treatment of neurodegenerative diseases: current state. Current pharmaceutical design, 12(27), pp.3509-3519.

Giurleo, J.T., He, X. and Talaga, D.S., 2008. β-lactoglobulin assembles into amyloid through sequential aggregated intermediates. Journal of molecular biology, 381(5), pp.1332-1348.

Greenwald, J. and Riek, R., 2010. Biology of amyloid: structure, function, and regulation. Structure, 18(10), pp.1244-1260.

Gupta, Y., Singla, G. and Singla, R., 2015. Insulin-derived amyloidosis. Indian journal of endocrinology and Metabolism, 19(1), pp.174-177.

Hamada, D. and Dobson, C.M., 2002. A kinetic study of β-lactoglobulin amyloid fibril formation promoted by urea. Protein Science, 11(10), pp.2417-2426.

Harper, J.D. and Lansbury Jr, P.T., 1997. Models of amyloid seeding in Alzheimer's disease and scrapie: mechanistic truths and physiological consequences of the time-dependent solubility of amyloid proteins. Annual review of biochemistry, 66(1), pp.385-407.

Hettiarachchi, C.A., Melton, L.D., Gerrard, J.A. and Loveday, S.M., 2012. Formation of β-lactoglobulin nanofibrils by microwave heating gives a peptide composition different from conventional heating. Biomacromolecules, 13(9), pp.2868-2880.

Hill, A.F., Barnham, K.J., Bottomley, S.P. and Cappai, R., 2011. Protein Folding, Misfolding, and Disease. Humana Press.

Hill, E.K., Krebs, B., Goodall, D.G., Howlett, G.J. and Dunstan, D.E., 2006. Shear flow induces amyloid fibril formation. Biomacromolecules, 7(1), pp.10-13.

Hoppenreijs, L.J.G., Fitzner, L., Ruhmlieb, T., Heyn, T.R., Schild, K., Van Der Goot, A.J., Boom, R.M., Steffen-Heins, A., Schwarz, K. and Keppler, J.K., 2022. Engineering amyloid

Hsieh, S., Chang, C.W. and Chou, H.H., 2013. Gold nanoparticles as amyloid-like fibrillogenesis inhibitors. Colloids and Surfaces B: Biointerfaces, 112, pp.525-529.

Hudson, S.A., Ecroyd, H., Kee, T.W. and Carver, J.A., 2009. The thioflavin T fluorescence assay for amyloid fibril detection can be biased by the presence of exogenous compounds. The FEBS journal, 276(20), pp.5960-5972.

Jakob-Roetne, R. and Jacobsen, H., 2009. Alzheimer's disease: from pathology to therapeutic approaches. Angewandte Chemie International Edition, 48(17), pp.3030-3059.

Jean, E., Ebbo, M., Valleix, S., Benarous, L., Heyries, L., Grados, A., Bernit, E., Grateau, G., Papo, T., Granel, B. and Daniel, L., 2014. A new family with hereditary lysozyme

amyloidosis with gastritis and inflammatory bowel disease as prevailing symptoms. BMC Gastroenterology, 14, pp.1-6.

Khurana, R., Coleman, C., Ionescu-Zanetti, C., Carter, S.A., Krishna, V., Grover, R.K., Roy, R. and Singh, S., 2005. Mechanism of thioflavin T binding to amyloid fibrils. Journal of Structural Biology, 151(3), pp.229-238.

Krebs, M.R., Devlin, G.L. and Donald, A.M., 2007. Protein particulates: another generic form of protein aggregation? Biophysical journal, 92(4), pp.1336-1342.

Krebs, M.R., Devlin, G.L. and Donald, A.M., 2009. Amyloid fibril-like structure underlies the aggregate structure across the pH range for β-lactoglobulin. Biophysical journal, 96(12), pp.5013-5019.

Krebs, M.R., Domike, K.R. and Donald, A.M., 2009. Protein aggregation: more than just fibrils. Biochemical Society Transactions, 37(4), pp.682-686.

Laemmli, U.K., 1970. Cleavage of structural proteins during the assembly of the head of bacteriophage T4. nature, 227(5259), pp.680-685.

Linse, S., Cabaleiro-Lago, C., Xue, W.F., Lynch, I., Lindman, S., Thulin, E., Radford, S.E. and Dawson, K.A., 2007. Nucleation of protein fibrillation by nanoparticles. Proceedings of the National Academy of Sciences, 104(21), pp.8691-8696.

Linse, S., Cabaleiro-Lago, C., Xue, W.F., Lynch, I., Lindman, S., Thulin, E., Radford, S.E. and Dawson, K.A., 2007. Nucleation of protein fibrillation by nanoparticles. *Proceedings of the National Academy of Sciences*, *104*(21), pp.8691-8696.

Maity, S., Pal, S., Parvej, H., Das, N., Sepay, N., Sarkar, M. and Halder, U.C., 2016. Facile synthesis and characterization of beta lactoglobulin–copper nanocomposites having antibacterial applications. RSC advances, 6(88), pp.85340-85346.

Maity, S., Sardar, S., Pal, S., Parvej, H., Chakraborty, J. and Halder, U.C., 2016. New insight into the alcohol-induced conformational change and aggregation of the alkaline unfolded state of bovine β-lactoglobulin. RSC advances, 6(78), pp.74409-74417.

Matulis, D., Baumann, C.G., Bloomfield, V.A. and Lovrien, R.E., 1999. 1-Anilino-8-naphthalene sulfonate as a protein conformational tightening agent. Biopolymers: Original Research on Biomolecules, 49(6), pp.451-458.

Maurer-Jones, M.A., Gunsolus, I.L., Murphy, C.J. and Haynes, C.L., 2013. Toxicity of engineered nanoparticles in the environment. Analytical chemistry, 85(6), pp.3036-3049.

Melkani, G.C., Trujillo, A.S., Ramos, R., Bodmer, R., Bernstein, S.I. and Ocorr, K., 2013. Huntington's disease induced cardiac amyloidosis is reversed by modulating protein folding and oxidative stress pathways in the Drosophila heart. PLoS genetics, 9(12), p.e1004024.

Mousavi, S.H.A., Bordbar, A.K. and Haertlé, T., 2008. Changes in structure and in interactions of heat-treated bovine β-lactoglobulin. Protein and Peptide Letters, 15(8), pp.818-825.

Muchowski, P.J., Schaffar, G., Sittler, A., Wanker, E.E., Hayer-Hartl, M.K. and Hartl, F.U., 2000. Hsp70 and hsp40 chaperones can inhibit self-assembly of polyglutamine proteins into amyloid-like fibrils. Proceedings of the National Academy of Sciences, 97(14), pp.7841-7846.

Murphy, S.R., Chang, C.C., Dogbevia, G., Bryleva, E.Y., Bowen, Z., Hasan, M.T. and Chang, T.Y., 2013. Acat1 knockdown gene therapy decreases amyloid-β in a mouse model of Alzheimer's disease. Molecular Therapy, 21(8), pp.1497-1506.

Naeem, A., Khan, K.A. and Khan, R.H., 2004. Characterization of a partially folded intermediate of papain induced by fluorinated alcohols at low pH. Archives of biochemistry and biophysics, 432(1), pp.79-87.

Navarra, G., Giacomazza, D., Leone, M., Librizzi, F., Militello, V. and San Biagio, P.L., 2009. Thermal aggregation and ion-induced cold-gelation of bovine serum albumin. European Biophysics Journal, 38, pp.437-446.

Nowacek, A., Kosloski, L.M. and Gendelman, H.E., 2009. Neurodegenerative disorders and nanoformulated drug development. Nanomedicine, 4(5), pp.541-555.

Pal, S., Maity, S., Sardar, S., Chakraborty, J. and Halder, U.C., 2016. Insight into the co-solvent induced conformational changes and aggregation of bovine β-lactoglobulin. International journal of biological macromolecules, 84, pp.121-134.

Palmal, S., Jana, N.R. and Jana, N.R., 2014. Inhibition of amyloid fibril growth by nanoparticle coated with histidine-based polymer. The Journal of Physical Chemistry C, 118(37), pp.21630-21638.

Papiz, M.Z., Sawyer, L., Eliopoulos, E.E., North, A.C.T., Findlay, J.B.C., Sivaprasadarao, R., Jones, T.A., Newcomer, M.E. and Kraulis, P.J., 1986. The structure of β-lactoglobulin and its similarity to plasma retinol-binding protein. Nature, 324(6095), pp.383-385.

Pepys, M.B., Hawkins, P.N., Booth, D.R., Vigushin, D.M., Tennent, G.A., Soutar, A.K., Totty, N., Nguyen, O., Blake, C.C.F., Terry, C.J. and Feest, T.G., 1993. Human lysozyme gene mutations cause hereditary systemic amyloidosis. Nature, 362(6420), pp.553-557.

Polymeropoulos, M.H., Lavedan, C., Leroy, E., Ide, S.E., Dehejia, A., Dutra, A., Pike, B., Root, H., Rubenstein, J., Boyer, R. and Stenroos, E.S., 1997. Mutation in the α-synuclein gene identified in families with Parkinson's disease. science, 276(5321), pp.2045-2047.

Pourrahimi, A.M., Liu, D., Pallon, L.K., Andersson, R.L., Abad, A.M., Lagarón, J.M., Hedenqvist, M.S., Ström, V., Gedde, U.W. and Olsson, R.T., 2014. Water-based synthesis and cleaning methods for high purity ZnO nanoparticles–comparing acetate, chloride, sulfate, and nitrate zinc salt precursors. RSC Advances, 4(67), pp.35568-35577.

Prabakaran, S. and Damodaran, S., 1997. Thermal unfolding of β-lactoglobulin: characterization of initial unfolding events responsible for heat-induced aggregation. Journal of Agricultural and Food Chemistry, 45(11), pp.4303-4308.

Radad, K., Al-Shraim, M., Moldzio, R. and Rausch, W.D., 2012. Recent advances in benefits and hazards of engineered nanoparticles. Environmental toxicology and pharmacology, 34(3), pp.661-672.

Roychaudhuri, R., Yang, M., Hoshi, M.M. and Teplow, D.B., 2009. Amyloid β-protein assembly and Alzheimer disease. Journal of Biological Chemistry, 284(8), pp.4749-4753.

Sakurai, K., Konuma, T., Yagi, M. and Goto, Y., 2009. Structural dynamics and folding of β-lactoglobulin probed by heteronuclear NMR. Biochimica et Biophysica Acta (BBA)-General Subjects, 1790(6), pp.527-537.

Sardar, S., Anas, M., Maity, S., Pal, S., Parvej, H., Begum, S., Dalui, R., Sepay, N. and Halder, U.C., 2019. Silver nanoparticle modulates the aggregation of beta-lactoglobulin and induces to form rod-like aggregates. International journal of biological macromolecules, 125, pp.596-604.

Sardar, S., Pal, S., Maity, S., Chakraborty, J. and Halder, U.C., 2014. Amyloid fibril formation by β-lactoglobulin is inhibited by gold nanoparticles. International journal of biological macromolecules, 69, pp.137-145.

Sciarretta, K.L., Gordon, D.J. and Meredith, S.C., 2006. Peptide-based inhibitors of amyloid assembly. Methods in enzymology, 413, pp.273-312.

Shang, W., Nuffer, J.H., Dordick, J.S. and Siegel, R.W., 2007. Unfolding of ribonuclease A on silica nanoparticle surfaces. *Nano letters*, *7*(7), pp.1991-1995.

Siddiqi, M.K., Shahein, Y.E., Hussein, N. and Khan, R.H., 2016. Effect of surfactants on Ra-sHSPI–A small heat shock protein from the cattle tick Rhipicephalus annulatus. Journal of Molecular Structure, 1119, pp.12-17.

Šimšíková, M. and Antalík, M., 2013. Interaction of cytochrome c with zinc oxide nanoparticles. *Colloids and Surfaces B: Biointerfaces*, *103*, pp.630-634.

Singh, R.P., Shukla, V.K., Yadav, R.S., Sharma, P.K., Singh, P.K. and Pandey, A.C., 2011. Biological approach of zinc oxide nanoparticles formation and its characterization. Adv. Mater. Lett, 2(4), pp.313-317.

Song, Y., Azakami, H., Hamasu, M. and Kato, A., 2001. In vivo, glycosylation suppresses the aggregation of amyloidogenic hen egg white lysozymes expressed in yeast. FEBS letters, 491(1-2), pp.63-66.

Sunde, M., Serpell, L.C., Bartlam, M., Fraser, P.E., Pepys, M.B. and Blake, C.C., 1997. Common core structure of amyloid fibrils by synchrotron X-ray diffraction. Journal of molecular biology, 273(3), pp.729-739.

Verma, M., Vats, A. and Taneja, V., 2015. Toxic species in amyloid disorders: Oligomers or mature fibrils. Annals of Indian Academy of Neurology, 18(2), pp.138-145.

Vertegel, A.A., Siegel, R.W. and Dordick, J.S., 2004. Silica nanoparticle size influences the structure and enzymatic activity of adsorbed lysozyme. *Langmuir*, *20*(16), pp.6800-6807.

Wu, W.H., Sun, X., Yu, Y.P., Hu, J., Zhao, L., Liu, Q., Zhao, Y.F. and Li, Y.M., 2008. TiO2 nanoparticles promote β-amyloid fibrillation in vitro. Biochemical and biophysical research communications, 373(2), pp.315-318.

Xiao, L., Zhao, D., Chan, W.H., Choi, M.M. and Li, H.W., 2010. Inhibition of beta 1–40 amyloid fibrillation with N-acetyl-l-cysteine capped quantum dots. Biomaterials, 31(1), pp.91-98.

Yagi, M., Sakurai, K., Kalidas, C., Batt, C.A. and Goto, Y., 2003. Reversible unfolding of bovine β-lactoglobulin mutants without a free thiol group. Journal of Biological Chemistry, 278(47), pp.47009-47015.

Yu, W.W., Chang, E., Falkner, J.C., Zhang, J., Al-Somali, A.M., Sayes, C.M., Johns, J., Drezek, R. and Colvin, V.L., 2007. Forming biocompatible and nonaggregated nanocrystals in water using amphiphilic polymers. Journal of the American Chemical Society, 129(10), pp.2871-2879.

Zhang, D., Neumann, O., Wang, H., Yuwono, V.M., Barhoumi, A., Perham, M., Hartgerink, J.D., Wittung-Stafshede, P. and Halas, N.J., 2009. Gold nanoparticles can induce the formation of protein-based aggregates at physiological pH. *Nano letters*, *9*(2), pp.666-671.

Zhang, S., 2003. Fabrication of novel biomaterials through molecular self-assembly. Nature Biotechnology, 21(10), pp.1171-1178.

Zhao, D., Li, L., Xu, D., Sheng, B., Qin, D., Chen, J., Li, B. and Zhang, X., 2018. Application of ultrasound pretreatment and glycation in regulating the heat-induced amyloid-like aggregation of β-lactoglobulin. Food Hydrocolloids, 80, pp.122-129.

Journal of Molecular Structure 1318 (2024) 139164

Contents lists available at ScienceDirect

Journal of Molecular Structure

journal homepage: www.elsevier.com/locate/molstr

Promotion and modulation of amyloid fibrillation of bovine beta-lactoglobulin by hydroxychalcones

Hasan Parvej [a], Ramkrishna Dalui [a], Shahnaz Begum [a], Swarnali Paul [a], Falguni Mondal [a], Sanhita Maity [b], Nayim Sepay [c], Umesh Chandra Halder [a,*]

[a] Department of Chemistry, Jadavpur University, Kolkata 700 032, India
[b] Department of Chemistry, Amity University, Ranchi, Jharkhand 834002, India
[c] Department of Chemistry, Lady Brabourne College, Kolkata 700017, India

ARTICLE INFO

Keywords:
Beta-lactoglobulin
Hydroxychalcone
Amyloid fibrillation
Protein aggregation

ABSTRACT

Hydroxychalcones are naturally occurring compounds having biological relevance. This work demonstrates the synthesis of some chalcones having hydrophobic and polar groups and the investigation of their effect on the stability of a model protein beta-lactoglobulin (β-lg). An easy and simple method (Simon-Smith) was utilized to synthesize the four chalcone compounds. The binding of the chalcone molecules to the protein destabilized the protein structure and subsequently exposed the hydrophobic cores resulting in the aggregation of β-lg under thermal conditions. Using multiple spectroscopic methods (UV-Vis, fluorescence, FT-IR), imaging techniques like TEM, and theoretical tools were used to monitor the formation of protein aggregation and to understand the underlying mechanism. Exposures of hydrophobic amino acid residues in the aqueous medium by binding of the chalcones are responsible for protein aggregation through protein-protein interactions. It is sensitive to the polarity of the hydroxychalcones. In this process, polar group-containing hydroxychalcones are less effective, and unsubstituted hydroxychalcones are most efficient in promoting the amyloid fibrillation of β-lg.

1. Introduction

Privileged compound chalcone, 1,3-diphenyl-2E-propene-1-one, contains two benzene rings and one α,β-unsaturated ketone functionality (having -C=O-CH=CH- group in their structure) and is used as an efficient template in drug discovery [1,2]. The moiety has been of interest for its synthesis, biosynthesis, and broad biological activities to organic chemists and biochemists for many decades [3,4]. It has more than a thousand years of therapeutic history. Derivatives of chalcone, found in a wide range of plants vegetables, fruits, and teas, are the root chemicals of various natural products [5,6]. Chalcone containing plants and herbs was used for treatments of different biological disorders like inflammation, cancer, diabetes, etc. [7]. Several compounds with chalcone moiety are being used as drug candidates (metochalcone, sofalcone). Chalcones, the secondary metabolites of edible or medicinal plants, are members of the flavonoid family [8,9]. Chalcones mainly consist of polyphenolic compounds whose colours vary from yellow to orange and contribute significantly to the pigmentation of the corolla of some plants [10]. Chalcones are found to act as an initial intermediate in the biosynthesis of several flavonoids, isoflavonoids, and aurones [11].

Protein aggregation causes different adverse physiological effects in the human body [12]. For example, aggregation of Aβ peptide, α-synuclein, insulin, etc. cause several neurodegenerative diseases like Alzheimer's, Parkinson's disease, and diabetics type II, respectively [13,14]. Many proteins have an alpha helix as their most prominent structural motif in their native conformation [15]. Under stress, proteins can undergo extensive conformational changes and acquire a beta-sheet structural motif. Native proteins become toxic due to these structural transitions [16]. In addition to native proteins, beta-sheets are also found in many functional proteins, such as immunoglobulins. However, amyloid deposits generally change from an alpha-helix conformation to a beta-sheet conformation [16]. Formation of cross β-sheet structure is the prerequisite condition of protein aggregation and thus amyloid fibril formation. Misfolding of the protein creates a fibrillar structure depending upon the physical and chemical stimulants. The binding of small molecules to the protein can change the protein structure causing its misfolding. Hence preventing the formation of these soluble aggregates during the fibrillation procedure could serve as the key to the

* Corresponding author.
E-mail address: uhalder2002@yahoo.com (U.C. Halder).

https://doi.org/10.1016/j.molstruc.2024.139164
Received 5 April 2024; Received in revised form 22 June 2024; Accepted 26 June 2024
Available online 28 June 2024

Check for updates

ChemistrySelect

Research Article
doi.org/10.1002/slct.202303699

Chemistry Europe
European Chemical Societies Publishing

www.chemistryselect.org

Anion–Induced Amyloid Fibrillation of Human Insulin *In vitro*

Shahnaz Begum,[a] Swarnali Paul,[a] Hasan Parvej,[a] Falguni Mondal,[a] Ramkrishna Dalui,[a] Anirban Pradhan,[b] Nayim Sepay,[c] and Umesh Chandra Halder*[a]

In the present study, we have focused on the effect of three biologically important salt anions on insulin aggregation. The result of the present study reveals that salts differing in their anions (NaI, NaOAc, and $NaNO_3$) induce the self–assembly formation of insulin even at low physiological (in the micromolar range) salt concentration with efficacy that follows the order $I^- > CH_3COO^- > NO_3^-$. Here, the anion–driven aggregation of insulin does not follow either the Hofmeister series or electroselectivity series at very low salt concentrations; instead, the binding of anions at low pH to the positively charged residues of insulin is determined by a mechanism where the salt anions promote the fibrillation of insulin and modify the morphology of the monomeric precursor molecule. Both the nucleation and fibril elongation are controlled by the electrostatic forces and hydrophobic interactions. Aggregation mechanism and aggregate morphology were investigated employing a combination of Thioflavin T (ThT) and ANS fluorescence, circular dichroism (CD), dynamic light scattering (DLS), and transmission electron microscopy (TEM). Overall, the present data will enhance the idea to rationalize the anion effects on the aggregation of amyloid-prone protein and to understand the influence of charged biomolecules in cellular compartments.

Introduction

Many proteins and peptides can form the stable self–assembly termed amyloid fibrils under stress due to misfolding.[1,2] Morphologies of these fibrils are independent of the nature of the proteins, albeit they consist of common cross-β sheet structure.[3] Efforts have been made to understand the formation of oligomeric intermediates of amyloid fibrils playing key roles in the pathology of amyloid diseases.[4] More than twenty diseases are associated with the phenomenon 'amyloidosis' in human. They include Alzheimer's disease, Parkinson's disease, cataracts, systemic amyloidosis, type 2 diabetes mellitus, and cardiovascular diseases.[5] Researchers devoted their time to investigate the fibril-forming events and the structural intermediates triggering the protein oligomerization process. Nucleation and subsequent growth of these oligomers induces to form worm-like protofibrillar assembly having less organized structures than the resultant fibrillar aggregates.[6]

Two factors generally can control the oligomerization rate and morphology of the aggregates arising from unfolded peptides and proteins. These are the amino acid sequence (intrinsic parameter) of the involved peptides or proteins and the surrounding physicochemical or environmental factors. The intrinsic parameter is thus related to the primary structure, types and distribution of the amino acid residues, the charge on the residues, and their beta-sheet propensity to adapt the crossed β-structure. Conversely, physicochemical or environmental factors are related to pH, temperature, salt ions, small additives, cosolvents, or solutes.[7–10]

Salts are abundantly present in our physiological system of cellular compartments at smaller concentrations (nanomolar to micromolar concentration range), acting as micronutrients. The ions of these salts can act as an essential environmental determinant during amyloid formation and have been observed to play a specific role in the aggregation of the α-synuclein,[7] Aβ peptide,[11] prion protein,[12] HypF–N[13] and bovine serum albumin.[9] The protein aggregation ability of various ions is generally related to the electroselectivity principle or the Hofmeister series, a ranking of the ions commonly employed to explain various chemical and biological science phenomena. The historic 'Hofmeister effect' is brought into play at moderate to high (> 0.3 M) concentrations of salts, wherein the 'kosmotropic' ions are assumed to make water structure and decrease protein solubility by increasing the conformational stability. On the contrary, the 'chaotropic' ions are assumed to break the water structure to increase protein solubility by decreasing the conformational stability.[14] However, the effects are considered negligible at lower and physiological salt concentrations. Below 0.1 M salt concentrations, the nonspecific electrostatic interactions mainly control protein–ion interactions and screen the charges on protein surfaces.[15] Still, literature shows many examples where ion–specific influences play important role in solubility[16] and stability of protein[17] and amyloid fibrillation[7] in this concentration range. Although some anions, like sulfates, precipitate the native protein solution, their action on non-native protein solution is complex, and fewer are reported. Again, some anions can stabilize the structure of the protein in nonnative conditions, thus decreasing the possibility of forming aggregation–prone structures. Ions of varying charges can

[a] S. Begum, S. Paul, H. Parvej, F. Mondal, R. Dalui, U. Chandra Halder
Department of Chemistry, Jadavpur University, Kolkata 700 032, India
E-mail: uhalder2002@yahoo.com

[b] A. Pradhan
Department of Chemistry, Birla Institute of Technology (BIT) Mesra, Jharkhand, 835215, India

[c] N. Sepay
Department of Chemistry, Lady Brabourne College, Kolkata 700017, India

NJC

ROYAL SOCIETY OF CHEMISTRY

PAPER

View Article Online
View Journal | View Issue

Check for updates

Cite this: New J. Chem., 2024, 48, 3120

In vitro retardation and modulation of human insulin amyloid fibrillation by Fe^{3+} and Cu^{2+} ions

Swarnali Paul,[a] Shahnaz Begum,[a] Hasan Parvej,[a] Ramkrishna Dalui,[a] Subrata Sardar,[a] Falguni Mondal,[a] Nayim Sepay[b] and Umesh Chandra Halder *[a]

Received 21st September 2023,
Accepted 4th January 2024

DOI: 10.1039/d3nj04431a

rsc.li/njc

Metal ions of the later part of the first-row transition series (Fe, Co, Ni, Cu, and Zn) can form bonds through the carboxylate, hydroxyl, thiol, and imidazole side chains of proteins and those bonds are significantly more stable than those formed by non-transition metals. Their adventitious binding to protein surfaces provides a great platform for maintaining the native structure of many biologically significant proteins and thus inhibiting the self-aggregation phenomenon of proteins. Aggregation followed by deposition of proteins used for therapeutic purposes either at the site of administration *in vivo* or during storage conditions *in vitro* is a major concern. In this work, human insulin is induced to form 'amyloid fibrils' at acidic pH and elevated temperature and then the inhibitory activities of two transition metal ions Fe^{3+} and Cu^{2+} towards insulin amyloid fibrillation were investigated. The results show that the formation of β-sheet-rich fibrillar structures was inhibited more with Fe^{3+} than Cu^{2+}-treated insulin. Dynamic light scattering and circular dichroism proved that Cu^{2+} was effective at lowering the interaction ratios with insulin, yet Fe^{3+} was effective in maintaining the size as well as the alpha-helical conformation of monomeric insulin. This metal complex (insulin-Fe^{3+} or insulin-Cu^{2+}) delayed the nucleation step of aggregation and Fe^{3+} is far better than Cu^{2+} in this endeavor. However, both of the metal ions proved their effectiveness in preventing amyloid fibrillation *in vitro* and can modulate the morphology of the aggregates as revealed by TEM studies. Overall the two transition metal ions Fe^{3+} and Cu^{2+} employed in this investigation are essential micronutrients too and are required in minute concentrations. The present study will encourage the applications of transition metal ions Fe^{3+} and Cu^{2+} as effective interrupters of amyloidogenesis in aggregation-prone proteins showing pathogenic amyloid deposition.

1. Introduction

There are many known human etiopathogeneses associated with the generation of oligomers and mature fibrils[1] by aggregation of therapeutic proteins at the sites of application or other places. To carry out their functions, proteins must remain in their folded conformation, which usually corresponds to the thermodynamically most stable state.[2] But secondary structures having marginal stability may act as nucleation sites for protein misfolding or aggregation due to deviation from its optimal physical state (called the native state) or under stress-inducing conditions.[3] The deviations include the conversion of the native protein into cross-β-sheet rich structures under different non-optimal conditions and causing the loss of their functional properties. This leads to the process of protein oligomerization resulting in the formation of amyloid-like fibrils.[4] Amyloid formation at the site of repeated injections in patients administered with insulin having diabetes mellitus is a common example of such protein aggregation.[5] Besides this, long term storage or keeping under improper conditions may lead to the generation of such clumps of many important therapeutic proteins/enzymes due to their unfolding followed by the misfolding phenomenon.[6,7] The functional properties of such cytotoxic[8] fibrillar forms are lost and deposited in various parts of the body like the shoulders,[9] arms,[10] thighs,[11] and abdominal walls[12] after injection, and thus can induce inflammation. The close relationship of neurodegenerative diseases and amyloidosis has been established.[13] Human insulin is a widely used model protein[14] for the investigation of the mechanism of amyloid formation as its fibrillar structure resembles the other amyloid prone proteins, like amyloid precursor protein (Aβ peptides causing Alzheimer's disease), atrial natriuretic factor (amyloid ANF causing atrial amyloidosis), and prion protein (causing spongiform encephalopathies), *etc.* Even during the

[a] Department of Chemistry, Jadavpur University, Kolkata-700032, India. E-mail: uhalder2002@yahoo.com
[b] Department of Chemistry, Lady Brabourne College, Kolkata-700017, India

RSC Advances

ROYAL SOCIETY OF CHEMISTRY

PAPER

View Article Online
View Journal | View Issue

Cite this: *RSC Adv.*, 2023, **13**, 34097

Structural modulation of insulin by hydrophobic and hydrophilic molecules†

Shahnaz Begum,[a] Hasan Parvej,[a] Ramkrishna Dalui,[a] Swarnali Paul,[a] Sanhita Maity,[a] Nayim Sepay,[b] Mohd Afzal[c] and Umesh Chandra Halder *[a]

Received 29th September 2023
Accepted 13th November 2023

DOI: 10.1039/d3ra06647a

rsc.li/rsc-advances

In the bloodstream, insulin interacts with various kinds of molecules, which can alter its structure and modulate its function. In this work, we have synthesized two molecules having extremely hydrophilic and hydrophobic side chains. The effects of hydrophilic and hydrophobic molecules on the binding with insulin have been investigated through a multi-spectroscopic approach. We found that hydrophilic molecules have a slightly higher binding affinity towards insulin. Insulin can bind with the hydrophilic molecules as it binds glucose. The high insulin binding affinity of a hydrophobic molecule indicates its dual nature. The hydrophobic molecule binds at the hydrophobic pocket of the insulin surface, where hydrophilic molecules interact at the polar surface of the insulin. Such binding with the hydrophobic molecule perturbs strongly the secondary structure of the insulin much more in comparison to hydrophilic molecules. Therefore, the stability of insulin decreases in the presence of hydrophobic molecules.

Introduction

Protein structure is very sensitive to their microenvironments.[1] Structural alteration of proteins is often observed due to several factors (modulators) like pH,[2] temperature,[2] salt concentration,[3] and different types of small molecules.[4,5] This change in the presence of physical and chemical modulators is significant because it may change the function of the proteins.[6,7] The study of the modulators' interactions with proteins has drawn attention from the scientific community.[8,9]

Human insulin is a protein hormone in the blood that regulates blood sugar levels.[10,11] Depending upon the exposure and availability of it in the body, several medical conditions like hypertension,[12] coronary heart disease,[13] stroke,[14] cancer,[15] and type II diabetes[16] are widespread nowadays. The small monomeric insulin contains fifty-one amino acids and is divided into two α-helical structures, joined together by three disulfide bonds (intra-chain and inter-chain).[17] This small monomeric form of insulin is highly unstable.[18,19] Again, insulin is one of the serum proteins that commonly interact with the polar poly-hydroxyl group containing molecules like glucose. However, in the serum, many hydrophobic molecules can affect the structure and function of the insulin. Thus, the structure of insulin may change in the presence of diverse molecules in the blood and these compound can initiate insulin-related diseases. Therefore, an investigation of the effect of molecules with hydroxyl groups and hydrophobic groups on the insulin's structure is highly essential.

Protein-small molecule interaction studies are used to investigate the structural effect on proteins in the presence of different microenvironments.[20,21] The tuning of the microenvironment is possible through the proper choice of small molecules.[22,23] Hydrophilic to hydrophobic molecules can be synthesized from simple organic reactions. The reaction of an aldehyde with primary amine is one of the simple organic reactions used to join two fragments through imine bond formation.[24] The products of the reaction are known as Schiff's base.[24] With the proper choice of the substituent attached to the amine and aldehyde part, the hydrophilicity and hydrophobicity of the molecule can be tunable. For this reason, Schiff's base is used in very diverse fields of science like coordination chemistry,[25,26] hydrogels,[27,28] sensing,[29] analytical chemistry, electronics, optics[25] *etc.*

In this study, we have synthesized one hydrophobic Schiff's base (*E*)-2-((*tert*-butylimino) methyl)-6-methoxyphenol and one hydrophilic Schiff's base (*E*)-2-((2-hydroxy-3-methoxybenzylidene) amino)-2-(hydroxymethyl)propane-1,3-diol. The interactions of these two molecules with insulin have been investigated here. Therefore, it will provide a scope to monitor the structure of insulin in two opposite microenvironments.

Results and discussion

Synthesis of Schiff's base and choice of compounds

Insulin binds with glucose, which is a polar poly-hydroxy compound. For this reason, a poly-hydroxy compound is

[a]*Department of Chemistry, Jadavpur University, Kolkata-700032, India. E-mail: juumesh.halder@gmail.com*

[b]*Department of Chemistry, Lady Brabourne College, Kolkata-700017, India*

[c]*Department of Chemistry, College of Science, King Saud University, Riyadh 11451, Saudi Arabia*

† Electronic supplementary information (ESI) available. See DOI: https://doi.org/10.1039/d3ra06647a

RSC Advances

ROYAL SOCIETY OF CHEMISTRY

PAPER

View Article Online
View Journal | View Issue

Cite this: RSC Adv., 2022, 12, 17020

Coumarin derivatives inhibit the aggregation of β-lactoglobulin †

Hasan Parvej,[a] Shahnaz Begum,[a] Ramkrishna Dalui,[a] Swarnali Paul,[a] Barun Mondal,[a] Subrata Sardar,[a] Nayim Sepay,[b] Gourhari Maiti[a] and Umesh Chandra Halder *[a]

The binding of a small molecule to a protein through non-covalent interactions mainly depends on its size and electronic environment. Such binding can change the stability of the three dimensional protein structure which sometimes may destabilize it to accelerate or to inhibit protein aggregation. Coumarin is a widely used fluorescent dye with several biological applications. Different substituents (electron-donating and electron-withdrawing) at different positions of the coumarin moiety can influence its molecular volume, physical and chemical properties. Here we investigate the effect of such substituents of coumarin on the aggregation of a model protein, beta-lactoglobulin (β-lg) through a multi spectroscopic approach. It was observed that coumarin methyl ester with an 8-hydroxyl group can inhibit the β-lg aggregation. This compound can bind the hydrophobic site of beta-lactoglobulin and stabilize a particular protein conformation through the formation of hydrogen bond and hydrophobic interactions. Thus a properly designed compound can inhibit protein–protein interactions through protein–small molecule interactions. Other coumarinoid compounds also are effective in the prevention of thermal aggregation of β-lg.

Received 16th February 2022
Accepted 15th May 2022

DOI: 10.1039/d2ra01029a

rsc.li/rsc-advances

Introduction

The formation of insoluble amyloid fibrils from normal soluble proteins is well known. Amyloid fibrils are impervious to degradation.[1] Proteins can form amyloid fibrils and each case brings a different characteristic disease. Aggregation of Aβ, α-synuclein, or prion proteins causes neurodegenerative brain disorders Alzheimer's disease, Parkinson's disease, or mad cow disease, respectively. It is also found that diseases like diabetes type 2 are disorders due to amyloid fibril formation of insulin.[1] Since amyloid fibrils are insoluble in physiological conditions, they can deposit around the cell and tissues and cause a pathogenic effect.[2] Aggregation of such proteins gives very stable systems and facilitates the process. Structurally, fibrillar assemblies are predominantly cross-β conformation of the proteins. Interestingly, the formation of fibrils is independent of protein size, shape, and sources. Recently, hydrophobins, curli, and melanosomes are identified as the expression of functional amyloidogenesis.[1]

To prevent the amyloid fibrils formation, a number of therapeutic strategies have been developed. Site-specific glycosylation of protein[3] and protein engineering[4] are of some example of prevention techniques. Most of the proteins have a very stable conformational structure in fibrillar form because it is in a global free-energy minimum.[5–7] Therefore, once a protein starts partial degradation to form a fibril, it is very hard to stop the process. Stabilization of the native conformer of a protein can slow down the partial degradation of protein and can deem fibrillation.[8] It is the most acceptable therapeutic strategy to prevent fibrils formation now. Therefore, the design of new anti-fibrillating molecules is in demand.

Coumarin, an aromatic heterocyclic lactone compound, is an important natural product found in many plants. Coumarin derivatives or coumarinoids have a large family containing thousands of compounds. They have very interesting photophysical,[9] biological, and medicinal[10] properties. Coumarin absorbs light at ~280 nm wavelength and shows fluorescence property by the emission at 410 to 470 nm. This photophysical property is very much tunable with the substituents attached to the moiety.[11] For this reason, these compounds are widely used as dyes. Some coumarinoids were designed for blue-green tunable organic laser dyes.[11]

Whey contains an important lipocalin protein, *i.e.* β-lactoglobulin (β-lg), which is of immense interest due to its nutritional and small molecule carrier properties.[12] Structurally, the protein is β-sheet enriched (eight anti-parallel β-sheets forms a barrel-like structure) and forms self-assembly upon thermal exposure. The protein can be isolated and purified in high yield

[a]Department of Chemistry, Jadavpur University, Kolkata 700 032, India. E-mail: uhalder2002@yahoo.com
[b]Department of Chemistry, Lady Brabourne College, Kolkata 700017, India

† Electronic supplementary information (ESI) available. See https://doi.org/10.1039/d2ra01029a

NJC

PAPER

View Article Online
View Journal | View Issue

Cite this: New J. Chem., 2018, 42, 19260

Inhibition of amyloid fibril formation of β-lactoglobulin by natural and synthetic curcuminoids†

Sanhita Maity,[a] Sampa Pal,[a] Subrata Sardar,[a] Nayim Sepay,[a] Hasan Parvej,[a] Shahnaz Begum,[a] Ramkrishna Dalui,[a] Niloy Das,[b] Anirban Pradhan[c] and Umesh Chandra Halder*[a]

The aggregation of proteins has been associated with several aspects of daily life, including food processing, blood coagulation and many neurodegenerative infections. However, the actual mechanisms responsible for amyloidosis, the irreversible fibril formation of various proteins, which is linked to disorders such as Alzheimer's disease, Creutzfeldt–Jakob disease and Huntington's disease, have not yet been fully elucidated. Curcumin, a potent anti-oxidant, exhibits anti-amyloid activity; however, its activity is limited due to its instability. Therefore, chemical modifications of curcumin have been performed to obtain molecules with enhanced stability and superior anti-amyloid activity. Herein, the main objective of this study is related to the inhibitory effects of three stable analogs of curcumin against bovine β-lactoglobulin (β-lg) fibrillization. We inferred that a pyrazole derivative of curcumin showed remarkable potency in arresting the fibrillization of β-lg, as revealed by biophysical techniques. Molecular docking demonstrated that pyrazole-mediated inhibition of β-lg fibrillogenesis may be initiated by interacting with aggregation-prone regions of the protein and preventing interactions between monomers, leading to suppression of the overall aggregation process. This work alludes to a possible broader scope for discovery of other small molecules that may exert similar effects against amyloid formation and its associated neurodegenerative diseases.

Received 27th June 2018,
Accepted 13th October 2018

DOI: 10.1039/c8nj03194k

rsc.li/njc

Introduction

The anomalous self-assembly and accumulation of misfolded proteins is known to have common cellular and molecular mechanisms, including protein aggregation, which is the known leading causative agent of a number of conformational diseases, such as Alzheimer's disease (AD), Parkinson's disease (PD), Huntington's disease (HD) and prion disease.[1,2] The aggregates consist of fibers with cross β-sheet structures, termed harmful 'amyloids', and their morphological features are not associated with behaviors of specific proteins. Although the proper aetiology of AD remains controversial, diverse factors appear to play vital roles in the pathophysiology of the disease; these include abnormal β-amyloid (Aβ) deposits in extracellular amyloid plaques, which lead to progressive neuronal death, tau protein hyperphosphorylation, metal ion dyshomeostasis, oxidative stress, and neurotransmitter system dysfunction.[3–7] Different peptides and proteins generate morphologically similar or different amyloid fibrils through dimer and oligomer formation; this has been hypothesized to occur in a stepwise fashion, with a slow phase of nucleation of the precursors of the amyloid fibrils followed by a relatively fast elongation phase.[8] Moreover, in the formation of amyloid fibrils, the incentive to assemble arises from favorable solvation energies and side-chain interactions accompanying the formation of β-sheet structures.[9] Currently, numerous clinical and experimental studies are revealing that soluble oligomeric and protofibrillar forms of proteins are potentially neurotoxic.[10,11]

Recently, the most challenging research task has focused on the inhibition of fibril formation[12–14] by the employment of small molecules. These potent modulators are believed to stabilize monomers by blocking the formation of toxic oligomers and to divert the monomeric proteins to off-pathway non-toxic intermediates. Small molecules are being developed to inhibit aggregation of Aβ,[15] α-synuclein[16] and prions.[17]

Much evidence has shown that polyphenols, which have structural constraints, are effective in the inhibition of amyloid fibrillation.[18,19] Curcumin, a classical active yellow lipid-soluble β-diketone dietary polyphenolic component, has been

[a] Organic Chemistry Section, Department of Chemistry, Jadavpur University, Kolkata 700032, India. E-mail: uhalder2002@yahoo.com
[b] Department of Chemistry, Durgapur Govt. College, Durgapur, West Bengal 713214, India
[c] Director's Research Unit (DRU), Indian Association for the Cultivation of Science, Kolkata-700032, India

† Electronic supplementary information (ESI) available. See DOI: 10.1039/c8nj03194k

J. Chem. Sci. (2020) 132:103
https://doi.org/10.1007/s12039-020-01796-z

REGULAR ARTICLE

Antioxidant ferulic acid prevents the aggregation of bovine β-lactoglobulin *in vitro*

SAMPA PAL[a], SANHITA MAITY[a], SUBRATA SARDAR[a], SHAHNAZ BEGUM[a], RAMKRISHNA DALUI[a], HASAN PARVEJ[a], KAUSHIK BERA[b], ANIRBAN PRADHAN[c], NAYIM SEPAY[a], SWARNALI PAUL[a] and UMESH CHANDRA HALDER[a,*]

[a]Organic Chemistry Section, Department of Chemistry, Jadavpur University, Kolkata 700 032, India
[b]Natural Products Laboratory, Department of Chemistry, The University of Burdwan, Burdwan 713 104, India
[c]Director's Research Unit (DRU), Indian Association for the Cultivation of Science, Kolkata 700 032, India
E-mail: uhalder2002@yahoo.com

MS received 20 November 2019; revised 27 April 2020; accepted 4 May 2020; published online 11 August 2020

Abstract. Amyloids, a well-ordered β-sheet-enriched structural network, can be broadly defined as insoluble protein aggregates that are linked to a wide variety of diseases including systemic amyloidosis and some neurodegenerative disorders. Ferulic acid (FA), a phenolic acid, abundant in antioxidant and efficient pharmaceutical has beneficial effects against several ailments. Based on this, we have investigated the protective role of FA on amyloid formation of bovine β-lactoglobulin (β-lg), a model globular protein. Using a set of *in vitro* biophysical methods, such as UV-Vis spectroscopy, fluorescence, circular dichroism, transmission electron microscopy, etc., our research group has concluded that FA significantly inhibits the heat-induced amyloid formation of β-lg and this inhibitory effect is dose-dependent. Exposed surface hydrophobicity of β-lg amyloid fibrils decreased significantly in the presence of FA. Docking study revealed that ionic and hydrogen bonding interactions between FA and β-lg prevented protein conformational changes leading to fibrillation. We anticipate that our finding would give an insight into the protein aggregation inhibited by the antioxidant compound, FA and pave the way for finding and developing other new small molecules (protein misfolding inhibitors) that give similar result against amyloid fibril formation and its allied neurodegenerative disorders.

Keywords. Antioxidant; ferulic acid; β-lactoglobulin; aggregation.

1. Introduction

In the present area of research, a very interesting topic is the alteration of native (often soluble) proteins into non-native folded fibrillar structures; these are often not soluble in various solvents as well as in water. These protein fibrils are usually called amyloid fibrils and are the hallmark for numerous ailments, including Alzheimer's, Huntington's, type II diabetes, Parkinson's, prion-associated encephalopathy diseases and others.[1–6] Amyloid fibrils are highly organised polypeptide aggregates and are rich in β-sheet secondary conformation.[7] These fibrils are stable against temperature,[8] hydrolytic pressure,[9] proteolytic enzymes[10] and denaturants.[11] Several proteins and peptides, e.g. amyloid β-peptide (Aβ), β-lactoglobulin (β-lg) islet amyloid polypeptide (IAPP), insulin, α-synuclein, and transthyretin have been identified as amyloidogenics,[12–16] but it has been observed that there is no similarity in primary structure among them.[17] The aggregation pattern of such peptides and proteins differs owing to their differential forms.[18–20]

In recent research work, a number of endeavours have been applied to find or design the compounds which can prevent the formation of these toxic oligomeric species or break up the pre-formed fibrils. Several working parameters, e.g. concentration of protein, pH of experimental solution, ionic strength of the reaction medium, reaction temperature, existence of co-solvents, etc., can be altered to modulate the aggregation process of β-lg into the oligomers or fibrils.[21–23]

Small organic molecules (either from natural origin or synthetically derived) play a significant role in

*For correspondence

International Journal of Biological Macromolecules 125 (2019) 596–604

Contents lists available at ScienceDirect

International Journal of Biological Macromolecules

journal homepage: http://www.elsevier.com/locate/ijbiomac

Silver nanoparticle modulates the aggregation of beta-lactoglobulin and induces to form rod-like aggregates

Subrata Sardar, Md. Anas, Sanhita Maity, Sampa Pal, Hasan Parvej, Shahnaz Begum, Ramkrishna Dalui, Nayim Sepay, Umesh Chandra Halder *

Organic Chemistry Section, Department of Chemistry, Jadavpur University, Kolkata 700032, India

ARTICLE INFO

Article history:
Received 10 September 2018
Received in revised form 23 November 2018
Accepted 2 December 2018
Available online 7 December 2018

Keywords:
Silver nanoparticle (SNP)
β-Lactoglobulin (β-lg)
Amyloid fibrillar aggregates
Rod-shaped aggregates
Scanning electron microscopy (SEM)
Transmission electron microscopy (TEM)
Docking

ABSTRACT

Silver nanoparticles (SNPs) have been increasingly used in medicines and biomaterials as a drug carriers and diagnostic or therapeutic material due to their smaller size, large surface area and cell penetration ability. Here we report the preparation of SNPs of diameter 10 ± 3 nm by using silver nitrate and sodium borohydride and the interaction of synthesized SNPs with our model protein β-lactoglobulin (β-lg) in 10 mM phosphate buffer at pH 7.5 after thermal exposure at 75 °C. Heat exposed β-lg forms amyloidal fibrillar aggregates whereas this protein aggregates adopt rod-like shape instead of fibrillar structure in presence of SNP under the same conditions. Size of the synthesized SNPs is confirmed by UV–Visible spectroscopy, SEM and TEM. Interactions and subsequent formation of molecular assembly of heat stressed β-lg with SNP were investigated using Th-T assay and ANS binding assay, DLS, RLS, CD, FT-IR, SEM, TEM. Docking study parallely also support the experimental findings.

1. Introduction

Silver nanoparticles (SNPs) play a significant role in catalytic reaction, wound dressing, optical property, electrical property, antimicrobial activity, purification of ground water, removal of some chemical hazards, medical implants, prevention in infection, drug delivery, cancer treatment, antifungal activity, molecular linkers, pharmacological application, etc. [1–4]. Silver nanocrystals encapsulated in mesoporous silica nanoparticles displayed antimicrobial activity against both Gram-positive and Gram-negative bacteria [5]. Some researchers applied silver nanoparticles in purification of ground water in a convenient way. This nanoparticle is suitably used to detect some chemical hazards like Hg^{2+}, Cu^{2+} and S^{2-} [6–7]. It is also increasingly used in cosmetics and it has also been proposed in medical implants and instruments for the prevention of infection [8–10]. The silver nanocrystals encapsulated with silica nanoparticles are now used for imaging and drug delivery purpose [11]. Very low concentrations of silver nanoparticles are effective in induction of apoptosis in cancer cells [12]. Recent study demonstrates the antitumor activity of green-synthesized SNPs against lung cancer in vitro and in vivo [13]. The interactions between SNPs and various DNA bases (adenine, guanine, cytosine, and thymine) are also used as molecular linkers because of their biological significance [14]. The interaction of silver nanoparticles with proteins like SNPs-BSA and SNPs-BSA-emodin, interactions over the protein structure as well in the protein-drug binding show that silver nanoparticles may play a good role in biomedical and pharmacological applications [15].

Several diseases are known to occur due to the misfolding and aggregation of the proteins that are naturally present for normal the functioning of our body. Protein misfolding and aggregation are associated with many neurodegenerative diseases like Alzheimer's (AD), Parkinson's (PD), amyotrophic lateral sclerosis (ALS), frontotemporal dementia (FTD), diabetes type II and Huntington's diseases are the notorious examples for this kind [16–20]. The pathologic characteristics of AD are the formation of amyloid-beta (Aβ) fibrils enriched with cross β-sheet structures caused by the misfolding of Aβ peptide [21,22]. The mechanism of the formation of the fibrils is formed based on the nucleation and growth mechanism [23]. In the progression, the monomers are transformed into oligomers and the oligomers act as nuclei for the formation of fibril followed by the elongation of the fibrils through the addition of the monomers [24]. In our previous study, we have shown that gold nanoparticles (GNP) inhibit the amyloid fibril formation of β-lg [25]. β-Lg has been extensively utilized in the study of protein folding and aggregation.

β-Lg is a predominantly β-sheet protein having 162 amino acid residues and molecular weight 18.4 kDa. Basically it is a well-known globular whey protein of pI 5.2. In its β-barrel structure there are 8 strands (A to H) which are succeeded by three turn α-helix and a final β-strand (strand I) [26]. At pH 7.0 the protein exists as a reversible dimer and extent of dimerization depends on pH, temperature, protein

* Corresponding author.
E-mail address: uhalder2002@yahoo.com (U.C. Halder).

https://doi.org/10.1016/j.ijbiomac.2018.12.039
0141-8130/

International Conference on Chemistry for Human Development (ICCHD-2018)

8–10th, 2018 January

Certificate

This is to Certify that Prof/Dr./Mr./Mrs. Ramkrishna Dalui

of Jadavpur University

has participated and presented a Paper (Oral/Poster) Delivered Talk in the International Conference on Chemistry for Human Development (ICCHD-2018) held at Heritage Institute of Technology, Kolkata

Jt. Convenor

Convenor

National Seminar on

CURRENT DEVELOPMENTS IN CHEMICAL SCIENCES (CDCS-2018)

(Wednesday, March 7, 2018)

under

Centre for Advanced Studies II Program

Organized by

Department of Chemistry, Jadavpur University, Kolkata 700 032

This is to certify that Ramkrishna Dalui *of* Jadavpur University *has participated/presented a poster in the seminar organized by the Department of Chemistry, Jadavpur University, Kolkata 700 032 on Wednesday, March 7, 2018.*

Date: 07-03-2018
Place: Kolkata

SAUBHIK HALDAR

PARTHA MAHATA

Conveners

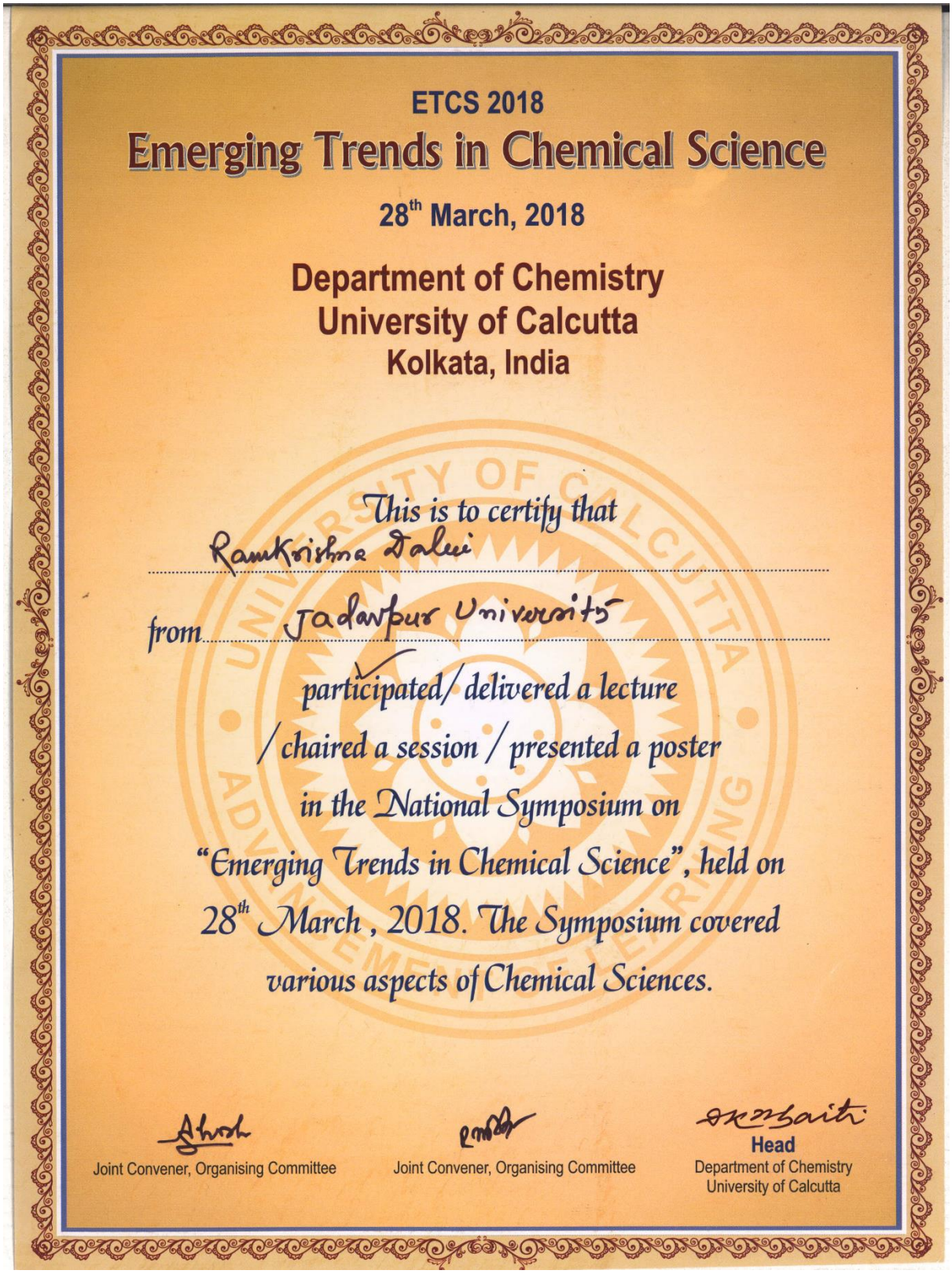

ETCS 2018

Emerging Trends in Chemical Science

28th March, 2018

Department of Chemistry
University of Calcutta
Kolkata, India

This is to certify that

Ramkrishna Dalui

from Jadavpur University

participated/ delivered a lecture / chaired a session / presented a poster in the National Symposium on "Emerging Trends in Chemical Science", held on 28th March , 2018. The Symposium covered various aspects of Chemical Sciences.

Joint Convener, Organising Committee

Joint Convener, Organising Committee

Head
Department of Chemistry
University of Calcutta

National Seminar on

CHEMICAL SCIENCES: TODAY AND TOMORROW (CSTT-2019)

(Thursday, March 14, 2019)

under

Centre for Advanced Studies II Program

Organized by

Department of Chemistry, Jadavpur University, Kolkata 700 032

This is to certify that RAMKRISHNA DALUI *of* Dept. of Chemistry

JADAVPUR UNIVERSITY *has delivered an invited talk /participated/ presented a poster in the seminar organized by the Department of Chemistry, Jadavpur University, Kolkata 700 032 on Thursday, March 14, 2019.*

Date: 14-03-2019
Place: Kolkata

Partha Roy
Co-Convener

Swapan Kumar Bhattacharya
Convener

RAC 2019

Organized by
Department of Chemistry

NATIONAL INSTITUTE OF TECHNOLOGY MEGHALAYA

Supported By

CSIR SERB NEC NIT Meghalaya TEQIP

CERTIFICATE OF PARTICIPATION

This is to certify that

Mr. Ramkrishna Dalui, Jadavpur University

participated and presented a poster

at **the National Conference**

on

Recent Advances in Chemistry (RAC 2019)

held in the **Department of Chemistry, NIT Meghalaya**

during **October 14-15, 2019**

Dr. Atanu Singha Roy
(Convener)

Dr. Amit Kumar Paul
(Convener)

Prof. Ayon Bhattacharjee
(Dean R & C, NIT Meghalaya)

National Seminar on

Emerging Trends in Chemical Sciences
(January 07, 2020)

under

Centre for Advanced Studies II Program

Organized by

Department of Chemistry, Jadavpur University, Kolkata 700 032

Certificate of Participation

This is to certify that Ramkrishna Dalui

of Jadavpur University *has* ~~*taken part*~~*/presented a poster in the seminar organized by the Department of Chemistry, Jadavpur University, Kolkata 700 032 on January 07, 2020.*

Date: 07-01-2020
Place: Kolkata

KAJAL KRISHNA RAJAK
Convener

SAMIT GUHA
Co-Convener